

ASD-TDR-63-96

## SUMMARY OF THE FIFTH REFRACTORY COMPOSITES WORKING GROUP MEETING

August 1961

Technical Documentary Report Number ASD-TDR-63-96

Directorate of Materials and Processes  
Aeronautical Systems Division  
Air Force Systems Command  
Wright-Patterson Air Force Base, Ohio

Project No. 7381

(Prepared by L.N. Hjelm, Materials Engineering Branch, Applications  
Laboratory, Directorate of Materials and Processes)

## NOTICES

When Government drawings, specifications, or other data are used for any purpose other than in connection with a definitely related Government procurement operation, the United States Government thereby incurs no responsibility nor any obligation whatsoever; and the fact that the Government may have formulated, furnished, or in any way supplied the said drawings, specifications, or other data, is not to be regarded by implication or otherwise as in any manner licensing the holder or any other person or corporation, or conveying any rights or permission to manufacture, use, or sell any patented invention that may in any way be related thereto.

ASTIA release to OTS not authorized.

Qualified requesters may obtain copies of this report from the Armed Services Technical Information Agency, (ASTIA), Arlington Hall Station, Arlington 12, Virginia.

Copies of ASD Technical Reports and Technical Notes should not be returned to the Aeronautical Systems Division unless return is required by security contractual obligations, or notice on a specific document.

ASD-TDR-63-96

SUMMARY OF THE FIFTH REFRACTORY COMPOSITES  
WORKING GROUP MEETING

August 1961

Technical Documentary Report Number ASD-TDR-63-96

Directorate of Materials and Processes  
Aeronautical Systems Division  
Air Force Systems Command  
Wright-Patterson Air Force Base, Ohio

Project No. 7381

(Prepared by L. N. Hjelm, Materials Engineering Branch, Applications Laboratory, Directorate of Materials and Processes)

## ABSTRACT

This report is a compilation of 38 papers describing most of the information discussed at the 5th Refractory Composites Working Group Meeting held at the Chance-Vought Corp., Dallas, Texas, on 8-10 August 1961. The representatives of approximately 50 organizations presented informal discussions of their current activities in the fields of development, evaluation, and application of inorganic refractory composites for use over approximately 2500°F.

This Technical Documentary Report has been reviewed and is approved.

W. P. Conrardy  
Chief Materials Engineering Branch  
Directorate of Materials and Processes



## FOREWORD

This report consists of a series of papers presented at the Fifth Refractory Composites Working Group Meeting held in Dallas, Texas on 8, 9, and 10 August 1961.

The meeting was co-chaired by J. J. Gangler of NASA and L. N. Hjelm of ASD, with the Chance Vought Corp. acting as host.

The assistance given by the Chance Vought Corp. and its personnel in acting as host are deeply appreciated. The assistance of the personnel of the University of Dayton Research Institute in preparation of this report is gratefully acknowledged.

## TABLE OF CONTENTS

- I. ATTENDANCE LIST
- II. INVITATION LETTERS AND DISTRIBUTION LIST
- III. PRESENTATIONS
  - 1. Wachtell, R.  
Chromalloy Corporation
  - 2. Withers, James C.  
American Machine and Foundry
  - 3. Dickinson, C. D.  
General Telephone & Electronics Laboratories
  - 4. Ingram, J. C. Jr.  
Aeronautical Systems Division
  - 5. Klopp, W. D.  
Battelle Memorial Institute
  - 6. Levinstein, M. A. for Dotson, L. E.  
General Electric Company
  - 7. Huffman, J. W.  
North American Aviation
  - 8. Chao, Pao Jen  
The Pfaudler Company
  - 9. Commanday, Maurice R.  
Chromizing Corporation
  - 10. Strauss, Eric L.  
The Martin Company
  - 11. Bergstrom, T. R.  
The Boeing Company
  - 12. Merrihew, F. A.  
Bell Aerosystems Company
  - 13. Browning, M. E.  
General Dynamics Corporation
  - 14. Geyer, N. M.  
Aeronautical Systems Division
  - 15. Sklarew, Samuel  
The Marquardt Corporation
  - 16. Beckley, Don A.  
Aerojet-General Corporation
  - 17. Herron, R. H.  
Bendix Corporation

# TABLE OF CONTENTS (Cont'd)

18.	Lefort, Henry Lawrence Radiation Lab., Univ. of Calif.	21
19.	Unger, Robert Plasmakote Corporation	22
20.	Accountius, O. E. Rocketdyne	23
21.	Flint, E. P. A. D. Little Company	24
22.	Kummer, D. L. McDonnell Aircraft Corporation	25
23.	Sutton, W. General Electric Company	26
24.	Huminik, John Jr. Value Engineering Company	27
25.	Mash, Donald R. Advanced Technology Laboratories	28
26.	Leeds, D. H. Aerospace Corporation	29
27.	Wurst, John C. University of Dayton	30
28.	Davis, L. Harvey Engineering Laboratories	31
29.	Burroughs, J. E. General Dynamics	32
30.	Walton, J. D. Jr. Georgia Institute of Technology	33
31.	Grisaffe, S. J. Lewis Research Center, NASA	34
32.	Johnson, R. L. for Wheildon, W. M. Norton Company	35
33.	Hill, V. L. Allison Division	36
34.	Armstrong, J. R. for Long, R. A. Narmco Industries, Inc.	37
35.	Levy, Milton Watertown Arsenal Laboratories	38
36.	Bradstreet, S. W. Armour Research Foundation	39
37.	Johnson, Ronald L. Plasmadyne Corporation	40

HEADQUARTERS  
**Aeronautical Systems Division**

AIR FORCE SYSTEMS COMMAND  
UNITED STATES AIR FORCE  
WRIGHT-PATTERSON AIR FORCE BASE, OHIO

REPLY TO  
ATTN. OF: ASRCEE-1 (Lt. L. N. Hjelm)

21 June 1961

SUBJECT: Refractory Composites Working Group Meeting

TO:

1. The Aeronautical Systems Division and the National Aeronautics and Space Administration are jointly planning the fifth meeting of the Refractory Composites Working Group. This meeting will be held on 8, 9, and 10 August 1961 at The Chance Vought Corporation in Dallas, Texas. This Group is concerned with the technical details of Government, Industry, and University efforts in the area of high temperature (over 2500°F) inorganic composites. The objectives of the Group are the coordination, collation, collection, and dissemination of detailed technical information on the research, development, and applications of refractory composites.
2. You or another qualified, capable representative of your organization are cordially invited to attend this Working Group Meeting if the following requirements can be met: the attendee must (a) be a technical investigator in the area of refractory composites as outlined in the above mentioned objectives, (b) be able and willing to discuss both in technical detail and philosophy the work of your organization in this area, (c) be free to prepare a written report on this work (d) be able to provide 85 copies of this report (plus a reproducible copy) to the chairman of the meeting before 15 July 1961 for distribution to the participants prior to the meeting.
3. It is imperative that these requirements be adhered to in order to accomplish the objectives of the meeting. Since this is a working group, each attendee must be an active participant. Therefore, attendance will be restricted to those who meet the requirements outlined above. A summary report will be published and made available to all others interested in this area. The usefulness of a meeting of this kind is dependent

upon the free exchange of significant technical information. In order to protect each organization's interests, truly proprietary information should be withheld. This may include specific compositions, modifications, techniques, processes, applications, etc. However, in order to interpret and discuss the efforts of the organization, the nominal or basic compositions, general techniques or processes, background information, side effects, etc., should be presented as a minimum.

4. The written report is required prior to the meeting so that it may be distributed to the attendees in advance of the meeting. They will then have the opportunity to study the reports, evaluate the results, and prepare for a discussion of the work. The reproducible copy is needed to prepare an ASD summary report of the meeting. This should include all glossy unscreened prints and black on white figures. Everything but the typing should be "originals". The typed material may be in any form, as it will be re-typed for printing.

5. Each attendee will be required to present a 2-3 minute oral presentation briefly describing the scope, results, applications, and significant aspects of the work described in the written report. This oral abstract will serve to initiate discussion and exchange of information and will be limited to about 10 minutes for each report. A blackboard, slide projectors, and 16 mm movie projector will be available for your use.

6. For planning purposes, and for the premeeting report distribution it will be necessary to know, as soon as possible, whether your organization plans to participate and who the attending technical investigator will be. Please address your immediate reply and 85 copies plus one reproducible of your report by 15 July 1961 to:

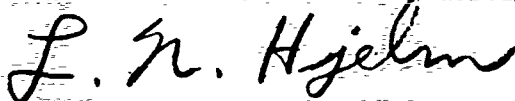
Lt. Lawrence N. Hjelm, Chairman  
Refractory Composites Working Group  
Aeronautical Systems Division  
Attn: ASRCEE-1  
Wright Patterson AFB, Ohio

7. Due to difficulties concerning clearance of papers encountered in the past, at least one day of the meeting will be held as a classified session. Therefore, papers up to and including confidential may be

presented. These will then be published as a classified supplement to the ASD report of the meeting. Since a classification restricts the dissemination of technical information, it is requested that the papers be kept unclassified if at all possible, or if necessary, that the classified portion of the paper be kept separate from the unclassified portion.

8. A letter will follow this shortly which will describe in more detail the meeting arrangements such as transportation, hotel accommodations, meeting place and time, procedures for filing security clearances, meeting agenda, distribution list, etc.

9. The Co-Chairman for this meeting will be Mr. J. J. Gongler of NASA Headquarters. Any questions or comments concerning this meeting should be addressed to the undersigned.



LAWRENCE N. HJELM, 1/Lt USAF  
Chairman, Refractory Composites  
Working Group

HEADQUARTERS  
**Aeronautical Systems Division**

AIR FORCE SYSTEMS COMMAND  
UNITED STATES AIR FORCE  
WRIGHT-PATTERSON AIR FORCE BASE, OHIO

REPLY TO  
ATTN. OF: **ASRCEE-1**

SUBJECT: **Refractory Composites Working Group Meeting**

TO:

1. This is to follow up the letter of 21 June 1961, inviting your organization to participate in the coming Working Group meeting.
2. As announced, Chance-Vought Corporation will host the meeting on 8, 9 and 10 August 1961 and will provide a tour of their facilities on the 11th for those interested.
3. A reservation card for the Statler Hilton Hotel is attached for your convenience.
4. Bus service will be provided daily from the Statler Hotel to the Chance-Vought Corporation. The bus will leave the hotel at 8:00 A.M. and return at the close of the meeting.
5. The small sub-committee of the Working Group that has been active in testing techniques will meet on 7 August 1961 to discuss current and future activities in high temperature testing and coating evaluation techniques as well as new efforts of interest to the group. This meeting will be at 9:00 A.M., 7 August 1961 in the Bluebonnet Room of the Statler Hotel. The results of this meeting will be summarized to the Working Group later in the week, so that only the active, interested members of the sub-group need attend this meeting.
6. One day of the meeting, the 10th, will be held as a classified session, for material to and including Confidential. Please send your clearance to:

Chance Vought Corporation  
Attn: Security Officer  
Box 5907  
Dallas 22, Texas

Person to be contacted: **Mr. Wm L. Aves**  
Subject: **Refractory Composites Working Group Meeting**

Also, please send an information copy of your clearance to the undersigned. The clearances will be used to prepare the name tags and passes, and will be required for attendance at the classified meeting. The classified preprints will be sent to cleared organizations and personnel thru normal channels.

7. The distribution list for the meeting is attached. Please notify the undersigned of your intention to attend so that preprints may be sent out and accommodations arranged for.

8. The meeting will be similar to the past in that the 8th and 9th will consist of unclassified discussions of the various organizations in the fields of protective coatings, sprayed material, material evaluation, high temperature composites, etc. The discussion on the 10th will consist of similar classified activities. As in the past, each attendee will present a short summary of his organization's activities of five minutes or less, with ten minutes for discussion. The co-chairman of the Working Group, Mr. J. J. Gangler of NASA, will act as moderator and referee of this meeting.

*Lawrence N. Hjelm*

LAWRENCE N. HJELM, 1/Lt USAF  
Chairman, Refractory Composites Working Group

2 Atch

1. Distribution List
2. Reservation Card



DISTRIBUTION LIST FOR THE INVITATIONS TO THE FIFTH WORKING GROUP MEETING

Mr. Donald Mash  
Advanced Technology Laboratory  
369 Whisman Road  
Mountain View, California

Mr. A. Levy  
Aerojet General Corporation  
Sacramento, California

Mr. S. Bramer  
Aerojet General Corporation  
Materials Laboratory  
Azusa, California

Mr. Mills  
Aeronutronic Div., F.M.C.  
Research Operation  
Ford Road  
Newport Beach, California

Mr. R. H. Singleton  
Allison Division  
General Motors Corporation  
Indianapolis, Indiana

Mr. S. W. Bradstreet  
Armour Research Foundation  
10 West 35th Street  
Chicago 16, Illinois

Mr. E. L. Olcott  
Atlantic Research Corporation  
Materials Group  
Alexandria, Virginia

Mr. G. A. Jensen  
Avco -RAD  
201 Lowell Street  
Wilmington, Massachusetts

Mr. Paul John  
Avco - RAD  
Materials Engineering, Dept T-422  
201 Lowell Street  
Wilmington, Massachusetts

Mr. H. R. Ogden  
Battelle Memorial Research Institute  
505 King Avenue  
Columbus 1, Ohio

Mr. R. H. Herron  
Bendix Aviation Corporation  
401 Bendix Drive  
South Bend 20, Indiana

Mr. W. M. Sterry  
Boeing Airplane Company  
Seattle, Washington

Mr. Frank M. Anthony  
Bell Aircraft Corporation  
Buffalo, New York

Chief,  
Bureau of Naval Weapons  
Attn: Mr. W. Cohen  
Code SP-2710  
Special Projects Office  
Navy Department  
Washington 25, D. C.

Chief,  
Bureau of Naval Weapons  
Attn: Mr. S. J. Matesky  
Code RMMP-23  
Missile Propulsion Division  
Navy Department  
Washington 25, D. C.

Dr Kenneth Smith  
Harvey Aluminum  
Torrence, California

Mr. K. M. Taylor  
Carborundum Company  
Research Laboratories  
Niagara Falls, New York

Mr. W. L. Aves  
Chance Vought Aircraft Company  
Engine Structures Material  
Dallas 22, Texas

Mr. R. L. Wachtell  
Chromalloy Corporation  
450 Tarrytown Road  
White Plains, New York

Mr. M. R. Commandy  
The Chromizing Company  
1721 East 47th Street  
Los Angeles 58, California

Mr. Gail F. Davies  
Clevite Research Center  
540 E. 105th Street  
Cleveland 8, Ohio

Mr. M. E. Browning  
General Dynamics Corporation  
Convair Division  
Materials & Processing Group  
Fort Worth, Texas

Mr. H. C. Sullivan  
General Dynamics Corporation  
Convair Division  
Mail Zone 6-181  
San Diego 12, California

Mr. Gaylord B. Smith  
E. I. DuPont Company  
Mechanical Development Laboratory  
101 Beach Street  
Wilmington 98, Delaware

Mr. R. H. Lorenz  
Fansteel Metallurgical Corporation  
2200 Sheridan Road  
North Chicago, Illinois

Mr. M. Levinstein  
General Electric Company  
Flight Propulsion Division  
Evendale, Ohio

Mr. G. R. VanHouten  
General Electric Company  
ANP Division  
Evendale, Ohio

Mr. J. D. Walton, Jr.  
Georgia Institute of Technology  
Engineering Experiment Station  
Atlanta, Georgia

Mr. Beasley  
Horizons Incorporated  
Cleveland 4, Ohio

Mr. H. Leggitt  
Hughes Tool Company  
Culver City, California

Mr. G. M. Skinner  
Linde Company  
1500 Polco Street  
Indianapolis, Indiana

Mr. W. Harper  
Lockheed Missile Division  
Department 5320  
Sunnyvale, California

Mr. J. Cox  
Lawrence Radiation Labs  
P. O. Box 808 , Livermore, Calif.

Mr. H. Lefort  
Lawrance Radiation Labs  
P. O. Box 808  
Livermore, Calif.

Mr. Don Kummer  
McDonnell Aircraft Company  
St Louis, Missouri

Mr. L. M. Raring  
Pratt & Whitney - Canel  
P. O. Box 611  
Middletown, Conn.

Mr. H. Pearl  
Republic Aviation  
Farmingdale Long Island, New York

Mr. Huminik  
Value Engineering  
2320 Jefferson Davis Highway  
Alexandria, Va.

Mr. Heoman  
Western Gear  
P. O. Box 182  
Lywood, California

Mr. M. L. Thorpe  
Thermal Dynamics Corporation  
Hanover, New Hampshire

Mr. Philip A. Ormsby  
Thiokol Chemical Corporation  
Huntsville, Alabama

Mr. R. A. Jefferys  
Thompson-Ramo-Wooldridge, Incorporated  
Cleveland, Ohio

Mr. M. A. Schwartz  
United Technology Corporation  
P. O. Box 358  
Sunnyvale, California

Mr. J. W. Rosenbery  
University of Dayton  
Research Center  
300 College Park  
Dayton 9, Ohio

Mr. Lloyd G. Mount  
Vitro Laboratories  
200 Pleasant Valley Way  
West Orange, New Jersey

Commander  
Aeronautical Systems Division  
Attn: ASRMDS (Mr. R.D. Guyton)  
Wright-Patterson AFB, Ohio

Commander  
Aeronautical Systems Division  
Attn: ASRCEE-1 (Lt L. N. Hjelm, 1/Lt)  
Wright-Patterson AFB, Ohio

Commander  
Aeronautical Systems Division  
Attn: ASRLMC (Mr. J.J. Krochmal)  
Wright-Patterson AFB, Ohio

Commander  
Aeronautical Systems Division  
Attn: ASRCMP-3 (Mr N. Geyer)  
Wright-Patterson AFB, Ohio

Commander  
Aeronautical Systems Division  
Attn: ASRCEE-1 (1/Lt L. N. Hjelm)  
Wright-Patterson AFB, Ohio

Commanding Officer  
Attn: A. P. Levitt  
Watertown Arsenal Laboratories  
Watertown, Massachusetts

Dr. R. M. Bushong  
National Carbon Company  
Niagara Falls, N. Y.

Commander  
Aeronautical Systems Division  
Attn: ASDRFM (J. R. Myers)  
Wright-Patterson AFB, Ohio

Commander  
Aeronautical Systems Division  
Attn: ASRCNE (R. VanVliet)  
Wright-Patterson AFB, Ohio

Mr. I. R. Kramer  
The Martin Company  
Baltimore 3, Maryland

Mr. S. Sklarew  
The Marquardt Corporation  
16555 Saticoy Avenue  
Van Nuys, California

Dr. Eliason  
Melpar, Incorporated  
Falls Church, Virginia

Mr. H. S. Ingham  
Metallizing Engineering Company  
of America  
Prospect Avenue  
Westbury, L.I., New York

Mr. S. Grissaffe  
NASA  
Lewis Research Center  
21000 Brookpark Road  
Cleveland 35, Ohio

Mr. Dan Gates  
M-RP, NASA  
Huntsville, Alabama

Mr. E. E. Matheuser  
NASA  
Langley Research Center  
Langley Field, Virginia

Mr. Roger A. Long  
Narmco Industries, Incorporated  
8125 Aero Drive  
San Diego 11, California

Mr. D. G. Moore  
National Bureau of Standards  
Enameled Metals Section  
Washington 25, D. C.

Mr. P. J. Clough  
National Research Corporation  
Metallurgical Research Department  
70 Memorial Drive  
Cambridge 42, Massachusetts

Commander  
U. S. Naval Ordnance Test Station  
Attn: Dept. 5557  
China Lake, California

Dr. N. N. Ault  
Norton Company  
Worcester, Massachusetts

Mr. J. W. Huffman  
North American Aviation, Inc.  
Materials & Processes  
International Airport  
Los Angeles 45, California

Dr. D. K. Priest  
Pflaudler Company  
Applied Research Department  
Rochester 3, New York

Mr. Jack Winzler  
Plasmadyne Corporation  
3839 South Main Street  
Santa Ana, California

Mr. J. L. Gohsen  
Plasmakote Corporation  
9024 Lindblade Avenue  
Culver City, California

Mr. J. V. Long  
Solar Aircraft Company  
2200 Pacific Avenue  
San Diego 12, California

Mr. J. J. Gangler  
NASA Hq  
1512 H Street, N.W.  
Washington 25, D. C.

Mr. R. Francis  
Mr. A. D. Little  
30 Memorial Drive  
Cambridge, Mass.

Mr. D. Leeds  
Aerospace Corporation  
5500 El Segundo Blvd.  
El Segundo, California

Mr. H. Jaffee  
ARDE - Portland Incorporated  
75 Austin Street  
Newark 2, N. J.

Mr. E. Gregory  
Air Reduction  
Central Research Department  
Murray Hill, N. J.

Mr. J. Withers  
American Machine & Foundry  
1025 N. Royal Street  
Alexandria, Va.

Mr. Don Hart  
AFFTC (Attn: FTROS)  
Edwards AFB, California

Mr. T. Bergstrom  
Boeing Airplane Company  
Seattle, Washington

Mr. Runck  
DMIC  
505 King Avenue  
Columbus 1, Ohio

Mr. W. H. Sutton  
General Electric MSVO  
3750 "O" Street  
Philadelphia 24, Pa.

Mr. D. Schiff  
High Temperature Materials  
31 Antwerp Street  
Boston 35, Mass.

Mr. T. A. Greening  
Lockheed Missile & Space Company  
R&D Materials Division  
3251 Hanover Street, Bldg 203  
Palo Alto, California

Mr. Clause Goetzal  
Lockheed Missile & Space Company  
Materials Division, Bldg 202  
3251 Hanover Street  
Palo Alto, California

Mr. A. D. Joseph  
Pratt & Whitney Aircraft  
Materials Development Laboratory  
East Hartford, Connecticut.

Mr. R. P. Frohberg  
Rocketdyne Division, NAA  
Materials Division  
6630 Canoga Avenue  
Canoga Park, California

Mr. D. L. Meehan  
Douglas Aircraft Company  
Missile Engineering Department 82-260  
300 Ocean Park, Blvd.  
Santa Monica, California

L. Sama  
Sylvania Electric Products  
Sylcor Division  
208 Willets Point Blvd.  
Bayside, L. I., New York

L. Seigle  
General Telephone & Electronics Laboratory  
Bayside Laboratories  
Bayside 60, New York

LIST OF ATTENDEES  
REFRACTORY COATING WORKING GROUP

August 8, 9, 10, 1961

Accountius, O. E.  
Rocketdyne Div., NAA

Armstrong, J. R.  
Narmco Industries, Inc.

Aves, W. L.  
Chance Vought Corp.

Beckley, D. A.  
Aerojet Gen. Corp.

Bergstrom, T.  
Boeing Company

Bliton, J. L.  
Armour Research

Bogart, A. T.  
NASA - Ames

Bourland, G.  
Chance Vought Corp.

Burroughs, J.  
Gen. Dynamics

Bradstreet, S. W.  
Armour Research Foundation

Bramer, S.  
Aerojet Gen. Corp.

Browning, M. E.  
Gen. Dynamics

Clough, W. R.  
Pratt & Whitney

Commandy, M. R.  
Chromizing Co.

Cothren, J. E.  
Douglas Missiles

Davis, Cal  
Martin Co.

Davis, L. W.  
Harvey Aluminum

Dickinson, C. D.  
General Telephone

Featherston, A. B.  
Chance Vough Corp.

Flint, E. P., Dr.  
A. D. Little

Forcht, B.  
Chance Vought Corp.

Gangler, J. J.  
NASA Headquarters

Geyer, N.  
Aeronautical Sys. Div.

Goleen, J. L.  
Plasma Products

Grissaffe, S.  
NASA - Lewis

Hart, R. A.  
Martin-Denver

Herron, R. H.  
Bendix

Hill, V. L.  
Allison

Hjelm, L. N.  
Aeronautical Sys. Div.

Huffman, J. W.  
NAA

Huminik  
Value Engineering

Ingram, J. C., M/Sgt.  
Aeronautical Sys. Div.

Jahn, P.  
Avco

Johnson, R. L.  
Plasmadyne

Klopp, W. D.  
DMIC

Kummer, Don  
McDonnell Aircraft

Khao, P. J.  
Pflaude Co.

Lavendel, H. W.  
Lockheed

Leeds, D.  
Aerospace

Levinstein, M.  
Gen. Elec.

Lefort, H.  
Lawrence Radiation Lab.

Levy, N.  
Watertown Arsenal Lab.

Martens, C.  
ARGMA

Mash, D.  
Adv. Tech. Lab.

Merrihew, F. A.  
Bell

Moore, D. G.  
Natl. Bureau of Standards

Meyers, J. R.  
Aeronautical Sys. Div.

O'Kelly, K. P.  
Chance Vought Corp.

Rosenbery, J. W.  
Univ. of Dayton

Ragnell, H. A.  
Chance Vought Corp.

Rudick, M. J.  
Chance Vought Corp.

Sklarew, S.  
Marquardt

Smith, F.  
Chance Vought Corp.

Strauss, E.  
Martin Co.

Strickman, R.  
Electro Therm. Ind.

Sutton, W. H.  
Gen. Elec.

Thomas, B.  
Edwards AFB

Unger, R.  
Plasmakote

Wachtell, R. L.  
Chromalloy

Walton, J. D.  
Georgia Inst. of Tech.

Withers, J.  
AM&F

Wurst, J. C.  
Univ. of Dayton

ACTIVITIES OF CHROMALLOY CORPORATION IN THE  
DEVELOPMENT OF COATINGS FOR FACTORY METALS

R. WACHTELL

Chromalloy Corporation  
West Nyack, New York



## I. INTRODUCTION

Due to the lack of high temperature oxidation resistance of the refractory metal tungsten, tantalum, molybdenum and columbium, these metals and their alloys must be provided with protective coatings if they are to be effectively used. They all possess high-temperature strength superior to conventional materials, especially at temperatures above 2000° F. Their oxidation resistance above 2000° F is, however, very poor.

If use is to be made of their superior high-temperature properties, they must be adequately protected from oxidation. CHROMALLOY has found that the cementation process can be adapted to coating these materials.

In the pack cementation process, the work piece is immersed in a powder mixture containing:

1. The elements to be transferred to the surface to be coated.
2. An inert material to prevent sintering of the powder pack.
3. An energizer, which upon vaporization, provides the mechanism of transfer of the coating elements to the surface of the work piece.

The retort containing powders and work pieces is placed in a furnace and heated to the desired coating temperature, and held there for a period of usually about 10 hours or more. After cooling, the retort is opened, and the parts are removed and cleaned.

Using variations of this technique, CHROMALLOY has successfully coated many different types of materials, including copper, superalloys, graphite, refractory metals, etc.

## II. PROGRAMS IN PROGRESS AT CHROMALLOY

### A. Molybdenum

By far, the technology of molybdenum and its alloys is the most advanced of the refractory metals. Likewise, coatings for molybdenum are also at the most advanced stage. About the best known and most reliable coating for molybdenum is CHROMALLOY'S proprietary W-2 coating. It is no longer a laboratory curiosity, and is currently being used in small scale production. No problems are foreseen in going to large scale production. Figures 1 and 2 depict W-2 coated Mo-0.5Ti, as coated with W-2 and after 10 hours at 2700° F.

The W-2 coating is silicide base in nature, and is "self-healing" in the temperature range above 2400°-2500° F. It has currently undergone an optimization program sponsored by the Air Force. The purposes of this program have been to establish reliability and reproducibility for the W-2 coating, thus, establishing a basis for Air Force specifications.

Battelle Memorial Institute has designed for CHROMALLOY a statistical experiment which would evaluate two levels each of what was felt were the nine most important variables. These variables and the two levels of each considered are:

#### Material Compound (Pack Mixture):

A. Purity	High (99.7% min.)	Commercial (98%)
B. Particle Size	-60 + 150 mesh	-230 mesh
C. Age	One month old	New
D. Mixing	Good	Poor

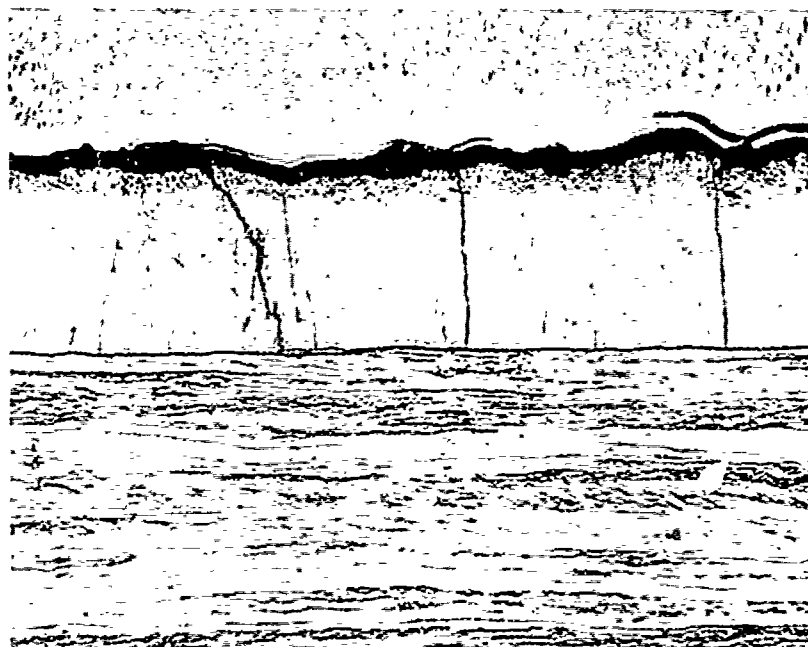


Figure 1. Mo-0.5Ti As Coated with W-2  
250X

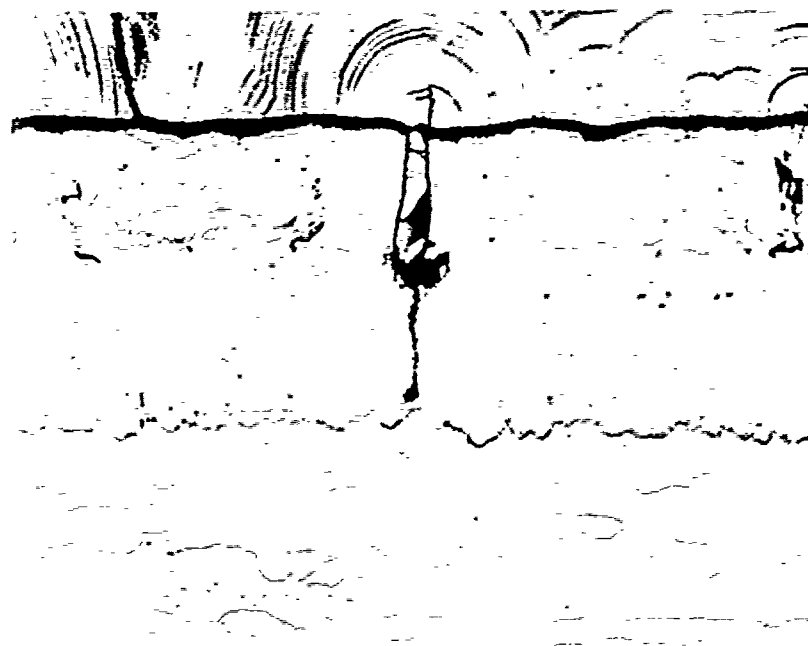


Figure 2. W-2 Coated Mo-0.5Ti After 10 Hours  
At 2700° F.

Substrate:

E. Soundness *	Contaminated by air	Uncontaminated
F. Surface Preparation	Etched **	As rolled

Process:

G. Time	Two twelve hour cycles	One twenty-four hour cycle
H. Temperature	1800° F	1900° F
J. Retort Composition	Mild steel	Mild Steel with molybdenum insert

The experimental design used was a one-eighth replica fractional factorial design. Incorporated in the design were sixty-four test units of the 512 possible, with nine variables at two levels each.

Experimental Program and Results:

Oxidation test life was used as a means of analyzing the affects of the nine variables. Tests were conducted at 2700° F which was the expected use temperature, and also since experimentally useful test life data could also be expected at this temperature.

W-2 coated Mo-0.5Ti tab specimens (1 inch X 0.5 inch X 0.035 inch) were tested in a gas fired tube furnace. Average lives of from two hours to 57 hours at 2700° F were obtained with specimens going as long as 76 hours before a hole was found.

\* The two materials being used are both Mo-0.5Ti. "Uncontaminated" material is the normally produced commercial grade sheet supplied by General Electric Corp. The second material was purposely surface contaminated by eliminating processing steps that normally prevent contamination by air. It was supplied by Universal Cyclops.

\*\* Specimens etched with 1:1, HNO<sub>3</sub>: H<sub>2</sub>O and then liquid honed, rinsed with water and washed in acetone. As rolled <sup>2</sup>material was washed in acetone only.

Statistical analysis of the data revealed that:

1. Time and temperature of processing were by far the most critical variables, with double processing and 1900° F the preferred levels of each respectively.
2. Purity and age of powder pack and retort composition were of no statistical significance, so that practical considerations would dictate the preferred levels of these variables.
3. The remaining four variables were, statistically, less important than time and temperature of processing.

Based on statistical results and practical considerations, the following are recommended levels of the nine variables considered:

<u>VARIABLE</u>	<u>RECOMMENDED LEVEL</u>
A. Purity of powder	Commercial
B. Mesh size of powder	-60, + 150 Mesh
C. Age of powder	Fresh or aged
D. Mixing of powder	Good
E. Soundness of substrate	Uncontaminated
F. Surface preparation	Etched and liquid honed
G. Processing time	Two 12 hour processes
H. Processing temperature	1900° F
J. Retort composition	Steel

This program also revealed that properly rounded sheet edges are a necessity if W-2 coated molybdenum is not to fail prematurely.

It was found that edge failures were randomly distributed among the oxidation test data. Since edge preparation was not included as a variable, and these failures were premature, it was decided to analyze the data with, and without edge failure data. The optimized coating described previously was the result of such an analysis\*.

---

\*See Final Report, "Development of a Powder and/or Gas Cementation Process for Coating Molybdenum Alloys for High Temperature Protection", by H. Blumenthal and Neil Rothman, Chromalloy Corporation, Contract No. AF33(616)-7383, Task No. 73811.

Part of this program entailed predicting the life of an optimum coating, and specifying the tolerance limits for these predictions. The predictions made are affected by whether or not edge failures are included in the data. Edge failures influenced the average lives of the coatings and the shape of the distribution curve for the oxidation test data. With edge failures included, the distribution curve assumes an extreme value configuration. Without edge failure data, the distribution is of the normal distribution type. This is important, since the tolerance limits are dependent upon the distribution type. The effects of edge failures are apparent from the predictions tabulated in Table I.

**TABLE I- PREDICTIONS OF MINIMUM LIVES OF OPTIMIZED W-2 COATINGS BASED ON EXTREME VALUE AND NORMAL DISTRIBUTIONS**

	<u>Tolerance Limit</u>	<u>Min. Life, Cycles** for Extreme Value Distribution</u>	<u>Min. Life, Cycles For Normal Distribution</u>
Edges in	99.9	2.1	10.1
" "	99.0	9.8	13.4
" "	95.0	15.4	16.3
Edges out	99.9	6.4	13.0
" "	99.0	12.7	15.7
" "	95.0	17.3	18.1

The most important conclusion to be derived from the above table is that in any molybdenum structure, it would be wise to design in such a way that

---

\*\* Two hours at 2700° F per cycle.

edges would be minimized and to avoid, where possible, having edges in the heat encountering zones. Such precautions would, in effect, make the structures more reliable, since a normal distribution without the inclusion of edges (Table I) would have a greater expected life at any tolerance limit than a similar structure with edges included.

Other coatings for molybdenum are under study at CHROMALLOY. Composite coatings consisting of alternately deposited layers have undergone study. Lives of over 100 hours at 2700° F have been obtained experimentally.

About the most promising coating developed has been the one known as Durak B. Tests currently in progress have indicated that a life of 150 hours at 2700° F may be expected. The bulk of the specimens being tested have survived 176 hours at 2700° F.

#### B. Columbium

Columbium base alloys are also coated by pack cementation. Modified W-2 coatings have survived over 200 hours at 2000° F, and over 125 hours at 2500° F. The greatest shortcomings of present CHROMALLOY produced coated columbium has been the brittleness induced in the base metal by the coating process. This effect is probably due to the susceptibility of columbium base alloys to embrittlement by air. During the heat-up portion of the coating cycle, the work pieces are contacted by the air present in the retort.

In some columbium materials it is possible to subsequently restore ductility by a post-coating heat treatment. Some alloys (particularly the D-31 alloy) are severely embrittled by air and, at present, ductility cannot be restored by heat treatment in these alloys.

Aluminum base alloys have been applied to columbium base alloys. Some of these coatings have withstood 2500° F for over 25 hours, but the coatings do not appear to be impervious to diffusion of oxygen to the base metal. In some

instances, weight gains of 100 or more milligrams have been recorded on apparently sound specimens (1 inch x 0.5 inch). Further work will be done to produce an impervious aluminum base coating.

### C. Tantalum and Tungsten

Less work has been done on coating tantalum and tungsten than on either molybdenum or columbium. Indications are, however, that silicon base coatings such as W-2 will protect these materials.

Both tantalum and tungsten are embrittled, as in columbium, by present techniques. Efforts will be made to eliminate or minimize this embrittlement.

Present silicon base coatings have protected tantalum for at least one hour at 2700° F. An alloy 50Mo-50W has survived over 60 hours at 2700° F after W-2 coating.



PROTECTIVE COATINGS FOR REFRACTORY METALS

JAMES C. WITHERS

American Machine and Foundry

Alexandria, Maryland

## PROTECTIVE COATINGS FOR REFRACTORY METALS

By James C. Withers

The American Machine and Foundry Company, or AMF as we are often designated, has been actively investigating protective coatings for the refractory group of metals: niobium, molybdenum, tantalum and tungsten. Protection in the temperature range of 2000 to 5000°F (1090 to 2800°C) has been of particular interest. The coatings investigated have been both the electroplated and diffusion types.

The electroplated coatings included:

- nickel
- chromium
- platinum
- rhodium
- cobalt-tungsten
- cermets of these metals

The diffusion coatings applied by pack cementation techniques consisted of a number of proprietary products designated as AMFKOTES. These are composed of various combination of elements including beryllium, boron, carbon, magnesium, aluminum, silicon, titanium, vanadium, chromium, iron, nickel, zinc, zirconium, niobium, molybdenum, tantalum, tungsten, and rhenium.

Both types of coatings were applied to the refractory metals.

Oxidation and thermal shock test were then made. Tests for the diffusion coatings were conducted in the region 2000° to 4200°F (1090 to 2320°C), whereas the electroplated coatings were tested only to 2500°F (1370°C).

Further, the electrodeposits were applied only to niobium and molybdenum.

### Electrodeposition

Electroplated coatings were applied to molybdenum by the technique developed by Brenner and his co-workers.<sup>1</sup> This consists of a base chrome and nickel plate followed by the finish deposit. After chromium plating, specimens were given a reverse current treatment in a mixture of 10% sulfuric acid in acetic acid, and then nickel plated.<sup>2</sup> After nickel plating, specimens were transferred to a controlled plating bath where five mil deposits were applied except in the case of platinum and rhodium. These latter deposits were only from one to two mils thick.

Cermets of  $Al_2O_3$ ,  $ZrO_2$ ,  $MoSi_2$  and  $SiO_2$  in combination with the other plating materials were electroplated by suspension of the ceramic particles in the electroplating baths. Deposits containing up to 50% by weight of ceramic phase were plated and tested.

### Diffusion Process

The diffusion coatings were applied by packing the specimens in powders of the coatings elements along with halide carriers. The pack was then heated in an inert atmosphere to 1500 - 2200°F depending on the combination of coating elements and base metal. A time interval of from 5 to

---

<sup>1</sup> J. Electrochem. Soc. 105, 8, 1958, p. 450

<sup>2</sup> J. Electrochem. Soc. 105, 2, 1960, p. 91

20 hours was used depending on the temperature and the desired thickness of coating.

The diffusion coatings for use on the refractory metals are designated by AMF as the AMFKOTE series of coatings. AMF designates these by numbers which define the elements in a coating and the base metal to which it can be applied. An example of this is our AMFKOTE-2 coating which is being used for coating molybdenum. This coating has been applied to a thickness of 2.5 mils with the nominal coating thickness being 1 to 1.5 mils. There is a slight weight increase of the base material when the coating is applied.

#### Oxidation Tests on Electrodeposits

All oxidation tests on electroplated materials were run in slow moving air in a resistance-heated silicon carbide furnace.

Few tests were performed on pure nickel, chromium, and alternate nickel-chromium coatings since it was considered this would be a duplication of Brenner's<sup>1</sup> earlier work. Sufficient work was performed to verify that the average lifetime was 300 hours at 2000°F. In a number of cases, protection for 500 to 700 hours was obtained.

At higher temperatures, the results were not encouraging. The average life of duplex chromium-nickel coatings at 2500°F was one hour. In like manner, the average life of 2 mil deposits at 2500°F was one hour for platinum and one-half hour for rhodium. Failure of the platinum and

rhodium deposits was found to be caused by porous stressed deposits. To demonstrate that this was the mode of failure, a 3 mil platinum sheet was hot rolled and then welded around a molybdenum specimen. This combination was tested for 24 hours at 2500°F. Then the platinum sheet was removed from the molybdenum and both metals were examined. It was found that slight oxidation had begun on one corner of the molybdenum and examination of the platinum sheet revealed a small pin hole in the same area. This demonstration showed that platinum can be used to protect molybdenum at 2500°F if the platinum can be applied in a stress-free, nonporous form. A number of new types of platinum and rhodium plating baths are being investigated. We have had some success in depositing low stress deposits about 5 mils thick and free of pin holes. A 5 mil deposit of platinum applied to tungsten was oxidation resistant for 5 hours at 3000°F.

Cermet deposits, as shown in Slide 1, have much improved oxidation resistance over the pure metal deposits. Depending on the metal-ceramic system, coatings in 5 mil thicknesses resisted oxidation at 2500°F for from 2 to 5 hours. At 2000°F, a cobalt-tungsten alloy-zirconium oxide cermet resisted oxidation for 468 hours.

The cermet electroplated coatings have not been tested extensively, but they appear to offer a good potential in coating applications. The amount of ceramic can be controlled and graded from a very small amount to almost pure ceramic. This ability can be used to advantage in matching the thermal

expansion of a base material and in applying a virtually pure ceramic material on a graded cermet.

### Test Results on Diffusion Coatings

Oxidation tests on diffusion coatings were conducted either in slow moving air in an electric furnace or under an oxidizing flame. Some test results of AMFKOTE-2 on molybdenum under those oxidating conditions were as follows:

19 to 45 hours at 2800°F in a furnace  
8 to 9 hours at 3000°F in an oxidizing flame  
8 hours at 3200°F in an oxidizing flame  
45 minutes at 4200°F in an oxidizing flame

The total normal emissivity of AMFKOTE-2 is 0.76 at 399°C, 0.9 at 615°C, and greater than 0.95 at 725°C.

The AMFKOTE-2 series of coatings are being tested at NASA, Langley Field, for leading edge coatings and the effect of the coating on the physical properties of the base metal.

In addition to the application on molybdenum, AMFKOTE series coatings have been developed and tested on such materials as niobium and tantalum. Results of oxidation tests at 2500°F are as follows:

	<u>Tantalum</u>	<u>Niobium</u>	<u>Molybdenum</u>
AMFKOTE-3	275 hrs	396 hrs	264 hrs
AMFKOTE-4	312 hrs	34 hrs	---

The AMFKOTE-2 coating has also been subjected to severe thermal shock tests. Two methods were used: a furnace test and a flame test.

In the furnace test, specimens at room temperature were put in a heated oven and held until they attained the oven temperature. The specimens were then removed to the atmosphere, cooled until they could be examined, and then reheated in the same manner. After ten cycles the coatings were still in excellent condition. In the flame test, the specimens were heated to test temperature, then the flame was removed until it cooled to red heat. The cycle was repeated ten times. No failures were found. AMFKOTE-2 has excellent self-healing properties above about 2300°F. After the first evolution of  $\text{MoO}_3$ , a specimen oxidizes at a very slow rate and maintains its shape and dimension for several hours. NASA reports have stated that the coating has remarkable self-healing properties at high temperatures.

AMFKOTE-3 and 4 coatings do not have as good thermal shock properties as those produced with AMFKOTE-2 but as indicated by the results given before, they provide good protection. In addition, AMFKOTE-4 has self-healing characteristics.

Several coatings are presently being evaluated on tungsten for operation at temperatures greater than 3500°F (1930°C).

Inasmuch as AMFKOTE refractory coatings are applied by a pack cementation-vapor technique, they can be used to protect large complex shapes. Size of the base piece is only limited by the oven required to heat the pack to about 2000°F. The application technique deposits the coating equally well in recesses, on corners, and over flat surfaces.

## Summary

Further test work similar to that I have described is being performed. As the results are determined, they will be reported. At this stage, I can say that AMFKOTE refractory coatings will provide good protection against oxidation at temperatures up to 4200°F (2320°C) even when severe thermal shock conditions are present. Tests with electrodeposited coatings were not as promising though cermet electrodeposits may offer good protection particularly at temperatures to 2500°F (1370°C).





SLIDE 1  
Nickel - SiO<sub>2</sub> Cermet

HIGH-TEMPERATURE REACTIONS AND PROTECTIVE  
SYSTEMS INVOLVING TUNGSTEN AND REFRACTORY COMPOUNDS

PART I. HIGH-TEMPERATURE REACTIONS BETWEEN  
TUNGSTEN AND SEVERAL REFRACTORY COMPOUNDS

R. RESNICK

R. STEINITZ

PART II. PROTECTION OF TUNGSTEN AGAINST OXIDATION AT  
ELEVATED TEMPERATURES

A. L. PRANATIS

C. I. WHITMAN

C. D. DICKINSON

General Telephone & Electronics Laboratories

Bayside, New York

# HIGH-TEMPERATURE REACTIONS AND PROTECTIVE SYSTEMS INVOLVING TUNGSTEN AND REFRACTORY COMPOUNDS

## PREFACE

In the overall research program on refractory metals and compounds at General Telephone & Electronics Laboratories, Inc., a number of separate experimental projects are under way which are directly related to the subject of the meeting. The scope of these projects has been separated for clarity in presentation into two areas, one dealing with a study of reactions that occur between components in a composite system at high temperatures and the other dealing with both the fundamental and applied aspects of the protection of tungsten at high temperatures. Therefore, this manuscript consists essentially of two separate research-in-progress reports.

The first report, entitled "High-Temperature Reactions Between Tungsten and Several Refractory Compounds," derived its original impetus from a need for fundamental information on composite materials that might be suitable for rocket nozzle applications; however, as the study progressed it became apparent that data in this relatively unexplored area had immediate applications in the protective coating of tungsten and other refractory metals as well as other areas requiring an understanding of high-temperature phenomena. In a coating system alone, there are two areas where high-temperature reactions could lead to failure. At the metal-coating interface the formation of a low-melting mixture or direct reaction could cause failure. At the coating--coating-oxide interface, a reaction could preclude the possibility of protection from the oxide. Therefore, the tools and techniques for studying high-temperature reactions as well as the results have important implications in research for the protection of any material suitable for high-temperature service.

The protection of tungsten from oxidation at high temperatures is being studied from two aspects. The first, an applied research project, has used existing information and theories to develop coating systems that have a potential for protecting tungsten against oxidation. In the evaluation of these coatings, a careful examination of the causes of failures and studies of variables that delay or decrease the probability of failure have played an important role in the evolution of the more protective systems.

The second aspect is being studied under the sponsorship of ASD (Contract AF-33(616)-8175). This project has more basic goals:

- (1) To determine those areas where the lack of fundamental information or principles are reducing the effectiveness of the applied research effort for the development of protective coating systems for tungsten at temperatures above 3350°F.
- (2) To design and conduct research experiments to obtain the needed information. Although work on this project has just begun, several basic principles with broad applications in coating systems have evolved, and in their rudimentary form, two of these have been described and used in explaining observed results. Ultimately, it is felt that the information and correlations developed in this project will lead to an understanding of existing systems as well as provide the basic information for predicting which other systems have a high probability of success in protecting tungsten from oxidation.

## 1. INTRODUCTION

In recent years considerable interest has been generated in the reactions at high temperatures between tungsten and various other refractory materials, since it is believed that combinations of these materials may provide the properties required in high-temperature use which are lacking in tungsten alone. Examples of approaches considered are the dispersion of fine particles of a refractory compound in a pure tungsten matrix in order to increase the elevated-temperature strength and coatings or layers of a compound on tungsten to provide improved resistance to corrosion and erosion. A somewhat novel proposal is to infiltrate a porous tungsten matrix with one of the lower-melting compounds, and also some metals, to provide evaporation cooling when the material is subjected to a high heat flux, as in rocket nozzles.

In general, it is required that the various combinations of materials be more or less inert at operating temperatures if required properties obtained during the fabrication of parts are to be retained during use. For example, a dispersion-hardening agent that rapidly dissolves in tungsten would, as a result, lose its strengthening power. Also, if materials used as evaporation coolants were to react with the tungsten skeleton, the structure would probably be weakened and also made dimensionally unstable. Thus one is interested not only in chemical reactions, but also metallurgical reactions such as interdiffusion and phase transformations which can cause changes in properties in periods of the order of one minute at temperature of 5400°F and above. It should be realized that, under these conditions, no system is likely to be completely inert. The reaction rates must

therefore be considered. If the rates are slow enough, the reactions that do occur may not destroy the usefulness of the system. However, at the temperatures of interest in this investigation, possible reactions should take place at quite rapid rates.

## II. PRELIMINARY CONSIDERATIONS

In studies of this type, it is often helpful to consider the free energy of reaction of various possible chemical reactions so that one might predict which will be the more stable systems. Unfortunately, the necessary thermodynamic data are available for only a few of the systems under consideration, and then the maximum temperature for which they are valid is only about  $2000^{\circ}\text{K}$  or  $3632^{\circ}\text{F}$ . In addition, one is not always certain as to the species of molecules involved in reactions taking place at very high temperatures. Nevertheless, the free energy of reactions has been calculated for several of the tungsten-refractory oxide systems where the data are probably good up to the temperature at which they are being applied. The results are given in Table I. The reaction temperature has been taken as  $2100^{\circ}\text{K}$  or  $3812^{\circ}\text{F}$  for these calculations, since it is the approximate temperature at which, according to Brewer,<sup>(1)</sup> the vapor pressure of  $\text{WO}_3$  is one atmosphere, and at which  $\text{WO}_2$  dissociates into solid tungsten and gaseous  $\text{WO}_3$ . Therefore  $\text{WO}_3$  is taken to be one of the reaction products in each case. Since the reacting specimens are to be heated either in a continuously evacuated chamber or in a flowing inert gas atmosphere, the fact that any of the reaction products are gaseous at elevated temperature will influence the calculated free energy. Thus the calculations have been made for two cases: first with the assumption that all gaseous reaction products have a partial pressure of one atmosphere, and second, with the realistic assumption that the partial pressure is one micron of mercury. The free energy is calculated from the following expression

$$\Delta F = \Delta F^{\circ} + RT \ln A$$

where  $\Delta F$  is the free energy change in the standard state,  $R$  is the gas constant,  $T$  is the absolute temperature, and  $A$  is the ratio of the product of the activities of the reaction products to the product of the activities of the reactants, each activity raised to a power equal to the number of moles involved in the reaction. The partial pressures can be substituted for the activity if it is assumed that the gases act ideally. Values for  $\Delta F^\circ$  have been tabulated or charted graphically by Coughlin,<sup>(2)</sup> Tripp and King,<sup>(3)</sup> and Ellingham,<sup>(4)</sup> among others.

A positive value for the free energy of reaction means that the indicated reaction should not take place. Allowing for considerable error in the published data, and for the fact that all of the experiments to be described below were conducted at considerably higher temperatures than those for which the calculations are made, the positive magnitude of  $\Delta F$  is still large enough in all but one case so that it seems that none of the reactions other than the reduction of  $MgO$  by tungsten is likely to take place even at temperatures of the order of  $5400^\circ F$ .

So little thermodynamic data are available for the refractory carbides and nitrides, that it is impossible to make even rough calculations of the free energies of reaction for systems of interest. Therefore, only the oxide-tungsten reactions are listed in Table I.

### III. EXPERIMENTAL DETAILS AND RESULTS

Two series of experiments were performed in an attempt to detect the high-temperature reactions. The first series yielded unsatisfactory results, but will be described in some detail, since it involved the use

of new apparatus, a carbon arc image furnace, and also might indicate some of the difficulties involved in this work. The specimens were small, 0.25" diameter by 0.12" thick, compacts pressed from tungsten powder mixed with rather large particles of compound. They were positioned in the arc image furnace in the manner illustrated schematically in Fig. 1.

The stabilized zirconia block serves not only as a support for the specimen but also acts as thermal insulation. The flow of argon passes out of the chamber through a port directly in front of the specimen. The existence of the port helps to eliminate distortion of the light beam and energy absorption which occurs in the curved surface of the Vycor tube, and also prevents the possibility of a film being evaporated onto the glass which would, of course, absorb still more of the energy. After heating, the specimens were mounted in an epoxy resin and sectioned and polished for the metallographic examination, and a piece analyzed by the Debye-Scherrer X-ray method in order to determine the reaction products. The results of these experiments were discussed in some detail in reference (5). Since they were inconclusive, and since the same systems have been investigated in what is considered a more satisfactory manner by the second method discussed below, they will not be covered here.

The second attempt to study the high-temperature reactions between tungsten and various metallic compounds involved the use of a basically different specimen design and furnace. The specimens consisted of small pieces, approximately  $1/8"$  x  $1/4"$ , of tungsten foil one to two mils in thickness. These were coated with a thin layer of powdered



compound and heated in the tungsten resistance furnace illustrated in Fig. 2. This technique represents a distinct improvement over the one described above in that the presence of an initially sharp interface between the tungsten foil and the compound assists in detecting the occurrence of a reaction, since the interface would be distorted in some way by a reaction. Furthermore, the specimens are heated uniformly and the temperature can be measured accurately with a brightness pyrometer by either sighting into the furnace through a small hole, in which case the black body temperature is read directly, or by correcting the brightness temperature read on the surface of the tungsten foil with the accurately determined emissivity of tungsten. (6) In addition, the smaller volume of unreacted material, as compared with the powder compact specimens, increases the accuracy of the X-ray analyses.

The results of these experiments are given in Table III, and Figs. 3 through 26 are typical microstructures.

#### IV. DISCUSSION OF RESULTS

The tungsten-thorium oxide specimens show no evidence of reaction up to a temperature of  $5430^{\circ}\text{F}$ .  $\text{ThO}_2$  particles will sinter to tungsten, but no sign of reduction can be seen in Fig. 3. Neither solid nor liquid  $\text{ZrO}_2$  appear to react with tungsten, as shown in Figs. 4 to 6. Again, as in the case of  $\text{ThO}_2$ , sintering takes place in the solid, and an adherent layer forms when molten. The copper indicated in the photomicrographs was electroplated onto the specimens after heat treatment in order to aid in the metallographic preparation.

Magnesium oxide is reduced by tungsten under the conditions indicated in the table. No reaction can be detected in the powder compact

specimens, since both reaction products are gaseous at these temperatures. Fig. 7 is a low magnification photograph of typical samples. The corroded surface of the foil can be clearly seen. Fig. 8, 9 and 10 show the progressively deeper corrosion of the foil in cross section. The reaction between MgO and tungsten has been recognized by other workers<sup>(7)</sup> for many years.

There appears to be some disagreement as to whether or not  $\text{Al}_2\text{O}_3$  reacts with tungsten. Ackermann and Thorn<sup>(8)</sup> found reaction in a tungsten effusion cell, and Wilson<sup>(9)</sup> reports a reaction using tungsten foil specimens similar to those used in these experiments. On the other hand, Brewer and Searcy<sup>(10)</sup> found no reaction by the effusion method up to  $300^\circ$  above the melting point of  $\text{Al}_2\text{O}_3$ , and Preston,<sup>(11)</sup> using the tungsten foil method, could find no reaction between these materials. In the present work, no evidence reaction was detected even at  $5430^\circ\text{F}$ . As may be seen in Figs. 11 and 12, the interface between the foil and the oxide remains sharp and regular. No sign of corrosion is present. A suggestion has been made by Ryshkewitch<sup>(12)</sup> that the reaction which has been reported is actually one between tungsten and residual oxygen or moisture in the atmosphere, with subsequent decomposition of the tungsten oxide in the alumina to form the observed droplets of tungsten. To test this idea, a specimen was run in an atmosphere of argon that was passed initially over ice held at a temperature of about  $-40^\circ$ . As anticipated, a reaction did occur, and a photomicrograph of the polished specimen Fig. 13 shows the deposits of tungsten in the alumina.

Figs. 14 and 15, illustrating the tungsten-yttrium oxide system, do not show any evidence of reaction. The same is true of tungsten-hafnium oxide shown in Fig. 16.

All of the tungsten-refractory carbide systems investigated thus far exhibit considerable reaction at elevated temperatures. Tungsten and tantalum carbide form a eutectic which melts at roughly  $5170^{\circ}\text{F}$ . The X-ray analysis shows the presence of three distinct phases, W, TaC, and a structure representative of  $\text{W}_2\text{C}$ , which no doubt is actually the solid solution  $(\text{W}, \text{Ta})_2\text{C}$ . Lattice parameter measurements have not been made to confirm this. Fig. 17, which illustrates a specimen heated below the melting point of the eutectic, clearly shows the formation of the new phase, and Fig. 18, heated slightly above the eutectic temperature, shows the rapid dissolution of the tungsten foil which takes place.

The W-HfC system differs from the W-TaC system in that there are no isomorphous lower carbides. A eutectic does form which melts at roughly  $5100^{\circ}\text{F}$  as seen in Fig. 19. The X-ray analysis shows the presence of an additional phase which has been tentatively identified as B.C.C. hafnium metal. This is probably a high-temperature phase that is stabilized at room temperature by being in solution with tungsten.

W-ZrC is another highly reactive system. Figs. 20 and 21 show the rapid dissolution of the tungsten at temperatures down to  $4900^{\circ}\text{F}$ . The X-ray analysis showed only the presence of W and ZrC. However, a metallic-looking phase can be seen metallographically and probably is zirconium present in too small an amount to be detected with the X-ray techniques used. The solid-solution carbide, (80% Ta - 20% Hf)C, was also tested in combination with tungsten. Again, reactions took place at moderate temperatures. The tungsten carbide phase can be seen in Figs. 22 and 23, and the melting reaction above  $5100^{\circ}\text{F}$  in Fig. 24.

The refractory nitrides TiN and ZrN have also been found to react quite readily with tungsten at temperatures below their melting points. Low melting eutectics form in both systems as shown in Figs. 25 and 26. In the case of TiN, the liquid nitride has diffused through the tungsten foil along the grain boundaries and thus a nitride phase appears on both sides of the foil.

#### V. CONCLUSIONS

With the exception of MgO, the refractory oxides are in general quite unreactive with tungsten. The refractory carbides and nitrides which have been examined are, on the other hand, much too reactive to be of use in combination with tungsten, since all of those tested formed reaction products that melt below 5150°F. Since ThO<sub>2</sub> has a melting point of about 5600°F, and is unreactive up to its melting point, it should be superior in most applications to any of the carbides in combination with tungsten.

#### VI. ACKNOWLEDGMENT

We thank the Aerojet-General Corporation, Sacramento, California for permission to publish some of the information presented in this paper.

### REFERENCES

1. Leo Brewer, "The Thermodynamic Properties of the Oxides and Their Vaporization Processes", Chemical Reviews, Vol. 52, No. 1, 1953.
2. James P. Coughlin, "Contributions to the Data on Theoretical Metallurgy: XII, Heats and Free Energies of Formation of Inorganic Oxides", Bureau of Mines, Bulletin No. 542, 1954.
3. Harlan P. Tripp and Burnham W. King, "Thermodynamic Data on Oxides at Elevated Temperatures", J. Am. Ceramic Soc., Vol. 38, No. 12, 1955.
4. H. J. T. Ellingham, "Reducibility of Oxides and Sulfides in Metallurgical Processes," J. of the Soc. of Chemical Industry, Vol. 63, No. 5, 1944, P. 125.
5. A. Machonis, E. Mazza, R. Resnick, and I. Strauss, General Telephone & Electronics Laboratories Report No. TR60-105.4, Nov. 30, 1960.
6. R. D. Allen, L. F. Glaser, Jr., and P. L. Jordan, "Spectral Emissivity, Total Emissivity, and Thermal Conductivity of Molybdenum, Tantalum, and Tungsten above 2300°K. J. Applied Physics, Vol. 31, No. 8, 1960, P. 1382.
7. G. E. Moore, "Reduction of Magnesium Oxide by Tungsten in Vacuum," J. Chem. Physics, Vol. 9, 1941, p. 427.

8. R. J. Ackermann and R. J. Thorn, "Reactions Yielding Volatile Oxides at High Temperatures etc.", Argonne Nat. Laboratory Report ANL-5824.
9. J. W. Wilson, "Tungsten and Rocket Motors", Stanford Research Institute Progress Report No. 9, Feb. 15, 1960. ASTIA No. AD233962.
10. L. Brewer and A. W. Searcy, "The Gaseous Species of the Al-Al<sub>2</sub>O<sub>3</sub> System," J. Am. Chem. Soc., Vol. 73, 1951, P. 5308.
11. O. Preston, "Tungsten and Rocket Motors," Stanford Research Institute Progress Report No. 4, July 9, 1959, ASTIA No. AD219161.
12. E. Ryshkewitch, Oxide Cermics, Academic Press, New York, N. Y. 1960, p. 228.

TABLE I

System	Possible Reactions	Free Energy of Reaction
W + ThO <sub>2</sub>	$2/3 W + ThO_2 \xrightarrow{2100^\circ K} 2/3 WO_3 (g-1 \text{ atm.}) + Th$	+ 139,000 cal/mol.
	$2/3 W + ThO_2 \xrightarrow{2100^\circ K} 2/3 WO_3 (g-1 \text{ micron}) + Th$	+ 101,900 cal/mol.
W + ZrO <sub>2</sub>	$2/3 W + ZrO_2 \xrightarrow{2000^\circ K} 2/3 WO_3 (g-1 \text{ atm.}) + Zr$	+ 112,000 cal/mol.
	$2/3 W + ZrO_2 \xrightarrow{2100^\circ K} 2/3 WO_3 (g-1 \text{ micron}) + Zr$	+ 74,500 cal/mol.
W + MgO	$2/3 W + 2 MgO \xrightarrow{2100^\circ K} 2/3 WO_3 (g-1 \text{ atm.}) + 2 Mg(g-1 \text{ atm.})$	+ 79,000 cal/mol.
	$2/3 W + 2 MgO \xrightarrow{2100^\circ K} 2/3 WO_3 (g-1 \text{ micron}) + 2 Mg(g-micron)$	-72,000 cal/mol.
W + Al <sub>2</sub> O <sub>3</sub>	$2/3 W + 2/3 Al_2O_3 \xrightarrow{2100^\circ K} 2/3 WO_3 (g-1 \text{ atm.}) + 4/3 Al(l)$	+ 100,000 cal/mol.
	$2/3 W + 2/3 Al_2O_3 \xrightarrow{2100^\circ K} 2/3 WO_3 (g-1 \text{ micron}) + 4/3 Al(l)$	+ 62,500 cal/mol.
W + Y <sub>2</sub> O <sub>3</sub>	$2/3 W + 2/3 Y_2O_3 \xrightarrow{2100^\circ K} 2/3 WO_3 (g-1 \text{ atm.}) + 4/3 Y(l)$	+ 120,000 cal/mol.
	$2/3 W + 2/3 Y_2O_3 \xrightarrow{2100^\circ K} 2/3 WO_3 (g-1 \text{ micron}) + 4/3 Y(l)$	+ 82,500 cal/mol.
W + HfO <sub>2</sub>	$2/3 W + HfO_2 \xrightarrow{2100^\circ K} 2/3 WO_3 (g-1 \text{ atm.}) + H_f$	+ 116,000 cal/mol.
	$2/3 W + HfO_2 \xrightarrow{2100^\circ K} 2/3 WO_3 (g-1 \text{ micron}) + H_f$	+ 78,500 cal/mol.

TABLE II

## RESULTS OF REACTIONS BETWEEN TUNGSTEN FOILS AND REFRACTORY COMPOUNDS

System	Temp. °F	Time (Minutes)	Metallographic Observations	Phases detected by the X-ray Analyses
W+ThO <sub>2</sub>	5070	1	Particles sintered to foil. No other reaction.	W, ThO <sub>2</sub>
	5430	1	same as above	
	5430	3	same as above	
W+ZrO <sub>2</sub>	4530	1	Particles sintered to foil. No other reaction.	W, ZrO <sub>2</sub> Lines prominent.
	5070	1	ZrO <sub>2</sub> partially molten. Adhered to the foil.	
			No evidence of other reaction.	
	5430	1	ZrO <sub>2</sub> Completely molten. Adhered well to the foil. No indication of other reaction.	
W + MgO	4000	1	Some slight sintering. Interface slightly irregular.	W
	4530	5	Interface severely eroded. All of the MgO reacted.	
	5430	1	Same as above	
W + Al <sub>2</sub> O <sub>3</sub>	4000	1	Al <sub>2</sub> O <sub>3</sub> molten. No reaction. Oxide did not adhere to the foil	W, Al <sub>2</sub> O <sub>3</sub>
	4530	5	Al <sub>2</sub> O <sub>3</sub> molten. Wet and adhered to foil. Interface is very sharp. No reaction.	
	5430	1	Same as above. Al <sub>2</sub> O <sub>3</sub> vaporizing fairly rapidly.	



TABLE II (cont'd)

System	Temp. °F	Time (Minutes)	Metallographic Observations	Phases detected by the X-ray Analyses
W+Y <sub>2</sub> O <sub>3</sub>	4000	2	Particles sintered to foil.	W, Y <sub>2</sub> O <sub>3</sub>
	4530	1	No other reaction.	
	5430		Y <sub>2</sub> O <sub>3</sub> molten. No other reaction. Y <sub>2</sub> O <sub>3</sub> molten. No other reaction.	
W+HfO <sub>2</sub>	5240	2	HfO <sub>2</sub> molten, wets tungsten. Slight reaction in the form of interdiffusion.	W, HfO <sub>2</sub>
			No new phases distinguishable.	
	5430	1	Same as above	
W+TiN	5070	1	No significant reaction.	W, TiN
	5240	2	TiN molten. Slight reaction at the interface.	
W + ZrN.	5070	1	Interface is slightly irregular. ZrN sinters to the W	W+ZrN + W <sub>2</sub> Zr
	5240	2	about the same as above.	
	5430	1	Severe irregularities at the interface. A metallic like phase is dispersed in the ZrN. New phase also appears at the interface.	
W+ TaC	4880	1	Sintering of TaC to tungsten foil.	W, TaC, and (W, Ta) <sub>2</sub> C
	4880	2	Similar to above	
	5160	1	Eutectic composition forms and melts.	
W + HfC	2800	2	A eutectic forms which melts at about this temperature.	W, HfC and b. c. c. Hf

TABLE II (cont'd)

System	Temp. °F	Time (Minutes)	Metallographic Observations	Phases detected by X-ray Analyses
W + ZrC	2700°C	1	A eutectic form which melts below 2700°C	W, ZrC
W + (80%Ta, 20%H <sub>f</sub> )C	2700°C	1	A eutectic form which melts below 2700°C	W, ZrC
	2800°C	2	Diffusion layer much thicker than above. Considerable erosion of the tungsten is evident.	(Ta, H <sub>f</sub> ) C, W
	2850°C	2	About the same as 2800°C specimen	

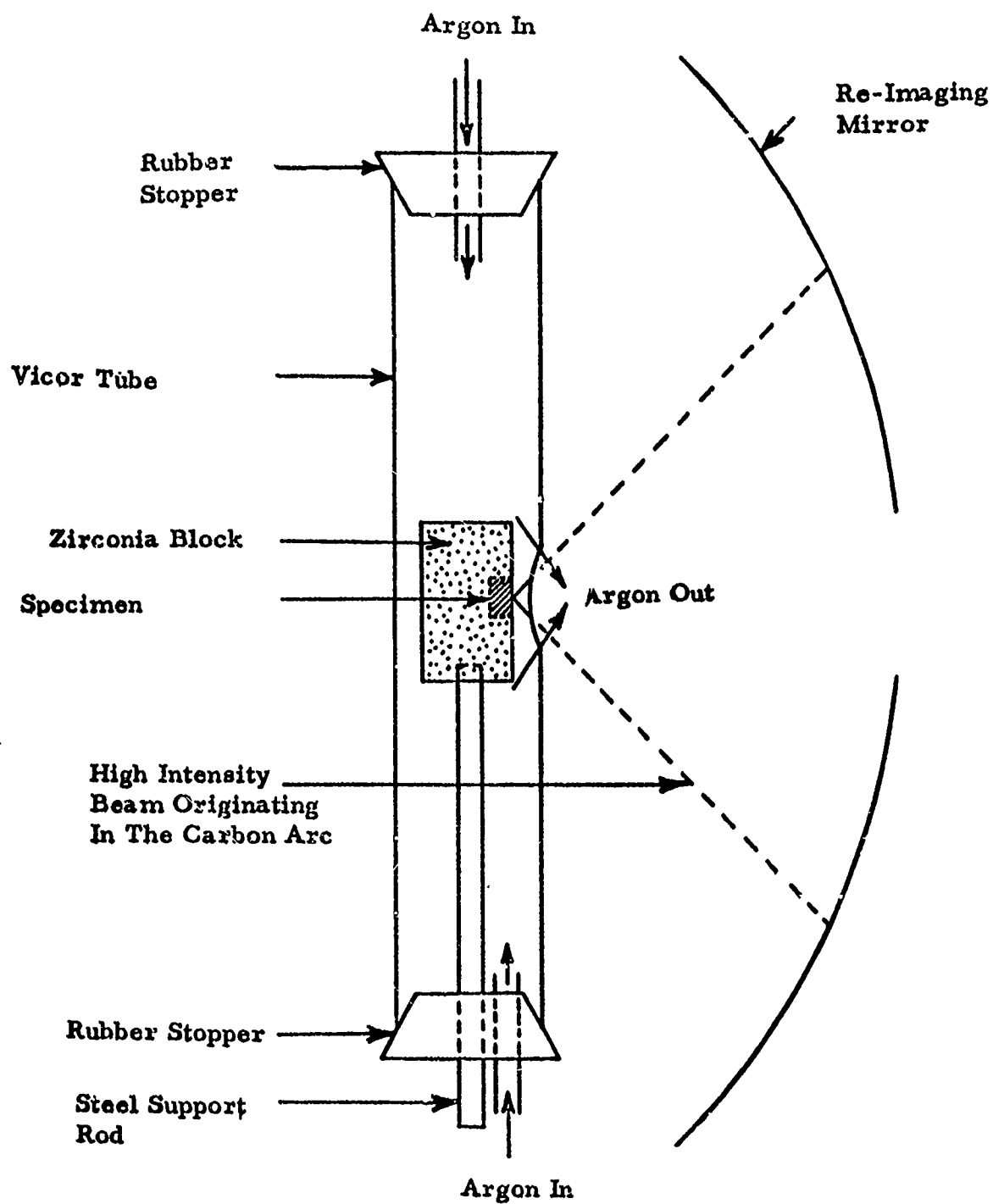
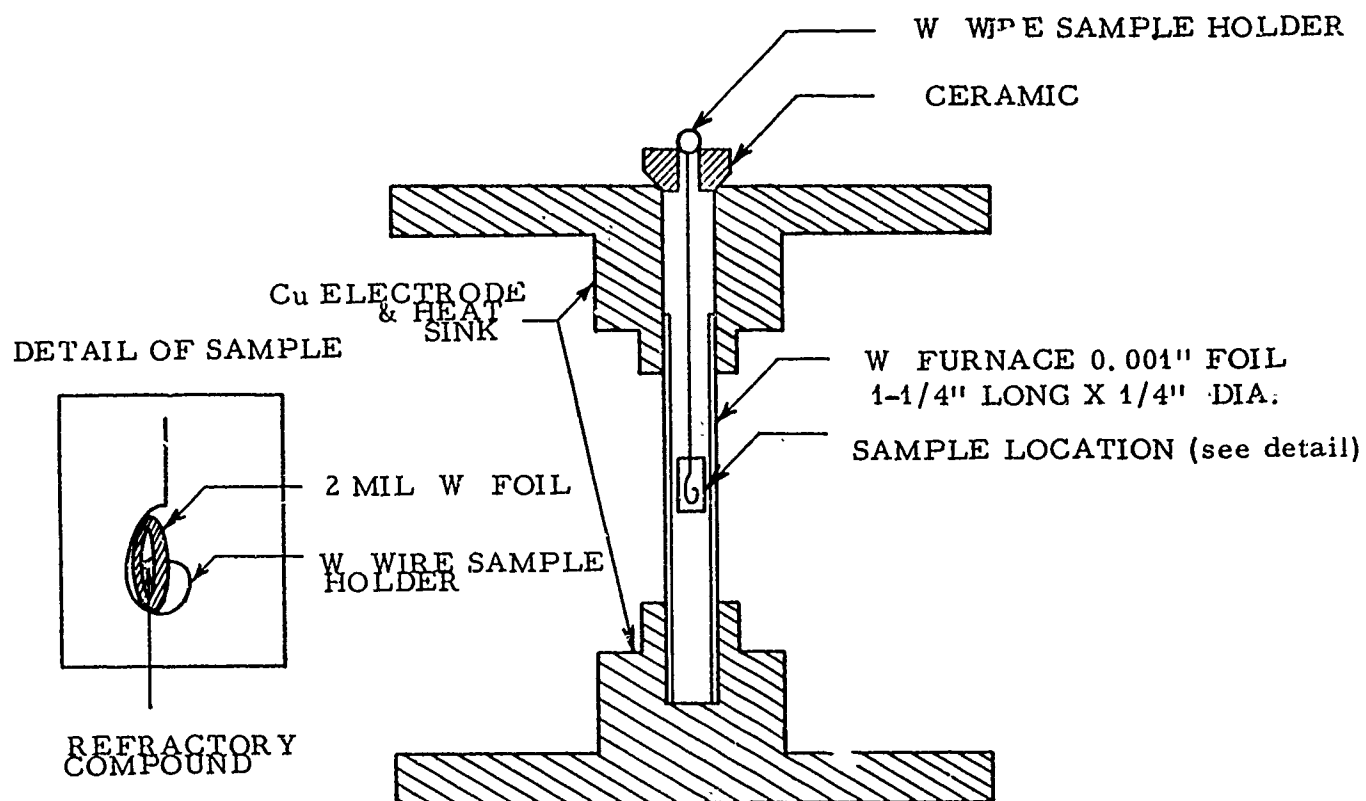


FIG. 1. SCHEMATIC REPRESENTATION OF INERT ATMOSPHERE SPECIMEN CONTAINER USED WITH ARC IMAGE FURNACE.

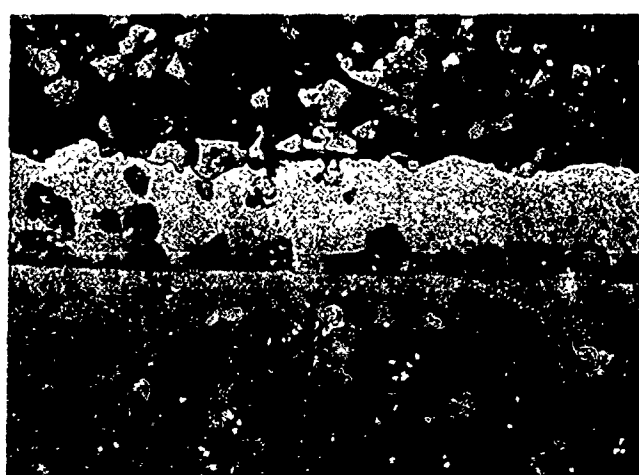
3000°C

W HIGH TEMPERATURE  
REACTION FURNACE



ENCLOSED WITHIN VACUUM OR GAS CHAMBER

FIG. 2



← Cu  
←  $\text{ThO}_2$   
← W  
← Cu

PLATE No. 23876

750 X

FIG. 3.  $\text{ThO}_2$  VS. W 3000°C - 2 MIN.

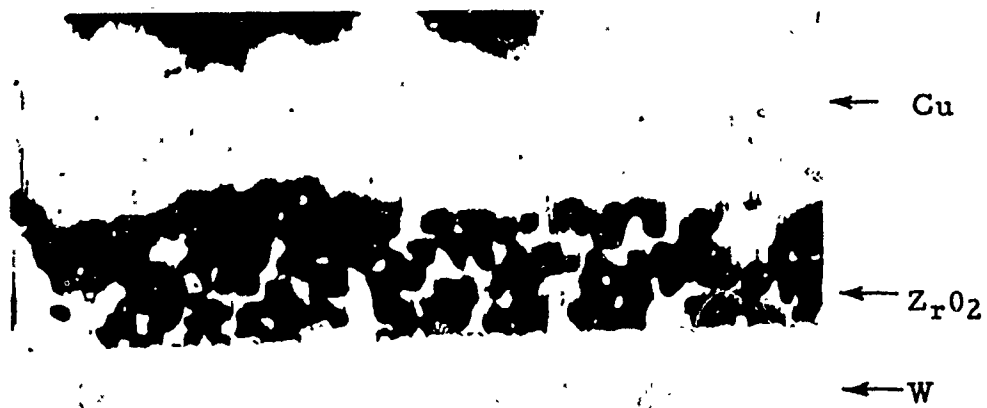


PLATE No. 23851

750 X

FIG. 4  $ZrO_2$  VS. W 2500°C - 1 MIN.

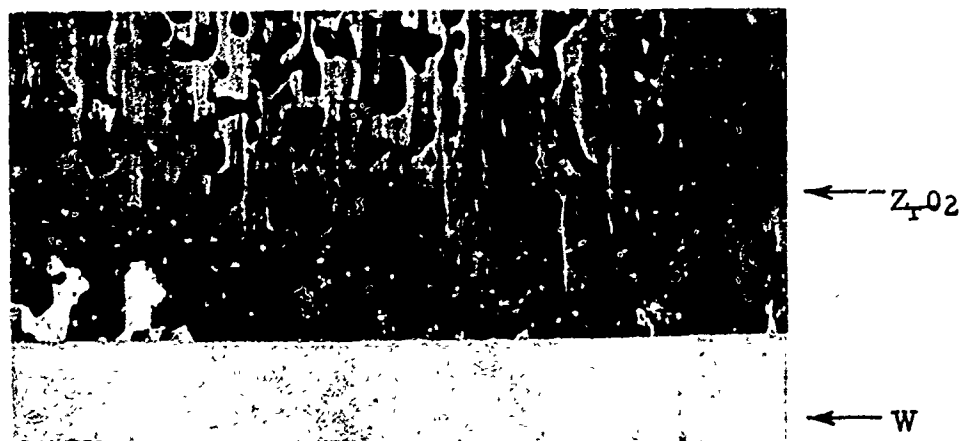


PLATE No. 23852

750 X

FIG. 5  $ZrO_2$  VS. W 2800°C - 1 MIN.

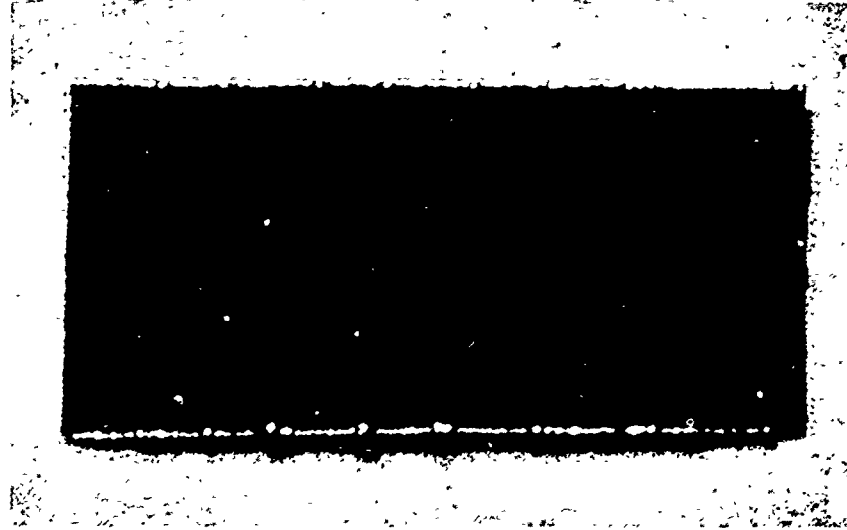


PLATE No. 23853

750 X

FIG. 6  $ZrO_2$  VS. W 3000°C - 1 MIN.

As received



2500°C 1 MIN.



3000°C 1 MIN.



FIG. 7 W + MgO

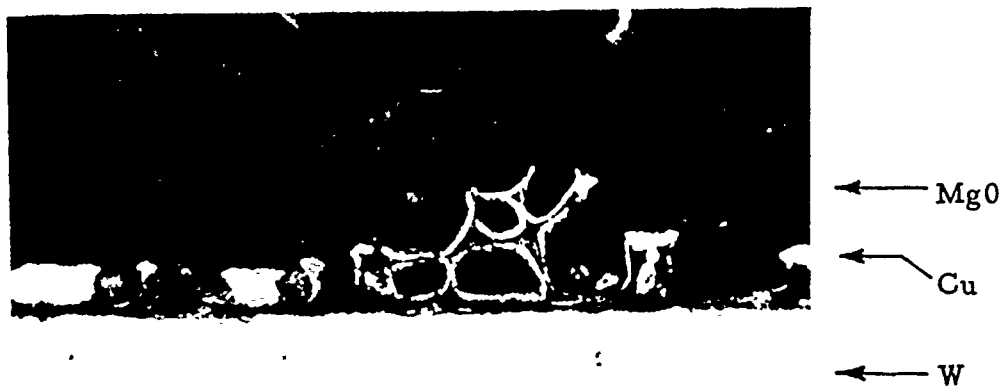


PLATE No. 23856

750 X

FIG. 8 MgO VS. W 2200°C - 1 MIN.

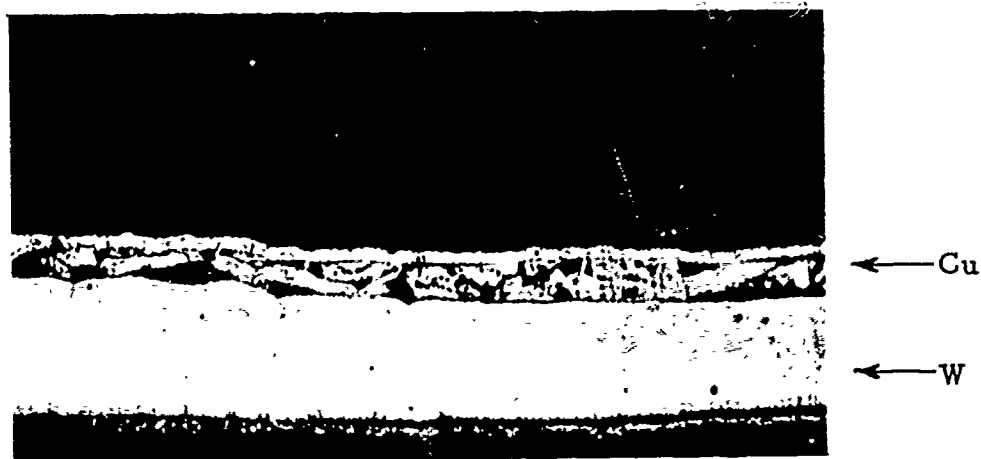


PLATE No. 23857

750 X

FIG. 9 MgO VS. W 2500°C - 5 MIN.



PLATE No. 23858

750 X

FIG. 10 MgO VS. W 3000°C - 1 MIN.





PLATE No. 23877

750 X

FIG. 11  $\text{Al}_2\text{O}_3$  VS. W 2500°C 1 MIN.

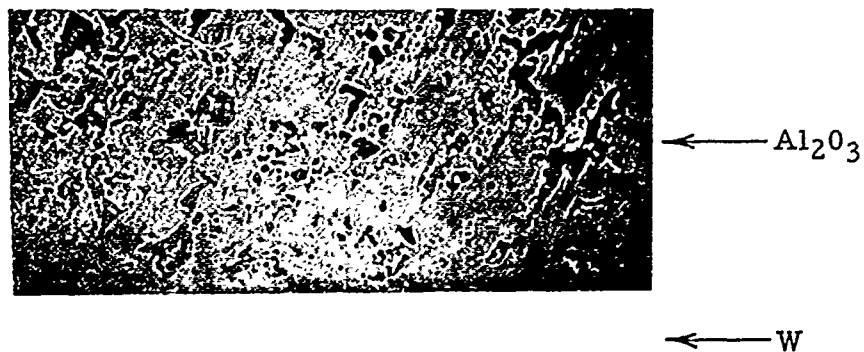


PLATE No. 23878

750 X

FIG. 12  $\text{Al}_2\text{O}_3$  VS. W 3000°C 1 MIN.

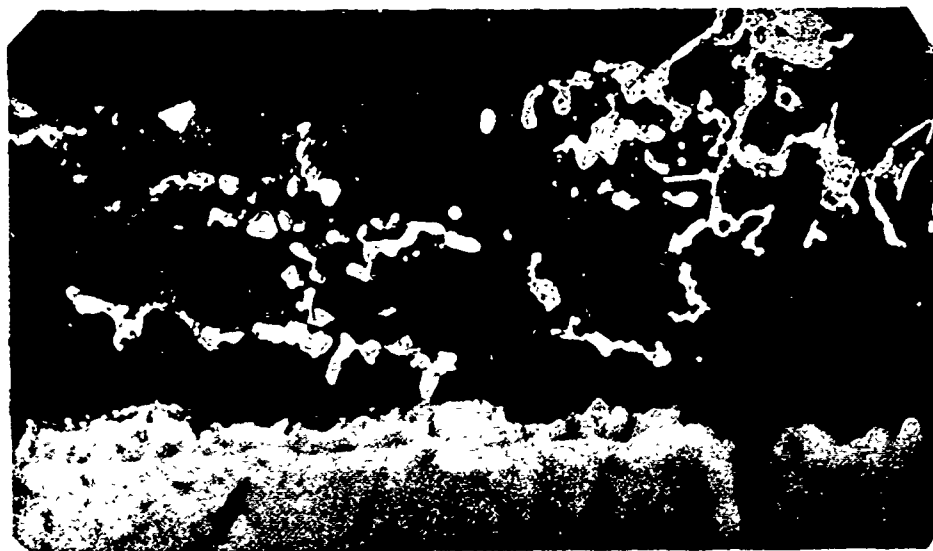


PLATE No. 24165

750 X

FIG. 13

W + Al<sub>2</sub>O<sub>3</sub>

HEATED IN WET ARGON FOR 2 MINUTES AT 2400°C



PLATE No. 23917

Mag. 750 X

FIG. 14  $Y_2O_3$  VS. W 2500°C - 1 MIN.



PLATE No. 23918

Mag. 750 X

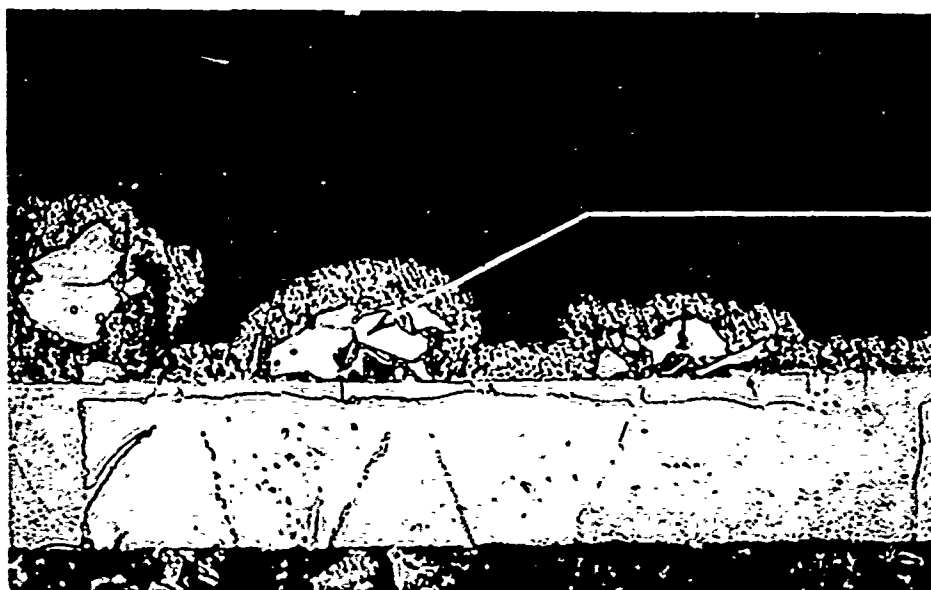
FIG. 15  $Y_2O_3$  VS. W 3000°C - 1 MIN.



PLATE No. 24152

750 X

FIG. 16      W +  $\text{HfO}_2$    3000°C   FOR 1 MIN.



← TAC  
← Cu  
←  $(Ta, W)_2C$   
← W  
← Cu

PLATE No. 23916

Mag. 750 X

FIG. 17 TAC VS. W 2700°C - 1 MIN.



← TAC  
← W  
← Cu

PLATE No. 23919

Mag. 750 X

FIG. 18 TAC VS. W 2750°C - 1 MIN.



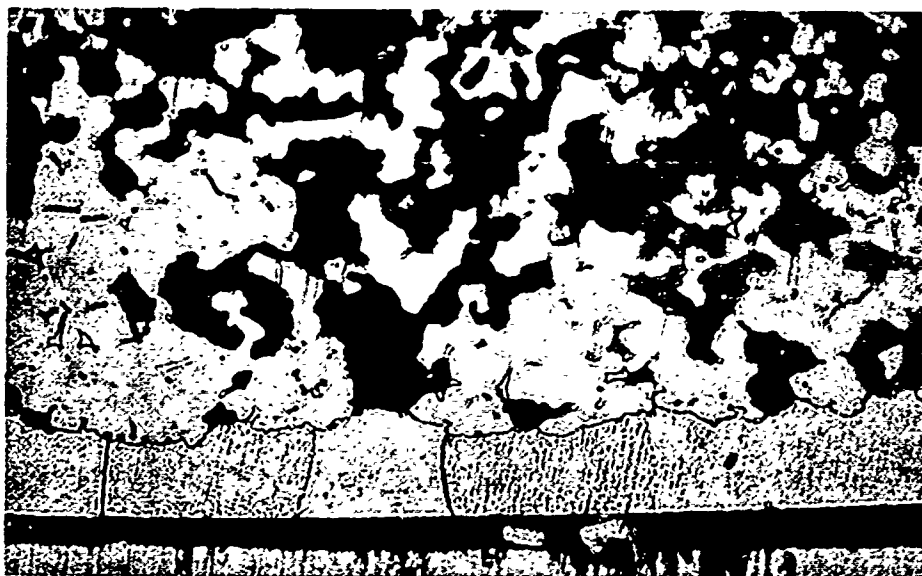
← HfC

← W

PLATE No. 23955

Mag. 750 X

FIG. 19 HfC VS. W 2800°C - 2 MIN.



←  $Z_rC$

← W

PLATE No. 23920

Mag. 750 X

FIG. 20  $Z_rC$  VS. W 2700°C - 1 MIN.



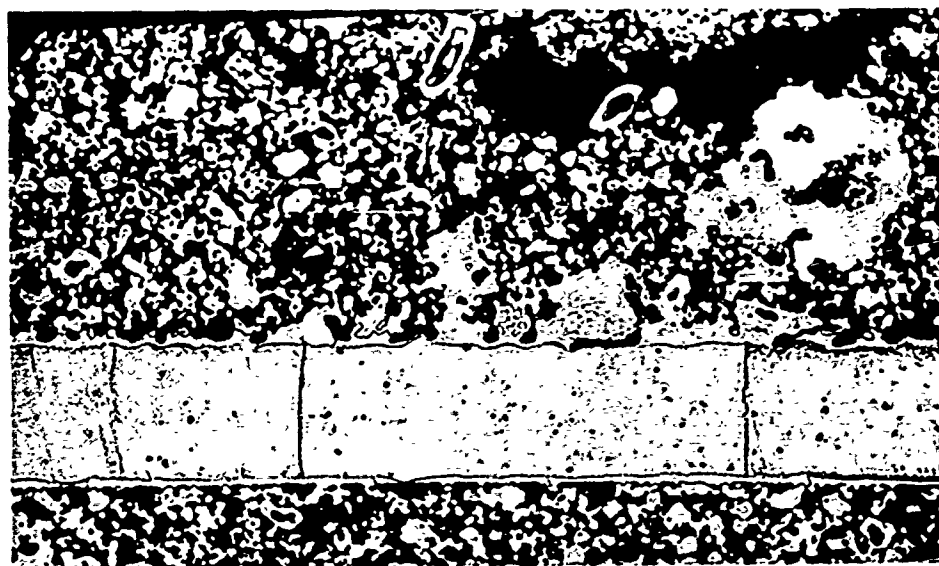
←  $Z_rC + W$

← W

PLATE No. 23921

Mag. 750 X

FIG. 21  $Z_rC$  VS. W 2900°C - 1 MIN.



← TAC + 20%  
HfC

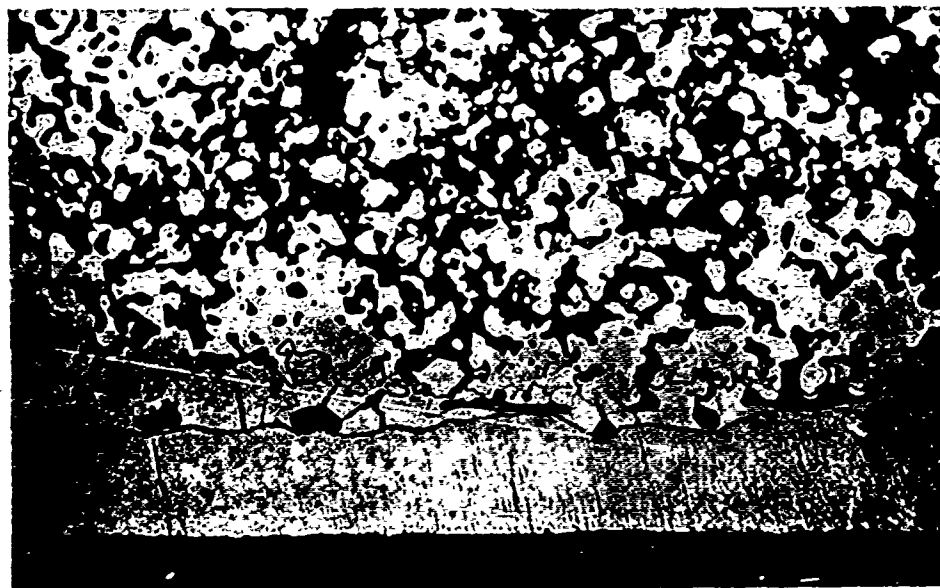
← DIFFUSION  
LAYER

← W

PLATE No. 23956

Mag. 750 X

FIG. 22 TAC + 20% HfC VS. W 2700°C - 1 MIN.



← TAC + 20%  
HfC

← W

PLATE No. 24151

Mag. 750 X

FIG. 23 TAC + 20% HfC VS. W 2800°C - 2 MIN.





PLATE No. 23954

Mag. 750 X

FIG. 24 TAC + 20% HfC VS. W 2800°C - 2 MIN.

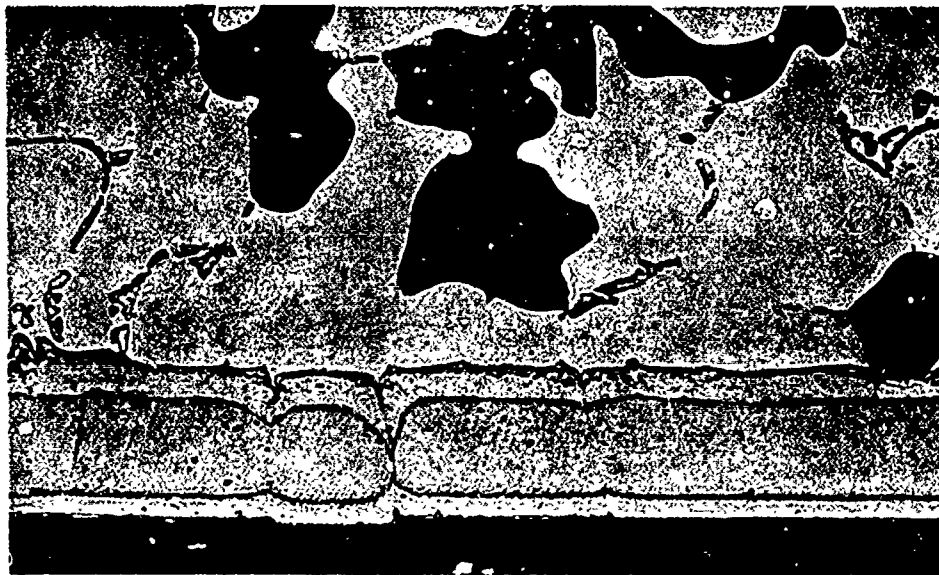
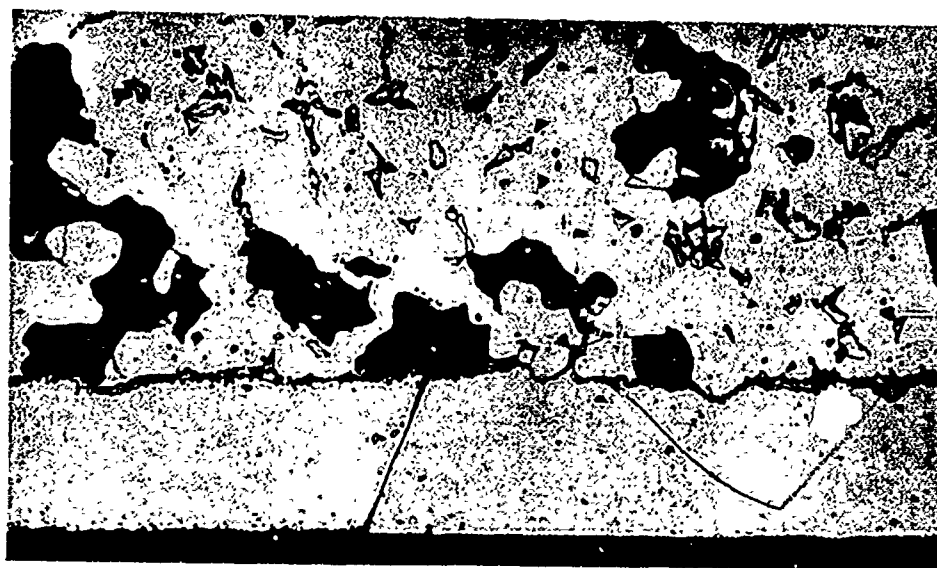


PLATE No. 24150

Mag. 750 X

FIG. 25      W + TiN   2900°C   -   2   MIN.



← Z<sub>r</sub>N

← W

PLATE No. 24156

Mag. 750 X

FIG. 26      ZN + W   3000° C   -   1 MIN.

PROTECTION OF TUNGSTEN AGAINST OXIDATION AT  
ELEVATED TEMPERATURES

A.L. Pranatis, C.I. Whitman and C.D. Dickinson

General Telephone & Electronics Laboratories  
Bayside, New York

ABSTRACT

Preliminary studies of protective coating systems for tungsten are reported. Particular emphasis is placed on silicide systems and their modifications for protection to 1800°C. Two new basic approaches are applied to the silicide system to demonstrate their usefulness in the analysis of coating systems.

## I. INTRODUCTION

Tungsten has obvious advantages as a material of construction for use at high temperatures, but its use as such is limited by a lack of oxidation resistance. It appears unlikely that simple alloying can supply a solution to this problem and therefore the development of a composite system is required. Consequently, a number of refractory coatings for tungsten are presently being studied at the General Telephone & Electronics Laboratories. Included in the materials selected for preliminary testing, several of which are still under consideration, were silicon, aluminum, chromium, tantalum, zirconium, titanium, and beryllium, applied both by cementation and as paint and sinter-type processes. On the basis of preliminary screening tests, silicon has been selected for intensive study, and this is a preliminary report of research in progress on this phase of the program.

## II. COATING PROCEDURES

Although other techniques have been, and are being, investigated, pack cementation has been the principal method used for coating preparation. Some typical experiments are outlined in Table I. After investigation of a number of activating agents and experimental techniques, the following more or less standard procedure was adopted.

Samples of tungsten to be coated are outgassed in vacuum at  $1000^{\circ}\text{C}$  after pickling in an  $\text{HF-HNO}_3$  acid mixture to remove any surface contamination. Typical specimens coated are 0.040" diameter tungsten rod in lengths of about 3 to 3-1/2". These tungsten rods are packed in a mixture consisting of 90%, 325-mesh silicon powder and 10% sodium fluoride. A vitreous silica tube is used as a container with each end

plugged with Fiberfray insulation. This tube is then placed within a Globar furnace in dry hydrogen and heated at  $1050^{\circ}\text{C}$  for times up to 16 hours.

The primary emphasis on this part of the program has been to provide samples for testing, and as a result, the various parameters influencing the process have not been explored to any great extent. However, a number of observations have been made on the basis of experience to date.

In pack cementation a tungsten disilicide coating is formed. Figure 1 indicates the typical structure of the as-coated 0.040" tungsten rods. The coating is metallurgically bonded to the substrate material and generally has radial cracks through to the tungsten in the metallographic sample. It is not clear whether these cracks exist in the samples as coated or whether they are produced on metallographic mounting. It appears most likely that they are present in the as-coated samples. The coating will form in recesses. It has been repeatedly observed that the coating will extend into cracks and other defects in the tungsten. Figure 2 illustrates this clearly. No difference in coating behavior has been noted between Sylvania NS and Zirtung grades of tungsten, in comparison with Puretung.

The coating thickness is parabolic with time or, in other words, diffusion controlled. Sixteen hours are sufficient to form an approximately 4.0-mil coating on tungsten. Taken in conjunction with the radial cracks, this suggests that the silicide coatings form by diffusion of silicon through the coating, reacting with tungsten at the silicide-tungsten interface.

Sodium fluoride has been the most effective activating agent used, as was also noted by Goetzel and Landler.<sup>(1)</sup> Coatings made with other alkali halides are much thinner. Ammonium salts have been difficult to use under these conditions because of their volatility. The effectiveness of sodium fluoride probably results from a higher partial pressure of silicon-containing vapors in the pack. The thermodynamic calculations listed in Table II substantiate this. On this basis, KF should also be an effective activating agent, although Goetzel and Landler noted coating thickness variations which they attributed to the melting of the KF. Under the conditions employed, up to 50% of the sodium fluoride can vaporize from the pack during the coating cycle. At 1050°C NaF has a vapor pressure of 1 mm, which can account for this loss. A satisfactory diluent for the silicon remains to be found. Alumina and silica have not been satisfactory to date because of increased sintering of the pack and alteration of the coating structure.

This work is continuing, and it is planned to explore the effect of process variables on the coating and on its oxidation resistance.

### III. COATING EVALUATION

Life-test data, combined with metallographic observations, have been used as the main method of evaluating coating effectiveness. The majority of tests have been carried out on coated 0.040" tungsten rods, heated by self-resistance to failure under static conditions. A few cycling tests were made with greatly shortened life times. Under usual test conditions, temperatures vary from the apparent test temperature at the center of the specimen to about 200° or 300°C at

the water-cooled grips. In addition to these experiments with resistance heated 0.040" rods, supplementary tests have been carried out, principally for the purpose of observing microstructure changes, on 0.040" rod and on 0.020" rolled strip heated for definite time periods, either in the resistance jigs or in platinum wound furnaces.

Although resistance-jig temperatures were standardized at 1090°C (2000°F), 1370°C (2500°F), 1650°C (3000°F) and 1818°C (3300°F), it soon became clear that, except at the highest test temperature (1818°C), failure usually occurred in the low-temperature region of the specimens, at temperatures between 1200°C and 1350°C. It has been found possible to extend substantially low-temperature life by modifying the silicide coatings. At 1818°C failure occasionally occurred in the center of the specimens, and examination of the specimens after failure revealed crater-like eruptions in the clear glassy oxide coating, suggesting the remnants of broken bubbles.

Tests attempted at temperatures above 1818°C failed, either through eutectic melting of the coating or through pronounced bubbling of the coating.

Temperatures were manually controlled and monitored with a Micro Optical pyrometer. Although calculations showed that no more than a 3- or 4-degree temperature variation need be expected across the cross-section of an uncoated tungsten rod, temperature variations across the actual test specimens with their thick intermetallic and oxide coating undoubtedly were of greater magnitude. A further factor complicated assignment of exact test and failure temperatures. Comparison of optical pyrometer temperatures with those obtained with a Shaw two-color pyrometer, revealed that temperature variations of as much as 70°C could occur in a few seconds, due both to chilling



of the specimens by drafts and to variations in voltage as other furnaces on the same power line were turned off and on.

For all these reasons, temperatures during these tests could be only roughly indicated, and in consideration of the following data, conclusions regarding the effect of temperature should be drawn cautiously. However, it was felt that the ease and rapidity with which screening tests could be carried out with resistance-jig heating so outweighed the disadvantages of inadequate temperature control that its continued use was justified.

A real variable affecting specimen life is coating thickness, and even in specimens that fail catastrophically by "pest" formation, the rate of oxidation appears to be diffusion controlled. Comparisons of coating effectiveness must therefore take this into account, as is done in Table III, which indicates the average test life of silicide coated 0.040" rod, and two modified silicide coatings designated A and B. For comparison, Table IV contains the life times observed with tungsten coated with various metals.

On the basis of data gathered so far, it appears that modifications could improve the life times of silicide coatings at 1650°C by a factor of about three. At other temperatures improvement is not as obvious because tests were arbitrarily terminated after ten hours. However, the beneficial effects of these modifications are apparent from visual and metallographic examination. At low test temperatures, modified coatings are characterized by a uniform dark color, in comparison with a milky white porous outer layer on the ordinary silicide coatings. Metallographic examination shows either absence of or a lower rate of penetration from the pest-type structures to be discussed below.

It must be emphasized again that the failures listed in Table III occurred almost entirely at low temperatures. However, some correlation between maximum specimen temperature and life seems to exist. On the other hand, the metallic coatings listed in Table IV were of a more ordinary nature and failure generally occurred in the specimen region of maximum temperature.

Metallographic examination of the coatings after failure revealed completely different structures for specimens tested at high and low temperatures. Figures 3 and 4 show the microstructures of the high- and low-temperature regions of an 0.040" tungsten rod coating with unmodified silicide. Failure occurred after about 13 hours in the region of approximately 1300°C. Maximum test temperature was about 1650°C. The structures are typical, but the phases present have been only tentatively identified.

In the high temperature region, the following phase sequence appears:

- (1) A thin layer of glassy oxide, most probably  $\text{SiO}_2$ , either pure or alloyed with tungsten.
- (2) A thin layer of either mixed  $\text{WSi}_2$  and  $\text{W}_5\text{Si}_3$ , or pure  $\text{W}_5\text{Si}_3$ , approximately the same thickness at the outer layer of  $\text{SiO}_2$ , resulting from the selective oxidation of Si in the original layer of  $\text{WSi}_2$ .
- (3) The residue of  $\text{WSi}_2$  with grain size corresponding to oxidation temperature.
- (4) A layer of  $\text{W}_5\text{Si}_3$ , the result of diffusion of Si from the  $\text{WSi}_2$  layer.
- (5) The tungsten rod, now alloyed with Si and with a grain size corresponding to the test temperature.

Similar structures have been noted by Goetzel and Landler<sup>(1)</sup>.

A completely different and much more complex structure is usually present in the regions of low-temperature failure. Due to its complexity, identification of the phase sequence is much less positive:

- (1) Again, but only probably, a thin layer of  $\text{SiO}_2$ .
- (2) A layer of glassy oxide, ranging in color under polarized light from white to pale blue, probably all of the same structure but varying in composition.
- (3) A mixed structure, consisting of islands of either  $\text{WSi}_2$  or  $\text{W}_5\text{Si}_3$  in the above oxide, with varying proportions of metal and oxide.
- (4) Prior to failure, the recrystallized  $\text{WSi}_2$ .
- (5) A thin layer of  $\text{W}_5\text{Si}_3$ .
- (6) In the failure zone, islands of  $\text{WO}_2$ , resulting from direct oxidation of tungsten, after complete consumption of the silicide coatings.

This phase sequence is the usual occurrence for low-temperature failures. Occasionally, a microstructure typical of the high-temperature regions appears associated with low-temperature failures. At present, it is not clear whether this is the result of the above sequence occurring in a localized fashion or of a different mechanism of failure.

These data, although scattered and undeniably erratic, permit some inferences which may be summarized as follows:

- (1) Failure at all test temperatures occur most generally at temperatures between  $1000^\circ\text{C}$  and  $1370^\circ\text{C}$  as a result of low-temperature oxidation. Coatings so attacked have a milky white appearance.
- (2) The silicide coatings can be modified to reduce the rate of low-temperature oxidation substantially.

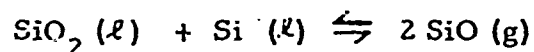
- (3) All types of silicide coatings have an upper service limit in the vicinity of 1818°C. Above this temperature the protective coating can be destroyed either through eutectic melting or through bubbling of the coating by gas formation.

#### IV. DISCUSSION OF OXIDATION BEHAVIOR

All the data to date clearly indicate that the silicide coatings possess remarkable high-temperature potentialities, but are presently limited in usefulness by their susceptibility to accelerated failure at low temperatures. Solution of this problem will undoubtedly permit extended life times up to temperatures between 1800°C and 1900°C.

The bubbling in the coating which occurs at these temperatures is a result of a reaction between  $\text{SiO}_2$  and the underlying silicide to form  $\text{SiO (g)}$  at the interface between these phases. These can be understood by considering the thermodynamics of the reaction.

Extrapolation of thermodynamic data<sup>(2)</sup> for the free energy of the reaction



estimates the equilibrium pressure of  $\text{SiO (g)}$  to reach 1 atm. at 1877°C with an uncertainty of about  $\pm 100^\circ\text{C}$ . In a silicide phase the activity of silicon will be less, of course, and the temperature for  $p(\text{SiO}) = 1 \text{ atm.}$  will be higher. A decrease in the activity to 0.1, a value reasonable for silicides, will increase this temperature by about  $200^\circ\text{C}$ . Experimentally the coating is observed to bubble at optical temperatures of  $\sim 1850^\circ$  to  $\sim 1950^\circ\text{C}$ . The true temperatures are probably  $75^\circ\text{C}$  higher if emissivity is taken into account, and therefore these observations are consistent with the thermodynamic estimates.

Unlike the high-temperature limitation, the basic cause of low-temperature failure is as yet not well understood. However, the particular phase sequences appearing at high and low temperatures suggest, if not a solution of the problem, at least its statement in comprehensible terms.

The oxidation of an alloy may be viewed as a problem in ternary diffusion and discussed on the basis of principles developed in the study of solid state diffusion. As is well known, a diffusion couple will, in solid phases, produce a series of layers of phases corresponding to the phase diagram for the particular system.<sup>(3,4,5)</sup>

For example, in the Sb-Sn system, a diffusion couple will show a layer corresponding to the  $\beta$ , Sn-Sb phase.<sup>(4)</sup> In ternary and higher systems, similar considerations hold with the additional complication that there is generally a choice of phase layers or "paths" for the diffusion couple. The path chosen by the system depends on the relative diffusion rates of the components.<sup>(3)</sup>

Although the phase diagram for the ternary system W-Si-O is not completely known, it is possible to "guess" intelligently at the phase diagram, as has been outlined by Sidebottom and White.<sup>(6)</sup>

To construct the tentative diagram shown in Fig. 5, we proceed as follows:

The free energy of the reaction  $2\text{WO}_3 + 3\text{Si} \rightarrow 2\text{W} + 3\text{SiO}_2$  ranges from -221 k cal at 1000°K to -196 k cal at 2000°K. The formation of silicide phases would make these  $\Delta F$  values more negative.

Therefore, the joins from the silicide phase should be to the  $\text{SiO}_2$ .

The existence of other ternary phases, which would modify the diagram, are quite possible and can be determined only by experiment. For  $\text{WSi}_2$ , however, this simple diagram is sufficient to account for what is known experimentally, emphasizing that no pretense is made of quantitative exactness.

At  $1650^\circ\text{C}$ , the phase sequence suggests a "zig-zag" diffusion path, as shown by the dotted lines of Fig. 5, and the formation of  $\text{SiO}_2$ , either by diffusion of silicon through the oxide and reaction at the oxide-gas interface, or alternatively, by diffusion of oxygen through the oxide and reaction at the oxide-silicide interface, but with such rapid diffusion of silicon in the silicide phases that no  $\text{WO}_3$  can be formed. It will be noted that the diffusion path is parallel to the tie-lines in the two-phase fields,  $\text{WSi}_2 + \text{W}_5\text{Si}_3$  and  $\text{W}_5\text{Si}_3 + \text{SiO}_2$ , and therefore, as demonstrated by Clark and Rhines,<sup>(3)</sup> no mixed phase regions will occur in the phase sequence. Protection is thus the result of the formation of a coherent, relatively pure outer layer of  $\text{SiO}_2$ . Since neither the diffusion coefficients nor the phase diagram are known, this overall picture, although plausible, is subject to modification. In any event, this semi-quantitative interpretation is quite satisfactory for describing the high-temperature oxidation of  $\text{WSi}_2$ .

The low-temperature case is much less clear since all the observed phases have not been identified positively. However, the observed phase sequence suggests a straight-line diffusion path, the dash-dot line of Fig. 5. The crossing of the two-phase regions and the tie-lines contained in them at an angle would then result in the formation of mixed two-phase regions, as has been indicated by Clark and Rhines.<sup>(3)</sup> The consequence would be that the outer layer would consist, not of

pure coherent  $\text{SiO}_2$ , but a non-protective mixture of  $\text{SiO}_2$  and  $\text{WO}_3$ , accounting for the relatively rapid oxidation. (There is a strong possibility that this outer layer may consist of  $\text{SiO}_2$  and an unknown ternary oxide phase, but this does not affect the qualitative validity of this argument.)

Since a straight-line diffusion path requires that the proportions of silicon and tungsten remain relatively constant throughout the entire phase sequence, it follows that at low temperatures the diffusion of oxygen relative to silicon is greater than at high temperatures. There are no data to indicate whether this represents a decreased mobility of silicon in the silicide phase or an increased oxygen mobility in the oxide phase. An increased oxygen mobility in the oxide phase could be the result of cracking in the outer  $\text{SiO}_2$  layer, so that oxygen diffusion occurs not through the lattice but through tiny microcracks. A decreased mobility of silicon in  $\text{WSi}_2$  compared with that of oxygen in  $\text{SiO}_2$  would mean that oxygen arrives at the interface more rapidly than silicon, and therefore combines with tungsten to form  $\text{WO}_3$  simultaneously with  $\text{SiO}_2$ , producing a non-protective layer. (The activation energy for diffusion of oxygen in  $\text{SiO}_2$  may be expected to be much lower than that for diffusion of silicon in  $\text{WSi}_2$ .) Other possibilities exist, such as the formation of ternary inter-oxide compounds that would be stable only at low temperatures but not at high, so that an entirely different phase diagram and phase sequences would occur. These possibilities, as well as others, are being investigated.

It is of interest to generalize on the implications of this analysis.

In general it is believed that oxidation-resistant silicides owe this property to the formation of a protective layer of silica. Reversing the argument, we can then say that for a silicide to be oxidation resistant, it should form a protective layer of essentially silica. (It is of course possible that oxidation resistance of a silicide could be obtained from a different oxide layer, but there is no case of this known experimentally). In the majority of cases, it is to be expected that for such a protective layer to be formed two conditions must be fulfilled:

- (1) Thermodynamically there must be a preference for oxidation of the silicon to form silica (i.e., the join must be from silicide to silica).
- (2) The diffusion of silicon must be sufficiently rapid so that  $\text{SiO}_2$  will in fact be formed preferentially as required by (1). This condition is adopted somewhat arbitrarily from the possibilities discussed previously.

On this basis, it is obvious that for the formation of a protective  $\text{SiO}_2$  layer in the initial stages of the oxidation, a higher mobility of silicon is required than when the protective layer is established. A reduced mobility of silicon can be tolerated for the maintenance of a protective film. Thus, it is possible that a silicide may resist oxidation quite well under a protective silica coat, yet be unable to establish the protective layer on its own.

This argument also implies that small changes in chemical composition of the silicide phases could be an important factor in whether or not rapid low-temperature oxidation will occur. The silicon in a silicon-rich  $\text{WSi}_2$  would have a greater mobility than in a silicon-deficient  $\text{WSi}_2$ , and



may be able to form a protective  $\text{SiO}_2$  layer. Preliminary experiments in these Laboratories have shown improved oxidation resistance with  $\text{WSi}_2$  bulk specimens containing excess silicon at normal pest temperatures. Any addition to  $\text{WSi}_2$  which, through one mechanism or another, increases silicon mobility may help in forming an  $\text{SiO}_2$  layer. These considerations should also apply to other oxidation-resistant intermetallics such as aluminides and beryllides. It is worth noting that pest-type oxidation phenomena have been observed in aluminides and found to be composition dependent (7).

$\text{WO}_3$  is volatile, especially above  $1200^\circ\text{C}$  and in the presence of water vapor. This fact has frequently been used in attempting to interpret the pest type phenomena and to account for high-temperature oxidation resistance. (8) It is clear, however, that while the  $\text{WO}_3$  volatility may assist in producing a protective  $\text{SiO}_2$  layer, or in avoiding pest at higher temperatures, it is not essential to the oxidation resistance. The thermodynamic and diffusion factors are basic to the establishment of a protective layer. Other experimental observations support this. For instance, weight is not lost on oxidation of  $\text{WSi}_2$ , indicating that little tungsten is lost by volatilization. Further,  $\text{TiSi}_2$  shows oxidation resistance and  $\text{TiO}_2$  is not volatile. Also,  $\text{TaAl}_3$  and  $\text{NbAl}_3$  are oxidation resistant through formation of a layer that is essentially  $\text{Al}_2\text{O}_3$ , and  $\text{Ta}_2\text{O}_5$  and  $\text{Nb}_2\text{O}_5$  are not volatile.

Although we have restricted our analysis here to the W-Si-O system, this type of analysis should be applicable to any oxidation that is diffusion controlled, including alloys as well as compounds and systems higher than ternary. This then suggests the following general conclusions:

- (1) In a series of silicides (aluminides, beryllides), e.g.  $\text{Mo}_3\text{Si}$ ,  $\text{Mo}_5\text{Si}_3$ ,  $\text{MoSi}_2$ , oxidation resistance is most likely in the silicon-rich material, since the diffusion of the silicon to the surface can occur more easily in this compound.

- (2) Since oxidation behavior may be strongly affected by slight changes in composition, previously reported results of poor oxidation resistance in other intermetallic compounds need to be reviewed to determine if this could be a factor influencing the observed behavior.
- (3) Pest-type oxidation processes are possible in other ternary systems. Exceptions would include SiC where the  $\text{CO}_2$  is volatile, and cases where the mobility of the oxide-former is sufficiently high to form a protective oxide until the temperature is so low that oxidation is negligible.
- (4) The establishment of the protective oxide layer at the start of oxidation is the most critical stage, since the diffusion of the oxide-forming constituent must be most rapid at this point.
- (5) Some of the problems of (4) may be alleviated through treatment either at low temperature or, preferably, at reduced oxygen pressure, so as to form a protective oxide layer.
- (6) A combination of a high-melting compound and a protective oxide may offer protection that neither is capable of alone (e.g.  $\text{W}_5\text{Si}_3$  and  $\text{SiO}_2$ ).

These conclusions are of course highly speculative, since the experimental data are meager. It is to be expected that this picture will be modified and refined in the future. However, the theoretical basis for this approach is quite sound, and in view of its potential usefulness in analysis of oxidation processes, a further elaboration of the theory of ternary diffusion is now proceeding.

REFERENCES

1. C.G. Goetzel and P. Landler, WADD 60-825, January, 1961.
2. H. L. Shick, Chem. Rev. 60, 331 (1960).
3. J.B. Clark and F.N. Rhines, Trans. ASM 51, 199 (1959).
4. L.S. Castleman, Nuclear Sci. & Eng. 4, 209 (1958).
5. F.N. Rhines, Trans. AIME 137, 246 (1940).
6. B.A. Sidebottom and J. White, Trans. Brit. Cer. Soc. 60, 96 (1961).
7. M.F. Judkins, private communication.
8. A.W. Searcy, J. Amer. Cer. Soc. 40, 931 (1957).

TABLE I

## TYPICAL SILICIDE COATING EXPERIMENTS

Pack Composition	Temp. °C	Time (hrs)	Coating Thickness (mils)
70% Al <sub>2</sub> O <sub>3</sub> 30% Si, -30+80 5% NaCl, KBr or NaI	1000	16	< 0.1
70% Al <sub>2</sub> O <sub>3</sub> 30% Si -30+80 5% NaCl, KBr or NaI	1200	16	~0.2
-325 Si I <sub>2</sub> sealed in quartz tube	1000	16	3.7
90% Si -325 10% NaF	1050	16	3.7
"	950	16	0.33 - 1.9 variable thickness
"	1050	4	2.0
" (reground pack)	1050	1	1.0
90% Si -60 + 150 10 NaF	1050	16	3.7

TABLE II

EQUILIBRIUM PRESSURES OF  $\text{SiX}_4$  FOR VARIOUS  
ACTIVATING AGENTS, CALCULATED FROM THERMO-  
DYNAMIC DATA.

<u>Activating Agent</u>	<u>P (<math>\text{SiX}_4</math>) at 1050°C (mm)</u>
NaF	0.79
KF	1.3
NaCl	0.001
KCl	0.0004

TABLE III

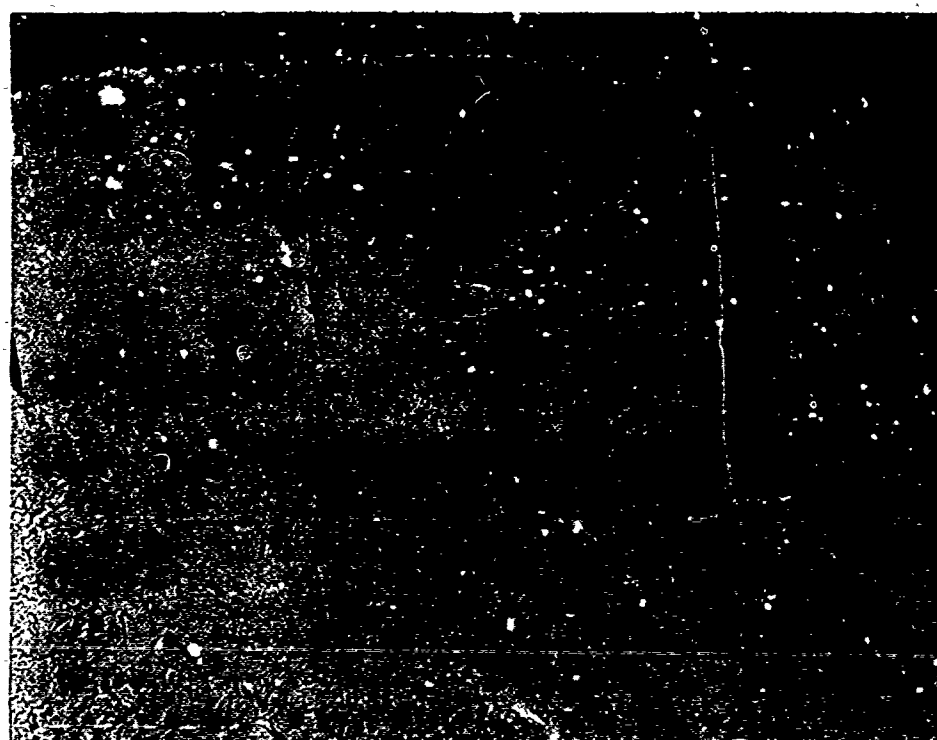
TEST-LIFE RANGE OF SILICIDE COATINGS

Temperature °C	Thickness (mil)	Time (hours)		
		Si	Si-A	Si-B
1095	1	1.5 - 3	5.5	6
	~ 2	6.5 - >10*	--	>10
	3 - 4	8 - >10	>10	--
1370	1	0 - 2.5	0 - 6	6
	~ 2	0 - >10	--	>10
	3 - 4	7.5 - >10	>10	--
1650	1	0 - 1.5	1	7
	~ 2	4 - 5	--	6 - 26
	3 - 4	6 - 9	>10 up to 26	--
1818	1	0 - 7.5	0	4.5
	~ 2	4 - 7	--	>10
	3 - 4	0 - >10	>10	

\* >10--Test terminated after 10 hours - specimen intact.

TABLE IV  
METAL COATING TEST LIFE

Temperature °C	Thickness (in.)	Time (Hours)			
		Al (pack coating)	Be	Cr(spray)	Ti (Pack)
650	<.001	7	--	--	7
1095		--	--	3.08	1.30
1500		--	<0.15	--	--



500 X

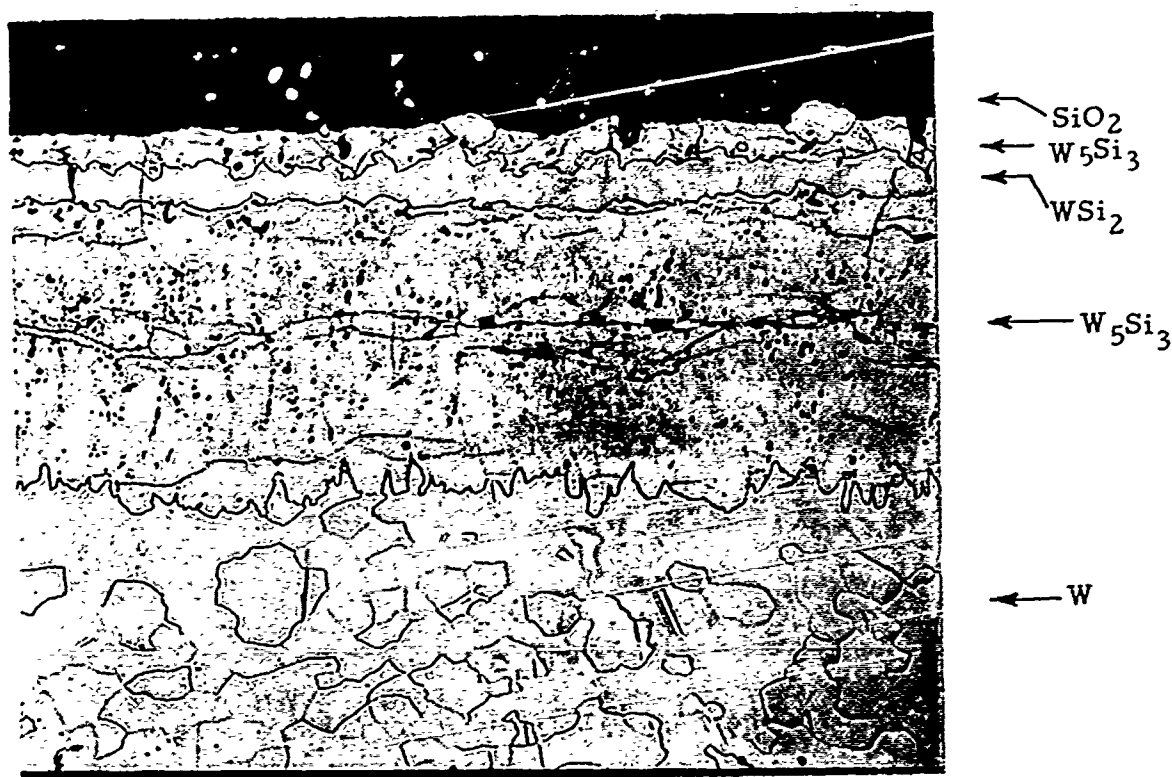
FIG. 1. CROSS-SECTION OF RUN 74-Si-2 IN THE AS-COATED CONDITION. THE BULK OF THE COATING IS  $WSi_2$ , BUT A VERY THIN, ALMOST INDISTINGUISHABLE LAYER OF  $W_5Si_3$  LIES BETWEEN THE  $WSi_2$  AND THE TUNGSTEN SUBSTATE. THE RADIAL CRACKS OCCASSIONALLY PENETRATE INTO THE TUNGSTEN METAL.





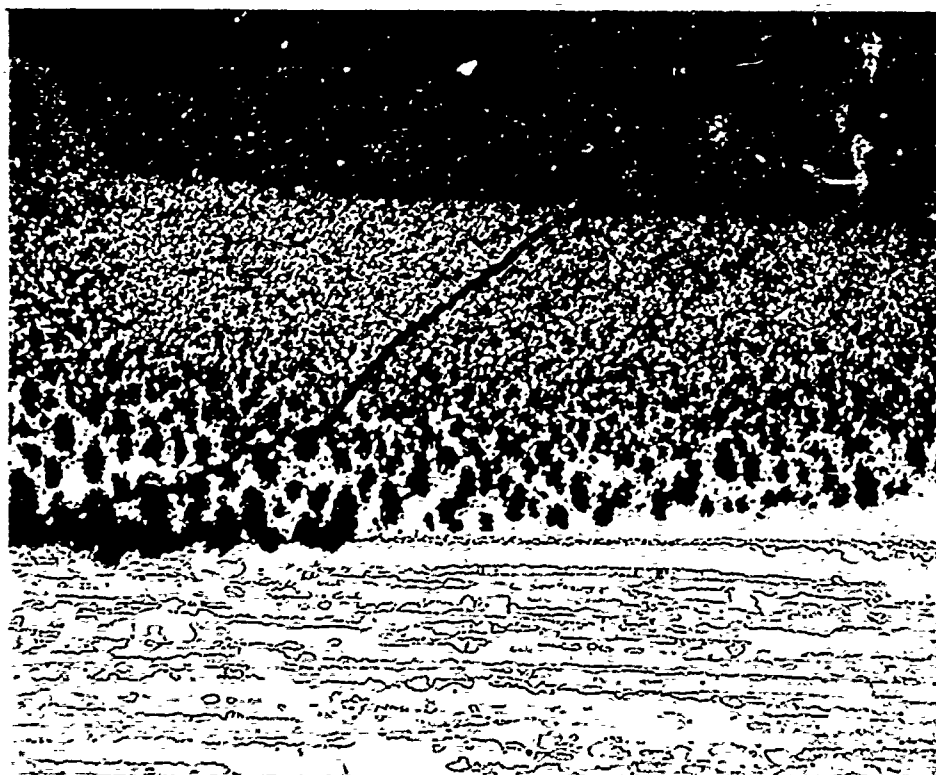
50 X

FIG. 2. RUN 89-Si-7 PENETRATION OF SILICIDE COATING INTO  
SPLIT END OF 0.040" TUNGSTEN ROD BY PACK CEMENTATION  
WITH NaF ACTIVATION.



250 X

FIG. 3. THE HIGH TEMPERATURE REGION OF A SILICIDE COATED TUNGSTEN ROD AFTER 13 HOURS OXIDATION AT 1650°C. THE PHASE SEQUENCE CORRESPONDS TO DOT-DASH DIFFUSION PATH OF FIG. 5.



←  $\text{SiO}_2$  (?)  
 ← Oxide  
 ← Oxide+ $\text{WSi}_2$   
 ←  $\text{WSi}_2$   
 ←  $\text{W}_5\text{Si}_3$   
 ←  $\text{WO}_2$   
 ← W

250 X

FIG. 4. THE LOW TEMPERATURE FAILURE ZONE ( $\sim 1300^\circ\text{C}$ )  
 OF THE SILICIDE COATED SPECIMEN OF FIG. 3 AFTER 13  
 HOURS OXIDATION. THE TENTATIVE PHASE IDENTIFICATIONS,  
 CORRESPONDS TO THE DOTTED DIFFUSION PATH OF FIG. 5.  
 THE  $\text{WO}_2$  PHASE DOES NOT BELONG TO THE SEQUENCE AND  
 IS THE RESULT OF DIRECT OXIDATION OF TUNGSTEN.

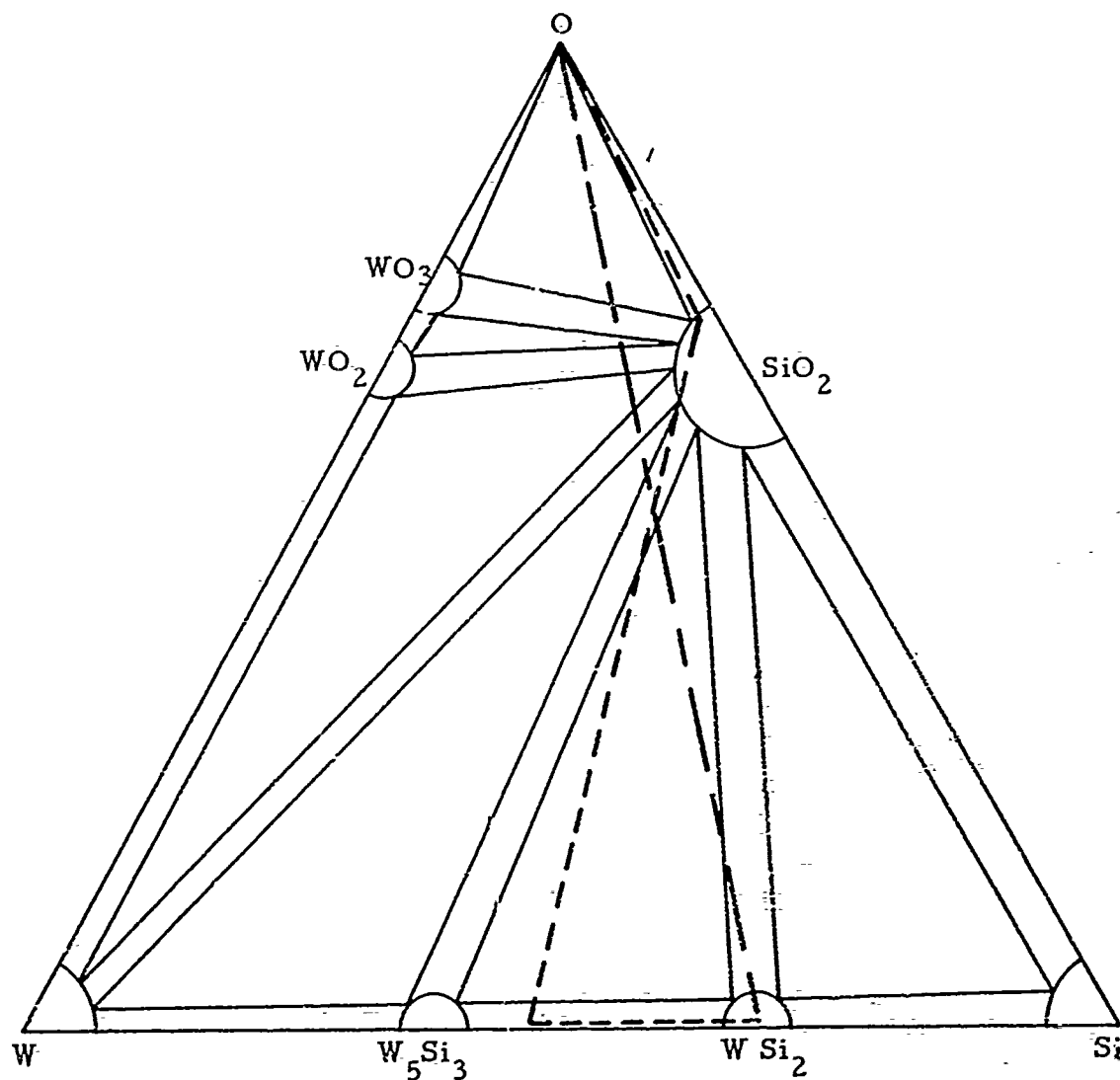


FIG. 5. A TENTATIVE PHASE DIAGRAM FOR THE W-Si-O SYSTEM AT 1370° AND 1650°C. THERE IS SOME EVIDENCE FOR A TERNARY PHASE NOT INDICATED HERE BETWEEN SiO<sub>2</sub> AND WO<sub>3</sub>. THE DOTTED LINE REPRESENTS THE HIGH TEMPERATURE DIFFUSION PATH AND THE DASH-DOT LINE, A LOW TEMPERATURE PATH.

STATUS OF EFFORTS ON REFRACTORY MATERIALS  
IN THE FLIGHT DYNAMICS LABORATORY, ASD

J. C. INGRAM, JR.

Aeronautical Systems Division  
Wright-Patterson Air Force Base, Ohio

## STATUS OF EFFORTS ON REFRACTORY MATERIALS IN THE FLIGHT DYNAMICS LABORATORY, ASD

The Flight Dynamics Laboratory has current and in procurement seven (7) major efforts in the field of refractories which include metallics, non-metallics and composites. Following is a brief summary of these programs:

### I. Refractory Metal Load-Carrying Structural Component

This program was initiated in June 1959 with McDonnell Aircraft Corporation for the design, fabrication and test of typical or representative structural component for a boost-glide, re-entry vehicle. The component should be capable of efficient operation for 30 minutes up to 2500°F and had to be fabricated from alloys of Cb or Mo. Either of these would have to be protected from oxidation.

After a survey, the F-48 Cb alloy was chosen and a coating had to be developed which eventually was the LB-2 cold slurry consisting of 10 Cr - 2 Si - Al. The basic coat, after baking out at 500°F, requires an Al slurry second coat (overlay) and this system is subsequently diffusion heat-treated in Argon at about 1900°F.

Extreme difficulty was experienced in obtaining the F-48 in the desired quality, sizes and gages and for some time the coating problem appeared to be as great. After two years, however, essentially enough material had been obtained, a satisfactory coating developed and the item fabricated. This was a replica of a fixed fin and deflecting rudder for a manned, lifting-drag, re-entry vehicle.

Test of the assembly was completed at McDonnell 15 July 1961; however, all test objectives were not met because the heating equipment was being overtaxed. The assembly withstood several cycles of temperatures up to 2425°F and several load cycles up to 150% of Design Ultimate Load. There was localized skin wrinkling in 5 or 6 panels and approximately 10 panel corners were warped. The coating held up well and no type of structural failure appeared to be imminent.

The program monitor is MSGT Jesse C. Ingram, Jr. with both technical and monetary assistance being given by the Applications Laboratory, Directorate of Materials and Processes.

### II. Refractory Metal Fasteners

This program was initiated in late May 1961 with Republic Aviation Corporation and requires the design, fabrication, protection and test of structural, mechanical fastening devices capable of utilization in the temperature range of 2000 - 4500°F. The items will be fabricated from alloys of Cb, Mo, W and (possibly) others.

The effort specifies modification of existing designs and introduction of new concepts. Both blind and quick-release fasteners are mandatory and production processes also will be developed. No coating development, per se, is allowed under the contract; instead, developments already proven and those which may become available, will be used.

Because of the newness of this effort, there is nothing significant to report. The program is being monitored by MSGT Jesse C. Ingram, Jr., with assistance being given by the Manufacturing Technology Laboratory, Directorate of Materials and Processes.

### III. Frontal Sections for Super-Orbital Re-entry

This contract was awarded Solar Aircraft in early July 1961 and requires design, fabrication and test of six (6) frontal sections for vehicles re-entering the earth's atmosphere from extremely high altitudes at near-escape velocities. Principal structural metals will be W and/or Ta with the two greatest problems being protection of the exterior and insulating (for heat block) the interior. Utilization temperatures are 4500°F externally and approximately 200°F maximum internally.

The effort is being monitored by MSGT Jesse C. Ingram, Jr. with augmentation being provided by the Applications Laboratory, Directorate of Materials and Processes, ASD.

### IV. High Temperature Composites (3000 - 4000°F)

This contract was awarded the Martin Company in July 1960 and will continue for approximately another year. The statement-of-work originally specified four nose units, 16" in diameter, but now it appears that we will get no more than 2 small (4" diameter) hemispheres and 2 large units.

Very early, it was found that SiC was no good and later, Zirconia was put aside; however, an effort to develop ZrO will now continue. At present, the only successful work has been done with Alumina. Future work will include thoria and hafnia, but emphasis will be on ZrO. The largest single piece unit that has been successful was 4" in diameter; anything larger has to be segmented.

Tests are made in a modified gas jet type of facility which employs multiple nozzles and various mixed combustibles. The parts are primarily radiation cooled but do have supplemental back-up cooling by water.

The program monitor is Robert T. Achard.

### V. Beryllium Structural Composites

This is a follow-on program with Aeronca and is just beginning. The old program is finished and the work primarily centered around stainless steel honeycomb, insulated, and filled with foamed ceramics. The new program is directed toward hot sections (principally underbodies) of lifting body vehicles. The old program was for 18 months and the new one is for the same duration, initially.

Materials to be used are stainless steels and Inconels for the honeycomb with Be for interfaces. Problems that are inherent with Be will probably result in having to decrease emphasis on that material. Insulants are of the fibrous type, e. g., Refrasil or Fiberfrax and ceramics will include SiO<sub>2</sub>, ZrO and Al<sub>2</sub>O<sub>3</sub>.

Ultimate utilization temperature is 3400°F for a period of one hour and no decibel rating specified except that a high limit is almost mandatory.

No coating, per se, will be developed.

Tests to be conducted will include ramjet, radiation, static, plasma and combinations of these where practical.

The program is being monitored by James F. Nicholson and Frank E. Barnett with monetary support being furnished by the Manufacturing Technology Laboratory of the Directorate of Materials and Processes.

#### VI. Ultra-High Temperature Active Cooling

This program is in P. R. status with letters of inquiry having been sent to many organizations. These are in an attempt to find out who has done what and some interesting replies are being received.

From the letters received, approximately 4 of the highest potential solutions will be chosen for further evaluation. From these, two will be investigated in detail.

Both ablation and transpiration methods and commensurate materials will be studied.

#### VII. Refractory Metal Honeycomb Sandwich Components

This program is presently in the procurement negotiation stage and a contract is expected in less than 60 days. Included in the development will be true thermal resistant heat-shields and also structural elements incorporating "double-wall" concepts. The heat-shields will be designed to withstand 3000°F temperatures and the structural elements 2500°F with the effort being divided between one Mo alloy and one Cb alloy which are yet to be chosen.

Honeycomb cores will be non-perforated and all core to face joining will be by brazing. It appears mandatory to develop brazing alloys; however, no specific coating development, per se, will be allowed.

In general, tests will be conducted in air using quartz lamp heat; however, thermal conductance tests will use a resistance heated "hot-plate" method and may be done in a vacuum or inert atmosphere. Hot sonic tests will be conducted up to 160 decibels.

The initial effort is for 14 - 15 months and is being monitored by P. P. Plank with both technical and monetary assistance being given by the Manufacturing Technology Laboratory of the Directorate of Materials and Processes.



DEVELOPMENT OF PROTECTIVE COATINGS  
FOR TANTALUM-BASE ALLOYS

W. D. KLOPP  
D. J. MAYKUTH  
H. R. OGDEN

Battelle Memorial Institute  
Columbus, Ohio

# DEVELOPMENT OF PROTECTIVE COATINGS FOR TANTALUM-BASE ALLOYS

by

W. D. Klopp, D. J. Maykuth, and H. R. Ogden

## INTRODUCTION

Tantalum alloys are currently being developed which maintain useful strength properties up to at least 3000 F. These high-strength alloys also exhibit good formability and ductility to as low as -320 F. However, all of these fabricable alloys have intrinsically poor oxidation behavior, at least at temperatures of 2500 F and greater, and, thus, will require protective coatings in order to serve satisfactorily in oxidizing environments.

The development of protective coatings for tantalum alloys was undertaken at Battelle Memorial Institute in May, 1960, under the sponsorship of the Aeronautical Systems Division, U.S. Air Force. The objectives of this program were to develop coatings for tantalum and tantalum alloys which exhibit static and cyclic oxidation resistance above 2500 F ideally, and which possess self-healing properties.

## EXPERIMENTAL RESULTS

### General

The results of a comprehensive literature survey indicated that five general types of coatings merited evaluation for protecting tantalum.

These included aluminum-base, beryllium-base, chromium-base, silicon-base, and oxide-glass coatings. The first two groups, aluminum-base coatings and beryllium-base coatings on tantalum, were under study at the Sylcor Division, Sylvania Electric Products, Inc., under separate Aeronautical Systems Division sponsorship; consequently, only limited studies of aluminide coatings were undertaken at Battelle.

The results of studies on seven types of coatings, as determined by static, continuous-weighing oxidation tests on 0.75 by 1-inch coated coupons, are summarized in Table 1.

Aluminum coatings showed good oxidation resistance in the range 2500 F to 2700 F when applied by either hot dipping or pack cementation.

Chromium coatings could not be applied in thicknesses over 0.7 mil and were not oxidation resistant at 2500 F. The most serious drawback to the use of high-chromium coatings is hardening of the substrate by chromium diffusion. Pack deposition of chromium at 2200 F hardened unalloyed tantalum to 600 KHN for a depth of at least 20 mils.

Silicide coatings were easily applied by pack deposition and showed good protection at both 2500 F and 2700 F, coupled with absence of diffusion hardening of the substrate either during silicon deposition or subsequent oxidation exposure.

Flame-sprayed  $Al_2O_3$ , with or without glass impregnation, was unprotective at 2500 F. The lack of protection was associated with partial oxidation of the substrate during flame spraying.

Titanium and hafnium coatings were evaluated as possible additions to other coatings. These metals were applied by pack cementation using NaF as the carrier, but the resultant coatings were thin and non-protective.

TABLE 1. SUMMARY OF RESULTS OF INITIAL COATINGS STUDIES

Coating	Method of Application	Coating Thickness, mils	Maximum Protective Life, hours		Substrate Hardening
			2200 F	2500 F	
Aluminum	Hot-dip 1800 F, heat in vacuum at 1700 F Pack cementation, (a) 16 hr at 2000-2200 F	2  2-4	>6	3.5  >7.5	None  None
Chromium	Electroplating, vapor deposition Pack cementation, 1800 F-2400 F	Nonuniform coatings 0.1-0.7	-	-	-  Severe
Silicon	Vapor deposition, 2370 F Pack cementation, 2000 F-2400 F	1 2-5	0 >6	0 >7	- None
Al <sub>2</sub> O <sub>3</sub> plus glass	Flame spray, paint, and sinter	5	0	0	Severe
Titanium	Pack cementation, 2000 F-2370 F	0.2-0.5	1.5	0	None
Hafnium	Pack cementation, 2200 F	0.3	2	0	-
Zinc	Vacuum distillation, hot dip	Coatings were mechanically adherent only and not oxidation resistant at 1700 F.			

(a) Pack mixtures contained 75 vol % Al<sub>2</sub>O<sub>3</sub> filler, 25 vol % coating element, plus 2 wt % halide carrier. Packs were heated in argon, generally for 16 hours.

Zinc coatings were evaluated briefly on the basis of the Naval Research Laboratory<sup>(1)\*</sup> results with columbium. No interdiffusion between tantalum and zinc was observed and the coatings were not oxidation resistant.

As a result of the above-described preliminary evaluation, major interest in the Battelle program has centered on silicide-coating systems.

### Studies of Silicide Coatings

#### Straight Silicide Coatings

A study of pack-deposition techniques indicated that marked improvements in the character and protectiveness of straight silicide coatings could be achieved by modifying the deposition conditions. Variables in this study included deposition temperature (2000 F to 2400 F); carrier (halides with elements from Groups I and II); proportions of  $Al_2O_3$ , silicon, and carrier in the pack;  $Al_2O_3$  particle size; and number of deposition cycles.

The deposition rates with various halides could be correlated with halide stabilities and boiling points. The halide of the coating element should be more stable than the corresponding tantalum halide but slightly less stable than the carrier halide. The coating element halide should also have a low boiling point. The preferred carrier for

---

\* Reference appears on page 14.

pack deposition of silicon was determined to be NaF. This carrier gives a 3-mil coating of primarily  $\text{TaSi}_2$  in 16 hours at 2200 F.

Increasing the silicon concentration of the pack from 10 vol % to 50 vol % slightly increases the deposition rate, but variations in the amount of NaF from 1 wt % to 8 wt % have no significant effect. Increasing the deposition temperature from 2200 F to 2400 F gave a thicker coating (5 mils compared to 3 mils), but the protective life at 2700 F remained about 2.5 to 3 hours.

Significant improvements in the protective life were obtained by application of the coating in two cycles instead of one and by employing coarser sized  $\text{Al}_2\text{O}_3$  in the pack. The average lives at 2700 F for tantalum coated with silicon in one cycle, two cycles, and two cycles using coarser (5-mil)  $\text{Al}_2\text{O}_3$  were 2.7, 4.8, and 9.8 hours respectively. The respective coating thicknesses were 3.2, 3.8, and about 5 mils. The improved protectiveness obtained by the latter technique is attributed to greater flow of the volatile silicon fluoride during deposition with coarser  $\text{Al}_2\text{O}_3$  and to healing of defects in the coating during the second coating cycle.

Failure of silicide-coated tantalum apparently occurs by oxidation of both tantalum and silicon simultaneously from the outer layer of  $\text{TaSi}_2$ . The principal scale formed is porous  $\text{Ta}_2\text{O}_5$ . Oxidation proceeds through the  $\text{TaSi}_2$  until the less oxidation-resistant lower silicides and tantalum substrate are exposed, at which time failure occurs. The microstructure of a typical sample after oxidation is shown in Figure 1. Growth of the subsilicide layer also occurs during exposure. The growth rates of this layer, which was about



500X

N77602

FIGURE 1. MICROSTRUCTURE OF SILICIDE-COATED TANTALUM  
EXPOSED IN AIR FOR 3.3 HOURS AT 2500 F

Initial coating thickness, 2.5 mils.

0.08 mil as deposited, are about  $2.9 \times 10^{-2}$  mil<sup>2</sup>/hour at 2500 F and  $1.1 \times 10^{-1}$  mil<sup>2</sup>/hour at 2700 F.

Ductility of the silicide-coated tantalum substrate is excellent at room temperature both as coated and after exposure at 2700 F. The coating itself is brittle at room temperature, having a hardness of about 1400 KHN.

#### Silicide Alloy Coatings

The protectiveness of silicide coatings on tantalum is significantly affected by alloy additions both to the coating and to the tantalum substrate. Beneficial additions include boron, manganese, vanadium, tungsten, and, to a slight extent, aluminum. The beneficial additions are characterized by their ability to flux the SiO<sub>2</sub> formed during exposure into an adherent, protective glassy oxide film.

Codeposition and two-cycle deposition of several silicide alloy coatings were studied using unalloyed tantalum substrates. Alloy coatings were applied by codeposition from packs containing silicon and aluminum (25 to 90 at. %), boron (1 to 20 at. %), chromium (25 to 75 at. %), molybdenum (20 and 33 at. %), titanium (25 to 75 at. %), and vanadium (2 to 10 at. %). In general, the results of the codeposition studies were unsatisfactory. Additions of chromium, molybdenum, titanium, and vanadium to the pack reduced the deposition rate of silicon and did not transfer to the coating in the charged ratios. Aluminum codeposited with silicon to a minor extent and tended slightly to vitrify the oxide film formed during subsequent exposure. Boron oxidized during codeposition with silicon.



Modification of the silicide coatings by alternate deposition of boron or manganese followed by silicon gave superior results. Silicon-boron coatings applied by two-cycle deposition formed glassy oxides and exhibited low weight gains during exposure. The short life of this coating at 2700 F, as seen in Table 2, is attributed to the high boron content (calculated at 79 at. %). Coatings of Si-26 at. % Mn formed glassy coatings on exposure which were protective for at least 24 hours at 2700 F. The microstructure of this coating, shown in Figure 2, shows no visible consumption of the coating by oxidation. This is in marked contrast to the oxidation of the straight TaSi<sub>2</sub> coating shown in Figure 1. The composition of this coating as well as the silicide-boride coating is amenable to modification by changing deposition conditions.

Alloy additions to the tantalum substrate also exhibit marked effects on the protectiveness of silicide and silicide-alloy coatings. Silicide-base coatings on Ta-10W and Ta-10Hf-5W alloys have given protection for up to 8 hours at 2700 F, as seen in Table 2. The aluminum-modified silicide coating appears superior to the straight silicide coating on these two alloys. The oxide films formed were thin and protective, although not as glassy as formed on the Si-B and Si-Mn coatings.

Vanadium and columbium in the tantalum substrate appear particularly beneficial in fluxing the SiO<sub>2</sub> into a protective glassy film. A binary Ta-7.5V alloy formed droplets of a black, glassy phase near the failure point, presumably a low-melting V<sub>2</sub>O<sub>5</sub>-SiO<sub>2</sub> complex oxide. The silicide-coated Ta-30Cb-5 and 10V alloys formed thin glassy oxide films and exhibited very low weight gains at 2700 F. The microstructure of

TABLE 2. SUMMARY OF SILICIDE COATINGS ON TANTALUM AND TANTALUM ALLOYS

Coating Composition, atomic per cent	Deposition Conditions (a)	Coating Thickness, mils	Protective Life At 2700 F, hr	Remarks
		<u>100Ta</u>		
100Si	Single cycle, 16 hr, 2200 F	3.2	2.7	Oxidation linear for straight silicide coatings
	Two cycles, 4 and 12 hours	3.8	5.8	
	Two cycles, coarse $Al_2O_3$	(5)	9.8	
Si-(2)Al	Two cycles, coarse $Al_2O_3$	(3)	7	---
Si-79B	Two cycles, Si over B	(4)	1.3	Glassy oxide
Si-26Mn	Two cycles, Si over Mn	9	>24	Glassy oxide
		<u>Ta-10W</u>		
100Si	Two cycles, coarse $Al_2O_3$	(4)	5.2	---
Si-(2)Al	Two cycles, coarse $Al_2O_3$	(4)	8	---
		<u>Ta-10HF-5W</u>		
100Si	Single cycle, 16 hr, 2200 F	3.3	0.6	Thin protective oxide film
Si-(2)Al	Ditto	(2.5)	6.5	
		<u>Ta-7.5V</u>		
100Si	Single cycle, 16 hr, 2200 F	(2.5)	2.8	Partly liquid oxide
		<u>Ta-30Cb-5,10V</u>		
100Si	Single cycle, 16 hr, 2200 F	3.4	>6	Very protective oxide film
Si-(2)Al	Ditto	(2.5)	>6	

(a) All coatings were deposited at 2200 F for a total of 16 hours. Two-cycle coatings were deposited in successive 4- and 12-hour cycles.



250X

N80525

FIGURE 2. MICROSTRUCTURE OF Si-26 AT. % Mn COATING ON TANTALUM AFTER EXPOSURE IN AIR FOR 24 HOURS AT 2700 F (NO FAILURE)

Initial coating thickness, 9 mils.

coated Ta-30Cb-10V after exposure is shown in Figure 3. The major result of exposure is thickening of the subsilicide layer. Macrophotographs of exposed silicide-coated tantalum and Ta-30Cb-10V alloy samples are compared in Figure 4. The exposed alloy sample exhibits only a thin, glassy oxide film, as compared to a thick  $Ta_2O_5$  scale formed on silicide-coated tantalum.

### CONCLUSIONS

The major conclusions from the current study are as follows:

1. Silicide-base coatings are quite attractive for protecting tantalum and tantalum alloys at temperatures above 2500 F. These coatings may be modified by alloying to give protection for at least 24 hours at 2700 F with no deleterious effects on the substrate. The glassy oxides formed also appear to have self-healing possibilities. The interdiffusion rates of the coating with the substrate are relatively low compared, for example, to silicide coatings on molybdenum.

2. Coatings must be tailored to the composition of alloy substrates. Additions such as vanadium, columbium, and tungsten to the substrate significantly improve the protectiveness of silicide coatings. In particular, vanadium appears especially beneficial through formation of  $V_2O_5$  which induces formation of a protective, glassy oxide film.

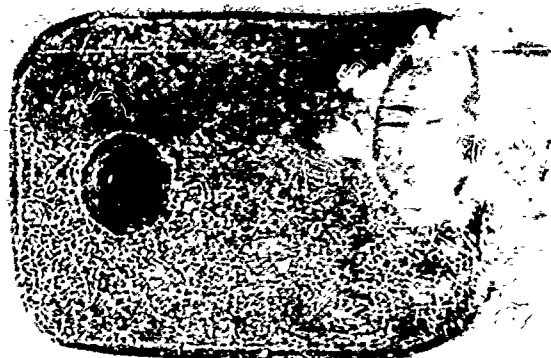


500X

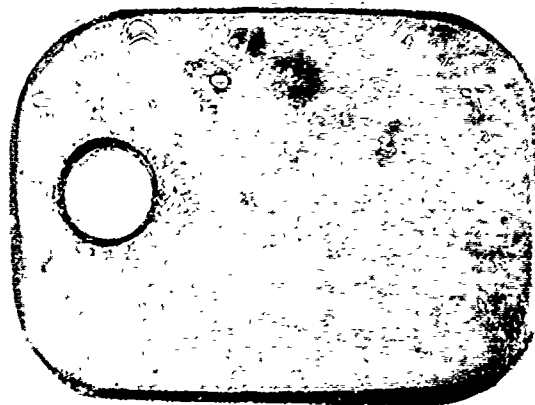
N7032

FIGURE 3. MICROSTRUCTURE OF SILICIDE-COATED Fe-30Cb-10V ALLOY AFTER EXPOSURE IN AIR FOR 7 HOURS AT 2700 F (NO FAILURE)

Initial coating thickness, about 4 mils. Coating cracked from substrate during sectioning.



4X A319  
a. Silicide-Coated Tantalum After 4.7 Hours at 2700 F



3X A189  
b. Silicide-Coated Ta-30Cb-10V After 7 Hours at 2700 F

FIGURE 4. SILICIDE-COATED TANTALUM AND SILICIDE-COATED  
Ta-30 Cb-10V AFTER EXPOSURE AT 2700 F

ACKNOWLEDGMENT

The support of the Aeronautical Systems Division of the U.S. Air Force in sponsoring this research is gratefully acknowledged.

REFERENCES

1. Sandoz, G., "Coating Columbium for High Temperatures", J. Metals, 12 (4), 340 (April, 1960).

WDK:JS  
July 17, 1961

LB-2 PROCESSING OF THE MC DONNELL  
F-48 FIN-RUDDER COMPONENTS

L. E. DOTSON

General Electric Company  
Evendale, Ohio



## Introduction

The application of the LB-2 coating to the McDonnell F-48 sub-structures and corrugated panels marks the first time the coating of such complex components has been successfully accomplished. This processing account is presented and some of the problems encountered are described.

Since the detailed processing description involves terminology and phenomena unfamiliar to most readers a brief rundown of the LB-2 coating process is first presented to clarify the actual processing procedure.

## LB-2 COATING PROCESS

The complete LB-2 process consists of (1) specimen surface preparation, (2) slurry application, (3) diffusion heat treatment, and (4) coating inspection and repair (if necessary).

### Surface Preparation

The specimen must have smooth, uncontaminated surfaces prior to coating. Sharp edges are rounded and holes are de-burred by grinding with an abrasive cone. Discolored areas, which indicate oxide film on the base metal, are also removed by grinding. In addition, subsurface oxygen contamination of the specimen surface is removed by pickling in nitric-hydrofluoric acid solution.

After pickling, thickness measurements are made at specific locations on the specimen to allow later determination of coating thickness.

Finally the specimen is prepared for coating with the two LB-2 slurries by suspending with tantalum wires or support hooks and washing with acetone to remove grease and foreign matter.

### Slurry Application

The base-coat slurry consists of 10% Cr-2% Si-Al alloy suspended in an acetone-xylene vehicle. The top coat slurry, hereafter referred to as 30 LN, consists of a Reynolds aluminum paste suspended in an acetone-xylene vehicle. Both slurries require thorough mixing before and during use to prevent the suspended alloy or metal from settling out. When the slurries are not in use the containers are tightly sealed to prevent evaporation of the solvent vehicle.

The slurries are applied to the specimen by dipping, painting, or spraying as dictated by the configuration or complexity of the part. The 30LN is more difficult to apply by painting than is the base coat. However, both slurries are easily applied by dipping or spraying. If the specimen to be coated is an assembled structure, the faying surfaces should be painted with the base coat prior to assembly.

The base coat slurry is applied to the specimen first and allowed to air dry for one hour. The 30LN slurry is then applied over the dry base coat and air dried for 2 - 24 hours.

#### Diffusion Heat Treatment

Following the air drying, the slurry coated specimen is ready for the diffusion heat treatment. The specimen is attached to a support rack which is inserted into a retort. The retort is sealed and checked for leak tightness. When leak tight, the retort is purged with purified argon by evacuating the retort and backfilling with argon. The argon is passed through a molecular sieve or silica gel dryer and a 1500°F Ti sponge train before it enters the retort.

After the retort is purged, it is placed in a cold furnace for the diffusion heat treatment cycle. Argon gas flow through the retort is maintained during the entire cycle and is exhausted through an oil seal to prevent air from backstreaming into the retort.

The temperature is increased to 500°F and maintained for 30 minutes during which time the evolution of organic material from the dried slurries begins. This phenomenon, called "boiloff", is evidenced by a dense grey smoke which issues from the retort exhaust system. After the 500°F soak, the temperature is increased to 1900°F. The "boiloff" continues until a temperature between 1000° and 1300°F is

reached. After one hour at 1900°F the retort is removed from the furnace and air cooled to room temperature.

#### Coating Inspection And Repair

After heat treatment, the coated specimen is cleaned, inspected, and repair coated if necessary.

Normally a grey-yellow residue is formed during heat treatment and is removed from exterior specimen surfaces by brushing and acetone rinsing. Interior surfaces are cleaned by gas blasting and acetone rinsing.

The cleaned specimen is remeasured and the coating thickness determined. The coating is considered adequate if the thickness increase totals 3 mils (0.003 inches) and both sides of the measured surface have a light grey appearance. Thinly coated areas have a dark blue-grey appearance and generally have a total coating thickness of 1.5 - 2.0 mils. These areas have a single intermetallic diffusion zone present whereas the standard coating has two discrete intermetallic zones. Uncoated areas present a dull, tan metallic lustre after heat treatment.

Questionable areas are ground lightly with an abrasive cone to determine if uncoated spots exist. Grinding of a normal coating or the intermetallic alone with an abrasive cone produces a shiny finish. Uncoated spots will appear dull by comparison. Uncoated areas and coated areas considered marginal with respect to oxidation resistance are repair coated. The surfaces are ground and/or pickled until visibly clean, the slurries are re-applied to the prepared areas, and the diffusion heat treatment is repeated.

The LB-2 coating protects FS-80, F-48, FS-82, F-50, and Cb-65 columbium alloys for two hours at 2500°F in static air.

This general description of the LB-2 coating process has not been directly related to the processing of a particular Cb alloy structure. Therefore the applicability of the process to complex structures is indicated by the following detailed account of the processing of the McDonnell F-48 sub-assemblies.

#### F-48 SUB-ASSEMBLY PROCESSING

The application of the LB-2 oxidation resistant coating to the McDonnell F-48 sub-structure and panels was accomplished in accordance with the previously mentioned operating steps.

- I. Pre-Coating Preparation
- II. Slurry Coating Application
- III. Diffusion Heat Treatment
- IV. Post-Coating Inspection And Repair

#### I. Pre-Coating Preparation

The pre-coating preparation involved surface preparation, mapping and measuring of all accessible surfaces, and the fixturing of each sub-assembly, i.e. fin, rudder, and panels, for coating and heat treatment.

##### Surface Preparation

To properly condition the structures and panels for coating, the surface preparations required were:

- (1) De-burring and rounding of all holes and sharp edges to insure adequate edge coatings;
- (2) The removal of all visible contamination by grinding or pickling to avoid uncoated areas;
- (3) Complete removal of all base coat slurry and foreign matter from non-faying surfaces.

All holes in the fin and rudder members were ground smooth except for those in blind areas and all sharp edges were rounded. The corrugated panels were processed in the same manner. However, some burred panel holes were inaccessible for conditioning.

All tan and/or blue discolorations were removed from the fin and rudder by grinding. Neither fin nor rudder was pickled since adequate rinsing was not possible. Discolorations and copper remaining from the spot welding operation were removed from the panels by pickling. Pickling time and solution strengths were such that 0.3 mils was the maximum reduction in sheet thickness.

Some of the sub-structures non-faying surfaces were partially covered by excess base coat slurry which was applied to the faying surfaces during fabrication. Experience has shown that the 30 LN slurry will not wet the base coat if it has dried for more than a few hours. Since some of this excess base coat was weeks old its complete removal was necessary. The fin and rudder was first wiped with dry cheese cloth and then with acetone saturated cheese cloth. In addition, the fin was sprayed thoroughly with acetone. The acetone also served to remove any grease or oil on the structure surfaces.

#### Mapping

The complexity of the sub-assemblies demanded that a map of each section be prepared to locate the various members for thickness measurements.

Both fin and rudder members were divided into ten groups. A map was made of each group and the thickness of each accessible member was measured and recorded on the map. The rudder was measured at 318 locations and the fin at 161 locations.

Seventeen of the corrugated panels were mapped and measured. The number of measurements varied from 1 - 8 for these panels depending on the individual panel construction. The remaining two panels could not be measured accurately.

### Fixturing

After mapping, each unit was attached to a holding fixture to assure safe, easy handling during the coating and heat treating operations.

The rudder trailing edge was too fragile to support the entire rudder weight. Thus the rudder was suspended by tantalum hooks and support wires as shown in Figure 1. The fin was wired into the same rack used for the rudder and being of stiffer construction rested on tantalum covered supports across the bottom of the rack. The corrugated panels were supported as shown in Figure 2. Tantalum was used exclusively for supporting all parts since it does not mar the coating in contact with it.

The fin and rudder were attached to the support rack before coating. The panels were supported after coating.

## II. Slurry Coating Application

### Rudder

The base coat was applied to the rudder with squirt bottle and paint brush in about two hours time. After a one hour drying period the base coat was inspected and all visible bare areas were spot-coated.

The 30 LN top coat could not be applied effectively by squirt bottle or paint brush due to its thixotropy (plasticity). Therefore, the bulk of the 30LN was applied to the rudder by manually operated spray gun. The entire operation required about 6 hours. Subsequent handling of the slurry coated rudder removed the 30LN from some areas. These spots were paint patched only 4 hours prior to heat treatment. Therefore 30LN drying time varied from 4 to 12 hours on the rudder.

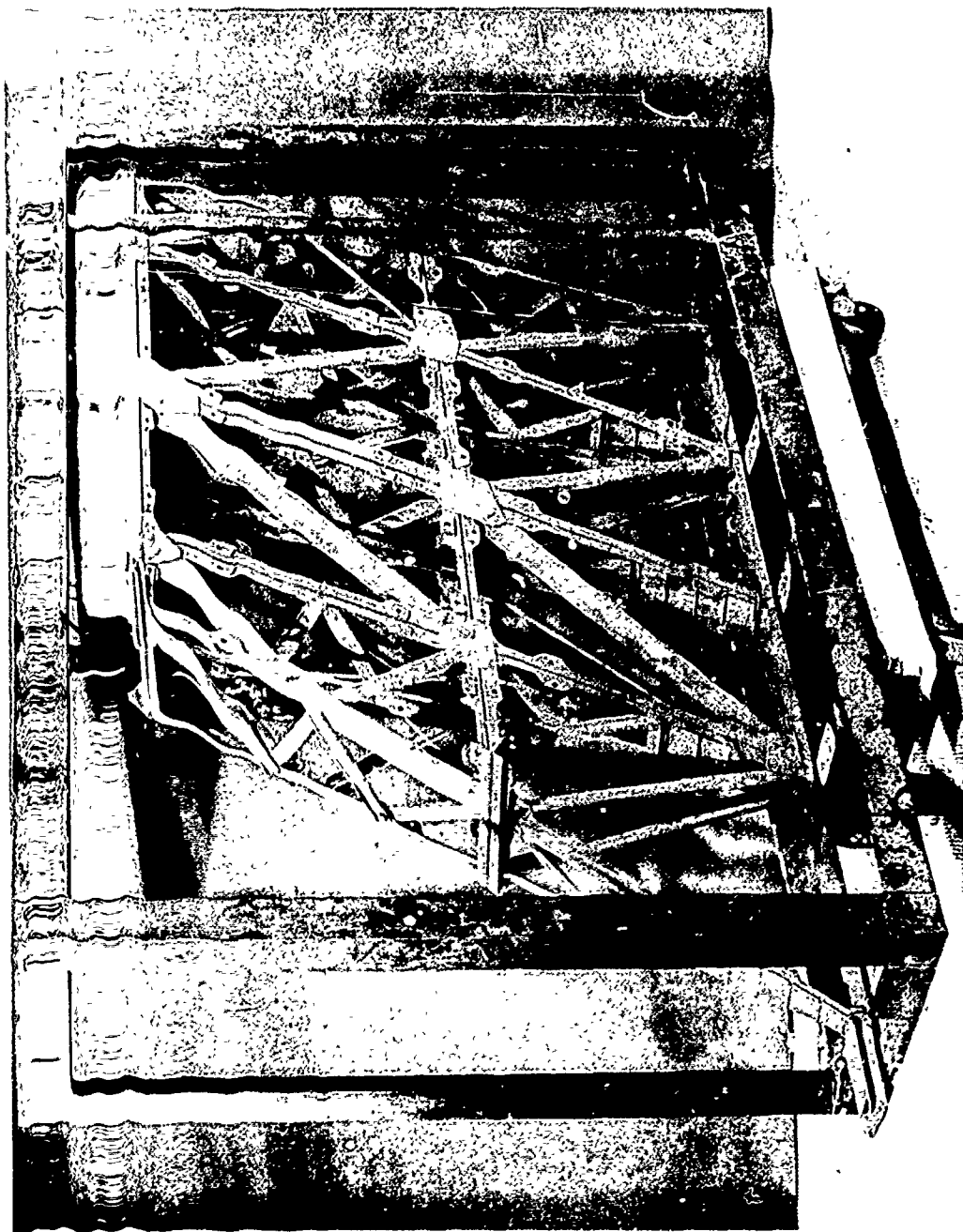


Figure 1 Columblum Alloy Rudder Sub-Assembly Coated By LB-2 Process



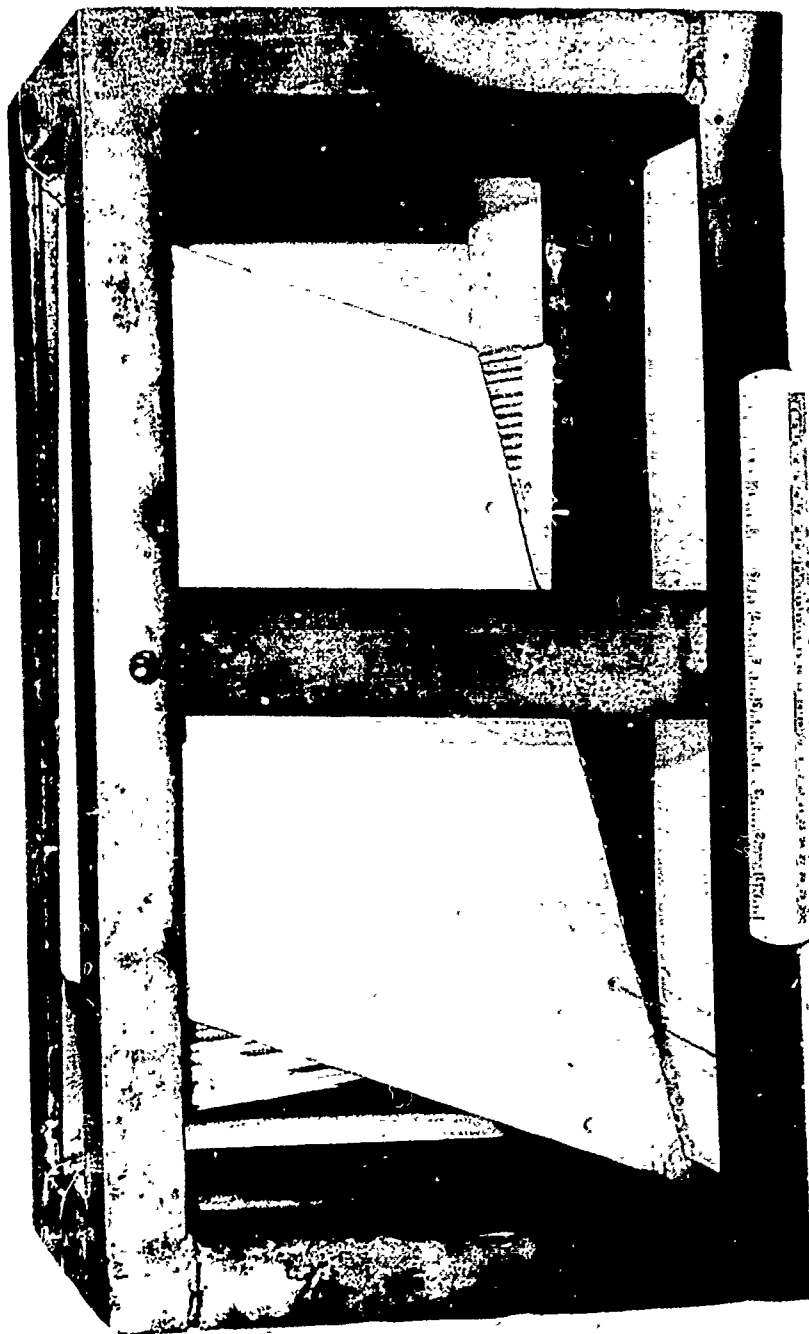


Figure 2 Slurry Coated Corrugated Panels In Support Rack

### Fin

The experience gained from coating the rudder indicated that the more complex fin should be sprayed with both slurries.

Therefore, after a thorough spraying with acetone, the fin was coated with both slurries in a paint spray booth using a standard air-operated paint spray gun. Total spraying time for both coats was about one hour. Base coat drying time was one hour while the 30 LN drying time was about 16 hours.

### Panel

The corrugated panel configuration required that a dipping or pouring method be used to obtain slurry coverage of all surfaces. Three panels were coated by pouring. The remaining 16 panels were hand-dipped.

### III. Diffusion Heat Treatment

During the LB-2 development program the heat treatments were conducted in small, easily operated equipment. The gas flow rate used was equivalent to 40 times the retort volume per hour. Retort pressure was maintained at 2 - 3 psig. The maximum surface area processed at one time was about 25 square inches - a surface area to retort volume ratio of  $150 \text{ in}^2/\text{ft}^3$ .

To duplicate these conditions in full scale equipment would have required an immense heat treatment system and a prohibitive gas consumption rate. Therefore simulated structure heat treatments were made to establish the process conditions and handling procedures necessary to permit the successful coating of the fin and rudder. The information gained from these "shakedown" runs led to the use of the equipment and process described as follows:

## Fin And Rudder

### 1. Equipment

The equipment used to accomplish the heat treatment of the fin and rudder consisted of (1) the angle iron rack shown in Figure 1, (2) the retort shown in Figure 3, (3) an argon purification system, and (4) a large General Electric box furnace.

The retort and retort lid were constructed from  $\frac{1}{2}$ " thick mild steel with peripheral braces formed from  $\frac{1}{2}$ " X 2  $\frac{1}{2}$ " angle iron. The number of welds needed to form the retort was minimized to reduce the probability of weld rupture during heat treatment. There were no horizontal corner welds. The retort inside dimensions were 15" wide, 45" high, and 65" long, the volume was 25.4 ft<sup>3</sup> and the weight was approximately 1600 pounds. The heat treat furnace was an open element electric resistance type with no atmosphere control. The furnace control calibration was Air Force certified.

### 2. Preparation For Heat Treat

The preparations required between coating and heat treatment included: (1) guying structures to rack and installing rack in retort, (2) sealing and purging retort, (3) painting retort and gas tubing. The structures were attached firmly to the rack with wires which had been attached to the structures before coating thus minimizing damage of the slurry coating during the guying operation. All areas marred during the wiring operation was patched with one or both slurries. A piece of T1 foil was attached to the rack to act as an internal getter during the heat treatment. The rack was then inserted into the retort and braced to prevent movement inside the retort. The lid was arc-welded to the retort, the retort was made leak-tight, and the air in the retort was removed

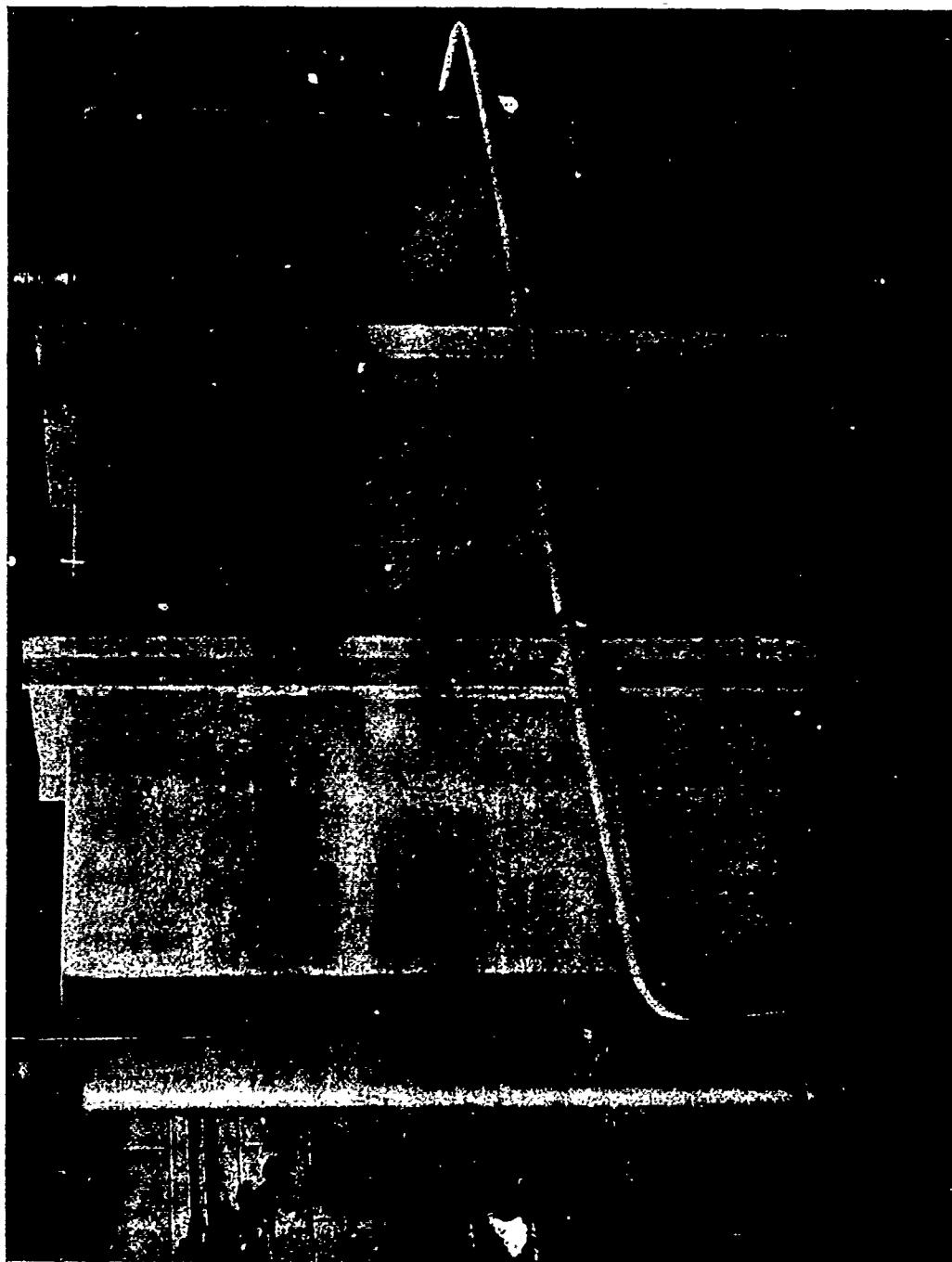


Figure 3 Retort Used For Diffusion Heat Treatment Of Fin And Rudder Sub-Assemblies.

by evacuating to 10-15" Hg absolute pressure and backfilling with argon to 1 psig three times. In addition, the retort was purged for a minimum of 30 minutes at 60 SCFH argon flow before heat treatment.

Finally, the necessary gas tubing was attached and the retort and tubing were painted with "NO-CARB"<sup>(1)</sup> to prevent decarburization and oxidation.

### 3. Diffusion Heat Treatment

The purged retort, with argon flowing through, was inserted into the furnace while the furnace temperature was 100-400°F and the diffusion heat treatment was conducted according to the standard cycle.

The temperature was increased to 500°F and held for 30 minutes. Then the temperature was increased to 1900°F at an average rate of 450°F per hour and held for 80 minutes followed by an air cool to room temperature. The additional 20 minutes at 1900°F was allowed to insure that the structure was at the 1900°F diffusion temperature for 60 minutes. The "boiloff" occurred in the 500-1300°F range and although it was quite vigorous for both fin and rudder it did not cause any noticeable pressure buildup in the retort. The argon flow was maintained at 50-60 SCFH during the entire heat treatment. The argon dewpoint was -80 to -95°F according to measurements made during the heat treatments. The argon was exhausted through an oil seal to prevent air from back streaming into the retort and to maintain a slight positive pressure in the retort.

The rudder had an estimated surface area of 5500 in<sup>2</sup> which gave a surface area to retort volume ratio of 220 in<sup>2</sup>/ft<sup>3</sup>. During LB-2 development this ratio did not exceed 150 in<sup>2</sup>/ft<sup>3</sup> and usually was much less. Surface area of the fin was not measured but was estimated to be less than that of the rudder.

---

(1) Park Chemical Company protective paint.

The NO-CARB protective paint effectively prevented scaling of the retort exterior. The retort interior was clean after each of the four sub-structure heat treatments thus indicating that a satisfactory atmosphere was maintained.

No deformation of the retort occurred until the sixth cycle when the rear end bulged slightly.

### Corrugated Panels

Processing of the corrugated panels also required a heat treatment system much larger than that used during the LB-2 development work. Again scale-up runs were made to define the equipment and process conditions required for processing the panels. The information gained from the scale-up runs is reflected in the following description of equipment and processing.

#### 1. Equipment

With the exception of one panel, which was coated during the second fin heat treatment, all corrugated panels were processed in an Inconel retort shown in Figure 4.

The retort dimensions were: 9" wide, 18" high and 52" long. The retort volume was about 5 ft<sup>3</sup>. The front lid was bolted on, gasket sealed, water cooled, and contained two thermocouple wells which ran the entire length of the retort.

The panels were supported in the angle iron rack shown in Figure 2.

The gas purification system was essentially the same as that used for the sub-structure heat treatments.

The Inconel retort was heated in a Waltz Glo-bar furnace.

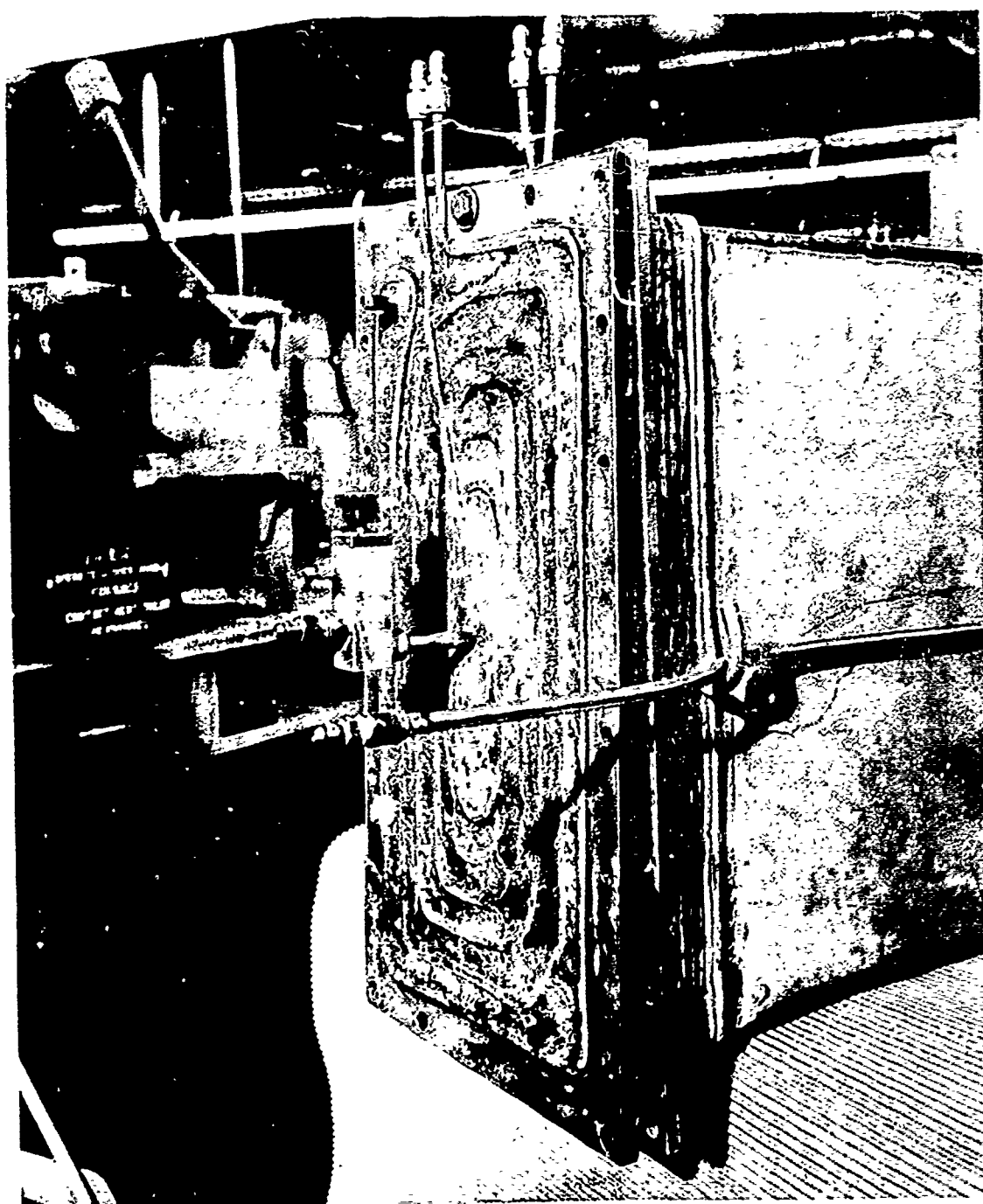


Figure 4 Inconel Retort (9" X 18" X 52")

## 2. Panel Heat Treat

The rack with slurry coated panels attached was inserted into the retort after the retort interior had been acetone cleaned. The lid was then bolted on and the retort made leak tight. The retort was purged by evacuating to 15" Hg absolute pressure and backfilling with argon three times and then inserted into the furnace. The furnace temperature was increased to 700°F in one hour. (This condition was arbitrarily chosen to replace the 1/2 hour soak at 500°F since the furnace control system did not program below 1000°F). Then the temperature was raised to 1900°F in 2 ½ hours and held for one hour.

The retort temperature actually varied from 1890-1940°F in the region where the panels were located. This temperature gradient was caused by the need for water cooling the front lid gasket. Experience had shown that no apparent change in oxidation resistance results from diffusion heat treating over this temperature range.

The argon flow rate was maintained at 15 SCFH for the panel heat treatments. The argon dewpoints varied from -90°F to -105°F during the panel heat treatments.

Panels were successfully processed in the Inconel retort with surface area to retort volume ratios up to 600 in<sup>2</sup>/ft<sup>3</sup>.

No retort surface preparation was required. Scaling of the retort exterior was negligible after more than 25 cycles.

## IV. Post Coating Examination And Repair

### Rudder

Preliminary visual inspection revealed apparently thin or uncoated areas. Subsequent measurement of these questionable areas showed the coating thickness



to be about 2.5 mils as compared to 7.6 mils average on the remainder of the rudder. Even so the thin areas did not appear to expose base metal. Intensive grinding of these areas resulted in less than one square inch of base metal being exposed out of a total rudder surface of about 5500 in<sup>2</sup>. Thus the thin areas definitely appeared to contain the protective intermetallic layer. However, this particular phenomenon had not been encountered before and to assure that the rudder would be adequately coated a series of tests were made to determine the cause of the thin areas and confirm repair capability of the LB-2 process. For these tests, the following panels were prepared:

1. Two F-48 panels were coated with 30LN only.
2. Two F-48 panels were coated with base coat only.
3. Two F-48 panels were contaminated in air at 2000°F; the contaminated surface from half of each panel was removed by grinding, the panels were then coated with both slurries.
4. Two F-48 panels contaminated by the boil-off during the rudder heat treat were ground clean and coated with both slurries.

These panels were given the normal diffusion heat treatment with the following results.(Figure 5)

1. Panels coated with 30LN only, had rough, metallic appearance and exhibited heavy edge failure after 2 hours at 24-2500°F in static air.
2. Panels coated with base coat only had the essential appearance of the thin areas on the rudder. Coating was about 1.5 mils thick. Only slight edge failure occurred after 2 hours at 24-2500°F in static air.
3. The panel which had been ground on one-half only had no coating on contaminated areas. The other half coated satisfactorily and with-



Figure 5. Test Panels Oxidized Two Hours At 24-2500°F

stood 2 hours at 24-2500°F without failure.

4. Panels which had been decontaminated by grinding coated satisfactorily and withstood the oxidation test even without edge preparation.

To test the feasibility of obtaining short time protection by the slurries without heat treatment, two panels were slurry coated and exposed to air at 2450°F. The slurry oxidized rapidly but remained intact for 15 minutes. After 25 minutes the oxide coating had spalled away from the base metal as shown in Figure 6.

From these tests the following conclusions were drawn.

1. The 30LN overcoat did not stay on the structure during the entire heat treatment in the thin areas.
2. The primary intermetallic zone is formed by the base coat.
3. Contamination, as expected, prevents the formation of a coating.
4. Grinding adequately prepares a contaminated surface for patch coating.
5. Un-heat treated slurry provides short time protection ( 15 minutes) to base metal.

Therefore all questionable areas on the rudder were thoroughly ground and the two slurries reapplied to the ground areas. The entire rudder was heat treated a second time. The patched areas gained an average of 3.4 mils additional coating i.e. from 2.8 mils to 6.2 mils average total coating. All patched areas had good coating appearance.

#### Fin

After heat treatment the fin also had some thinly coated areas. Grinding of these areas produced no base metal exposure but to assure adequate coating the fin was also patch coated. A coating increase of 2.8 mils average was obtained going from 2.5 to 5.3 mils. The average coating thickness on the fin

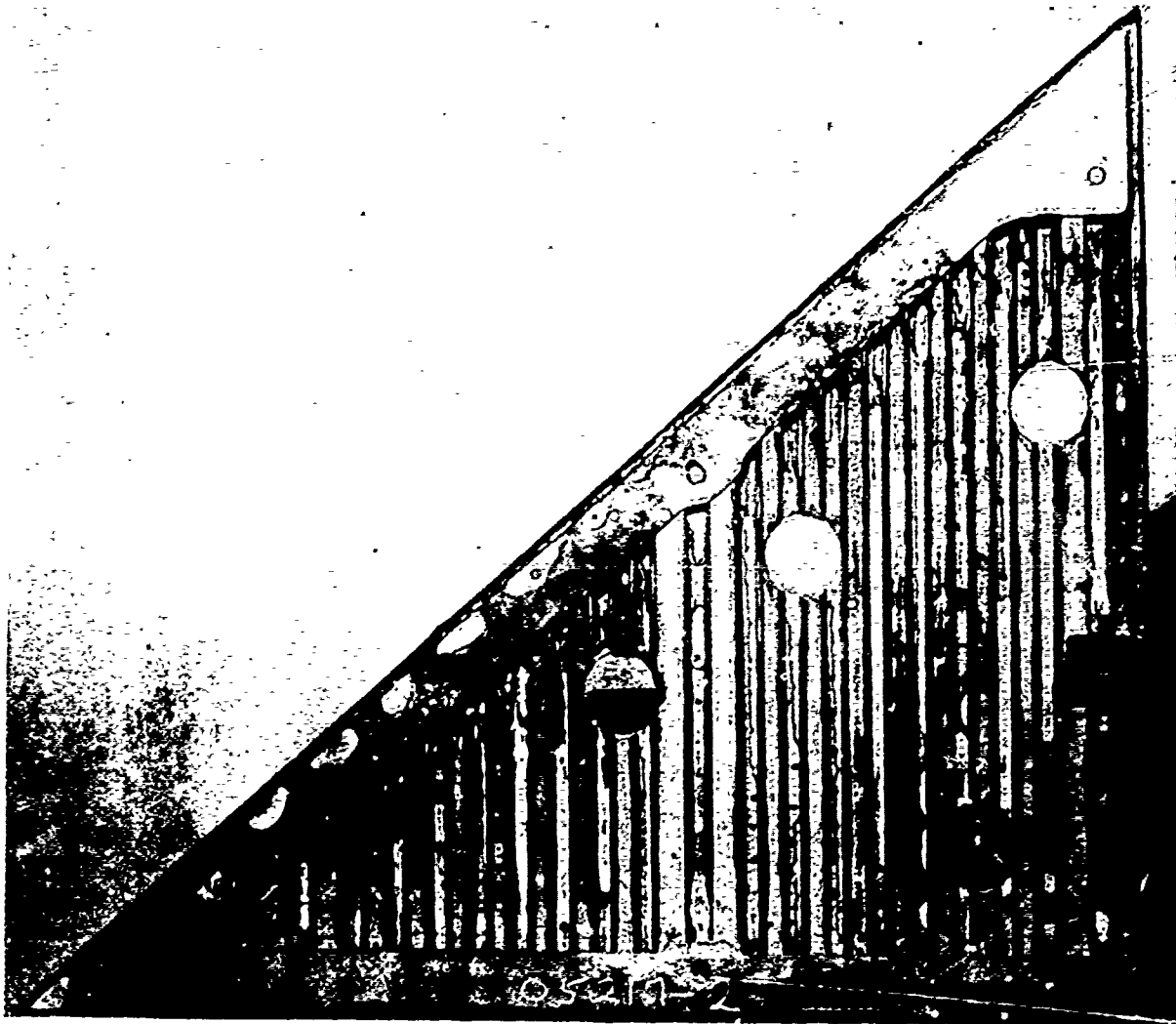


Figure 6. Coated Corrugated Panel With Uncoated Areas In Channel

was 6.1 mils which is about 1.5 mils lower than obtained on the rudder. This is believed due to the fact that spraying the 30LN top coat onto the fin produced a thinner top coat and consequently a thinner overall coating.

#### Panels

Whereas no truly uncoated spots were found on either fin or rudder, uncoated spots were found on 16 of the 19 panels processed. Figure 6 shows one of three panels which had extensive uncoated areas in the spot welded sections of the corrugations. The remaining 13 panels had uncoated spots primarily in small edge areas near 90° bends with only isolated and infrequent uncoated spots occurring in the corrugations.

All uncoated spots are believed to have resulted from contamination invisible to the naked eye yet deep enough into the base metal that the light pickle used prior to coating would not remove it.

The three panels which had extensive uncoated areas near the spot welds in the corrugations were swab pickled both inside and outside the corrugations after a light alundum grit blast, and completely recoated with both slurries to assure that no uncoated spots remained inside the corrugations. The inside surfaces of the panel corrugations were inspected visually and presented the same appearance as the outside surfaces in all cases. No uncoated spots were detected inside the corrugated surfaces.

The remaining 13 panels were processed by grinding the uncoated areas, painting the base coat on the ground areas, and coating the entire panel with 30LN slurry to avoid discoloration of the unpatched surfaces during heat treatment.

A total of 13 panel heat treatments were required. In six of these runs control panels were coated for oxidation testing. All control panels successfully withstood the standard 2 hours at 2500°F in static air -- even without edge preparation. Panel coating thickness averaged 7.9 mils in a 4-10 mil range.

CONCLUSIONS:

The foregoing discussion has shown that the LB-2 slurry coating process is readily applicable to large, complex Cb alloy structures. True, the final evaluation of the oxidation resistance of the coated fin-rudder assembly cannot be made until after the structure tests are conducted. However, past experience has shown that no LB-2 coated F-48 which had the coating thickness and appearance of the fin, rudder, and panels has ever failed during 2 hours at 2500°F in static air.

All components had average coating thicknesses well above the 1.5 mils per side considered adequate. The rudder averaged 3.8 mils per side, the fin 3.0 mils per side, and the panels 4 mils per side.

Thus it is believed that the McDonnell fin-rudder assembly has the best oxidation resistant coating obtainable from the LB-2 process at the present state of the art.

INVESTIGATION OF PROTECTIVE COATINGS FOR  
REFRACTORY METALS

J. W. HUFFMAN

M. WEISMAN

North American Aviation

Los Angeles, California

## 1. INTRODUCTION

North American Aviation, Inc. is conducting studies of hypersonic recoverable booster systems and of re-entry vehicles. In these advanced designs, it will be necessary to use refractory metals for critical structural components with operating temperatures from about 1800 F up to about 3000 F. However, the efficient use of refractory metals is conditioned upon the effectiveness of protective coatings for prevention of oxidation and gas absorption. The effective protection of mechanical joints is of particular concern since some of the refractory metals may not be readily weldable. The Los Angeles Division of North American is therefore conducting an investigation intended to determine the feasibility of protecting refractory metal structures from the effects of extreme environments. The program will also support the advanced design studies of the Space and Information Systems Division of North American. Coating systems developed by outside organizations and by North American are being studied.

## 2. EVALUATION OF COATING SYSTEMS DEVELOPED BY OUTSIDE ORGANIZATIONS

### 2.1 Screening Tests

2.1.1 Four refractory metals, along with a number of available protective coatings, were used during initial screening tests:

<u>Refractory Metal</u>	<u>No. of Coatings</u>
Molybdenum TZM	3
Columbium FS-82	3
Columbium F-48	3
Tantalum, unalloyed	2

Simple test coupons were submitted to the various suppliers for application of their protective coatings. The coated coupons were then tested by (1) a succession of 1 1/2 hour thermal cycles (each cycle including 1/2 hour at maximum temperature) in a static, sea-level air environment, at maximum temperatures up to about 3000 F, and (2) a continuous exposure to a high velocity gas stream at temperatures up to about 3000 F. Molybdenum TZM alloy with Durak coating and Columbium FS-82 alloy with LB-2 coating were selected for further testing. The selection of these metal-coating systems was based not only upon the screening test results, but also on the cost and availability of the base metals and the coatings. Some of the significant screening test results are as follows:



<u>Sample</u>	<u>Test</u>	<u>Temp. (F)</u>	<u>Results</u>
TZM/Durak	Thermal Cycle	2800	4 cycles with 1.6% weight loss. Edge and surface failure.
TZM/Durak	Erosion	3000	1.5 hr. with 0.05% weight loss. Edge failure only.
FS-82/LB-2	Thermal cycle	2600	4 cycles with 0.6% weight gain. General failure.
FS-82/LB-2	Erosion	2600	45 min. with 5.6% weight loss. Edge failure only.

2.1.2 Columbium F-48 alloy was not selected for further testing due to procurement difficulties, and tantalum due to unavailability of a suitable coating.

## 2.2 Coated Mechanical Joints

2.2.1 The effectiveness of the selected coatings for protecting mechanical joints will be determined by subjecting simple riveted lap joints, 1 1/4 in. wide, to (1) erosion in a high velocity gas stream and (2) thermal cycling, under stress, in a static sea-level air environment. The Molybdenum TZM/Durak specimens will be tested at temperatures up to about 3000 F, and the Columbium FS-82/LB-2 specimens up to about 2600 F. These temperatures were selected in accordance with the results of the screening tests. Some of the test specimens have been coated and testing has commenced. However, no test results are available at this date.

2.2.2 Following the completion of the simple riveted joint testing, a more complex specimen will be designed, fabricated, coated, and tested by thermal cycling and erosion.

2.3 Effects of High Temperature Exposure on Mechanical Properties of Coated Refractory Metals - An investigation of the deteriorating effects of high temperatures on the mechanical properties of coated refractory metals has been initiated. Tensile, creep, and riveted joint coupons of Columbium FS-82 alloy and Molybdenum TZM alloy are being prepared and coated. The tensile and

riveted joint specimens will be heated up to about 3000 F for various times and then tested for mechanical strength in comparison with unheated specimens. Creep strength, and static strength after exposure to creep conditions, will be determined. Specimens subjected to various test conditions will be examined for progressive diffusion of the coatings into the base metals. Testing has commenced but no results are available at this date.

### 3. DEVELOPMENT OF COATING SYSTEM FOR COLUMBIUM

3.1 Description - An aluminizing coating for columbium is being developed at North American and was first reported at the Fourth Meeting of the Refractory Composites Working Group. The coating slurry is composed of a mixture of aluminum and ceramic powders in an organic vehicle, and is applied by spraying, dipping, or brushing. After drying, the slurry coated parts are heated to 1900 F, in argon, for one hour. A protective columbium aluminide surface is formed by diffusion and surface reaction.

#### 3.2 Preliminary Tests

3.2.1 In preliminary oxidation testing, aluminized Columbium FS-82 alloy specimens were exposed at 2600 F for three hours in a static oxidizing atmosphere without visible harmful effects.

3.2.2 Tensile coupons of aluminized FS-82 were subjected to various elevated temperature exposures and then tested at room temperature. The tensile properties thus determined are listed below, in comparison with unheated materials:

<u>Exposure</u>		<u>Strength (KSI)</u>		<u>Elongation</u>
<u>Temp. (F)</u>	<u>Time (hr.)</u>	<u>Ultimate</u>	<u>0.2% Yield</u>	<u>(% in 2 in.)</u>
1850	1	64.9	45.0	23.5
1850 plus 2540	1 1 1/2	69.0	54.8	22.9
1850 plus 2580	1 3	74.5	62.1	25.4
(Unexposed, uncoated base metal)*		68.4	47.6	19.8
(Unexposed, coated)*		64.0	43.7	18.5

\* Control tests

The above results are preliminary in nature and represent single point data. However, the data indicated that strength has in-

creased, without attendant loss of ductility, with increasing exposure time. This apparent strengthening effect cannot be explained at this date.

### 3.3 Future Work

3.3.1 The results of the exposure tests (Section 3.2) will be verified by further investigation, and then compared with the results of similar tests of other columbium-coating systems.

3.3.2 Aluminized columbium will be tested for oxidation resistance by exposure to a high velocity gas stream and by thermal cycling in a static, sea-level air environment.

3.3.3 The capability of protecting columbium mechanical joints with the aluminizing coating will be investigated.

3.3.4 The applicability of the aluminizing coating to other metals, refractory and non-refractory, will be investigated.

RECENT DEVELOPMENT  
OF  
OXIDATION RESISTANT COATINGS AT PFAUDLER

PAO JEN CHAO  
JANEZ ZUPAN  
DAVID K. PRIEST

The Pfaudler Company  
Rochester 3, New York

## ABSTRACT

The present metallic coatings effort of Pfaudler Research is concerned with (1) advanced study of the statistically evaluated reliable and reproducible PFR-6 coating process for protection of molybdenum base alloys against oxidation at 3000°F, and (2) development of protective coatings for columbium base alloys. Production size capability and evaluation data for PFR-6, and results of oxidation resistance tests on coatings for columbium base alloys are presented and discussed.

## CONTENTS

	Page
1. Introduction . . . . .	1
2. PFR-6 Coating for Molybdenum Base Alloys . . . . .	2
3. Scale-up of the PFR-6 Coating Process . . . . .	13
4. Protective Coatings for Columbium Base Alloys . . . . .	18

## LIST OF TABLES

Table	Page
1. PFR-6 Analysis of Variance Study. Statistical Evaluation Summary of Oxyacetylene Torch Test Data . . . . .	4
2. Coating Life of PFR-6 at Several Temperatures . . . . .	5
3. Coating Life of PFR-6 at 1800°F and 2000°F . . . . .	8
4. Cumulative Oxidation Tests of PFR-6 . . . . .	9
5. Thermal Shock Tests of PFR-6 from 80°F to Test Temperature . .	10
6. Bend Ductility Test of PFR-6 Coated Mo-0.5% Ti at Low Temperature . . . . .	11
7. Post-bend Life of PFR-6 in the Oxyacetylene Torch . . . . .	12
8. Coatings for Columbium and Columbium Base Alloys . . . . .	20

## LIST OF FIGURES

Figure	Page
1. Microstructure of PFR-6 Coated Mo-0.5% Ti Specimen . . . . .	3
2. Coating Life as a Function of Coating Thickness . . . . .	6
3. Calibration Run No. 1 for Furnace No. 7 . . . . .	14
4. Thermocouple Hot Junction Location in 18.5 in. x 18.75 in. x 22.25 in. Retort . . . . .	15
5. PFR-6 Coated Nozzle Configuration. . . . .	16
6. PFR-6 Coated Electrodes for Glass Melting Furnaces . . . . .	17
7. Two-cycle Cementation Coating on C-103 Columbium Base Alloy. .	19
8. Single-cycle Cementation Coating on FS-82 Columbium Base Alloy .	19

## 1. INTRODUCTION

Many coating processes have been extensively studied in Pfaunder Research Department for the development of protective coatings for several refractory metal substrates. The best coating technique has appeared to be the pack cementation process. Three general process concepts were used in the development work associated with an oxidation resistant protective coating for molybdenum. These were: (1) Single-cycle codeposition; (2) Multicycle codeposition; and (3) Multicycle deposition.

Employing these concepts, 41 protective coatings were developed for molybdenum base alloys and were statistically evaluated for reliability and reproducibility to meet Air Force requirements. A final selection of a single-cycle codeposition coating, designated PFR-6, was made and this coating was optimized and extensively evaluated.

The columbium base alloy systems are much more complicated than those of molybdenum. However, because of some similarities in behavior between columbium and molybdenum, similar coating concepts have been applied to the development of oxidation resistant coatings for columbium base alloys. A great deal of additional basic study is being carried out in order to produce suitable protective coatings for particular columbium base alloys. Preliminary modifications of coating processes have been investigated, however, and promising results have been obtained.

## 2. PFR-6 COATING FOR MOLYBDENUM BASE ALLOYS

After a year's intensive study of coating processes and the statistical evaluation of coating properties, an outstandingly reliable and reproducible coating designated PFR-6 was achieved from 41 coating systems studied. This work was sponsored under Contract AF 33(616)-7192. The PFR-6 coating, a single-cycle codeposit, has a process time shorter than that of any coating produced by a multicycle process. Therefore, PFR-6 not only possesses desirable properties but also is economical to produce. It also allows adequate limits for process variances since time and temperature of processing are easy to control. The microstructure of PFR-6 on Mo-0.5% Ti sheet is shown in Figure 1.

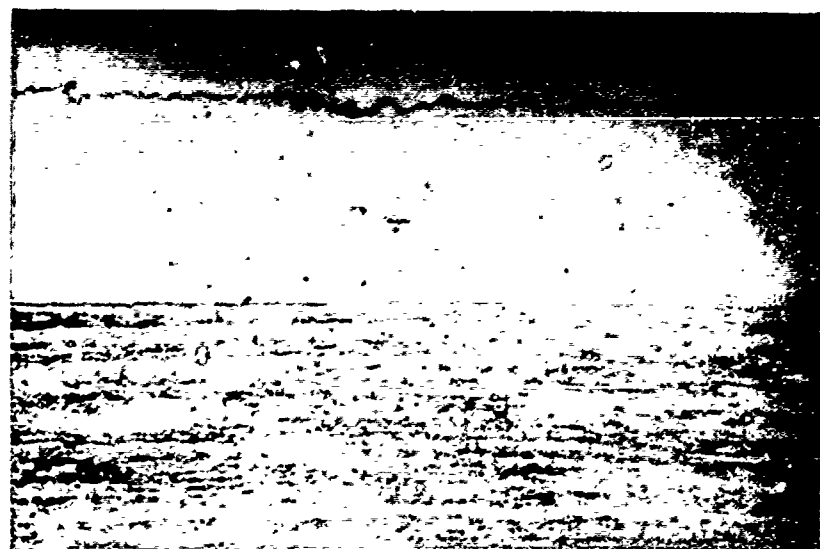
Extensive evaluation of PFR-6 has been carried out in this laboratory and by the Climax Molybdenum Company. The most important coating property to be determined is that of coating lifetime in a specific oxidizing environment. While high temperature oxidizing environments ranging from so-called static tests to plasma jet tests were considered, an oxidizing oxyacetylene torch test was selected for evaluation of PFR-6. This choice was dictated by ease of test control and calibration, availability of equipment, and the speed of testing required in evaluating large (statistically significant) numbers of samples.

A triple torch test was devised and calibrated statistically. A 22/8 flow rate ratio of oxygen to acetylene was employed, exposing the test samples to an excess oxygen flame. The data obtained from this test were treated statistically with respect to batches, operators, and torch reproducibility. On the basis of an Analysis of Variance Study (Table 1) PFR-6 has been shown to be reliable and reproducible.

While lifetime at 3000°F (optical) is relatively short (although sufficient for probable re-entry profiles), data taken in the torch environment at a series of other surface temperatures (Table 2) show that a lifetime of 10-15 hr at 2800°F may be anticipated, with correspondingly shorter lifetimes at higher temperatures. These data are averages of only three tests at each temperature and should not be considered statistically reliable.

Another parameter of importance is the influence of coating thickness on lifetime and correlation of high-temperature oxidation resistance and coating thickness for structural design purposes. Preliminary data (Figure 2) indicate that thicker coatings do result in extended life. The data shown are based on metallographic thickness measurements and oxyacetylene torch test data compiled from the optimization study of the PFR-6 coating. Few data are available for very thin coatings, however, and because of the considerable scatter of data, only a tentative conclusion should be drawn.





Iron plating

PFR-6  
coating

Substrate

FIGURE 1. Microstructure of PFR-6 coated Mo-0.5% Ti specimen. Average coating thickness is 3.8 mils. Potassium ferricyanide etch. 250X.

TABLE 1. PFR-6 ANALYSIS OF VARIANCE STUDY.

STATISTICAL EVALUATION SUMMARY OF OXYACETYLENE TORCH TEST DATA.

Variable	Average coating life at 3000° F. <sup>a, b</sup> hr	Variance, hr	Standard deviation, hr
	$\bar{X}$	$s^2$	$s$
Operator No. 1	1.32	0.067	0.258
Operator No. 2	1.38	0.163	0.403
Operator No. 3	1.41	0.169	0.410
Batch No. 1	1.37	0.099	0.315
Batch No. 2	1.47	0.113	0.336
Batch No. 3	1.37	0.104	0.322
Batch No. 4	1.34	0.167	0.408
Batch No. 5	1.26	0.099	0.315
Torch No. 1	1.58	0.159	0.394
Torch No. 2	1.27	0.068	0.261
Torch No. 3	1.21	0.075	0.273
All Samples	1.36	0.111	0.333

Calculation of confidence limit for all samples

$$\begin{aligned}
 95\% \text{ confidence limit} &= \bar{X} \pm 1.96 \sigma \\
 &= 1.361 \pm 1.96 (0.333) \\
 &= 1.361 \pm 0.653 \\
 &= 0.71 \text{ hr to } 2.01 \text{ hr}
 \end{aligned}$$

<sup>a</sup> 3000° F assuming emissivity of 1.0 (3125° F assuming emissivity of 0.8)

<sup>b</sup> Sample thermal shocked with 30 psi air blast every 0.5 hour

TABLE 2. COATING LIFE OF PFR-6 AT SEVERAL TEMPERATURES.

<u>Temperature, °F<sup>a</sup></u>	<u>Coating life, hr</u>
2800	12.5
2900	4.4
3000	---
3125	2.1
3230	0.5

<sup>a</sup>Estimated true temperature based on emissivity of 0.8.

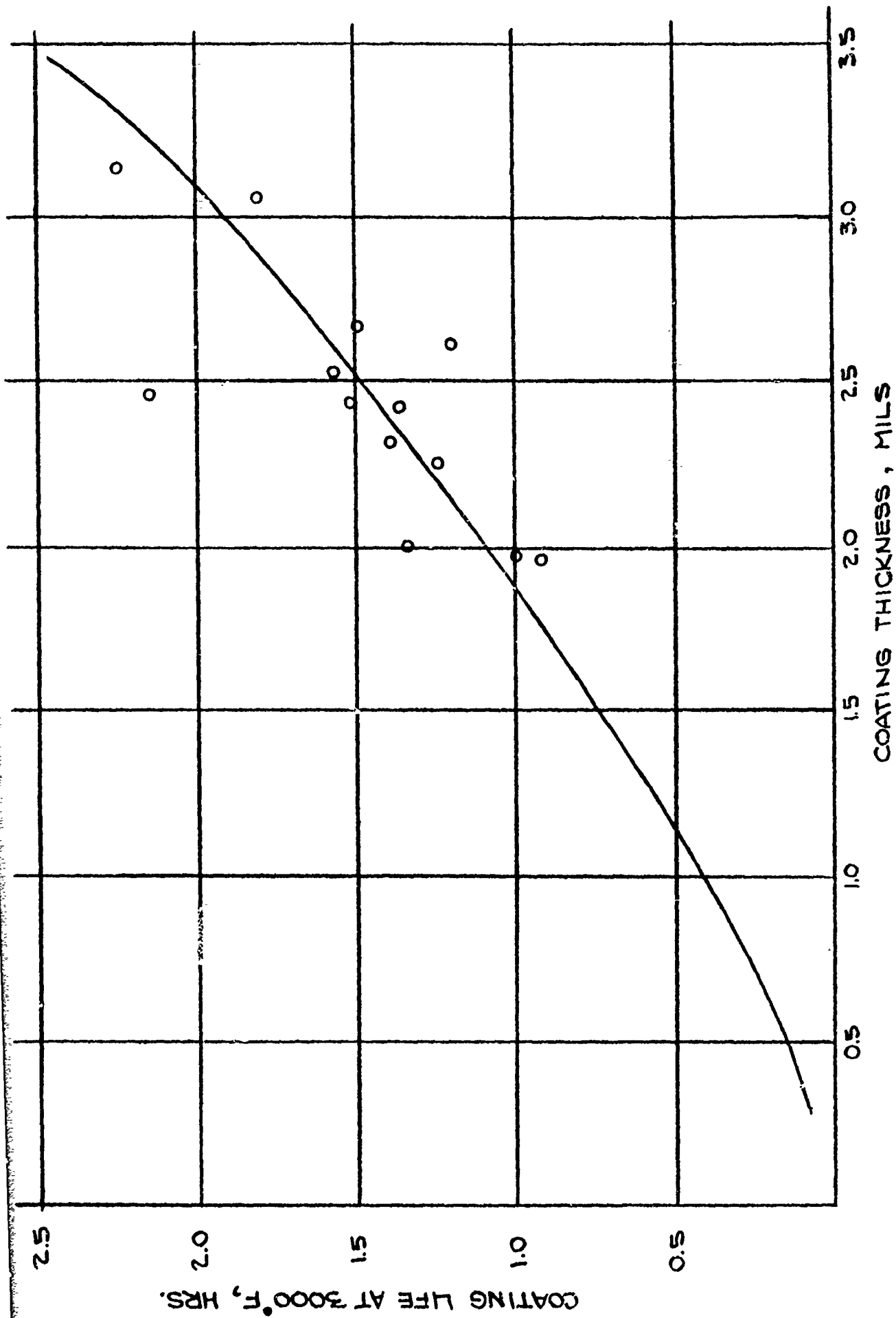


Fig. 2 Coating Life as a Function of Coating Thickness.

Long oxidation tests at 1800°F and 2000°F and cumulative oxidation testing at a series of elevated temperatures have been carried out by the Climax Molybdenum Company on PFR-6. The tests were carried out by heating each sample in a separate compartment in an electrically heated muffle furnace. Air was introduced at the rear of each compartment and was regulated to flow over the sample at a velocity of about 25 ft per min. During the test, samples were closely observed for evidence of failure indicated by evolution of molybdenum trioxide and were also inspected at intervals, at room temperature, to find visible flaws. Data obtained at 1800°F and 2000°F (Table 3) indicate that PFR-6 exhibits a life of approximately 1000 hr in this temperature range, although the reproducibility of the coating life could be improved. Within this test regime, however, minimum life was 812 hr and maximum life at least 1000 hr.

The cumulative oxidation data (Table 4) indicate that PFR-6 protects Mo-0.5% Ti substrate for time periods up to 25 hr within the temperature range 1800°F to 2600°F. As much as 6 hr of this test exposure was at 2500-2600°F. The wide variations in coating life reported at elevated temperatures are associated with a range of test temperatures. The apparent variability in lifetime would be reduced if the results could be correlated with accurate temperature determinations.

It should be pointed out that the data in Tables 3 and 4 were obtained with PFR-6 samples prepared in January 1961. Since then the reproducibility of PFR-6 has been improved.

Thermal shock tests on PFR-6 were also conducted by Climax. A specially constructed thermal shock cycle apparatus was used in which the samples were heated from 80°F to testing temperatures in 30 sec, held at testing temperature for 15 sec, then cooled to 80°F in 45 sec by air blast. Every 10 cycles the samples were allowed to cool in still air so that failures might be detected. The data developed in these tests (Table 5) indicate excellent thermal shock tests for the PFR-6 coating.

Data obtained from low temperature ductility tests (Table 6) indicate that the PFR-6 coating process does not severely impair the mechanical properties of the substrate.

In the Pfaudler Laboratory, oxidation tests were carried out on bent samples to determine the extent of damage brought about by bending. Samples were bent over a 1.5 in. radius die at 150°F prior to the oxyacetylene torch test. Since in earlier, more severe bending tests failure appeared on the concave side of the bent samples, the torch flame was directed onto the concave side of the sample for the oxidation tests. As in previous work, the 3000°F test temperature was measured by an optical pyrometer assuming an emittance of 1.0. (Assuming an emittance of 0.8, the test temperature would be 3125°F.) In addition to the Climax test results, these post-bend oxyacetylene torch test data (Table 7) indicate that the bend ductility of the PFR-6 coated Mo-0.5% Ti substrate is adequate in the working range explored.

**TABLE 3. COATING LIFE OF PFR-6 AT 1800°F and 2000°F<sup>a</sup>.**

<b>Sample No.</b>	<b>Total hours at 1800°F</b>	<b>Total hours at 2000°F</b>	<b>Remarks</b>
1	500	500	OK.
2	500	312	Failure at surface and edge.
3	500	312	Complete failure.
4	500	336	Failure at one end.
5	500	356	Failure due to small blister.
6	500	500	OK.
7	500	428	Failure at surface.
8	60	-	Coating was broken due to im- proper handling.

<sup>a</sup>Data courtesy of Climax Molybdenum Company.

TABLE 4. CUMULATIVE OXIDATION TESTS OF PFR-6<sup>a</sup>.

Sample No.	Accumulated coating life in hours at					
	1800°F	2000°F	2200°F	2400°F	2500-2600°F	2700-2900°F
9	8	4	4	4	5.5 <sup>b</sup>	-
10	8	4	4	4	6.0	5 <sup>b</sup>
11	8	4	4	4	5.5 <sup>b</sup>	-
12	8	4	4	4	6.0	5 <sup>b</sup>
13	8	4	4	4	4.0	Not completed
14	8	4	4	4	5.0	Not completed
15	8	4	4	4	5.0	Not completed
16	8	4	4	4	4.0	Not completed

<sup>a</sup>Data courtesy of Climax Molybdenum Company.

<sup>b</sup>Failed.

**TABLE 5. THERMAL SHOCK TESTS OF PFR-6 FROM 80°F TO TEST TEMPERATURE<sup>a</sup>.**

Sample No.	Thermal shock cycles		"1800°F test";	Remarks
	End A <sup>b</sup>	End B	True temp, °F	
17	500+	500+	1780-1810	OK.
18	500+	500+	1780-1810	OK.
19	500+	400	1780-1810	End B failed due to small blister.
			"2000°F test;" True temp, °F	
20	500+	500+	2000-2080	OK.
21	500+	500+	2000-2080	OK.
22	271	500+	2000-2065	End A failed with evolution of MoO <sub>3</sub>

<sup>a</sup>Data courtesy of Climax Molybdenum Company.

<sup>b</sup>The two ends of each specimen, designated "A" and "B", were tested simultaneously.



TABLE 6. BEND DUCTILITY TEST OF PFR-6 COATED Mo-0.5% Ti AT LOW TEMPERATURES<sup>a</sup>.

Condition of sample <sup>b</sup>	Temperature, °F	Bend angle degrees	Remarks
Uncoated	-80	7	Failed.
Mo-0.5% Ti	-70	6	Failed.
	-60	45	Failed.
	-20	150	Limit of fixture <sup>c</sup> .
	30	150	Limit of fixture <sup>c</sup> .
	78	150	Limit of fixture <sup>c</sup> .
As coated	78	8	Failed.
	110	20	Failed.
	120	16	Failed.
	125	35	Failed.
	130	150	Limit of fixture <sup>c</sup> .
	150	150	Limit of fixture <sup>c</sup> .
Coated samples exposed for 500 hr at 1800°F plus 25 hr at 2000°F	78	4	Failed.
	150	3	Failed.
	175	75	Failed.
	200	150	Limit of fixture <sup>c</sup> .

<sup>a</sup>Data courtesy of Climax Molybdenum Company.

<sup>b</sup>30 mil thick substrate.

<sup>c</sup>No failure.

**TABLE 7. POST-BEND LIFE OF PFR-6 IN THE OXYACETYLENE TORCH**

<u>Batch No.</u>	<u>Post-bend coating life at 3000°F, hr<sup>a</sup></u>
1	1.53
	1.43
	1.95
2	1.47
	1.57
	1.38
3	1.68
	1.85
	1.98
4	1.82
	1.57
	1.80
5	1.42
	1.98

<sup>a</sup> 3000°F assuming emissivity of 1.0 (3125°F assuming emissivity of 0.8). Sample thermal shocked with 30 psi air blast every 0.5 hr.

### 3. SCALE-UP OF THE PFR-6 COATING PROCESS

The PFR-6 coating has been shown to produce optimum protection when processing conditions are controlled over specific time and temperature ranges. These specific processing conditions, which are well established for furnaces and retorts of laboratory size, must be maintained in scale-up operation. The initial calibration of the temperature and time gradients in larger furnaces and retorts was performed in 75 KVA Globar and gas fired furnaces with retort sizes of 18.5 in. x 18.75 in. x 22.25 in. and 24 in. x 24 in. x 42 in., respectively.

A time-temperature calibration curve typical of those obtained is shown in Figure 3. These data were obtained from the thermocouple placement shown in Figure 4.\* At present, specially designed retorts are used for large structures with particular shapes. By this means temperature-time gradients can be effectively and economically controlled.

Furnaces available for metallic coating at Pfaudler range from 0.70 to 15.0 cu ft in working capacity and can handle loads to 5400 lb. However, for larger structures additional facilities and more extensive calibration of temperature-time gradients are needed to produce the PFR-6 coating.

Currently, intermediate sized objects are being coated with PFR-6. For example, a molybdenum nozzle configuration (Figure 5) 15.875 in. in maximum diameter and 14.375 in. in height has been coated. A number of molybdenum electrodes (Figure 6) have been coated also. These range from 1.5 in. to 4 in. in diameter and 14 in. to 18.875 in. in length.

Problems currently under study or to be investigated in the near future include edge and corner coverage for thin substrates, special geometry, fabricability and assembly of coated components, coating repairability, and the development of data applicable to engineering performance trade-offs.

---

\*An extensive discussion of retort calibration is contained in Pfaudler Report PF61-12, Quarterly Progress Report No. 1, covering period March 1 to June 10, 1961, for Contract AF 33(616)-8125.

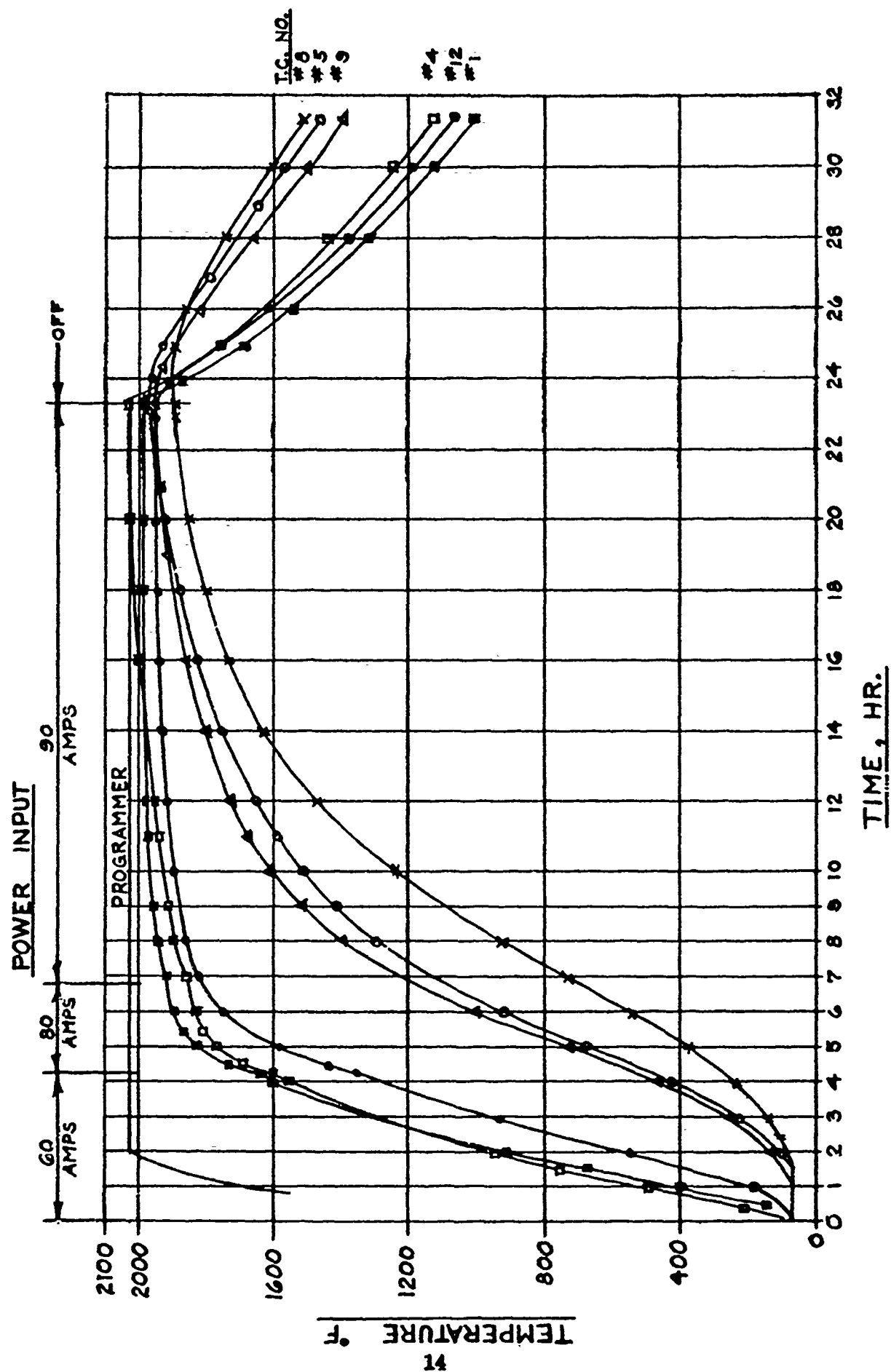
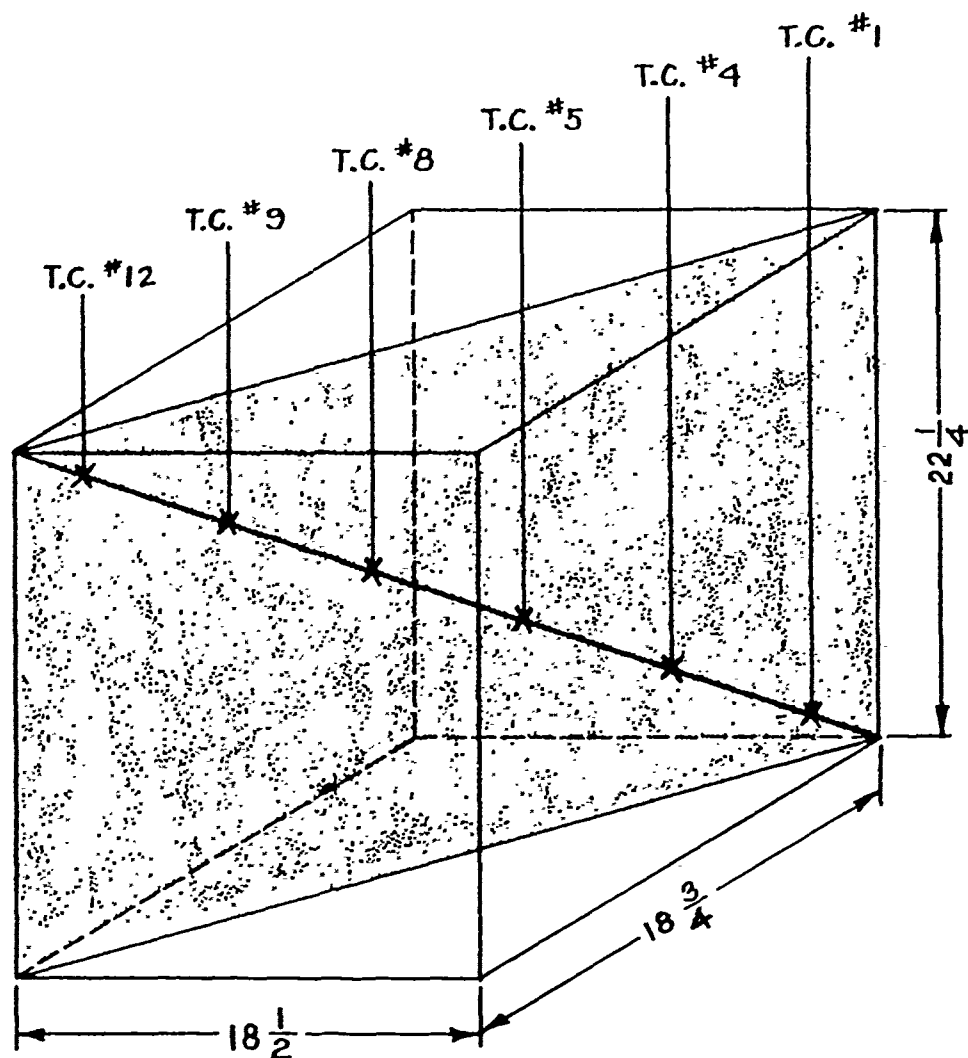


Fig. 3 - Calibration Run No. 1 for Furnace No. 7.



THERMOCOUPLE NO.	DEPTH FROM TOP SURFACE (IN.)	DISTANCE ON FACE DIAGONAL FROM CORNER (IN.)
1	20.7	2.0
4	16.9	6.5
5	13.1	11.0
8	9.3	15.5
9	5.5	20.0
12	1.7	24.5

Fig. 4 - Thermocouple Hot Junction Location in 18.5 in. x 18.75 in. x 22.25 in. Retort

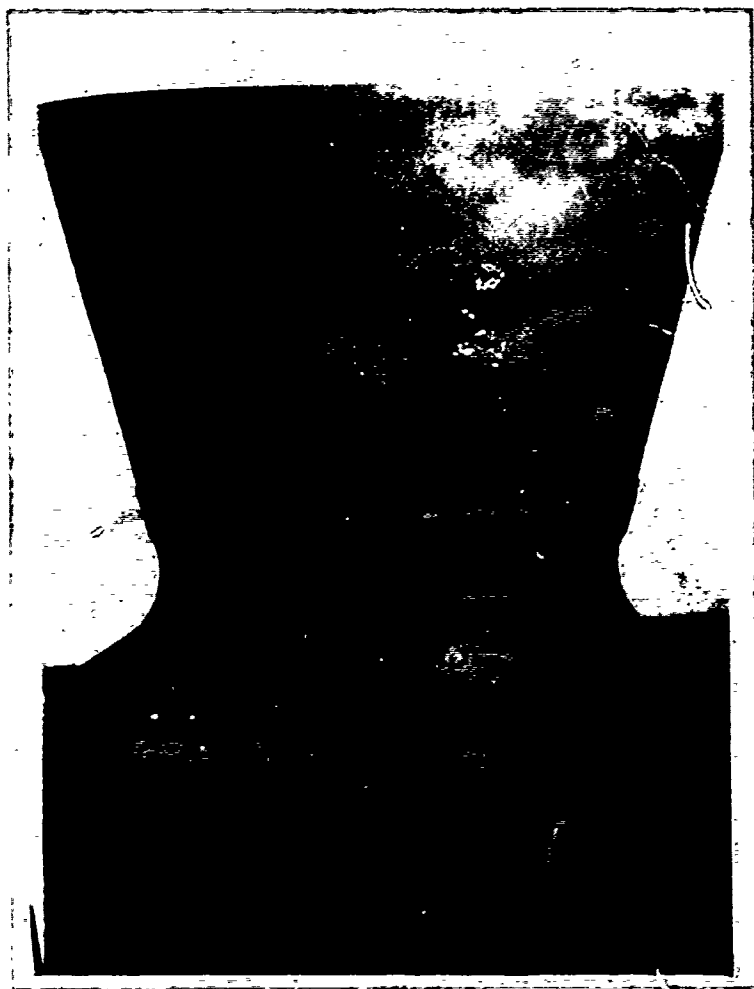


Fig. 5 PFR-6 Coated Nozzle Configuration



Fig. 6 PFR-6 Coated Electrodes for Glass Melting Furnaces

#### 4. PROTECTIVE COATINGS FOR COLUMBIUM BASE ALLOYS

The concepts employed in the pack diffusion coating processes for columbium base alloys are somewhat similar to those for molybdenum base alloys, but unique problems are presented by columbium. One of the problems considered of most importance in producing diffusion coatings on columbium base alloys is the occlusion of hydrogen by the substrate. Hydrogen is present as the reducing agent throughout the actual pack diffusion process and unless its absorption is controlled, severe embrittlement of the substrate will occur. Some attempts have been made to avoid the absorption of hydrogen by using high processing temperatures, since the occlusion of hydrogen by columbium is exothermic. Unfortunately, high processing temperatures may cause recrystallization of the columbium alloy substrates and may impair their mechanical properties. Removal of hydrogen by post-heat treatment under vacuum has also been tried. This treatment not only requires high temperatures but is dependent upon the permeability of the coatings to hydrogen. It can also cause recrystallization of the substrate.

While ammonium salts have been employed in the pack cementation processes, the use of these salts for cementation coating on columbium would introduce the problem of nitride contamination of the columbium. This, like hydrogen occlusion, must also be avoided.

Large amounts of alloying elements are needed to bring about the favorable mechanical properties of columbium base alloys. The presence of these alloyed substrates in the pack cementation process makes the process of diffusion more complex by the formation of certain materials which may not be compatible with a given coating system or technique. For example, the diffusion rate of certain elements is reduced by the presence of titanium and zirconium in the substrate. It is necessary, therefore, to design coating systems which take into account not only the presence of the columbium, but also those alloying elements present.

Solutions to these problems have been experimentally confirmed in Pfaudler Research. Following completion of experimental screening involving a number of coating compositions for columbium base alloys, two alloy coating systems have proved worthy of further investigation.

The first columbium alloy coating system which has been investigated to a moderate extent includes substrates of D-31 alloy, Cb-1% Zr alloy, F-48 alloy, C-103 alloy, FS-82 alloy, and unalloyed columbium. These are protected by a two-cycle cementation process (Figure 7). The first cycle consists of a pre-coating cementation treatment and the second cycle is a codeposition of silicon and an alloying element. Several alloy ratios have been investigated for maximizing performance. Typical lifetimes of from 7 to 18 hr are obtained when samples are tested in a dynamic oxy-acetylene torch facility at an optically measured temperature of 2600°F (Table 8). The torch facility used is identical to that employed in the research work on molybdenum. It is fully instrumented for oxygen and acetylene flow rates and it has been statistically calibrated. The flame yields an excess oxygen environment. Further work is proceeding on optimizing the performance of this coating.





Iron Electroplate

PFR-2M-C-103  
Coating

C-103 Alloy

PFR-2M-C-103  
Coating

Iron Electroplate

Figure 7. Two-cycle cementation coating on C-103 columbium base alloy.

250X

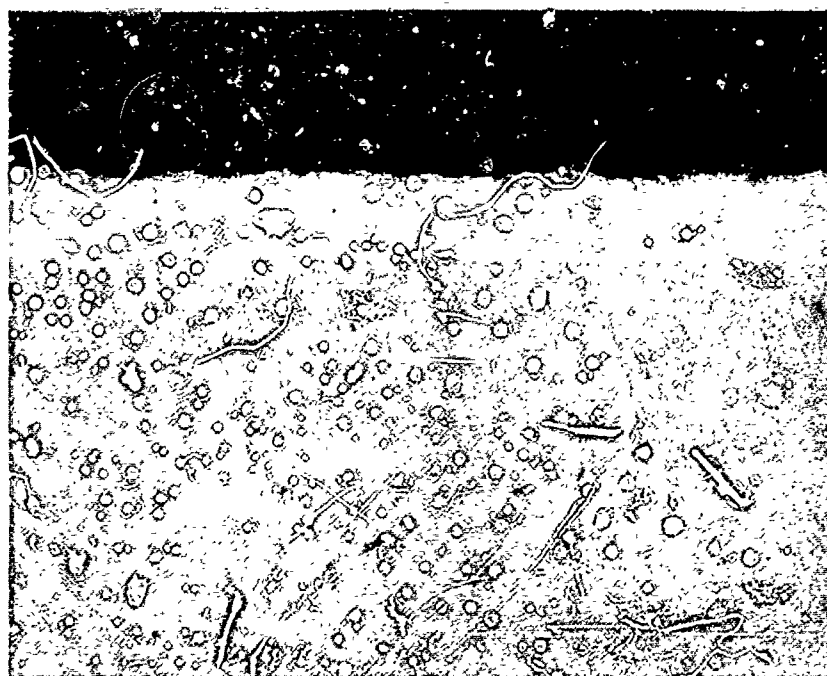


Figure 8. Single-cycle cementation coating on FS-82 columbium base alloy.

250X

TABLE 8. COATINGS FOR COLUMBIUM AND COLUMBIUM BASE ALLOYS.

Substrate	Coating Designation	Oxyacetylene Torch Oxidation Test Life		
		at 2600°F <sup>a</sup>	at 2800°F <sup>a</sup>	at 3000°F <sup>a</sup>
D-31 (2 cycles)	PFR-1A-D-31	Few min - 3 hr		
	PFR-2A-D-31	Few min - 13 hr		
	PFR-3A-D-31	5 - 28 hr		
	PFR-4A-D-31	2 - 14 hr		
	PFR-1-D-31	5 - 14 hr		
	PFR-2-D-31	15.8 hr and 15.3 hr (Two samples tested)		
	PFR-1M-D-31	16.3 hr and 26.3 hr (Two samples tested)	5 - 11 hr	2 - 4 hr
FS-82 (1 cycle)	PFR-1S-FS-82	2 - 6 hr		
FS-82 (2 cycles)	PFR-1M-FS-82	The same as above or slightly better.		0.5 - 0.75 hr
Cb-1%Zr (2 cycles)	PFR-1M-Cb-1Zr	3 - 4 hr	1 - 4 hr	0.5 - 4 hr
C-103 (2 cycles)	PFR-2M-C-103	Coated 5 mil - thick foil did not fail after 3 hr.	0.5 - 1 hr	
Cb (2 cycles)	PFR-2M-Cb	3.5 - 6 hr		0.5 - 1 hr
F-48 (2 cycles)	PFR-2M-F-48			0.25 - 1 hr

<sup>a</sup>Temperatures were measured with optical pyrometer assuming coating emittance of 1.0.

A second columbium alloy coating system involves the FS-82 substrate protected by a single-cycle alloy codeposition coating with alloying elements applied by the cementation process (Figure 8). Preliminary performance data (Table 8) indicate that lifetimes of from 4.5 to 7.5 hr at 2600°F can be obtained reproducibly. As in the previous case, evaluation was carried out in the calibrated oxyacetylene torch facility.

It should be noted again that in all of the evaluation work temperatures were measured optically and determined on the basis of a coating emittance of 1.0. It is believed that the actual emittance for these coatings is considerably less and therefore that true temperatures are higher.

PROGRESS REPORT ON PROTECTIVE COATINGS

MAURICE R. COMMANDAY

Chromizing Corporation

Hawthorne, California

## Introduction

The purpose of this report is to acquaint the Working Group with the experience level and performance background of two of our coating techniques.

## DURAK-B High Reliability Coating for Molybdenum Base Alloys

The DURAK-B Coating is a modified cementation applied silicide coating for use on molybdenum alloys.

The need for drastic improvement of disilicide coatings for the protection of molybdenum alloys against oxidation under dynamic stress and high temperature became evident to us during the early application of W-2 and DURAK coatings to various high temperature problems. Typically, simple "first generation" disilicide coatings show a wide scatter of service life and a tendency towards the development of unpredictable failures, particularly on edges and corners. In addition, we experienced cracking and gross spalling of outer coating layers on earlier coatings which, while they did not prevent the coating from meeting most of the needs prevalent at that time, certainly lowered service life, emissivity and, at least, psychologically affected confidence in the finished article.

In addition, an urgent need developed for a coating to meet the requirements of the Tory II-A Nuclear Reactor Project which involved high reliability oxidation resistance at a maximum service temperature of the order of 2000/2200°F. For reasons still obscure, we found that earlier coatings could not be depended upon in this temperature range for this application.

The DURAK-B coating was developed about year ago on a corporate funded project. Since that time, we have treated approximately 30,000 sq. in. of molybdenum alloy in sections ranging from .008" diameter wire to massive sections machined

from bar stock. We are pleased to be able to say at this time that we have yet to observe a single coating failure of any kind occurring during post treatment oxidation. In addition to the elimination of random failures, we have observed that the DURAK-B coating possesses a more consistent, even, dark color after being heated. It is interesting to note the Aerojet emissivity test data on DURAK-B which shows a total emissivity of approximately .94 at temperatures over 2600°F.

Complete freedom from the "superficial spalling" seems to be typical of DURAK-B. In addition, cracking of the external coating layers, particularly along small radii, is rarely observed on DURAK-B.

The mode of failure of DURAK-B coating is highly encouraging. This mode of failure seems to be general and time-temperature dependent, with no particular preference for edges or corners. Also, it has been observed, both here and at the Chromalloy laboratory in Nyack, that the service life scatter is greatly reduced. We recently had occasion to test a DURAK-B coating which was applied to a half dozen specimens and found that all the specimens failed within one hour of each other. There is also strong evidence that the DURAK-B coating offers about three to four times the service life of W-2 coatings of equivalent case depths. Systematic study of this is now underway.

Another advantage offered by this improved technique is the ability to coat fine wire without undue embrittlement. We have coated wire as fine as .008" diameter which repeatedly provides protection for 20 hours at 3100°F. in air.

## CONTENTS

	Page
Foreword . . . . .	ii
Introduction . . . . .	I-1
Evaluation of Coatings for Molybdenum . . . . .	II-1
High Temperature Composite Structure . . . . .	III-1
Resin-Impregnated Porous Ceramics . . . . .	IV-1



Further, DURAK-B seems to have a much greater tolerance for substrate defects than any previous coating. We were called upon to coat a number of 3" diameter wire screens. These were made up of molybdenum wires approximately .030" in diameter, woven on 1/8" centers. The cross-over shaded area between the wire strands, in effect, produces the equivalent of a controlled and reproduceable surface defect. Earlier coatings were unable to protect this shaded area, but the DURAK-B coating has consistently shown adequate protection in these critical points. In addition, we have successfully coated .008" diameter wires that were twisted around one another prior to coating. One explanation may relate to the observation that on the basis of dimensional change versus case depth measurements, DURAK-B coatings show significantly greater diffusion than do earlier coatings.

Some idea of service life of DURAK-B coated molybdenum alloy can be derived from the following data which were obtained by heating test specimens in slowly moving air with the specimens being withdrawn for cooling to room temperature at 12-hour intervals. 2000°F., no failures after 7500 hours. These tests are still in progress. 2700°F., 180 hours.

At this date, over 100 different applications have been made of the DURAK-B coating. As far as we know, all of these applications have been successful. We are unaware of a single instance where DURAK-B has failed to live up to expectations.

### DURAK-MGF Coating for Tungsten

This coating was recently applied to a welded tungsten liquid-fueled (hydrazine, nitrogen tetra-oxide) rocket motor of approximately 3/4" diameter throat. Under test, the estimated gas temperature was 4600°F. The estimated internal metal temperature was 3600°F., and the measured external metal temperature was 3100°F. An uncoated motor, after a single 80-second cycle, showed failures consisting of feather-like extrusions of tungsten, protruding out of the nozzle. The DURAK-MGF coated motor experienced two 300-second cycles. There was no failure with the exception of a minor pin hole on an external metal surface. There was no visible damage in the throat area.

RECENT INVESTIGATIONS OF  
REFRACTORY COMPOSITES

ERIC L. STRAUSS

The Martin Company  
Baltimore, Maryland

## I. INTRODUCTION

Since presenting a report<sup>(1)</sup> to the 4th Meeting of the Refractory Composites Working Group in November 1960 (which summarized Martin investigations of refractory composites during the preceding five years), The Martin Company has continued materials investigations in three distinct areas:

### 1. Evaluation of Coatings for Molybdenum

This work has been conducted under the sponsorship of the U. S. Navy, Bureau of Weapons, Contract NOW 60-0321c. The investigation was made to evaluate the performance of coatings for molybdenum under conditions, relevant to re-entry vehicle environments, that would serve to aid in the establishment of design criteria.

### 2. High Temperature Composite Structure

This work is sponsored by the Aeronautical Systems Division, Wright-Patterson Air Force Base, Ohio, under Contract AF33(616)-7497, Project No. 1368, Task No. 13719. The purpose of this program is the design, development, fabrication, test and evaluation of a nose cone-type heat shield, capable of efficient operation with surface temperatures in the range of 3000° to 4000° F. This component will be a representative structural element complete with details suitable for efficient structural use on hyperthermantic vehicles.

### 3. Resin-Impregnated Porous Ceramics

This effort involves the continuation of research, initiated by The Martin Company several years ago, to develop effective heat shield materials which will thermally protect the body of glide and lifting re-entry vehicles, without undergoing a change in shape.

---

(1) "Summary of Martin Investigations of Refractory Composites,"  
E. L. Strauss, The Martin Company, ER 11540, October 1960.

## II. EVALUATION OF COATINGS FOR MOLYBDENUM

Environmental factors affecting the performance of coated molybdenum structures include dynamic pressure airloads and resultant structural strains, temperature and time. To investigate these parameters, test conditions were selected to include:

- (1) Temperatures from 2000° F to the maximum at which the coatings afforded protection.
- (2) Pressures from 0.01 to 1 atmosphere.
- (3) Strains from 0 to 1%.
- (4) Time at temperature to 1-1/2 hr maximum.

The experimental test program was formulated on the assumption that two basic types of failure might be expected to occur in diffusion-type coatings: (1) cracking failures and (2) diffusion failures. Cracking failures are characterized by discrete separations in the coating, exposing the base metal to oxidation. This type of failure is primarily a function of temperature and strain. Diffusion failures, in contrast, are always time-dependent since, by definition, they occur as a result of gradual changes in the protective barrier as diffusion progresses.

Four coatings for Mo-0.5% Ti alloy were selected for evaluation. These included:

- (1) W-2 (Chromalloy Corp.)
- (2) Al-Si (National Research Corp.)
- (3) Al-Cr-Si (Climax Molybdenum Corp.)
- (4) GE System 300 coating (General Electric Co.).

Three types of tests were conducted:

- (1) Tensile tests, at both room and elevated temperature, to evaluate the strength and ductility of the coated material.
- (2) Strain tests to determine the deformation which the coatings could tolerate before cracking.
- (3) Oxidation tests to evaluate the effects of temperature, pressure and strain on coating life. (Coating failure was signified by the appearance of the volatile  $\text{MoO}_3$  oxide.)

The results of these studies are documented in a report <sup>(2)</sup> prepared for the U. S. Navy Bureau of Weapons.

The effect of temperature on tensile strength and ductility of coated Mo-0.5% Ti alloy is shown in Figs. II-1 and II-2. This coating drastically reduced the room temperature ductility of all samples. However, coated specimens did exhibit ductility in the temperature range of 500° to 3000° F but these tests provide no measure of coating ductility as such. Strain to coating failure tests revealed the strains which could be tolerated before cracking occurred. These strains first increased gradually with temperature, then increased abruptly as shown in the data for W-2 coating (Fig. II-3). Data obtained from the Al-Si and the Al-Cr-Si coatings suggested that they exhibit ductility at somewhat lower temperatures than the W-2 coating. However, differences observed in two lots of the same coating (Fig. II-3) were as large, in some cases, as differences among the various coatings.

Oxidation tests were conducted in the test fixture shown in Fig. II-4. Tests were set up and analyzed on a statistical basis. For the W-2 coating, tested at temperatures below 3100° F, failures did not, in general, occur within 90-min maximum exposure time employed. Tests at higher temperatures, however, revealed that temperature is a highly significant factor in the time necessary for the coating to fail. The ambient pressure did not have any measurable effect on coating life. Strain levels below those which crack the coating had no measurable effect on coating performance. Overall data for the W-2 coating suggested that strain at the 2500° to 2650° F temperature level should be limited to somewhat less than 0.5% while at 2800° F and above strains can be tolerated to at least the 1% level.

Tests on the Al-Si coating, conducted in the temperature range from 2500° to 3100° F, revealed that temperature is again the overriding factor influencing coating life (Fig. II-5). Pressure and strain did not grossly affect coating performance within the range studied. Tests conducted on the Al-Cr-Si coating, in the range of 2000° to 3100° F, gave extremely erratic results due to variations in the coated specimens. Coating failure, as revealed by the formation of the volatile molybdenum trioxide, was observed during heating to the test temperatures in numerous specimens. The GE 300 coating is a duplex coating consisting of a 5-mil chromium plate and an additional flame-sprayed layer of aluminum oxide. Tests indicated that this coating has a limited but consistent coating life to temperatures up to 3000° F, but the coating life decreases rapidly thereafter. Pressure and strain to 1% above 2800° F did not grossly

---

(2) "Evaluations for coatings for molybdenum," C. Wilkes and H. Magalotti, The Martin Company, ER 11462-6, Final Report, Contract N0w 60-0321c, June 1961.

affect coating performance.

In summary, it was concluded that the W-2 coating exhibits the best temperature capabilities with extended life to about 3000° F. The GE 300 coating has limited life at 3000° F and the temperature capabilities of the Al-Si and Al-Cr-Si coatings are still further restricted. The W-2 coating has less strain tolerance before cracking at 2500° to 2650° F than the other coatings, but exhibits adequate ductility at higher temperatures. All coatings are quite brittle at room temperature but exhibit ductility above 1600° F.

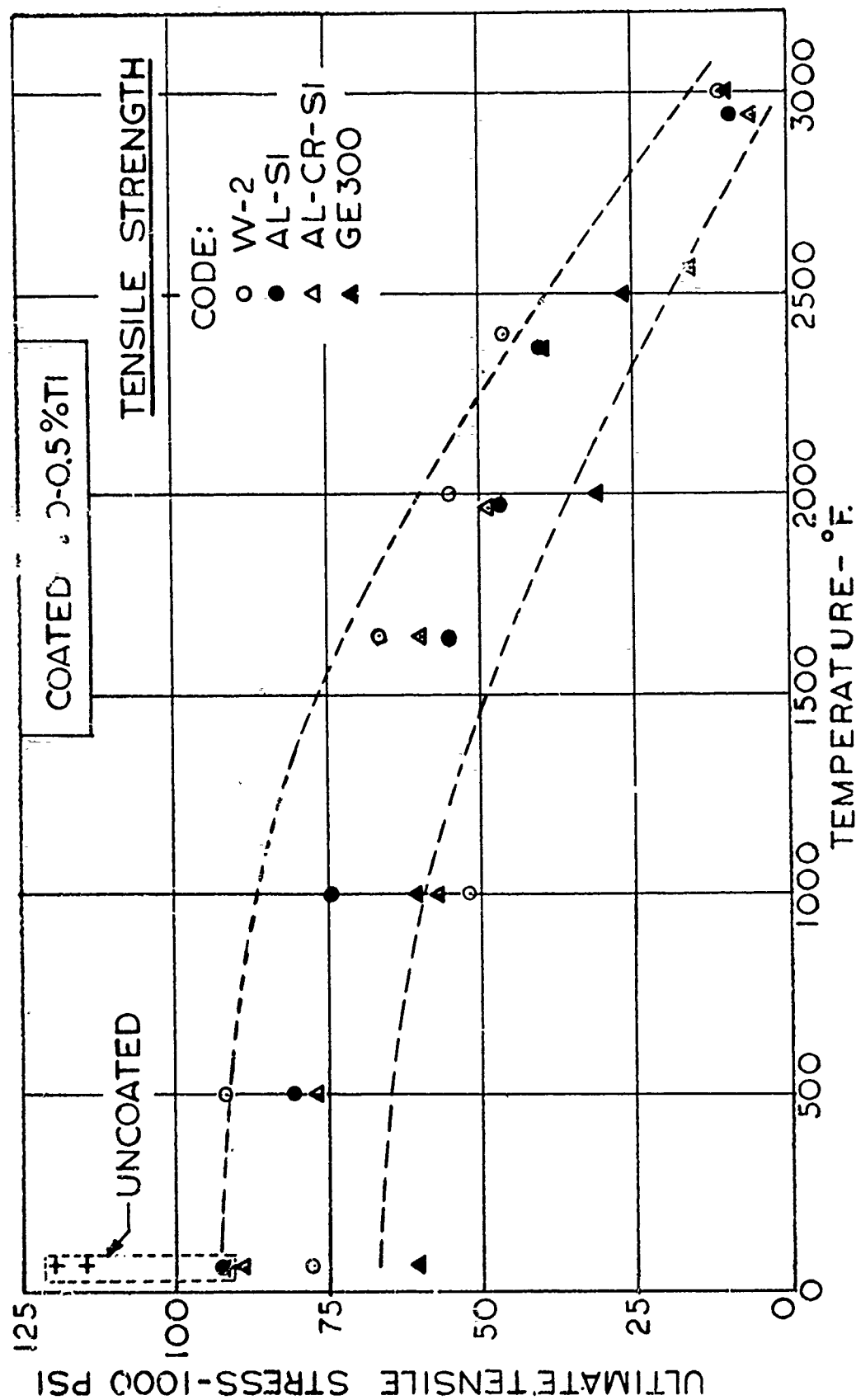


Fig. II-1. Effect of Temperature on Tensile Strength of Coated Mo-0.5% Ti Alloy



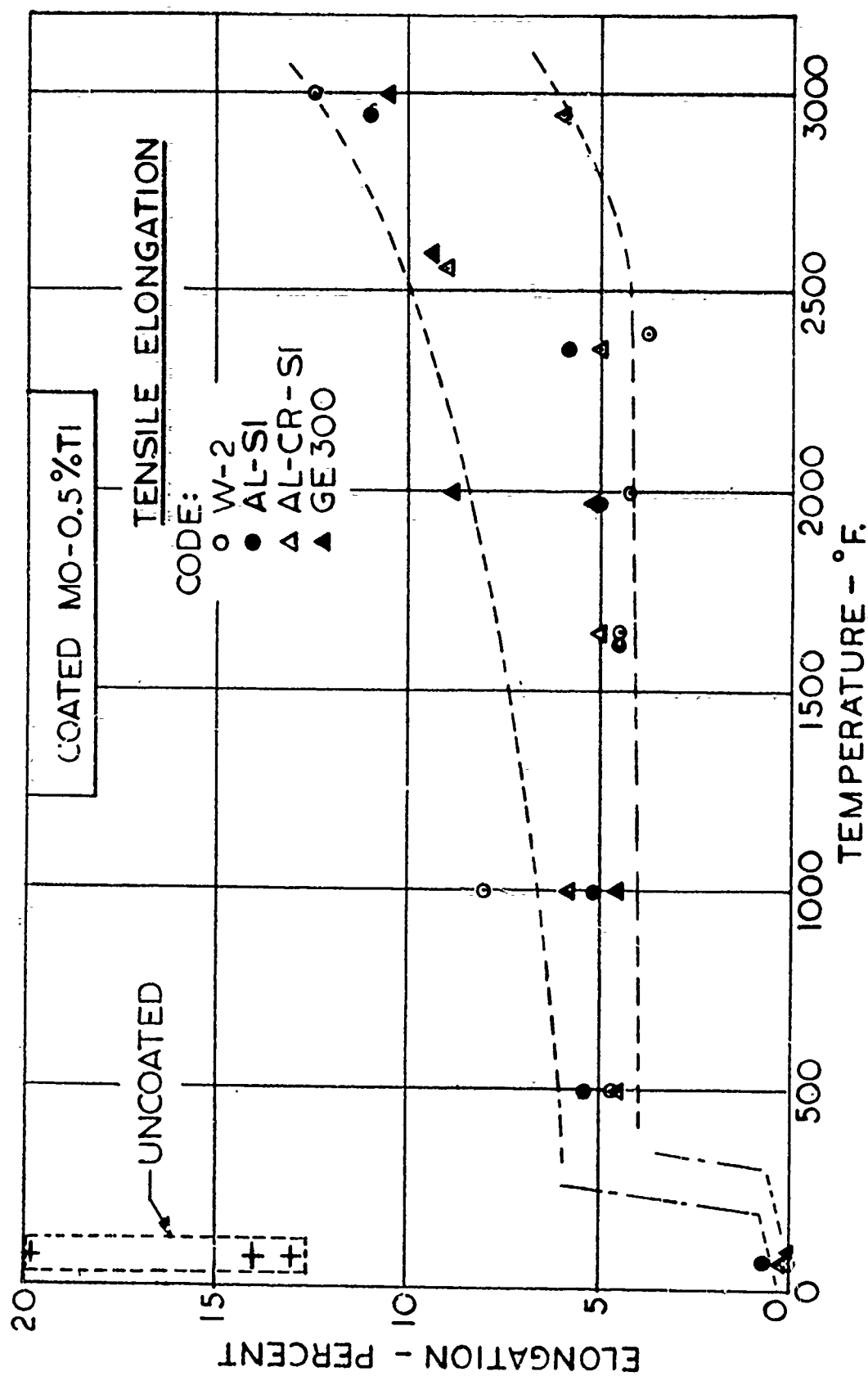


Fig. II-2. Effect of Temperature on Tensile Ductility of Coated Mo-0.5% Ti Alloy

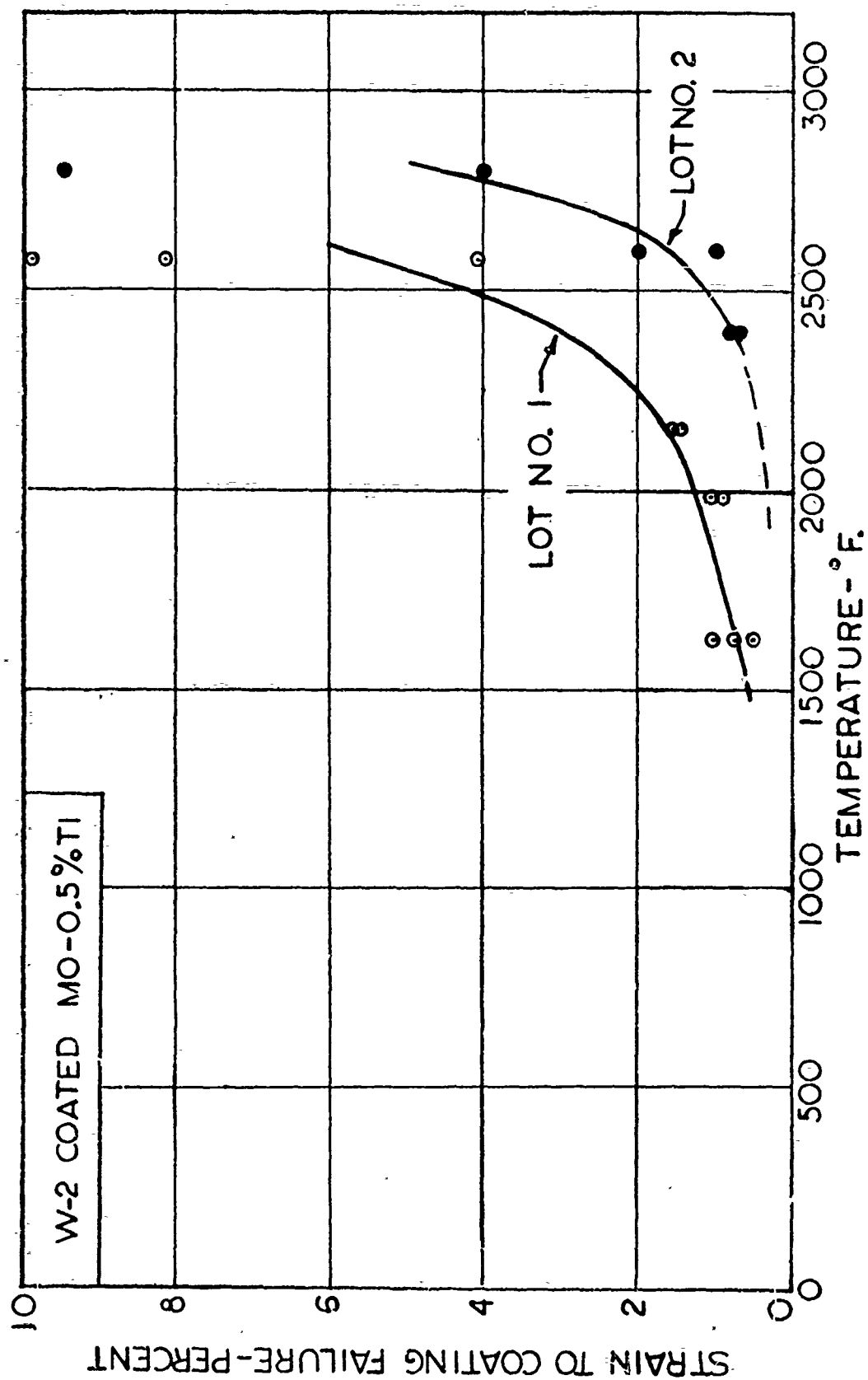


Fig. II-3. Effect of Temperature on Strain-to-Coating Failure of W-2 Coated Mo-0.5% Ti Alloy

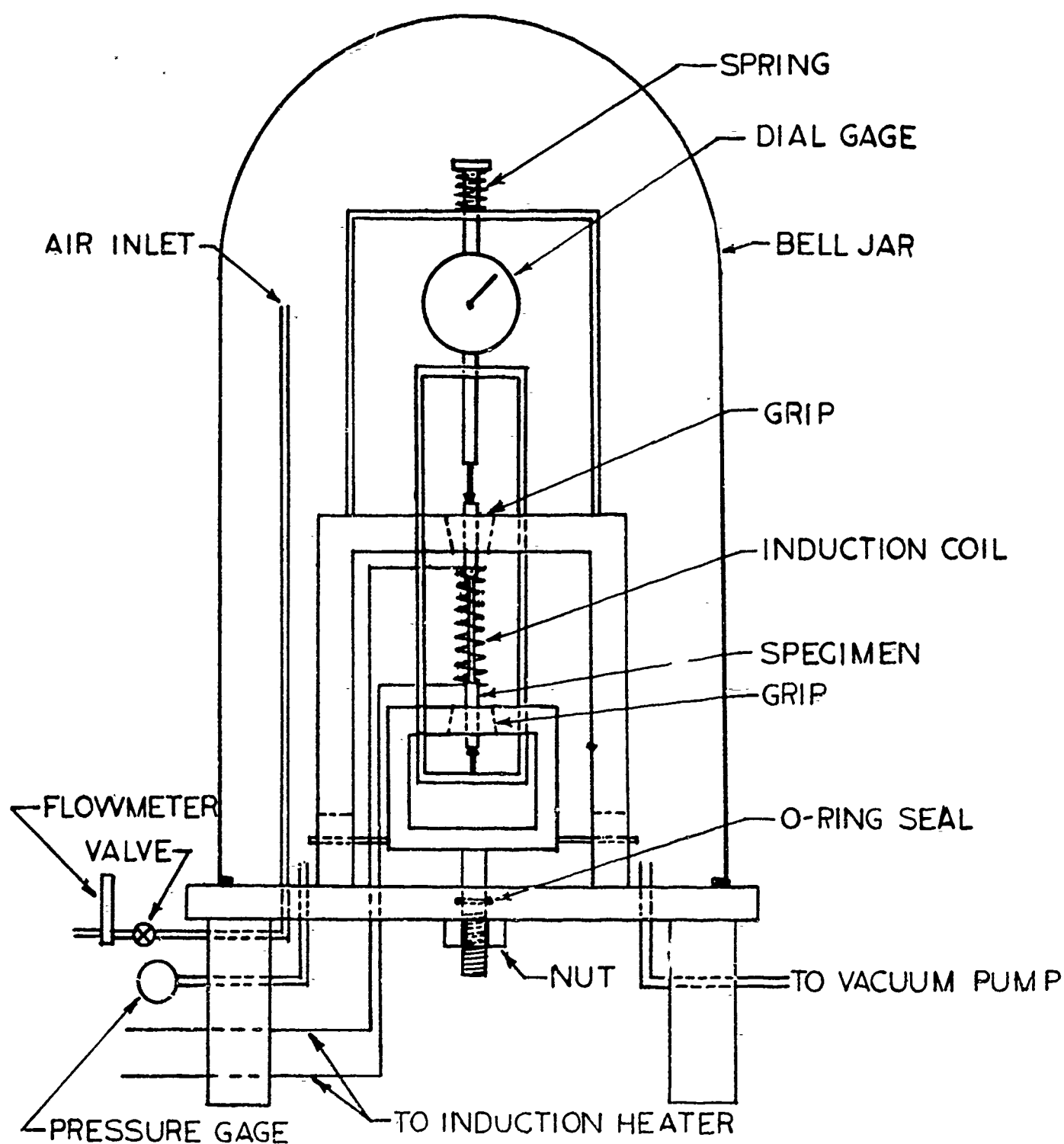


Fig. II-4. Plan View of Oxidation Test Fixture

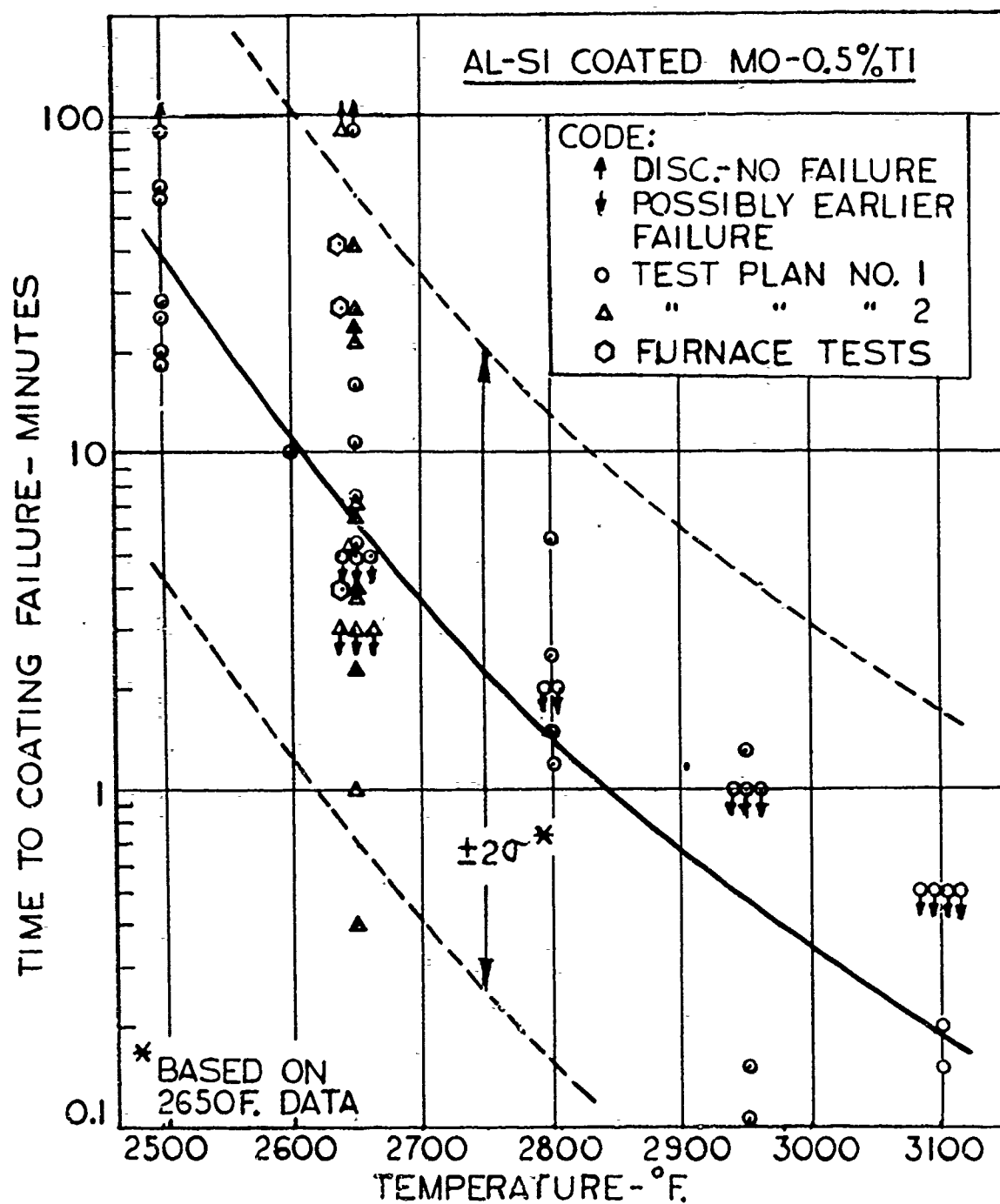


Fig. II-5. Effect of Temperature on Time-to-Coating Failure of Al-Si Coated Mo-0.5% Ti Alloy

### III. HIGH TEMPERATURE COMPOSITE STRUCTURE

The work accomplished on this program, from October 1960 through March 1961, has been reported.<sup>(3)(4)</sup> The heat shield design<sup>(5)</sup> consists of an exterior layer which sustains the high surface temperature and carries the local loads. Since this layer also induces a temperature gradient through its thickness, the temperature of the attachment to the inner surface is considerably lower than the surface temperature. This design utilizes a highly porous ceramic (such as a ceramic foam) for the outer layer material. The structure is represented by a water-cooled aluminum panel. The ceramic foam is either bonded directly to the aluminum with a silicone rubber adhesive, or it is ceramic bonded to inconel clips which, in turn, are adhesive bonded to the aluminum structure.

Tests to evaluate the chemical and dimensional stability of foamed ceramics were conducted in an arc-image furnace and a gas-fired furnace. The basic silicon carbide foam is limited to a maximum temperature of 3100° F by oxidation but when treated with zirconia it can withstand 3300° F without serious oxidation occurring. An aluminum oxide foam of 31-lb/ft<sup>3</sup> density is limited by shrinkage and by loss of strength to 3300° F maximum temperature. A zirconia foam of 45-lb/ft<sup>3</sup> density can be utilized to a temperature of 4000° F (zirconia foam experiences slight shrinkage at 4000° F).

The thermal conductivity of foamed alumina and of foamed zirconia was measured in a guarded hot plate apparatus and test points are compared with theoretically predicted thermal conductivities in Fig. III-1.

The effect of thermal strain on ceramic foam panels has been investigated both analytically and experimentally. The specimens were simply supported modules of the ceramic foam 3/4-in. thick. The test environment consisted of a linear temperature rise to the maximum

- 
- (3) "Second Quarterly Progress Report, High Temperature Composite Structure," Contract AF33(616)-7497, The Martin Company, ER 11585, January 1961.
  - (4) "Third Quarterly Progress Report, High Temperature Composite Structure," Contract AF33(616)-7497, The Martin Company, ER 11722, April 1961.
  - (5) "First Quarterly Progress Report, High Temperature Composite Structure," Contract AF33(616)-7497, The Martin Company, ER 11506, October 1960.

temperature, 5-min exposure at the maximum temperature, followed by a linear temperature drop. Some pertinent data are summarized in Table III-1. These data reveal that a 4-in. x 4-in. foamed alumina module can withstand a temperature rise rate of 30° F/sec without cracking. A 2-in. x 2-in. foamed zirconia module withstood a heating rate of 10° F/sec without cracking. However, cracking occurred at higher heating rates and also at 10° F/sec when module sizes larger than 2 in. x 2 in. were tested.

Additional tests were run in a hot gas test facility generating a steam temperature of approximately 4400° F, a dynamic pressure of 370 psf, and a sound level of 150 db.<sup>(6)</sup> Alumina samples (2 in. x 2 in.) exhibited no damage when exposed to a temperature rise rate of 8° F/sec to maximum of 3250° F. Four larger alumina panels (4-in. diameter) were tested in the hot gas environment at the above temperature conditions. Two samples withstood the test cycle without failure while the remaining two samples spalled or fractured during the cooldown portion of the test cycle. Both samples which failed were cut from the same alumina brick while the other two samples were cut from a different brick. A zirconia sample of similar diameter failed during the heatup portion of the test cycle.

On the basis of preliminary tests described, as well as quality and availability of ceramic foams, porous alumina was selected as the prime material for construction of the heat shield component. The possible use of zirconia foam will be further explored under a limited development program.

---

(6) "Fourth Quarterly Progress Report. High Temperature Composite Structure," Contract AF33(616)-7497. The Martin Company, ER 11821, July 1961.

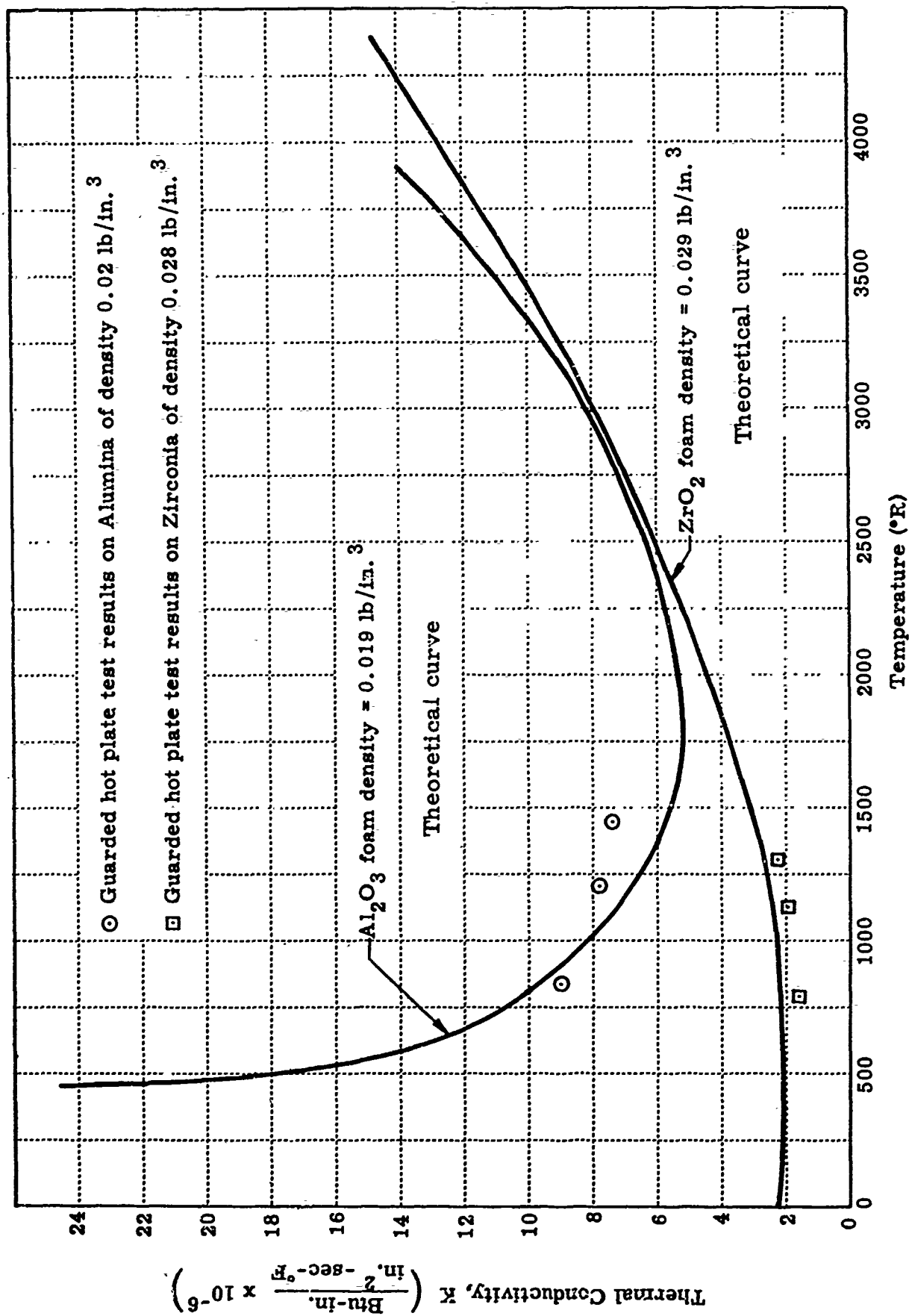


Fig. III-1. Thermal Conductivity Versus Temperature for Alumina and Zirconia Foam

TABLE III-1  
Thermal Stress Tests of Foamed Ceramics

Material	Module Size (in.)	Heating Rate (° F/sec)	Maximum Temperature (° F)	Appearance
Zirconia	3/8 x 3/6	10	2600	No effect
Zirconia	7/8 x 7/8	21	2600	Cracked
Zirconia	2 x 2	16	2650	Cracked
Zirconia	2 x 2	10	3000	No effect
Zirconia	2-1/2 x 2-1/2	10	2600	Hairline cracks
Zirconia	3 x 3	16	2650	Cracked
Zirconia with high-fired zirconia face	4 x 4	10	2800	Cracked
Alumina	4 x 4	14	2000	Good
Alumina	4 x 4	14	2850	Good
Alumina	4 x 4	30	2560	Good
Alumina	4 x 4	70	2600	Bowed
Alumina with high-fired alumina face	4 x 4	13	2680	Slight cracks



#### IV. RESIN-IMPREGNATED POROUS CERAMICS

Resin-impregnated porous ceramics are a new materials concept developed in our laboratory for application to re-entry body heat shields, and especially for thermal protection of glide and lifting body re-entry vehicles. The resin-impregnated porous ceramic is a composite material consisting of a porous ceramic matrix which is impregnated with an organic resin. It, therefore, combines the low thermal conductivity, high specific heat, and the mass transfer cooling effects of plastics with the heat resistance and thermal stability of ceramics. (7)

Tests were conducted in an oxyacetylene torch facility to measure back wall temperature rise and heat flow through resin-impregnated porous ceramics when exposed to a rectangular heating pulse. Foamed alumina, foamed zirconia and foamed silicon carbide were utilized as the ceramic matrices in these test specimens. To measure back wall temperature rise, 1-1/2-in. thick specimens (whose back faces were thermally insulated to prevent extraneous heating or cooling) were tested at cold wall heating rates of 25, 50 and 75 Btu/ft<sup>2</sup>-sec. Results of these tests (summarized in Table IV-1) reveal that heat transfer through resin-impregnated porous ceramics is fairly insensitive to heating rate. The fact that the back wall temperatures rose faster at a heat transfer rate of 50 Btu/ft<sup>2</sup>-sec than at 75 Btu/ft<sup>2</sup>-sec, can be attributed to inefficient pyrolysis of the resin at 50 Btu/ft<sup>2</sup>-sec. Thermocouples, located within the samples, established the temperature distributions through the thicknesses of resin-impregnated porous ceramics. Consequently, the temperature rise at any point below the heated surface can be calculated. This, in turn, permits a comparison of the three materials on an equal weight basis by considering the elapsed time for a 300° F temperature rise at a given weight thickness beneath the surface. Table IV-2 shows a clear superiority of alumina and zirconia over silicon carbide on an equal weight basis.

To measure heat flow through resin-impregnated porous alumina and zirconia, specimens were instrumented (with a heat sink-type

---

(7) "The Application of Resin-Impregnated Porous Ceramics to Re-entry Vehicle Heat Shields," E. L. Strauss paper prepared for the July 25 Conference on Aerodynamically Heated Structures, sponsored by the Office of Scientific Research and Arthur D. Little, Inc., June 1961.

TABLE IV-1  
Back Wall Temperature Rise of Resin-Impregnated Porous  
Cermals Exposed to an Oxyacetylene Flame  
(materials compared on an equal thickness basis)

Material	Thickness (in)	Weight (lb/ft <sup>2</sup> )	Elapsed Time for 300° F Rise on Back Face (min)	
			$\dot{q} = 25 \text{ Btu/ft}^2\text{-sec}$	$\dot{q} = 50 \text{ Btu/ft}^2\text{-sec}$
SiC and phenolic	1.5	8.75	--	4.5
Al <sub>2</sub> O <sub>3</sub> and phenolic	1.5	9.75	11.5	9.25
ZrO <sub>2</sub> and phenolic	1.5	11.25	20.9	15.4
				16.3
				5.7
				10.6

TABLE IV-2  
Back Wall Temperature Rise of Resin-Impregnated Porous Ceramics  
Exposed to an Oxyacetylene flame  
(materials compared on an equal weight basis)

Material	Thickness (in.)	Weight (lb/ft <sup>2</sup> )	Elapsed Time for 300° F Rise on Back Face (min)		
			$\dot{q} = 25 \text{ Btu/ft}^2\text{-sec}$	$\dot{q} = 50 \text{ Btu/ft}^2\text{-sec}$	$\dot{q} = 75 \text{ Btu/ft}^2\text{-sec}$
SiC and phenolic	1.50	8.75	- -	4.5	5.7
Al <sub>2</sub> O <sub>3</sub> and phenolic	1.35	8.75	10.6	8.4	9.2
ZrO <sub>2</sub> and phenolic	1.17	8.75	12.7	8.4	10.4

calorimeter attached to their back walls) and tested at a cold wall heating rate of  $75 \text{ Btu/ft}^2\text{-sec}$  in the oxyacetylene torch facility. Specimens of 1/2-in., 1-in. and 1-1/2-in. thickness were tested. Figure IV-1 shows that heat flow through the back face of these samples commences after an initial time delay and reaches a quasi-steady value. The heat transfer characteristics of resin-impregnated porous ceramics are, therefore, uniquely different from those of charring ablators (which do not tend to approach this quasi-steady value). The charring ablators are characterized by a long time delay and heat flow increases rapidly as the char line approaches the back face (Fig. IV-2). The quasi-steady heat flow rate is plotted versus heat shield weight in Fig. IV-3. This curve shows that for the particular conditions of these tests, the quasi-steady flow through resin-impregnated zirconia is 50 to 60% of the heat flow through an equal weight thickness of resin-impregnated porous alumina. The curves also show that the insulation efficiency of resin-impregnated ceramics increases with increasing heat shield weight (i. e., a threefold increase in the weight of a resin-impregnated zirconia heat shield from 4 to 12  $\text{lb/ft}^2$  reduces the quasi-steady heat flow rate by a factor of 4.25).

The oxyacetylene tests have clearly demonstrated the thermal superiority of foamed zirconia over foamed alumina and foamed silicon carbide as the ceramic matrix in resin-impregnated porous ceramics. The quasi-steady heat flow characteristics of resin-impregnated porous ceramics make these materials very suitable for heat shield applications where a "no shape change" outer insulation layer is combined with a cooled structure.

Figures IV-4 and IV-5 show some construction details for a resin-impregnated porous ceramic nose cap, which was fabricated primarily to check out manufacturing techniques and procedures for this type of construction. The completed 15-1/2-in. diameter spherical cap is shown in Fig. IV-6. The ceramic was 1-1/2-in. thick silicon carbide foam, which was impregnated with a phenolic base resin. The nose cap was assembled from 21 individual ceramic modules which are shown in Fig. IV-4. The ceramic was machined prior to resin impregnation, the outer surface was contoured to a 11-3/16-in. spherical radius, and the inner surface was contoured to a 9-11/16-in. spherical radius. The ceramic modules were then assembled on a steel shell (Fig. IV-5) and bonded in place with epoxy adhesive. The 0.040-in. wide wedge-shaped gap between adjacent modules was filled with a heat resistant filler material.

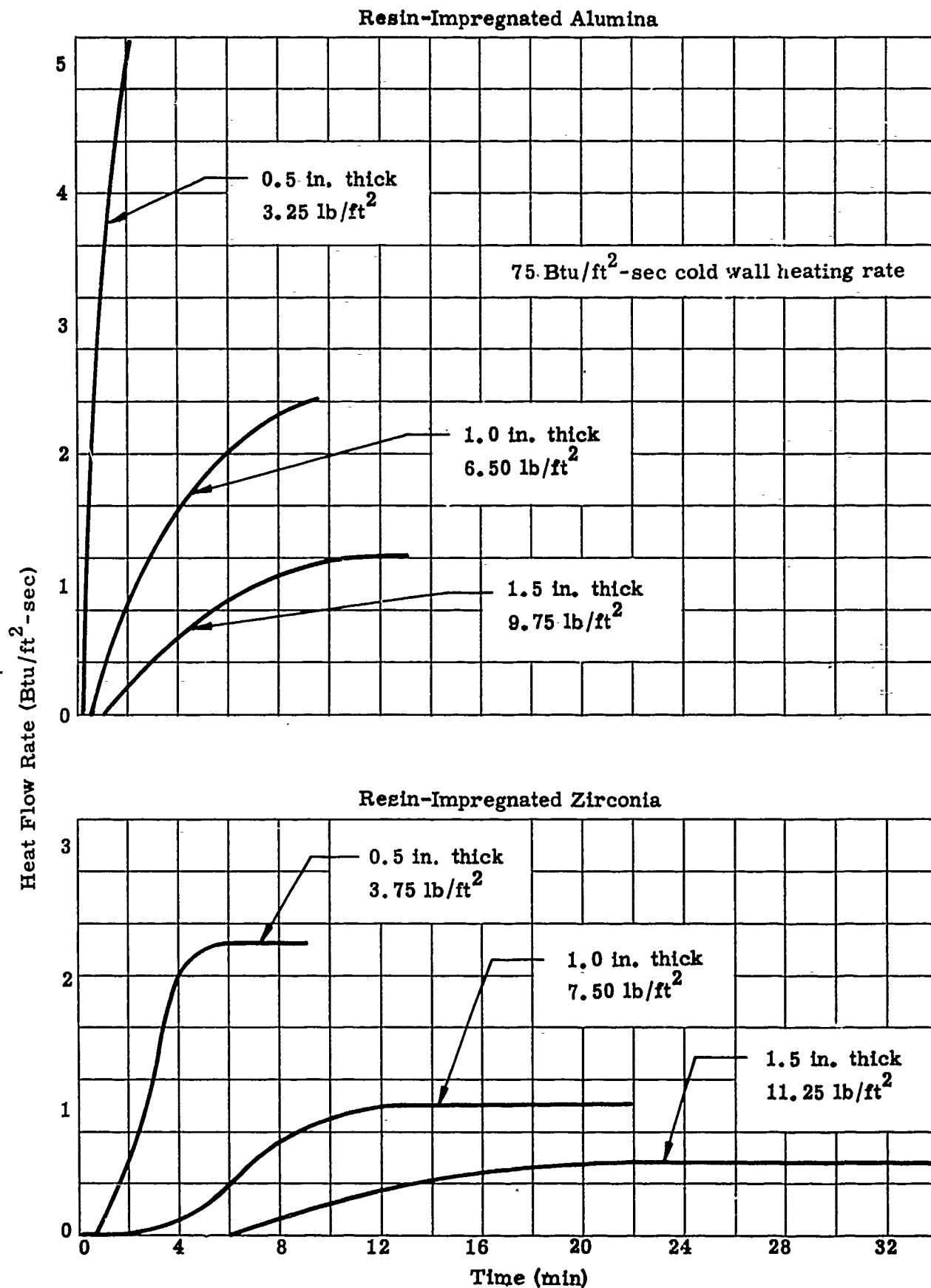


Fig. IV-1. Heat Flow Through Resin-Impregnated Porous Alumina and Zirconia Samples of Various Thicknesses

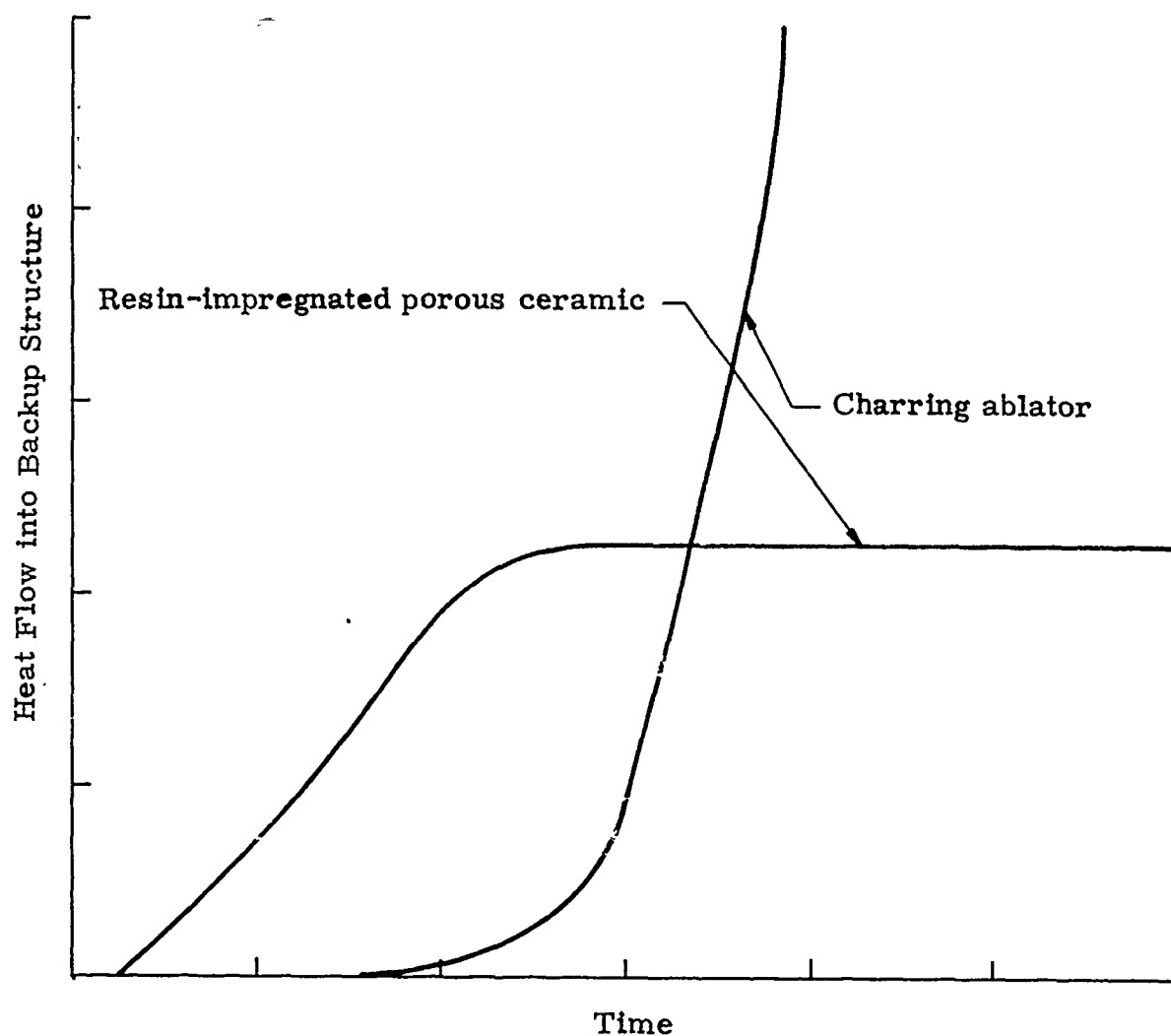


Fig. IV-2. Comparative Heat Transfer Characteristics of Resin-Impregnated Porous Ceramics and Charring Ablators

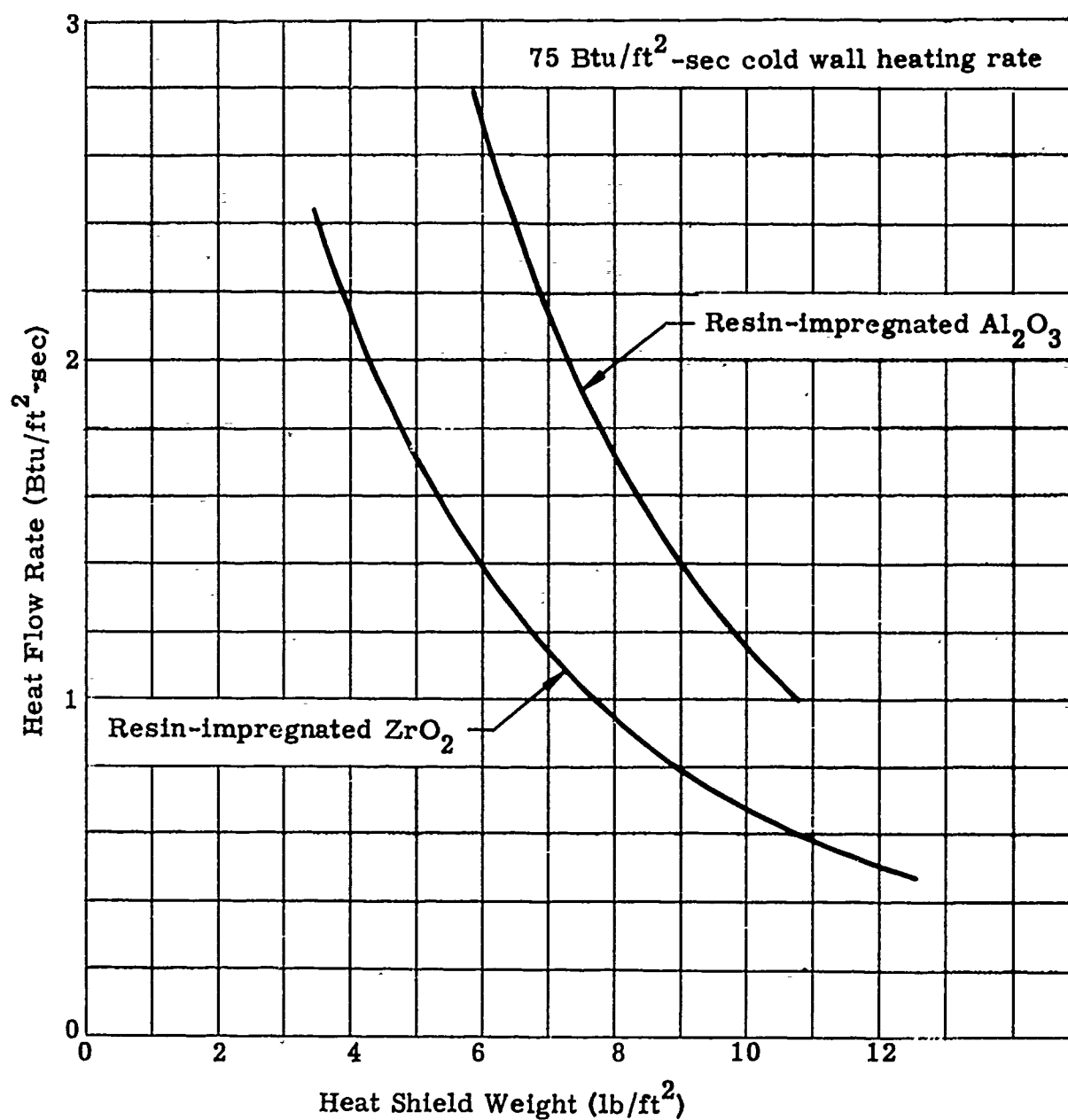


Fig. IV-3. Quasi-Steady Heat Flow Rate Through Resin-Impregnated Porous Ceramics

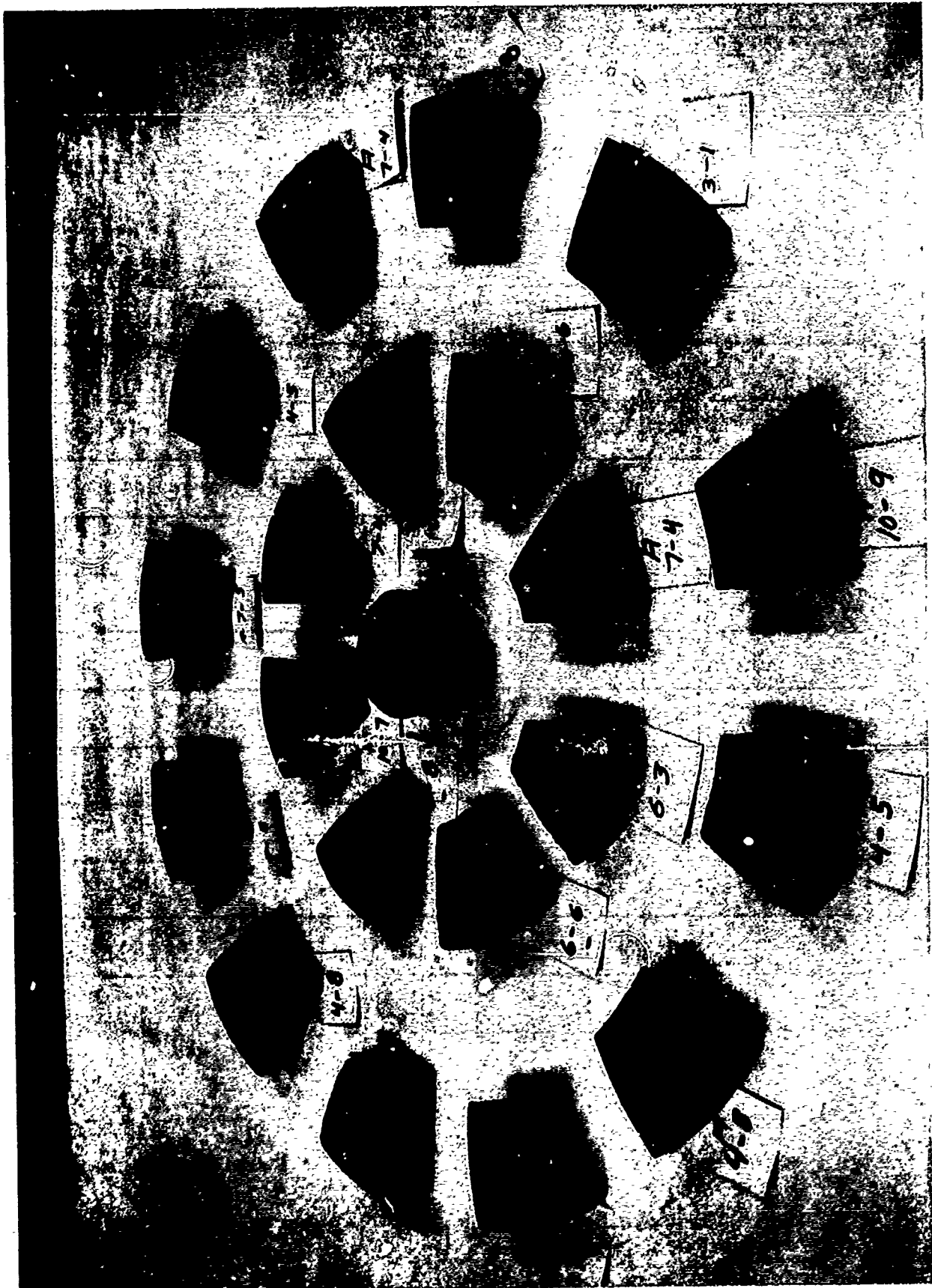


Fig. IV-4. Impregnated Ceramic Modules for Nose Cap



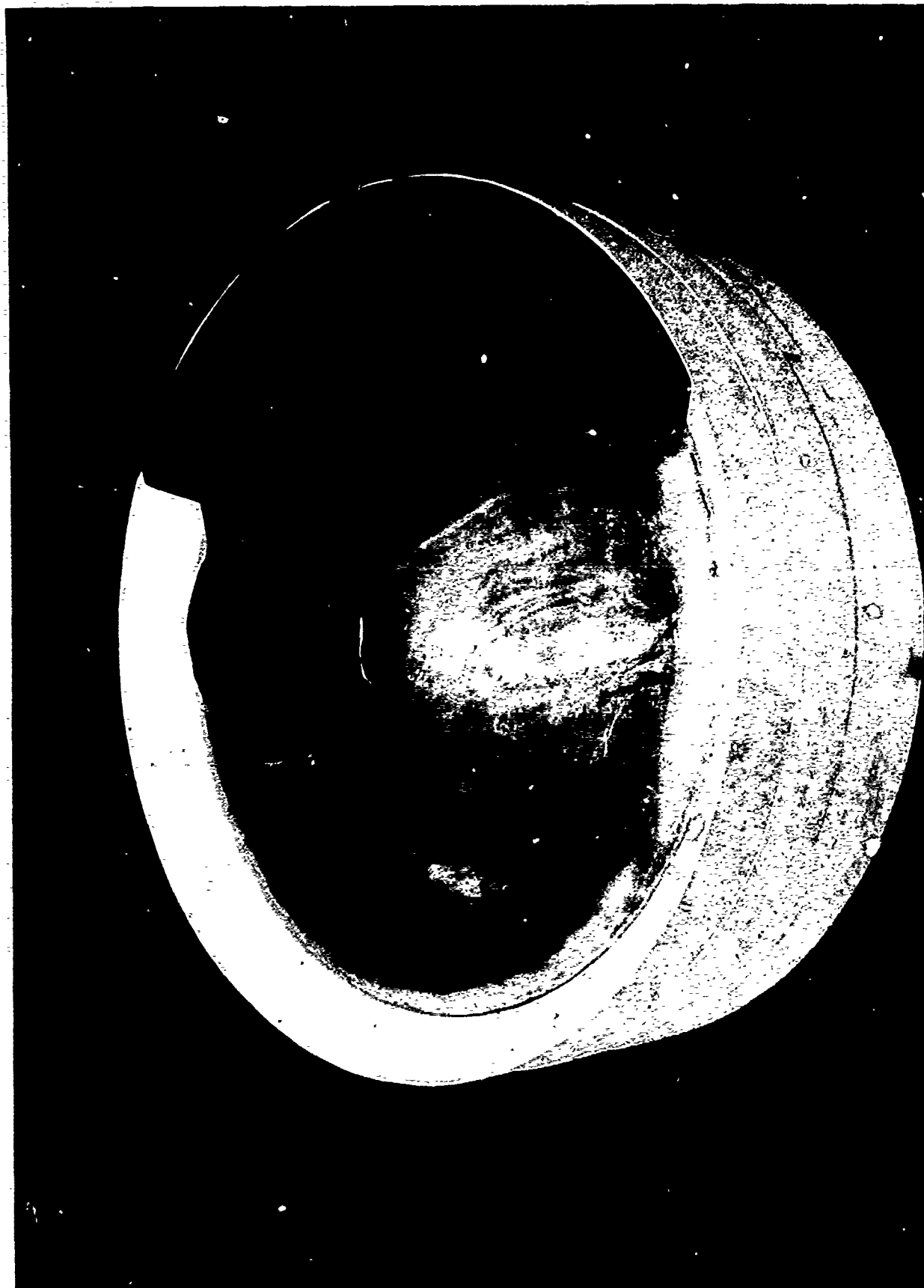


Fig. IV-5. Ceramic Modules Assembled on Backup Structure

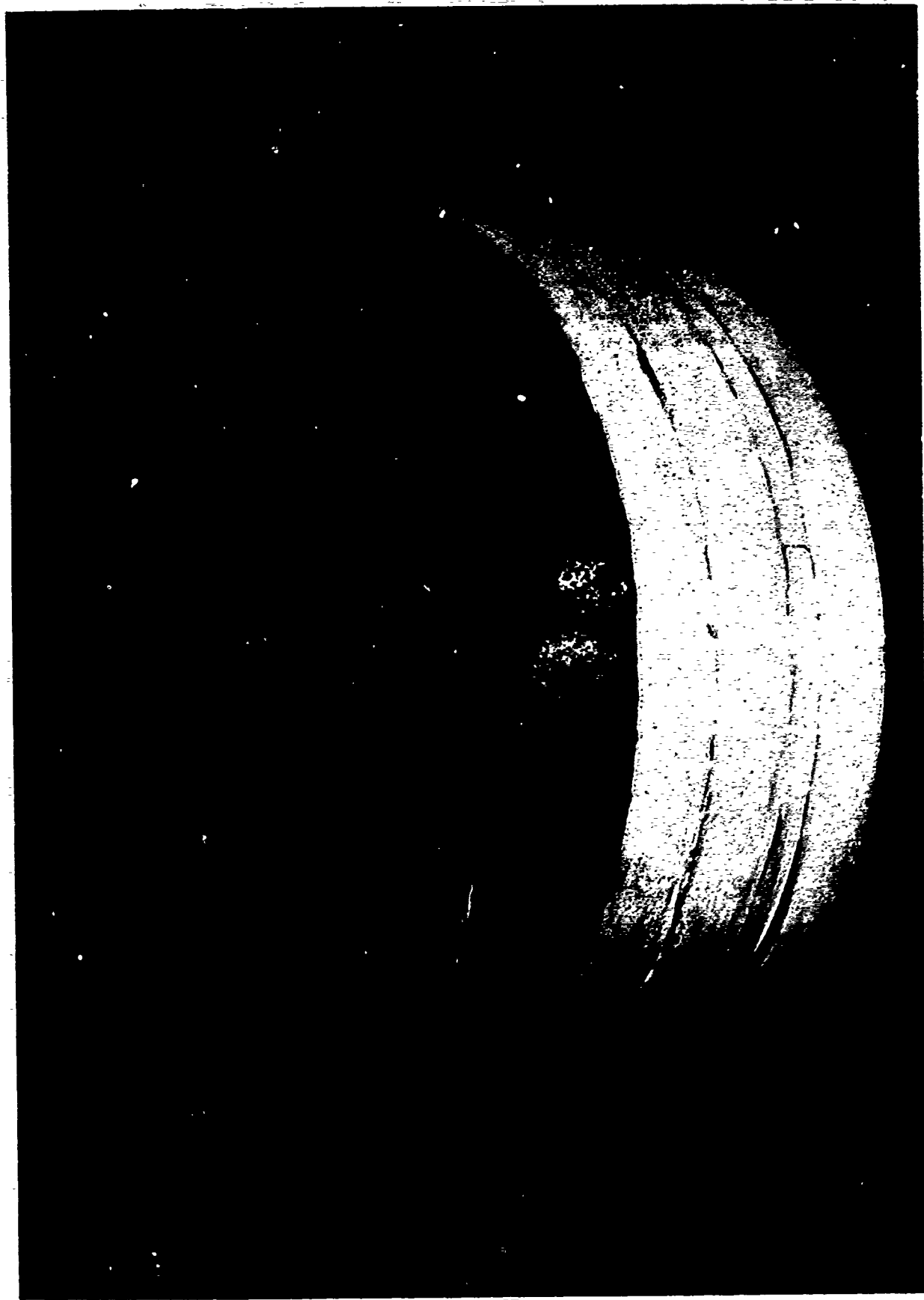


Fig. IV-6. 15-1/2-Inch Diameter Spherical Nose Cap Made of Resin-Impregnated Porous Ceramic

Q

A REPORT ON  
THE APPLICATION OF THE FLUIDIZED BED  
TO THE COATING OF REFRACTORY METALS

T. R. BERGSTROM

The Boeing Company  
Seattle, Washington

## INTRODUCTION

The Boeing Company has evaluated several systems to protect alloys of molybdenum and columbium from the environment that is anticipated in leaving and entering the earth's atmosphere at relatively high velocities. This work has indicated that metal silicide conversion coatings, properly applied, are adequate to protect the base metal if surface temperatures do not exceed 3000°F by any appreciable amount. Boeing has expended a great deal of effort in the development and testing of silicide conversion coatings that are compatible with design requirements. It has been necessary to investigate the effects of processing time and temperature, reactant particle size and purity, small additions of supplemental reactants, carrier gas concentration, inert additives, metal surface condition and contamination level in relation to coating thickness, oxidation resistance, exittance, mechanical properties, etc. The information that has been generated during these investigations is voluminous and will not be mentioned herein as the data are being reported under Contract AF 33(600)-41517.

It is more appropriate for this meeting to discuss the application of a unique process technique to the problem of applying or obtaining silicide conversion coating on alloys of columbium and molybdenum. In our developmental work the conventional pack cementation retort process and the relatively new fluidized bed reactor technique have been investigated. It has been concluded that the newer process method utilizing the fluidized bed is superior to the older pack cementation process for applications where large quantities of complex parts must be coated on a scheduled basis.

## The Fluidized Bed Reactor for Coating Refractory Metals

Probably the most significant characteristic of the fluidized bed reactor is its ability to quickly and uniformly heat parts.<sup>1, 2</sup> Many of the problems associated with the use of large scale pack cementation retorts to coat refractory metals were associated with poor heat transfer. It was, therefore, natural to postulate that the adaptation of the fluidized bed for the application of the silicide coatings to the refractory metals would be very desirable. This assumption has since proven to be entirely correct.

The fluidized bed as used for coating is illustrated in Figure 1. The principal flow lines and the primary reactions are indicated. The bed consists of a thin-walled metallic cylinder filled with reactant (usually powdered silicon metal). Heat is applied to the outside of the cylinder and the reactant is agitated by the upward flow of gas through a porous brick or metal plate at the bottom of the cylinder. The iodine gas used as an intermediate reactant is produced outside the fluidized bed in a generator. The iodine is mixed with argon in the generator and the mixture is injected into the bed with the main flow of argon. Figure 2 is a photograph of the Boeing 18" diameter fluidized bed.

The superiority of the fluidized bed process is the result of the fluidizing action and the rapid heat transfer obtained. The fluidizing action permits the insertion of complex fabricated parts into the reactor while at the desired coating temperature. The excellent heat transfer characteristics insure that the parts are heated rapidly and uniformly when they are inserted into the bed.

The two main process advantages realized from the fluidized bed reactor can be summarized as follows:

1. Processing time can be reduced to the actual time required for the coating to be deposited. The fluidized bed is run continuously at the desired process temperature and the parts are lowered into the hot reactor. In the pack cementation retorts, the major portion of the processing time is in the heat-up and cool-down cycles. It is difficult to eliminate or shorten these cycles as an acceptable way has not been found to place refractory metal parts into a pack retort while the retort is at the coating temperature. Total processing time using each process is, of course, a function of many things including alloy, coating thickness desired, and process temperature. Specific comparisons have shown that the fluidized bed can cut the total coating process time by a factor of three to as much as twelve. This consideration is particularly significant in assessing plant capability to coat large numbers of components on tight schedules.
2. Problems associated with uncontrolled reactions during the heating cycle can be avoided. In the pack cementation process a carrier halide is usually present during the heating cycle. Although reaction rates are generally very slow below the temperature range used for coating, certain anomalous reactions have been observed at lower temperatures. The long time required to heat the retort to the coating temperature allows these reactions and the normal coating reactions to occur in a variable manner within the retort. The severity of this problem increases as the size

and complexity of the component part increases. Conversely, in the fluidized bed the parts are brought to temperature extremely rapidly and uniformly; consequently, undesired reactions are minimized.

In addition to these basic advantages other processing gains are achieved. Studies of the pack cementation process revealed that the density of packing and the uniformity of the pack mixture had to be closely controlled. Localized pockets of slightly different composition had to be avoided. The natural agitation and mixing of the fluidized bed automatically eliminated these complex variables. It is normal practice to replace the silicon in the pack process after each retort run, and as a consequence only one batch of parts is coated per charge of silicon. The fluidized bed operates continuously with only minor additions of silicon and many batches of parts can be coated before the silicon must be replaced.

Historically, the main difficulty associated with the use of coated columbium alloys was a result of the base metal embrittlement caused by the pack cementation coating process. Columbium alloys have an affinity for oxygen, nitrogen, and hydrogen and when these gases are present during the coating process the interstitial impurity level of the alloy to be coated will increase. Any alloy of columbium will behave in a brittle manner if sufficient quantities of these contaminating elements are absorbed. It is therefore necessary to preclude interstitial pickup during any columbium alloy coating process if the metal is to remain ductile. It was determined that the use of a vacuum to pull the impurity gases out of a pack retort during the heating cycle would eliminate the embrittlement problem on the low strength-ductile columbium alloys. However, a high temperature vacuum purge of a retort full of powder is not a desirable

addition to a process cycle that is of itself lengthy. It was obvious that to be useful the fluidized bed process would have to be able to coat columbium alloys without impairing the base metal ductility. Fortunately, it has been found that the fluidized bed process can be used to coat the low strength-ductile columbium alloys and not seriously impair their ductility. All coated specimens tested to date have been ductile in impact bend tests at room temperature.

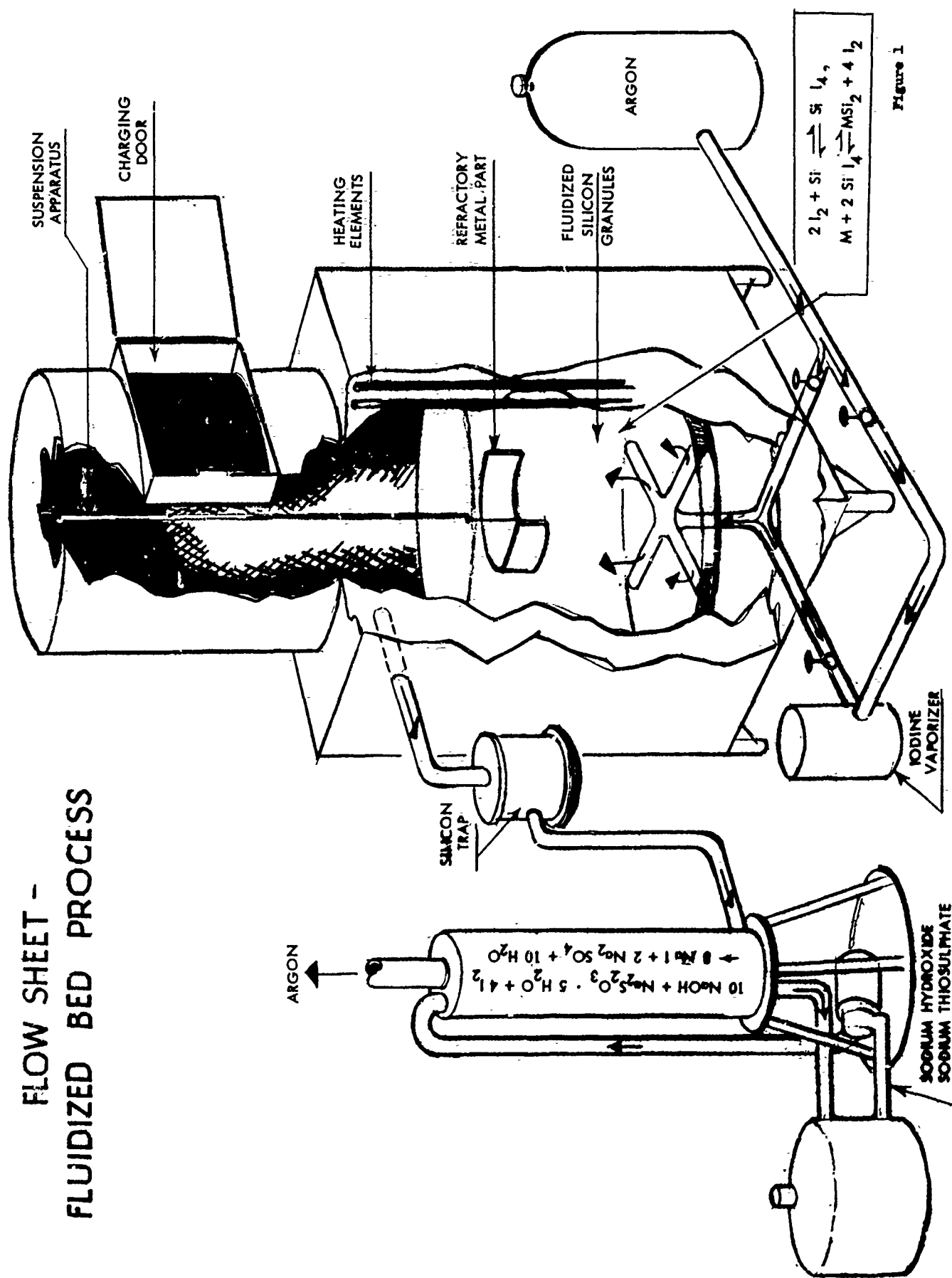
It is true that there are certain disadvantages associated with the use of the fluidized bed. However, the overall analysis of the situation, considering product quality, processing economics, plant capabilities, schedules, etc., has clearly shown that fluidized bed processing is superior to pack cementation processing for airframe type applications.



### References

1. Principles of the Fluid Bed; J. D. Stauffer and C. O. Pedersen, Metal Progress, April 1961, 78-81.
2. Heat Treating in The Fluid-Bed Furnace; C. Bennell and C. Jung, Metal Progress, April 1961, 82-87.

# FLOW SHEET - FLUIDIZED BED PROCESS



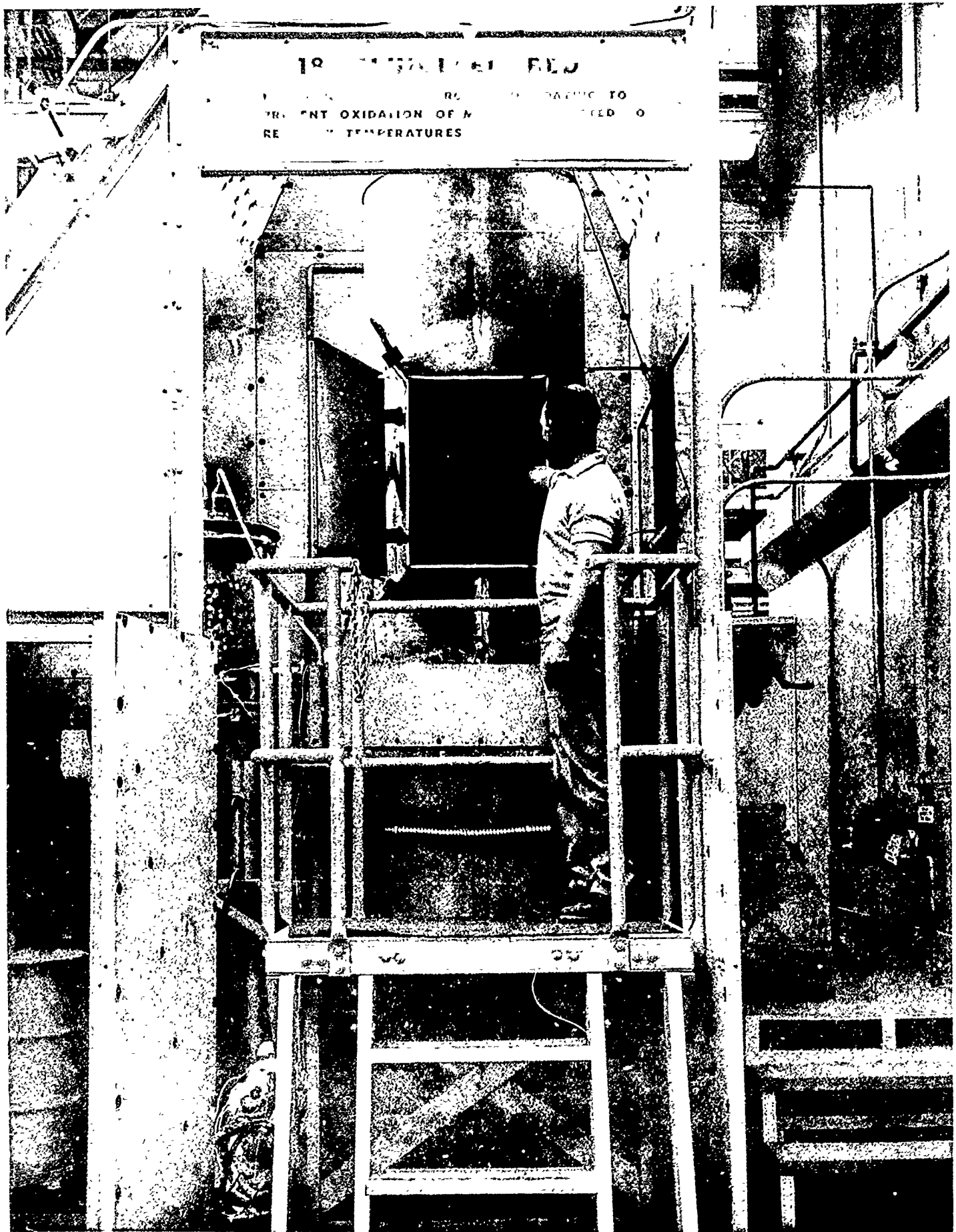


Figure 2

2A 66772

DESIGN, FABRICATION AND TESTING OF A  
MOLYBDENUM ALLOY OUTER WALL HEAT SHIELD

F. A. MERRIHEW  
FRANK M. ANTHONY

Bell Aerosystems Company  
Buffalo, New York

# DESIGN, FABRICATION AND TESTING OF A MOLYBDENUM ALLOY OUTER WALL HEAT SHIELD\*

## INTRODUCTION

Since the last Working Group Meeting, Bell Aerosystems Company's activities in the area of refractory composites have included engineering, fabrication and experimental studies of coated refractory metals for airframe and rocket applications. One portion of this work which has proceeded to the completion of its first phase is the subject of this paper, namely the development of a molybdenum alloy heat shield designed for a maximum operating temperature of 2700F.

## DESIGN REQUIREMENTS AND APPROACH

The molybdenum outer wall heat shield development was initiated about a year ago as a step toward extending the temperature capability of the Bell Double Wall radiation thermal protection system. This system, consisting of heat resistant outer wall shields, thermal insulation and a low temperature aluminum load carrying structure, is shown schematically in Figure 1, and its practicality has been demonstrated experimentally at temperatures of 2000F. Increasing demands for greater vehicle performance can only be met by increasing the operating temperature capability of the system, particularly that of the outer wall.

---

\*This work was supported by the United States Air Force Under Contract AF 33(600)-40100, monitored by the Manufacturing and Materials Technology Division, AMC Aeronautical Systems Center, Wright-Patterson Air Force Base, Ohio.

The function of the outer wall is to provide a smooth external surface and to protect and retain the insulation. A typical application might be that of protecting the lower surface of a manned hypersonic glider. Temperatures may follow those shown in Figure 2 with a rapid rise to about 1550F in 2 minutes of boost, a gradual increase to about 2600F after 21 minutes total followed by a gradual decrease to 1000F after 36 minutes total. The temperature variation shown in Figure 2 actually represents that used for the test program as directed by our customer. The design work was based on a somewhat longer time period and a maximum temperature of 2700F.

Transient conditions may impose pressure loadings, but since the outer wall is not sealed pressure differentials are rapidly equalized, thus reducing potential creep problems. During low to moderate temperature portions of flight, such as boost and landing phases where course correction maneuvers will be required, pressure differentials of up to 5 psi may exist but during the high temperature portion of flight pressures will be about an order of magnitude lower. Significant acoustic loadings also exist particularly during boost phase.

Requirements for the outer wall therefore include:

1. Inertness to the atmospheric environment while at temperatures of up to 2700F
2. Resistance to acoustic loadings
3. Adequate strength to resist surface pressures with minimum deformation.
4. Resistance to thermal stresses
5. Light weight
6. Low cost
7. Reusability

In meeting the requirements it is necessary to recognize the shortcomings in the present state of the art. These shortcomings were primarily in the areas of fabrication and coating technologies. Forming methods for molybdenum alloys were fairly well established, however, difficulties were expected because of the variability of sheet material. Assembly techniques were much more restrictive. Reliable brazing and fusion welding techniques were not available. Spot welding appeared to offer promise but even here the techniques employed could not insure reliably reproducible results. Riveting appeared to offer the most attractive approach for assembly. Experience had shown that edges of sheet material presented difficulties with regard to oxidation protection by coating systems. Also, questions existed as to the sequence of coating and assembly steps.

The design approach employed for this molybdenum outer wall panel was based on the utilization of available materials and the most promising fabrication procedures. Since holes and edges were potential weak spots with regard to coating protection, these were to be minimized and, if it all possible, eliminated from direct contact with the boundary layer airflow.

#### DESIGN CONSIDERATIONS

In accordance with the requirements and the approach established, the construction material selected was the 0.5% titanium alloy of molybdenum. The protective coating chosen was Chormalloy W-2. Tests of numerous coatings at Bell over the past several years had indicated the superiority of this coating. At the time of coating selection evaluations had not been conducted on the Pfadler, Chance Vought, or Boeing coatings.

Initially, corrugated sandwich panels of various types were considered assuming assembly by spot welding or riveting. Experimental evaluations of spot welding indicated a need for more extensive development of this process. Hence, it was not considered to be completely available as required. Riveting, therefore, was selected as the means of assembly. This choice tended to make corrugated sandwich panels quite unattractive. With such designs a large number of rivets were required and approximately half of the rivets were exposed to the boundary layer airflow. The panel size being considered was approximately 12" x 12" x 1/4". Structural analysis indicated that 5 mil material would be adequate to withstand the expected loadings. With a reasonable corrugation pitch, it is obvious that a large number of rivets would be required for assembly of the face sheets to the corrugation. For designs of this type the number of rivets involved ranged from about 150 to 200. Not only would these introduce a large number of potential failure points, but they result in an expensive design to produce.

Experimental evaluations of 5 mil sheet material indicated little hope of adequately protecting such thin gages. Relatively severe embrittlement resulted from the application of the protective coating. Attempts to reduce the embrittlement by the use of thinner coatings resulted in a loss of adequate oxidation protection. Edges were the primary problem, but numerous failures were also encountered on flat surfaces. Concurrent evaluations of 10 mil material indicated much better results although perfect performance was not achieved. On the thicker material edge failures were the major problem.



Since it was felt that the minimum sheet thickness practical, from a coating point of view, for the outer wall panel was 10 mils, additional designs were considered in an attempt to simplify the construction and to reduce the number of rivets required. As a result of these studies a design assembled from the details shown in Figure 3 was selected. This design consists of ten 10 mil channels riveted internally to two 30 mil beams. Each beam is supported on two 30 mil support legs. Each channel is attached to each beam by four internal rivets. The panel contains a total of 88 rivets, none of which are exposed to the boundary layer airflow. One end of each channel is joggled so that it nests within the preceding outer wall panel. Hence, only one edge is exposed to boundary layer airflow. The weight of the coated panel is 1.82 pounds. The completed panel is shown in Figures 4 and 5 and measured 12" x 12.12" in plan form.

#### FABRICATION CONSIDERATIONS

In producing the detailed parts for the selected panel design conventional forming techniques were employed in conjunction with heated tools. Initially edge cracks were encountered in the forming of the detailed parts. This problem was resolved by greater attention to the edge preparation in the sheet metal blanks prior to forming. Extreme care was required to provide well rounded edges necessary for both consistent forming results and for achieving good coating protection.

For the preliminary studies of riveting techniques molybdenum alloy rivets were procured from commercial sources. It was found that a relatively large number of these rivets contained small

cracks in the heads. It was decided, therefore, to produce the rivets required at Bell. Suitable procedures were quickly established and rivets of the flat head type were formed at 1200F.

In establishing the coating and assembly sequence, consideration was given to the following factors:

1. The W-2 coating process consists of two cycles.
2. Coating penetration around rivets after installation was somewhat questionable.
3. The greater the coating thickness, the greater was the embrittling effect on the substrate.

As a result of these considerations, it was decided to apply approximately one-half of the desired coating thickness to the detailed parts and rivets prior to assembly. This would result in a degree of protection to all surfaces. In addition, the embrittling effect would be minimized. Assembly would follow the first coating and the assembled part would be recoated. Studies with coated rivets indicated that a temperature of approximately 1600F was required to properly set the rivet without introducing cracks.

Using the techniques briefly described above, two outer wall panels were fabricated; one was uncoated, while the second was coated and assembled in the manner described. During assembly of the coated panel, however, one 10 mil channel was cracked and had to be replaced. Unfortunately, there were no spare channels to which the first coating step had been applied and an uncoated channel was installed.

### TEST RESULTS

The uncoated panel was subjected to an acoustic loading of 145 db for a period of 30 minutes. No failures of any kind were detected. Through the frequency range of 20 to 9600 cycles per second, only minor amplification of the noise input was found at frequencies of 250 and 650 cps.

The coated panel was subjected to an oxidation proof test at 2000F in still air for 30 minutes. Slight smoking was noted when the assembly was removed from the furnace. Post test examination indicated numerous locally oxidized regions along the edges of the 10 mil channels, see Figures 4 and 5. Figure 6 provides a close-up view of a typical edge failure. A few local edge failures were noted on the 30 mil parts. Only one small pinhole was detected on the flat surfaces. This was on one of the 10 mil channels but did not penetrate the channel thickness. Measurements of surface recession at the local failure points indicated maximum values of .03 inch with average recession of about .01 inch. In many regions the recession was too small to be measured but visual inspection indicated that failures had occurred.

After the oxidation proof test edge failures were apparent along about .2 inch of the 30 mil material out of a total linear distance of about 56 inches. For the 10 mil material only about 100 inches of the 240 inch total edge length was visible. Of this 100 inches local failures or suspicious indications were apparent along about 20 inches.

After the oxidation proof test a thermal exposure test program was conducted using the temperature-time history shown in Figure 2. A quartz lamp bank provided the heat flux. The test panel was bolted to a water cooled inner wall at its four support points and fibrous insulation was used to minimize heat flow from the panel to the cooled wall.

The first four cycles were terminated prematurely, because of lamp failures, after times of 9.2, 15.5, 17.2 and 19.5 minutes. Maximum temperatures reached during these cycles were 2310F, 2450F, 2530F and 2640F, respectively. After these four attempts, higher capacity quartz lamps were installed and two complete 36 minute cycles were conducted. During the next cycle the control thermocouple malfunctioned causing the panel to reach a temperature of 2960F after 15 minutes.

The panel is shown after testing in Figures 7 and 8. Considerable degradation is apparent. The failures were of two basic types, pinholes, or edge failures.

The 30 mil material suffered only edge failures and then only about 10% of the total edge length was damaged. Note that the structural integrity of the 30 mil parts does not appear to be reduced.

Damage of the 10 mil material was more extensive. Careful examination of Figures 7 and 8 will indicate the extreme degradation of the channel that had only one coating application, the second channel from the top. Consider first the pinhole failures. Of the nine channels which received two coating applications, three contained no pinhole failures, two had just one failure each,

two had 4 failures each, one had 5 failures, and one had 8 failures. At the end of the testing the pinhole noted after the oxidation proof test had grown to .48 inch in diameter. The next two largest pinholes were .38 and .32 inch. The remainder were quite small as can be seen in Figures 7 and 8. In Figure 7 it can be seen that most of the pinholes seem to fall within a fan-shapes region originating on the left hand side of the panel at the second channel from the top. During one of the first tests a plug in an air cooling line came loose and the panel was sprayed with an oil residue from within the coolant line. This foreign material may have accelerated oxidation failure.

Failures along the right hand and left hand edges of the panels were quite general. The different amounts of surface recession on the various channels indicate that these failures began at different times. The maximum linear recession from an edge was .35 inch. All of the edges around the 1/4 inch access holes, two in each of the third channels from the top and bottom, failed during the test. The maximum recession from these edges was .17 inch. The final shape of these holes also indicates that failures occurred at different times.

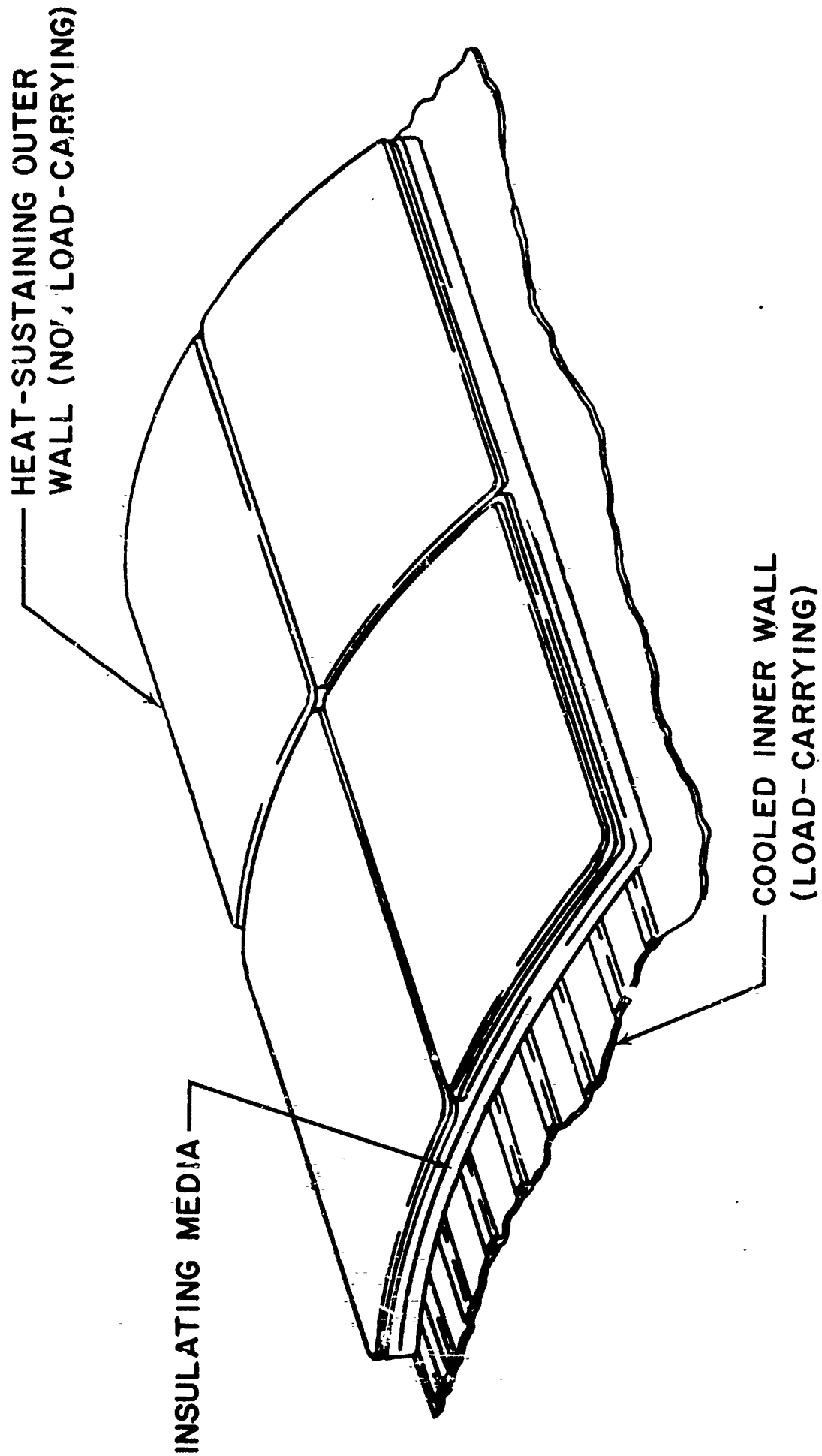
Of the 88 rivets installed, evidence of oxidation was found in the vicinity of only three. In one instance the shank of the rivet was almost completely burned away.

## CONCLUSIONS

The results obtained during the test program point out quite vividly the shortcomings which exist and restrict the use of coated molybdenum alloy for structural applications. The panel produced and tested is considered satisfactory for one, and perhaps two missions. Reusability beyond that point is extremely questionable. In general, coating performance on flat surfaces is only slightly below tolerable standards. A major problem, however, still exists at edges despite the extreme care taken with edge preparation. In this regard performance of 30 mil material is vastly superior to that of 10 mil material.

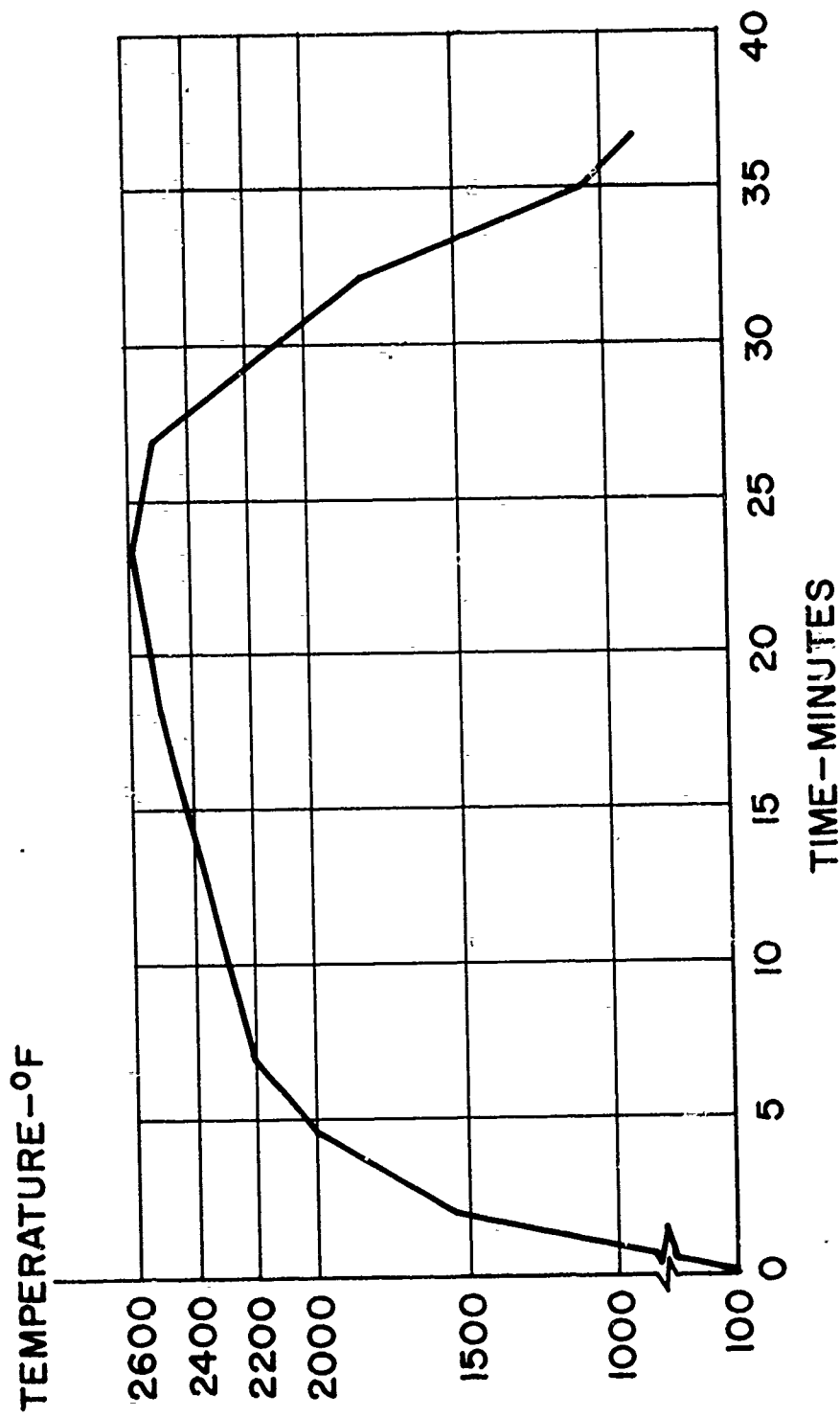
The assembly sequence of applying a partial coating thickness to all detailed parts and rivets, hot riveting, and recoating appears to result in good protection at the joints.

Many of the problems involved in the successful utilization of coated molybdenum for structural components have been solved. The major problem area requiring attention appears to be that of providing adequate protection to edges of thin material.



DOUBLE-WALL CONSTRUCTION

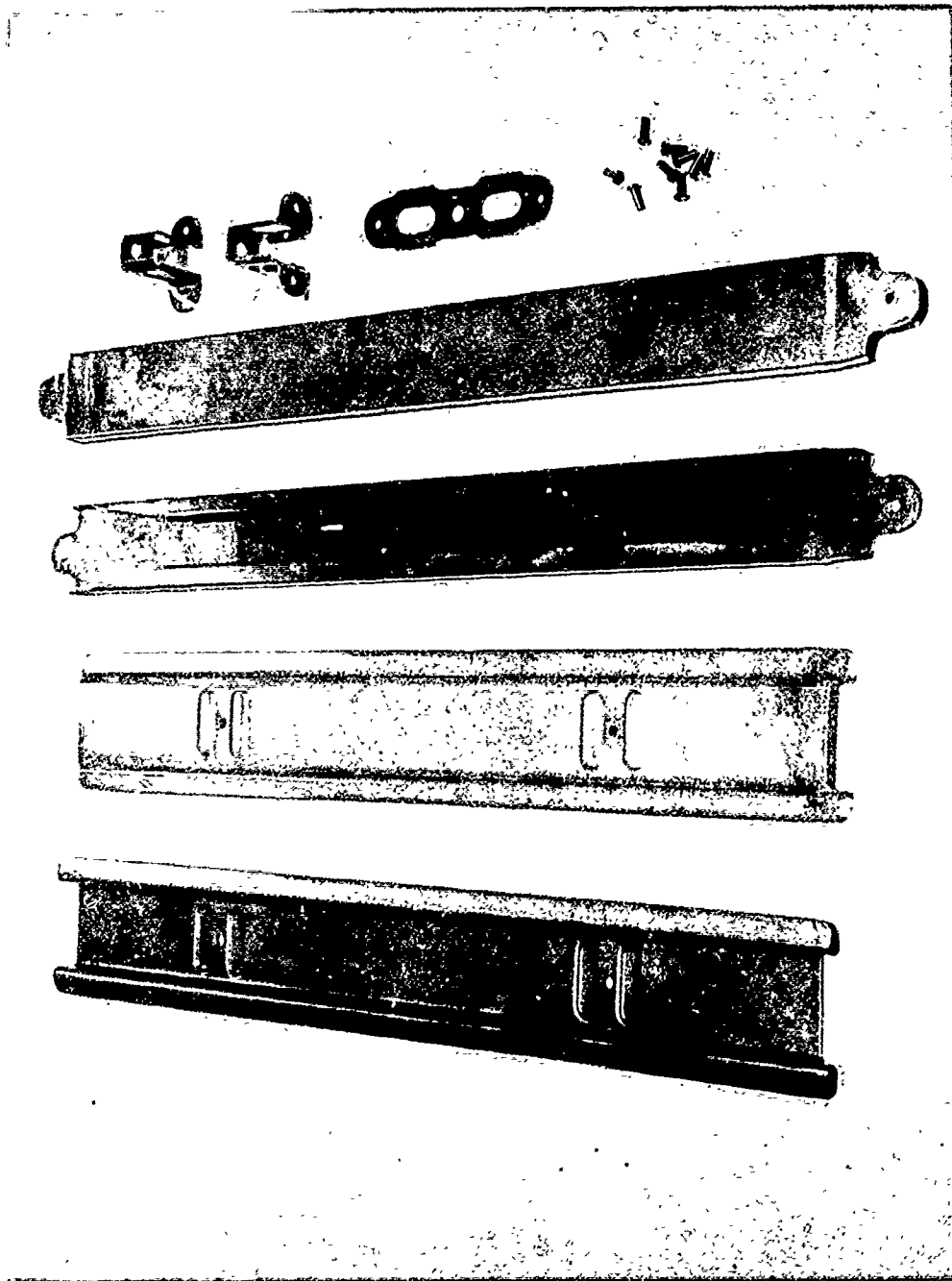
Figure 2



TEST TEMPERATURE-TIME HISTORY

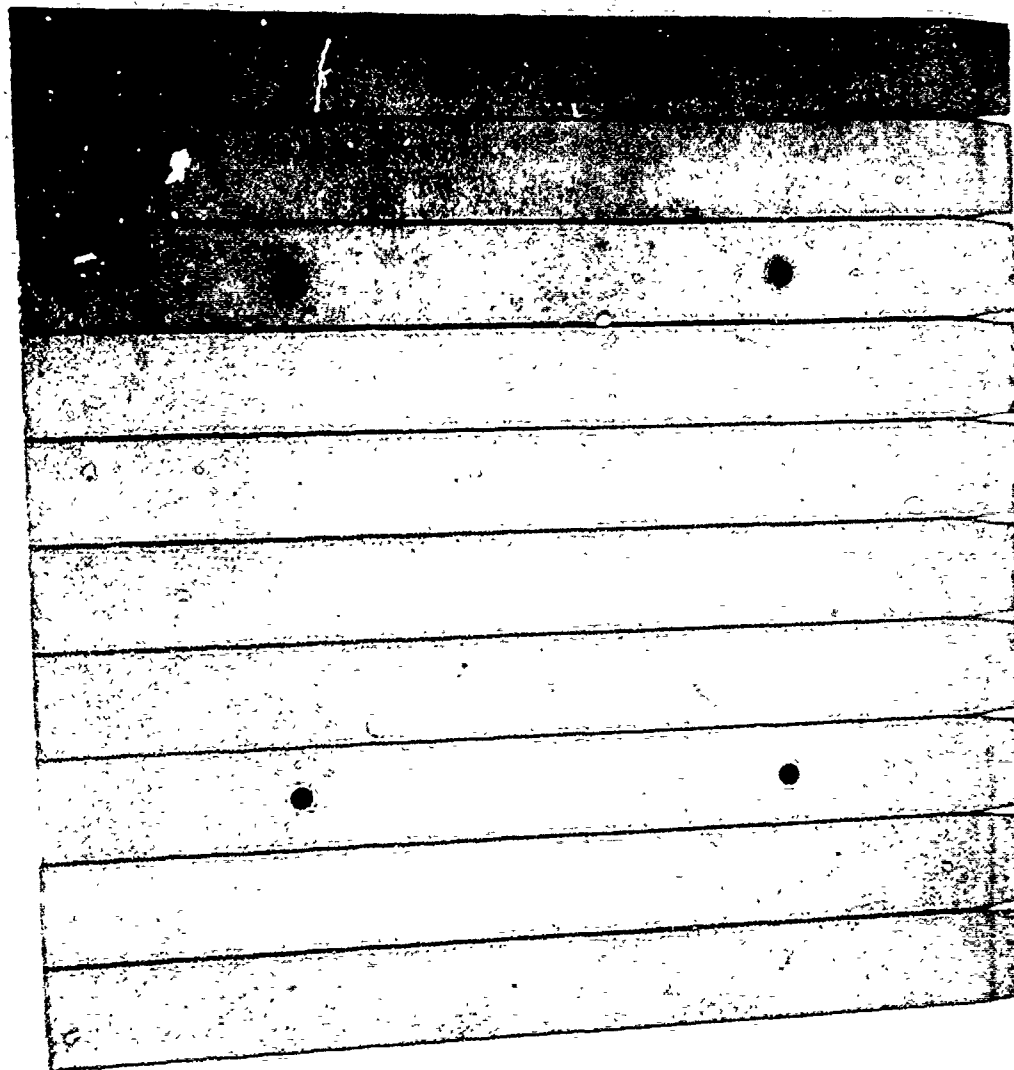


Figure 3



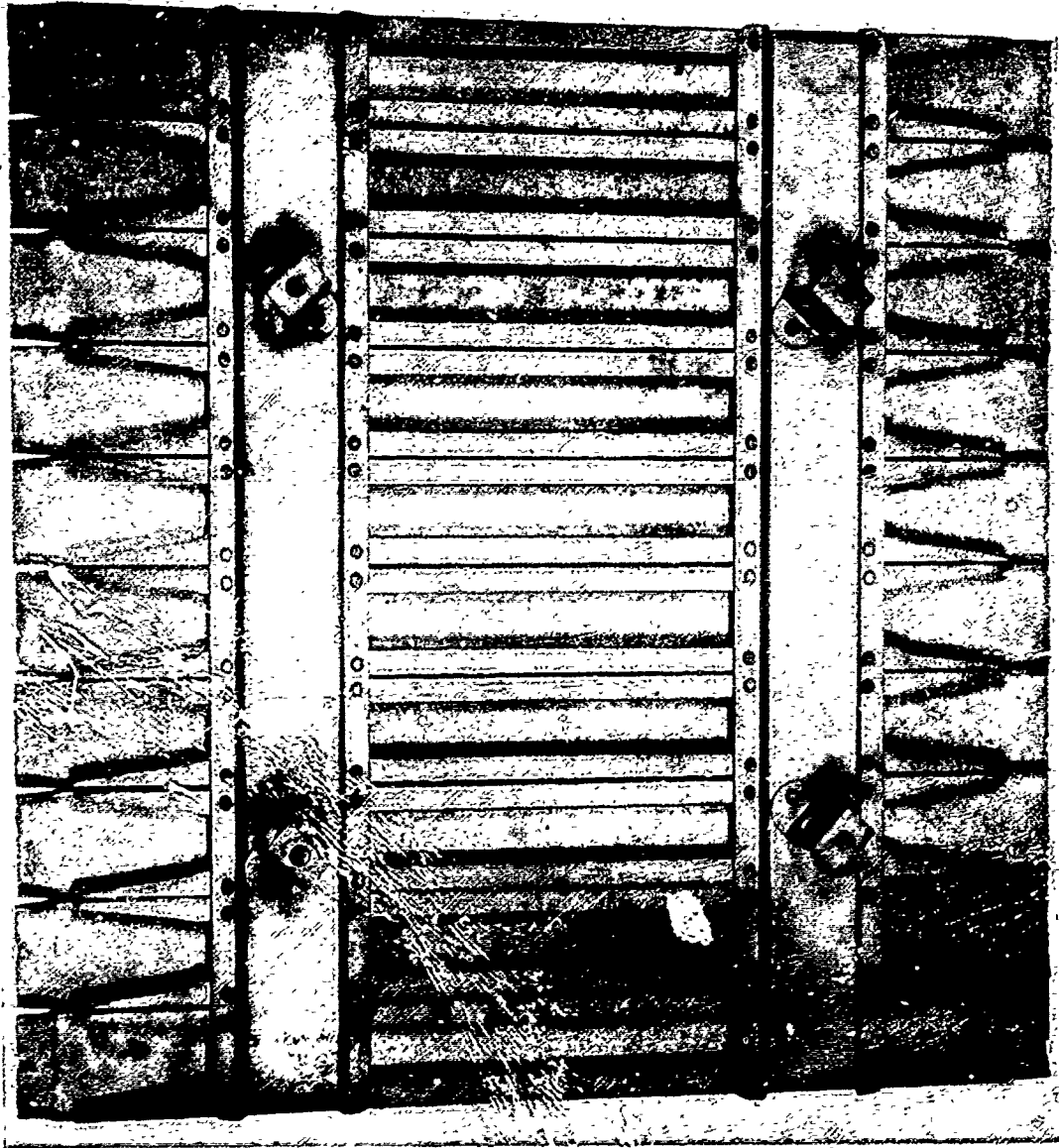
DETAILS FOR MOLYBDENUM ALLOY OUTER WALL PANEL

Figure 4



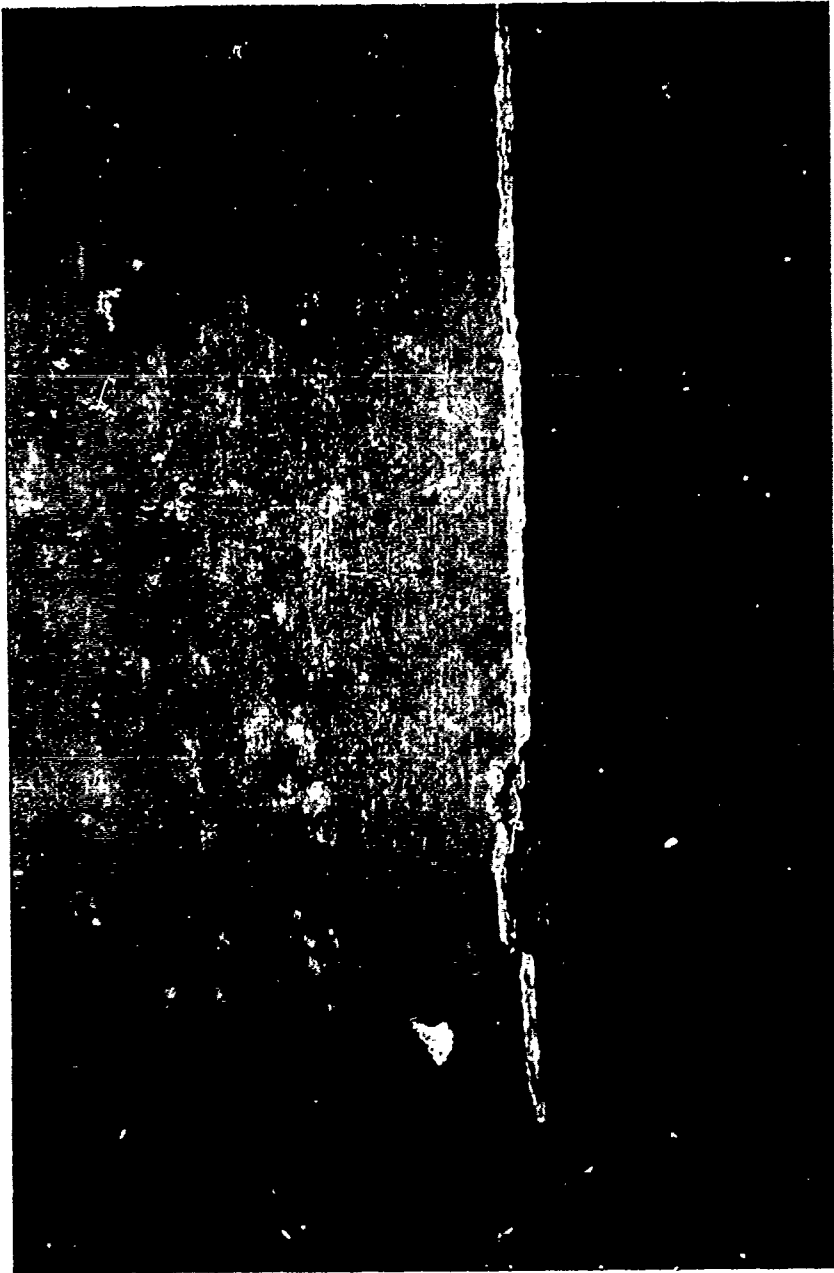
COATED MOLYBDENUM ALLOY OUTER WALL PANEL  
AFTER OXIDATION PROOF TEST, TOP VIEW

Figure 5



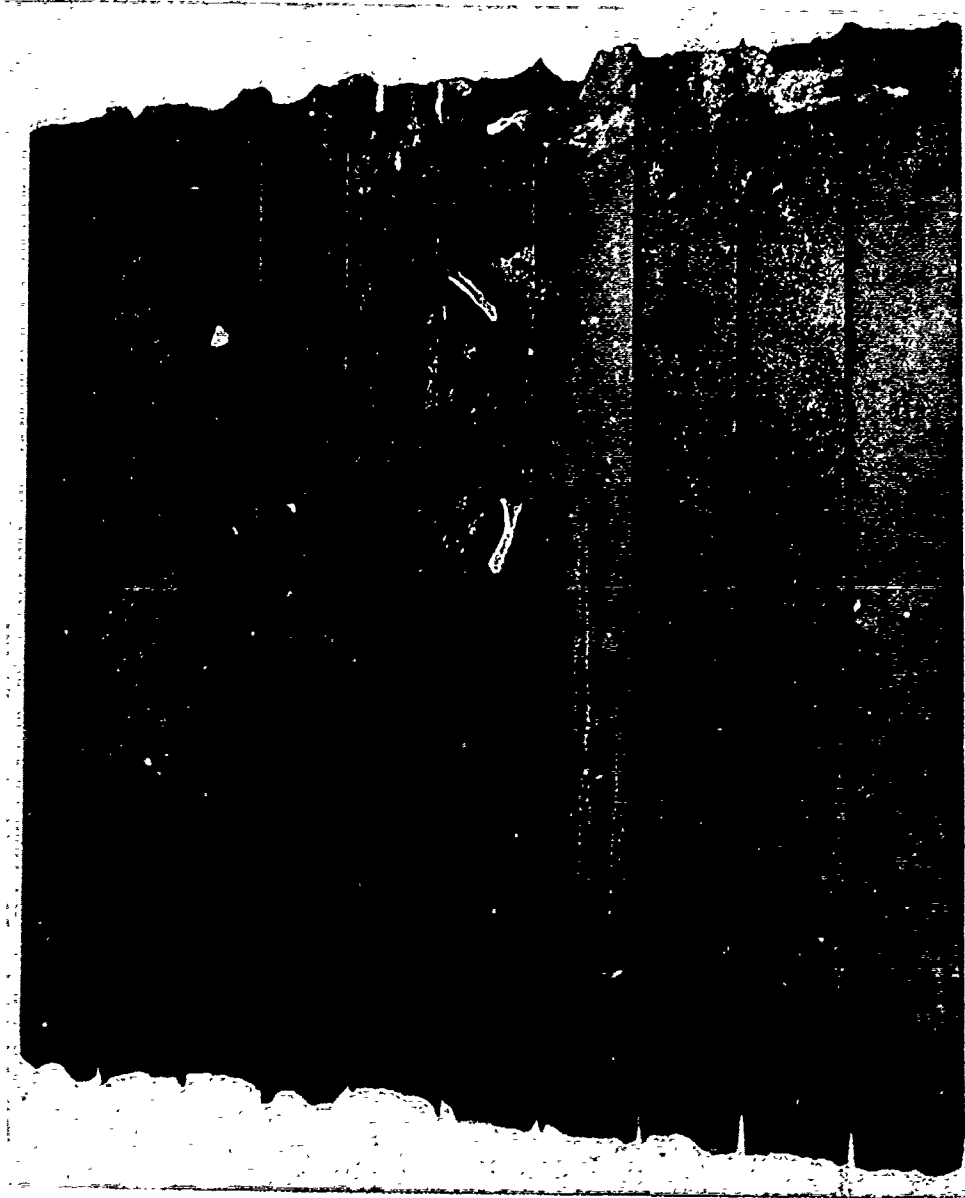
COATED MOLYBDENUM ALLOY OUTER WALL PANEL  
AFTER OXIDATION PROOF TEST, BOTTOM VIEW

Figure 6



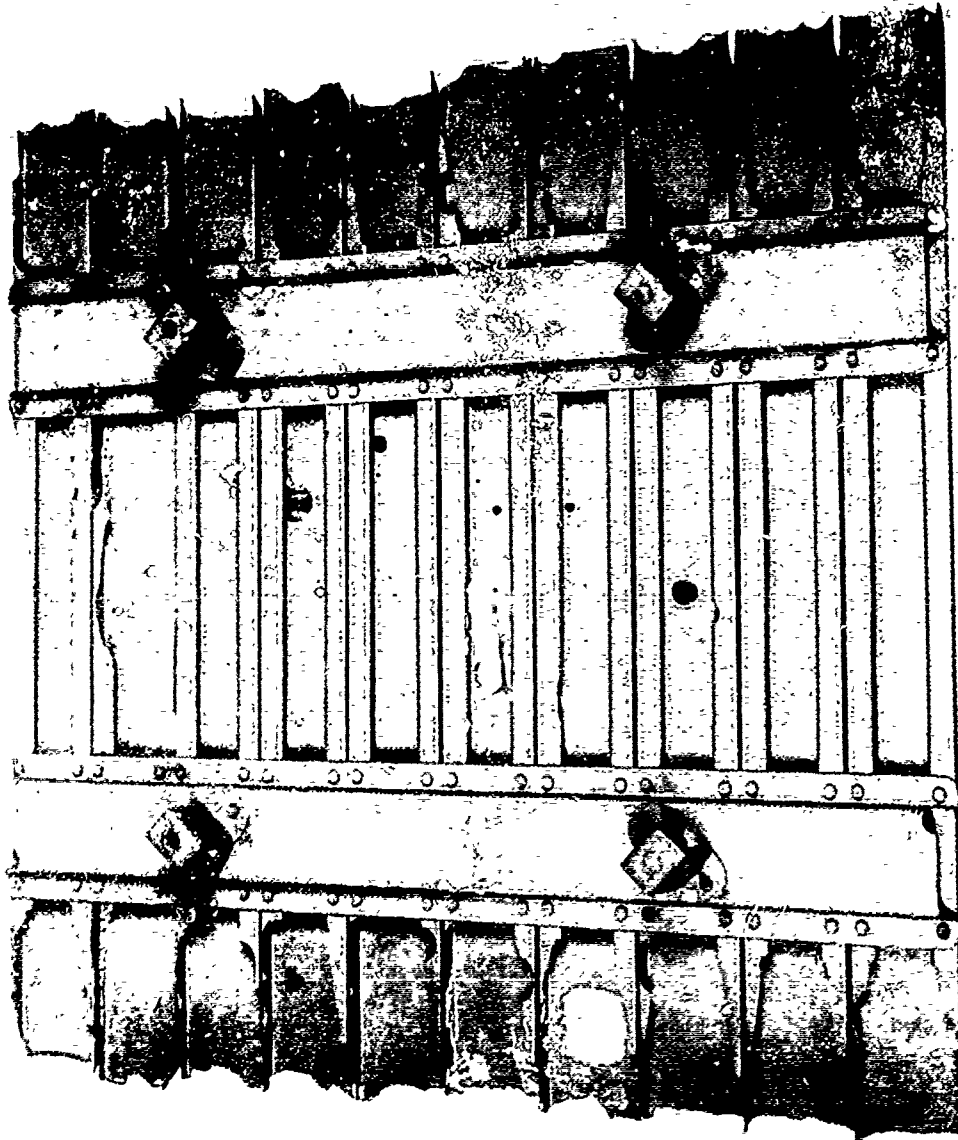
TYPICAL EDGE FAILURE AFTER OXIDATION PROOF TEST

Figure 7



COATED MOLYBDENUM ALLOY OUTER WALL PANEL  
AFTER THERMAL EXPOSURE TESTING, TOP VIEW

Figure 8



COATED MOLYBDENUM ALLOY OUTER WALL PANEL  
AFTER THERMAL EXPOSURE TESTING, BOTTOM VIEW

A question was asked by Mr. M. Levinstein of General Electric regarding acoustic loading of the Chromalloy W-2 coated molybdenum panel. Only the uncoated panel underwent acoustic loading. The test program called for acoustic loading of the coated panel after thermal cycling at the time-temperature history shown in Figure 2 of the paper. This portion of the program, however, was cancelled due to the condition of the panel after the thermal cycling.

During the limited program conducted an uncoated panel was fabricated to check manufacturing and assembly procedures. This successfully passed acoustic testing. This test was to determine the existence of major problems. Since the acoustic loading problem should be more severe with coated material, it was unfortunate that such tests could not be conducted within the scope of the Double-Wall Program. Tooling, test equipment and experience are available, however, and could be employed for the continued evaluation of this typical structural component made from various refractory metal alloys and protected by various coating. In fact, our current company funded R&D will investigate a columbium alloy panel of the same construction.

DEVELOPMENTAL WORK IN HIGH TEMPERATURE  
PROTECTIVE COATINGS FOR REFRACTORY METALS

M. E. BROWNING

General Dynamics

Fort Worth, Texas



The development of high temperature protective coatings differs throughout the country because of three major considerations:

1. Design objectives
2. Structural requirements
3. Environmental parameters

Each coating formulation is evolved taking these three factors into consideration plus such pertinent facets as metal or material involved, method of application, and dimensional tolerances required. The essence of this is that specific applications require specialized coatings based on the individual requirements of the job to be accomplished. Where weight is considered important (and where isn't it?), a super-abundance of protective coating may over-balance design weights and have a critical effect on final design objectives. Naturally, too thin a coating will be susceptible to premature failure and catastrophic results.

The effect of the coating on the basis metal (both at room temperature and at operational temperatures) is vitally important in the majority of design considerations. Serious

reduction of physical properties in the basis metal caused by properties of the coating, the method of application, or a combination of both can also nullify a good design.

Ease of application and convenience of repair are ultimate objectives in any coating development work. This type of evaluation should be considered in final screening tests. Finally, the environmental parameters (e.g. time-at-temperature, number of thermal cycles and temperature involved, type of exposure expected, etc.) must be carefully considered.

The developmental work referenced herein represents a part of the exploratory high temperature coatings work being carried on at General Dynamics/ Fort Worth and was chosen to typify research in protective coatings for columbium and tantalum alloys.

#### PROCESSES INVOLVED

Processes involved in developing protective coatings at General Dynamics/ Fort Worth include:

1. Spray techniques
2. Electrodeposition
3. Vapor Deposition

4. Pack Cementation,

and 5. Multi-cycle combinations of the above.

These were examined for most advantageous metallic and intermetallic coating application.

Two fields of interest predominate in the work reported herein. These are:

- A. Close control coatings for thin substrates ( under 0.020" ), and
- B. High integrity coatings for heavier substrates ( over 0.020" thickness ).

Screening tests were used to eliminate those potential coatings which did not show the necessary characteristics for production development. In the study reported, careful examination of step in processing was necessary. In nearly all cases it was found that the preparation of the basis metal was critical. In this regard, basis metal specimens had to be handled with special precautions prior to coating application.

Columbium Coatings

Three environmental conditions were used as "go - no go" limits for those coatings preliminarily screened and accepted for second phase oxidation testing. Temperatures used in the three conditions mentioned were 2300° F, 2500° F, and

2700° F. A wide cone producing oxy-acetylene blast fixture (with or without indexing device) was used as the major test criteria. Zirconia tube furnaces and/ or R.F. chambers were available for long term exposure tests.

A. Coatings Constituents:

Elements of these developmental coatings for columbium included Al, Ti, Cr, Si, Ni, Ir, and Rh.

B. Metal Substrates Tested:

Representative columbium alloys examined included FS-82, D-31, and C-103.

C. Coating Performance:

A comparison was made of several types of coatings applied to test specimens of the same alloy cut from the same sheet. A rated comparison is offered as Table I.

Tantalum Coatings

Protective coatings for use on tantalum alloys were examined in light of the three environmental realms mentioned under the columbium coating evaluation. However, in this program the temperatures were raised 200° F. This results in three categories using 2500° F, 2700° F, and 2900° F. The same equipment was made available for testing in this work.

TABLE I

COMPARISON OF COATINGS ON VARIOUS REPRESENTATIVE  
COLUMBIUM ALLOYS USING A PERFORMANCE RATING

ALLOY	COATING CONSTITUENTS	TEMPERATURE CLASS	RATING **
FS-82	Si	(a)	2
"	Si	(b)	1
FS-82	Al + Ti	(a)	5
"	Al + Ti	(b)	3
FS-82	Cr + Ti + Si	(a)	10
"	Cr + Ti + Si	(b)	8
"	Cr + Ti + Si	(c)	3
FS-82	Cr + Si + Al	(a)	7
"	Cr + Si + Al	(b)	5
"	Cr + Si + Al	(c)	1+
D-31	Ti + Al + Ti	(a)	4
"	Ti + Al + Ti	(b)	2
D-31	Cr + Ti + Al	(b)	6
"	Cr + Ti + Si	(c)	2
D-31	Al + Rh	(a)	3
"	Al + Rh	(b)	2
D-31	Ni + Al + Ir	(a)	4
"	Ni + Al + Ir	(b)	4
"	Ni + Al + Ir	(c)	1
C-103	Si	(a)	2
"	Si	(b)	1
C-103	Al + Ti	(a)	3
"	Al + Ti	(b)	2+

\* Highest temperature class for which satisfactory reproducible coatings of minimum thickness appear feasible.  
(a) 2300° F, (b) 2500° F, and (c) 2700° F.

\*\* Rated from 1 to 10 based on appearance after exposure, edge protection, and integrity in the temperature class for the specific alloy involved.

A. Coatings Constituents:

Elements of these developmental coatings for tantalum included Al, Ti, Cr, Ir, and Rh.

B. Metal Substrates Tested:

Only the 10 W - Tantalum alloy was tested in this early portion of the tantalum protective coating program.

C. Coating Performance:

A comparison was made of several types of coatings applied to the 10 W - Ta alloy cut from the same sheet.

A rated comparison is offered as Table II.

CONCLUSIONS

General conclusions which can be evolved as a result of this portion of the high temperature coatings test program are as follows:

- I. Coatings, applied by the same methods, examined on several different columbium<sup>Alloys</sup> reveal that exposure to oxidizing atmosphere induce different effects.
  - A. D-31 appears to be somewhat harder to apply a uniform coating than does FS-82. The C-103 tested appears to be less homogeneous than either of the other two.
  - B. The same coating will not give exactly the same protection on different alloys even when applied with the most exacting care.
- II. Aluminate coatings applied to tantalum ( 10W- Ta ) appear to have greater promise as a reproducible production coating than others tested.

TABLE II

COMPARISON OF COATINGS ON 10 W - TANTALUM  
USING A PERFORMANCE RATING

ALLOY	COATING CONSTITUENTS	TEMPERATURE CLASS *	RATING **
10 W- Ta	Al + Ti	(a)	5
" "	Al + Ti	(b)	3
10 W- Ta	Cr + Ti + Si	(a)	4
" "	Cr + Ti + Si	(b)	2
10 W- Ta	Si + Cr	(a)	4
" "	Si + Cr	(b)	1
10 W- Ta	Al + Ir	(a)	3
" "	Al + Ir	(b)	1
10 W- Ta	Al + Ti + Rh	(a)	7
" "	Al + Ti + Rh	(b)	4

\* Highest temperature class for which satisfactory reproducible coatings of minimum thickness appear feasible. Temperatures of (a) 2500° F and (b) 2700° F were used. Tests for (c) 2900° F have not yet been fully completed.

\*\* Rated from 1 to 10 based on appearance after exposure, degree of edge protection, and integrity in the temperature class for 10 W- Ta.

ASD CONTRACTS FOR  
PROTECTION OF REFRACTORY METALS

N. M. GEYER

Aeronautical Systems Division  
Wright-Patterson Air Force Base, Ohio



ASD continues to support a number of efforts toward development of refractory metal coatings. Included among those programs currently sponsored by the Directorate of Materials and Processes (i. e. - Metals and Ceramics Lab. or Applications Lab.) are:

<u>Contract Number</u>	<u>Contractor</u>	<u>Description of Effort</u>	<u>Status of Reports</u>
AF 33(616)-7184	Battelle	"Dev. of Ta Coatings"	4 QPR's (15 May 61)*
" " 7215	TRW	"Dev. of Alloy Coating for Cb"	3 QPR's TR 61-66 Pt I & Pt II
" " 7383	Chromalloy	Establish Reliability of W-2 for Mo"	3 QPR's (15 April 61)
" " 7462	Sylcor	"Dev. of Aluminide Coatings for Ta"	3 QPR's (Mar 61) TR 61-233
" " 7896	Chance-Vought	"Dev. of Silicide Coatings for Cb"	1 QPR (May 61)
" " 8125	Pfautler	"Optimization of PFR-6 Coating for Mo"	1 QPR (June 61)
" " 8154	GE-FPLD	"Dev. of Std. Test Tech. for Refractory Metals Coatings"	1 QPR (July 61)
" " 8188	TRW	"Dev. of Coatings for W"	---
" " 8175	GT&E Labs/	"Studies on Protection of W"	---
AF 61(052)-353	Metallic Surfaces Rsch. Labs. (Eng)	"Study of Oxid. Res. Coat. for Mo"	Annual Summary Rept (31 Mar 61)

Three contracts were completed since last November:

AF 33(616)-6868	NYU	"Investigation of Si-coatings for W"	TR 60-825
AF 33(616)-6807	AMF	"Electrodeposited Cermet Coatings for Mo & Cb"	TR 60-718
" " 7192	Pfautler	"Dev. of Pack Silicide Coatings for Mo"	TR 61-241

In addition to these efforts several contractual programs in the nature of supporting research on diffusion, oxidation, etc. are being sponsored by M&C Lab:

AF 33(616)-5770	Westinghouse Rsch. Lab.	"Kinetics of W-oxidation"	TR 59-575 Pt II
" " 6354	Mfg. Lab., Inc.	"Diffusion Barrier Studies"	TR 60-343, 7 QPR's. (July 61)
" " 8005	OSU Research Foundation	"Oxy-carburization of W"	No repts available.

AF 33(616)-7675	OSU Rsch. Found.	"Oxidation of Ta"	No repts available.
AF 61(052)-460	Central Inst. for Ind. Rsch. (Norway)	"Rsch. on Defect Structure of Metal Oxides (Nb & Ta)"	" " "

\*Dates in parenthesis indicate latest Quarterly Progress Report.

FURTHER DEVELOPMENTS IN REINFORCED REFRACTORY  
COATINGS AT THE MARQUARDT CORPORATION

SAMUEL SKLAREW

The Marquardt Corporation  
Van Nuys, California

## FURTHER DEVELOPMENTS IN REINFORCED REFRACTORY COATINGS AT THE MARQUARDT CORPORATION

### Introduction

Under Air Force sponsorship and over a period of about six years, The Marquardt Corporation has been actively engaged in developing systems of reinforced refractory coatings and devising techniques for their application.

These systems fall into two categories:

1. Refractory ceramic structures with metallic reinforcements embedded therein.
2. Metallic substructures, to one side of which reinforced refractory ceramic coatings are adfixed.

In the latter category, the nodes of the corrugated metallic reinforcement strip are spot welded to the substructure, thereby forming the attachment means.

Periodically, at the various meetings of the Refractory Composites Working Group, the evolution of these systems was discussed and illustrated. The majority of the attendees are familiar with the details. However, for the newcomers and those who wish to refresh their memories, it is suggested that the proceedings of the previous meetings of this group be reviewed and also the following WADC reports:

31 May	1956	TR 56-250	Unclassified
15 Aug.	1957	TR 57-577, Part I	Unclassified
15 Aug.	1957	TR 57-577, Part II	Confidential
28 Feb.	1959	TR 59-102, Part I	Confidential
30 April	1960	TR 59-102, Part II	Unclassified

The purposes of this paper are to bring the state of the art up to date, to discuss the potentials, and to point out areas for further exploration.

### Ceramic Development

Under our present contract, number AF 33(616)-8209, we have made improvements in the coating compositions, are exploring improved coating application techniques, and are making ready to prepare model test hardware for 4000°F plus service temperature with cyclic and/or extended service life.

Our best compositions, prior to the initiation of the present contract, were based on lime stabilized zirconia grain bonded with fluorophosphoric acid. These are excellent compositions. They are readily prepared, applied, and cured at 450°F to give hard, strong bodies capable of service to 4300°F. Fluorophosphoric acid is, however, a noxious liquid. The fumes attack the mucous membranes, which tends to make life in its presence a bit difficult. This, however, can be lived with if suitable precautions are observed. Many pieces of high temperature hardware have been prepared, such as plasma arc chambers, rocket nozzles, etc., which have performed very satisfactorily with these coatings.

New coatings, based on lime stabilized zirconia with bonding agents newly discovered, are a marked improvement over the fluorophosphoric acid bonds. Composites have been tested to 4725°F without deterioration during multiple test cycles totaling over one hour at 4700°F. Traces of glaze have appeared in the torched area distinguishing tested from untested panels. The thermal drop on a 1/4 inch thick refractory coupon is 11°F per thousandth of thickness at 4725°F front face temperature. Other benefits of these new type

compositions are greater compatibility with people, stronger and harder cured ceramics with lower shrinkage at temperature. Optimization of these formulations is currently underway.

In trying to cope with material surface temperatures in excess of 4000°F, one is confronted with a choice. He can try to find a material with adequate structural strength at temperature or else insulate a material with adequate structural strength at some lower temperature, so that the insulation provides thermal protection while the substrate provides structural adequacy. We have chosen to develop the latter approach. A second choice now faces us. We can go the route of utilizing a refractory metal as a substrate, employing a refractory metal reinforcing media and utilizing a comparatively thin refractory coating to insulate the substrate. Such a system can operate if suitable anti-oxidation coatings are used on the substrate and reinforcement, and if one is willing to operate at substrate temperatures of near 3000°F range. Unfortunately, reliability of such systems are of a low order. The alternate to the above route is the one we have chosen to follow.

If we can keep the substructure sufficiently cool to operate with steel, stainless steel or super alloys, we need no longer worry about anti-oxidation coatings for refractory metal substrates. Our only concern in this direction is to protect refractory metal reinforcing strip against oxidation. This is a simpler and more easily achieved goal because the reinforcement with its oxidation protective coating becomes completely encapsulated in the refractory ceramic insulating coating. Penetration of oxygen through such-a coating is relatively slow and so this coating forms a strong front line of defense around the reinforcement. The anti-oxidation coating can now function as a

strong, impervious second line of defense, increasing reliability of the system. It cannot be flaked or lost from the reinforcement through differential thermal expansion, because it is physically confined by the encapsulating refractory insulating coating.

We have investigated about twenty five dip coatings for the tantalum corrugated strip reinforcement we are presently using on N-155 substrate. Several have shown good promise. Chrome powder suspended in Nicrobrazo liquid, zirconia paint, and Phosphotherm, a proprietary phosphate glass were superior to the others tried. We plan to try siliconized refractory metal coatings including W-2 and Pfaudler's chromized coating as well as other dip formulations.

Refractory insulating ceramic coating application techniques have improved over the hand troweling method formerly used exclusively. We have discovered how to prepare thixotropic compositions which can be readily cast. The part with the attached reinforcement is placed in a mold which delineates the outline of the coating to be cast. The mold and part are mounted on a vibratory platform and the ceramic mix vibrated into the cavity. When the annulus is filled, the vibration is stopped and the cast is permitted to set up for several hours before removal of the mold. At present, the cast is air dried before being baked. We have a humidity drying and baking oven under construction which will be utilized for controlled curing when completed. Present curing temperatures are in the order of 300-450°F. We have started a series of differential thermal analyses to fix curing temperatures and times more accurately.

Under preparation is some model test hardware nose caps and leading edges. These should be ready in a few months. In the past, we have made and tested ramjet combustion chambers, leading edges for reentry vehicles, ceramic components for plasma chambers, rocket nozzles, ceramic tooling, linings for pebble bed heater ducting, etc. The majority of these items performed very well.

#### Future Work

We plan to optimize our present zirconia based compositions and to ultimately move into the plus 5000°F service range with thoria based compositions. If a way can be found to lighten the composite structure, without sacrificing strength, reliability, abrasion resistance and ease of formability, we plan to pursue such development. Improved reliability and extended service life and application to structural hardware on an enlarged scale is our goal.



COMPOSITE THROAT INSERT MATERIALS  
PERFORMANCE IN SUBSCALE ROCKET MOTORS

DON A. BECKLEY

Aerojet-General Corporation  
Sacramento, California

## TABLE OF CONTENTS

	<u>Page</u>
ABSTRACT . . . . .	ii
INTRODUCTION . . . . .	1
EXPERIMENTAL DETAIL . . . . .	2
RESULTS AND DISCUSSION . . . . .	2
CERAMIC COMPOSITES . . . . .	2
MIXED COMPOSITES . . . . .	4
LAMINAR COMPOSITES . . . . .	5
MICRO COMPOSITES . . . . .	6
MACRO COMPOSITES . . . . .	6
SUMMARY AND CONCLUSIONS. . . . .	7

### ABSTRACT

The performance of composite throat insert materials is discussed, when exposed to a 6000°F flame in a subscale rocket motor. Results from 15 test firings are included, with emphasis placed on defining the problem areas associated with the use of ceramic, laminar, mixed, micro, and macro composite material systems.

## INTRODUCTION

Aerojet General Corporation has for the past year been conducting rocket motor firing evaluations of composite throat insert materials capable of withstanding theoretical propellant flame temperatures in excess of 6000°F. The material development efforts have been conducted in cooperation with several manufacturing laboratories. In this report, the results of subscale Material Evaluation Rocket Motor (MERM) tests are disseminated, with emphasis placed upon characterizing the State-of-the-Art and problems encountered in utilizing each type of composite material.

This work, sponsored by the POLARIS program under contract number LMSC 18-2211, is scheduled for presentation at the fifth meeting of the Refractory Composites Working Group of the Aeronautical Systems Division.

## EXPERIMENTAL DETAIL

The MERM characteristics and programmed test conditions are tabulated as follows:

- (1) motor type - end burning
- (2) propellant type - nitroplasticized/polyurethane
- (3) theoretical flame temperature - 6180°F
- (4) chamber pressure - 800 to 1000 psi
- (5) duration - 60 seconds
- (6) propellant consumed - 70 pounds per test
- (7) throat type - see Figures 1 - 3 (P/N 1-306428, 0-331516 and 1-314376).

## RESULTS & DISCUSSION

The detailed test results are appended as TABLE I and discussed by reference to the type of composite, firing number and insert material.

### CERAMIC COMPOSITES

SY-2 - The TaC insert fabricated by plasma arc spraying was reported by the vendor, General Telephone and Electronic Laboratories, to be a combination of TaC and Ta<sub>2</sub>C due to decarburization of the TaC powder in the plasma. Despite the mixed carbide system, the insert appeared to fire well until 28.8 seconds, when it is believed that degradation of the asbestos-epoxy back-up material permitted ejection of the insert. Use of plastic insulation type back-up material was dictated by the desire to

minimise the thermal gradient and hence the thermal shock potential on the insert. Review of the firing movies indicated no pyrophoric tendency of the TaC in this fuel, nor tendency to thermal shock, in this relatively (1/4-inch) thin section. But this firing does illustrate the need for a suitable high temperature insulation material that will not degrade under heat.

It has been suggested, but not tried, that laminates of TaC which are relatively poor thermal conductors be used as its own insulation.

SY-37 - Firing of a TaC insert (also from GT&E) with a large ATJ graphite heat-sink resulted in a spalling thermal-shock type of failure. The difference in insert performance, when compared to SY-2, is attributed to the influence of a heat-sink versus insulating type back-up material.

SY-32 - The  $TiB_2$  insert (from GT&E), fabricated by plasma arc spraying, is an example of the thermal shock problem which must be avoided in using brittle inorganic materials. This insert ejected incandescent particles of  $TiB_2$  from ignition until it was completely consumed at 14 seconds. The use of National Carbon's C-6 cement was an attempt to provide a moldable back-up material for inserts, thereby minimizing assembly and fit-up problems. Its use was not successful.

SY-44 - Despite the conclusive results in Table I labeled, "insert completely eroded," this firing of HfC (fabricated by Firth Sterling) is regarded as inconclusive, since neither the physical characteristics nor fabrication technique could be adequately documented. The problem of know-

ing "what" composite is being tested cannot be overly emphasized, since in most cases the raw materials and fabrication technique provide the only insight to a subsequent development sequence.

#### MIXED COMPOSITES

SY-18, 20 and 49 - These firings represent an approach to minimizing the thermal shock tendencies of carbides by hot pressing them with graphite powder. The fabrication technique, involving a gradation in the respective amounts of carbide and graphite at various depths below the flame surface, has been under development by the Carborundum Company. Although the inserts did not display thermal shock cracks, they did erode more than standard graphites in this propellant.

The TaC-ZrC-C (graphite) insert eroded more than its TaC-C (graphite) counterpart and introduces the question - Do the 3/1 and 4/1 TaC/ZrC material combinations actually possess melting points which are greater than TaC? As part of the answer, AGC-Azusa has received TaC-ZrC-C (graphite) samples from Carborundum for determination of the melting point.

SY-19 - With an addition of ZrC (30% by weight) less erosion resistance was exhibited than that of the parent ZT type graphite developed by the National Carbon Company. This statement serves as a generalization for all additives tested thus far although, an additive which is capable of minimizing graphite chemical reactivity is still being sought.

SY-16 - Mix 6214 (Kennametal) is an example of a carbon exchange metal. In theory at firing temperatures, two lower melting materials (that

are fabricable) revert to higher melting materials as shown in the following reaction -



Under 5500°F propellant conditions, the concept appeared sound. A post-fired metallurgical examination disclosed that the reaction had proceeded partially through the insert from the flame surface.

Under 6180°F flame conditions, the ratio of refractory product materials to less refractory reactant materials was not great enough and melting occurred. To alleviate the problem, the Kennametal Corporation altered the material ratios, initiated the reaction by pre-sintering and incorporated an additional degree of thermal shock resistance by infiltrating the void spaces with copper. This new material designated Mix 6707 Cu is scheduled for testing.

#### LAMINAR COMPOSITES

SY-36 and -38 - Tungsten backed with TaC on the OD and TaC backed with tungsten on the OD represent two laminar material systems. Neither approach fired successfully; a list of potential causes of failure is listed as follows:

- a. With TaC on the OD the tungsten is denied a heat-sink; it is forced to operate at higher temperatures and ultimately suffers erosion.
- b. Conversely, with tungsten on the OD the TaC is provided a heat sink and an unnecessarily large thermal gradient.
- c. However, a more probable cause has been provided by studies of the fabricator, General Telephone and Electronic Laboratory. In an



arc image furnace at 5400°F a third phase is formed during a three minute exposure when tungsten powder surrounds a larger TaC particle. At 5800°F nearly complete W-TaC solution occurs in one minute producing a product identified as  $(W, Ta)_x C_y$ .

#### MICRO COMPOSITES

SY-73 - SY-73 typifies a group of firings which featured the addition of carbides to a hot pressed tungsten matrix. In this case the tungsten was 88% of theoretical density. In all instances, carbide additions increased the crack sensitivity, compared to unalloyed tungsten, and the tendency for carbide tungsten reactions were observed in the post-fired matrix when viewed on a metallograph. Purposeful inclusion of carbides has been discontinued.

#### MACRO COMPOSITES

SY-24 - The Armour approach to utilization of composite materials incorporates a tungsten wire matrix with a vacuum infiltration of carbide particles into the interstices. The macro composite mixture is then hot pressed in a graphite die. The firing results with less refractory carbides, ZrC and TiC (in 5500°F fuel), appear promising although erosion in the ZrC instance is regarded as excessive. Future firings will incorporate TaC-W and HfC-W composites.

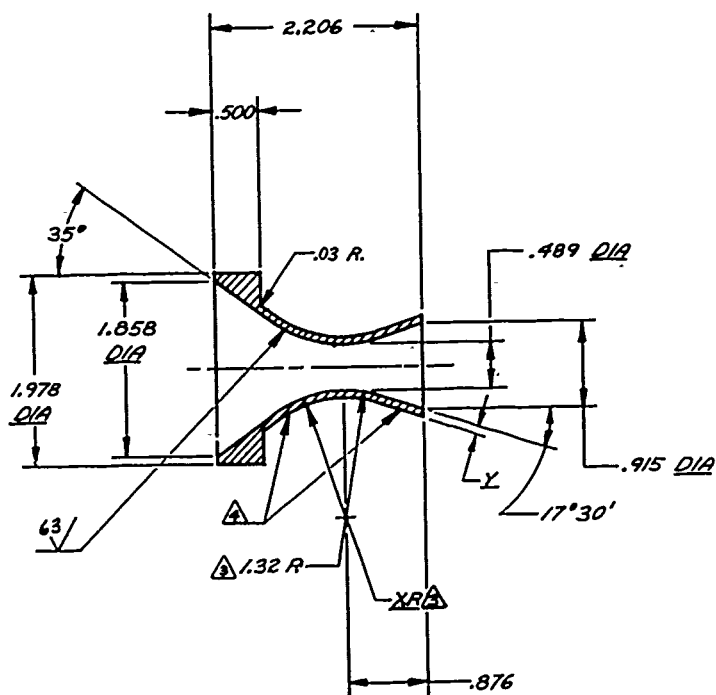
SY-78 and 80 - The use of a tungsten metal honeycomb to restrain a high temperature carbide filler and improve its shock resistance fired successfully with 5500°F propellant. However, when exposed to the added

thermal loading and flame chemistry of the 6200°F fuel, both TaC-W honeycomb and NbC-W honeycomb exhibited excessive erosion.

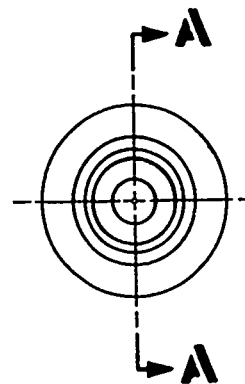
#### SUMMARY and CONCLUSIONS

Based upon a requirement of minimal erosion, none of the composite insert materials tested to date have displayed a value of utility when used with this propellant. The principle problem appears to be thermal shock or the means to overcome thermal shock, which creates a material system that is chemically reactive with itself (W-TaC reactions) or the propellant at high temperatures.

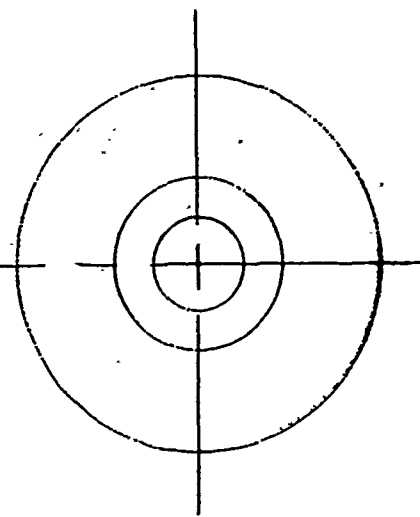
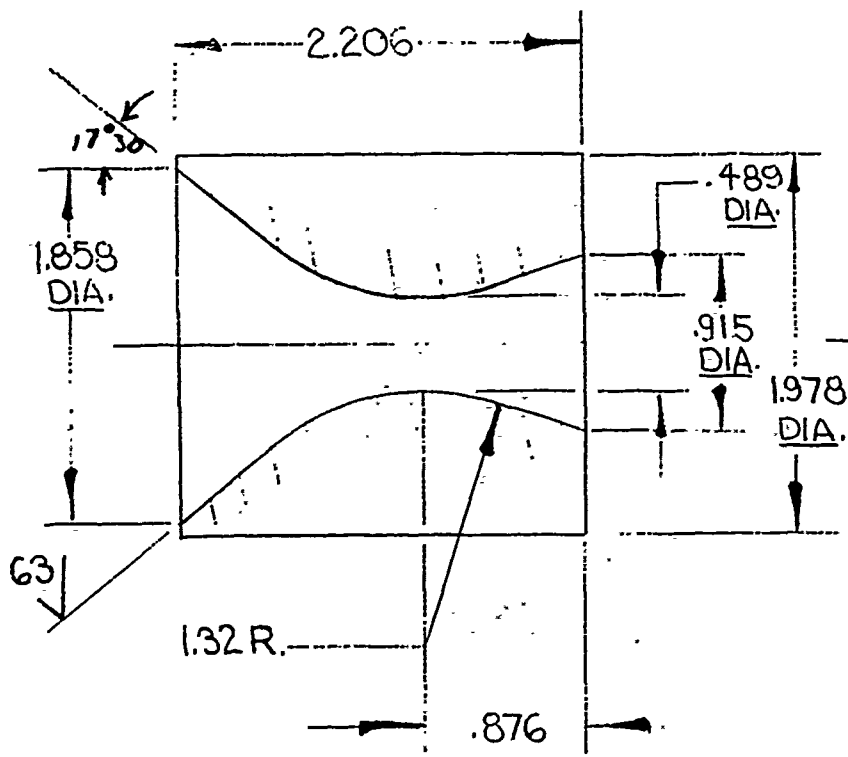
The reactivity of thin stoichiometric carbide coatings with combustion products is not established, partially due to the back-up material and design problems inherent in testing thin coatings.

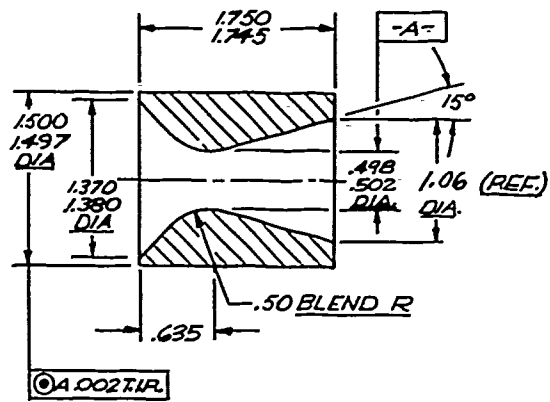
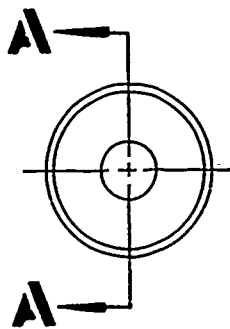


**SECTION A-A**



PART NO.	XR	Y
-2	1.26 R	.060
-4	1.20 R	.120
-6	1.07 R	.250
-8	1.00 R	.320
-10	0.75 R	.570





SECTION A-A

TABLE I

MEMO

## Ceramics and Composites

## 1st STAGE

Firing No. D-50131-	HTC/Vendor	Configuration/ Thickness	Diameter (in.) Initial Final	% Area Change	Erosion Rate (mil/sec)	Pressure (psig) Max.	Duration (sec.)	Pressure Loss/ Time of Loss	Firing Purpose	Result and Comment (All P-T Curves Regressive) Typical
2	Tac/UT&E	O-331516/ Astroble Epoxy	.188	-	-	800	24.8	-	Eval. Tac p. 4e.	Insert ejected 28.8 sec.
16	6214 mix/ Kennametal	1-306428	.176	.702	1.7	1095	450	67	Compare P/N 8 (5500- 6180F)-O eros-f)	Irregular erosion; melting
18	Tac-ZrC-C/ Carborundum	1-306428	.178	.777	2.0	1040	478	74	Evaluate S.P.O. car- bide material	Irregular erosion;
19	30% ZrC-C (zt)/ Nat. CarCo	1-306428	.170	.702	1.7	1070	309	67.5	ZrC protective film	ZrC not beneficial; oval shaped erosion
20	NbC-C/ Carborundum	1-306428	.178	.660	1.4	1010	365	65.6	Evaluate S.P.O. car- bide material	Moderate even erosion
24	ZrC - W wire/ Armour Research	1-311376	.500	.591	.70	825	304	66.	Eval. wtl system @ 6200F compare 5500F	Jagged erosion; thermal shock not evident
32	TiB <sub>2</sub> /GT&E	O-331516-6/ Astrolite C-6	.185	-	-	855	132	14.	Eval. TiB <sub>2</sub>	Insert spalled & ejected; probable failure of C-6 back-up also.
36	W-Tac on OD/ GT&E	O-331516-6/ Astrolite C-6	.185	-	-	940	206	32.	Eval. laminar composite	One half insert eroded; probable failure of C-6 back-up
37	Tac/UT&E	O-331516-4/ ATU	.185	.769	2.0	823	206	70.	Eval. Flamarc Tac	Insert spalled during firing.
38	W-Tac on ID/ GT&E	O-331516-6/ C-6	.185	.634	2.2	978	240	34.	Eval. laminar com- posite	Insert tipped in holder; probable failure of back-up; throat eroded.
44	HFC/Firth Sterling	1-311376/ ATU	.195	-	-	735	103	97.	Eval. pressed and sintered	Insert completely eroded; 55% pressure loss in 10 seconds.
49	Tac-C/ Carborundum Co.	1-306428/ Astrolite	.184	.695	1.44	865	295	73.	Evaluate S.P.O. material	Severe and very irregular erosion
73	90W 107AC (88%)/ Haynes Stellite	O-331516-4/ ATU	.184	.522	16.3	905	688	58.	Eval. carbide addi- tion to HP tungsten	Upstream area of throat ejected during firing; downstream still in place.
78	Tac-W (honeycomb)/ AVCO	1-306428	.185	.767	111.0	904	153	76.	Evaluate S.P.O. carbide material	Severe erosion; chipped-out during firing @ exit section and burned through behind insert
80	CbC-W (honeycomb)/ AVCO	1-306428	.193	.889	2.5	904	153	82	Evaluate S.P.O. carbide material	Severe irregular erosion; pulling out of carbide indicating bond failure; W-carbide chemical reactions during firing;

COMPOSITE MATERIALS REPORT

R. H. HERRON

Bendix Corporation

South Bend, Indiana

## COMPOSITE MATERIALS REPORT

The work at Bendix since the last working group meeting has been concentrated in two principal areas. One is further development of the tungsten base composites which exhibit the microtranspiration cooling effect and the other is further development and testing of the chromium composite materials. Preliminary work in both of these basic compositions was reported in the last working group meeting.

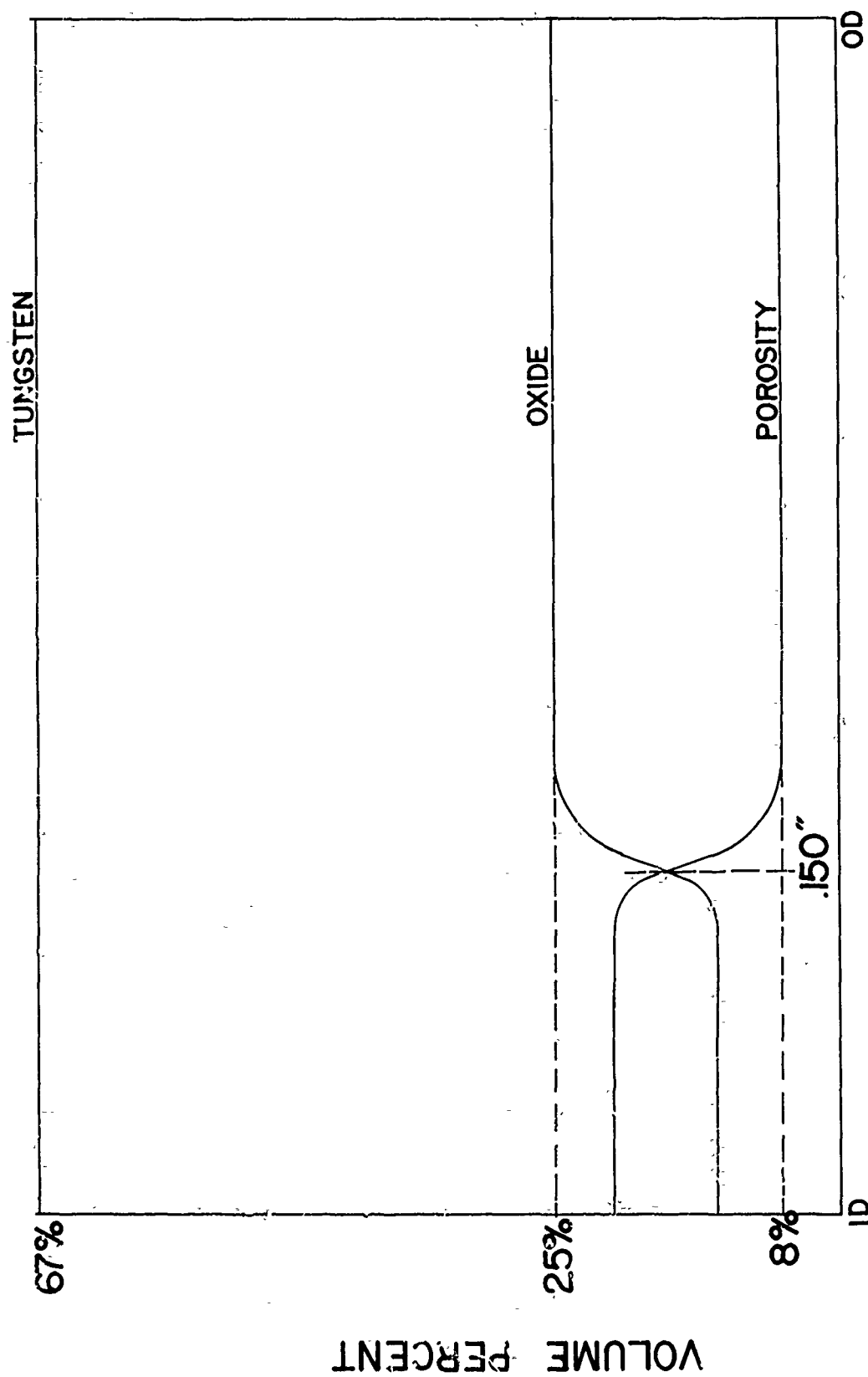
### Tungsten Composite Materials

The work with the tungsten composite materials has included further compositional development, further experimental evaluation in solid propellant rocket nozzles, and additional theoretical analysis on the potential heat absorption effect of this type of structure. The principal basis for the microtranspiration theory is shown in linear analysis of Figure 1. This analysis was made from a tungsten-beryllium oxide composite throat insert fired on a second-stage Minuteman rocket motor. The analysis shows the loss of the oxide to a depth of approximately .150" and a corresponding increase in the porosity of the microstructure with a negligible reduction in the tungsten matrix material. The analysis also shows the rapid change from an area of oxide loss to an area of no oxide loss indicating removal of the oxide phase as a gaseous phase rather than a liquid phase.

In the area of compositional development, two important factors have been determined with the microtranspiration materials. The first of these was that aluminum oxide could be substituted on a volume basis for the beryllium oxide with equivalent test results and equivalent loss of the oxide phase. This demonstrates that the microtranspiration mechanism functioned with both oxide materials. Aluminum oxide was introduced into the composition after formulating the microtranspiration hypothesis which would dictate that the melting point of the oxide is secondary to its potential energy absorption. The fact that a lower melting oxide has functioned as well as the higher melting beryllium oxide is, perhaps, the best experimental evidence that a cooling mechanism is effective in these tungsten composite materials.

The other important development from a compositional standpoint is that a catalyst is required to create the oxide loss noted in the tungsten-aluminum oxide or tungsten-beryllium oxide materials. Figure 2 shows the microstructure of a tungsten-aluminum oxide composite after testing in identical conditions. One composition contained the catalyst and the other composition did not. A copper infiltration process has been used after testing and prior to mounting both materials so as to determine the void spaces and continuous porosity present in the microstructure prior to metallographic preparation. The dark areas in the photomicrograph are





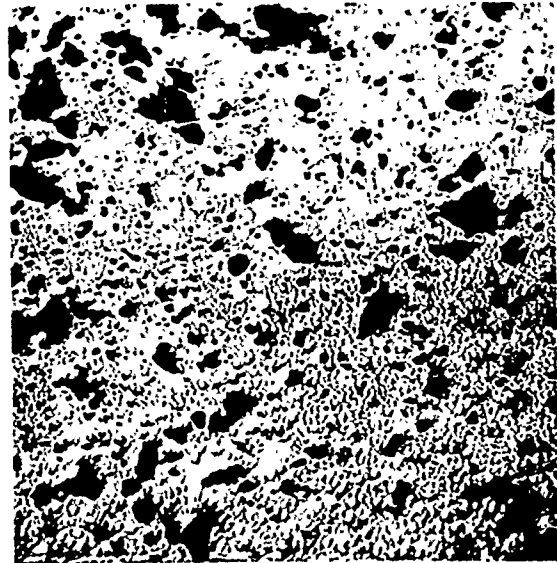
LINEAR ANALYSIS OF TUNGSTEN COMPOSITE  
(AFTER FIRING)

Figure 1.



WITH CATALYST

1000 IN. -1



WITHOUT CATALYST

## EFFECT OF CATALYST ON OXIDE LOSS OF A TUNGSTEN COMPOSITE

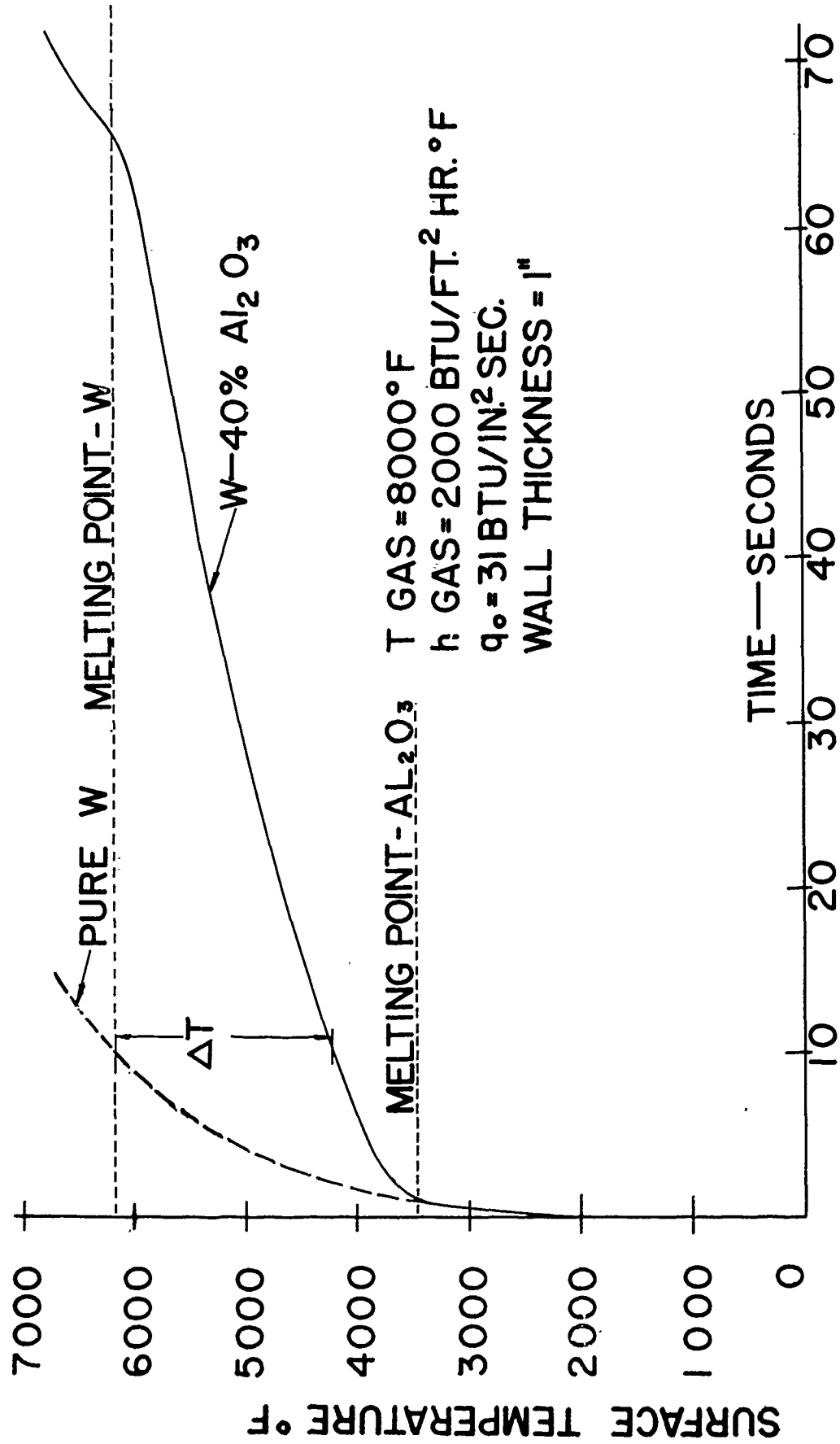
the aluminum oxide grains and the orange colored areas represent the void spaces (copper infiltrated). These photomicrographs clearly indicate the loss of the oxide phase when the catalyst is present and the retention of this phase when the catalyst is absent.

In order to determine the potential energy absorption of the proposed microtranspiration cooling mechanism, the work from Ingram & Associates at the University of Chicago\* was studied to determine the chemical species present in tungsten-oxide systems at high temperatures. Ingram's work was extrapolated to 5500°F from 4300°F, and at this temperature it was determined that the equilibrium species of a tungsten-alumina system include aluminum metal 49% and oxygen 35% which indicates the degree of dissociation of the oxide in this temperature range. From a knowledge of the species present, the potential capabilities of a tungsten-aluminum oxide composite to absorb heat during a rocket firing were calculated. Using this data, a heat transfer analysis was made and the results are shown in Figure 3. The assumptions used in this analysis are indicated in the figure. This analysis shows that a tungsten-aluminum oxide composite material utilizing the microtranspiration cooling mechanism can survive an 8000°F flame temperature firing for over 60 seconds where a pure tungsten material would reach its melting temperature in slightly over 10 seconds.

As mentioned previously both the tungsten-aluminum oxide and the tungsten-beryllium oxide composite materials have been successfully tested in solid propellant nozzle inserts. Table I summarizes the testing with these materials and lists the conditions of the various tests. As indicated in this Table, the tungsten-beryllium oxide material (Compound 2410-135) has received more extensive testing than the tungsten-aluminum oxide (Compound 3870-1). Microscopic examination of these tests has indicated oxide loss similar to that illustrated in the linear analysis of Figure 1. The depth of oxide loss has been dictated by the thermal environment of the particular test. The oxide loss in the inserts containing beryllium oxide has not led to any toxic air contamination. Air samples were taken on all full-scale tests and the maximum beryllium content was less than one-fiftieth of the allowable short time limit established by the A.E.C. The test conditions listed in Table I are not severe enough to determine the effectiveness of the microtranspiration mechanism, since pure tungsten materials have survived most of these test conditions without erosion. These tests do indicate the ability of the tungsten composite materials to withstand present propellant conditions. The theoretical analysis on the potential heat absorption of the microtranspiration mechanism discussed above indicates the ability of the tungsten composite material to withstand more severe test conditions than can be tolerated by pure tungsten material.

The listing of these successful tests is not meant to imply that all tests with these materials have been successful. Structural failures have occurred in several tests. The importance of the successful tests is the fact that these materials possess

\*Ingram and Drowart, International Symposium On High Temperature Technology, p. 219, McGraw-Hill, 1960.



THROAT MATERIALS COMPARISON IN HYPOTHETICAL EXTREME ENVIRONMENT

Figure 3.

TABLE I

ROCKET MOTOR TEST RESULTS

<u>Throat Material</u>	<u>Propellant</u>	<u>Throat Diameter (In.)</u>	<u>Flame Temperature (°F)</u>	<u>Chamber Pressure (PSI)</u>	<u>Test Duration (Sec.)</u>	<u>No. Of Tests</u>	<u>Results</u>
2410-135*	Thiokol	7.40	5500	600	55	1	No Erosion
2410-135	Thiokol	4.30	5500	600	60	5	No Erosion
2410-135	Thiokol	.880	5500	500 & 800	40	3	No Erosion
2410-135	Aerojet	4.30	5500	500	57	3	No Erosion
2410-135	Hercules	3.51	6700	280	62	2	No Erosion
2410-135	Grand Central	.57	5000	975	9.9	1	No Erosion
2410-135	Hercules	1.10	6700	274	62	2	No Erosion
2410-135	Hercules	.75	6700	500	40	3	No Erosion
2410-135	Rohm & Hass	.530	6200	900	9.5	1	No Erosion
3870-1**	Hercules	.75	6700	500	40	5	No Erosion
3870-1	Rohm & Hass	.534	6200	800	9.9	1	No Erosion

\*W - BeO

\*\*W - Al<sub>2</sub>O<sub>3</sub>

adequate structural properties when properly supported and the nozzle is properly designed. All of the materials currently under investigation for use as inserts with higher temperature propellants are more brittle than the tungsten inserts currently in use. If these materials are to be successful, more attention will have to be given to better definition of design parameters and development of design concepts which will minimize stresses in the throat inserts.

### Chromium Composite Material

The chromium composite material, as reported in the last working group meeting, is composed of chromium with one of the Group II oxides. The principal composition evaluated to date is the Bendix Chrome-30 material which is composed of chromium and magnesium oxide. The improved erosion resistance of this material over pure chromium was reported at the last working meeting. This improvement is believed due to a modification of the oxide protective layer formed on the surface of the material when exposed to a high temperature oxidizing environment. This modification eliminates the eutectic between chromium oxide and chromium and enhances adherence of the protective coating.

The principal improvements obtained with this material since the last working group meeting have been achieved through hot working of the sintered material. Through the cooperation of Wright Field personnel and using Wright Field equipment, the Chrome-30 material was extruded at temperatures of 2200° F and extrusion ratios ranging from 6:1 to 12:1. The properties obtained from the extruded material are shown in Table II. The most significant improvement in the physical properties after extrusion was the ductility obtained in tensile test specimens. Figure 4 shows a room temperature stress-strain curve of a material extruded at a 10:1 area ratio. No special precautions were used during the extrusion to protect these materials from contamination and the tensile bar was tested as machined. The degree of ductility obtained in this material at room temperature after extrusion was important, but even more important with a chromium base material is the ductility after reheating in air. Figure 5 shows the deflection versus maximum fiber stress in a simple bend test of the extruded material compared to the deflection obtained on the same material after reheating in air to 1800° F for one hour. This data indicates that ductility has been achieved in a chromium base material without special precautions, such as sheathing during the processing, using a high purity grade chromium raw material, or special surface removal and that this ductility is retained after reheating to a temperature which normally causes embrittlement in pure chromium.

Long time oxidation tests have been conducted on extruded Chrome-30 material and the results of these tests are shown in Figure 6. The improved oxidation resistance of this material over pure chromium is attributed to the modification of the protective coating which is formed on the surface of the material when exposed to temperatures in the order of 1800° F in air. The modified coating not only reduces the rate of oxidation in the lower temperature range, but greatly improves the coating adherence which is a major problem with pure chromium materials above 1600° F.

**TABLE II**  
**PROPERTIES OF CHROME-30**

Tensile Strength, Extruded Bar . . . . .	56,500 psi @ 72° F
(Extrusion Ratio 10:1)	23,000 psi @ 1800° F
	4,800 psi @ 2500° F
Elongation, Extruded Bar Over 1-1/4" Length. . . .	15% @ 72° F
	19% @ 600° F
Tensile Strength, Forged . . . . .	35,000 psi @ 72° F
	18,000 psi @ 1800° F
	6,300 psi @ 2600° F
	1,800 psi @ 3100° F
Hardness As Extruded . . . . .	R <sub>B</sub> 81
Density . . . . .	0.238 lbs/cu. in.
Oxidation, 100 Hours @ 2000° F . . . . .	0.003 gms/cm <sup>2</sup> wt. gain
Conductivity, Thermal . . . . .	35 BTU/hr/ft <sup>2</sup> °F/ft @ 78° F
Expansion @ 0-1200° F . . . . .	4.1 x 10 <sup>-6</sup> in/in ° F
1200-2000° F . . . . .	5.2 x 10 <sup>-6</sup> in/in ° F
Electrical Resistivity. . . . .	4.8 x 10 <sup>-5</sup> ohm-cm
Emissivity, 1200° F And Above . . . . .	0.90

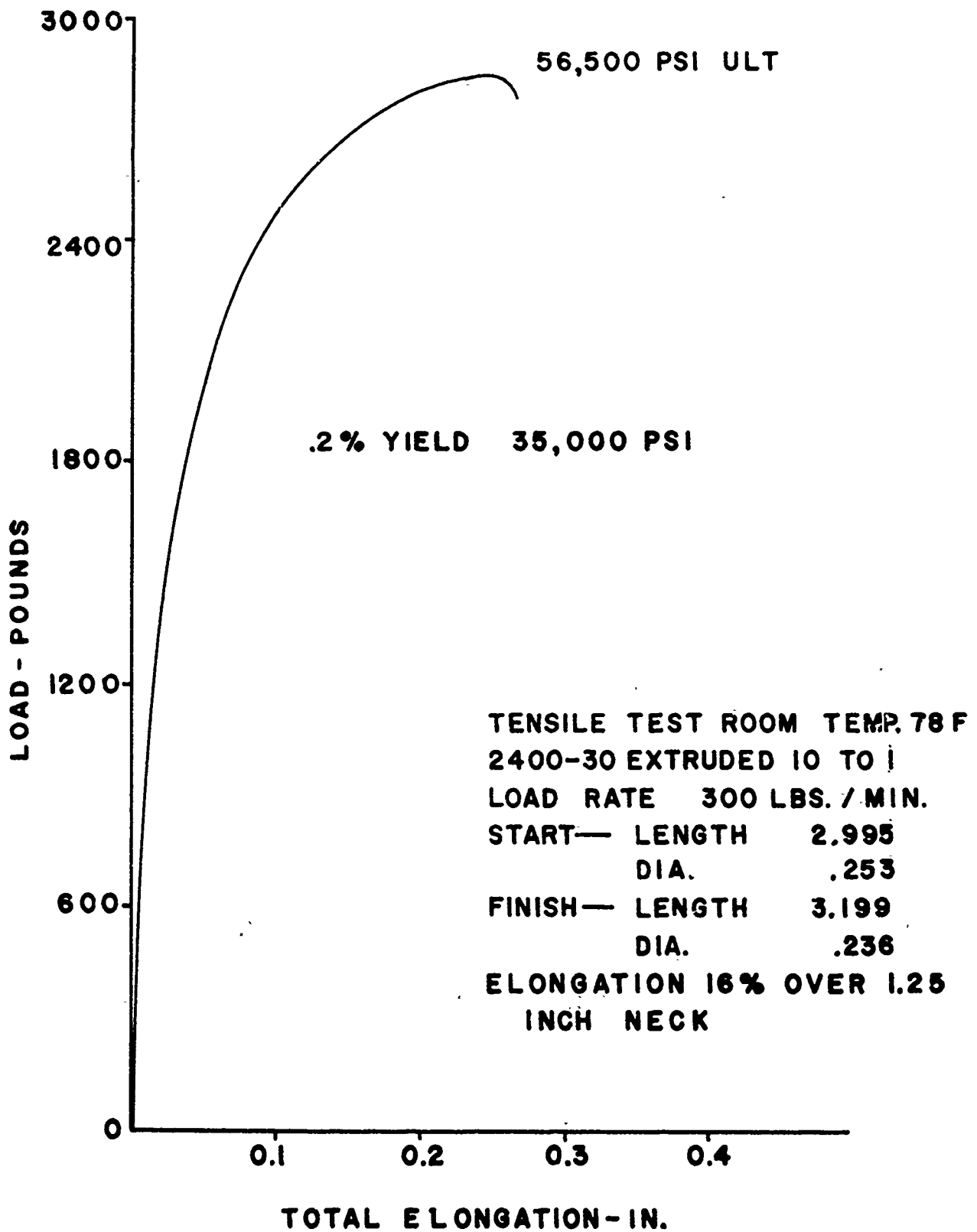
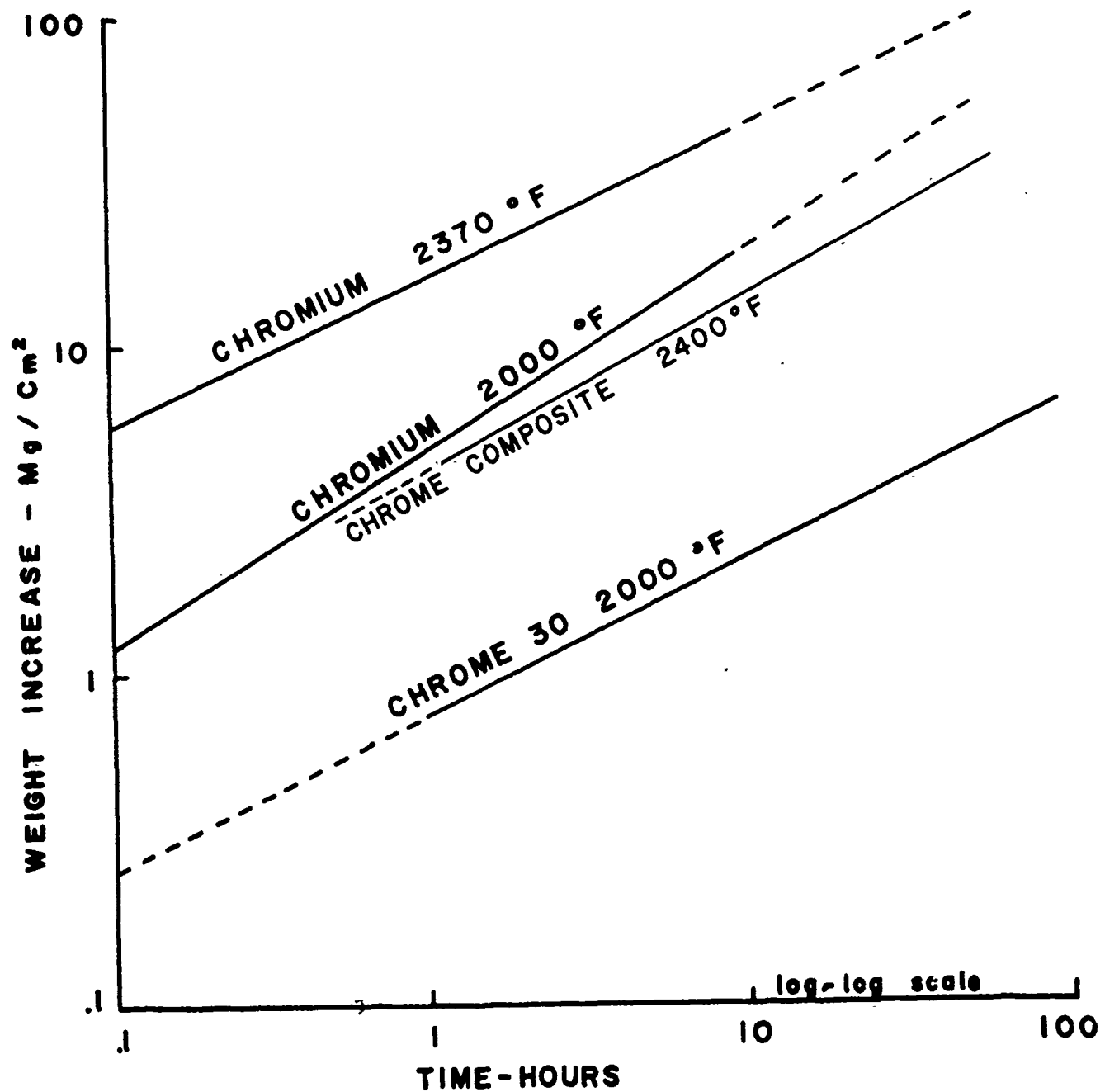


Figure 4. Tensile Test Of Extruded Chrome-30.





## OXIDATION WEIGHT GAIN

Figure 5. Bend Test Of Chrome-30.

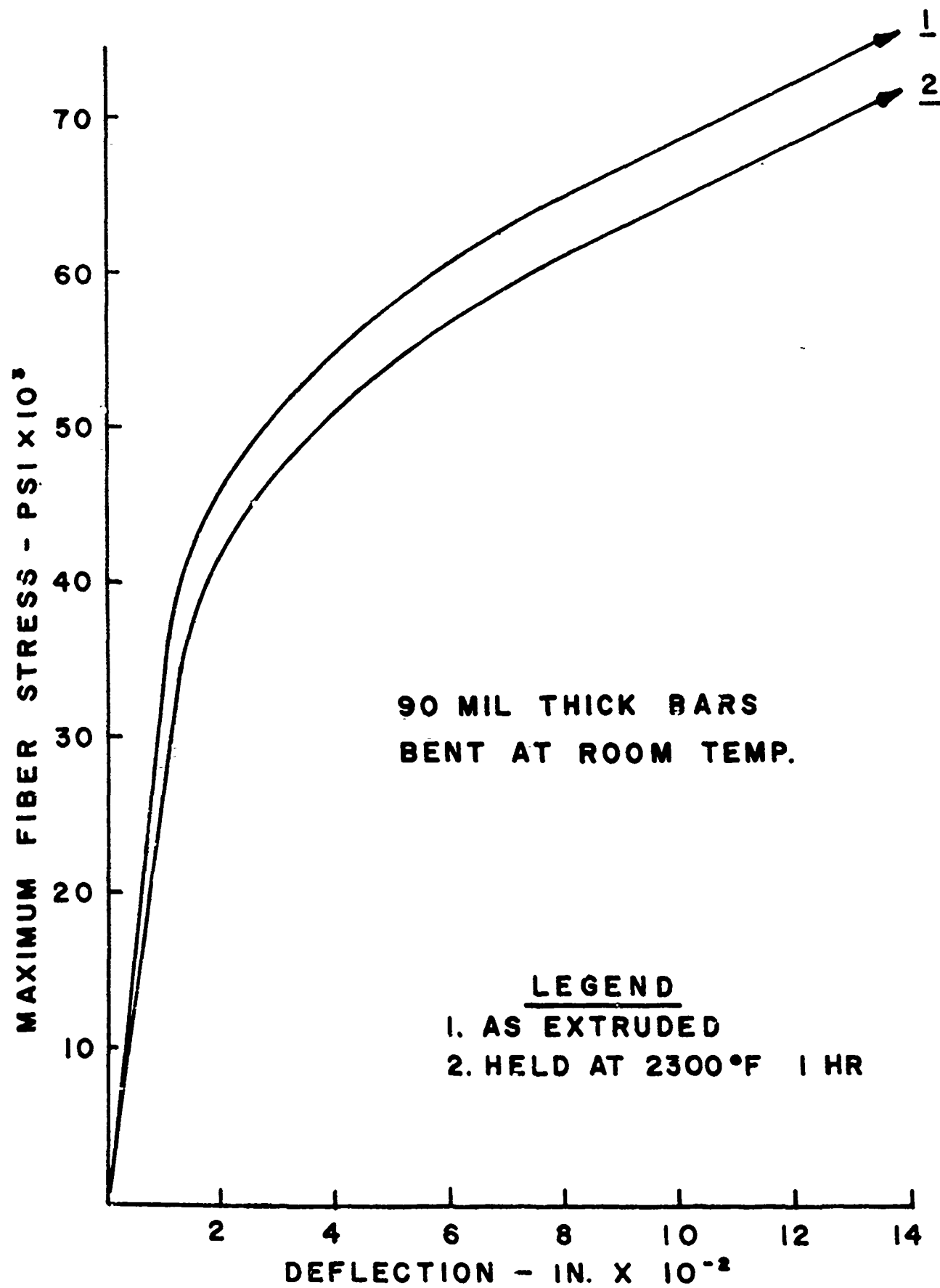


Figure 6.

In addition to the extrusion work previously discussed, Chrome-30 material has been extruded, forged, and rolled both hot and cold (600° F). The data obtained from a material which was extruded at a ratio of 10:1 at 2200° F hot forged 50%, hot rolled 50% and cold rolled at 600° F for 50% is presented in Table III. This data was obtained from the limited number of test samples and is not considered statistically significant. It does indicate, however, the potential which can be obtained with this material by cold working and heat treating processes.

**TABLE III**  
**EFFECT OF WORKING AND HEAT TREATMENT OF CHROME-30**

<u>Condition</u>	<u>Yield*</u> <u>Strength</u> <u>(PSI)</u>	<u>Ultimate*</u> <u>Strength</u> <u>(PSI)</u>	<u>Deflection</u> <u>Inches</u>
As extruded	31,000	51,000	.20
As rolled 50% @ 600° F	-	83,000	0
Rolled and annealed at 1850° F for 1 hour in air	40,000	100,000	.20

\*Maximum fiber stress in bend sample - .1" x .3" - span length 1".

CERAMIC COATING CONSIDERATIONS FOR  
REACTOR COMPONENTS

HENRY LEFORT

Lawrence Radiation Laboratory, University of California

Livermore, California

## CERAMIC COATING CONSIDERATIONS FOR REACTOR COMPONENTS

Henry Lefort

Lawrence Radiation Laboratory, University of California  
Livermore, California

Research and development work on Project Pluto at Lawrence Radiation Laboratory is largely classified. The details of development work on materials, techniques of fabrication and the operating conditions (temperatures, etc.) for reactor components cannot be specifically discussed on an unclassified basis. Consequently, only general considerations for coating reactor components can be made in this presentation.

The ceramic group at Lawrence Radiation Laboratory is presently engaged in studying many basic and developmental problems of ceramic application in elevated-temperature nuclear reactors. One particular area of interest is concerned with ceramic or oxide coatings for protection of BeO-UO<sub>2</sub> reactor components. Specifically, it is desired to protect the BeO from moisture attack at high temperatures and pressures. Attack of this type is to be expected if a reactor operates in air at high temperatures.

Fuel elements based on the BeO-UO<sub>2</sub> composition are being considered for use in many new high-temperature reactor experiments. Application may be found in the nuclear propulsion field, for example, Project Pluto and the now defunct Aircraft Nuclear Propulsion project. Pluto is a nuclear ramjet engine for a low-flying, Mach three, air-breathing missile.

In considering the use of BeO in moderators or in fuel-moderator combinations, it becomes necessary to estimate the operating conditions which

may be encountered. It is conceivable that a hollow cylindrically shaped piece of dense  $\text{BeO-UO}_2$  will be exposed to temperatures well in excess of  $2000^\circ\text{F}$  for long periods of time and possibly at high pressure in moist air. McKisson<sup>1</sup> indicated that the  $\text{BeO-H}_2\text{O}$  interaction will not limit the feasibility of operation of an open-cycle  $\text{BeO}$ -moderated power reactor at passage surface temperatures up to  $1560^\circ\text{F}$ . At higher temperatures, however, volatilization of  $\text{BeO}$  in the presence of water vapor may become important enough to consider methods of minimizing it.

A ceramic coating for a  $\text{BeO}$  body must first of all meet the neutronic requirements (i. e., low absorption cross section). It should have significantly better resistance to water attack than  $\text{BeO}$ . Consequently, for some reactor applications,  $\text{SiO}_2$  and the silicates will not be satisfactory for use due to their soluble nature at high temperatures in high gas flows.

Consideration must also be given to thermal expansion match, chemical stability, and crystalline stability as compared to  $\text{BeO}$ . The coating should have a fairly close thermal-expansion match to the  $\text{BeO}$  body, should be resistant to chemical reaction with the gas flow or with the  $\text{BeO}$  substrate, should have low vapor pressure, and should not exhibit phase changes which might disrupt its adherence to the substrate. One soon finds that there are only a few materials that may meet such coating requirements.  $\text{Al}_2\text{O}_3$  and  $\text{ZrO}_2$  are two which may be satisfactory because of their low cross sections and refractory nature.

The next question is, how does one apply such materials to obtain a dense inert coating on a  $\text{BeO}$ -base substrate. In many cases the shape factor (such as a small hollow cylinder) will rule out any type of flame-spray method. However, there still remain such methods as slip dipping, vapor deposition, vacuum deposition, vapor transport, and such chemical reactions as

the pack cementation process. If one is concerned with production amounts (perhaps several thousand pieces or more), the coating method may be a limiting factor.

The temperature of coating application is important regardless of the application method. There seems to be no lower limit, but the upper limit is governed by the extent of the coating-BeO reaction. If at too high a temperature for too long a time, the BeO may penetrate through to the coating surface and be available for water attack. As an example, if  $\text{Al}_2\text{O}_3$  were slip-dipped on and fired to a dense or vitreous coat, then a beryllium aluminate such as chrysoberyl ( $\text{BeO} \cdot \text{Al}_2\text{O}_3$ ) could form at a maturing temperature slightly above  $3100^\circ\text{F}$ . Young<sup>2</sup> has shown that this compound is also subject to moisture attack.

Coating application methods such as vapor deposition of  $\text{Al}_2\text{O}_3$  from a reaction of anhydrous  $\text{AlCl}_3$  with  $\text{H}_2$  and  $\text{CO}_2$  are described by Powell et al.<sup>3</sup> Since such a reaction can take place near  $1900^\circ\text{F}$ , it seems possible that the formation of beryllium compounds within the coating material could be eliminated. However, such coating adherence may be questionable. That is, one could expect more mechanical adherence than chemical-bond adherence with this method. Consequently, spalling may take place more readily with a slight thermal mismatch, or with a phase change in the coat.

Some aspects of the problems involved in coating BeO-base ceramic components have been considered. A few advantages of a coating for BeO are:

1. By using a uniform thin coat the smallest weight and volume of foreign material is introduced into a reactor.
2. The coating may protect against other corrosive vapors or conditions.

3. Coatings, especially of the simple oxide type such as  $\text{Al}_2\text{O}_3$ , can be fairly easily included in a production step when manufacturing large numbers of pieces.

4. Application can be made to selected areas, and more than one type of coating can be applied to one piece or component if conditions require it.

#### REFERENCES

<sup>1</sup>R. L. McKisson, "An Evaluation of the Beryllia-Water-Vapor Reaction in an Open-Cycle Air Cooled Reactor," J. Nuclear Materials 2 (1959)

p 26.

<sup>2</sup>W. A. Young, "The Reactions of Water Vapor with Beryllia and Beryllia-Alumina Compounds," J. Phys. Chem. 64 (1960)p 1003.

<sup>3</sup>C. F. Powell, I. C. Campbell, and B. W. Gonsér, Vapor Plating, John Wiley and Sons, Inc., New York, 1955, 158 pp.



COMPOSITE PLASMA DEPOSITIONS

ROBERT UNGER

Plasmakote Corporation

Culver City, California

A coating is one of the many possible composite structures. A graded coating consists of two or more components, either metallic or non-metallic, whose proportions vary continuously according to a preselected pattern from the substrate to the outer face.

The principal objectives in producing a graded coating as compared to a monolithic or single component coating are improved thermal shock characteristics and therefore increased adherence levels. Once the base material and operating environment over the temperature range of interest have been established, the proper thermal expansion of the desired coating can be produced by gradation techniques. A smooth transition is desired for maximum structural integrity.

The initial step in producing a graded coating is to apply a suitable metal undercoating to the substrate whose coefficient of expansion closely matches that of the base material.

Common undercoating materials would include the lower melting nickel-chromium base alloys where suitable, as well as molybdenum or tungsten for more refractory applications. Initial gradation investigations were directed towards producing acceptable systems for thin tubular wall regeneratively cooled, liquid rocket engines. It has since been expanded to include dense graphite shapes as well.

The actual method for producing the gradation zone in a composite coating structure is straightforward. For example, to produce a smooth transition from a nichrome base to a stabilized zirconia outer insulating layer two to five discrete mixtures are deposited in a transition zone. The initial mixtures contain large volumetric proportions of the metal rich structure. The final passes are deposited with the materials present in approximately inverse proportions to those previously laid down. However, it has been found that the "as sprayed" composite material differed greatly from the pre-mixed powder feed. In order to resolve the problem of determining the percent of oxide and metal that deposits from a feed of known proportions, semi-quantitative spectrographic analysis determinations were run with a series of mixed powders. It should be pointed out that while several methods exist for producing suitable cermet powders for this spray purpose, no known supplier is currently producing them. Therefore, the experimental coatings deposited in these studies were all pre-mixed and not pre-alloyed. Particle diameters generally ranged from 15 to 75 microns. An example of the type of study that must be run prior to producing depositions of known proportions is listed in Table I.

Table I. Analysis of "as mixed" and "as sprayed"  
ZrO<sub>2</sub> - Nichrome V Systems

<u>Powder Mixture Analysis</u>		<u>Sprayed Deposition Analysis</u>	
<u>Nichrome V</u>	<u>Zirconia</u>	<u>Nichrome V</u>	<u>Zirconia</u>
73.7	26.3	92.5	7.5
		89.9	10.1
		91.8	8.2
60.0	40.0	76.0	24.0
		75.5	24.5
		81.0	19.0
48	52.0	68.2	31.8
		68.5	31.5
		70.5	29.5

Hopper segregation of the nichrome (apparent density 184.3 lb./ft.<sup>3</sup>) and zirconia (apparent density 21.2 lb./ft.<sup>3</sup>) probably account for data being not wholly reproducible. A material with a lower heat of fusion and high specific gravity will of course deposit at a more rapid rate from a mixed feed. This would indicate the rapid buildup of the metallic component of gradated coatings in early investigations.

To achieve an effective nichrome V - Zirconia gradation then, the volumetric mixtures would be about as follows:

1st gradation	70 volume % Nichrome	30 volume % zirconia
2nd "	50 "	50 "
3rd "	30 "	70 "
4th "	10 "	90 "

One concept that has been built would allow instantaneous mixture control from a series of four hoppers feeding into a common manifold, each individually controlled by a solenoid valve.

In the course of W. A. D. D. contract AF 33(616)-7323 a problem similar to that previously discussed was encountered with nickel-alumina gradations. A summary of the spectrographic analysis of several mixtures is listed in Table 2.

Table 2. Analysis of "as mixed" and "as sprayed"  
Nickel-Alumina Gradations

<u>Powder Mixture Analysis</u>		<u>Sprayed Deposition Analysis</u>	
<u>Nickel</u>	<u>Alumina</u>	<u>Nickel</u>	<u>Alumina</u>
61.0	39.0	77.5	22.5
47.0	53.0	51.0	49
17.5	82.5	48.5	51.5

Current efforts are directed towards combining the erosion resistant properties of refractory carbide compounds with other materials in composite plasma sprayed systems.

Referring again to the W. A. D. D. sponsored activities at Plasmakote, Table 3 lists a summary of the carbon chemistry of several refractory carbide systems.

TABLE 3 SUMMARY OF CARBON ANALYSIS OF CARBIDE MATERIALS

Carbide Material	Theoretical percent carbon	% Carbon as received	% Variation from Theoretical	% Carbon after being sprayed in air	% Variation from Theoretical	% Carbon after being sprayed in argon	% Variation from Theoretical
TaC <i>Kennametal</i>	6.2	6.4	+ 3.1	4.3	31.0	5.4	12.9
ZrC <i>Norton</i>	11.6	13.0	+ 12.1	6.6	43.1	10.2	12.1
CbC	11.4	11.2	- 1.8	4.9	57.0	9.4	17.6
HfC	6.3	6.0	- 4.8	4.5	28.5	5.6	11.1
4TaC: 1HfC	6.2	6.3	+ 1.62	4.1	33.9	5.3	14.5

A brief literature survey has shown some variation in accepted physical and chemical constants of these materials, due undoubtedly to the presence of minute traces of contaminants. The contamination remains present in current investigations. Particular carbide powder lots are generally free of pure metallic elements except in trace quantities. However, Hafnium Carbide, for example, has been received with as much as 4 weight percent Zirconium Carbide present. This would undoubtedly be explained in terms of mutual solubility based only on slight variation in their lattice constants. (i. e.  $\text{ZrC}^1$  4.685Å°,  $\text{HfC}^2$  4.64Å°.) The problem, in actual coating practice, would be one of conjecture only, being that under oxidizing conditions both Zirconium and Hafnium Carbide form refractory insulating oxides.

It should be noted that both Hafnium and Columbium Carbides were received in a carbon deficient condition. Zirconium and Tantalum Carbide were received with an excess carbon content, accounted for by uncombined carbon.

As has been mentioned, gradation type systems have been produced on graphite. In this instance it was deemed necessary to first obtain preliminary data on the refractory carbides, as

---

<sup>1</sup> Metallurgy of the Rarer Metals, Miller, 2nd Ed., 1957

<sup>2</sup> Refractory Hard Metal, Schwarzkopf and Kieffer, 1953

such, prior to mixing these systems.

Current efforts then, are directed towards translating these basic sprayed materials data into usable solid propellant throat inserts, exit cones and related hardware.



REFRACTORY COMPOSITE RESEARCH AT ROCKETDYNE

O. E. ACCOUNTIUS

Rocketdyne  
Canoga Park, California

---

**REFRACTORY COMPOSITE RESEARCH AT ROCKETDYNE**

By O. E. Accountius\*

Rocketdyne, A Division of North American Aviation, has had an abiding interest in refractory composite materials for the past several years. This interest arose as a natural consequence of desire for product improvement. Most of the effort, however, has been in the development field. Recently, in view of the increasingly greater demand for new and improved materials in missile technology, a materials research section has been initiated within the Research Department. This materials section has been placed on the same level and in the same environment as the other research disciplines. At the present time, a separate materials research laboratory is being constructed and equipped.

Within the materials research section, a unit has been established for refractory composite materials. While the function of this group is essentially research, members also act in an advisory capacity to development and manufacturing operations.

Refractory composite areas to be covered by this unit are coatings and free-standing bodies. The adopted philosophy is that coatings will provide a more immediate but only temporary solution to many of the high-temperature structural problems. The long range and final objective is to develop refractory free-standing composite bodies for missile use.

At present, a company supported research program on refractory composites is being carried on. The objective of this program is to investigate the physico-chemical properties of refractory metals and ceramics, for the ultimate purpose of their

\* Senior Technical Specialist, Research Department, Rocketdyne

combination into light weight or high strength-to-weight ratio refractory composites. An effort will be made to attain this objective by subdivision of the overall problem into limited areas and investigation of the phenomena involved in each area. This program will be carried out over a considerable period of time and this report may be considered as the first in a series and, as a result, will be introductory in nature.

In implementing this program, literature information has been gathered on potential systems as a means of pin pointing the problem areas involved. Until these problem areas are elucidated, selection of a specific composite composition has been considered unwise since the approach selected is basic. Predilection for specific materials and an urgency to make them fulfill the desired need could obscure the basic information sought. Nevertheless, consideration must be given to the types of materials that will eventually be used in such refractory composites. As indicated earlier, these will consist of the refractory metals and ceramics.

Potential systems, however, are being investigated for chemical compatibility and theoretical predictable mechanical properties such as strength and modulus, using data and techniques reported in the literature. This survey is being supplemented by another survey of methods of producing fibers, whiskers and flakes of ceramic materials to serve as the reinforcing phase. From the literature, we have arrived at the conclusion that the final selection of materials will be in a large part based on amenability to the physical processing.

Both whiskers and flakes are being considered as the reinforcement. Flakes are of interest because some of the most interesting materials do not grow into whisker configuration. The laboratory program will, thus be initiated with investigation

into the parameters involved in producing whiskers and flakes of selected materials, e.g. alumina and boron nitride. The whisker growth studies are necessary if a process is to be devised whereby whiskers can be grown in usable amounts and qualities. Methods of increasing the uniformity of the whiskers will also be determined. Subsidiary physical processing studies which must be carried out are methods of harvesting which do not damage the whiskers and methods of orienting the extremely small fibers.

Methods of flake formation have not received the attention in the literature that methods for whisker growth have. Applicable methods of preparing refractory ceramic flakes that might be productive are: flattening out of spheres of refractory materials at their softening or sintering temperature, cleavage of single crystals by thermal or explosive shock, thin films formed by vapor deposition, spraying, etc., and chemical thinning. The need for having a high ratio of diameter-to-thickness considerably complicates the problem. In any event, some chemical method will probably be necessary to remove rough corners to eliminate stress concentration in the composited materials.

Selection of matrix materials for incorporation with the reinforcement materials will be investigated from consideration of the optimum bonding with the reinforcement and the refractory nature of the matrix material. Factors to be considered are wettability, establishment of a chemical bond and stress transfer between matrix and reinforcement. This is visualized to be a difficult problem because of the possible loss of strength of the reinforcement due to interaction with the matrix and the high temperature required during the infiltration process.

Selection and preparation of the appropriate reinforcement and matrix materials and establishment of their compatibility will permit formulation of these materials into composite bodies for testing. Major efforts in this area will be to obtain the proper orientation and composition for the optimum mechanical properties and to obtain the proper distribution and texture of the matrix materials.

The final task, in event that satisfactory solutions are found for the major problems mentioned above, will be to determine the tensile strength and elastic modulus of the composites at a number of temperatures covering the useful temperature range and in the environment in which the composites will be expected to function.

In conclusion, it may be observed that this program is very ambitious. A good probability exists that no clear answers can be obtained for some of the problems brought out. The need for high-strength refractory composites, however, is great and any significant step forward will eventually lead to more efficient rocket propulsion systems.

PYROLYTIC BORON NITRIDE COATINGS

E. P. FLINT

A. D. Little Company  
Boston, Massachusetts

## PYROLYTIC BORON NITRIDE COATINGS

Pyrolytically-formed compounds with high melting points, resistance to oxidation, and anisotropic in properties are potential materials as coatings for easily oxidizable metals and nonmetals.

The work described in this paper has been directed toward the preparation of pyrolytic boron nitride coatings on graphite and on tungsten.

A compound that has especially attractive possibilities for the synthesis of pyrolytic boron nitride by gas-phase thermal decomposition is borazole, a 6-membered ring structure,  $B_3N_3H_6$ , which is an analogue of benzene. As the cost of borazole is prohibitive and since the compound suffers from the disadvantage of instability toward polymerization when stored at room temperature, we used trichloroborazole (TCB) as a source material in a vacuum system designed so that the TCB vapor would be impinged on an inductively heated susceptor.

Initial experiments served to determine proper circumstances for satisfactory deposition. They essentially summarize to the use of a flow rate given by warming the TCB sample to 45° C and pumping its vapor past the graphite susceptor maintained at 1500-1800° C in a scrupulously air-tight system. A photograph of typical products obtained as deposits on AGSR graphite is shown in Figure 1. Although the products shown here are virtually white in color, other runs have given material of varying shades of yellow and brown, when small amounts of impurities are present.

The effect of the susceptor material has been considered briefly. It was of interest to determine whether a highly polished graphite susceptor would alter the structure of the deposit and no apparent difference was found. A tungsten susceptor was employed to

eliminate any possibility of codeposition of pyrolytic graphite together with pyrolytic boron nitride, such as was felt might occur. Adherence of the deposit was greatly inferior on the tungsten to that on the graphite substrate. However, photomicrographs of cross-sections still showed the columnar, conical formations characteristic of pyrolytic boron nitride. Also, X-ray fluorescence and diffraction analysis gave no indication of the formation of tungsten boride or nitride in the bulk of the deposit.

Attempts have been made to heat hot-pressed boron nitride inductively at very high frequencies as a possible susceptor material. An induction heater operating at 120 megacycles was used without success.

In a series of experiments designed to determine the maximum practical rate of deposition of pyrolytic boron nitride, it was found that increasing the temperature of the vapor generator to 70° C, corresponding to a trichloroborazole vapor pressure of about 6 mm., gave a deposition rate of about 25 mils per hour.

Considerable work has been done on determining the structure of the pyrolytic boron nitride deposit. This material, in polished cross-section, displays the cone-shaped columnar structure that is characteristic of pyrolytic graphite. Photomicrographs of pyrolytic boron nitride deposited on pyrolytic graphite are shown in Figures 2 and 3.

Preliminary tests have shown that pyrolytic boron nitride coatings have considerably better oxidation resistance than pyrolytic graphite coatings at all temperatures up to 1800° C.

The work summarized in this report was carried out under Contract No. NOW 60-0277(FBM) with the Bureau of Naval Weapons.



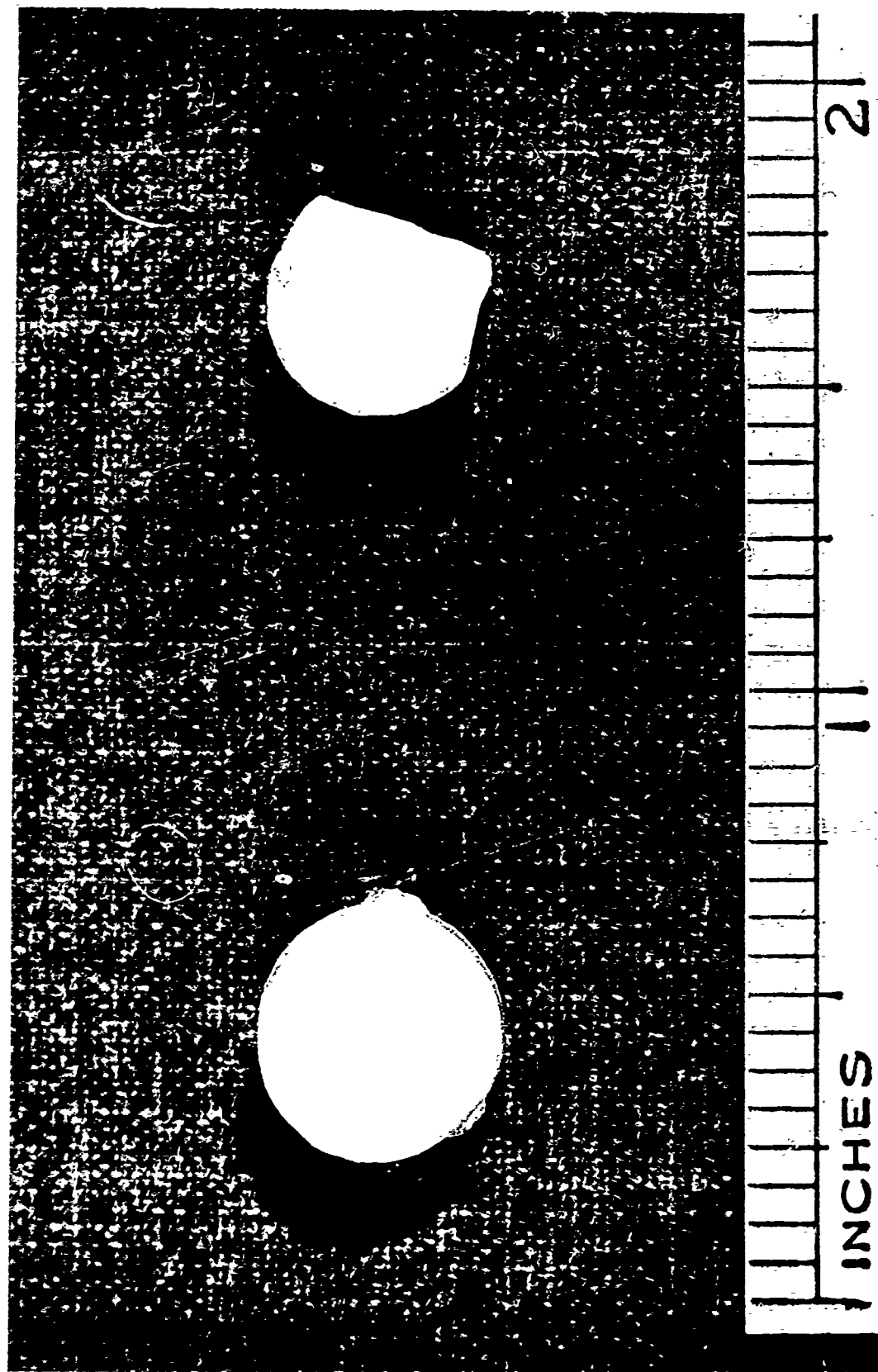


Figure 1

Pyrolytic Boron Nitride Deposited on AGSR Graphite

Figure 2

Pyrolytic Boron Nitride Deposited Normal to Cone Structure of Pyrolytic Graphite Substrate

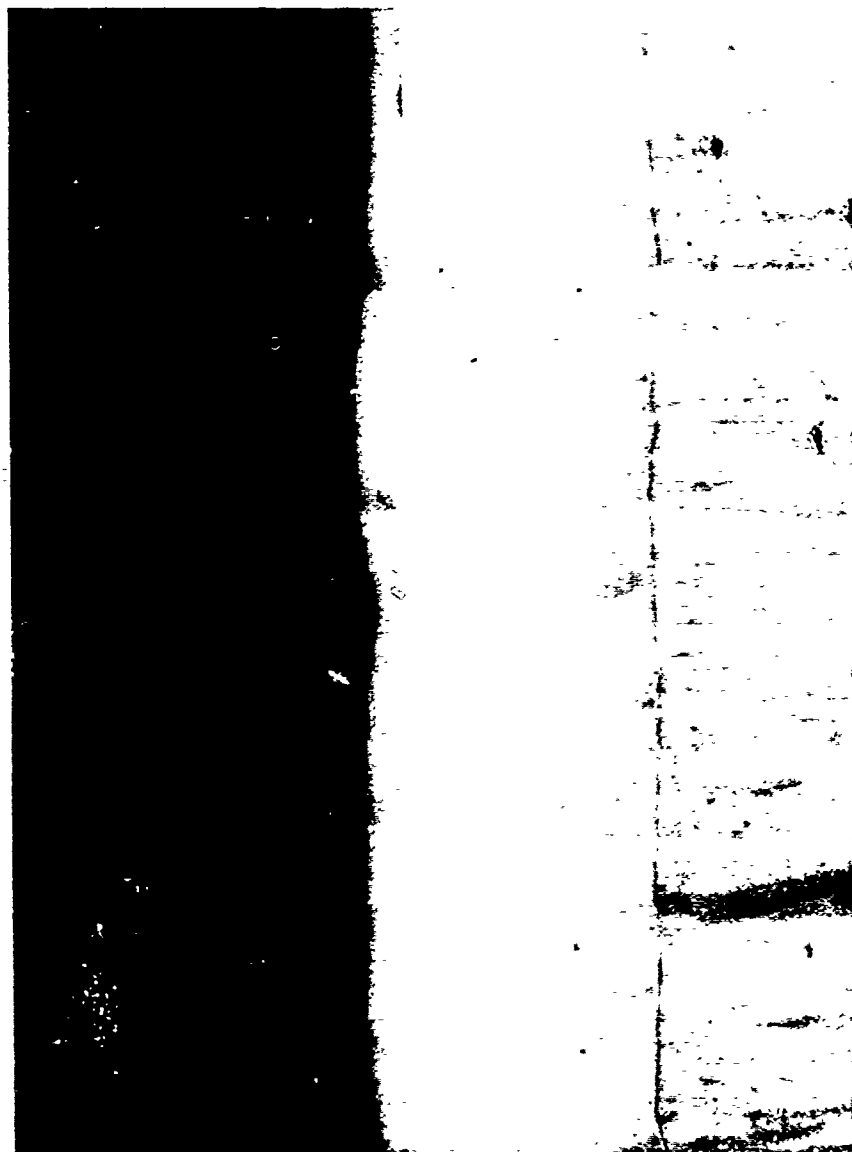


Figure 3

Pyrolytic Boron Nitride Deposited Perpendicular to  
Cone Structure of Pyrolytic Graphite Substrate



REFRACTORY COMPOSITE INVESTIGATIONS

D. L. KUMMER

McDonnell Aircraft Corporation

St. Louis, Missouri

## 1. INTRODUCTION

Refractory composite investigations at McDonnell Aircraft have been primarily directed toward hypersonic glide re-entry vehicle applications. This involves areas aerodynamically heated to 2500 to 4400°F with relatively long time exposures and oxidizing conditions. The composites discussed utilize essentially existing materials, however, these materials are applied in a manner which minimizes the shortcomings of a material and provides a reliable state-of-the-art composite.

## 2. GRAPHITE-ZIRCONIUM OXIDE COMPOSITE NOSE CAP

The object of this investigation was to provide a passive, radiation cooled, reusable nose cap capable of relatively long time operation in air at stagnation point temperatures of 4200°F. The three primary approaches taken were: (a) thin shelled ceramics, (b) ceramic filled metal honeycomb and (c) small ceramic elements in a graphite retainer.

Initial plasma jet tests of the various materials and composites are listed in Figure 1. The maximum predicted flight temperature as listed in Figure 1 varies with material, because, for a given heat input, material temperature is a function of the thermal properties of the material; primarily emissivity and thermal conductivity.

Only ceramic materials such as silicon carbide, silicon carbide bonded graphite and siliconized graphite were considered for the thin shell approach because of the requirement for very good thermal shock resistance. Although this family of materials would attain the lowest temperature for a given heat input, the temperatures are sufficiently high to cause appreciable strength reduction and/or oxidation. However, the specimens tested did not oxidize appreciably even though the plasma jet was 100% air stabilized. This is contrary to other data, therefore, we believe oxidation was somewhat retarded

in this test series. Plasma is a complex environment, particularly when contamination is present from the plasma jet electrodes and nozzle.

Limited investigation and testing of ceramic filled honeycomb did not provide promising results. The tantalum and columbium honeycomb was not specially coated for oxidation protection, but only surrounded with the ceramic filler material. The zirconia and thoria-silica filler materials offered very little oxidation protection and in one case the columbium appeared to autoignite. Although existing oxidation protective coatings for refractory metals are not normally useful at 4200°F, their employment together with a filler material may be helpful.

The third approach utilizes adjacent, small diameter, oxide ceramic elements in a graphite retainer. By utilizing the oxide ceramic materials as individual small elements, the thermal shock problems normally associated with the refractory oxide ceramics are greatly alleviated. Of course, the oxide ceramics are very desirable for use at the high temperatures due to their excellent chemical stability. The primary oxide ceramic investigated was a coarse grained, porous, partially stabilized zirconium oxide. This material proved to be very thermal shock resistant as no failures resulted during any of the testing. One-quarter inch diameter free standing rods and tubes, both clustered and individually, were tested. Also, two one-inch diameter solid spheres were tested at the normal heating rate of 44°F/second. One sphere was coated with flame sprayed molybdenum to determine if this would improve thermal shock resistance by distributing the heat more uniformly over the surface and, to a degree, provide short time surface temperature control due to oxidation. However, neither sphere failed from thermal shock. A free

standing 1/4" diameter rod of magnesium oxide, a thermal shock sensitive material, was successfully heated at a rate of 440°F/second which substantiates the shock resistance of small elements. Also, a free standing 1/4" diameter zirconia rod was heated at a rate of 440°F/second to 4500°F, cooled and reheated without failure.

This small ceramic element approach gave the most promising results, therefore, a 3 1/4" diameter model, pictured in Figure 2, was assembled and tested. The model, which contains sixty-two 1/4" diameter zirconia rods, has been heated to a temperature above 4100°F and cooled in still air three times without any failure. A protective coating was not applied to the graphite, therefore, some oxidation took place.

A very important consideration in a radiation cooled composite is emissivity. The high temperature emissivity of the refractory oxide ceramics is moderate to low; therefore, an attempt was made to increase emissivity. Cobalt oxide, sometimes applied as the nitrate, was selected as a promising material for increasing emissivity. Although cobalt oxide has a relatively low melting point, when in combination with large percentages of zirconia, a fairly high liquidus temperature can be obtained. Subsequent high temperature measurement of the emissivity of cobalt oxide containing materials has not shown this material to be as promising as originally contemplated.

Initial investigation of ways to increase the temperature resistance of siliconized graphite was accomplished. Although additional investigation is required, flame spraying the siliconized surface with zirconia appears most promising. The zirconia apparently stabilizes the silica protective layer that is formed upon oxidation of the siliconized graphite. Thus, a more refractory zirconium silicate glass-zirconia coating is formed. An undesirable result of the application of zirconia is the emissivity reduction.

A typical nose cap utilizing the zirconia rods or tubes in a graphite retainer is shown in Figure 3. The stable oxide ceramic material in a thermal shock resistant configuration is used at the hottest portions of the nose cap. The graphite retainer has good thermal shock resistance and a good high temperature strength to weight ratio. The materials and design are within the current state-of-the-art and the composite appears to have good reliability. The design also facilitates instrumentation which may be an important part of a nose cap. A surface roughness results from the rods or tubes, however, an initial look at this problem indicates that this surface condition is satisfactory.

This basic concept may be altered in numerous ways to include radial placement of the ceramic elements or filling the interstices between ceramic elements with a ceramic cement or slurry to provide a smooth surface. Radial placement may require machining of the ceramic elements which is difficult, but has been successfully accomplished on the zirconia material. More refractory ceramic elements and elements of different size and geometry may be substituted for the 1/4" diameter zirconia rods or tubes.

### 3. EXTERNAL THERMAL INSULATION FOR SKIN PANELS

A most critical problem for any vehicle which encounters 3000 to 4000°F temperatures is the design of the hot skin panels. This temperature range is currently beyond the reliable employment of structural refractory metals, therefore, a method of applying efficient external thermal insulation was investigated.

One approach to this problem is to use an oxide ceramic as the outer covering with efficient thermal insulation between the outer ceramic covering and



the metal structure. The ceramic outer covering is attached to the structural substrate by a coated refractory metal wire mesh.. Figure 4 shows a typical composite panel.

An oxide ceramic material is very desirable for the outer covering due to the high temperature chemical stability, refractoriness and insulating value of this family of materials. However, the thermal shock and attachment difficulties must be overcome for effective incorporation into a composite. In this approach, thermal shock is minimized by dividing the ceramic into thin tiles with the dimensions being controlled primarily by the expansion coefficient of the ceramic material. The resultant expansion joints would be a requirement in almost any case due to the large differential growth between the outer surface and structural substrate when a large thermal gradient is maintained across the section. The expansion joints can be sized so that the joint is closed at the maximum temperature. The problem of attachment is solved by using the ceramic material in a cement (chemical or colloidal bonded) and/or flame sprayed condition. Thus the ceramic is primarily mechanically trapped by the refractory metal mesh. Of course, all processing, particularly elevated temperature curing, must be compatible with the other materials which make up the composite. Aluminum phosphate and zirconium phosphate based materials have shown promise as the outer covering.

The coated refractory metal mesh serves to reinforce and hold the outer ceramic shell, contain the thermal insulation and transfer air loads to the structural substrate. This refractory metal mesh will attain a temperature approximately equal to the external surface temperature except for very transient heating conditions. However, because the mesh is surrounded by the ceramic material,

the metal is not exposed to as severe an environment as if it were the external surface. Also, the mesh is not structural and limited isolated oxidation would not result in failure of the composite. The mesh may be attached to the structural substrate mechanically or metallurgically, the latter being preferred. Tantalum alloys have shown promise as a mesh material.

The thermal insulation material is a very important part of the composite and will have primary influence in determining the weight efficiency of this composite. The more refractory fibers such as zircon and zirconia and mixed powders are primary candidates. Due to the large amount of radiant heat transfer at high temperatures, very small pores and the incorporation of radiation suppressing materials is very desirable. Small pores, of course, are also important for minimizing heat transfer by air conduction which can be particularly effective at reduced pressures. Dependent upon the location of the panel on the vehicle, a substantial amount of heat may be radiated from the interior panel surface to cooler portions of the vehicle, therefore, enabling a substantial thermal gradient between outer surfaces and structural substrate.

The metal substrate carries the primary loads and may be of any efficient structural design. The material may be either refractory metal or super alloy.

Figure 5 shows an assembled test specimen before and during test. This specimen was constructed to obtain additional information concerning this insulation concept. The ceramic outer facing is aluminum phosphate bonded aluminum oxide cast in place and cured at 800°F. The metal reinforcement is 25 mesh, .009" wire diameter stainless steel screen resistance welded to the stainless steel single faced corrugation structural substrate. The thermal insulating material is Fiberfrax. This specimen was rapidly heated with radiant lamps to a surface temperature of 2400°F, cooled and reheated without any detrimental effects.

Evaluations to date indicate that this approach to panel insulation is valid, however, additional development and testing is required. The ceramic cements, although readily utilized, suffer from sintering shrinkage at very high temperatures and the phosphate bonded materials are somewhat corrosive. At temperatures above 3200°F, oxidation protection of the refractory metal mesh is a problem, particularly because of the limited allowable assembly sequences. Steps to minimize weight and the determination of surface roughness effects due to the expansion joints must also be undertaken.

FIGURE 1  
PLASMA JET TEST SUMMARY FOR PASSIVE NOSE

(Tests run on 100% air)

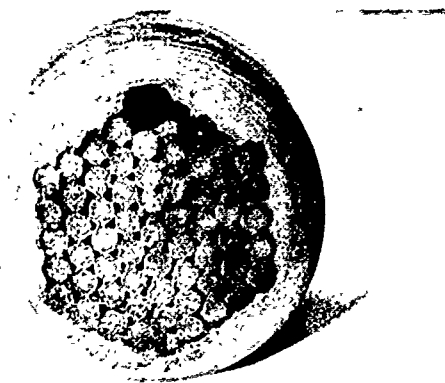
TEST NO.	SPECIMEN	TEST RESULTS								REMARKS
		MAXIMUM PREDICTED FLIGHT TEMP. (°F)	MAXIMUM MATERIAL TEMP. (°F)	TEMP. OF GAS ENTERING NOZZLE (°F)	AVERAGE RATE OF HEATING (°F/SEC.)	TIME AT MAXIMUM TEMP. (MINUTES)	APPROXIMATE MAXIMUM Q (BTU/FT. <sup>2</sup> /SEC.)	TOTAL TIME (MIN.)	TYPE OF FAILURE	
1	KT Silicon Carbide Blunted Nose Cone	3600	3600	5700	22	2.0	270	4.95	None	No apparent oxidation.
2	Silicon Carbide Coated Graphite Blunted Nose Cone	3600	3600	5900	22	2.0	190	6.28	None	No apparent oxidation.
3	Blunted Nose Cone Silicon Carbide Bonded Graphite Coated with Zirconia, Coated with Co	4000	4000	6000	22	0.5	235	3.95	None	No apparent change in specimen.
4	Cluster of 7 Zirconia Rods Coated w/CoO	4100	4100	5800	22	0.5	200	3.76	None	No apparent change in specimen.
5	Cluster of 7 Zirconia Tubes Coated w/CoO	4100	4150	6100	22	0.5	215	3.54	None	No apparent change in specimen.
6	ZrO <sub>2</sub> ball in contoured sting coated w/CoO	4100	4100	6000	22	0.5	200	3.21	None	No apparent change in specimen.
7	Zirconia ball Coated with Molybdenum	4100	4250	6100	44	0.5	235	2.59	None	The molybdenum coating had totally oxidized as predicted. No damage to the zirconia ball. Specimen was overheated.
8	Tantalum Honeycomb filled with Zirconia Coated with Co	4100	4500	6100	44	0.5	255	4.32	Melted some ZrO <sub>2</sub> -CoO and oxidized tantalum severely.	Specimen was overheated.
9	Tantalum Honeycomb filled with Zirconia Coated with Co	4100	4300	5400	44	0.5	255	3.61	Tantalum oxidized severely.	Tantalum after test was in brittle flakes, and severely oxidized.
10	Columbium Honeycomb filled with Thoria - Silicia Mixture	4100	3400	5800	44		215	2.37	Columbium oxidized, silica melted and fused.	A flash of light occurred which apparently was the columbium honeycomb igniting.
11	Zirconia Honeycomb	4500	3550	5700	44		145	4.18	Failed due to thermal shock.	Honeycomb broke off in segments.
12	Magnesia Rod (1/4")	4500	4500	6200	44	0.5	255	3.15	None	No apparent change in specimen.
13	Zirconia Rod (1/4")	4500	4500	6300	440	0.17	200	0.63	None	Specimen rotated into 200 BTU/ft. <sup>2</sup> 2sec. plasma position. No apparent change in specimen.
14	Zirconia Coated Graphite Nose Tip	4500	4600	5000	20	1.0		6.01	Zirconia cracked on heating and also upon cooling down.	During heating the Zirconia cracked off resulting in severe graphite oxidation. 50% air and 50% nitrogen.
15	Zirconia Rods in 3-1/4" Diameter Uncoated Graphite Shell	4100	4700	6000	44	0.17 (above 4200° F)	235	5.00	Small corner of Zirconia Rods melted	Specimen was at 4200° F when holder moved, causing specimen to reach 4700° F in local area, resulting in melting.

FIGURE 2  
MAC PLASMA JET TEST

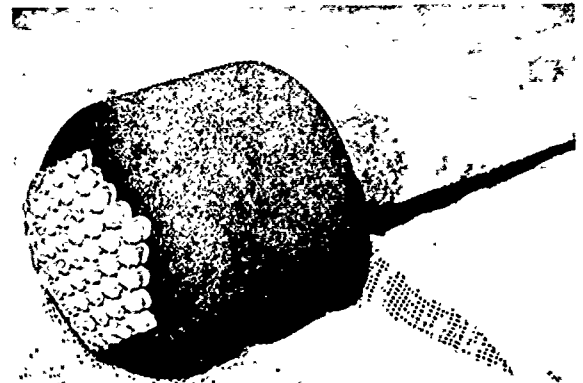
$3\frac{1}{4}$ " DIA. NOSE TIP



DURING



BEFORE



AFTER

FIGURE 3  
NOSE CAP DESIGN

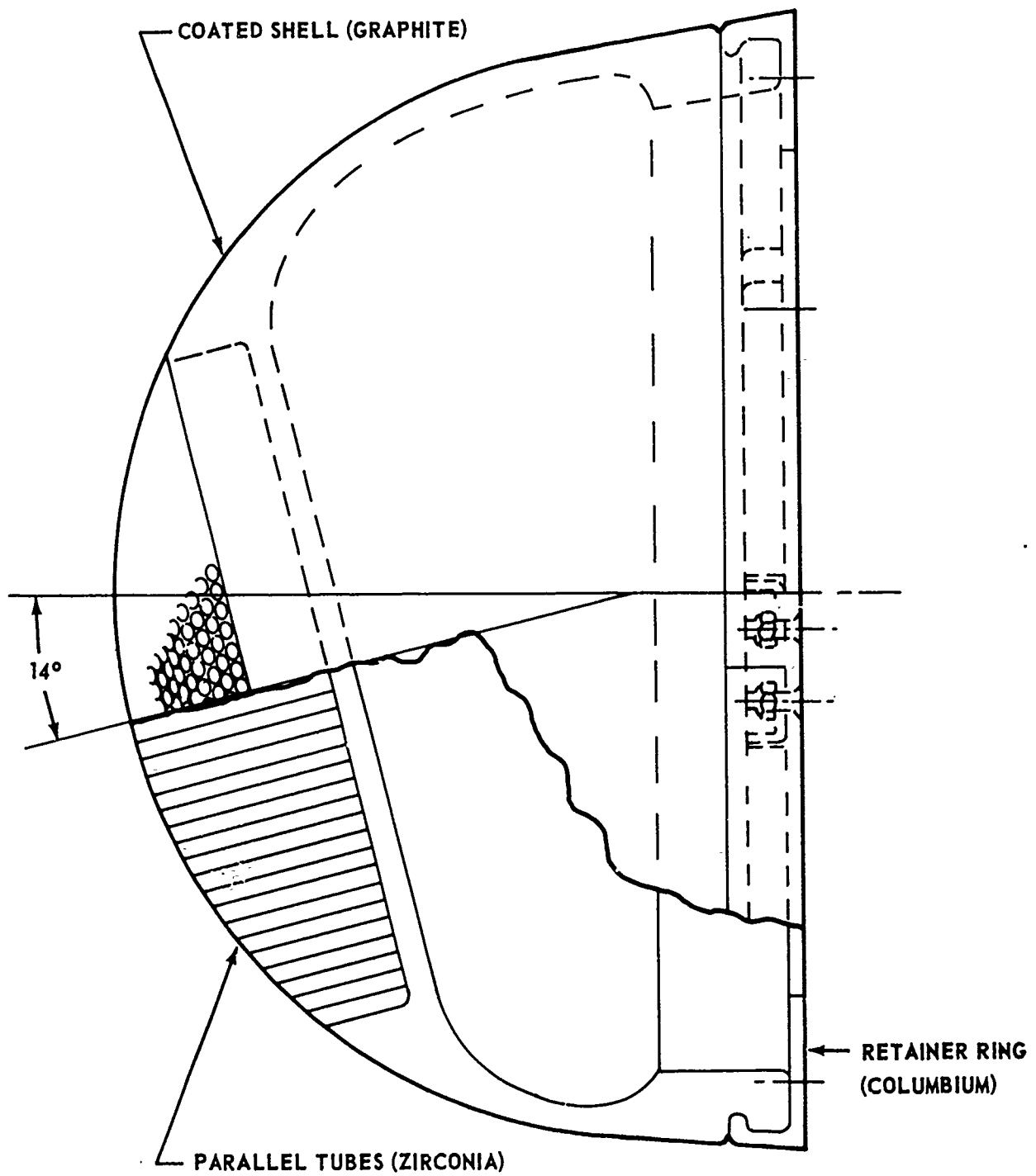


FIGURE 4  
INSULATED PANEL

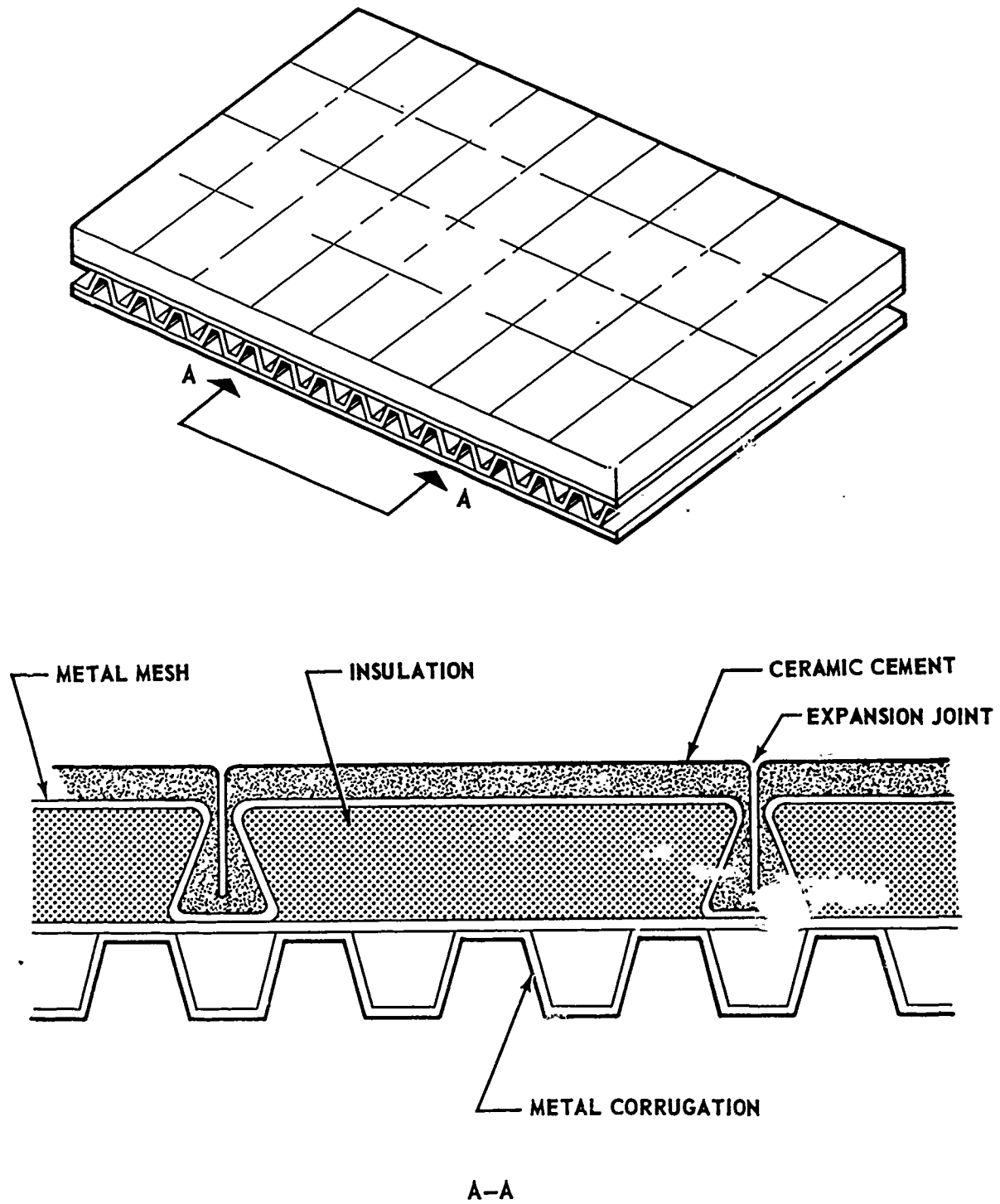
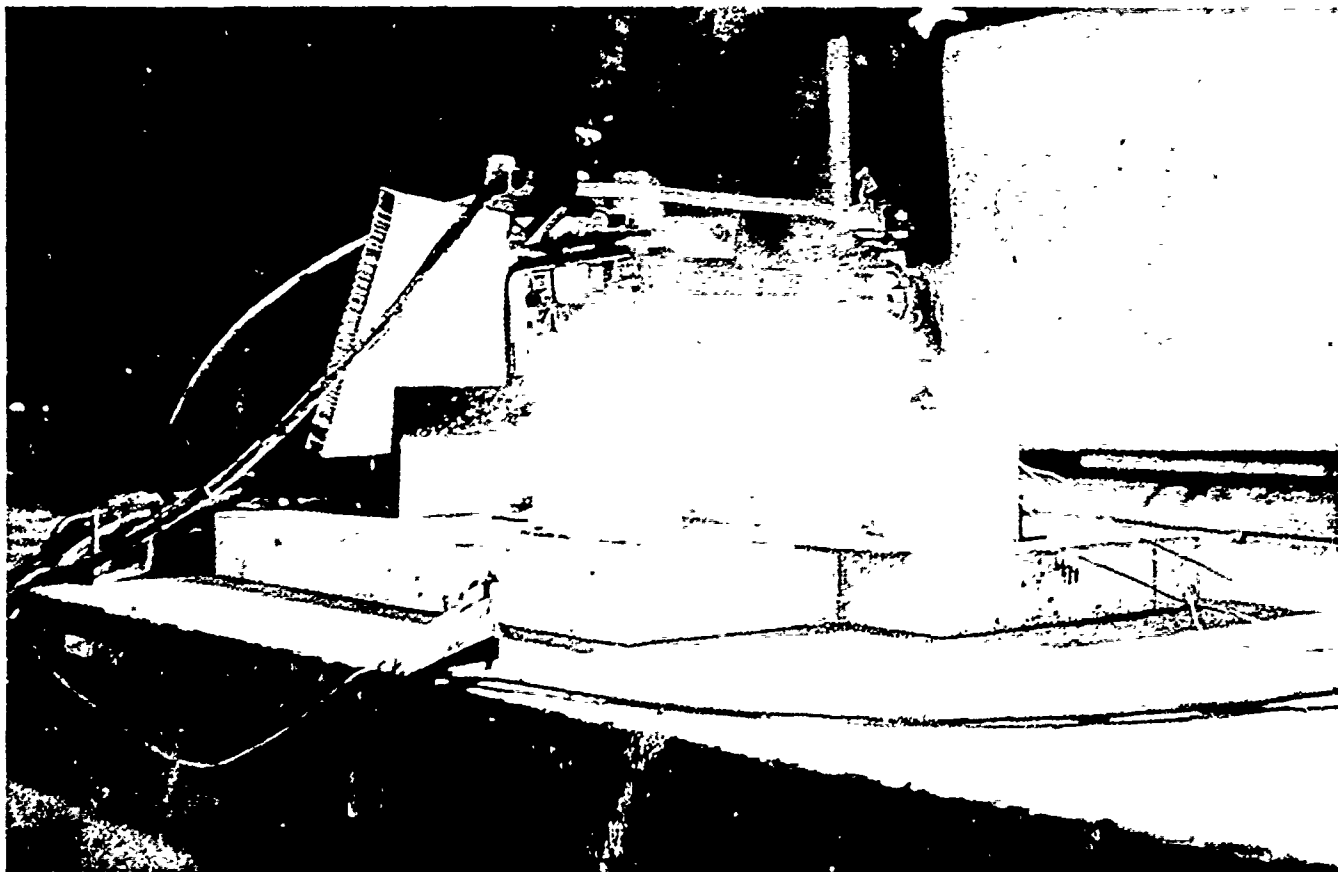
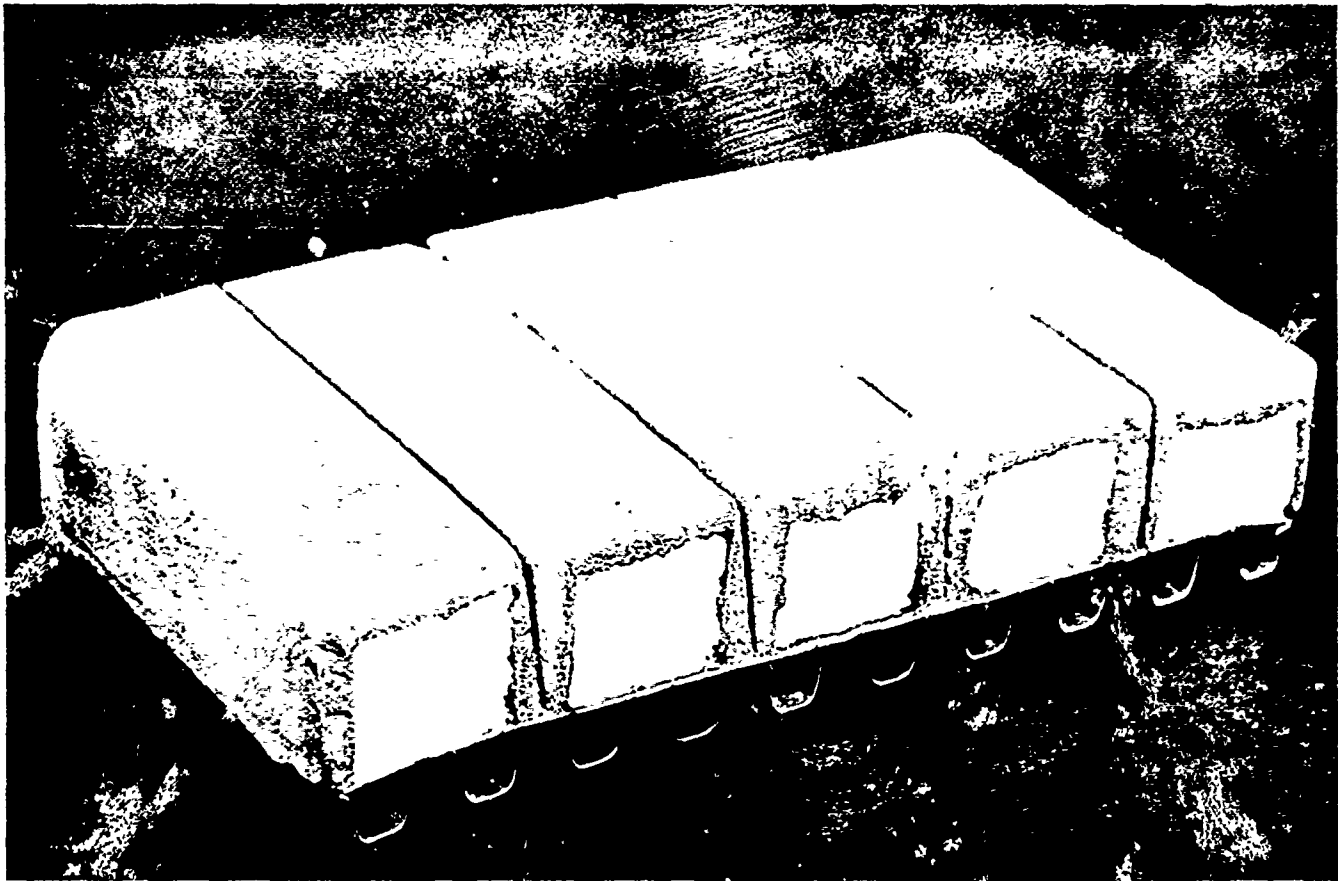


FIGURE 5

INSULATED PANEL BEFORE AND DURING TEST





DEVELOPMENT OF WHISKER - REINFORCED  
METALLIC COMPOSITES

W. SUTTON

General Electric Company  
Philadelphia, Pennsylvania

## DEVELOPMENT OF WHISKER - REINFORCED METALLIC COMPOSITES

Although metals reinforced with whiskers, or filamentary single crystals, are laboratory curiosities at the present time, they offer a new approach to the development of ultra high-strength, refractory materials. During the past year, a study has been conducted at the Space Sciences Laboratory of the General Electric Company, under the sponsorship of the United States Navy, Bureau of Weapons (Contract NOw 60-0465 d) in order to investigate the feasibility of whisker reinforcement. Sapphire ( $\alpha$  -  $\text{Al}_2\text{O}_3$ ) whiskers were selected because of their refractoriness, chemical compatibility with metals at elevated temperatures, and because they retain a considerable portion of their strength at temperatures near their melting point ( $3750^\circ\text{F}$ ). Individual tensile tests at room temperature have revealed fracture strengths as high as 1,400,000 psi.

The program was divided into three areas of investigation:

1. Whisker growth
2. Structural Analyses
3. Composite Fabrication

## WHISKER GROWTH

Sapphire Whiskers can be grown by a vapor deposition process, whereby molten aluminum, heated in a ceramic boat at 2500°F in a hydrogen atmosphere, is volatilized. Traces of moisture provide the oxygen necessary to oxidize the aluminum vapor, which then deposits on the upper surfaces of the boat. Growth occurs very rapidly along one prominent direction, so that needle-like crystals result. Growth parameters, such as temperature, time, dew point, substrate material, and hydrogen flow rate, have been investigated.

In more recent studies, sapphire whiskers have been grown during periods as short as 10 minutes. At the present time, whiskers are being grown in batches weighing about a gram. However, the feasibility for continuously growing whiskers looks promising and a study for establishing a continuous process is underway.

## STRUCTURAL ANALYSES

Theoretical studies were conducted in order to assess the various parameters affecting the strength of a composite reinforced with parallel, discontinuous (short) fibers. Calculations of stresses arising from an applied axial load showed that the stress disturbances, near the whisker ends, are local and particularly that the shear stress between the whisker and matrix is apt to rise to a high peak value at these discontinuities.

The strength of composite consisting of F-48 alloy (15W-5Mo-1 Zr-79 Cb) reinforced 50 <sup>v/o</sup> <sup>\*</sup> Al<sub>2</sub>O<sub>3</sub> whiskers was calculated. It was

<sup>\*</sup>v/o = volume percent

assumed that the two phases elongated equally and that each contributed to the composite strength proportionate to their concentration. Modifications were also made based on statistical deviations of individual whisker strengths and orientation. Figure 2 shows the results of these calculations and indicates the improvement in strength-to-density ratio ( $\sigma/\rho$ , in inches) at various temperatures of alloy F-48 reinforced with whiskers.

### COMPOSITE FABRICATION

Techniques for fabricating composites were investigated; most of the emphasis was placed on vacuum injection of molten metal into a whisker bundle contained in a mold. Problems of the wetting, bonding, porosity, and occluded gases were studied extensively. Aluminum and aluminum alloys were used for preliminary vacuum impregnation studies. Improvements of 200% in the yield strength were achieved whisker reinforcement, but these values were short of the improvements expected. The cross section of an aluminum tensile specimen reinforced with

$\alpha$  -  $\text{Al}_2\text{O}_3$  whiskers, is shown in Figure 2. The ends of 'a' type (retangular) and 'c' type (hexagonal cross-section) whiskers can be seen. Composites of silver similarly reinforced showed much greater improvements in strength. One sample containing 12.5 % whiskers exhibited a five-fold improvement (118,000 psi ultimate tensile strength) over that of the unreinforced specimens.

Future work will be directed towards the reinforcement of more refractory metals/alloys, and an investigation of their properties at elevated temperatures will be conducted.

Legend

Figure 1 - Photomicrograph of Aluminum -  $\text{Al}_2\text{O}_3$  Whisker Composites.

Cross Sectional View of tensile specimen showing ends of 'c' and 'a' type whiskers. (Magnification 750X)

Figure 2 - Strength-to-Density Ratio ( $\sigma/\rho$ ) at various temperatures for F-48 Alloy Unreinforced and Reinforced with  $\text{Al}_2\text{O}_3$  whiskers.

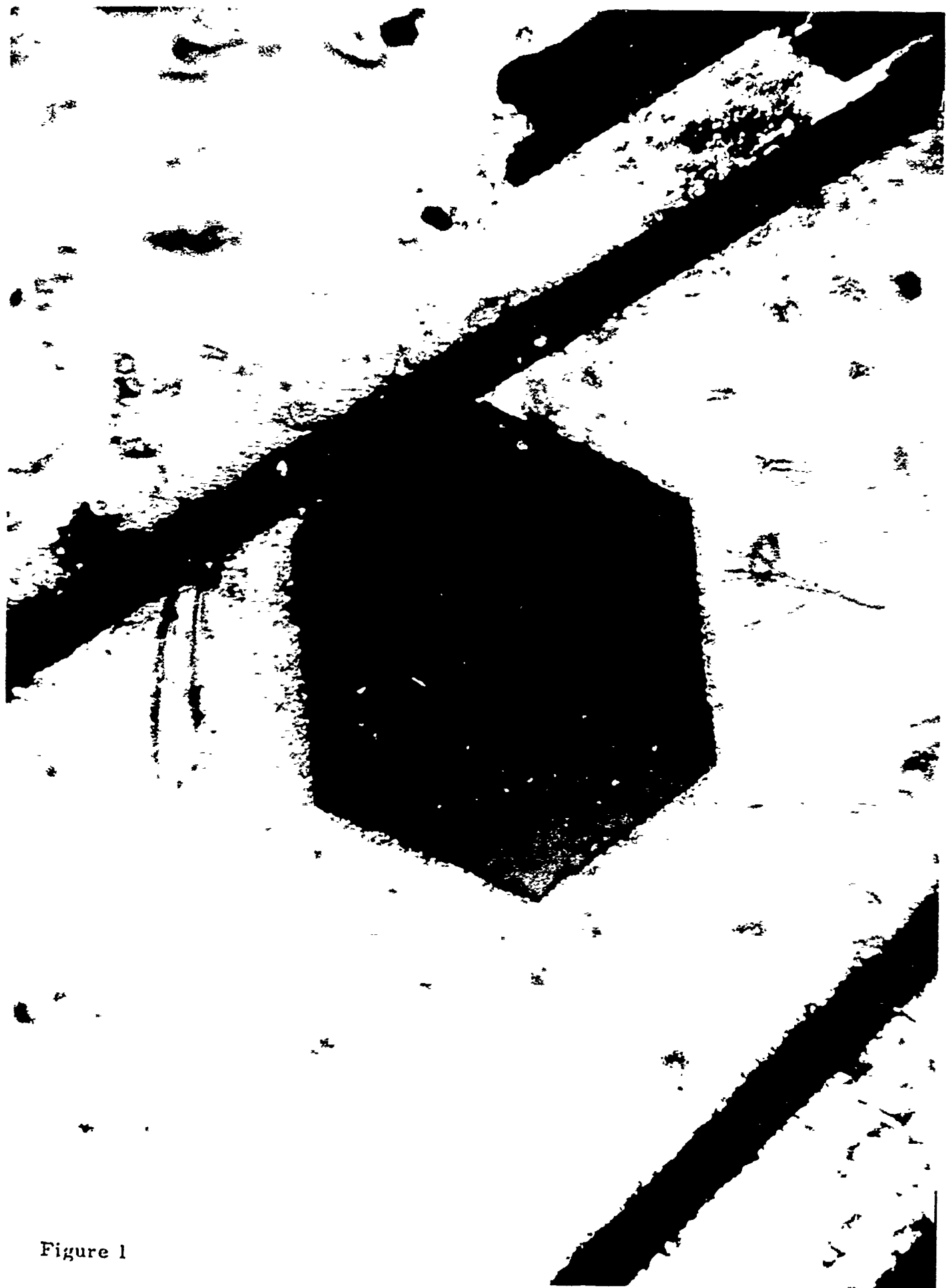


Figure 1

STRENGTH-TO-DENSITY RATIO FOR F-48 ALLOY  
UNREINFORCED AND REINFORCED WITH  $\text{Al}_2\text{O}_3$  WHISKERS

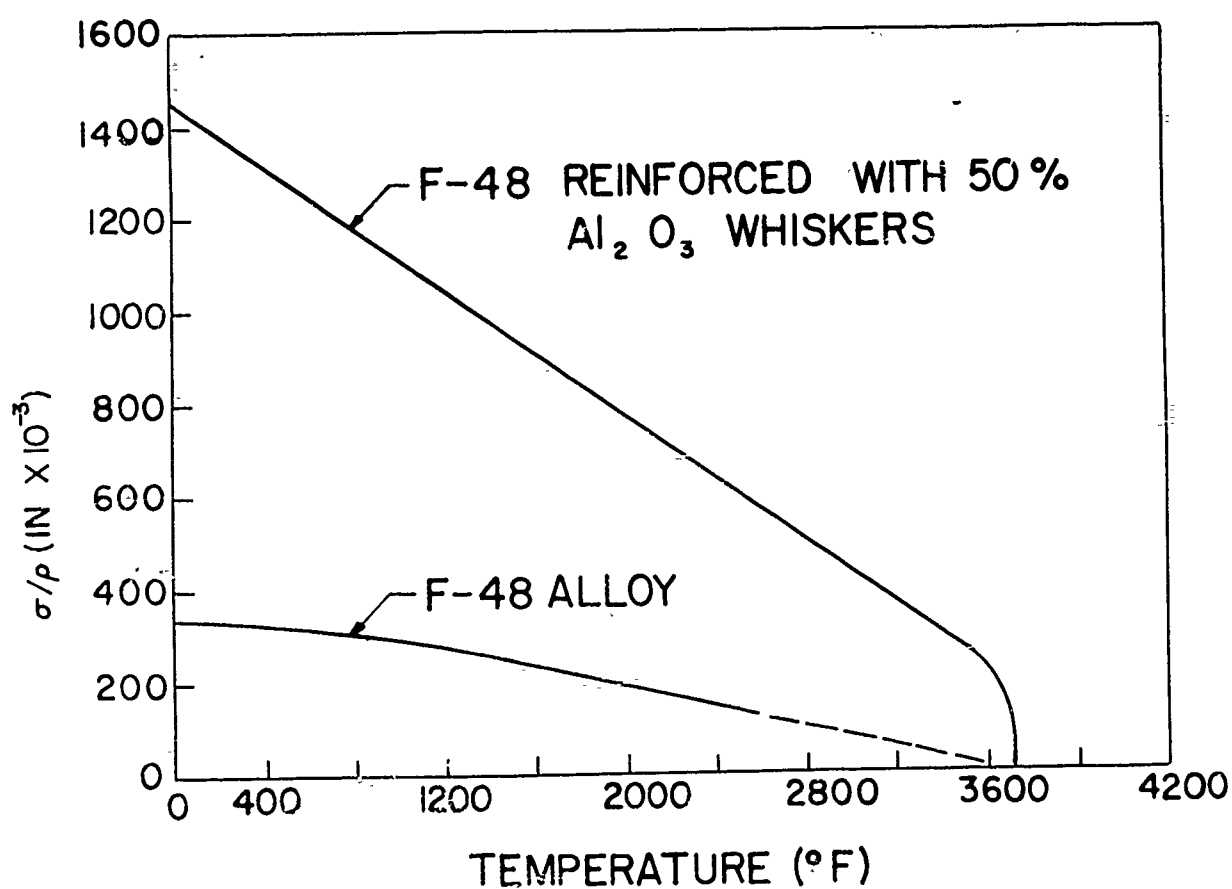


Figure 2

DEVELOPMENT AND TESTING OF  
ELECTRODEPOSITED CERMETS

JOHN HUMINIK, JR.  
GIOVANNI G. F. BARGERO

Value Engineering Company  
Alexandria, Virginia



Value Engineering Company is engaged in the deposition of ceramic-metal compositions from aqueous solutions by fairly conventional techniques. The program presently includes coating on the refractory metals and graphite with any of the following ceramics in a chromium matrix:

Tantalum Carbide	Silicon Nitride
Tantalum Boride	Silicon Carbide
Hafnium Boride	Zirconium Boride
Niobium Carbide	Zirconium Boride plus Molybdenum Silicide
Hafnium Carbide	Zirconium Oxide
Boron Nitride	Tungsten Boride

\* \* \* \* \*

The program thus far is restricted to systems utilizing the chromium matrix due to its relatively high melting point and economical availability. However, if higher melting matrix materials are desired, rhodium, rhenium or iridium could be used.

The advantages of using aqueous electrodeposition are that control of the solutions is relatively easy; thickness can be controlled to better than .001 inches; the process is adaptable to any shape nozzle; and the choice of compositions available for use in this process are numerous. Another advantage is that no machining or mechanical processing seems necessary on the deposited coating.

The present Navy sponsored research effort is concentrating on the following specific areas utilizing graphite as the substrate:

1. Effect of various thickness on performance (.003 to .050 inches)
2. Effect and uniformity of particle shape and size.
3. Effect of heat treatment on electrodeposited cermet coatings.
4. Effect of particle concentration in final coating.

\* \* \* \* \*

Another portion of the overall program which is under Army sponsorship consists of coating small metal nozzles and test firing some of them in the VECO test rocket motor and some of them at the Army Rocket and Guided Missile Agency static firing facility in Huntsville, Alabama.

This program will prove the comparability of results from two types of test facility and will also serve to furnish more test data on the electrodeposited coating.

Several static firings of the chromium and zirconium boride coating (Valcoat 12) have been made.

The results of these firings have shown that this coating is effective in greatly reducing erosion on the inside surface of nozzles.

It is felt that the Valcoat 12 is the best available coating today. However, with different propellants perhaps other compositions will perform better. It is anticipated that several of the other combinations of metal and ceramic which are under investigation will also be successfully adapted to rocket nozzles.

### TESTING

A standard test was sought wherein actual rocket flame chemistry and thermodynamic conditions could be approximated in the laboratory on a continuous basis.

As a result of a comprehensive evaluation of all methods used for high temperature materials evaluation, it was decided that a rocket engine utilizing hydrogen and oxygen gas for a fuel could produce the appropriate thermochemical parameters for direct correlation with actual firing.

On complete examination of the actual rocket environments, it was agreed that the "sand-blast" effect of solid propellants must be also available in this test rocket motor. Therefore, a special device was designed to insert solid particles at a controlled and continuous rate throughout the lengths of the firing time.

From a thermochemical analysis of the propellant system in this test motor, the required chamber pressure, the chamber temperature, mean molecular weight of exhaust gases, the ideal specific impulse, and the specific heat ratio can be found.

An appendix to this paper gives the necessary calculations for obtaining the data necessary for correlation of the test motor results with actual rocket motor parameters.

## SPECIFICATIONS

Propellant	Hydrogen and Oxygen Gas
Flame Temperature	(Variable) 5740° F MAX.
Chamber Pressure	(Variable) 300 - 500 psi
Flame Chemistry	(Variable) Oxidizing or Reducing
Thrust	150 psi
Nozzle Throat Diameter	.600 inches
Firing Time	(Variable) 60 seconds Max.

\* \* \* \* \*

The test motor is completely instrumented to record 14 parameters during the entire firing time. The entire system is operated by one experienced rocket propulsion engineer who can view the entire test by instrumented or visual methods.

The cost of making a 60 second instrumented firing and interpreting the data coming from the recorders is approximately \$100.00.

Other tests such as hardness, chemical analysis, metallographic and thermal shock tests are used in conjunction with the rocket motor to enable us to have a fairly complete understanding of the materials under investigation.

Other portions of VECO's test program are engaged in developing the techniques for measuring the physical properties of coatings or solid bodies. The particular properties presently being sought are thermal conductivity.

Other studies are going on to develop methods for determining accurately the erosion rate and specific heat of both coatings and solid nozzle bodies.

## SUMMARY

As a result of the program which has been conducted in the past year Value Engineering Company considers that the cermet electrodeposited coatings have progressed to the point where it is necessary to conduct realistic laboratory tests to get a further indication as to its adaptability to the rocket motors.

It is felt that by use of the test rocket motor constructed by VECO and with data obtained from large motors, it will be possible to understand far more than has ever been known before on the relationship between these two results.

We feel that the program is proceeding at a rapid and satisfactory rate. Also since the number of promising metal-ceramic combinations yet to be investigated are so numerous that it is felt that no barrier to this novel and complete approach is in sight.

## APPENDIX

It is believed that the following data is a complete treatment of the factors necessary to compare laboratory test results with actual rocket motor firings.

### Theoretical Evaluation of a Gaseous $H_2$ - $O_2$ Rocket Chamber.

A complete step by step sample calculation in computing temperature, the equilibrium gas composition of the reaction products, and the theoretical performance of the  $H_2$ - $O_2$  rocket motor in use at Value Engineering Company is given in this paper.

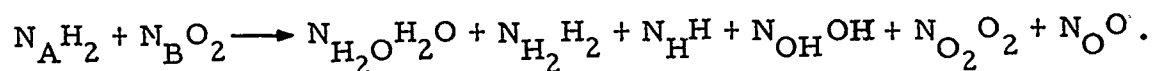
Calculations for various  $O_2/H_2$  ratios and for various motor specifications were conducted in conformity with the method described by G. Sutton in "Rocket Propulsion Elements." This paper covers the calculations for a  $H_2$ - $O_2$  rocket motor with the following specifications:

Propellant	(gas) Hydrogen and Oxygen
Mixture Ratio	$O_2/H_2 = 2.75$
Chamber Pressure	300 psia
Atm. Pressure	14.7 psia
Thrust	100 lbs.

The chamber was designed for a cylindrical combustion chamber, helically wound cooling duct, and water as coolant.

### Thermochemical Analysis.

A general equation taking into consideration all the resulting elements of a gaseous  $H_2$ - $O_2$  reaction is



Hydrogen peroxide and ozone are not likely to occur at the conditions under which the chamber operates.

From the given data the molar proportions for the reactions can be determined by selecting an arbitrary basis of the weight involved in the reaction. By using an arbitrary weight of 20 lbs. we have

$$\begin{aligned} O_2/H_2 &= 2.75 & O_2 &= 2.75 H_2 \\ O_2 + H_2 &= 20 \text{ lbs.} & H_2 &= \frac{20}{3.75} \text{ lbs} = 5.333 \text{ lbs} \end{aligned}$$

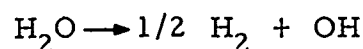
$$O_2 = 20 - \frac{20}{3.75} = 14.667 \text{ lbs.}$$

$$N_A = \frac{5.333}{2.016} = 2.645$$

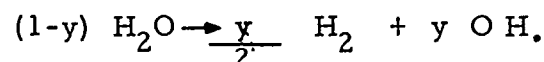
$$N_B = \frac{14.667}{32} = .458.$$

## Dissociation

The effect of dissociation for



is now taken into consideration by letting  $y$  be the number of moles dissociated per mole of  $\text{H}_2\text{O}$ . Then



The total number of moles dissociated will then be

$$\sum N_i = N_{\text{H}_2\text{O}} + N_{\text{H}_2} + N_{\text{OH}} = 1-y + \frac{y}{2} + y = 1 + \frac{y}{2}.$$

The partial pressure will be

$$P_i = P \frac{N_i}{\sum N_i} \text{ where } P \text{ in our case} = \frac{300}{14.7} = 20.4 \text{ atm.},$$

thus using  $P = 20.4 \text{ atm.}$

$$P_{\text{H}_2\text{O}} = 20.4 \frac{1-y}{\frac{2+y}{2}} = \frac{40.8(1-y)}{2+y}$$

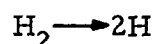
$$P_{\text{H}_2} = 20.4 \frac{\frac{y}{2}}{\frac{2+y}{2}} = 20.4 \frac{y}{2+y}$$

$$P_{\text{OH}} = 20.4 \frac{y}{\frac{2+y}{2}} = 40.8 \frac{y}{2+y},$$

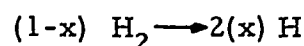
and the constant -pressure equilibrium constant  $K_p$  is

$$K_p = \frac{(P_{\text{OH}})(P_{\text{H}_2})^{1/2}}{(P_{\text{H}_2\text{O}})} = \frac{4.517 y \sqrt{y}}{(1-y) \sqrt{2+y}} = \left[ \frac{20.4 y^3}{2-3y+y^3} \right]^{1/2}, \text{ or } K_p^2 = \frac{20.4 y^3}{2-3y+y^3}.$$

The effect of dissociation for



is likewise taken into consideration by letting ( $x$ ) be the moles dissociated per mole of  $\text{H}_2$ . Then:



the total number of moles is  $\sum N_i = N_{\text{H}_2} + N_{\text{H}}$

$$\sum N_i = 1-x + 2x = 1+x,$$

and the partial pressure

$$P_i = P \frac{N_i}{\sum N_i} \quad \text{where again } P = 20.4 \text{ atm.}$$

$$P_{H_2} = 20.4 \frac{x}{1+x}$$

$$P_H = 20.4 \frac{2x}{1+x}.$$

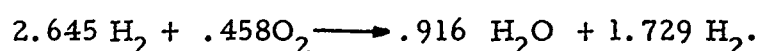
The constant-pressure equilibrium constant is then, by definition,

$$K_p = \frac{[P_H]^2}{[P_{H_2}]} = \frac{[20.4(2)x]^2}{[1+x]^2} \frac{[1+x]}{20.4 x} = \frac{81.6 x}{1+x}.$$

#### Determination of the Approximate Reaction Temperature

In order to find the dissociation in terms of (x) and (y) we must employ a value for the equilibrium constant,  $K_p$ , which is correct for the reactive temperature under consideration. Thus two avenues of approach are open. (1) The reaction temperature is assumed, or (2) a slightly higher than actual temperature is calculated by neglecting the dissociation reactions taking place in the reaction chamber.

The reaction-equation for a dissociation free  $H_2$ - $O_2$  reaction is



The theoretical (adiabatic) flame temperature is then calculated using the heat of reactions and the enthalpy change of the gases.

$$\begin{aligned} [Q_R]_{T_o} &= \sum [n (Q_f) \text{ product}] - \sum [n (Q_f) \text{ reactants}] \\ [Q_R]_{T_o} &= \sum \left[ n_p \int_{T_o}^T (C_p) dT \right] = \Delta h, \end{aligned}$$

where  $[Q_R]_{T_o}$  is the heat of reaction of the propellant combination at the reference temperature  $T_o$ ;  $\int_{T_o}^T (C_p) dT$  is the enthalpy change necessary to heat one mole of each gas product from  $T_o$  to  $T$ ;  $C_p$  is the specific heat in Btu/lb mole  $^{\circ}R$ ; and  $T_o$  is the reference temperature,  $77^{\circ}F = 537^{\circ}R$ . The heat of reaction of the propellant combination (oxidizer and fuel) will now be determined and equated to the enthalpy gain of the product gases.

A temperature,  $T$ , is assumed, and if the change in the enthalpy of the product,  $\Delta h$ , equals the heat of reaction of the reactant,  $Q_R$ , the assumed reaction temperature is the correct one. If  $\Delta h < Q_R$ , the assumed temperature is too low.

Let us assume  $T = 4702^{\circ}R$   
 $T = 4242^{\circ}F$ .

# Heat of Reaction

Gas	n	$Q_F$	$n Q_F$
$H_2O$	.916	104,042	95,302.47
$H_2$	1.729	0	0
$O_2$	0	0	0

Heat of Reaction  $Q_R = 95,302.47/\text{Btu}/20 \text{ lb. prop.}$

# Enthalpy Gain

Gas	n	$\int_{T_o}^T C_p dT$	Enthalpy
$H_2O$	.916	44,357	40,631
$H_2$	1.729	31,654	54,729

$\Delta h =$  Enthalpy gain of product gases = 95,360 Btu/20 lbs. prop.

Since  $\Delta h \approx Q_R$  a temperature of  $4242^\circ\text{F} = 4702^\circ\text{R}$  can be safely assumed.

Since the adiabatic combustion temperature is lower when dissociation takes place, a value lower than  $4242^\circ\text{F}$  will be used in determining the values of  $K_p$ .

Using a temperature value of  $4180^\circ\text{F}$  the values of  $K_p$  are

$$\text{for } H_2O \rightarrow 1/2 H_2 + OH \quad K_p \text{ at } 4130^\circ\text{F} = 7 \times 10^{-3}$$

$$\text{and } K_p^2 = \frac{20.4 y^3}{2 - 3y + y^3} = 49 \times 10^{-6}$$

$$y^3 = \frac{49 \times 10^{-6}}{20.4} = 2.4 \times 10^{-6}$$

$$y = .0135$$

$$(1-y) H_2O = \frac{1}{2} y H_2 + y OH$$

$$.916 (1-y) H_2O = \frac{.916}{2} y H_2 + .916 y OH$$

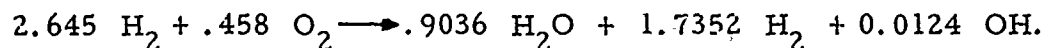
$$H_2O = (.916) (1 - .0135) = .9036$$

$$H_2 = (.916) (.0135) (.5) = .0062$$

$$OH = (.916) (.0135) = .0124$$

Since, for this particular ratio, the amount of hydrogen dissociated ( $H_2 \rightarrow 2H$ ) is of the order of  $10^{-5}$ , this amount is disregarded.

Then the complete equation for the reaction is



As before, the heat of reactions and the enthalpy change in the product gases are evaluated to determine the degree of accuracy of our temperature assumption.

Heat of Reaction			
Gas	n	$Q_F$	$nQ_F$
$H_2O$	0.9036	104,042	94,012
OH	0.0124	-10,620	-131
Heat of reaction $Q_R = 93,881 \text{ Btu/20\#}$			

Enthalpy Change			
$H_2O$	0.9036	44,116	39,863
$H_2$	1.7352	30,922	53,656
OH	0.0124	31,335	389

Enthalpy gain of product gases  $\Delta h = 93,908 \text{ Btu/20lb.}$

Since  $Q_R \approx \Delta h$ , the assumed temperature of  $\approx 4200^\circ F$  or  $4660^\circ R$  is correct.

Specific Heat,  $C_p$ , Molecular Weight,  $M$ , Gas Constant,  $R$

From the values found in the preceding pages. using the equations given below, we now can find:

the specific heat of the product gases:

$$C = \sum (X c_x);$$

the gas constant

$$R = R^1/M,$$

where  $R^1 = \text{Universal gas constant} = 1554 \text{ ft/}^\circ R$

$M_x = \text{Molecular weight of gas (x) in lb/mole;}$

and the molecular weight

$$M = \sum (X M_x).$$



The mole fraction (X) of the gases can now be found.

$$X_{H_2O} = \frac{.9036}{2.6512} = .3408$$

$$X_{H_2} = \frac{1.7352}{2.6512} = .6544$$

$$X_{OH} = \frac{0.0124}{2.6512} = .0048$$

Gas	X	M <sub>x</sub>	X M <sub>x</sub>	C <sub>p</sub>	X C <sub>p</sub>
H <sub>2</sub> O	.3408	18	6.1344	12.8	4.3622
H <sub>2</sub>	.6544	2	1.3088	8.6	5.6278
OH	.0048	17	0.0816	8.8	0.0422
	<u>1.0000</u>		<u>7.5248</u>	<u>30.2</u>	<u>10.0322</u>

$$M = (X M_x) = 7.5248 \text{ lb/mole}$$

$$R = R^1 / M = 1554 / 7.5248 = 206.5$$

$$C_p = 10.0322 \text{ Btu/mole}^{\circ}\text{F} = \frac{10.0322}{7.5248} = 1.333$$

Specific Heat Ratio, K

$$K = \frac{C_p}{C_p - 1.99} = \frac{10.0322}{8.1322} = 1.233$$

Ideal Exhaust Velocity

The ideal exhaust velocity of the system can now be calculated using

$$\text{where } v = \frac{2 g K}{K-1} \frac{R^1}{M} T_1 \left[ 1 - \left( \frac{P_2}{P_1} \right)^{\frac{K-1}{K}} \right]$$

$$g = \text{acceleration of gravity} = 32.2 \text{ ft/sec}^2$$

$$K = \text{specific heat ratio} = 1.233$$

$$R^1 = \text{universal gas constant} = 1544 \frac{\text{ft-lb}}{\text{mole}^{\circ}\text{F}}$$

$$M = \text{molecular weight of gas mixture, lb/mole}$$

$$R^1/M = \text{gas constant of system} = 206.5 \text{ ft}^{\circ}\text{F}$$

$$T_1 = \text{combustion temperature } 4200^{\circ}\text{F}$$

$$P_1 = \text{Combustion chamber pressure } 300 \text{ psia}$$

$$P_2 = \text{nozzle exhaust pressure} = 14.7 \text{ psia}$$

$$\frac{2 g K}{K-1} = 340.79 \text{ ft/sec}^2 \quad \frac{R^1}{M} T = 8.673 \times 10^5 \text{ ft}$$

$$\frac{P_2}{P_1}^{\frac{K-1}{K}} = (.049)^{.18896}$$

$$\begin{aligned}
 x &= (.049)^{.18896} \quad \ln x = .18896 \ln .049 \\
 \ln x &= -.5699 \\
 x &= .565
 \end{aligned}$$

$$\left[ 1 - \left( \frac{P_2}{P_1} \right) \frac{K-1}{K} \right] = 1 - .565 = 0.435$$

$$v = 11340 \text{ ft/sec}$$

### Specific Impulse

The theoretical specific impulse is then given by

$$\begin{aligned}
 I_{sp} &= \frac{v}{g}, \text{ or } I_{sp} = \frac{11340}{32.2} \text{ sec}^{-1} \\
 I_{sp} &= 352 \text{ sec}^{-1}
 \end{aligned}$$

### Mach Number

Since the velocity of sound at  $0^\circ\text{C} = 1087 \text{ ft/sec}$ , at  $4200^\circ\text{F} = 2316^\circ\text{C}$ , the speed of sound will be

$$v_{2316^\circ\text{C}} = v_{0^\circ\text{C}} \sqrt{\frac{T_1}{T_2}}$$

$$v_{2316^\circ\text{C}} = 1087 = \sqrt{\frac{273 + 2316}{273}} = 3348 \text{ ft/sec}$$

The ideal velocity in Mach number will then be

$$v = \frac{11340 \text{ ft/sec}}{3348 \text{ ft/sec}} = 3.387$$

$$v = \text{Mach } 3.387$$

The actual exhaust velocity is then found by correcting the theoretical exhaust velocity by a velocity correction factor experimentally found to be of the order of 0.94.

$$\text{Then } v = \text{Mach } 3.18.$$

### Nozzle Configuration

The exhaust coefficient,  $C_f$ , is calculated using

$$C_P = \sqrt{\frac{2K^2}{K-1} \frac{2}{K+1} \frac{K+1}{K-1} \left[ 1 - \frac{P_2}{P_1} \frac{K-1}{K} \right] + \frac{P_2 - P_3}{P_1} \frac{A_2}{A_t}},$$

and since  $P_2 = P_3 = 14.7 \text{ psia}$ , the last term is dropped.

$$\frac{2K^2}{K-1} = 13.05 \quad \left( \frac{2}{K+1} \right) \frac{K+1}{K-1} = .348 \quad \left[ 1 - \left( \frac{P_2}{P_1} \right) \frac{K-1}{K} \right] = 0.435$$

$$C_f = \sqrt{(13.05) (.348) (.435)} = 1.405$$

The characteristic exhaust velocity is given by

$$C^* = \frac{v}{C_f} = \frac{10,660}{1.405} = 7587 \text{ ft/sec.}$$

$$C^* = \text{Mach } 2.27$$

The nozzle throat area is calculated from

$$A_t = \frac{F}{\xi_f C_f P_1} = \frac{100}{(0.96)(1.405)(300)} = .247 \text{ in}^2.$$

The nozzle throat diameter then is

$$D_t = \sqrt{\frac{4 A_t}{\pi}} = .561.$$

The nozzle exit area can now be computed from

$$A_2 = \frac{\dot{w} v_2}{v_2} = \frac{F g V_1}{(v_2)^2} \left( \frac{P_1}{P_2} \right)^{1/K} = \frac{F g T_1 R_1}{(v_2)^2 P_1 M} \left( \frac{P_1}{P_2} \right)^{1/K}.$$

where

$A_2$  = exit area

$V_1$  = volume of combustion chamber

$v_2$  = ideal exhaust velocity = 11340 ft/sec

$F$  = thrust = 100 lb.

$P_1$  = chamber pressure = 300 psia

$P_2$  = atmospheric pressure = 14.7 psia

$g$  = gravitational acceleration

$T_1$  = chamber temperature = 4200°F

$R^1/M$  = gas constant = 206.5 ft/°F

$K$  = specific heat ratio = 1.233.

then

$$A_2 = .372 \text{ in}^2$$

$$D_2 = .688 \text{ in.}$$

The nozzle area expansion ratio is consequently obtained from the equation

$$\epsilon = \frac{A_2}{A_1} = \frac{.372}{.247} = 1.51.$$

## Summary of Nozzle Parameters

Throat area	= .247 sq. in.	Exit area	= .372 sq. in.
Throat diam.	= .561 in	Exit diam.	= .688 in
Nozzle diffuser		Exhaust velocity	= 10,660 ft/sec
half angle	= 15°		
	L* = 106		

## Injector Design

The propellant weight flow is calculated as follows:

$$\dot{w} = \frac{F g}{v} = \frac{100 \times 32.2}{10660} = .302 \text{ lb/sec}$$

The oxidizer and fuel flow are, respectively,

$$\dot{w}_O = \frac{\dot{w} r}{r+1} = \frac{(.302)(2.75)}{(2.75+1)} = 0.222 \text{ lb/sec} = 2.48 \frac{\text{cu. ft.}}{\text{sec}}$$

$$\dot{w}_f = \frac{\dot{w}}{r+1} = \frac{.302}{(2.75+1)} = 0.080 \text{ lb/sec} = 14.26 \frac{\text{cu. ft.}}{\text{sec}}$$

## Calculation of Line Pressure and Injectors Area

$$\frac{\dot{w}}{A} = C_D \sqrt{\frac{K g}{R} \left( \frac{2}{K+1} \right) \frac{K+1}{K-1} \frac{P^2}{T}}$$

For oxygen:

$$K = 1.4$$

$$\dot{w}_O = \text{oxygen flow} = .222 \text{ lb/sec}$$

$$T_{O_2} = \text{temperature of } O_2$$

$$P_{O_2} = \text{oxygen line pressure}$$

$$R = 48$$

$$C_{D_{O_2}} = 0.68$$

$$\left( \frac{2}{K+1} \right) \frac{K+1}{K-1} = .334$$

For hydrogen:

$$K = 1.41$$

$$\dot{w}_{H_2} = \text{hydrogen flow } 0.8 \text{ lb/sec}$$

$$T_{H_2} = \text{temperature of } H_2$$

$$P_{H_2} = \text{hydrogen line pressure}$$

$$R = 766.5$$

$$\left( \frac{2}{K+1} \right) \frac{K+1}{K-1} = .335$$

$$\frac{\dot{w}_{O_2}}{1.5779 \times 10^{-2} A_{O_2}} = P_{O_2}$$

$$\frac{\dot{w}_{H_2}}{4.6 \times 10^{-3} A_{H_2}} = P_{H_2}$$

$$D_{t_{O_2}} = 0.93 \text{ in}$$

$$6 A_{O_2} = .0407 \text{ in}^2$$

$$P_{O_2} = 346 \text{ psia}$$

$$D_{t_{H_2}} = .240 \text{ in}$$

$$A_{H_2} = .0452 \text{ in}^2$$

$$P_{H_2} = 385 \text{ psia}$$

## Heat Transfer

By assuming an average heat transfer of  $4.5 \text{ Btu/in}^2 \text{ sec}$ , the total heat transfer can be calculated by the product of the average heat transfer times the average surface of the combustion chamber. In our case, the total heat transfer is equal to

$$4.5 \times 61 = 274.5 \text{ Btu/sec.}$$

The amount of heat to be absorbed by the coolant (water) is given by

$$A \bar{q} = \dot{w}_{\text{H}_2\text{O}} \frac{1}{c} \Delta T,$$

$$\text{and } \Delta T = \frac{274.5 \text{ Btu}}{\dot{w}_{\text{H}_2\text{O}} \frac{\text{lb}}{\text{sec.}} 1.005 \text{ Btu/lb}^\circ\text{F}}$$

By selecting an arbitrary value for the temperature differential,  $\Delta T$ , the flow of the coolant can be computed.

The assumption of the average heat transfer was made to allow a good safety factor. Although the value can actually be as low as 1 or 2  $\text{Btu/in}^2 \text{ sec}$ ., a value of  $4.5 \text{ Btu/in}^2 \text{ sec}$ . was selected so as to give a safe value of the speed, amount, and pressure of the coolant, thus preventing the melting of the combustion chamber.

Because of the high value selected we can safely compute the related parameter using the maximum allowable value for  $\Delta T$ , namely

$$140^\circ\text{F i.e. } 140^\circ\text{F} + 70^\circ\text{F} = 210^\circ\text{F}.$$

$$\dot{w}_{\text{H}_2\text{O}} \approx 1.8 \text{ lb/sec.}$$

The evaluation of the cooling coefficient depends on the Reynolds number and Prandtl number. The coil passage will be rectangular in cross-section and will wind around the chamber in a helical fashion.

Since the cross-section area =  $.177 \text{ in}^2$ , and the injection volume flow

$$Q_o = \frac{\dot{w}_{\text{H}_2\text{O}}}{\rho_{\text{H}_2\text{O}}} = \frac{1.8 \text{ lb/sec. } 1728 \text{ in}^3/\text{cu.ft.}}{62.3 \text{ lb/cu.ft.}} = 50 \text{ in}^3/\text{sec.},$$

the injector velocity is

$$v = \frac{Q}{A} = \frac{50 \text{ in}^3/\text{sec}}{.177 \text{ in}^2} = 282.5 \text{ in/sec.}$$

$$v_{\text{H}_2\text{O}} = 23.5 \text{ ft/sec.}$$

The value of  $D$  to be used in the calculation of the Reynolds number equals four times the hydraulic radius.

$$h_e = 0.023 \text{ Cp } \frac{\dot{w}}{A} \left( \frac{D v \rho}{g} \right)^{-0.2} \left( \frac{\mu g c}{K} \right)^{-0.67},$$

where

$$\dot{w}_{H_2O} = 1.8 \text{ lb/sec}$$

$$C_p = 1.005 = c \text{ Btu/lb}^\circ\text{F}$$

$$g = 32.2 \text{ ft/sec}^2$$

$$A = \text{cross-section-area of coolant coil} = .177 \text{ in}^2$$

$$D = 4 \times \text{hydraulic radius, } 4 \times 0.0039 = 0.0156 \text{ ft}$$

$$\text{Hydraulic radius} = \frac{1}{2} \frac{\text{Area}}{\text{Wetted perimeter}} = 0.0039 \text{ ft}$$

$$v = \text{coolant velocity} = 23.5 \text{ ft/sec}$$

$$\text{Wetted perimeter} = 1.876 \text{ in}$$

$$\rho = \text{density of water} = 2.2 \text{ lb/cu. ft.}$$

$$\mu = \text{viscosity of water} = 0.92 \times 10^{-5} \frac{\text{lb-sec}}{\text{sq. ft}}$$

$$K = \text{thermal conductivity} = 0.45 \times 10^{-5} \frac{\text{Btu}}{\text{sec ft}^2 \text{ } ^\circ\text{F}}$$

$$h_e = 0.0124 \text{ Btu/in}^2 \text{ sec}^\circ\text{F}$$

The heat transfer across the liquid film is given by

$$q = h_e (T_{we} - T_e)$$

and the temperature on the liquid side

$$T_{we} = \frac{q}{h_e} + T_e = \frac{5}{0.0124} \frac{77 + 140}{2} \approx 500^\circ\text{F},$$

which is the temperature estimate of the outside wall surface.

If the wall is 0.25 in. thick the equivalent film coefficient for the wall would be

$$h_w = \frac{K_w}{t_w}$$

Since K for Copper is 10.75 Btu/in<sup>2</sup> hr °F/in

$$h_w = \frac{10.75}{0.25 \times 3600} = 0.0119 \frac{\text{Btu}}{\text{in}^2 \text{ sec } ^\circ\text{F}}$$

The wall temperature on the gas side then is equal to

$$T_{wg} = \frac{5}{0.0119} + 500^\circ\text{F} \approx 940^\circ\text{F}$$

To select the appropriate feed pressure

$$\Delta p = f \frac{L \rho v^2}{D 2g}$$

$$\begin{aligned}
 \text{where } f &= 1.15 \times 0.038 \\
 v &= 23.5 \text{ ft/sec} \\
 L &= (7.5)(4.71) \\
 D &= .1888 \text{ in.} \\
 \rho &= 62.2 \text{ lb./cu.ft} \\
 \Delta p &= 30.30 \text{ psia.}
 \end{aligned}$$

### Critical Flow Orifice

The critical flow orifice diameters for measuring the oxidizer and fuel flow are calculated using the general equation

$$\dot{w} = C_D \gamma Y A_2 \sqrt{\frac{2 \Delta p}{\rho}} \quad \text{where} \quad \gamma = \frac{P_1}{R T}$$

For  
Oxygen

$$\begin{aligned}
 C_D &= 0.98 \\
 Y &= 0.86 \\
 \dot{w} &= .222 \text{ lb/sec} \\
 \gamma &= 1.73 \text{ cu.ft/sec} \\
 \rho &= 8.921 \times 10^{-2} \text{ lb/cu.ft.} \\
 \Delta p &= 200 \text{ psia} \\
 \dot{w} &= .222 = (.8428)(1.63)A_{O_2}
 \end{aligned}$$

$$\begin{aligned}
 &\sqrt{\frac{2(144) \Delta p}{8.921 \times 10^{-2}}} \\
 \frac{7.18 \times 10^{-6}}{\Delta p} &= A_{O_2}^2
 \end{aligned}$$

In our case, where a  $\Delta p = 200$  psia in both lines was desired,

$$A_{O_2}^2 = 3.59 \times 10^{-4} \text{ in}^4 \quad A_{H_2}^2 = 6.043 \times 10^{-4} \text{ in}^4$$

$$A_{O_2} = 1.90 \times 10^{-2} \text{ in}^2 \quad A_{H_2} = 2.458 \times 10^{-2} \text{ in}^2$$

$$D_t = 0.1555 \text{ in} \quad D_t = 0.1769 \text{ in.}$$

For  
Hydrogen

$$\begin{aligned}
 C_D &= 0.98 \\
 Y &= 0.86 \\
 \dot{w} &= .08 \text{ lb/sec} \\
 \gamma &= 0.1205 \text{ ft}^3/\text{sec} \\
 \rho &= 5.61 \times 10^{-3} \text{ lb/cu.ft} \\
 \Delta p &= 200 \text{ psia} \\
 \dot{w} &= 0.08 = (.8428)(.1205)A_{H_2}
 \end{aligned}$$

$$\begin{aligned}
 &\sqrt{\frac{2(144) \Delta p}{5.61 \times 10^{-3}}} \\
 \frac{12.077 \times 10^{-6}}{\Delta p} &= A_{H_2}^2
 \end{aligned}$$

REFRACTORY COATINGS RESEARCH AT  
ADVANCED TECHNOLOGY LABORATORIES

DONALD R. MASH

Advanced Technology Laboratories  
Mountain View, California

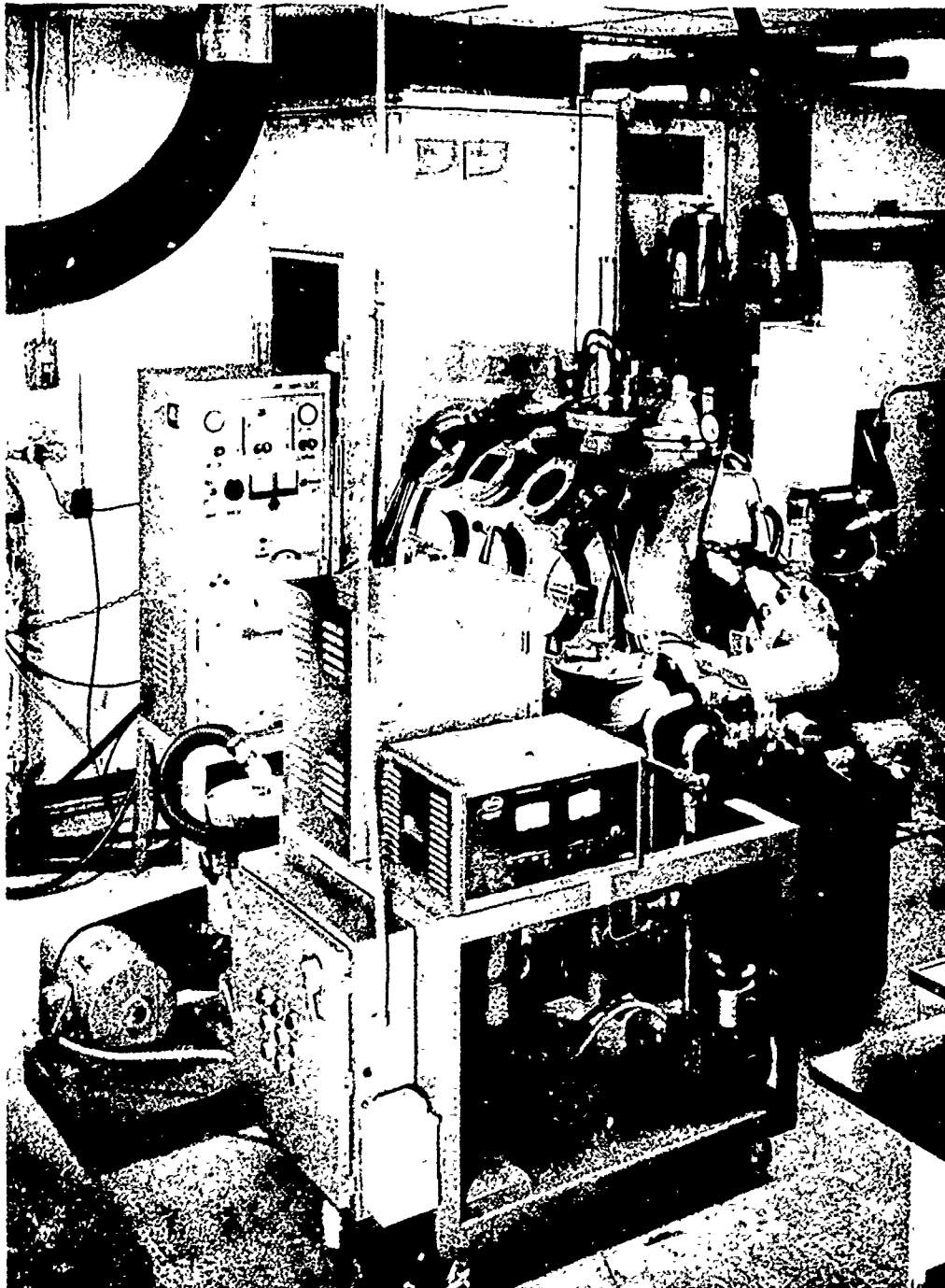


## REFRACTORY COATINGS RESEARCH AT ADVANCED TECHNOLOGY LABORATORIES

Over the past several years, the Materials Laboratory, ATL, has been conducting a wide range of investigations of plasma-jet spraying of composite materials for nuclear, missile, and industrial applications. In this work, emphasis is placed on systematic development of data relating the numerous process variables associated with plasma-jet spraying techniques. Experimental results have been reviewed in several recent publications.<sup>1,2</sup> Equipment and procedures used at ATL are described in these documents. Typical laboratory installations are shown in Figures 1 and 2.

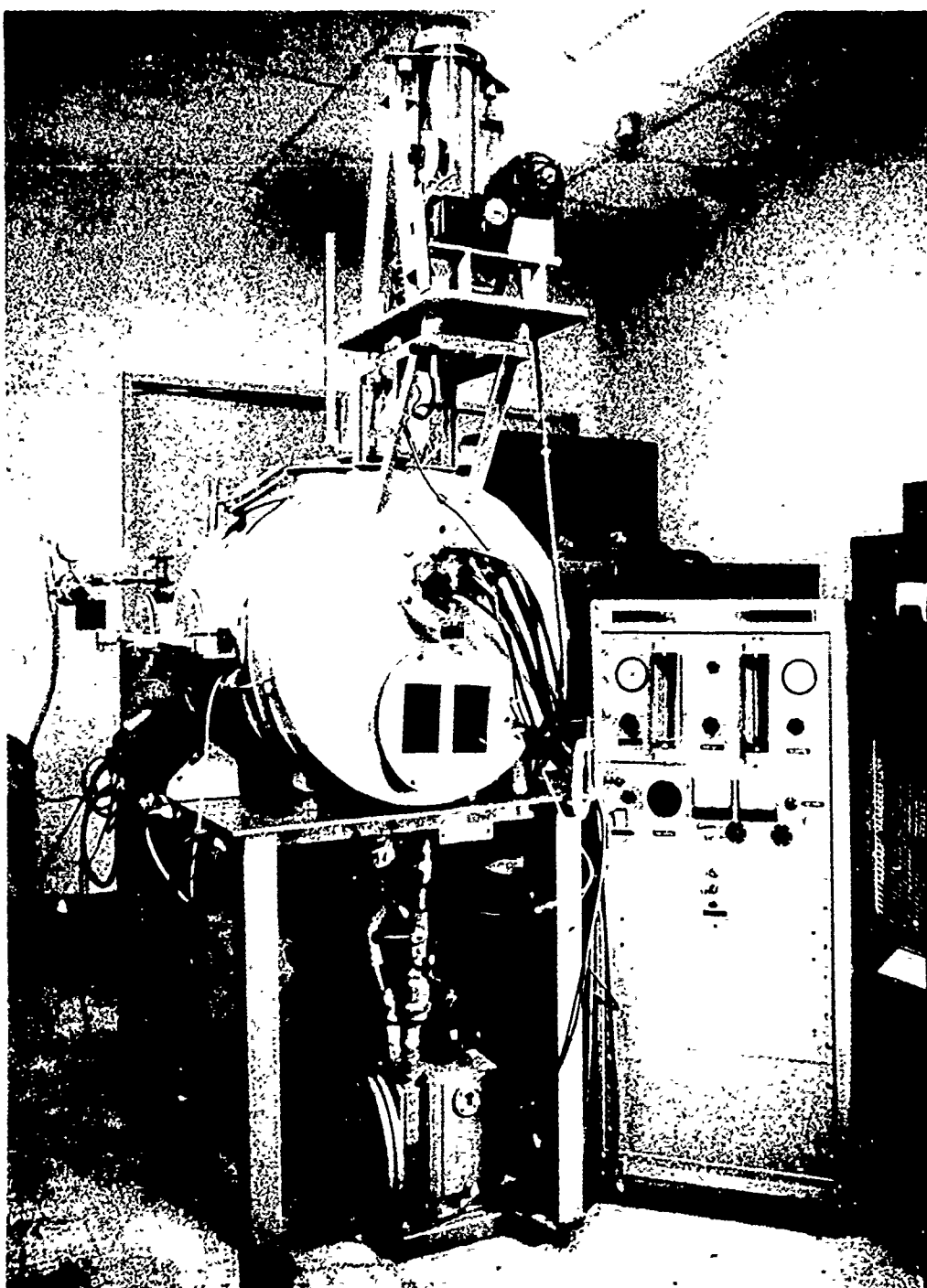
This brief report summarizes recent information accumulated in connection with plasma-jet spraying of metals and refractory compounds of interest to this Group and serves to indicate the current activities of the Materials Laboratory in the area of refractory composites research. Investigations to be discussed are concerned with a variety of high-temperature coatings on several different substrates as well as with free-standing shapes. Materials of interest in the current discussion are included in Table I, in which a number of pertinent properties are compared. It will be noted that each material is characterized by parameters indicating relative ease of spraying and available powder quality. Both parameters are useful in initiating programs involving a variety of materials of widely different characteristics.

- 
1. Mash, D. R., Weare, N. E., and Walker, D. L., "Process Variables in Plasma-Jet Spraying," presented March 23, 1961 at the AIME technical session, Western Metals Congress, Los Angeles, Calif., Journal of Metals, 13, No. 7, July 1961.
  2. Walker, D. L. and Kirby, R. S., "Process Variables in Plasma-Spraying Refractory Coatings on Beryllium," ATL-574, 1 March 1961, for Lockheed Aircraft Corporation, Missiles and Space Division, P. O. 18-2449 under Contract NOrd 17017.



LARGE INERT-ATMOSPHERE PLASMA SPRAY CHAMBER

FIGURE 1



SMALL INERT-ATMOSPHERE PLASMA SPRAY CHAMBER

FIGURE 2

TABLE I  
COMPARISON OF PROPERTIES OF  
MATERIALS USED FOR PLASMA-SPRAYED COATINGS

Material	Melting Point (°C)	Density (gm/cc)	Specific Heat, C <sub>p</sub> (cal/gm-°C)	Thermal Conductivity, k (cgs)	Thermal Expansion (10 <sup>-6</sup> /°C)	d <sub>max</sub> (micron)	* Relative Ease of Plasma Spraying	** Available Powder Quality
4340 Steel	1500	7.84	0.13	0.08	12.0	104	1	A
304 SS	1410	7.90	0.122	0.039	17.0	82	3	A
Nichrome	1400	8.4	0.107	0.036	17.6	73	3	A
Colmonoy No. 6	1010	7.5	-	-	-	-	-	A
Tungsten	3380	19.3	0.033	0.4	4.5	280	1	A
Alumina	2050	3.98	0.21	0.059	6-9	97	2	B
Tungsten Carbide	2870	15.8	-	0.16	5.2	-	-	B
Boron Carbide	2450	2.52	0.443	0.065	4.5	90	2	C
Zirconium Diboride	3050	6.13	0.115	0.055	4.5	102	1	B
Titanium Nitride	2950	5.43	0.19	0.070	-	96	2	C
Zirconium Dioxide	2690	6.27	0.16	0.005	8.7	26	5	A
Uranium Dioxide	2880	10.96	0.075	0.20	10	58	4	B
Titanium Carbide	3250	4.93	0.201	0.04	7.5	72	3	A
Tantalum Carbide	3900	14.65	0.038	0.053	8.2	110	1	A
Zirconium Carbide	3530	6.73	0.15	0.05	6.7	82	3	C

\* Calculated maximum particle diameter for reaching a center temperature of 0.9 melting point in 100 microseconds residence time in the plasma jet.

\*\* Based on d<sub>max</sub>. Indicates the degree of control necessary for spraying satisfactory coatings over five groups of ranges. Group 1 indicates a wide range of control; Group 5 indicates a relatively narrow range.

† Legend refers to performance of commercially available powder in plasma-spraying experiments: A = Good, B = Acceptable, C = Poor.

## I. Refractory Compounds and Metals<sup>\*</sup>

Operating parameters for a number of typical plasma-jet sprayed coatings are summarized in Table II. Substrates employed included stainless steel, mild steel, aluminum, and graphite. Besides being of practical importance, systematic studies yielding such data contribute to an understanding of the general problem of achieving optimum deposition characteristics by plasma-jet spraying techniques.

High deposition efficiency and density can be achieved only with complete particle melting. For a given material and particle size range, therefore, it is worthwhile to examine these deposition characteristics as a function of plasma enthalpy, since this factor determines complete particle melting. Power input and arc-gas flow rate, in turn, determine plasma enthalpy. In addition, arc-gas flow rate influences deposition efficiency by fixing particle residence time in the plasma jet and contributes to density as a result of the impact velocity imparted to the injected particles. Such effects can be separated to some extent by comparing deposition characteristics as a function of arc-gas flow rate at constant enthalpy. Optimum process parameters are established when both density and deposition efficiency are maximized.

Typical data for a number of metallic materials are shown in Figure 3, where both deposition efficiency and coating density are plotted as a function of plasma enthalpy. Each quantity reaches maximum value at a different enthalpy level, indicating that optimum conditions have not been established. Deposition-efficiency curves can be moved to the right by increasing average particle size, using a narrower range of particle sizes, and by increasing powder feed rate. Deposition efficiency provides a sensitive measure of particle melting conditions; however, comparison with density data is essential to determine optimum spray conditions for a given material. An interesting correlation between coating hardness and plasma enthalpy is given in Figure 4, which closely follows density-increase data shown on the previous figure.

---

\* Investigators include D. L. Walker, R. S. Kirby, J. G. Hill, and E. Buchanan.

TABLE II  
OPERATING PARAMETERS FOR PLASMA-SPRAYED COATINGS

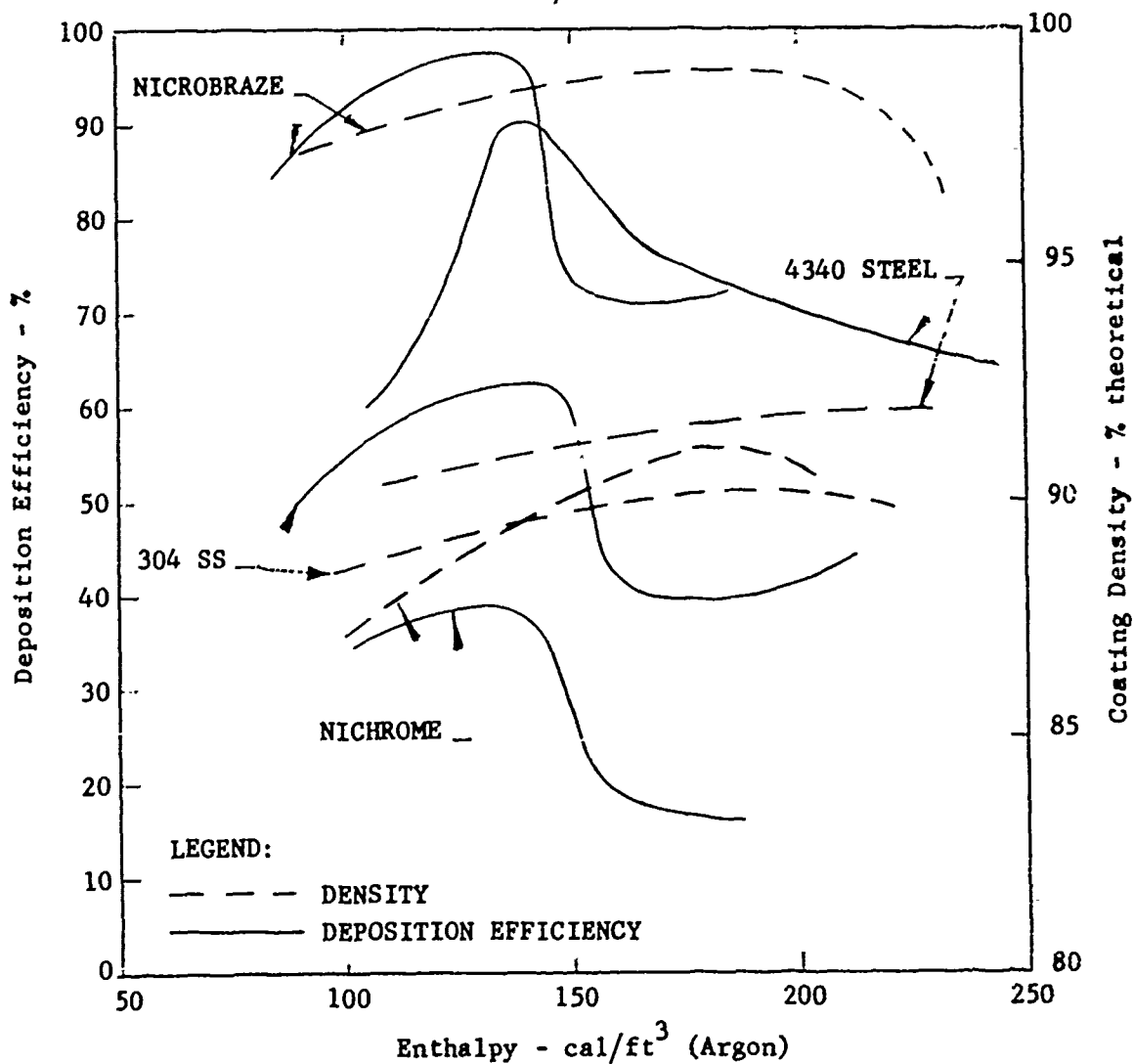
Sprayed Material	Power Input (kw)	Arc Current (amp)	Arc-Gas Flow* (cfh)	Powder-Carrier-Gas Flow (cfh)	Cover-Gas Type	Cover-Gas Flow (cfh)	Powder Feed Rate (gm/min)	Spraying Distance (in.)	Powder Size (mesh)	Traverse Speed (in./min)
304 SS	11-12	400-450	45-50	6.5	He	250	16-18	3½	-200 +325	72
AISI 4340 Steel	10	400	40-50	6.5	He	160	12-13	3½	-200 +325	45
Nichrome (80 w/o Ni- 20 w/o Cr)	9-15	400-600	36-40	6.5	None	None	16	3½	-200 +325	72
Colmonoy No. 6	11-19	450-700	50	6.0	None	None	15-30	3½	-200 +325	72
Tungsten	18	600	60	8.0	He	250	40	2½	-200 +325	45
Alumina	15-16	650-700	50-60	8.0	None	None	7	4	-325	-
Tungsten Carbide	23-25	750	50-60	6.5	None	None	34-50	4	-200 +325	45
Zirconium Diboride	15-19	650-700	25	5.0	He	250	14-15	3½	-325	45
Boron Carbide	19-20	750	20	5.0	He	315	5-6	3½	-200 +325	45
Zirconium Dioxide	>20	750	60	5.0	None	None	<10	4	-200 +325	70
Uranium Dioxide	25	750	60	6.0	He	400	30	3	-200 +325	70
Titanium Carbide	>19.5	750	25	6.0	He	250	<12	3½	-325 +12μ	72
Zirconium Carbide	16	700	30	6.0	He	250	12	2	-325 +12μ	40
Tantalum Carbide	>21	750	30	6.0	He	>160	<15	3	-325 +12μ	72

\* Arc gas was 100% argon for all materials except tungsten, for which 95% argon-5% hydrogen mixture was employed.

MATERIAL	POWER (KW)	POWDER SIZE (MESH)	POWDER FEED RATE (GM/MIN)
NICROBRAZE	11	-200 +325	22
304 SS	11	-200 +325	19
NICHROME	9	-200 +325	16
4340 STEEL	10	-200 +325	13

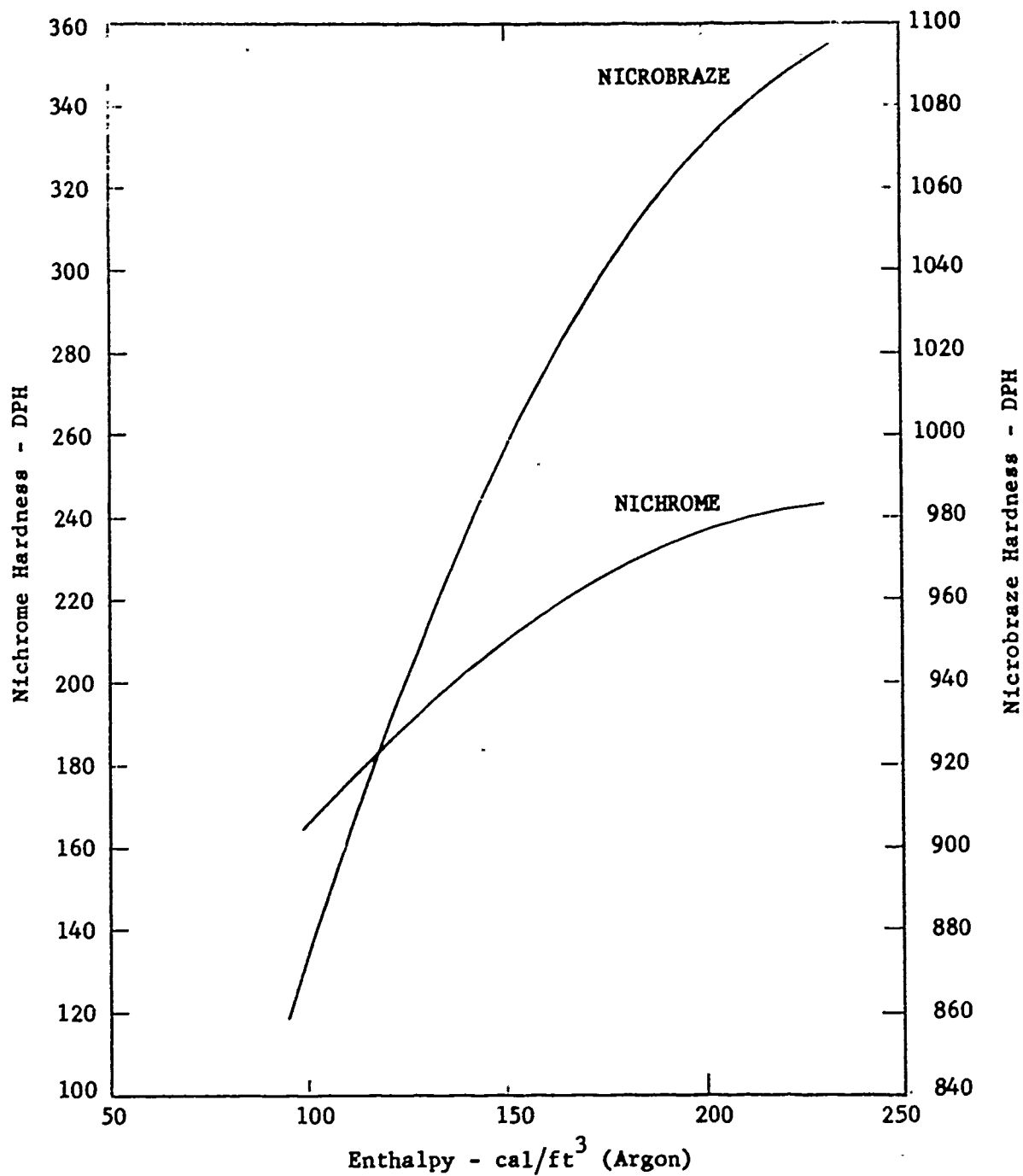
SPRAY DISTANCE:  $3\frac{1}{2}$  IN.

TRAVERSE RATE: 45-72 IN./MIN



EFFECT OF PLASMA ENTHALPY AT CONSTANT POWER INPUT ON  
COATING DENSITY AND DEPOSITION EFFICIENCY OF  
VARIOUS METALLIC MATERIALS

FIGURE 3



HARDNESS OF METALLIC COATINGS ON  
TYPE 304 STAINLESS STEEL SUBSTRATES AS A FUNCTION OF  
PLASMA ENTHALPY

FIGURE 4



A much closer correspondence between deposition efficiency and density maxima was obtained for a number of refractory compounds as a function of plasma enthalpy (Figure 5). Deposition conditions relating enthalpy, particle size, and material properties appear to be more closely established than in the metallic case, possibly due to better control of particle size range and to lower vapor pressure of the refractory materials.

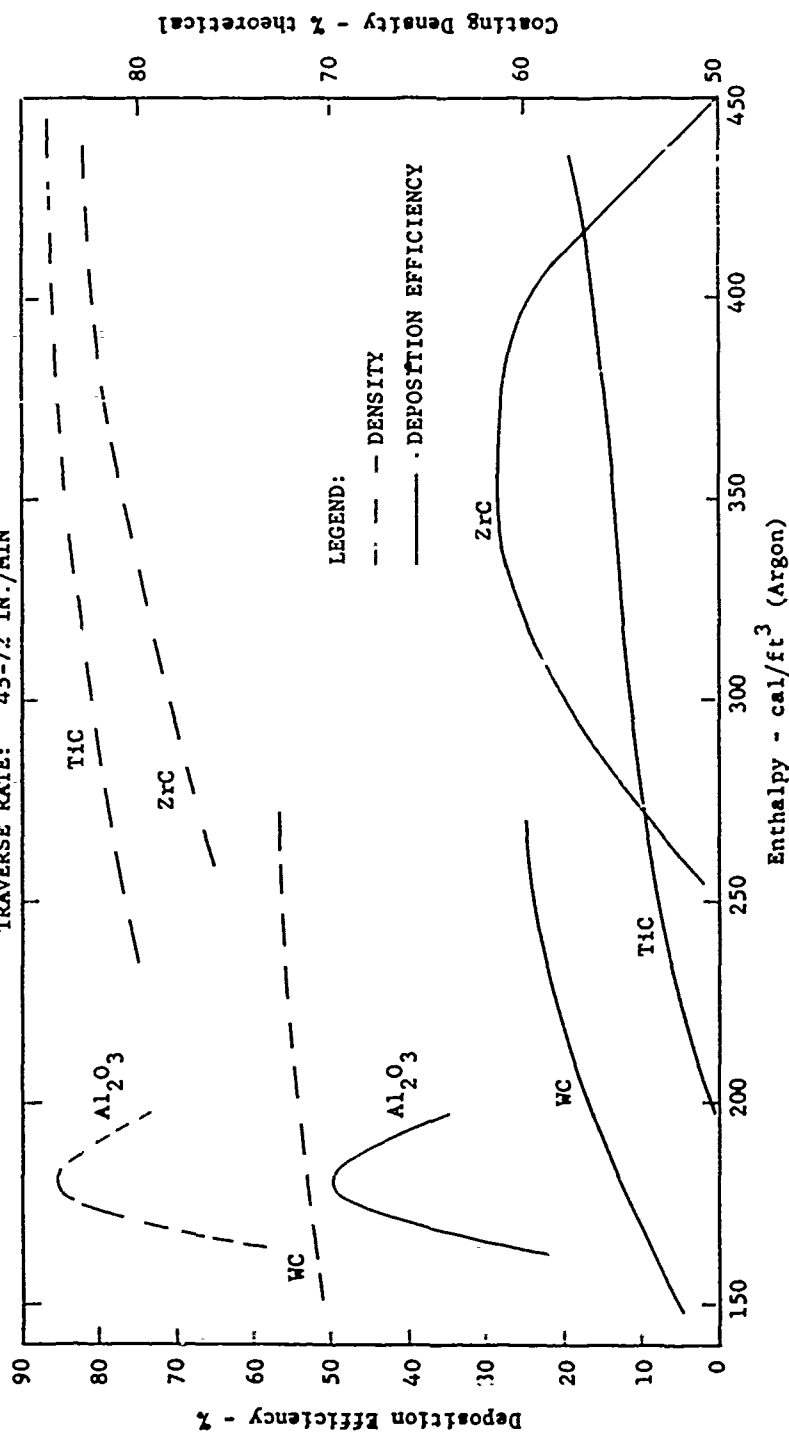
Tungsten free-standing shapes are of considerable interest currently and have been studied rather extensively at ATL. Figure 6 presents density-versus-enthalpy data for plasma-sprayed tungsten in which the effect of adequate particle melting and the supplementary influence of particle velocity are combined. This latter effect can be separated, as shown in Figure 7, where density is plotted against arc-gas flow at constant enthalpy. Maximum density of about 85% of theoretical was achieved, using argon arc gas. Addition of about 5% hydrogen to the arc gas resulted in densities of greater than 90% of theoretical density, chiefly as a result of improved heat-transfer properties of the mixed plasma. Other variables studied include spray distance, traverse rate, and particle size. A spray distance of  $2\frac{1}{2}$  inches produced maximum density, while the influence of traverse rate was minor except for the beneficial influence on surface finish obtained with increasing traverse rate. Density increased somewhat with decreasing particle size.

Representative samples were examined metallographically to observe structural details, especially with respect to porosity and grain size, and to determine apparent degree of melting.

Figures 8 and 9 are photomacrographs of typical samples. Figure 8 illustrates gradual improvement in melting and decrease in porosity with increased enthalpy during spraying. The major porosity still evident in Figure 8.d is between the layers of the coating. Figure 9 illustrates results of attempts to eliminate this interlayer porosity by heating the substrate during spraying (9. a), adding 5% hydrogen to the arc gas to improve heat transfer (9. b), and hot rolling (9. c). It is evident that the addition of hydrogen almost eliminates the interlayer porosity and increases the density to 90%, and that hot rolling accomplishes the same objective.

MATERIAL	POWER (KW)	POWDER FEED RATE (GM/MIN)
TiC	19	14.5
ZrC	17.3	11.2
WC	24	40
Al <sub>2</sub> O <sub>3</sub>	15.5	7

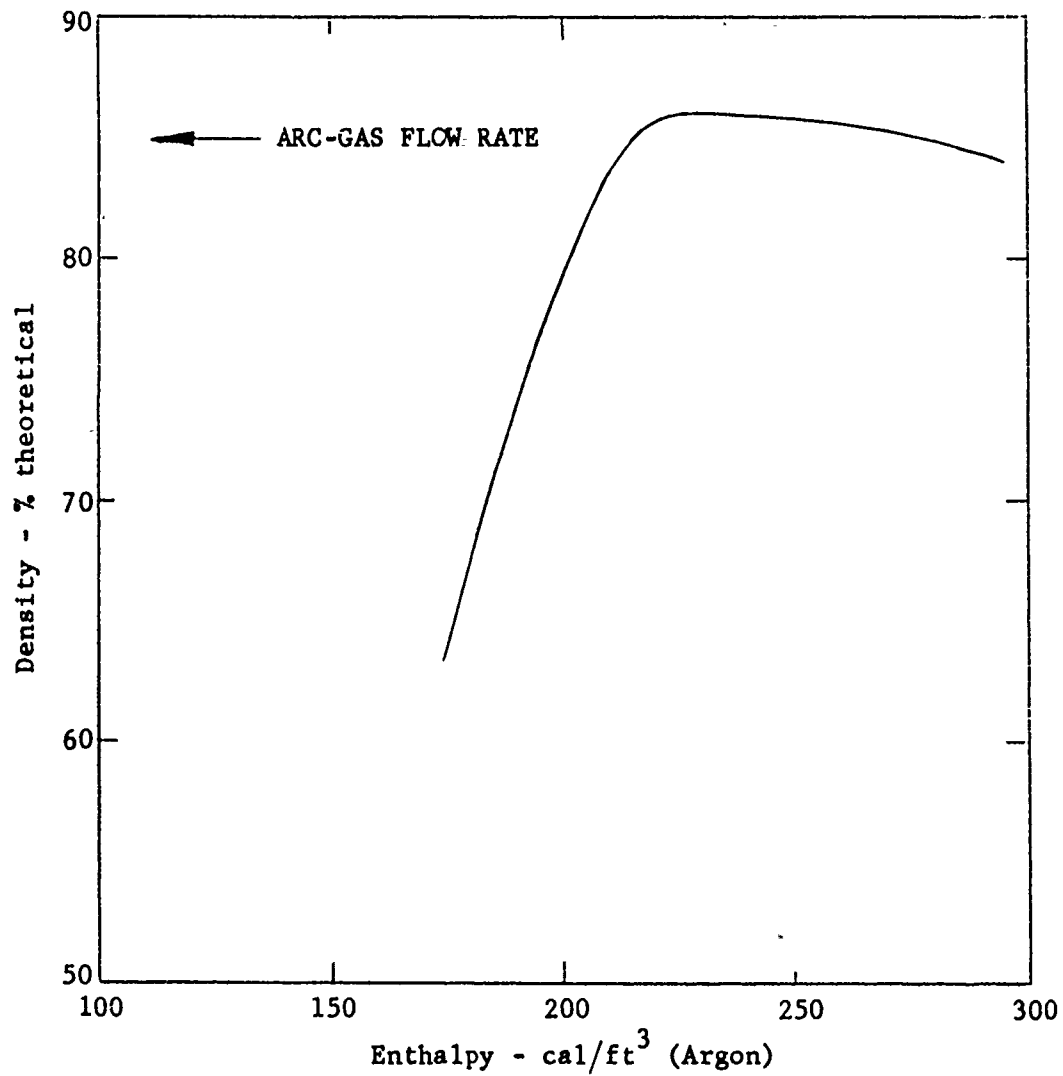
SPRAY DISTANCE: 2½-3½ IN.  
TRAVERSE RATE: 45-72 IN./MIN



EFFECT OF PLASMA ENTHALPY AT CONSTANT POWER INPUT ON  
COATING DENSITY AND DEPOSITION EFFICIENCY OF  
TYPICAL REFRACTORY COMPOUNDS

FIGURE 5

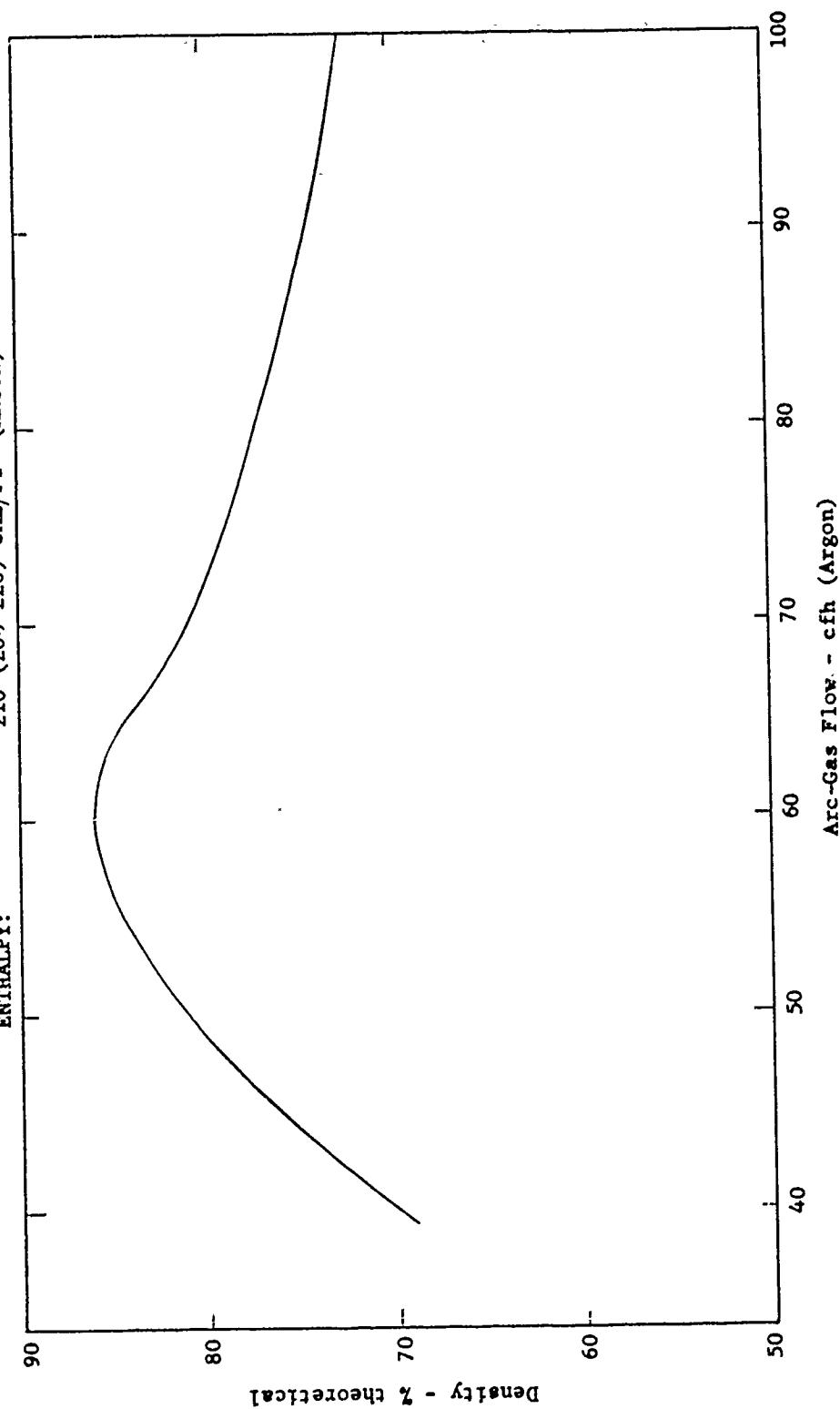
POWER INPUT: 20 KW  
SPRAY DISTANCE: 2½ IN.  
TRAVERSE RATE: 45 IN./MIN  
POWDER FEED RATE: 40 GM/MIN  
DEPOSITION EFFICIENCY: ~70%



EFFECT OF PLASMA ENTHALPY AT CONSTANT POWER INPUT ON  
THE DENSITY OF PLASMA-SPRAYED TUNGSTEN

FIGURE 6

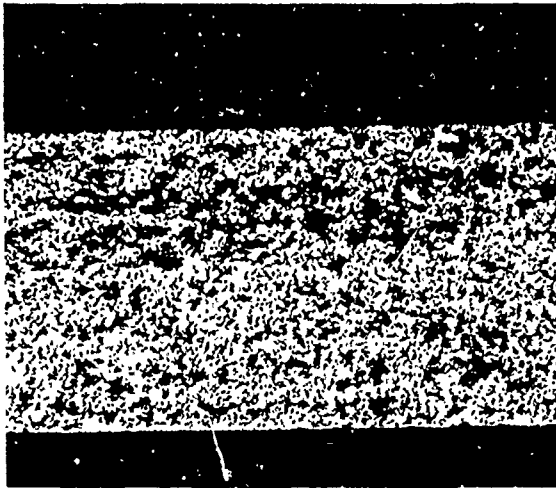
SPRAY DISTANCE: 2½ IN.  
 TRAVERSE RATE: 45 IN./MIN  
 POWDER FEED RATE: 40 GM/MIN  
 DEPOSITION EFFICIENCY: ~70%  
 ENTHALPY: 210 (200-220) CAL/FT<sup>3</sup> (ARGON)



EFFECT OF ARGON ARC-GAS FLOW AT CONSTANT PLASMA ENTHALPY ON  
 THE DENSITY OF PLASMA-SPRAYED TUNGSTEN

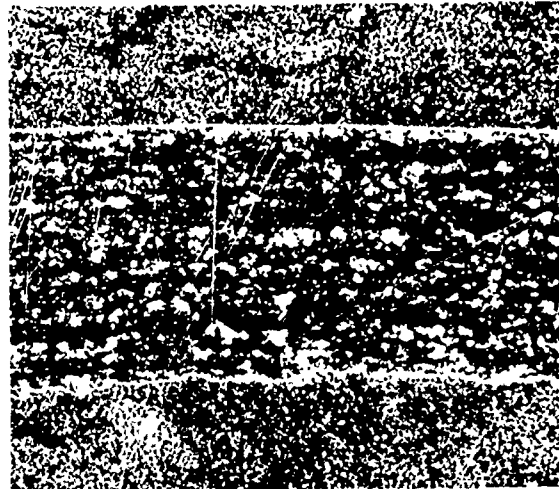
FIGURE 7

a. W-4-1



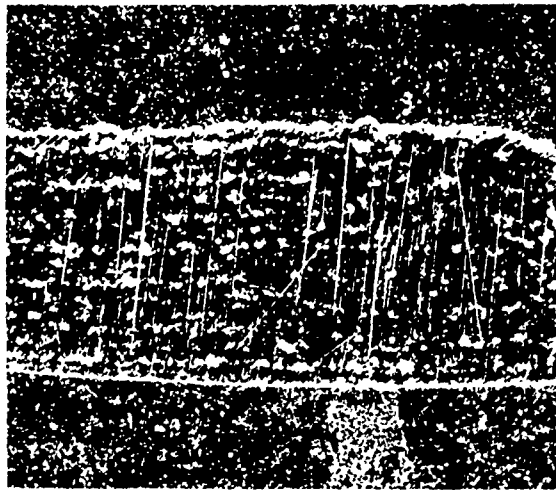
12x  $\rho = 55.8\%$   
 Current = 400 amp  
 Power = 10.8 kw  
 Arc-Gas Flow = 50 cfh argon  
 Spray Distance =  $3\frac{1}{2}$  in.  
 Powder Feed = 35 gm/min

b. W-6-1



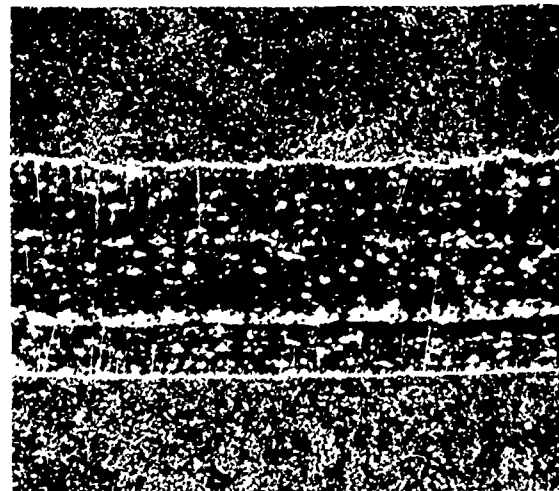
12x  $\rho = 78.2\%$   
 Current = 500 amp  
 Power = 14 kw  
 Arc-Gas Flow = 50 cfh argon  
 Spray Distance =  $3\frac{1}{2}$  in.  
 Powder Feed = 35 gm/min

c. W-11



12x  $\rho = 83.5\%$   
 Current = 600 amp  
 Power = 18.3 kw  
 Arc-Gas Flow = 60 cfh argon  
 Spray Distance =  $2\frac{1}{2}$  in.  
 Powder Feed = 35 gm/min

d. W-14



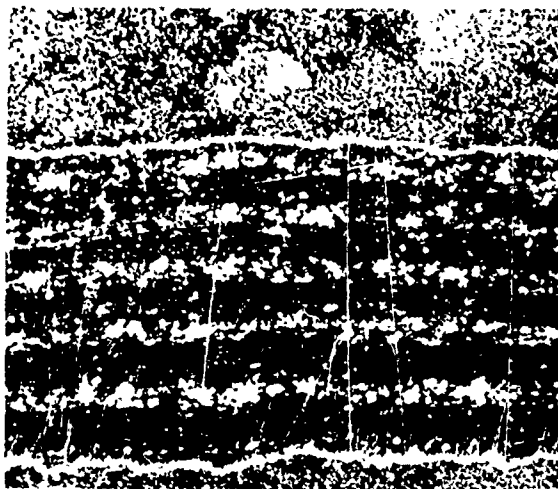
12x  $\rho = 85.3\%$   
 Current = 750 amp  
 Power = 24 kw  
 Arc-Gas Flow = 60 cfh argon  
 Spray Distance =  $2\frac{1}{2}$  in.  
 Powder Feed = 35 gm/min

All sprayed with 280-cfh helium cover gas;  
 traverse rate of 45 in./min.

# PLASMA-SPRAYED TUNGSTEN

FIGURE 8

a. W-41

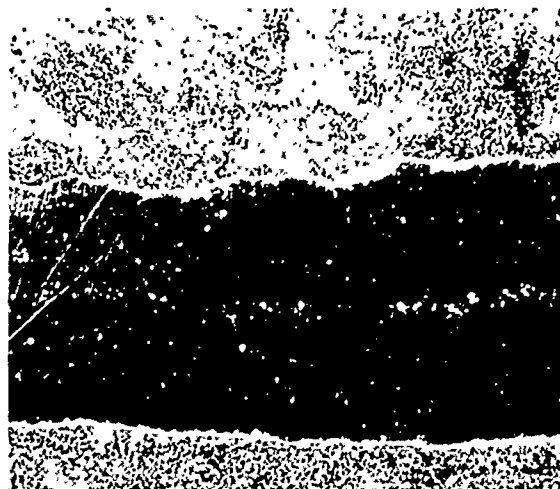


12x

$\rho = 85.3\%$

Current = 600 amp  
Power = 18.3 kw  
Arc-Gas Flow = 60 cfh argon  
Spray Distance =  $2\frac{1}{2}$  in.  
Powder Feed = 35 gm/min  
No cover gas  
Hot substrate

b. W-45

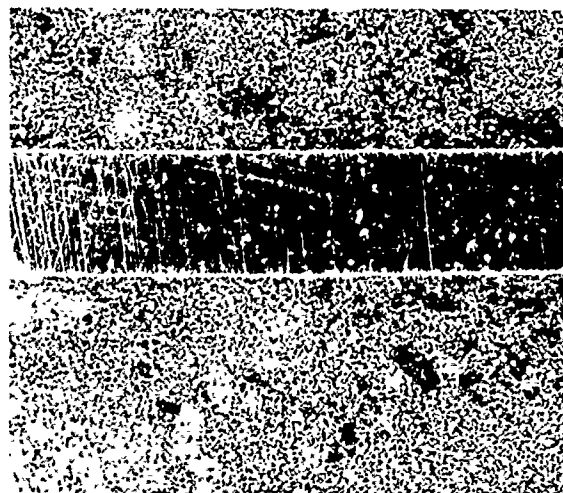


12x

$\rho = 90.4\%$

Current = 600 amp  
Power = 28 kw  
Arc-Gas Flow = 60 cfh (95A-5H<sub>2</sub>)  
Spray Distance =  $2\frac{1}{2}$  in.  
Powder Feed = 35 gm/min  
No cover gas  
5% H<sub>2</sub> mixed with argon arc gas

c. W-37-2



12x

$\rho = 92.1\%$

Current = 600 amp  
Power = 18.3 kw  
Arc-Gas Flow = 60 cfh argon  
Spray Distance =  $2\frac{1}{2}$  in.  
Powder Feed = 35 gm/min  
280-cfh helium cover gas  
Hot reduced 30% by rolling  
Density before rolling = 80%

# PLASMA-SPRAYED TUNGSTEN

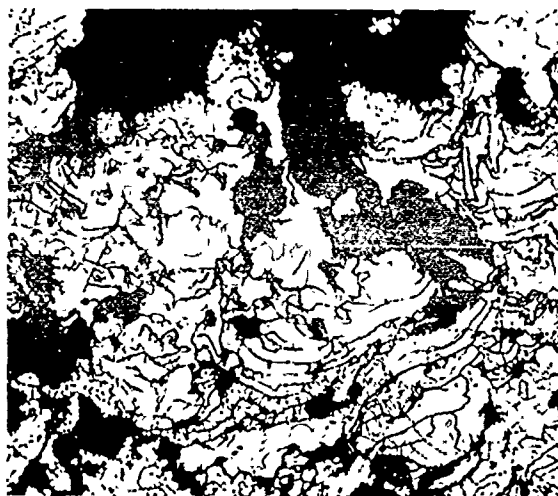
FIGURE 9

Figures 10 and 11 are photomicrographs of the same samples after etching. Equiaxed, fine-grain structures can be obtained when sufficient heat is available to adequately melt the particles. Similar structures can be produced by hot rolling.

Oxygen analyses (vacuum fusion) were performed on as-received powder, sample W-29 (argon arc gas), and sample W-45 (95 argon - 5 hydrogen arc gas). Results were as follows:

As-received powder	0.019%
W-29 (argon)	0.044%
W-45 (95A-5H <sub>2</sub> )	0.0078%

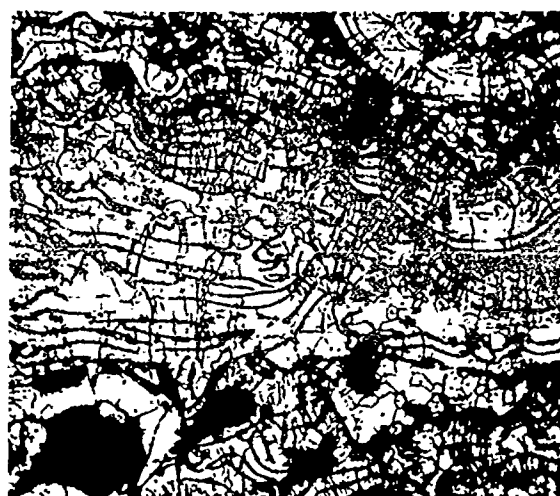
a. W-4-1



250x  $\rho = 55.8\%$

Current = 400 amp  
Power = 10.8 kw  
Arc-Gas Flow = 50 cfh argon  
Spray Distance =  $3\frac{1}{2}$  in.  
Powder Feed = 35 gm/min

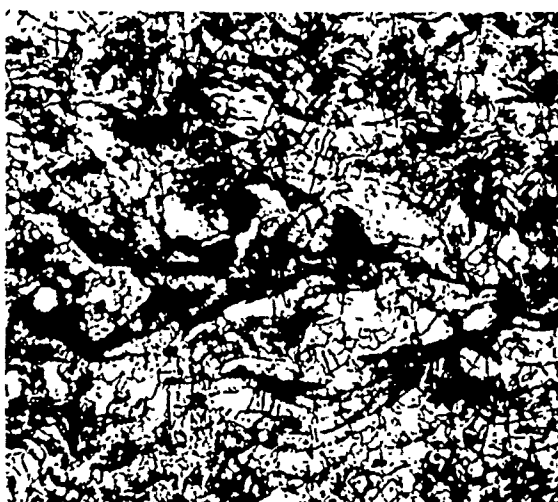
b. W-6-1



250x  $\rho = 78.2\%$

Current = 500 amp  
Power = 14 kw  
Arc-Gas Flow = 50 cfh argon  
Spray Distance =  $3\frac{1}{2}$  in.  
Powder Feed = 35 gm/min

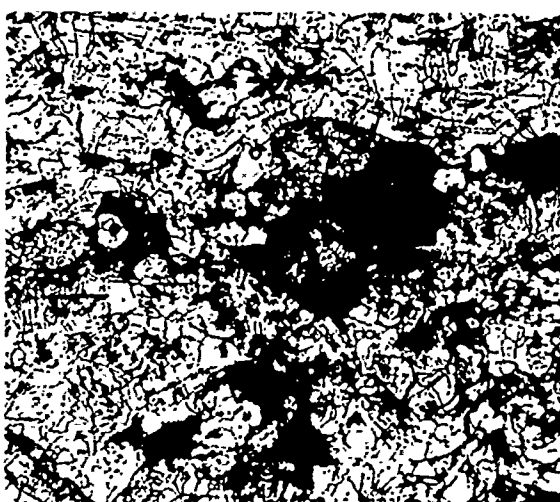
c. W-11



250x  $\rho = 83.5\%$

Current = 600 amp  
Power = 18.3 kw  
Arc-Gas Flow = 60 cfh argon  
Spray Distance =  $2\frac{1}{2}$  in.  
Powder Feed = 35 gm/min

d. W-14



250x  $\rho = 85.3\%$

Current = 750 amp  
Power = 24 kw  
Arc-Gas Flow = 60 cfh argon  
Spray Distance =  $2\frac{1}{2}$  in.  
Powder Feed = 35 gm/min

All sprayed with 280-cfh helium cover gas;  
traverse rate of 45 in./min.

# PLASMA-SPRAYED TUNGSTEN

FIGURE 10



a. W-41



250x  $\rho = 85.3\%$

Current = 600 amp  
Power = 18.3 kw  
Arc-Gas Flow = 60 cfh argon  
Spray Distance =  $2\frac{1}{2}$  in.  
Powder Feed = 35 gm/min  
No cover gas  
Hot substrate

b. W-45



250x  $\rho = 90.4\%$

Current = 600 amp  
Power = 28 kw  
Arc-Gas Flow = 60 cfh (95A-5H<sub>2</sub>)  
Spray Distance =  $2\frac{1}{2}$  in.  
Powder Feed = 35 gm/min  
No cover gas  
5% H<sub>2</sub> mixed with argon arc gas

c. W-37-2



250x  $\rho = 92.1\%$

Current = 600 amp  
Power = 18.3 kw  
Arc-Gas Flow = 60 cfh  
Spray Distance =  $2\frac{1}{2}$  in.  
Powder Feed = 35 gm/min  
280-cfh helium cover gas  
Hot-reduced 30% by rolling  
Density before rolling = 80%

# PLASMA-SPRAYED TUNGSTEN

FIGURE 11

## II. Development of Clad Ceramic Fuel Plates by Spray-Coating Techniques\*

The over-all objective of this program is to develop plate-type uranium dioxide nuclear-reactor fuel elements, using plasma-jet spraying techniques, and to evaluate properties and potential cost savings of these fuel elements. Advantages of a sprayed plate-type oxide fuel element include improved heat-transfer characteristics due to geometry and to the bond between fuel and cladding, and potentially lower fabrication costs.

Phase I, currently in progress, is concerned with investigation of spray-coating variables and evaluation of coating characteristics. Initially, the effects of the process variables were screened by spraying calcium-stabilized zirconia as a stand-in for uranium dioxide. This portion of the program has been completed, and uranium dioxide coatings are currently being evaluated. Emphasis has been placed on density, adherence, and efficiency of deposition.

### Materials and Procedure

Arc-fused uranium dioxide powder has been used throughout most of this investigation. Coatings have been made on 304 stainless steel, and on Zircaloy-2 substrates. Substrate thicknesses as low as 0.020 inch have been sprayed with coatings up to 0.100 inch thick.

Uranium dioxide is sprayed in a vacuum-purged inert-atmosphere chamber under argon (Figure 1). This procedure is necessary to prevent oxidation to  $U_3O_8$  or an intermediate oxide. The importance of spraying atmosphere on the stoichiometry of  $UO_2$  is illustrated by Table III.

### Coating Density and Deposition Efficiency

Densities as high as 90 to 91% theoretical (10.98 gm/cc) have been obtained. Variables studied include power input, spray distance, the use of cover gas, arc-gas flow, powder type, and powder size. Increasing power input and decreasing spray distance resulted in improved coating densities, but increased the tendency for cracking and spalling of the coatings. Cracking and spalling were reduced or eliminated by use of helium cover gas to provide surface cooling.

---

\* Work performed under AEC-Euratom sponsorship on Contract AT(04-3)-250, Project Agreement No. 4. Investigators include N. E. Weare, Dr. H. Marchandise, and E. Buchanan.

TABLE III  
OXYGEN-TO-URANIUM RATIO OF AS-RECEIVED  $\text{UO}_2$  POWDER  
AND COATINGS SPRAYED UNDER VARIOUS ATMOSPHERES

<u>Spraying Conditions:</u>	Powder Type	Fused
	Powder Size	-200, +325 mesh
	Power Input	25 kw
	Arc-Gas Flow (Argon)	75 cfh
	Spray Distance	4 to 6 inches
	Powder Feed	60 gm/min
<u>Spraying Atmosphere</u>		<u>O/U Ratio</u>
As-Received Powder		1.95
Argon, double purge		1.93, 1.98
Argon, slight contamination of atmosphere		2.05, 2.08
Air		2.34, 2.41

The general relationship obtained between deposition efficiency and plasma enthalpy is shown in Figure 12. The separate influence of arc-gas flow rate on coating density at constant enthalpy is shown (Figure 13) to be very significant. Maximum densities of 88 to over 90% of theoretical, depending on spray distance, were observed at values of about 75 cfh argon. Deposition efficiencies were maximized at about 60 cfh argon, and somewhat lower enthalpy values achieved (Figure 14) indicated the need for close particle-size control to establish optimum parameters. The influence of powder feed rate on deposition efficiency is shown also in Figure 14.

Fused  $\text{UO}_2$  powder produced coatings of higher density than did sintered powders. This is due primarily to the fact that the fused particles are nearly 100% of theoretical density, while the sintered particles contain a considerable amount of porosity. Similar effects were noted previously when spraying fused and sintered zirconia powders.

Powder particle size is more critical when spraying uranium dioxide than zirconia. Various powder sizes are currently being sprayed under constant spraying conditions to fully evaluate the effect of particle size. The best results to date have been accomplished using -200, +250 mesh powder.

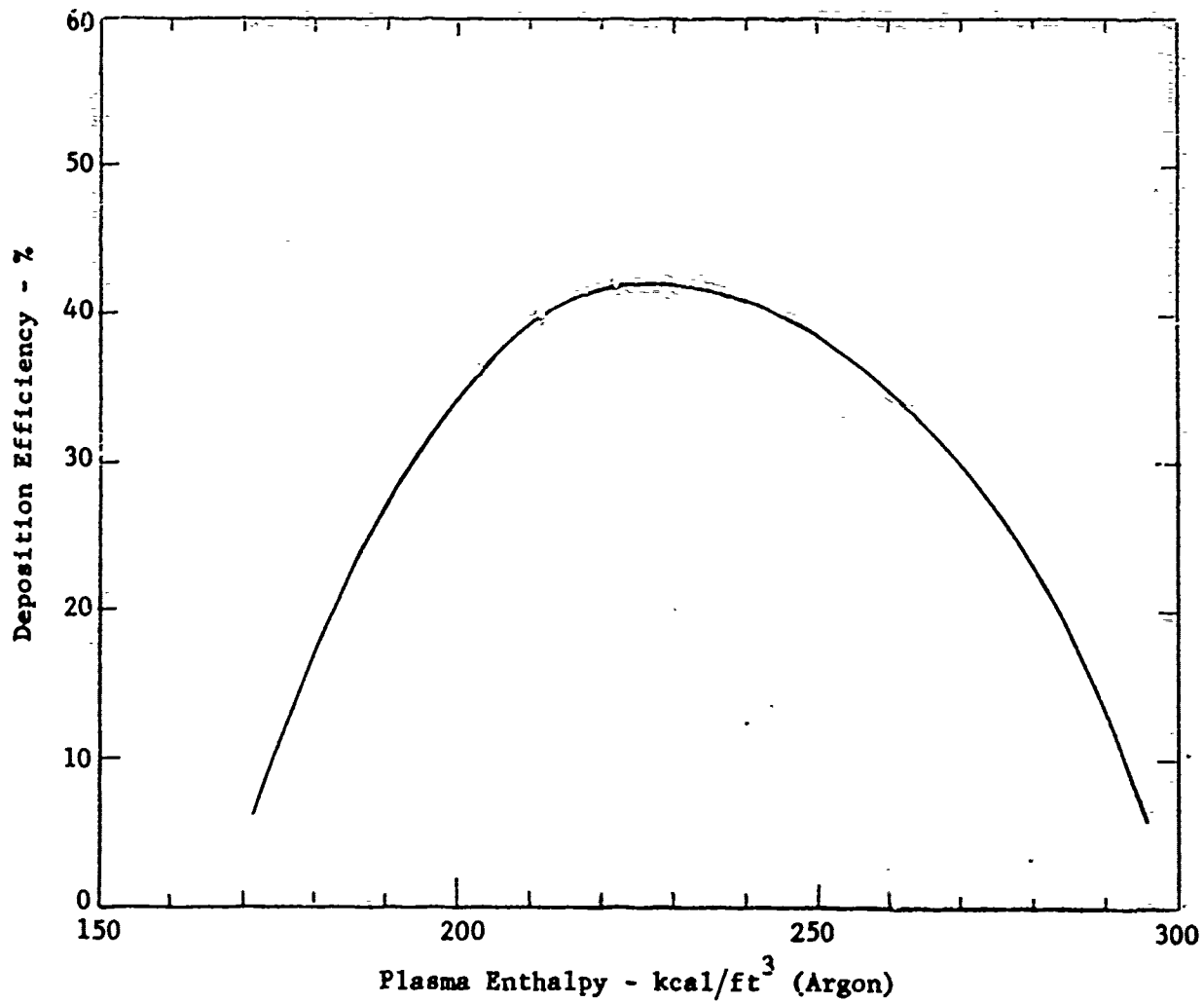
One major problem is the friability of  $\text{UO}_2$  powders. For example, powder screened to -200, +250 mesh breaks up in the feed system to 53% (-200, +250), 44% (-250, +225), and 3% (-325 mesh).

#### Coating Adherence

A major advantage of a sprayed fuel element is an integral bond between the fuel and the cladding. Adherence of sprayed  $\text{UO}_2$  fuel is therefore of prime importance. Coating adherence has been found to be a function of substrate type, surface preparation, thermal history during spraying, geometry of the spray pattern, and coating thickness.

More adherent coatings are produced on Zircaloy-2 substrates than on stainless steel because slightly rougher surfaces are produced on Zircaloy under identical grit-blasting conditions and because Zircaloy possesses a thermal-expansion coefficient about 40% of that for stainless steel.

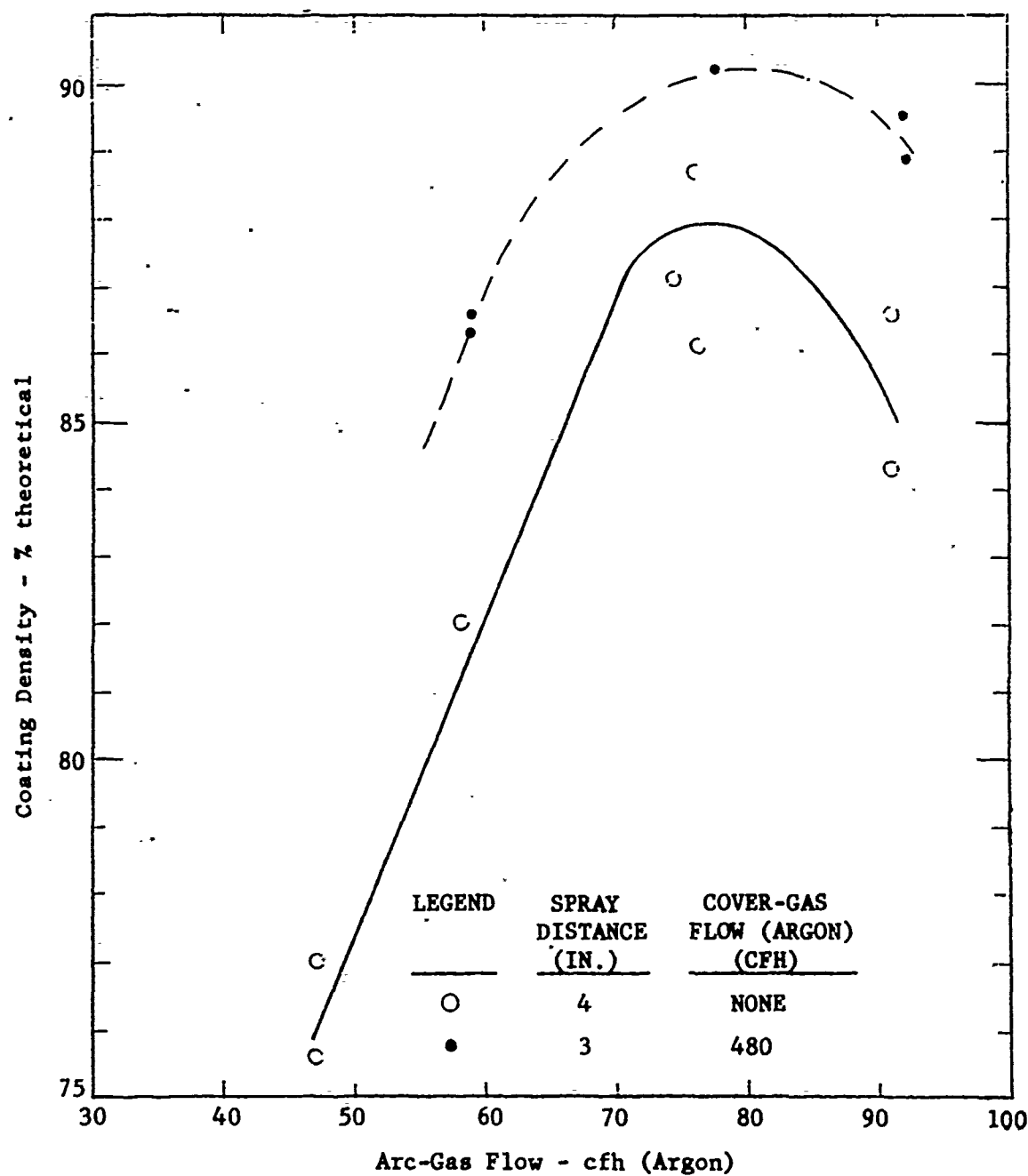
POWDER: FUSED  $\text{UO}_2$  (-200, +325 MESH)  
POWER INPUT: VARIABLE  
ARC-GAS FLOW: VARIABLE  
SPRAY DISTANCE: 4 IN.  
TRAVERSE RATE: 50 IN./MIN  
POWDER FEED RATE: 30 GM/MIN  
POWDER GAS FLOW: 6-7 CFH (ARGON)



EFFECT OF PLASMA ENTHALPY ON  
THE DEPOSITION EFFICIENCY OF URANIUM DIOXIDE

FIGURE 12

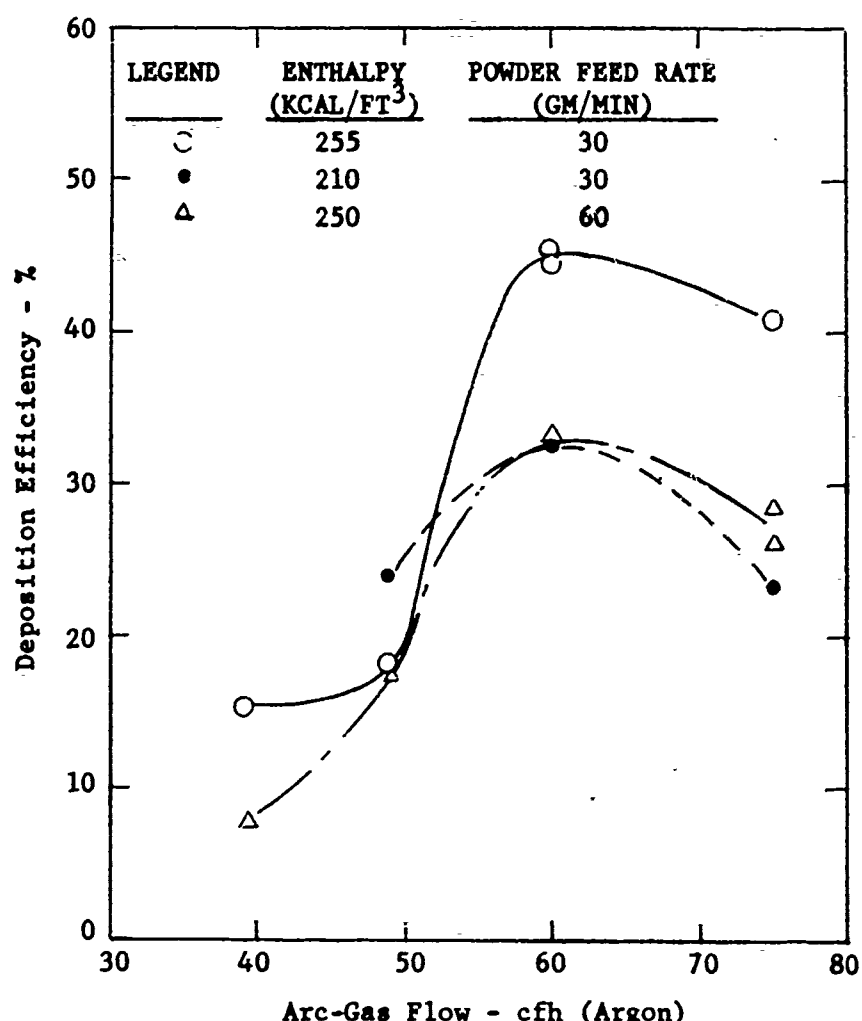
POWDER: FUSED  $\text{UO}_2$  (-200, +325 MESH)  
 ENTHALPY: 265 KCAL/FT<sup>3</sup>  
 TRAVERSE RATE: 70 IN./MIN  
 POWDER FEED RATE: 60 GM/MIN  
 POWDER GAS FLOW: 10 CFH (ARGON)



EFFECT OF ARC-GAS FLOW ON THE COATING DENSITY OF URANIUM DIOXIDE AT CONSTANT PLASMA ENTHALPY

FIGURE 13

POWDER: FUSED  $\text{UO}_2$  (-200, +325 MESH)  
 SPRAY DISTANCE: 4 IN.  
 TRAVERSE RATE: 50 IN./MIN  
 POWDER GAS FLOW: 6-7 CFH



EFFECT OF ARC-GAS FLOW ON THE DEPOSITION EFFICIENCY OF URANIUM DIOXIDE AT CONSTANT PLASMA ENTHALPY

FIGURE 14

To date, substrate surfaces have been prepared by gritblasting to provide a strong mechanical bond. On thin substrates, this is followed by straightening and annealing. Silicon carbide, sand, garnet, and iron blasting media have been tried. Of these, sand is the least desirable. Although the remaining three media provide an adequate surface, silicon carbide is preferred since it provides the cleanest surface for spraying. Bend tests have been made of coatings sprayed on 0.030-inch-thick substrates. Figure 15 shows four specimens bent around a 1-inch radius. Even though cracks occurred during bending, the coatings remained adherent in all cases, except for surfaces blasted with sand.

Additional studies are being conducted using chemical etching, presprayed bond layers, and gradated coatings as methods of improving coating adherence.

The effect of thermal history on the distortion resulting from spraying and on coating adherence has been studied. Conclusions of this study were:

- 1) Substrate temperatures must be kept below 500 C, while the coating must be maintained at a temperature below 870 C. Helium cover gas can be used to provide the required degree of temperature control.
- 2) The substrate must be in the fully annealed condition prior to spraying.
- 3) At spray distances below 1 inches, without the use of cover gas, traverse rates of 71 in./min or higher must be used at power levels of 22 to 25 kw and arc-gas flow rates of 55 to 75 cfh argon.

Under the best spraying conditions and a 3-inch spray distance, the deposition pattern is nearly circular and about 1/2 inch in diameter. Slight variations in arc-gas flow rate result in a very hot, narrow, deposition pattern about 1/8 inch wide by about 1/4 inch long. With this type of pattern, the coating will crack along each side of the pass and will subsequently peel off the substrate.

Coating thickness also influences adherence, since increasing coating thickness results in increased residual stresses at the interface. Coating thicknesses up to 0.050 to 0.060 inch are very adherent. However, coatings about 0.100 inch thick are less adherent and will not accept a severe bend such as that shown in Figure 15.





IRON

GARNET

SiC

SAND

BLASTING MEDIA

SUBSTRATE THICKNESS: 0.030 IN.

COATING THICKNESS: 0.050 IN.

BEND-TESTED COUPONS OF URANIUM DIOXIDE ON  
STAINLESS STEEL SUBSTRATES PRESSURE-BLASTED  
WITH FOUR BLASTING MEDIA

FIGURE 15

### III. Conclusions

Available results indicate the technical and economic feasibility of fabricating  $\text{UO}_2$  plate-type fuel elements by plasma-jet spraying techniques. Adherent deposits of adequate density have been produced in relatively thick sections. Final conclusions as to the importance of this approach to reactor fuel-element design must be reserved until in-pile behavior is investigated and compared to that of alternative designs.

INTERFACE BONDING STUDIES AND  
A NEW PLASMA ARC SPRAY GUN  
ACCOMPLISHMENTS AND PLANS

D. H. LEEDS

Aerospace Corporation  
El Segundo, California

INTERFACE BONDING STUDIES AND A NEW PLASMA ARC SPRAY GUN  
ACCOMPLISHMENTS AND PLANS

Under contract AF 04(647)-165, a 40 kw plasma arc spray facility was established (see figures 1 and 2). Accordingly, a plasma spray gun was designed and built and subsequently improved upon. Figures 3, 4 and 5 show the progressive changes which have been made over the past year in gun design.

Generation one design was used solely with a 3 1/2 kw (250 Amp) welding generator, and worked on softened tap water. This unit was thoroughly checked for thermal efficiency and other correlative theoretical design data with oscilloscopes, thermocouples and pressure gages. The design operated at from 51 to 67 percent efficiency, depending upon mass flows and power. No powder was sprayed through this unit since the current (250 Amps) was insufficient to heat even the minimum powder flow.

Generation two design, made with the identical heat transfer surfaces as generation one, was operated successfully at 27.5 kw (1100 Amps). The main advantage of this unit over the first generation design was the mechanical interchangeability of parts. The first unit was entirely soldered together. Hose connections on generation two utilized polyflow tubing which was subsequently found unreliable because of the effect of proximate heat on inner pressurized polyethylene hosing. A strong reliance on epoxy resined gas sealing joints, and on the water sealing capability of multicycled force fit parts, soon initiated the third generation design. Again, however, the heat transfer surface relationships seen by the cooling water, remained unchanged.

Generation three design may be completely disassembled into interchangeable parts - several varied shape cathode tip designs and several anode nozzle designs are possible. The parts are standardized and virtually trouble free. Some

difficulty was encountered with anode to cathode arcing contours, and some hole stoppage by tungsten melts was seen, but at this writing these troubles have been largely overcome.

Figures 6 and 7 show some of the breakdown assemblies of the anode, and cathode of generation three design. Figure 8 shows the most recent anode to cathode configuration. Figure 9 shows a full size assembly cross section schematic of the still later generation four spray gun.

The foremost incentive in attempting to design a spray gun was to significantly improve on plasma spray gun designs. Thus a rear electrode powder introduction (which had unsuccessfully been attempted in the past) was incorporated into the new design. A thoroughly water cooled cathode was included to allow a greater latitude in power capability (i.e., the new unit is designed for 80 - 100 kw using 5 gpm 60 psi tap water).

While gun design matured, the system was operational. "As deposited" coating densities were studied. Relationships at low power level were established between tungsten plasma coating deposit efficiency and the variables of anode and cathode mass flow (figure 10), enthalpy (figure 11) distance of substrate from spray nozzle face (figure 12) and finally rear to forward electrode configuration (see figure 8). It is believed that this last variable precluded other investigators from using rear electrode powder introduction. Figure 13 is a tabular compilation of the experimentally noted variables which could affect spray deposit efficiency.

Early photomicrographs (figures 14, 15 and 16) of sprayed tungsten indicate that for a given low enthalpy the latest plasma spray gun design results in decreased coating porosities over commercial designs. Densities on

the order of 89 percent of theoretical were measured.

A simple "Jolly Balance" (which utilizes Archimedes principle) was used to carefully measure these densities which ranged from 86 to 90 percent with the bulk of the measurements at 89 percent level. Commercial coating samples from local vendors which had been made at 20 kw ranged from 84 to 88 percent theoretical tungsten density, enjoying a higher deposit efficiency. The deposit efficiencies that we measured were done on a seventeen inch diameter aluminum plate which for the bulk of the experiments was not grit blasted. This plate was coated over a two inch area - one inch from the outer circumference, the plate was rotated and translated before the stationary spray gun, at  $90^{\circ}$  to the gun. It is felt that this represents a rather severe test for deposit efficiency from the standpoint of excessive cooling. It is postulated that the gain in electrical and thermal efficiencies over commercial designs is accomplished by virtue of the spray particles having a longer dwell time in the plasma carrier gas and a closer proximity to - if not a passing through, the electric arc. The increased available heat flux to the particles (i.e., increased over other designs) would result in a more plastically deformable material upon impingement.

With a more pliable particle, the limiting factor in coating formation would be the substrates receptivity.

Primary emphasis in the months to follow will be on a more detailed study of the nature of the bond between the substrate and the sprayed material including the investigation of improved substrate preparation techniques. Specific studies to determine bonding variables will be carried out in the following order:

- (1) Establish an experimental control with simple shear bond strength tests.

- (2) Study mechanisms of bonding by sequential discrimination.
- (3) Investigate methods of inducing surface activity.
- (4) Perform shear bond strength tests to establish a correlation between (1) and (3).
- (5) Perform thermal shock and conductivity tests to establish the usefulness of (4).
- (6) Investigate optimum shape and size of spraying materials.

The Aerospace axial rear electrode powder introduction has minimally an order of magnitude more latitude for increasing powder and intrainment gas mass flow over the existing commercial transverse powder introduction designs (i.e. transverse to the plasma column).

Recent work by Levinstein and Johnson at G.E.<sup>(1)</sup> includes the effects of the different spraying variables on coating density. In the course of the research program a device to measure velocities of spray particles in transit was made to determine the effect of this variable on density. After collaboration with G.E., a velocity meter similar to their design was built by Aerospace Corporation, for use in studying the effect of spray particle (coating) and grit blasting velocities on coating bond strengths.

Refractory and ablative coating systems are used under severe shear stress conditions in both internal and external vehicular environments where they allow usage of common structural substrate materials. Ceramic sprayed coatings achieve a maximum room temperature tensile bond strength on order of 500 to 1000 psi (refractory metal coatings achieve from 2000 to 3000 psi) tested until failure of the adhesive bond. The preceding work has been and is being carried out in a research program at the Aerospace Corporation which is aimed at studying the coating to substrate interface bonding characteristics, and applying the knowledge gained therefrom toward drastically increasing the bonding characteristics of future plasma sprayed coatings.

# REFERENCES

1. M. A. Levinstein, C. E. Johnson, "Properties of Plasma Sprayed Materials", January - March, 1961, General Electric Company, DM 61-102.



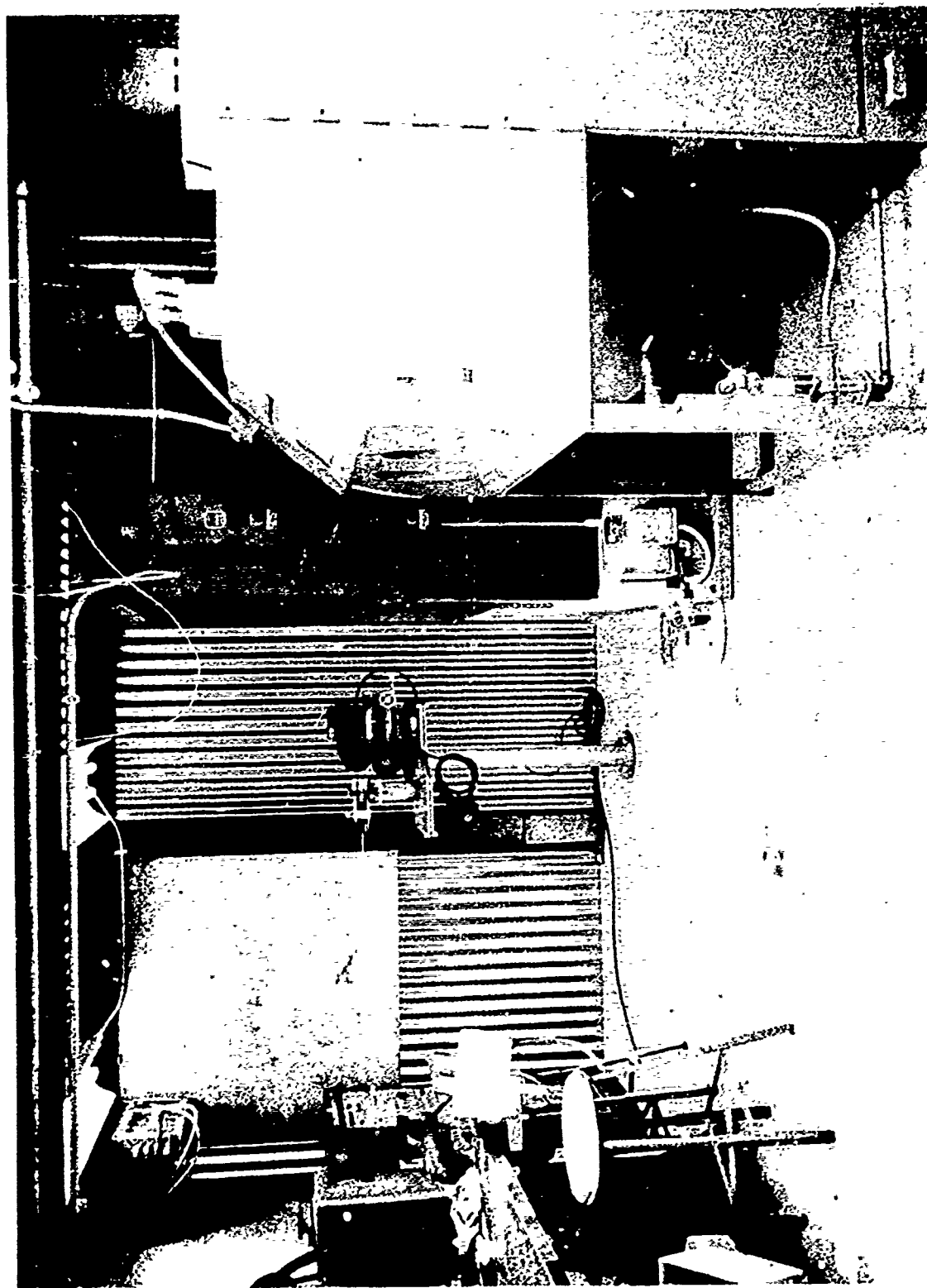


Figure 1. ARC SPRAY LABORATORY

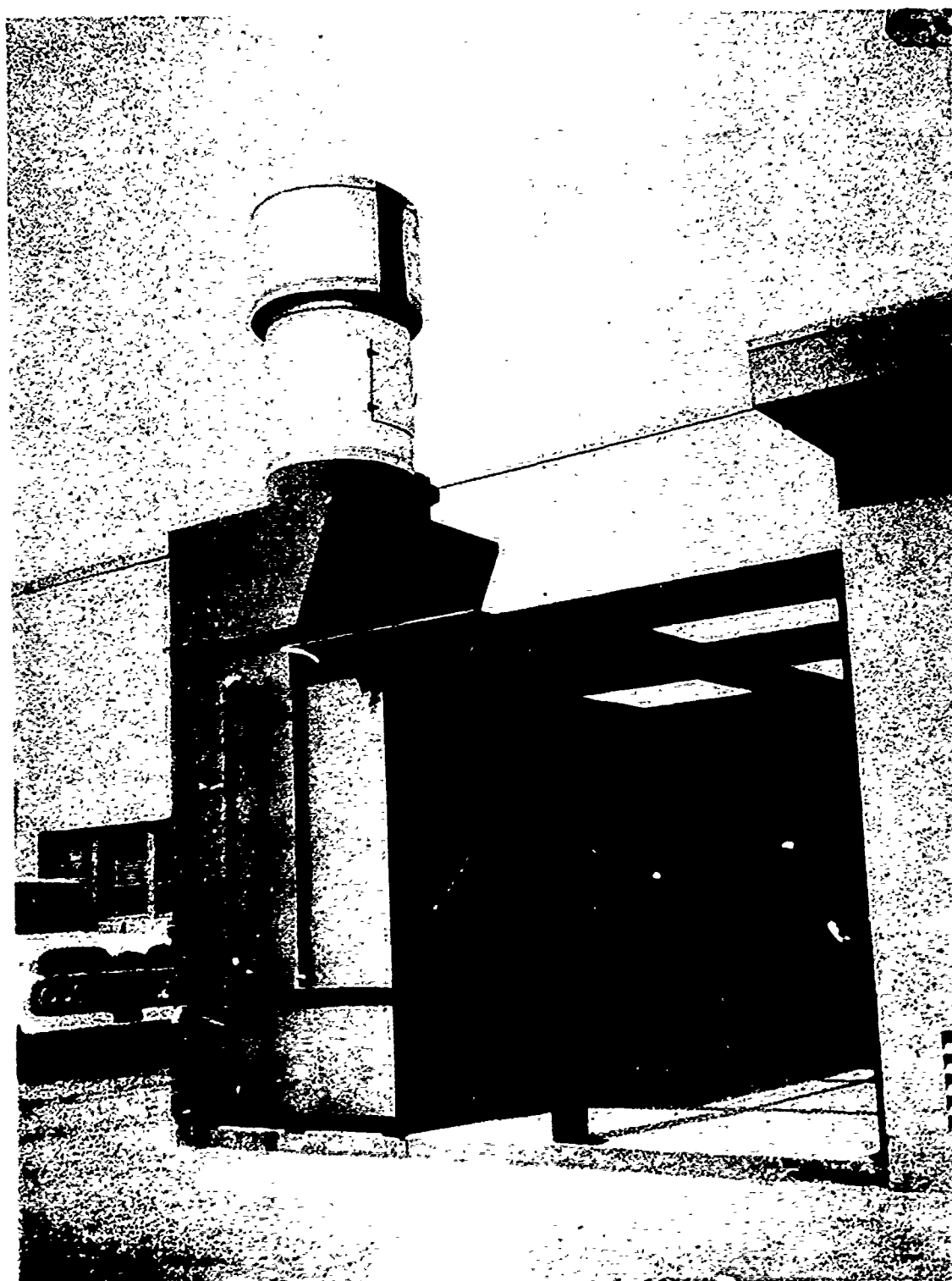


Figure 2. ARC SPRAY LABORATORY FACILITY

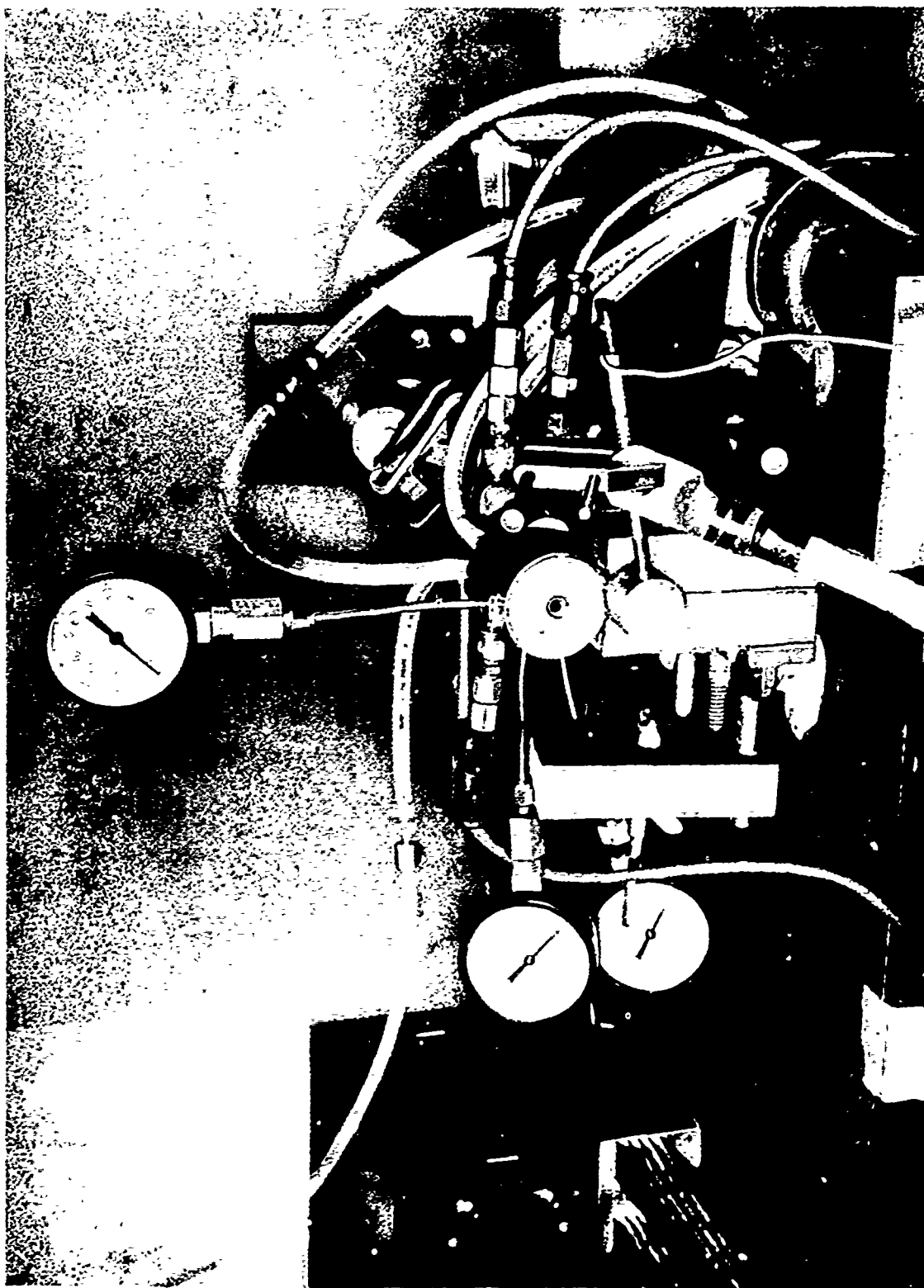


Figure 3. GENERATION ONE PLASMA ARC SPRAY GUN

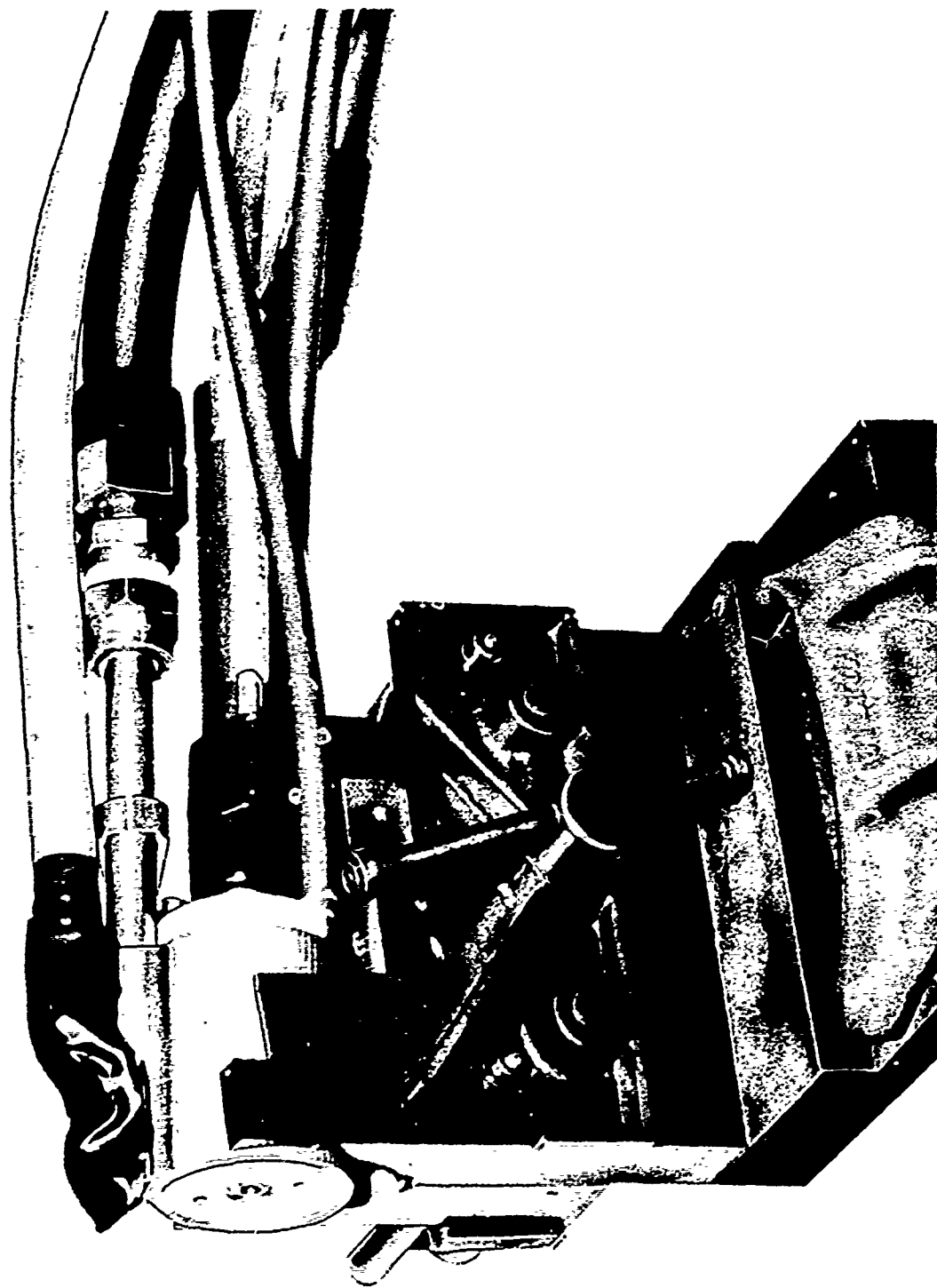


Figure 4. GENERATION TWO PLASMA ARC SPRAY GUN

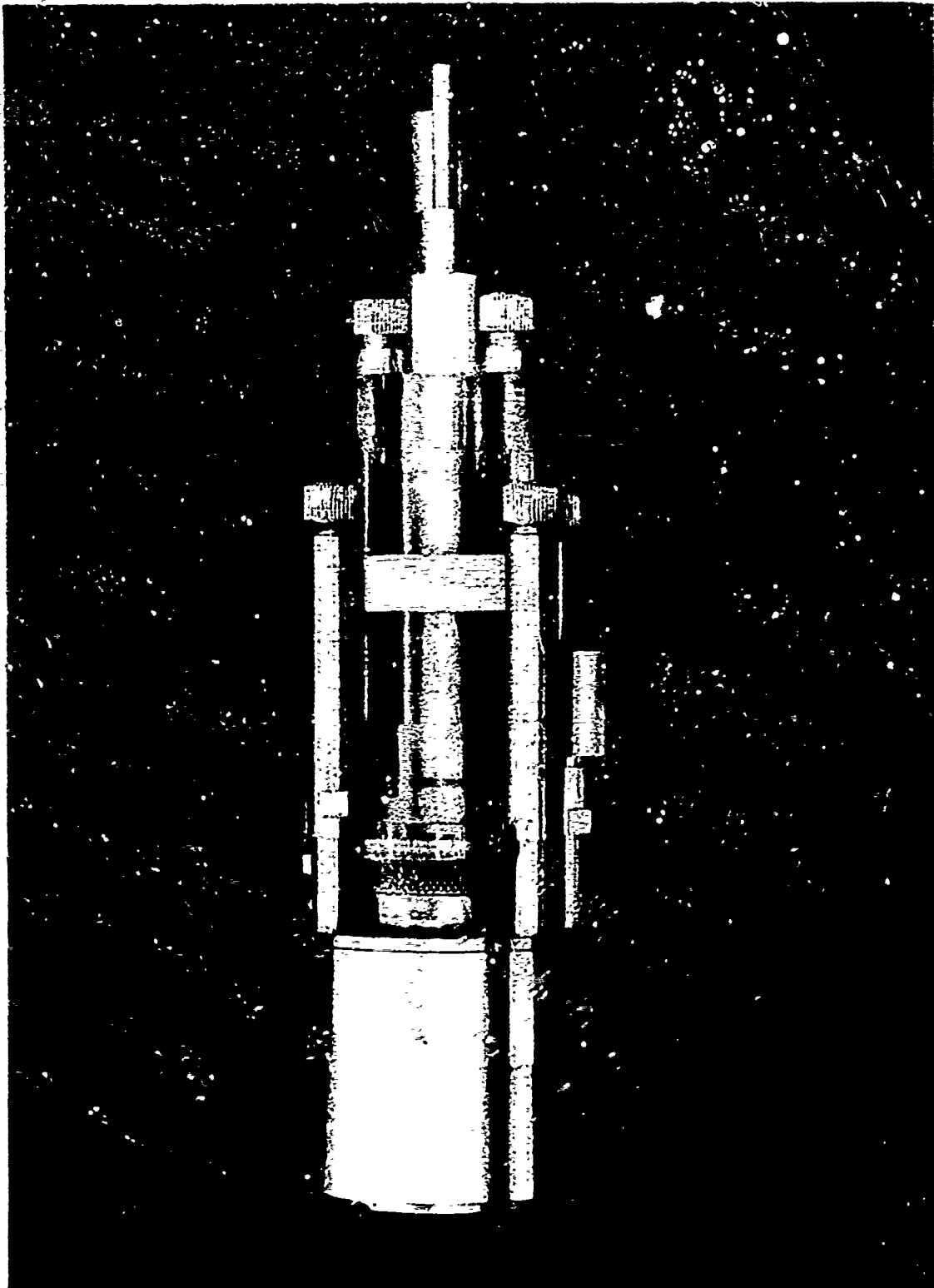


Figure 5. GENERATION THREE PLASMA ARC SPRAY GUN

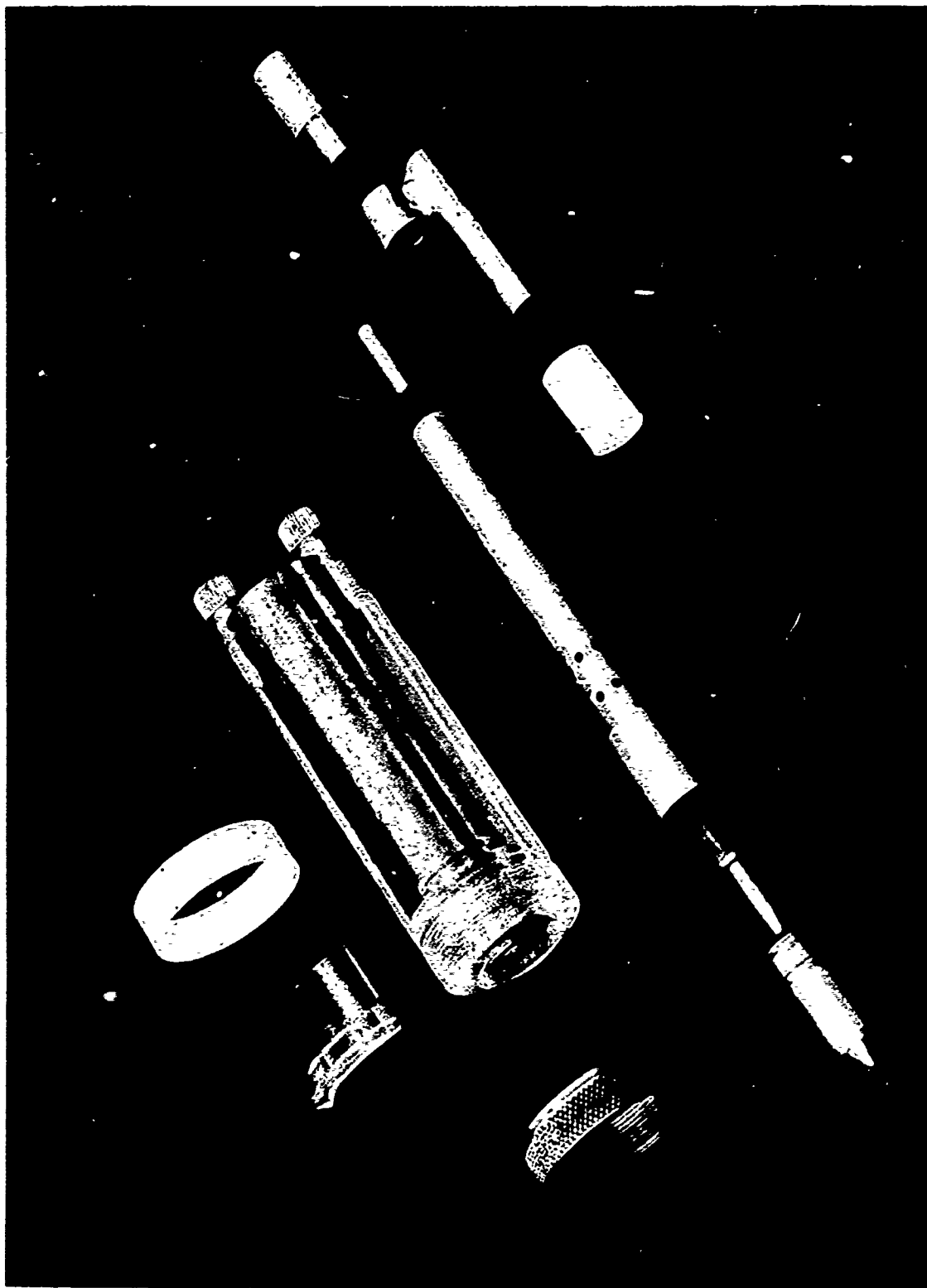


Figure 6. CATHODE SUBASSEMBLIES PLASMA ARC SPRAY GUN

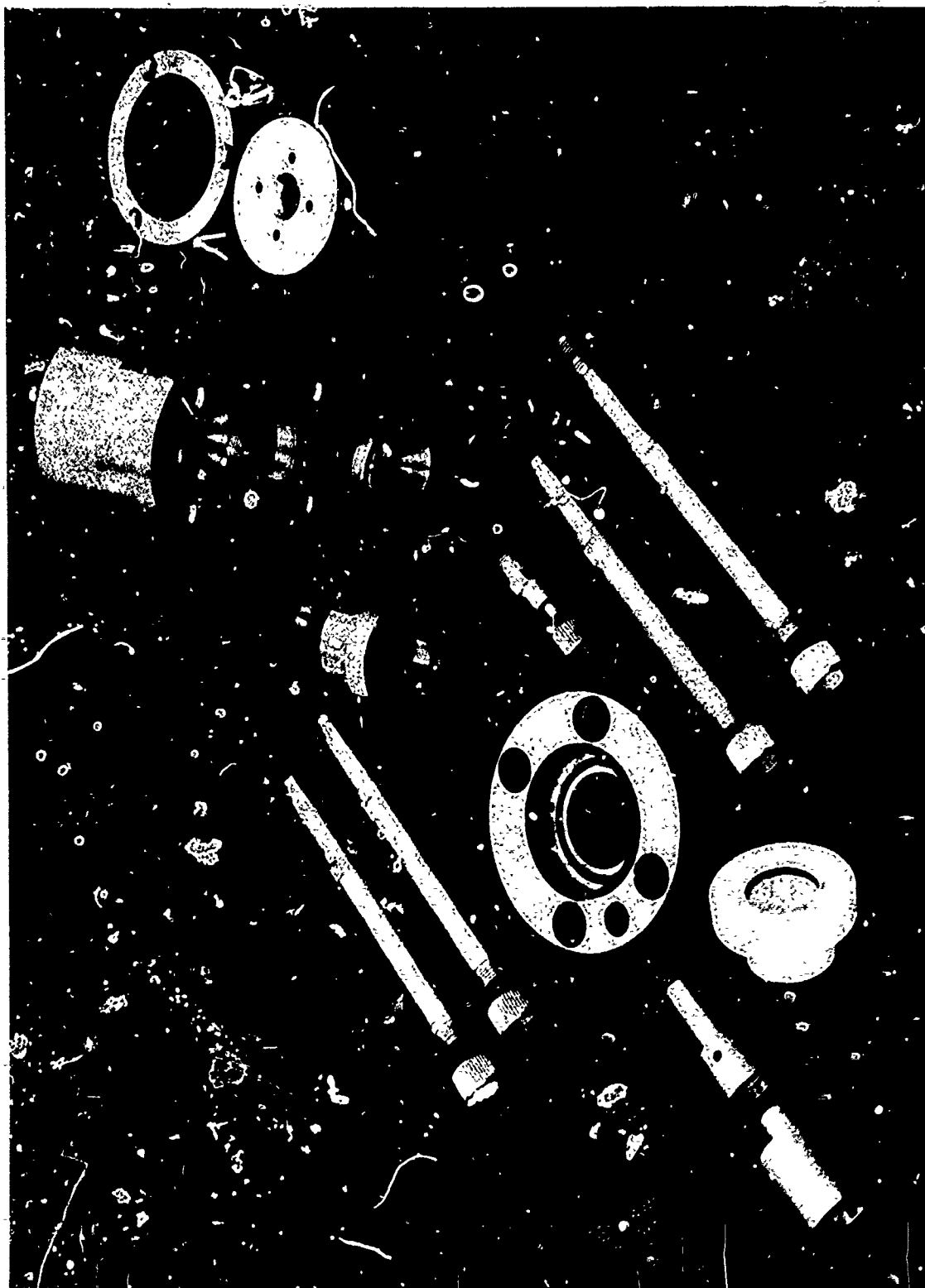
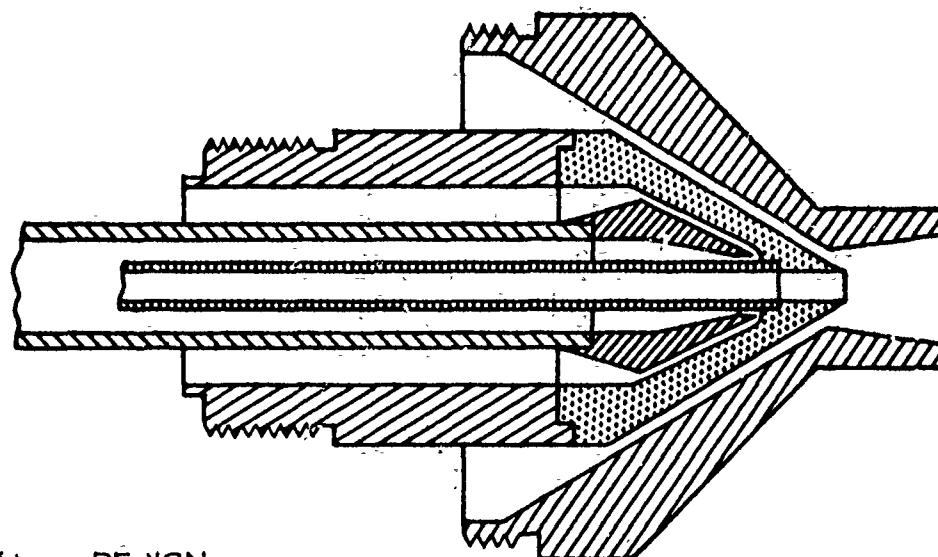
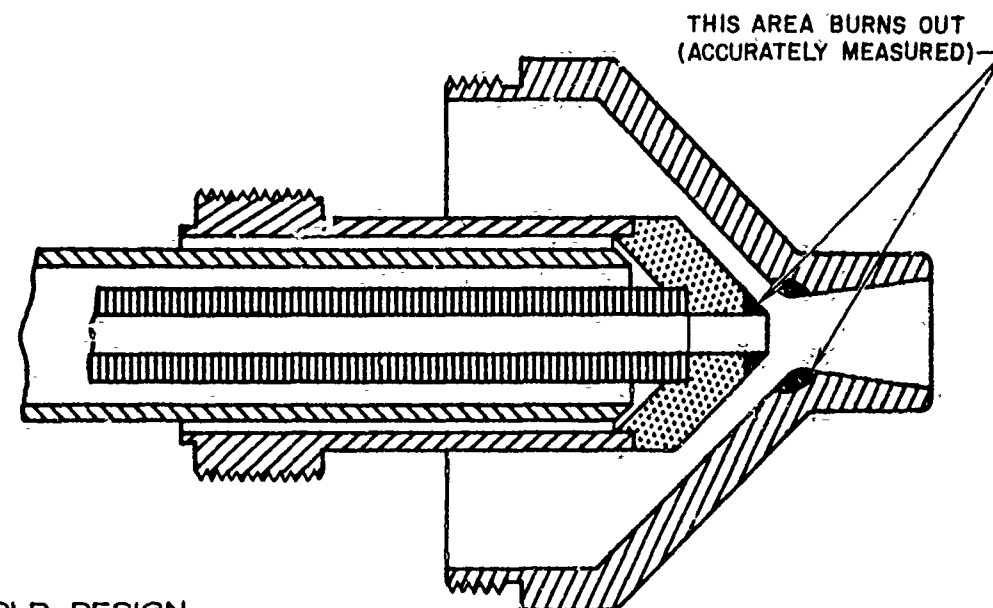


Figure 7. ANODE SUBASSEMBLIES PLASMA ARC SPRAY BUN



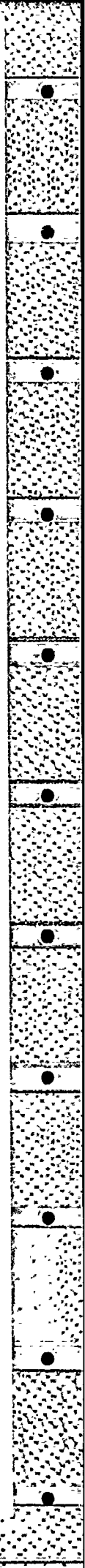
NEW DESIGN



OLD DESIGN

Figure 8. ANODE - CATHODE WATER AND GAS PASSAGE CONFIGURATIONAL RELATIONSHIPS





10

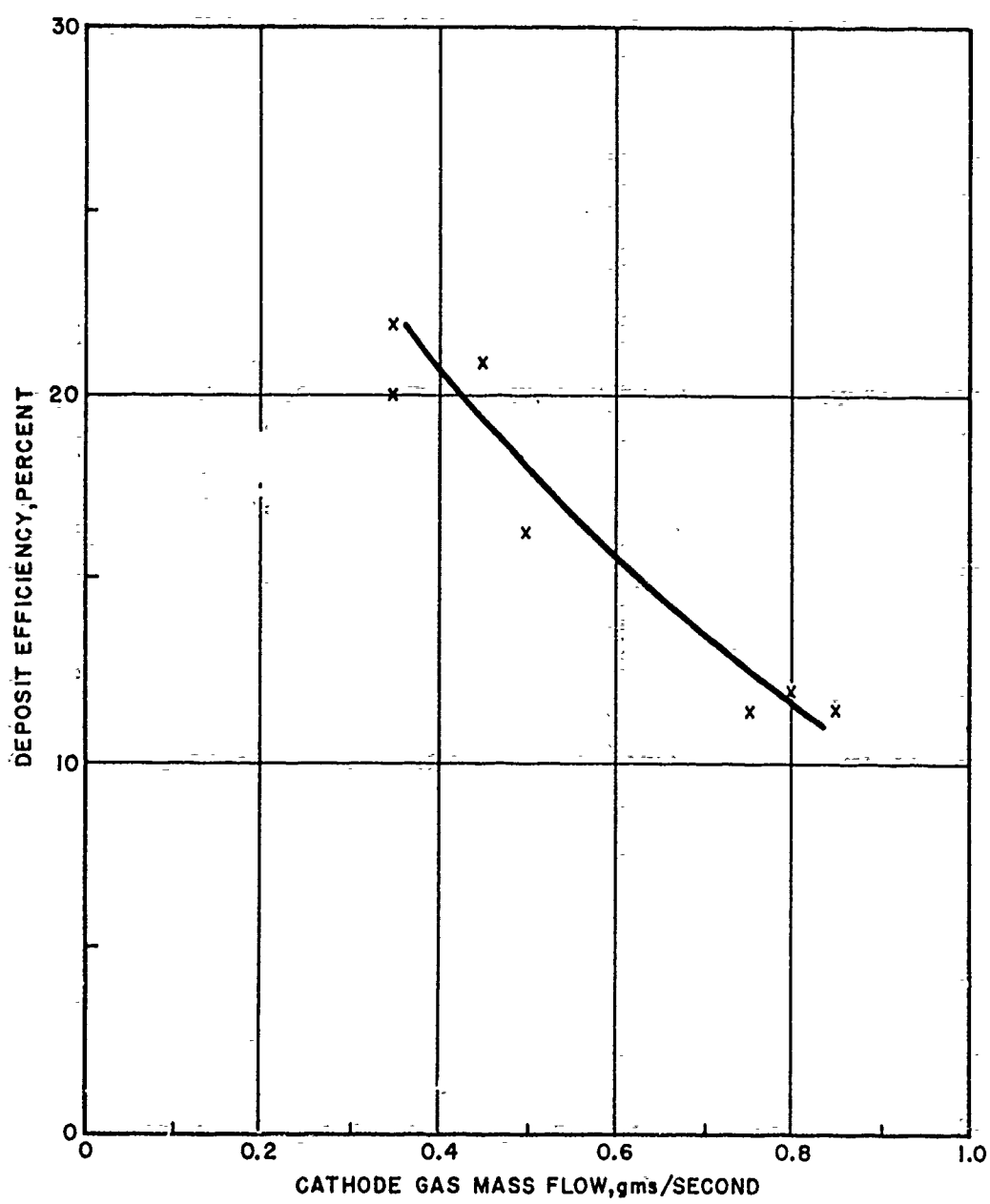


Figure 10. CATHODE MASS FLOW VS DEPOSIT EFFICIENCY (LOW POWER)

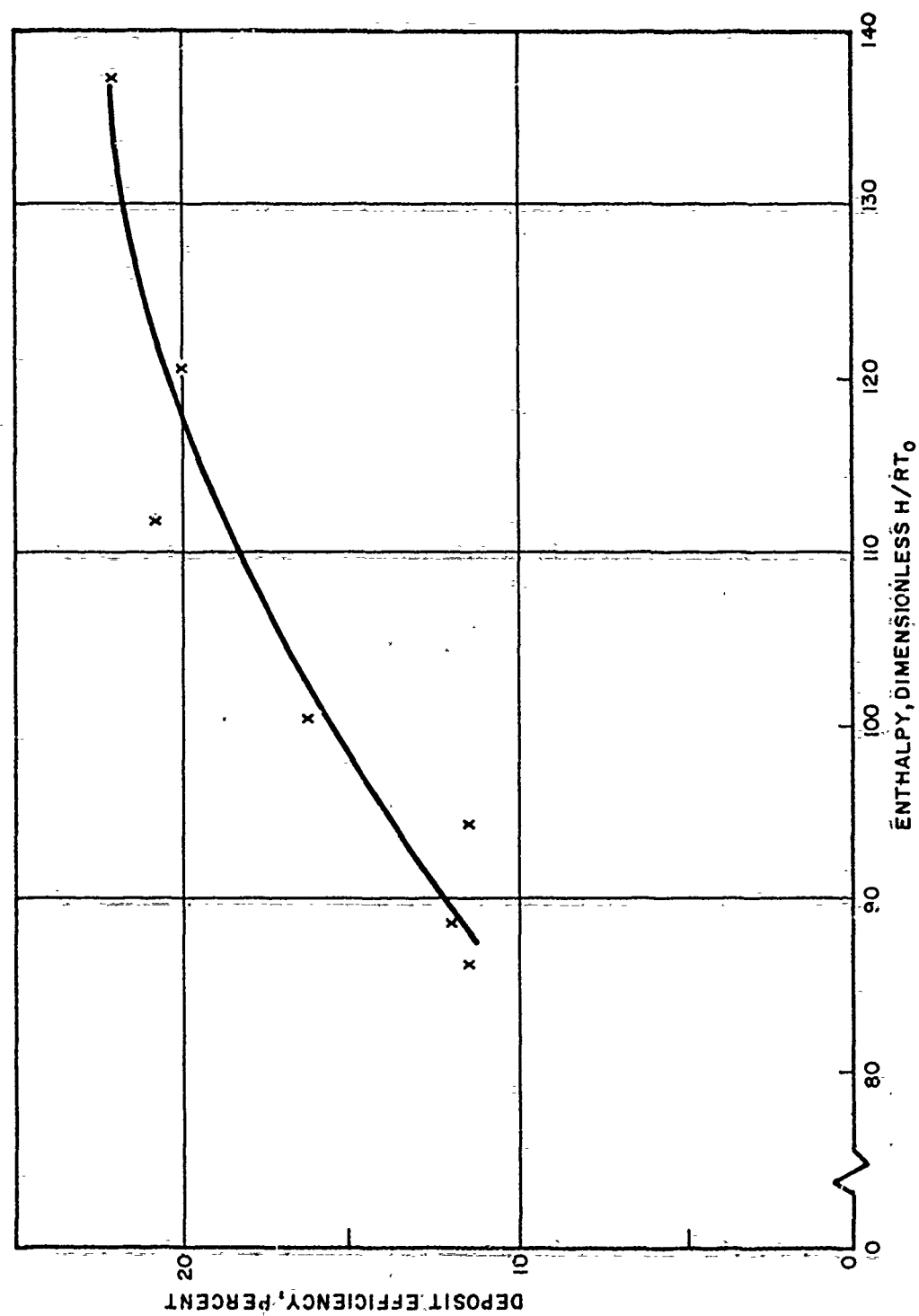


Figure 11. ENTHALPY VS DEPOSIT EFFICIENCY (LOW POWER)

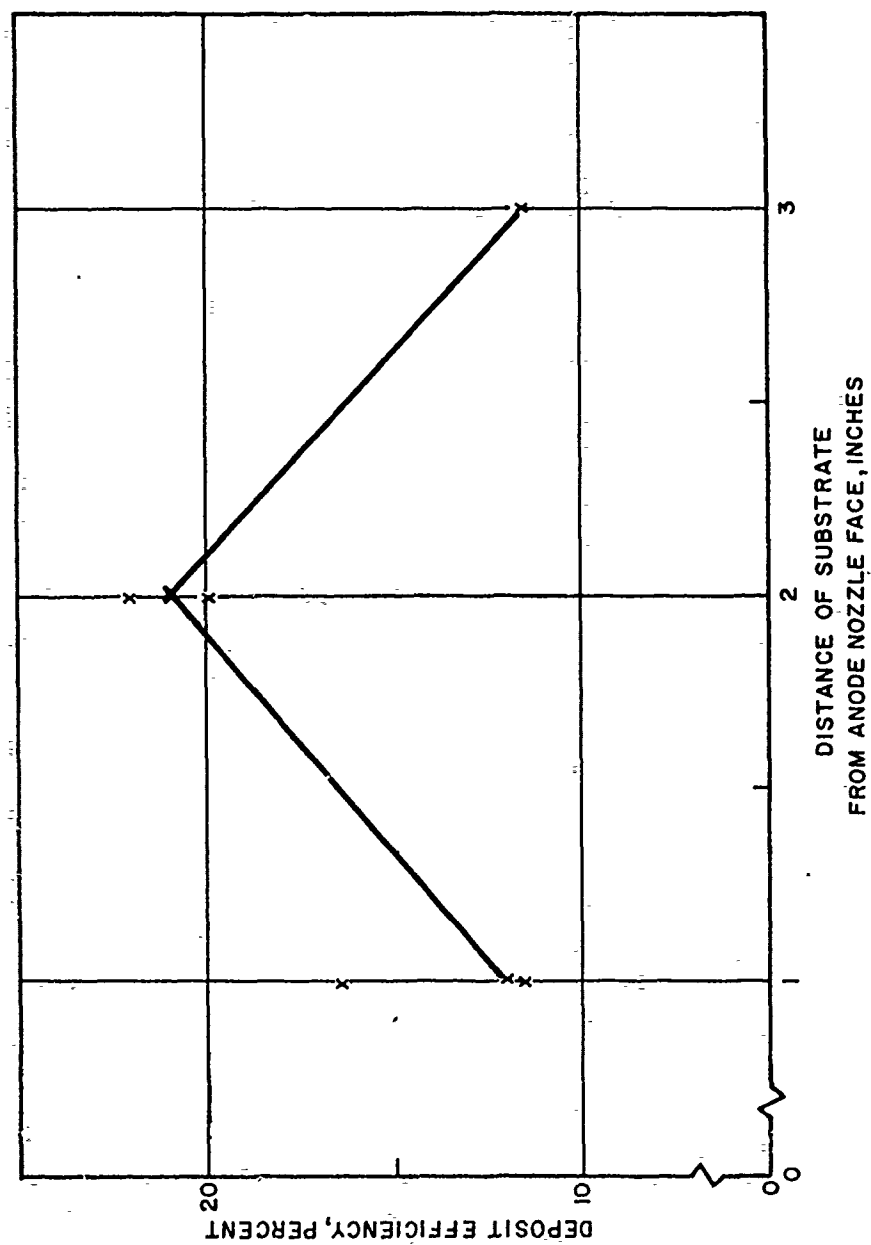
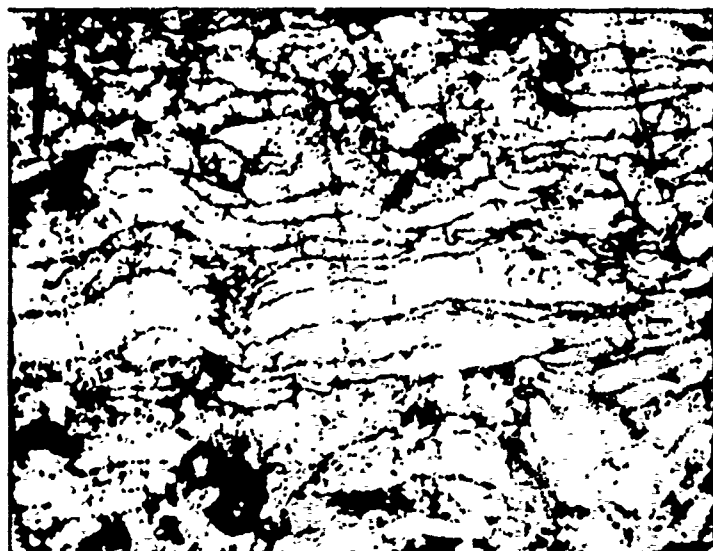


Figure 12. DISTANCE OF SUBSTRATE FROM SPRAY NOZZLE FACE VS DEPOSIT EFFICIENCY (LOW POWER)

Specimen Number	Deposit Efficiency Percent	Preheated	Grit Blasted?	Cleaning Gas?	Gap Setting (Inches)	Distance Setting Work (Inches)	Total Mass Flow (g/s)	Powder Mass Flow (g/s)	Anode Mass Flow (g/s)	Cathode Mass Flow (g/s)	Enthalpy H/RT
1	22.1	No	No	Yes	0.125	Two	2.55	1.45	0.75	0.35	137.28
2	20.9	Yes	Yes	Yes	0.075	Two	2.80	1.45	0.90	0.45	111.86
3	20.0	No	Yes	Yes	0.125	Two	2.70	1.45	0.90	0.35	120.81
4	16.3	Yes	No	Yes	0.075	One	2.75	1.25	1.00	0.50	100.67
5	12.0	Yes	No	Yes	0.075	One	3.15	1.45	0.90	0.80	88.83
6	11.5	Yes	No	Yes	0.075	Three	3.20	1.45	1.00	0.75	86.29
7	11.5	No	No	Yes	0.075	One	2.65	1.05	0.75	0.85	94.38

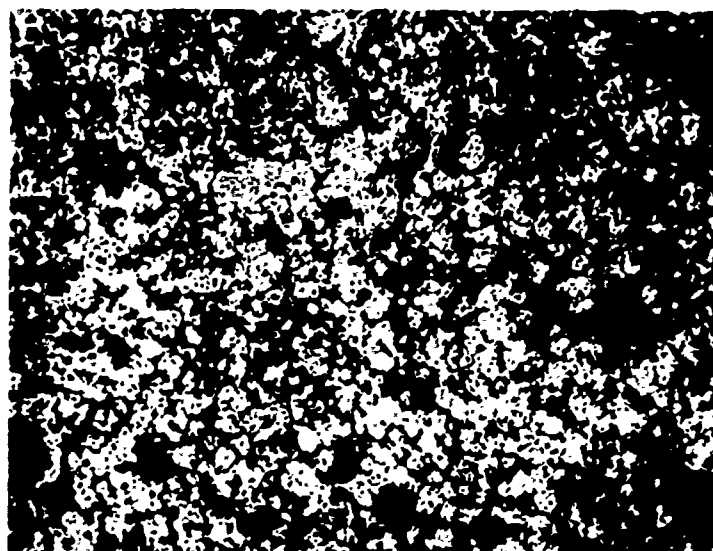
ANODE AND CATHODE GASES ARE ARGON      600 AMPS AT 22 VOLTS (13.2 KW)

FIGURE 13. EXPERIMENTALLY NOTED VARIABLES WHICH COULD AFFECT SPRAY DEPOSIT EFFICIENCY



Dark Denotes  
Porosity

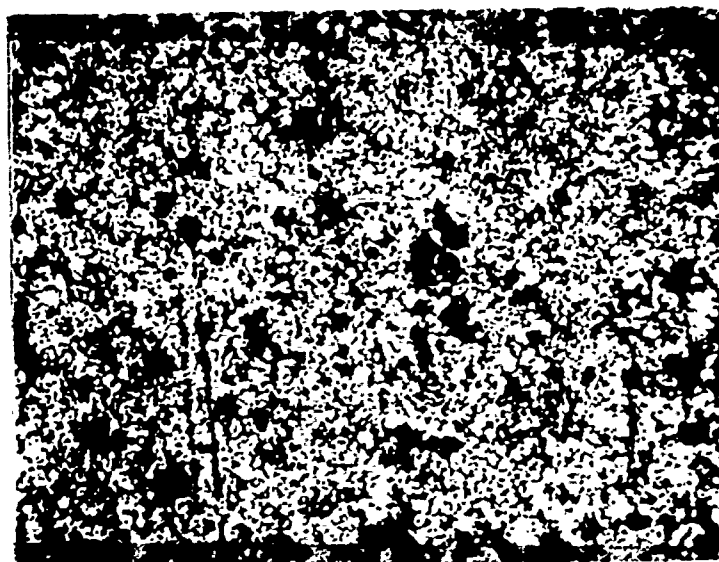
Plasma sprayed tungsten 533X  
Company B Arcspray Gun  
700 AMPERE (20KW Power)



Dark Denotes  
Porosity

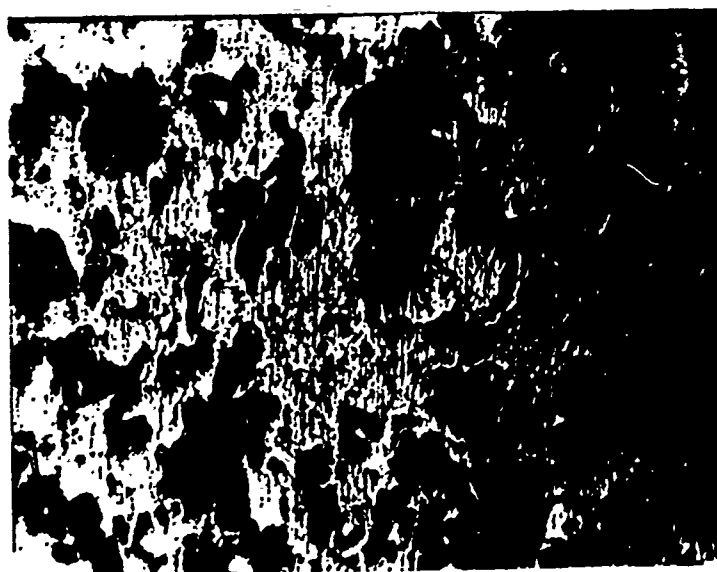
Plasma sprayed tungsten 533X  
Aerospace Arcspray Gun  
600 AMPERE (13KW Power)

Figure 14. "AS COATED" TUNGSTEN POROSITY COMPARISON  
PHOTOMICROGRAPHS



Dark  
Denotes  
Pores

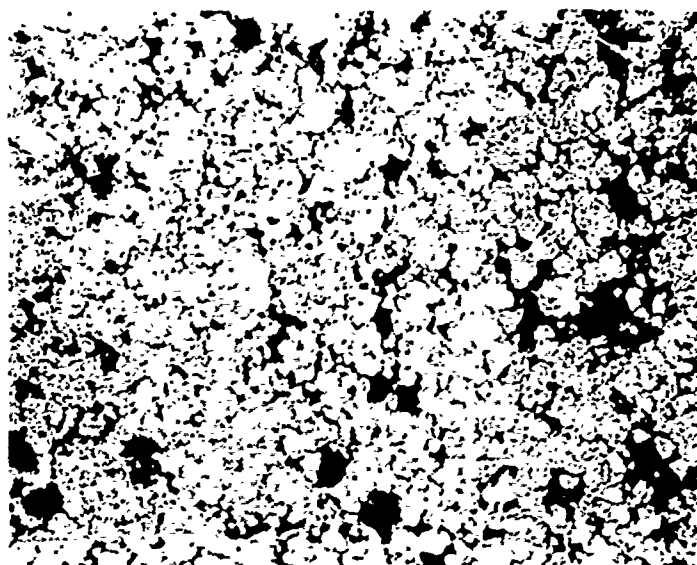
Plasma sprayed tungsten 266X  
Aerospace Arcspray Gun  
600 AMPERE (13KW Power)



Light  
Denotes  
Pores

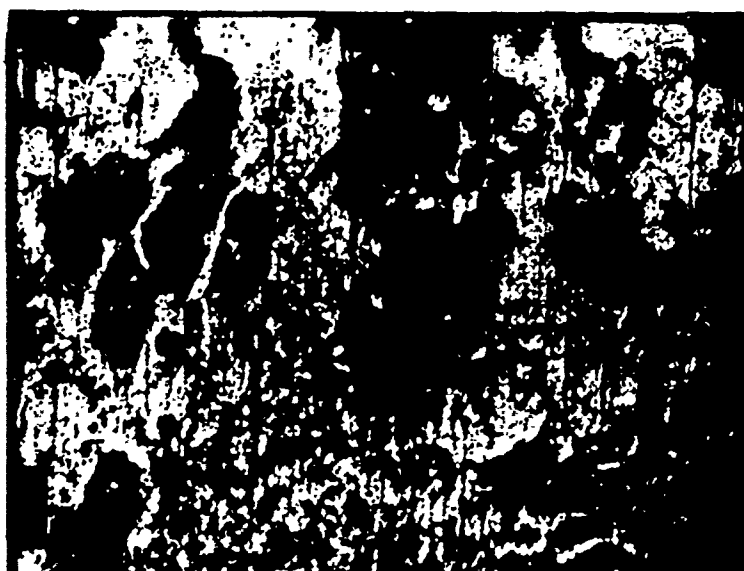
Plasma flame sprayed tungsten 200X  
Company A Arcspray Gun  
600 AMPERE (19KW Power)

Figure 15. "AS COATED" TUNGSTEN POROSITY COMPARISON  
PHOTOMICROGRAPHS



White  
Denotes  
Porosity

Plasma sprayed tungsten 533X  
Aerospace Arcspray Gun  
600 AMPERE (13KW Power)



Black Denotes  
Porosity

Plasma flame sprayed tungsten 400X  
Company A Arcspray Gun  
600 AMPERE (19KW Power)

Figure 16. "AS COATED" TUNGSTEN POROSITY COMPARISON  
PHOTOMICROGRAPHS



HIGH TEMPERATURE MATERIALS EVALUATION

JOSEPH W. ROSENBERY

JOHN C. WURST

University of Dayton

Dayton, Ohio

## 1. INTRODUCTION

The University of Dayton Research Institute has been continuing its evaluation of potential materials for various high temperature applications. The arc-plasma-jet screening test as proposed by a committee of this Working Group was generally followed and, wherever possible, improved upon. Special tests were also developed and utilized to evaluate materials for specific requirements and applications. Primary emphasis at the University during the past nine months has been in this area of materials evaluation and development of suitable test techniques.

## 2. X-15 ROCKET ENGINE STUDIES

The X-15 aircraft is powered by a liquid fueled engine utilizing a regeneratively cooled stainless steel nozzle. The nozzle is flame sprayed with a nichrome primer and Rokide Z insulating layer to provide thermal protection for the stainless steel and to minimize the heat transferred to the fuel. Some Rokide Z loss is normally experienced during engine operation, but during very short-term operation of several chambers complete Rokide losses were experienced in several areas, ultimately resulting in bursting failure of a tube.

Metallographic evaluation of a failed engine led to the following conclusions:

1. Extensive erosion of the Rokide Z coating subsequently resulted in complete tube failure due to surface erosion of the stainless steel and the formation of a brittle diffusion zone at the inside diameter of the tube.
2. The primary cause of engine failure would appear to be poor adherence of the Rokide Z coating to the stainless steel tubes.

Based upon these conclusions it appeared some type of thermal shock test was required to evaluate the adherence of Rokide Z and experimental type coatings. The test as finally developed at the University of Dayton consisted of a series of 10 cycles exposure at various power levels in the arc-plasma-jet. Each thermal shock cycle consisted of heating for 10 seconds and cooling for 10 seconds. Power levels were based upon settings of the power supply control variac with an initial setting of 45. If no failure occurred after 10 cycles at this power level the variac setting was raised to 50 for an additional 10 cycles. This practice was repeated for an additional 10 cycles each at variac settings of 55, 60, 65, 75, 90, 105 and 110 (wide open) or until failure occurred. For reporting purposes only the total number of cycles to failure are shown, it being understood that each successive 10 cycles were at a higher variac setting. The test samples were sections from an actual engine and were approximately 4 x 8 inches. The samples were potted in plastic at each end and water circulated through the tubes during test to simulate the fuel. A typical specimen after test is shown in Figure 1. The size of each specimen was such that four distinctly separate test areas were available on each panel.

Appreciable scatter in results was observed for all types of specimens. In addition, several modes of failure were also observed. These included spalling due to thermal shock during the heating cycle, partial separation of the coating from the base metal due to poor adhesion permitting mechanical removal of the coating, cracking of the coating, and actual melting of the coating. As a result of

the large amount of data acquired, statistical analysis based upon the probability of failure at less than a given number of cycles was utilized to evaluate the thermal shock test results. A probability plot of these data is presented in Figure 2. This plot has as its abscissa the percentage of specimens expected to fail at less than the indicated number of cycles and the total number of cycles as its ordinate. Curves are shown for Rokide Z coated sections obtained from Reaction Motors Division of Thiokol Chemical Corporation and for various experimental coatings applied by Plasmakote Corporation. A description of the Plasmakote coatings may be found in Table 1. From Figure 2 the Plasmakote samples number 21, 22, 23, and 24 appear decidedly superior to all others evaluated in this particular test.

In order to evaluate heat transfer rates through these various coatings 1/2 inch diameter 347 stainless steel tubes were sprayed with these various coatings and exposed to the arc-plasma effluent. A differential thermocouple circuit was employed to measure the temperature increase of the cooling water flowing through the tubes. In this manner a value for  $q$ , the rate of heat transfer to the water in Btu/sec., could be determined. In general the Plasmakote gradated coatings were comparable to Rokide Z and no serious heat transfer problems appear likely.

Studies have indicated gradated type coatings may offer a decided improvement in ceramic to metal bond strengths. Preliminary evaluation of a 100% alumina coating and a 50% alumina - 50% nickel gradation, both on an Inconel substrate and utilizing various grit blasting media, indicated a higher bond strength for the gradated material. Experimental techniques were such that the gradated type coating usually failed at an adhesive bonded surface rather than the ceramic/metal interface, while the 100% alumina coating consistently failed at this interface.

Further studies are currently planned to attempt a correlation of bond strength and thermal shock resistance for some of those coatings evaluated in the X-15 program.

### 3. COATINGS FOR REFRACTORY METALS

Two types of test for evaluating the oxidation protection afforded refractory metals by various coatings have been established. Both tests utilize the arc-plasma-jet as a heat source. The first test consists of exposing a specimen at increasing heat flux levels for a period of time, usually five minutes at each level until failure. Front surface temperatures are monitored by an optical pyrometer and a total radiation pyrometer, while back surface temperatures are determined by a Shawmeter, thereby avoiding possible reactions between the coating and a contact thermocouple.

The second test is intended to supplement the first by introducing the additional factor of thermal cycling. Test conditions are similar to those utilized in the first test, except the specimen is heated for 20 seconds and cooled for 20 seconds and this thermal cycling continued until failure or until a maximum of 15 cycles have been accomplished at a given heat flux rate. Heat flux is incrementally increased until failure occurs. Front and back surface temperatures are monitored as described previously.

An alternative method for these tests is to establish the testing levels based on the surface temperature of the specimen. In the few preliminary tests to be

described in this report, this surface temperature technique was utilized. There are, however, serious limitations to this method which make the thermal flux rate a more desirable standard since it is insensitive to specimen emittance. When emittance is unknown, surface temperature becomes an extremely nebulous value since true temperature cannot be determined. If the environment is standardized by measuring the heat flux rate to a water cooled, copper calorimeter surface temperatures measured will be an indication of the surface emittance of the sample and all materials will be evaluated in an essentially constant environment.

A series of coated Ta-10% W sheet samples have been evaluated by the surface temperature method described above. These 2 x 2 inch sheet specimens were coated with an Al-Sn mixture. Sheet samples of columbium, molybdenum, and tungsten with similar type coatings were also evaluated.

The continuous exposure test (Type 1) on the coated Ta-10% W alloy indicated the coating afforded adequate protection of the substrate at temperatures up to 3340°F for 5 minutes. A similar coating provided comparable protection for molybdenum and tungsten, although a columbium specimen failed at 2820°F after very short-term exposure.

Thermal cycling of the coated Ta-10% W alloy produced failure at about 2900°F in 5 of 5 tests, the one exception being a failure at 3150°F. A single molybdenum specimen survived 15 thermal cycles at 3270°F, but failed on further heating to 3450°F.

Additional samples representing commercial or semi-commercial coatings for molybdenum and tantalum are presently available and will be evaluated in the near future. These tests will be performed in a constant environment based upon thermal heat flux to a water cooled, copper calorimeter.

#### 4. OTHER TESTING

In addition to the previously described tests a number of other "standard" type tests were conducted according to the procedure outlined by the subcommittee of this Working Group. Materials evaluated have included ablative systems, elastomers, and heat sink type materials. Since most of these materials are proprietary in nature the results will not be reported.

Only one additional laboratory has reported further results on the group of standard materials sent out for "round-robin" testing. Preliminary test data have been submitted for statistical analysis by University of Dayton personnel. The basic problem of insufficient data under identical conditions still presents considerable difficulty in this analysis, however, because of the poorly defined limits of experimental error. Attempts will be made, nevertheless, to analyze the data statistically and determine which environmental parameters and specimen performance data are of primary significance and to ultimately evaluate the data from all participating laboratories.

In conjunction with evaluation programs for ablative materials a rod type specimen configuration has been experimentally determined which provides essentially linear ablation independent of the ablation mechanism.

## Arc-Effluent Measurements

The accurate definition of environmental parameters is important in a materials screening test for meaningful comparisons of specimen performance.

The basic effluent properties now being measured in the screening test are heat flux and stagnation pressure at the sample location and enthalpy at the nozzle exit. Heat flux is measured with a 1/2 inch diameter cold wall copper calorimeter and stagnation pressure with a large, flat face water cooled pitot tube, both of the designs recommended by the subcommittee on screening tests. It is generally recognized that neither design is completely satisfactory and that measurements with these instruments could be misleading and contain serious inaccuracies. Nevertheless, since no more convenient means of obtaining these measurements is now available, these designs have been established as intermediate standards.

Effluent enthalpy at the torch exit is useful only as a relative quantity, since air entrainment, recombination and radiation losses extract a significant portion of the effluent energy before it reaches the sample. Knowledge of enthalpy and effective temperature at the sample would enhance the value of the data. Some experimental efforts have been directed toward a better evaluation of the effluent properties. Temperature profiles (Figure 3) for relatively low power operation of the arc have been obtained with a transient probe shown in Figure 4. This probe consisted of an equispaced array of chromel-alumel thermocouples. Temperature-time histories of each thermocouple were obtained at several locations in the cooler regions of the effluent to determine the relationship between thermocouple response time and equilibrium temperature. Effluent temperatures were then determined in the hotter regions of the stream as a function of response time for short-term exposures of the probe.

Pressure distributions within the effluent have been measured with a pointed water cooled pitot tube assembly (Figure 5) designed to reduce the flow disturbance incurred with use of the "standard" pitot tube. A typical pressure profile obtained with this instrument is shown in Figure 6.

Various calorimeter designs both the hot and cold wall variety as well as smaller pitot tube assemblies are being considered. Methods for determining air entrainment and the quality of effluent mixing are also under consideration.

Freeman of American Cyanamid<sup>1</sup> has reported a probe for measuring temperature and enthalpy as a function of effluent conductivity, a technique which according to the author appears to be independent of effluent pressure and composition. Application of such a probe has been evaluated in preliminary tests; however, additional testing will be required to adequately explore the possibilities of such a technique.

## New Arc-Plasma-Jet Facility

With the present 50 KW plasma-jet, screening tests have been limited to a maximum heat flux of 500 Btu/ft<sup>2</sup>-sec. To extend this limit to approximately

<sup>1</sup>"Plasma Jet Diagnosis Utilizing the Ablating Probe," M. P. Freeman, American Cyanamid Co., Stamford, Conn., presented at the Symposium on Temperature Its Measurement and Control in Science and Industry, Columbus, Ohio, March 27 - 31, 1961, p. 107, sponsored by the American Institute of Physics.

1000 Btu/ft<sup>2</sup>-sec. and also to develop a test capability for larger specimen configurations a plasma-jet designed for operation in the range of 20 to 150 KW is being installed at the University.

The new facility consists of a Plasmadyne M-4 torch with nitrogen electrodes modified to produce a 1/2 inch diameter effluent. DC power for this unit will be supplied by 16 Miller rectifiers. In preliminary tests this unit has been operated to 90 KW at a nitrogen flow rate of 0.0086 lb./sec. (7.0 SC FM). The operating efficiency at this power level was 62% and the effluent enthalpy calculated at the front electrode exit was 6000 Btu/lb.

Techniques for air simulation similar to those now employed with the 50 KW unit will be applied to the new torch. While primarily intended for nitrogen and simulated air tests, the arc controls and power supply have been designed for operation with other gases.

The 50 KW plasma-jet will continue to play an active role in research programs at the University. While the bulk of materials testing will be shifted to the new facility, electrode and diagnostic probe development efforts will be pursued with the smaller unit.

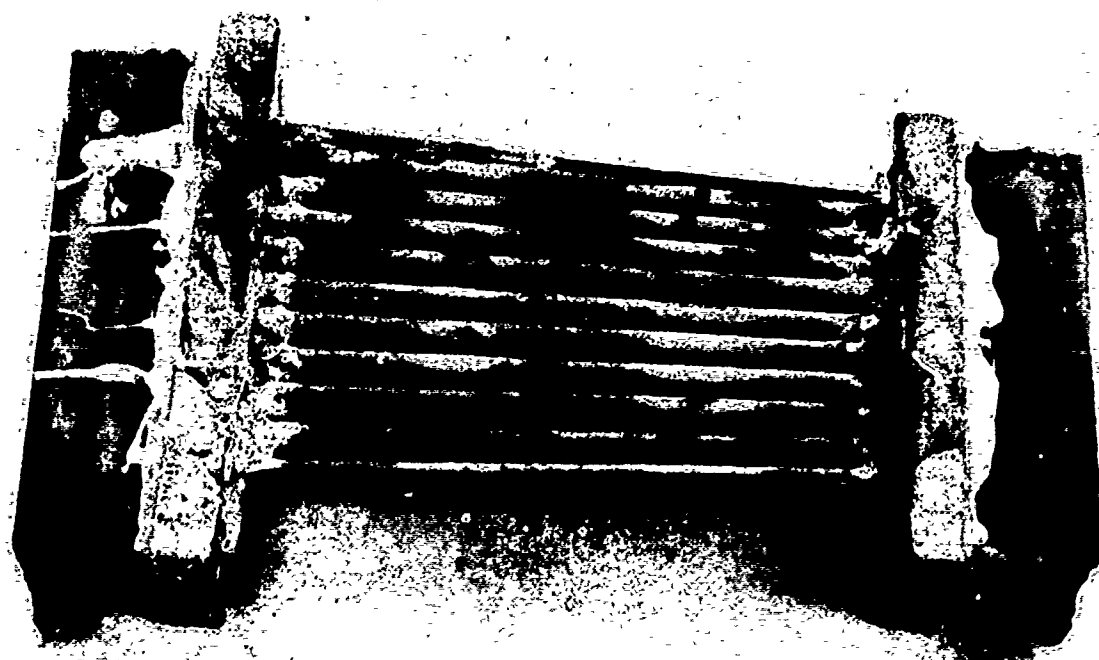


Figure 1. Typical X-15 Specimen after Test.

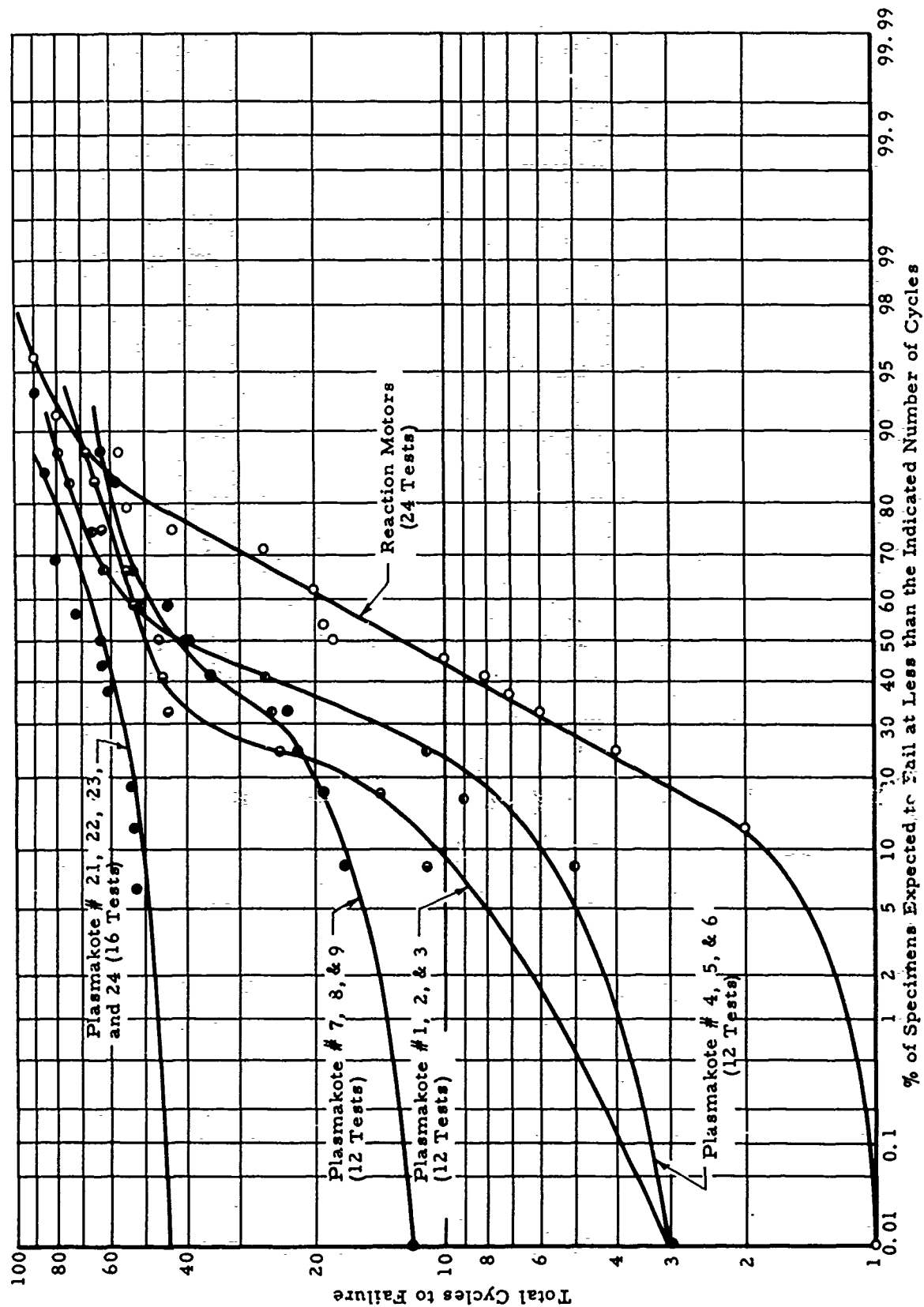


Figure 2. Probability of Comparing Thermal Shock Resistance of X-15 Rocket Section with Various Coatings



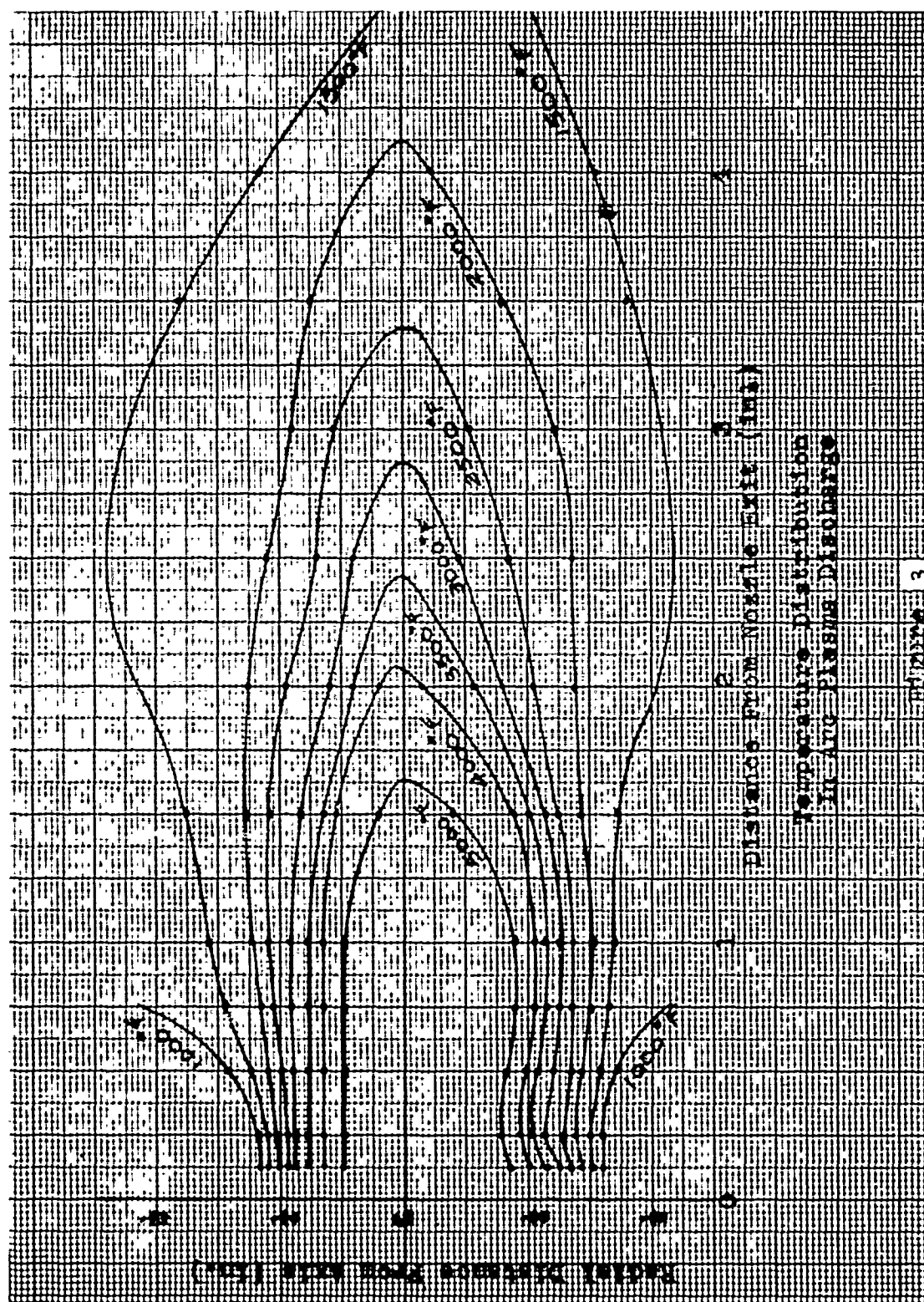
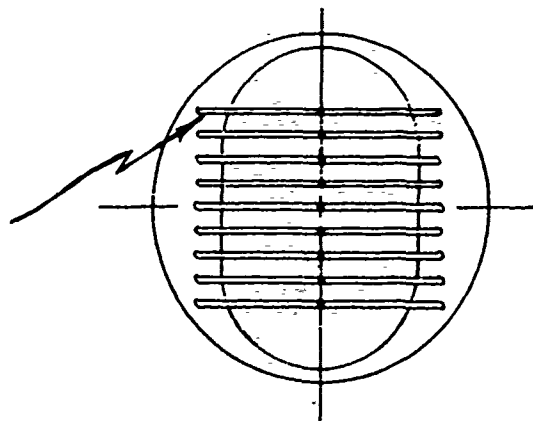
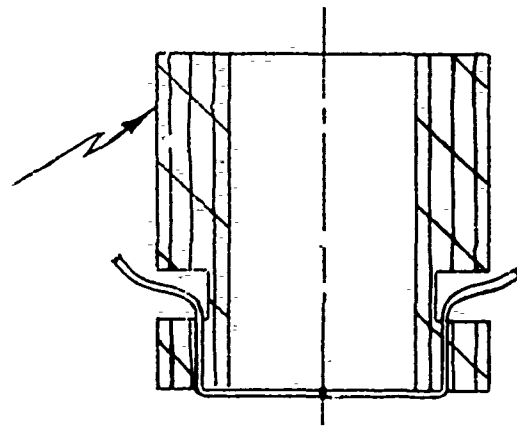


Figure 3

Chromel-Alumel  
Thermocouples



Phenolic Holder



Transient Temperature Probe

Figure 4

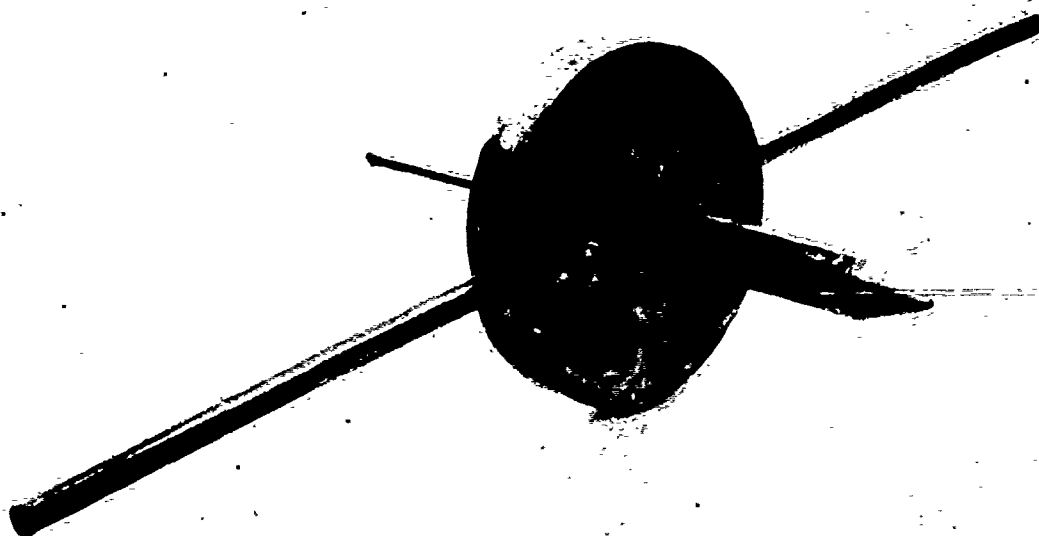


Figure 5. Pointed Pitot Tube Assembly.

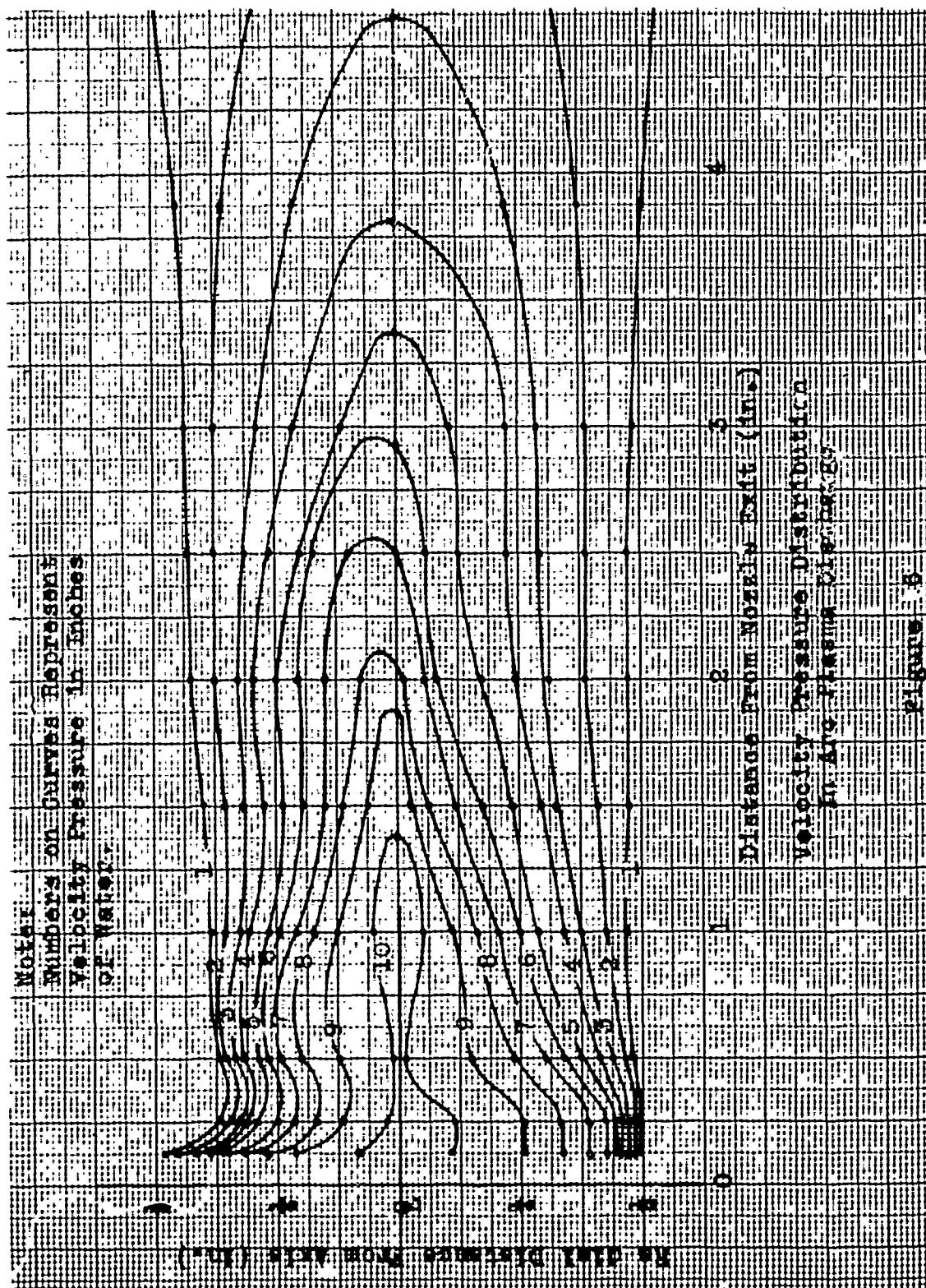


Table 1: Identification of Plasmakote Specimens

Specimen Number	Primer Coat	Gradation 1	Gradation 2	Gradation 3	Surface
1, 2, and 3	80 Ni - 20 Cr	70 NiCr - 30 ZrO <sub>2</sub>	30 NiCr - 70 ZrO <sub>2</sub>		ZrO <sub>2</sub>
	0.002"	0.002"	0.002"		0.006"
4, 5, and 6	80 Ni - 20 Cr	75 NiCr - 25 ZrO <sub>2</sub>	50 NiCr - 50 ZrO <sub>2</sub>	25 NiCr - 75 ZrO <sub>2</sub>	ZrO <sub>2</sub>
	0.002"	0.002"	0.002"	0.002"	0.005"
7, 8, and 9	80 Ni - 20 Cr	75 NiCr - 25 ZrO <sub>2</sub>	50 NiCr - 50 ZrO <sub>2</sub>	25 Ni - 75 ZrO <sub>2</sub>	ZrO <sub>2</sub> + 1% Ni
	0.002"	0.002"	0.002"	0.002"	0.005"
21 and 22	Molybdenum	70 Nichrome - 30 ZrO <sub>2</sub>	30 Nichrome - 70 ZrO <sub>2</sub>		ZrO <sub>2</sub>
	0.002"	0.002"	0.002"		0.004"
23 and 24	Molybdenum	50 Nichrome - 50 ZrO <sub>2</sub>	10 Nichrome - 90 ZrO <sub>2</sub>		ZrO <sub>2</sub>
	0.002"	0.002"	0.002"		0.004"

ACTIVITIES IN THE HIGH TEMPERATURE,  
INORGANIC REFRACTORY COATINGS FIELD

L. DAVIS

Harvey Engineering Laboratories  
Torrence, California

## TABLE OF CONTENTS

<u>SECTION</u>	<u>TITLE</u>
I	INTRODUCTION
II	GRAPHITE NOZZLE COATING
III	AL <sub>2</sub> O <sub>3</sub> COATINGS FOR NOZZLES
IV	HIGH REFRACTIVE INDEX GLASS
V	CERAMIC COATING FOR ALUMINUM
VI	COATINGS FOR EXTRUSION DIES
VII	HEAT TRANSFER STUDIES

## **I. INTRODUCTION**

SEVERAL PROJECTS IN THIS FIELD HAVE BEEN CARRIED ON BY HARVEY ENGINEERING LABORATORIES SINCE THE LAST REFRACTORY COMPOSITES WORKING GROUP MEETING SPONSORED BY WADD AND NASA AT CINCINNATI, OHIO, IN NOVEMBER 1960.

THOSE PROJECTS WHICH MAY BE OF INTEREST TO THE GROUP ARE REPORTED IN THE FOLLOWING SIX SECTIONS.



## 11. GRAPHITE NOZZLE COATING

AN EXPERIMENTAL COATING WAS DEVELOPED AND APPLIED TO GRAPHITE NOZZLE INSERTS FOR USE IN A SOLID PROPELLANT ROCKET. THIS COATING WAS APPLIED BY THE PLASMA TORCH AND CONSISTED OF TWO LAYERS. FIRST, TANTALUM METAL WAS APPLIED TO THE GRAPHITE SURFACE. THIS LAYER WAS .003" TO .005" THICK AND SERVED AS A BOND BETWEEN THE OUTER LAYER AND THE GRAPHITE. IT ALSO PROVIDED A SUBSTANCE IN CONTACT WITH THE GRAPHITE THAT HAD NO TENDENCY TO REACT CHEMICALLY WITH THE GRAPHITE OR WITH THE OUTER LAYER. THE SECOND LAYER WAS COMPOSED OF A MIXTURE OF 50% HAFNIUM OXIDE ( $\text{HfO}_2$ ) AND 50% THORIUM OXIDE ( $\text{ThO}_2$ ) FORMED BY MIXING THE POWDERS BEFORE PLASMA FLAME DEPOSITION.

WHILE THE PHASE DIAGRAM OF  $\text{HfO}_2 - \text{ThO}_2$  IS SOMEWHAT INDEFINITE IT APPEARS THAT THE 50-50 COMPOSITION HAS A SHORT RANGE BETWEEN THE LIQUIDUS AND SOLIDUS LINES (LESS THAN  $100^\circ\text{C}$ ) AND THE WHOLE COATING WILL HAVE A MELTING POINT IN THE VICINITY OF  $3000^\circ\text{C}$ .

THE OXIDES WERE APPLIED TO A THICKNESS OF APPROXIMATELY .030". SIMPLE THERMAL TESTS ON THIS COATING INDICATED GOOD RESISTANCE TO THERMAL SHOCK. THIS IS QUITE A CONTRAST TO A 100% THORIUM OXIDE COATING WHICH IS QUITE SHOCK SENSITIVE. REPORTS ON THE SERVICE TESTS OF THESE COATED NOZZLE INSERTS ARE NOT AVAILABLE AT THIS TIME.

### III. AL<sub>2</sub>O<sub>3</sub> COATINGS FOR NOZZLES

IN A SOMEWHAT SIMILAR APPLICATION TO THAT DESCRIBED IN SECTION II, A QUANTITY OF STEEL NOZZLES AND BULKHEADS HAVE BEEN COATED WITH THE USUAL AL<sub>2</sub>O<sub>3</sub> PROTECTIVE COATING. THIS COATING HAS BEEN APPLIED IN THE CUSTOMARY WAY WITH THE OXY-ACETYLENE TORCH AND, WITH THE PROPER TECHNIQUES, VERY GOOD COATINGS CAN BE SECURED. HOWEVER, IT HAS BEEN FOUND THAT APPRECIABLE IMPROVEMENT IN BOTH THE DENSITY AND THE HARDNESS OF THE COATING CAN BE ACHIEVED BY AN ADDED OPERATION. IF A LOW VELOCITY PLASMA FLAME IS PLAYED ON THE COATING FOR A VERY SHORT PERIOD OF TIME (15-30 SECONDS) A GLAZING EFFECT IS OBTAINED FROM FUSION OF THE OUTER SURFACE OF THE COATING. AGAIN, NO SERVICE RESULTS ARE AVAILABLE BUT IT APPEARS OBVIOUS THAT THIS IS MORE PROTECTIVE THAN THE USUAL ALUMINA COATING.

#### IV. HIGH REFRACTIVE INDEX GLASS

SOME WORK HAS BEEN CARRIED ON IN COOPERATION WITH NUCLEAR CORPORATION OF AMERICA IN THE DEVELOPMENT OF GLASSES HIGH IN RARE EARTH OXIDE CONTENT. SUCH GLASS WILL HAVE A VERY HIGH REFRACTIVE INDEX. RE-MELTING IMPROVES THE CLARITY OF THE GLASS. SEVERAL COMPOSITIONS WERE MELTED WITH THE LOW VELOCITY PLASMA FLAME. NO DIFFICULTY WAS ENCOUNTERED IN MELTING THIS MATERIAL BUT THE DIRECT APPLICATION OF THE FLAME TO THE MATERIAL CAUSED BUBBLING AS THE MELTING OCCURRED BECAUSE THE GAS VELOCITY WAS STILL TOO HIGH TO PERMIT QUIET MELTING. SUFFICIENT CLEAR GLASS WAS OBTAINED TO INDICATE THAT THE COMPOSITIONS AND THE PROCESS HAVE CONSIDERABLE MERIT. FURTHER EXPERIMENTS ARE PLANNED IN WHICH THE GLASS WILL BE CONTAINED IN A CRUCIBLE THAT IS IN A CHAMBER. THE PLASMA FLAME WILL BE USED TO HEAT THE ENTIRE CHAMBER AND CRUCIBLE TO A TEMPERATURE AT WHICH THE GLASS WILL MELT AND CONSOLIDATE.

## V. CERAMIC COATING FOR ALUMINUM

SAMPLES HAVE BEEN SUBMITTED AND A CONTRACT HAS BEEN RECEIVED FOR THE APPLICATION OF A CERAMIC COATING TO AN ALUMINUM LANDING MAT. THE CERAMIC FRIT IS APPLIED TO THE SURFACE OF THE MAT AND THE SECTION IS PUT IN A HEAT TREATING FURNACE WITH THE COATED SURFACE IN A HORIZONTAL POSITION. AT THE HEAT TREATING TEMPERATURE THE CERAMIC REACTS WITH THE ALUMINUM TO PRODUCE A SURFACE THAT IS A COMBINATION OF ALUMINUM BORATES AND SILICATES CONTAINING TITANIA. THIS SURFACE LAYER IS CHEMICALLY BONDED TO THE ALUMINUM.

THE COATING HAS A HIGH THERMAL SHOCK RESISTANCE AND IS NOT DAMAGED BY THE QUENCH OF THE ALUMINUM PART AFTER THE HEAT TREATING OPERATION. THIS COATING IS TO BE APPLIED TO THOSE AREAS OF PORTABLE ALUMINUM LANDING MATS THAT ARE EMPLOYED AS LAUNCHING PADS FOR SMALL MISSILES.

## VI. COATINGS FOR EXTRUSION DIES

DURING RECENT MONTHS AN IMPORTANT CONTRIBUTION TO THE "STATE OF THE ART" HAS BEEN ACHIEVED BY THE USE OF CERAMIC FACED DIES FOR HIGH TEMPERATURE EXTRUSION. DIES COATED WITH ALUMINUM OXIDE EXTENDED THE PRACTICAL EXTRUSION TEMPERATURE RANGE TO 3200°F AND, RECENTLY, THE USE OF ZIRCONIUM OXIDE FACINGS HAS EXTENDED THIS RANGE TO AT LEAST 4150°F. ALTHOUGH HIGHER TEMPERATURES ARE UNDOUBTEDLY POSSIBLE, THEY HAVE NOT YET BEEN ATTEMPTED.

IN CONTRAST WITH THE HIGH SPEED STEEL DIES PREVIOUSLY USED FOR THIS WORK WHICH WASHED AS MUCH AS 1/4" WHILE PRODUCING A SINGLE EXTRUSION 20" LONG AT A TEMPERATURE OF 2800°F, A CERAMIC (ZIRCONIA) FACED DIE WILL CONSISTENTLY PRODUCE A BAR OVER 40" LONG AT TEMPERATURES ABOVE 4100°F WITH A DIAMETRAL VARIATION OF ONLY  $\pm 0.005$ " OVER THE 40" LENGTH. IT WAS ALSO FOUND THAT SUCH DIES CAN FREQUENTLY BE USED FOR MORE THAN ONE EXTRUSION WITHOUT RECOATING; AND WHEN THE DIE COATING IS DAMAGED DURING EXTRUSION IT IS EASILY RESTORED TO ACCEPTABLE CONDITION BY RECOATING. IF THE DIE COATING IS PROPERLY APPLIED IT IS SELDOM NECESSARY TO DISCARD A DIE BLANK BECAUSE OF DAMAGE RESULTING FROM EXTRUSION.

VARIOUS COATING METHODS AND MATERIALS HAVE BEEN TESTED WITH VARYING DEGREES OF SUCCESS. THEY ARE AS FOLLOWS:

FLAME SPRAYED ALUMINUM OXIDE POWDER

ACCEPTABLE COATINGS HAVE BEEN APPLIED BUT ARE DIFFICULT TO ACHIEVE, ARE LESS CONSISTENT, AND ARE LESS ADHERENT THAN COATINGS APPLIED BY OTHER METHODS.

FLAME SPRAYED ALUMINUM OXIDE ROD (ROKIDE)

THIS COATING HAS BEEN ADOPTED FOR PROCESS WORK BELOW 3200°F. IT IS INEXPENSIVE, RELATIVELY EASY TO APPLY CONSISTENTLY BY AN EXPERIENCED OPERATOR, AND PRODUCES A DEPENDABLE COATING.

FLAME SPRAYED ZIRCONIUM SILICATE ROD (ROKIDE)

ALTHOUGH THIS COATING HAS SOME OF THE VIRTUES OF THE ABOVE  $Al_2O_3$  COATING, THE MATERIAL HAS A GLASSY PHASE AT 3000°F AND THUS IS SUITABLE ONLY FOR RELATIVELY LOW TEMPERATURES.

FLAME SPRAYED ZIRCONIUM OXIDE ROD (ROKIDE)

HAS BEEN ADOPTED FOR HIGH TEMPERATURE PROCESS WORK AND CAN BE USED INTERCHANGEABLY WITH THE  $Al_2O_3$  ROD SPRAY COATING AT LOWER TEMPERATURES. IT IS SOMEWHAT MORE DIFFICULT TO APPLY AND SLIGHTLY MORE EXPENSIVE THAN  $Al_2O_3$ , BUT IS OTHERWISE HIGHLY ACCEPTABLE,

## ARC PLASMA SPRAYED ZIRCONIUM OXIDE POWDER

ALTHOUGH THIS COATING IS SOMEWHAT SUPERIOR TO THE ABOVE IN TERMS OF BOND STRENGTH AND COATING DENSITY, IT HAS BEEN USED IN ONLY A FEW TESTS BECAUSE OF ITS HIGHER APPLICATION COST. HOWEVER, SINCE HIGHER TEMPERATURE MATERIALS CAN BE APPLIED WITH THE PLASMA FLAME, IT HAS A GREAT DEAL OF PROMISE FOR FUTURE WORK.

DIFFICULTIES IN OBTAINING CONSISTENTLY ADHERENT CERAMIC FACINGS HAVE BEEN ENCOUNTERED BECAUSE OF THE NECESSITY OF DEVELOPING COATING TECHNIQUES. THROUGH EXPERIENCE WITH THE PROCESS, IT WAS FOUND THAT REJECTIONS CAN BE REDUCED IF CLOSE CONTROL IS EXERCISED AS FOLLOWS:

1. SURFACE PREPARATION: THE MOST CRITICAL STEP IN THE COATING PROCESS IS THE PREPARATION OF A ROUGH SURFACE WHICH PROVIDES THE BASIS FOR A GOOD MECHANICAL BOND BETWEEN DIE STEEL AND THE SUBSEQUENT COATING. THE STEEL BLANK MUST BE ROUGH MACHINED NO SMOOTHER THAN RMS-200 AND IT SHOULD NOT BE HARDER THAN Rc46 TO PERMIT SUBSEQUENT GRIT BLASTING. IT SHOULD BE WELL BLASTED, AT A 45° ANGLE, WITH #G-18 STEEL GRIT TO PRODUCE A VERY ROUGH SURFACE WITH SOME

UNDERCUTTING IF POSSIBLE. TO ACHIEVE THE REQUIRED ROUGHNESS, CENTRIFUGAL PRESSURE BLASTING EQUIPMENT IN TOP OPERATING CONDITION WITH AT LEAST 110 POUNDS AVAILABLE PRESSURE SHOULD BE USED. AFTER BLASTING, THE DIE FACE SHOULD NOT BE TOUCHED WITH BARE HANDS, OILY RAGS, ETC., UNTIL COMPLETELY COATED.

2. APPLICATION OF UNDERCOAT: A FLASH COATING OF NICKEL-CHROMIUM ALLOY IS USED BETWEEN THE DIE SURFACE AND THE CERAMIC MATERIAL TO (A) PROVIDE CORROSION RESISTANCE AND (B) TO PROMOTE BONDING. CARE MUST BE EXERCISED TO KEEP THIS COATING THIN (NOT MORE THAN 0.005"); A HEAVY COATING WILL FILL THE ROUGH STEEL SURFACE AND PREVENT MECHANICAL BONDING.

3. APPLICATION OF CERAMIC COATINGS: OPERATOR TECHNIQUE IS CRITICAL IN THIS FINAL OPERATION. WITH ALL OF THE PROCESSES INVESTIGATED, ACCEPTABLE RESULTS HAVE BEEN CONSISTENTLY PRODUCED ONLY BY EXPERIENCED OPERATORS.

IN ADDITION TO IMPROVED DIE LIFE AND A MARKED INCREASE IN THE PRACTICAL EXTRUSION TEMPERATURE RANGE, THE USE OF CERAMIC FACED DIES HAS RESULTED IN A GENERAL REDUCTION OF EXTRUSION PRESSURES. A MORE RELIABLE CORRELATION OF EXTRUSION PRESSURES AND



TEMPERATURES (ESTIMATION OF THE K FACTOR), HAS ALSO BEEN PROVIDED AS WELL AS MARKED IMPROVEMENT IN THE SURFACE CONDITION OF AS-EXTRUDED BARS. THE CONCURRENT USE OF A RELATIVELY SOFT DIE STEEL BLANK THAT IS HELD INSIDE OF THE MASSIVE CONTAINER HAS ELIMINATED DIE BREAKAGE AND THE USUAL DIFFICULTIES ASSOCIATED THEREWITH.

TO SUPPLEMENT THE INVESTIGATION OF DIE COATING MATERIALS AND METHODS, A STUDY OF DIE DESIGNS INCORPORATING VARIOUS ENTRANCE ANGLES HAS BEEN MADE. THE STANDARD DIE USED IN THIS PROJECT HAS A  $90^{\circ}$  INCLUDED ANGLE APPROACH. SINCE DIES HAVING GREATER ANGLES ARE WIDELY USED THROUGHOUT THE EXTRUSION INDUSTRY, A TEST OF THE VALIDITY OF THIS ANGLE SEEMED TO BE IN ORDER. ENTRANCE ANGLES OF  $110^{\circ}$  AND  $130^{\circ}$  WERE USED, AND EACH WAS RUN IN DIRECT COMPARISON WITH A  $90^{\circ}$  DIE UNDER THE SAME CONDITIONS. THE RESULTS ARE AS FOLLOWS:

<u>DIE ENTRANCE ANGLE</u>	<u>EXTRUSION NUMBER</u>	<u>MATERIAL</u>	<u>TEMP OF</u>	<u>START TONS</u>	<u>REMARKS</u>
$110^{\circ}$	318	W+10Mo+.01C	3000	610	FAIR SURFACE
$90^{\circ}$	307	W+10Mo+.01C	3000	518	SMOOTH SURFACE
$130^{\circ}$	355	Mo+.50Ti+.08Zr +.25C	2800	518	SMOOTH SURFACE
$90^{\circ}$	354	Mo+.50Ti+.08Zr +.025C	2800	426	SMOOTH SURFACE

THE ADVANTAGE IN USING THE  $90^{\circ}$  APPROACH DIE IS, OF COURSE, THE MARKED REDUCTION IN STARTING FORCE. THE TUNGSTEN ALLOY AT  $3000^{\circ}\text{F}$  REQUIRED 18% MORE STARTING FORCE FOR THE  $110^{\circ}$  DIE THAN IT DID FOR THE  $90^{\circ}$  DIE, AND THE MOLYBDENUM ALLOY AT  $2800^{\circ}\text{F}$  REQUIRED 22% MORE STARTING FORCE FOR THE  $130^{\circ}$  DIE THAN IT DID FOR  $90^{\circ}$  DIE. AN ADDITIONAL ADVANTAGE OF THE  $90^{\circ}$  DIE IS THAT THE BAR IS COMPLETELY EJECTED AT THE END OF EXTRUSION. DIES WITH WIDER ANGLES ARE NOT AS EFFECTIVE IN THIS WAY, AND THEY FREQUENTLY RESULT IN THE EXTRUDED BAR REMAINING ATTACHED TO THE DIE WHICH PRESENTS A REMOVAL PROBLEM AND PARTICULARLY INTERFERES WITH PLACING THE HOT EXTRUDED BAR INTO A SLOW COOLING MEDIUM. THE DIE COATING IS ALSO MORE SUBJECT TO CHIPPING AND PEELING WHEN THE TAIL OF THE BAR STICKS IN THE DIE, AND CONSEQUENTLY DIE LIFE IS GENERALLY SHORTENED.

SOME DIFFICULTIES HAVE BEEN ENCOUNTERED IN APPLYING CERAMIC FACINGS TO DIES FOR PRODUCING WIDE FLAT BARS, DUE TO THE DEEP NARROW SIDES. FURTHER EFFORTS WITH COATING TECHNIQUES HAVE RESULTED IN PRODUCING RECTANGULAR DIES THAT ARE AS SERVICEABLE AS COMPARABLE ROUND DIES. HOWEVER, MORE CAUTION SHOULD BE EXERCISED TO PREVENT OVERUSE BECAUSE OF THE HIGHER INITIAL COST.

THE MOST DIFFICULT REFRACTORY ALLOY SHAPES THAT HAVE BEEN EXTRUDED DURING THIS PROJECT HAVE BEEN AN 8:1 RECTANGULAR BAR, 2" X 7/16" AND AN 18.8:1 ROUND BAR OF 0.706" DIAMETER. BOTH HAVE BEEN EXTRUDED THROUGH CERAMIC FACED STEEL DIES WITH A CONICAL ENTRANCE A. IT IS POSTULATED THAT WITH CAREFUL CONSIDERATION THIS DESIGN COULD BE EXTRAPOLATED FOR USE IN THE EXTRUSION OF A MORE COMPLEX SHAPE.

## VII. HEAT TRANSFER STUDIES

A SOMEWHAT RELATED PROJECT WHICH DID NOT, HOWEVER, INVOLVE COATINGS WAS A STUDY OF THE RATE OF HEAT TRANSFER THROUGH VARIOUS TYPES OF SOIL. VARIOUS PLASMA NOZZLES WERE EMPLOYED, INCLUDING THE USUAL HIGH VELOCITY NOZZLE, THE LOW VELOCITY NOZZLE AND THE TRANSFERRED ARC TORCH. A NUMBER OF DIFFERENT GASES AND GAS COMBINATIONS WERE ALSO USED. BY FAR THE BEST RESULTS WERE OBTAINED WITH THE LOW VELOCITY PLASMA FLAME.

HYPERTHERMAL RESEARCH FACILITY  
PROGRESS REPORT

R. A. STEVENS  
J. E. BURROUGHS

General Dynamics  
Fort Worth, Texas

The Hyperthermal Research Facility (HRF) is currently undergoing design and construction at GD/FW and is expected to be in check-out and calibration in the fall of 1961. Figure 1 is a schematic of the facility. It will be a high enthalpy, free jet hypersonic tunnel, and will use high pressure air as the primary working fluid. The air will be heated in a magnetically stabilized electric arc plasma generator, expand through an axisymmetric nozzle into a free jet test section, and exhaust to the atmosphere through a diffuser, cooling section, and steam jet ejector system. The plasma generator was designed and fabricated by Vidya, Inc., to GD/FW specifications.

Intended applications of the HRF include ablation studies, simulation of the thermal environment of high temperature structures, materials and vehicles, heat transfer and pressure distribution measurements, research on flow characteristics of high energy gases, and similar aero-thermodynamic studies. Running times ranging from several seconds to several minutes are required for adequate simulation of these phenomena. To accomplish these objectives it was necessary to design the facility to operate at high enthalpy levels and high Mach numbers. Particular emphasis was placed on simulating stagnation point heat transfer rates on reasonably sized models at total enthalpies corresponding to actual flight conditions.

The facility will also be capable of low temperature operation (below dissociation levels) and will thus be extremely useful as a conventional hypersonic wind tunnel.

Predicted capabilities of the HRF are:

- (1) Air supply pressure - 1 to 30 Atm
- (2) Stream total enthalpy - 500 to 10,000 Btu/lb at max. air supply pressure  
500 to 15,000 Btu/lb at lower pressure
- (3) Maximum test section Mach number - 15 to 20
- (4) Maximum power input - 1.8 megawatts D.C.
- (5) Running time - 3 minutes at max. power, continuous at half power

With the initial nozzle, the performance is predicted to be as follows:

- (1) Nozzle exit diameter - 8 inches

- (2) Air supply pressure - 460 psia
- (3) Test section Mach number - 12.5
- (4) Maximum test section total enthalpy - 8,000 to 10,000 Btu/lb.

Currently the installation of most of the major components of the HRF is complete. Operation will begin when the plasma generator and nozzle are received from the subcontractors.

Initially, calculations of the expansion process in the nozzle assumed chemical and thermodynamic equilibrium throughout. However, later analytical and experimental work has indicated that the chemical composition of the flow will "freeze" at some point in the nozzle. Current calculations, based on the studies of K.N.C. Bray (Ref. 1), predict chemical freezing upstream of the throat for plenum conditions of 10,000 Btu/lb enthalpy and 30 atm. pressure. The effect of freezing on test section conditions is to lower the static pressure and temperature and to increase the Mach number. Also, the problem of making measurements adequate to define test section conditions becomes more complicated.

Early in the program it became apparent that convective heat transfer rates from the hot gas to the nozzle walls would be very high, particularly at the throat section. Therefore, an extensive literature survey was conducted which revealed several methods for predicting nozzle convective heat transfer; however, none had been verified for the extreme conditions to be experienced in the HRF nozzle. The approximate solution of Bartz (Ref. 2) was used. Investigations of radiant heat transfer from the gas to the nozzle revealed that radiative losses would be negligible in the divergent section but would be very high in the plenum chamber and convergent section where the static temperature and pressure are high.

Based on predicted heat transfer rates, it was found that heat transfer coefficients sufficiently large to prevent melting of the nozzle wall could not be obtained on the coolant (water) side using ordinary forced convection. Therefore, the best available empirical data on forced convective nucleate boiling and burnout were used to design the cooling passages. In the critical area around the throat the water velocity was optimized according to the well known Gunther correlation (Ref. 3) with a safety factor of two on the burnout heat flux.

The design of the diffuser was based on experimental correlations available in the literature. Due to the lack of adequate theoretical means for predicting supersonic diffuser performance, a very simple configuration was selected which could be built with a minimum investment. It is hoped that empirical data obtained from inexpensive diffusers of this type will lead to a more sophisticated future design. With the initial diffuser, total pressure recovery greater than 0.6 of normal shock total pressure ratio (NSPR) is not expected. Approximately 0.20 NSPR is required

to operate the tunnel with the initial nozzle.

Considerable attention has been given to the problem of measuring test stream flow properties. By means of an error analysis (Ref. 4) it was established that the quantities which must be measured to yield meaningful accuracy in calculating the remaining flow properties are: static and total pressure, static temperature, and the degrees of dissociation of the various constituents.

Probably of more interest to attending personnel is the materials testing capabilities of the facility. The overall internal dimensions of the test chamber are four and one-half feet cubed. The first nozzle to be available will have a circular cross-section and will provide an estimated test stream diameter of approximately six inches. Nozzle exit diameter is eight inches. An automatic model positioning device will move the test specimen into position in 0.5 sec. and with reproducible positioning within 6 minutes of a degree. Twenty inch diameter windows allow excellent visual observation of the test specimen and easy access to removal and insertion of new specimens.

Heat transfer rates to models in the test stream can be controlled by controlling the total enthalpy of the gas, the size of the model the total pressure of the test stream, and by providing additional nozzles to vary the test stream Mach number. With control of these variables, model stagnation point heat transfer rates can be varied from extremely low values up to at least 2000 Btu/ft<sup>2</sup> sec.

Several special instrumentation techniques will be required in the HRF. First, spectroscopic techniques appear to offer the most promise for the measurement of test stream static temperatures and for determining the degrees of dissociation of the constituents. Test stream static temperatures are predicted to be of the order of 200-300°K at test section Mach numbers of 12-14. Second, the need to measure very small differential temperatures in the cooling water circuits, in order to make an energy balance, has prompted the design of a special thermistor bridge which has demonstrated its ability to measure small differential resistance (i.e. small  $T$ ) to 1.0% accuracy. Also, two types of water cooled probes have been designed for use in the test stream. One is a 30 degree blunt wedge with static pressure taps on the upper and lower surfaces, and the other is a cylinder with protruding pitot pressure taps along the stagnation line. The wedge will be used to check for vorticity in the flow and the cylindrical probe will be used as a pitot pressure rake. Future plans include the design and fabrication of a cooled calorimeter probe, and a sphere drag device for the measurement of local dynamic pressure.

It is anticipated that a considerable checkout and calibration effort will be required to define the test section conditions prior to actual model testing. Theoretical work in this area is continuing in an effort to develop a comprehensive theory to predict the nature of the flow. Such a theory, with experimental



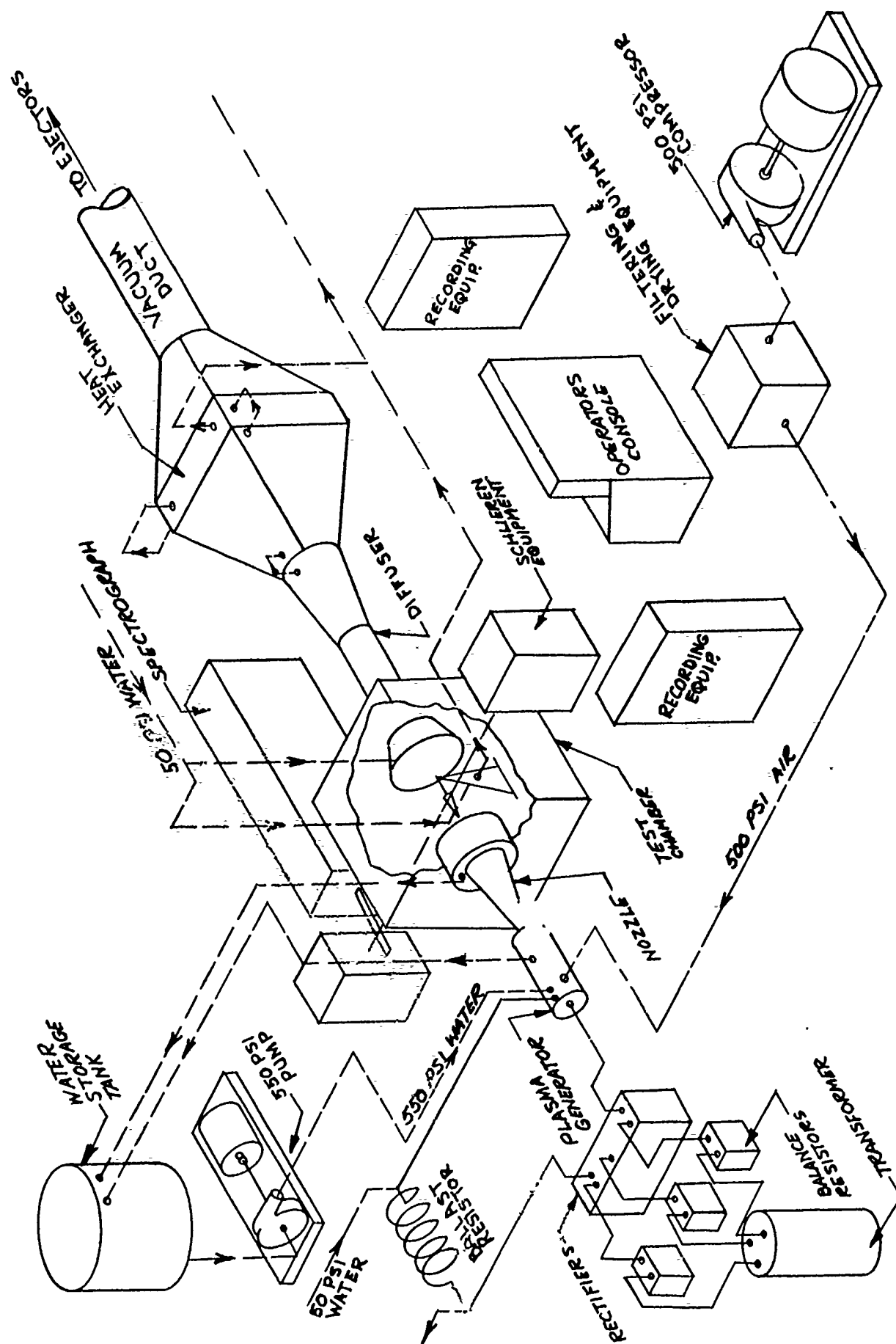
verification obtained in the HRF, would in itself be a significant contribution to the state of the art.

Additional information pertaining to the Hypertermal Research Facility may be obtained by contacting R. N. Oliver, Chief of Aerothermodynamics, General Dynamics/Fort Worth

## REFERENCES:

1. Bray, K. N. C., "Atomic Recombination In A Hypersonic Wind Tunnel Nozzle," J. Fluid Mech., Vol. 6, Part 1, July 1959.
2. Bartz, D. R., "An Approximate Solution of Compressible Turbulent Boundary Layer Development and Convective Heat Transfer in Convergent-Divergent Nozzles," Prog. Rept. No. 20-234, Jet Propulsion Laboratory, Calif. Inst. of Technology, July 9, 1954.
3. Gunther, F. C., "Photographic Study of Surface-Boiling Heat Transfer to Water with Forced Convection," Trans. ASME, 73 115-123, February 1951.
4. Brock, O. R., "Measurements Required in a Hypersonic Dissociated Air Stream To Define Stream Conditions," ERR-FW-029, Convair (Fort Worth), Dec. 1960.

FIGURE 1  
HYPERTHERMAL RESEARCH  
FACILITY SCHEMATIC



THIN ARC-SPRAYED SHAPES - III

C. A. MURPHY

N. E. POULOS

J. D. WALTON, JR.

Georgia Institute of Technology

Atlanta, Georgia

# THIN ARC-SPRAYED SHAPES - III

By

C. A. Murphy, N. E. Poulos, and J. D. Walton, Jr.

## I. INTRODUCTION

Again, as was the case in the last report to this group, most of the work reported in this paper is concerned with forming thin shapes using the arc-spray process. The arc spray equipment in use is a "Plasma Flame" F-40 Unit.

## II. PATTERNS

### A. Shapes for Physical Properties Measurements

The tubular tensile shape described in the last report has produced data with a deviation as great as that obtained with the hour-glass shape. However, this shape is much easier to fabricate and is presently being evaluated for reproducibility using a completely mechanized spray process. This is described later in the paper.

### B. Mandrels for Nozzle Insert Shells

At the time the last report was given techniques had been developed for obtaining complete arc-sprayed nozzle inserts from tungsten. Application of these techniques, using the same mandrel, to the fabrication of inserts from refractory oxides and carbides met with limited success. The major problem encountered during these attempts was the rupturing of the nozzle shell in the entrance and exit cones.

The following modifications or procedures were evaluated as means of reducing or eliminating this problem.

1. To reduce the effect of differential expansion of the insert on the mandrel, the mandrel was redesigned so that it was held together at

the point of minimum diameter with a dowel pin arrangement under low spring tension, using maximum mandrel preheat temperatures and building up an arc-sprayed shell of sufficient strength so that when the mandrel was cooled it would be pulled apart rather than cracking the shell. This design, however, was not successful in eliminating the rupturing of the nozzle shell in the entrance and exit cones.

2. The mandrel was further modified to increase the length of the entrance and exit cone sections as shown in Figure 1. It was thought that by not spraying this mandrel its entire length, the edges would not come to an abrupt end, possibly eliminating points where the insert shell could begin to crack on mandrel cool down. This design also was not successful.
3. A small furnace was constructed to provide uniform heat over the entire mandrel length both before and during spraying. It was thought that it would reduce mandrel temperature gradients and their effect on stresses within the coating, and/or variable contraction and expansion within the mandrel.

Preliminary investigations were conducted to form complete nozzle insert shells by arc spraying onto preheated mandrels of brass, stainless steel, and inconel. The surface of each mandrel was oxidized slightly to evaluate the effectiveness of the oxide film as a parting agent between the mandrel and the arc-sprayed coating and the temperature of the furnace was held at 1000° F. Stabilized zirconia was used as the spray powder.

Initial attempts at applying coatings to the mandrel at this temperature resulted in cracking and buckling of the coating after a very thin

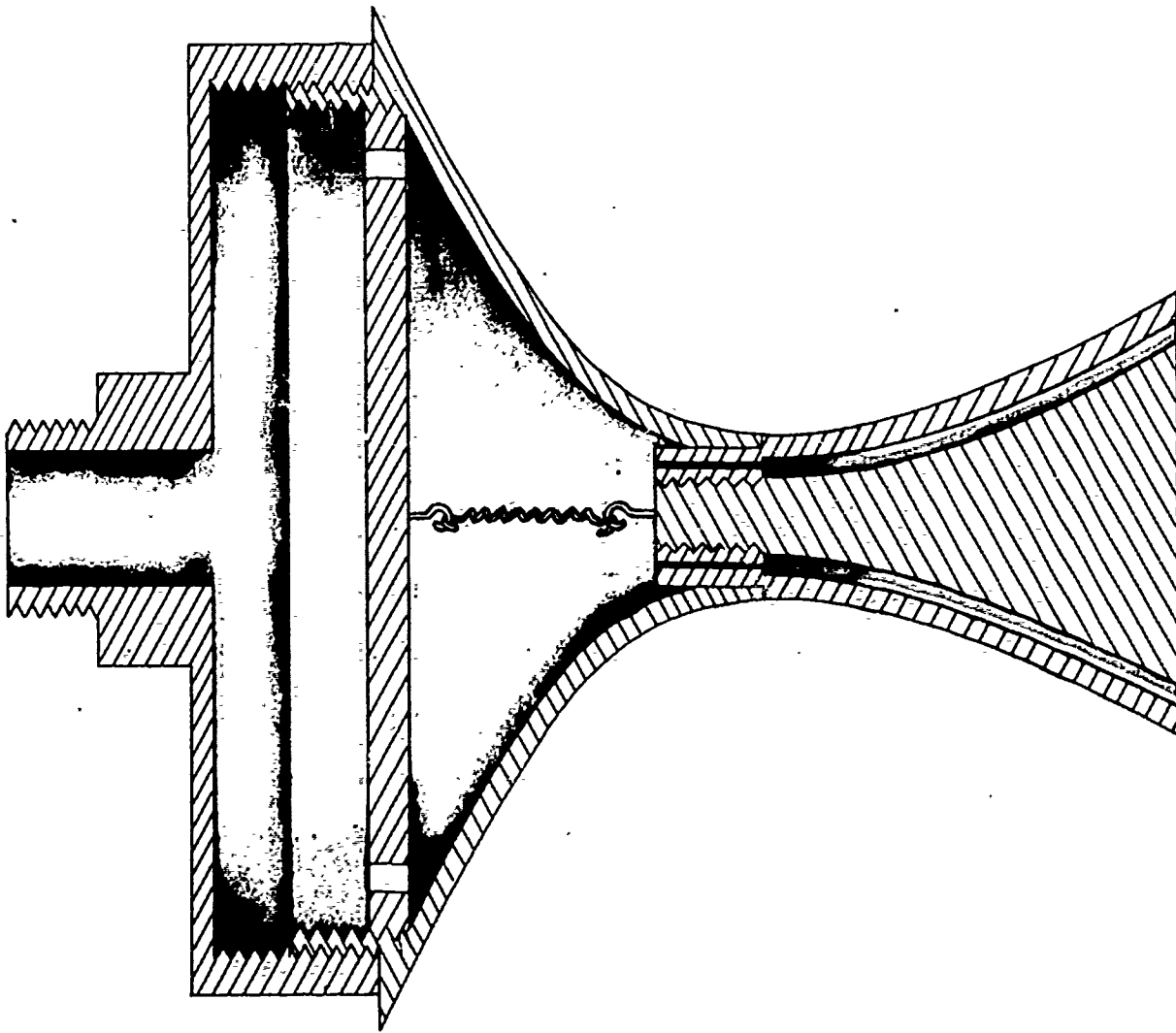


Figure 1. Drawing of Modified Insert Mandrel.

layer had been applied. Making faster passes with the arc gun and increasing the time lag between passes eliminated this problem.

As experience was gained, complete nozzle insert sections could be arc sprayed to a thickness of about 1/16-inch, but longitudinal cracking of these sections still occurred and resulted in a gap that required a moderate pressure to close. It was then thought that this cracking was the result of a residual tensile stress build-up in the coating which eventually exceeded the tensile strength of the coating and as a result, caused a rupture.

The National Bureau of Standards<sup>1</sup> has concluded that a residual stress gradient exists in flame-sprayed alumina and is the result of rather complex mechanisms. They have also indicated that expressions for calculating these stresses may be forth-coming<sup>2</sup>. Therefore, it is considered reasonable to conclude that residual stresses are present in the arc-sprayed coatings and that the magnitude of such stresses will vary from one arc-sprayed powder to another.

4. Attempts to eliminate this cracking of the arc-sprayed coatings by increasing the mandrel temperature from 1000° to 2000° F were unsuccessful. Although these nozzle throat sections were defective, there appeared to be a pronounced decrease in the porosity of the samples, indicating that better per cent theoretical densities had been attained. Exact measurements of this decrease were not taken, however.

---

<sup>1</sup>"Basic Studies of Particle-Impact Processes for Applying Ceramic and Cermet Coatings", National Bureau of Standards, Report No. 6453, Progress Report No. 4, Page 20, Contract No. AF(33-616)-58-19, April 1, 1959 to June 30, 1959.

<sup>2</sup>Ibid, Progress Report No. 8, Page 9.



The difficulties encountered in these attempts to obtain arc-sprayed nozzle insert shells from oxides and carbides necessitated a change in the configuration of the insert that excluded the fabrication by arc spraying of the entrance and exit cones of the nozzle; only the nozzle throat is arc-sprayed. The entrance and exit cones are made of graphite and the arc-sprayed nozzle throat is machine fitted in the graphite (See Figure 2). This change was made in an effort to obtain more information on the behavior of arc-sprayed materials in the solid fuel rocket motor. This information is considered necessary before more intensive effort is placed on obtaining complete, or larger, arc-sprayed nozzle insert shells from any one material.

Throat inserts of tungsten, chrome carbide, alumina, and a mixture of tungsten and zirconia have been successfully obtained by arc-spray techniques. Photomicrographs taken from the end surface of each insert are shown in Figures 3, 4, 5, and 6. The nozzle throat inserts were arc sprayed onto air-cooled inconel mandrels. A drawing of this mandrel is shown in Figure 7. Prior to the arc-spray operation, the surface of each mandrel was oxidized slightly in a furnace at an indicated temperature of 2200<sup>0</sup> F for 10 minutes. The temperature of the mandrel was held below 200<sup>0</sup> F during the arc-spray operation by using maximum mandrel cooling air and arc-gun flame-deflecting air.

Initial attempts at arc spraying the mixture of tungsten and zirconia were made by using two powder hoppers and injecting each powder into a separate port on the arc-gun nozzle. This resulted in the powders being discharged from the arc-gun nozzle in two separate streams with little or no mixing of the two powders taking place. To eliminate this, the powder feed tubes were joined with a "y" type connection and the powder mixture injected into a single powder port on the arc-gun nozzle.



Figure 2. Photograph Illustrating Composite Nozzle Insert Assembly.

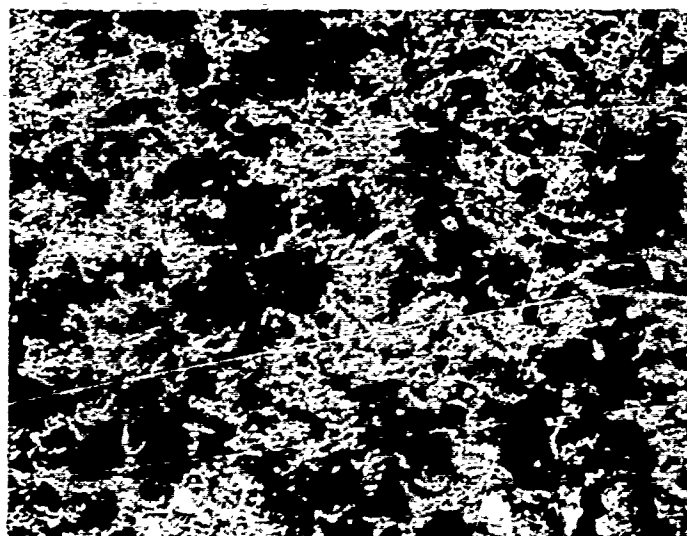


Figure 3. Photomicrograph of Tungsten Throat Insert  
No. 1264-22-1 (200 X).

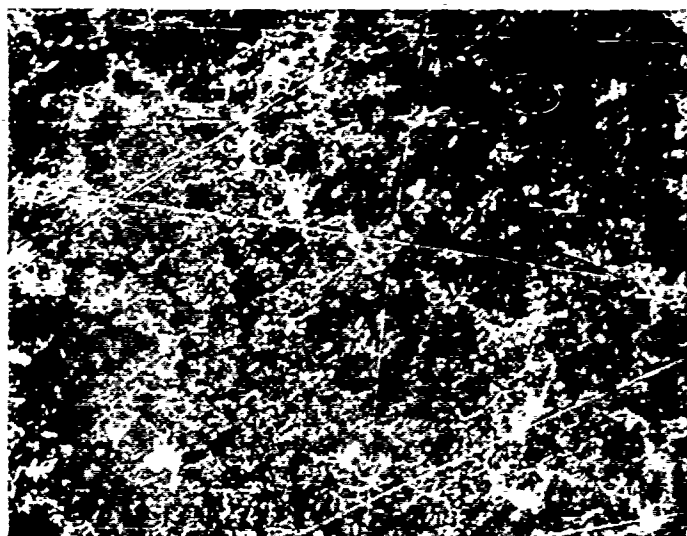


Figure 4. Photomicrograph of Chrome Carbide Throat Insert  
No. 1264-27-1 (200 X).

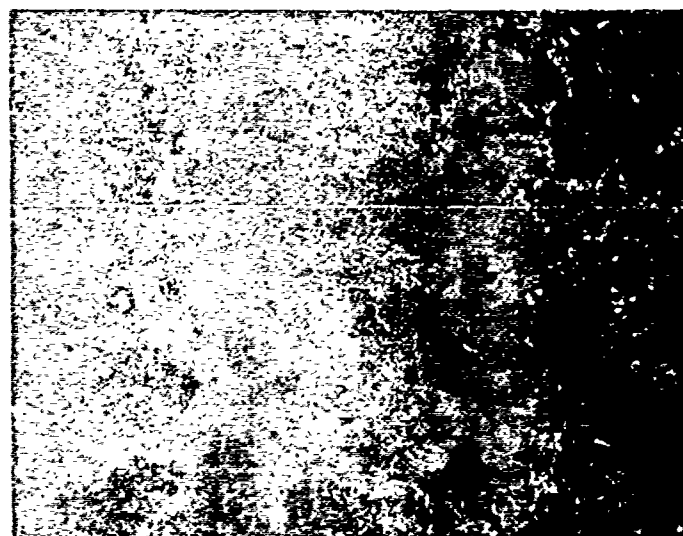


Figure 5. Photomicrograph of Alumina Throat Insert  
No. 1264-26-1 (200 X).

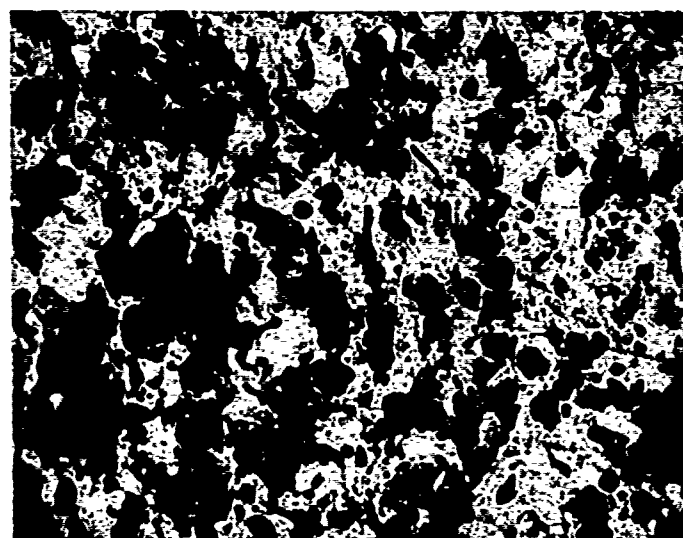
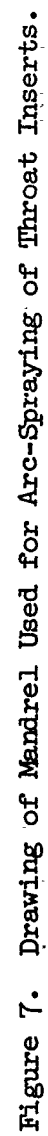


Figure 6. Photomicrograph of Tungsten-Zirconia Throat Insert  
No. 1264-33-1 (266 X).



### III. ACCESSORY EQUIPMENT

#### A. Controlled Atmosphere Chamber

Preliminary operation of the arc plasma torch in the inert atmosphere chamber described in the last report indicated a need to change several features of this design: (1) burn-out of the gun entrance diaphragm after approximately 2 minutes of operation, (2) no flexibility of the arc gun when sufficient coolant flow to eliminate burn-out was provided, and (3) numerous pin-hole water leaks constantly occurring in the chamber during operation.

Concurrently with this work, the Station's 80-kw arc plasma jet wind tunnel was nearing completion. Because of the limited amount of materials testing which would require the use of this tunnel it was considered advisable to adapt this facility to accomodate arc spraying as well as materials testing.

This tunnel is essentially a three component unit: (1) the primary chamber, (2) a particle trap and a heat exchanger for cooling the plasma gases, and (3) a vacuum pump--Kinney Model KDH-250. A schematic of this unit is shown in Figure 8. Spraying can be conducted in this unit from above atmospheric pressure down to 2 cm. Hg.

As originally designed, the operation of the 80-kw wind tunnel was to be limited to a few minutes test duration with a Pyrex cross as the primary chamber. Pyrex was adequate for the time and temperature necessary for materials testing, but it was found that prolonged arc-spray work in this chamber heated the cross beyond its maximum recommended working temperature of 425° F and made it necessary to fabricate an alternate primary chamber of steel.

To eliminate adverse heat and powder abrasion effects all electrical and mechanical components have been placed outside the vacuum system. These

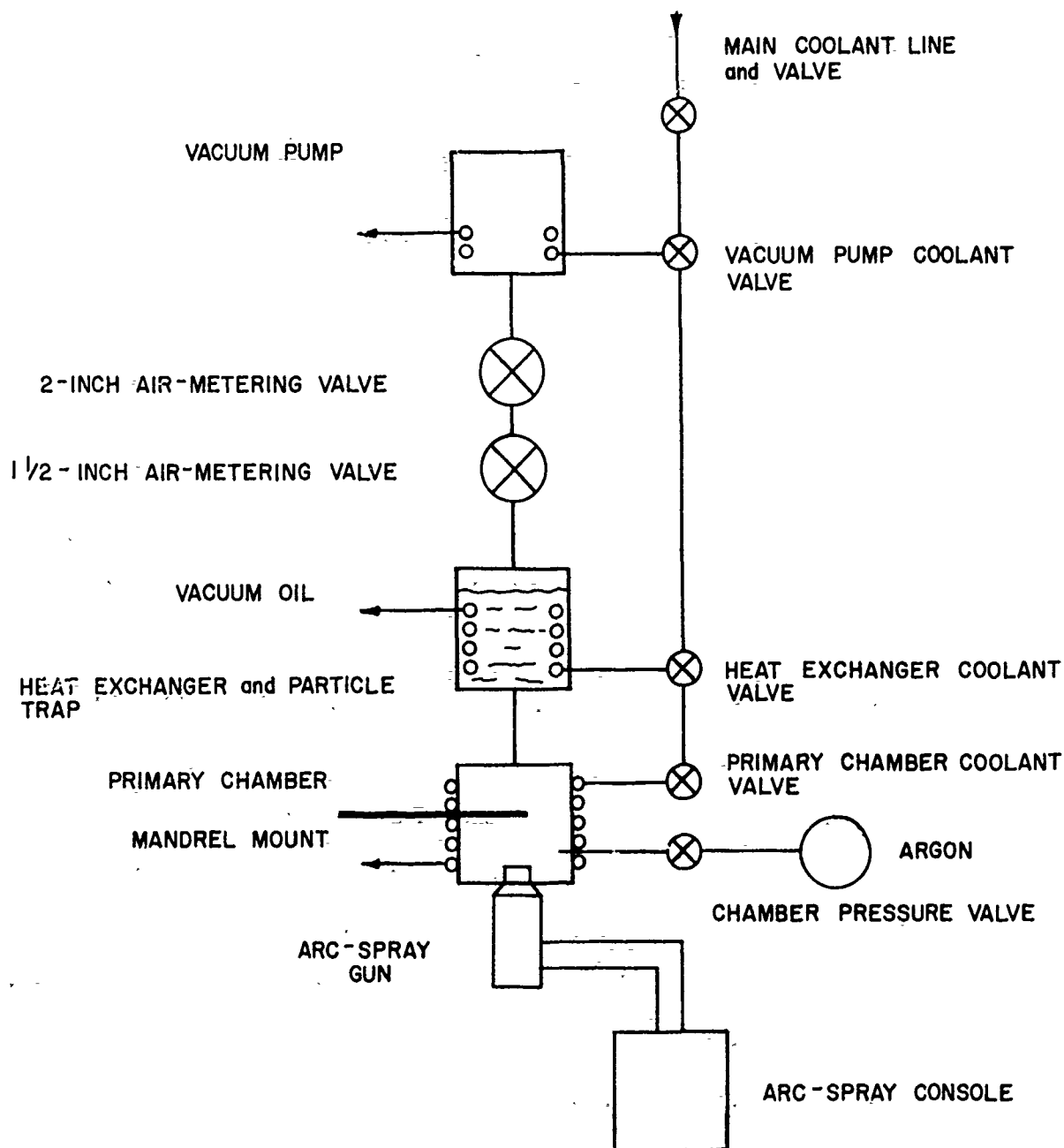


Figure 8. Schematic Drawing of 80-KW Wind Tunnel.

include a two stage table which controls the movement of the mandrel in the primary chamber. This unit is shown in Figure 9. The upper stage of the table consists of a 1/4-hp motor and a Zero-Max variable speed gear box for controlled rotation of the mandrel from 0 to 488 rpm in both clockwise and counterclockwise directions. The mandrel is connected to but not supported by the Zero-Max unit. From a flexible coupling a length of stainless steel rod is positioned by an O-ringed brass bushing which acts as the support and vacuum seal.

The second stage of the table controls the horizontal traverse of the upper stage. A small ratiomotor, with variable speeds from 16 to 65 rpm, was equipped with a pulley and push rod which allows varied reciprocating travels of 1-1/2, 2, and 2-1/2 inches.

Although the arc-spray gun is in the primary chamber, construction of the mounting device has put only a portion of the nozzle in the vacuum system. The gun is mounted in a steel cylinder closed at one end which is supported by two O-ringed brass rings. This is shown in Figure 10. The standoff distance can thus be controlled and held constant by means of a flange attached to the opposite end of the steel cylinder. The assembled system is shown in Figure 11.

Studies are now underway to determine the effect of chamber and arc-gun parameters on the physical properties of alumina.

#### B. Infrared Preheat Furnace

The furnace constructed to permit arc spraying onto preheated mandrels of brass, inconel, and stainless steel uses General Electric quartz infrared lamps 50-T3 as heating elements with power supplied by a Standard Electric Products Co., Adjust-A-Volt variable autotransformer. The lamp terminals



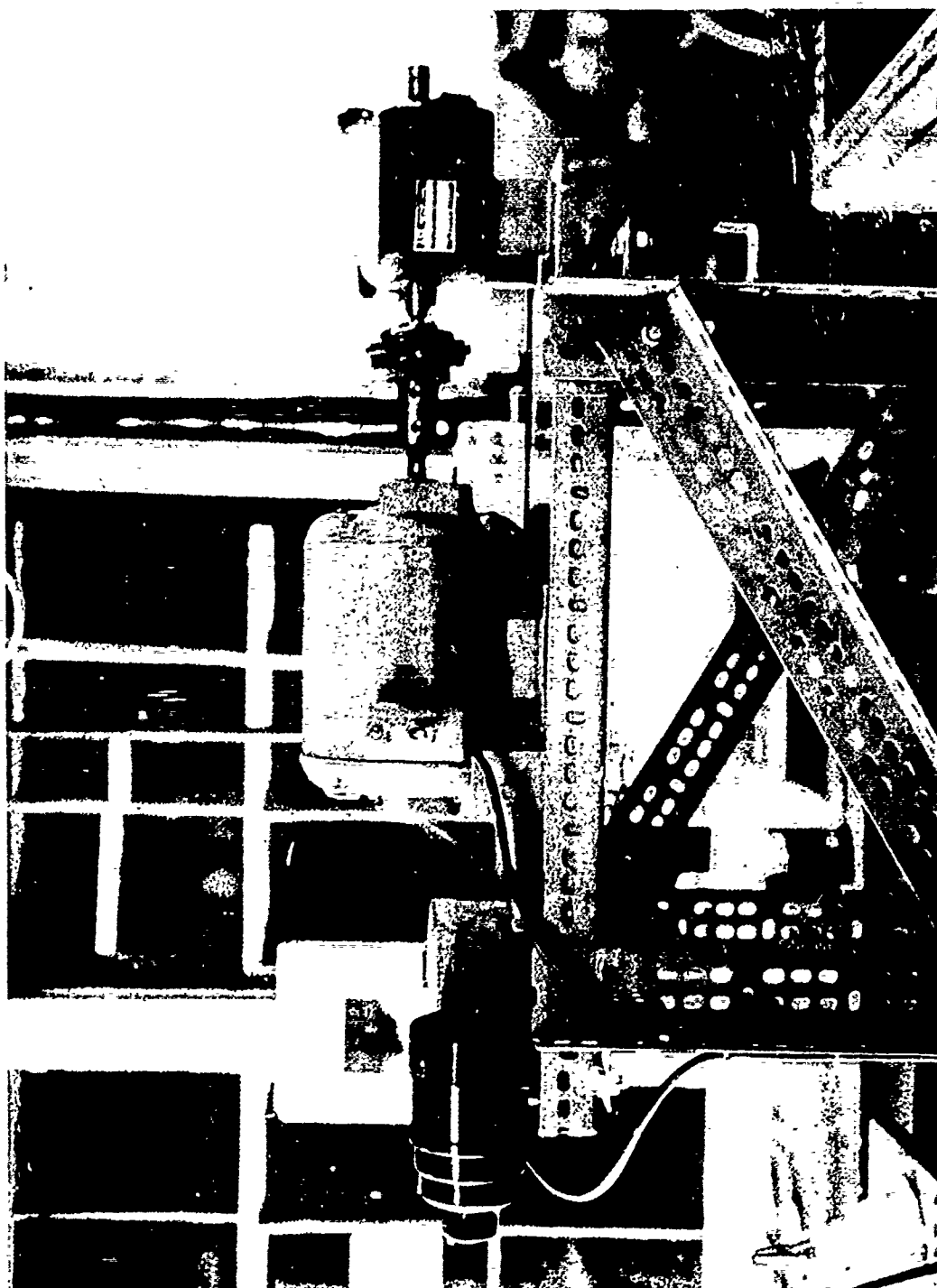


Figure 9. Mechanism Used to Rotate and Traverse Mandrel in Controlled Atmosphere Chamber.

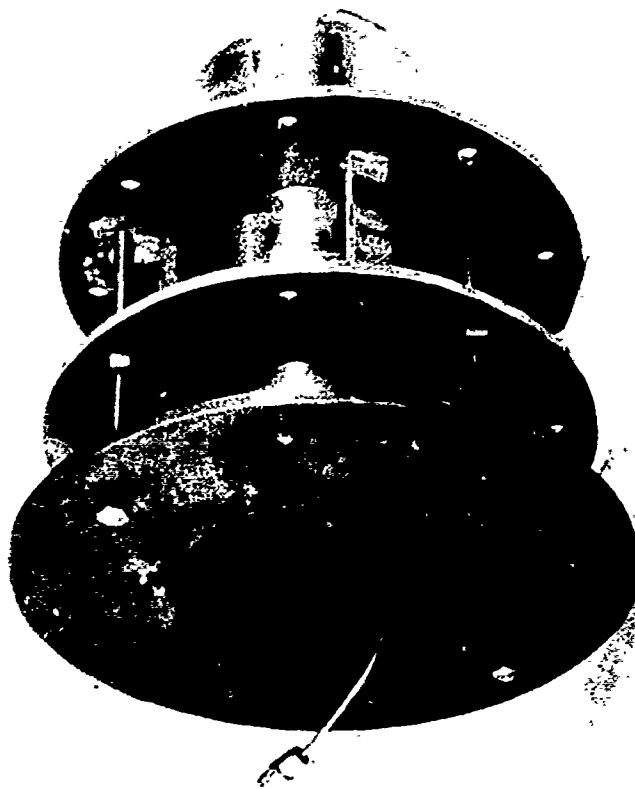


Figure 10. Device Used for Supporting and Positioning Arc-Spray Gun in Controlled Atmosphere Chamber.

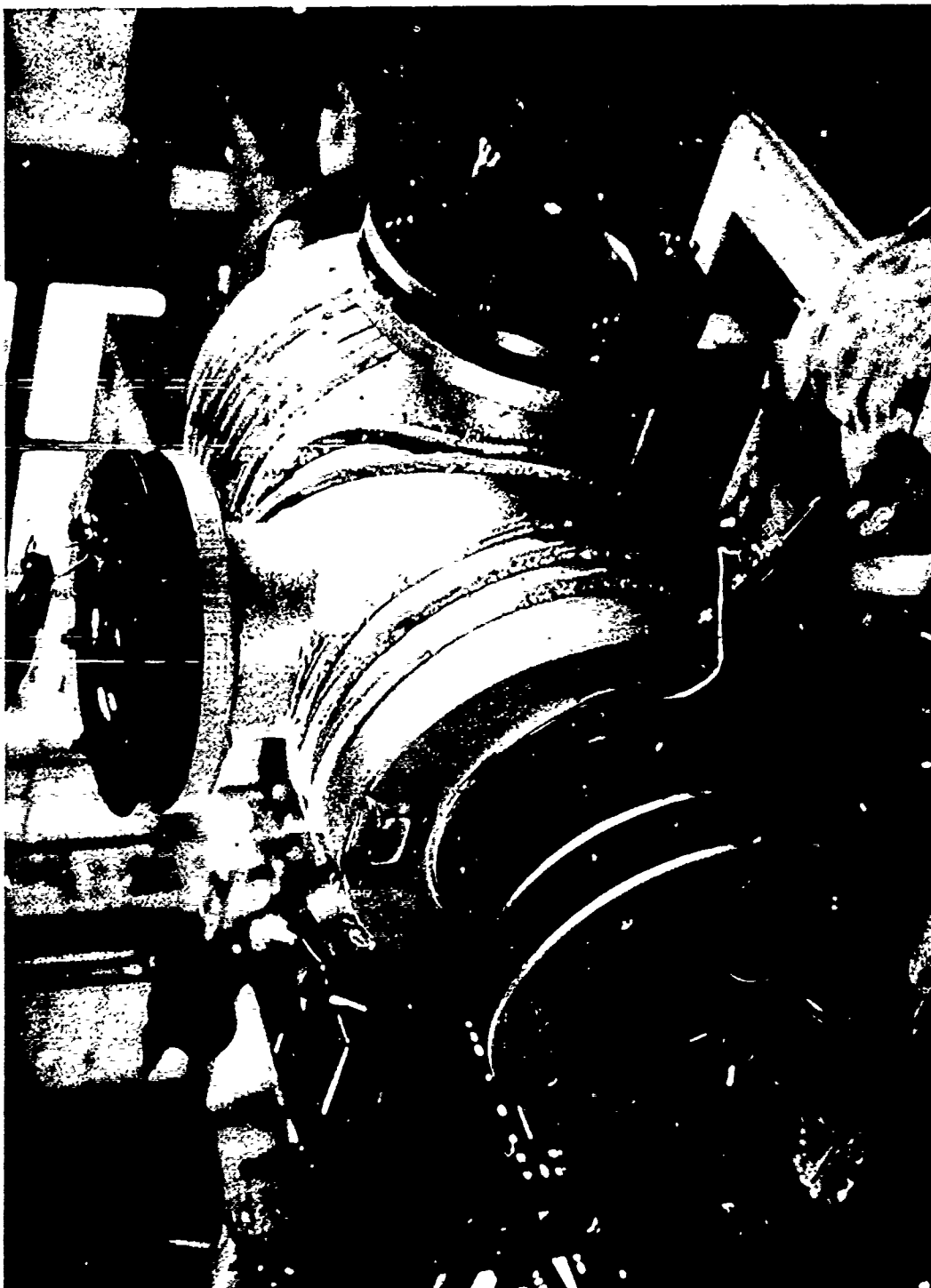


Figure 11. Photograph of Modified 80-KW Wind Tunnel Used for  
Controlled Atmosphere Arc-Spray Work.

are positioned in a water-cooled brass block to hold the lamp seals below the recommended 650° F maximum temperature.

Two pieces of Glasrock fused silica foam were carved to the configuration desired to allow an arc-spray operation through the furnace; the front and back of the furnace are open to prevent a material build-up in the furnace during the arc-spray operation. Three lamps are positioned in each half of the furnace. These halves are mounted in a slotted angle which permits an adjustment of these halves for the insertion of a mandrel. A grinding head from a surface grinder was modified to be used for mandrel rotation. The furnace can be used to preheat mandrels up to 2000° F and is shown in operation in Figure 12.

#### C. Syntron Vibratory Powder Feed Unit

Prior to its use in the arc-spray system, it was necessary to evaluate the Syntron vibratory feed system reported in the last paper in order to obtain powder feed rates comparable to those obtained with the metco powder hopper.

The Syntron unit was removed from its enclosure to gain free access of the instrument and permit close observation of the behavior of the test powder in the loading funnel and the trough. Preliminary tests of the unit revealed that the power output of the rheostat furnished with the Syntron unit was too great to be used for efficient arc-spray operations. A Variac power-stat was therefore utilized as a coarse adjustment, allowing the rheostat to be used as a fine control of the power supplied by the power-stat.

Tungsten, stabilized zirconia and fused silica powders were used to determine the feeding characteristics of the Syntron vibratory feeder. The tungsten and zirconia powders consisted of particles finer than 325 mesh,

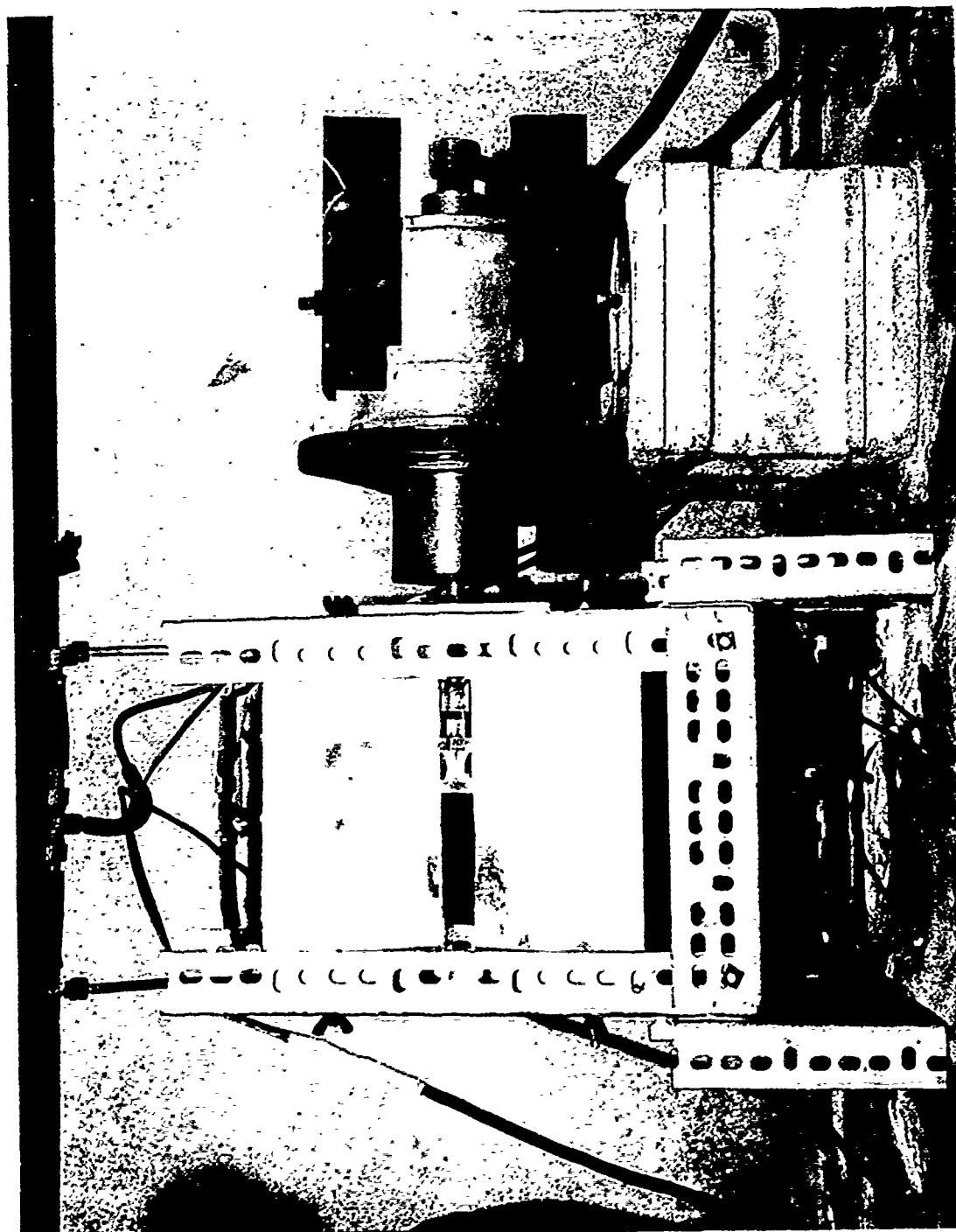


Figure 12. Photograph of Small Fused Silica Furnace Used to Preheat and Hold Mandrels at Elevated Temperatures.

whereas the fused silica powder had a screen analysis of:

+200 mesh	22.6 per cent
-200+230 mesh	7.9 per cent
-230+270 mesh	12.3 per cent
-270+325 mesh	10.7 per cent
-325 mesh	46.5 per cent

These powders were dried at 230° F for 12 hours before using.

The cumulative powder weight was measured for each run and plotted as a function of time. These curves are shown in Figures 13, 14 and 15.

The effect produced by atmospheric moisture that was adsorbed on the particles of powder was readily evident from Figure 15. The decrease in the flow rate of the silica after being fed through the powder feed unit was very pronounced.

When the Syntron feeder was replaced in its enclosure for further testing it was found that the enclosure leaked and could not be sealed. Therefore, a more compact unit was designed which was made of standard rectangular steel tubing with an access port at one end as shown in Figure 16. The new chamber measures 4 x 10 x 14 inches externally. It was necessary to shorten the trough of the Syntron vibratory feeder to fit this new chamber. A powder hopper was constructed of 2-1/2-inch-diameter brass tubing with a stainless steel funnel brazed to one end and a mounting flange attached to the other. A small hole was drilled at the top of the tubing to equilibrate the pressure in the hopper and the chamber. A baffle was placed in the trough of the Syntron unit to restrict the powder flow. This restriction was necessary to obtain an even flow of the powder down the length of the trough during operation and to eliminate any initial change of powder feed rate during startup. Powder feed

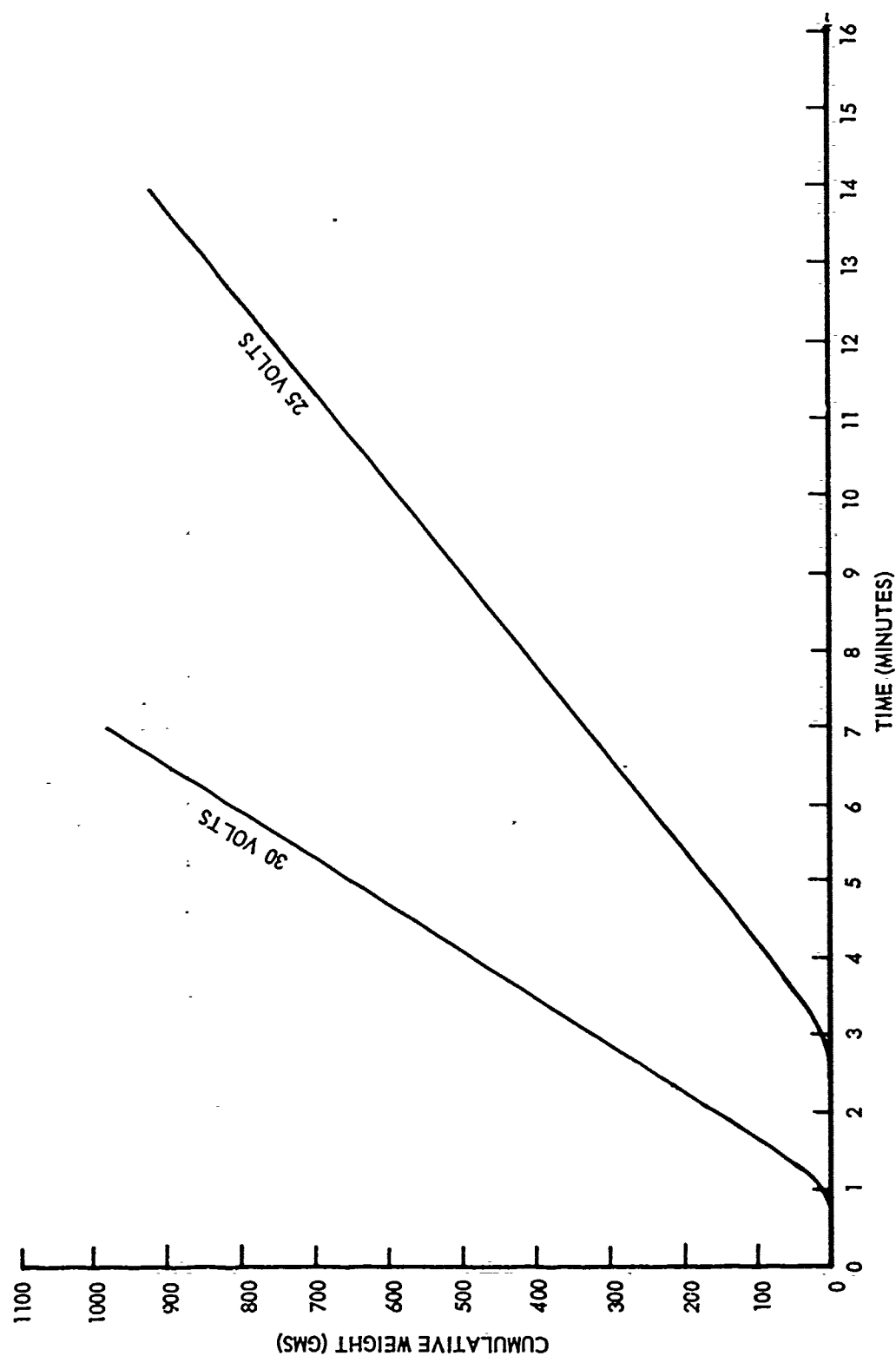


Figure 13. Weight Vs. Time of Tungsten Fed from the Syntrol Vibratory Feeder.

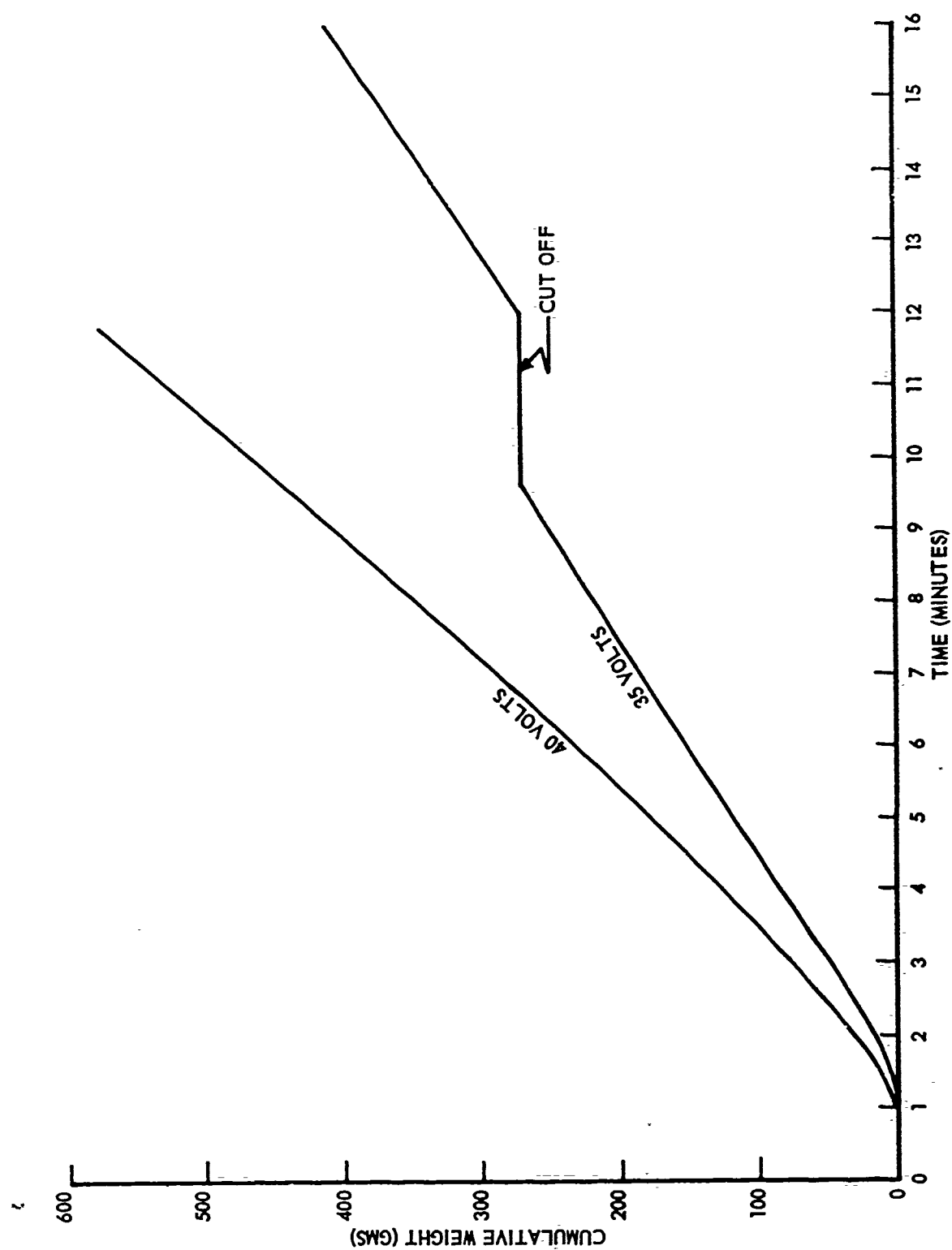


Figure 14. Weight Vs. Time of Zirconia Fed from the Syntrol Vibratory Feeder.



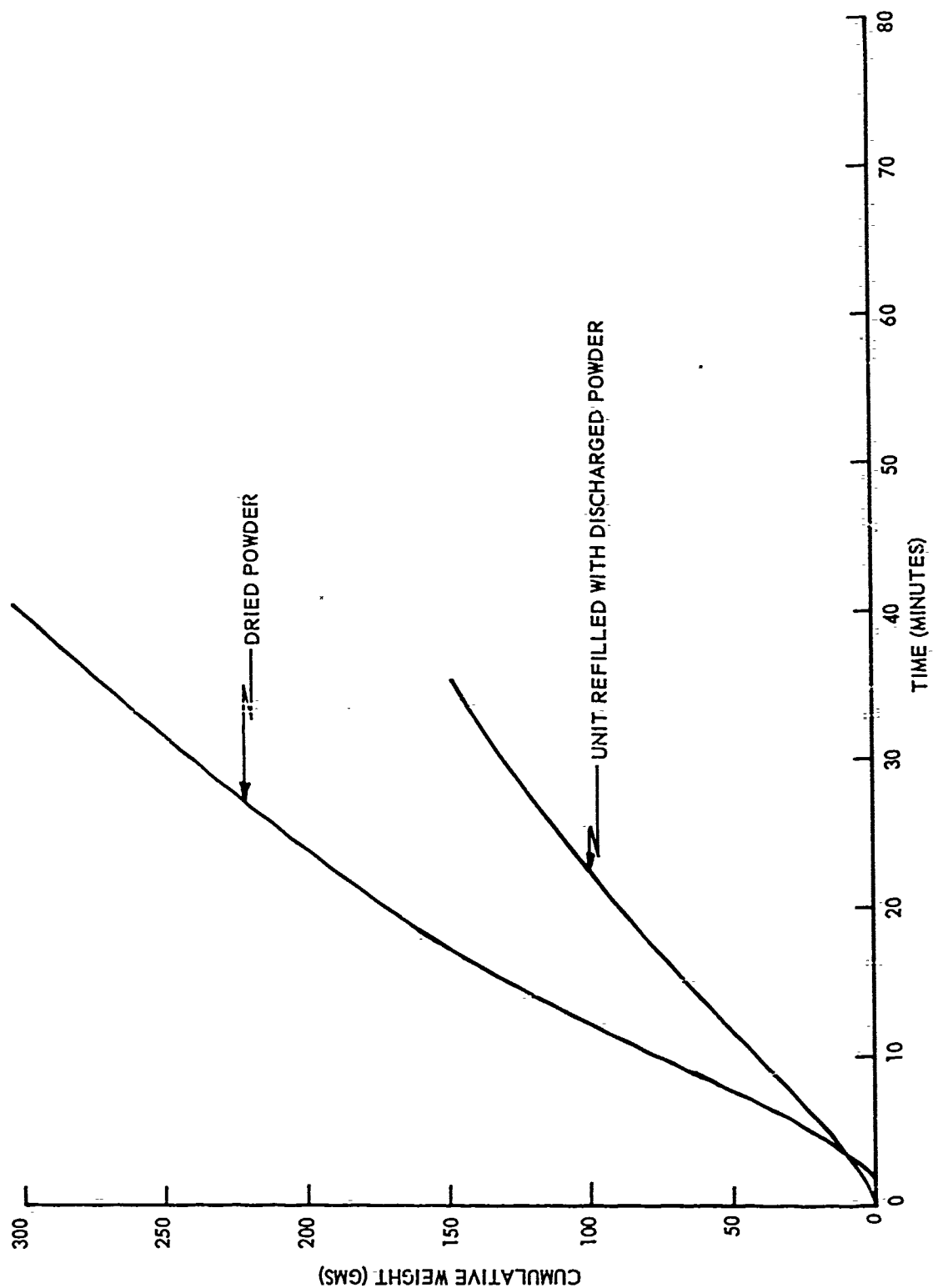


Figure 15. Weight Vs. Time of Silica Fed from the Syntrol Vibratory Feeder.

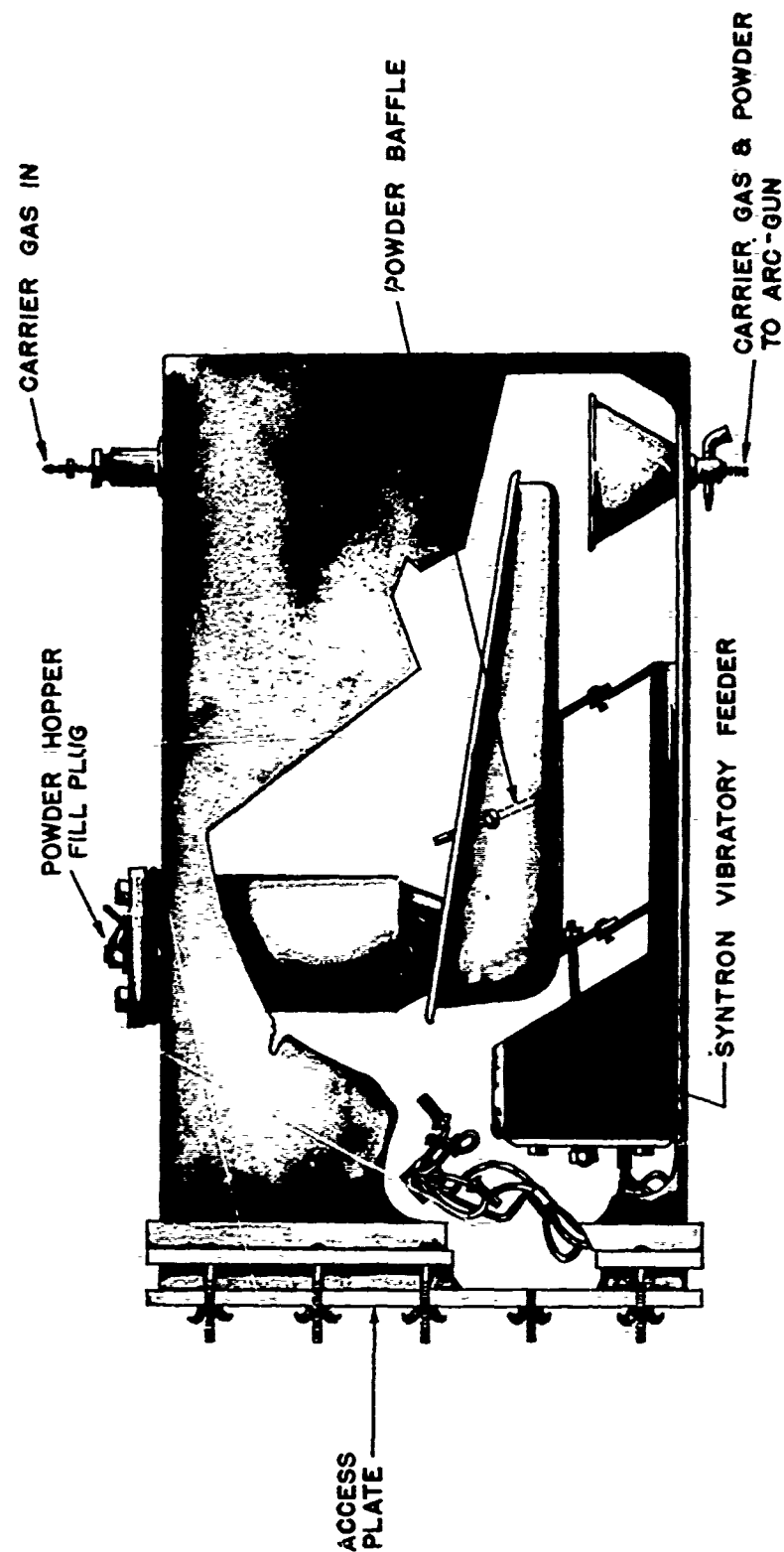


Figure 16. Drawing of Modified Syntron Vibratory Powder Feed Unit.

as a function of time at 28, 29, and 31 volts using -325 mesh tungsten powder is shown in Figure 17. Note the absence of the initial curvature in these curves over previous curves.

Comparison of the feed curves for tungsten in Figures 13 and 17 would seem to indicate the insertion of the baffle in the trough caused the feed rate to be reduced considerably at the same applied voltage. This, however, is not the case. The decreased feed rate was due to an adjustment of the vibrator mechanism which lowered the intensity of vibration at the same voltage. This was done to lower the feed rate of the unit to a range usable for spray work without lowering the applied voltage below a point where the vibrator would stop.

An attempt was made to feed -10 micron stabilized zirconia powder which had been dried for 4 hours at 300° F. A satisfactory feed rate could not be attained because the powder would not flow from the hopper to the trough. An external vibrator was mounted on the powder hopper to attempt inducement of a more effective powder flow into the trough. This had no effect. It was then thought that the failure of the powder to flow was the result of incomplete drying of the powder at 300° F.

A simple device for vacuum drying of the powder at 500° F was constructed and an observation port added to the feed unit enclosure to observe the powder flow mechanisms. The vacuum dried -10 micron zirconia would flow satisfactorily from the hopper to the trough and down the trough into the funnel. However, frequent bridging over of the powder in the funnel prevented the acquisition of any feed curves using this powder. Modification of the trough and funnel to eliminate this problem is presently underway.

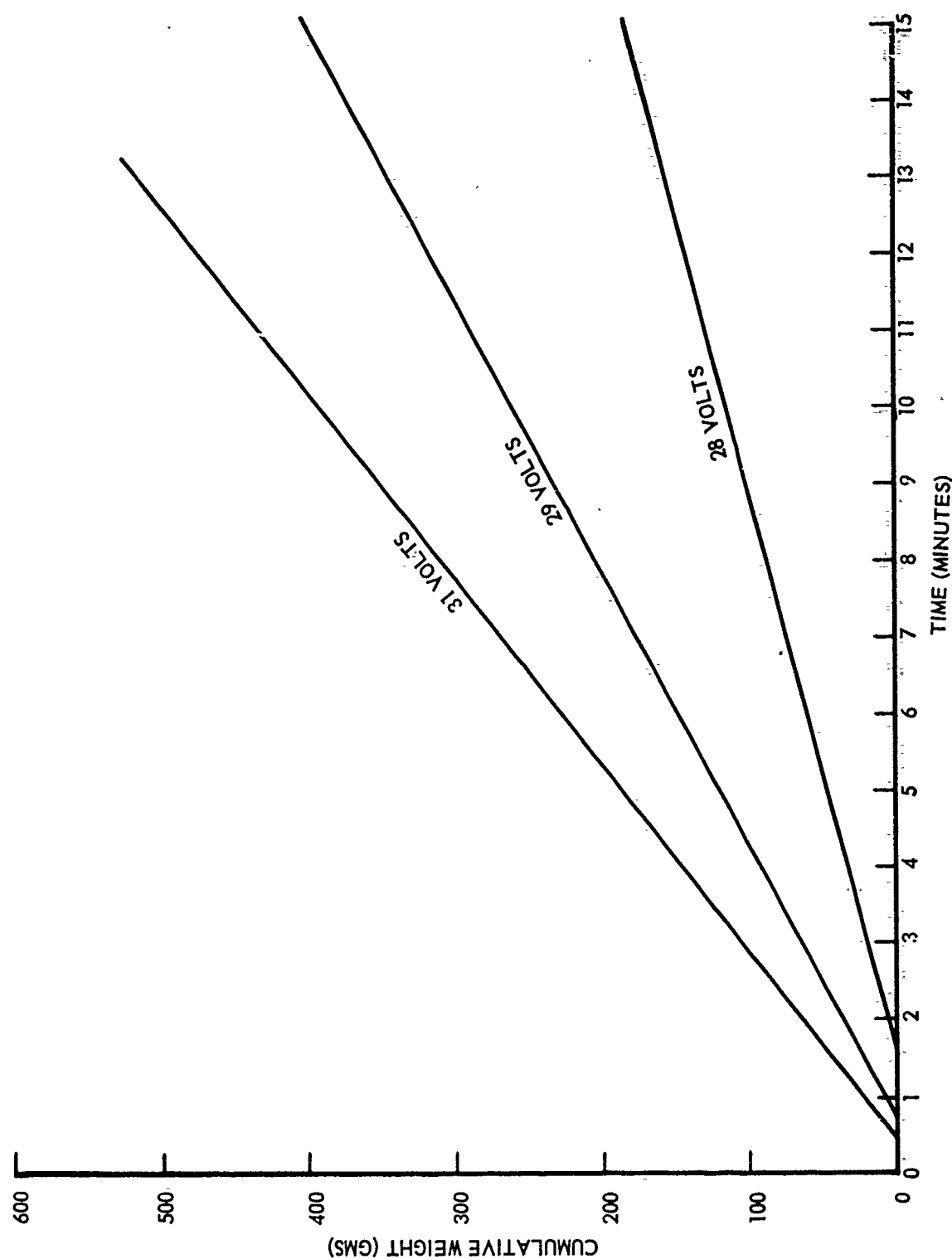


Figure 17. Weight Vs. Time of Tungsten Fed from the Syntrol Vibratory Feed Unit at 28, 29, and 31 Volts.

#### IV. PROPERTIES OF POWDERS AND ARC-SPRAYED SHAPES

##### A. Powders

The powders used in the investigations described in this paper are described briefly in Table I. The comments listed under the heading "treatment" in this table include all treatments which have been tried to date. In all cases the last treatment listed for each powder is the one which appears to be the most satisfactory.

##### B. Tensile and Density Data

Table II lists tensile strength, density data, and spray parameters on arc-sprayed circular cylinders of  $-240 +325$  mesh alumina. Average values are not given because of the erratic nature of the data.

It is felt that the erratic nature of the tensile data may be the result of testing samples which contain imperfections that are not readily seen with the eye. As a result two groups are being re-sprayed and closer control of the specimens made before testing using non-destructive optical techniques in conjunction with organic dye techniques.

##### C. Nozzle Insert Shells

Several arc-sprayed tungsten insert shells have been evaluated in a small solid fuel test motor in efforts directed towards development of a suitable ceramic castable back-up material for uncooled rocket nozzles. None of the materials tested were as satisfactory as graphite for this application.

The fabrication of nozzle throat inserts from several different materials is considered to be an important development in the effort to fabricate ceramic materials by arc-spray techniques for use in this area. The arc-spray equipment settings used to fabricate these throat inserts are given in Table III.

TABLE I

## BRIEF DESCRIPTIONS OF ARC SPRAYED POWDERS

<u>Powder</u>	<u>Source</u>	<u>Designation</u>	<u>Approx. Purity (%)</u>	<u>Major Impurity (%)</u>	<u>Particle Size As Received (Mesh)</u>	<u>Treatments</u>	<u>Comments</u>
Tungsten	Kennametal Inc.	MP-10	99	Fe + C 0.25 ea.	-100	None or Dry Screen to -200 mesh depending on lot or Dry Ball Mill and screen to -44 $\mu$	Good Coating, very good deposit efficiency when sprayed as received - better coating when milled but oxidizes unless care is taken to keep substrate cool.
Zirconia	Zirconium Corp. of America	Zircoa	93	CaO-5	-200 +20 $\mu$	Dry Ball Mill to -44 $\mu$	Good, high density coatings - fair deposit efficiency
Alumina	American Graded Sand Co.	White $Al_2O_3$ #240	-	-	-240	Washing tower -65 +44 $\mu$ and -44 $\mu$	Low deposit efficiency - hydrogen must be used
Chromium Carbide	Electro-Metallurgical Co.	Type M	-	-	-10	Dry Ball Mill + Dry Screen to -44 $\mu$	Low deposit efficiency-good strong coating with metallic appearance

TABLE II

TENSILE STRENGTH, DENSITY, AND PER CENT THEORETICAL DENSITY  
OF ARC-SPRAYED ALUMINA

<u>Sample No.</u>	<u>Indicated Tensile Strength (psi)</u>	<u>Bulk Density (gms/cc)</u>	<u>Per Cent Theoretical Density</u>
23-4-A	6250	3.5	88.2
23-4-B	300	3.4	85.7
23-5-B	3520	3.5	88.2
23-6-B	2020	3.3	83.1
23-1-C	10390	3.4	85.6
23-2-C	9450	3.6	90.7

Arc-Spray Equipment Parameters: 600 amps, 55 volts, 110 SCFH A,  
10 SCFH H<sub>2</sub>, 1/4 turn on powder feed  
hopper, stand-off distance 3 inches

Chamber Parameters: Chamber pressure 76 cm Hg, mandrel  
rotation 488 RPM, mandrel traverse  
32.5 passes per minute (P/M) on  
2-1/2 inch spray length

23-2-A	430	3.6	90.7
23-5-A	3810	3.3	83.1
23-6-A	600	3.5	88.2
23-1-B	5100	3.5	88.2
23-2-B	2060	3.4	85.6
23-3-B	7640	3.6	90.7

Arc-Spray Equipment Parameters: Same as Group 1

Chamber Parameters: Chamber pressure 76 cm Hg, mandrel  
rotation 380 RPM, mandrel traverse  
36 P/M on 2-1/2 inch spray length

TABLE II (Continued)

TENSILE STRENGTH, DENSITY, AND PER CENT THEORETICAL DENSITY  
OF ARC-SPRAYED ALUMINA

<u>Sample No.</u>	<u>Indicated Tensile Strength (psi)</u>	<u>Bulk Density (gms/cc)</u>	<u>Per Cent Theoretical Density</u>
23-3-C	9670	3.6	90.7
23-4-C	7890	3.5	88.2
23-5-C	6990	3.6	90.7
23-1-D	770	3.5	88.2
23-2-D	10230	3.5	88.2

Arc-Spray Equipment Parameters: Same as Group 1

Chamber Parameters: Chamber pressure 76 cm Hg, mandrel  
rotation 288 RPM, mandrel traverse  
40 P/M on 2-1/2 inch spray length

23-1-E	4020	3.4	85.6
23-2-E	6500	3.5	88.2
23-3-E	2430	3.5	88.2
23-4-E	2690	3.6	90.7
23-5-E	2540	3.5	88.2
23-6-E	2690	3.2	80.6

Arc-Spray Equipment Parameters: Same as Group 1

Chamber Parameters: Chamber pressure 72 cm Hg, mandrel  
rotation 488 RPM, mandrel traverse  
32.5 P/M on 2-1/2 inch spray length



TABLE II (Continued)

TENSILE STRENGTH, DENSITY, AND PER CENT THEORETICAL DENSITY  
OF ARC-SPRAYED ALUMINA

<u>Sample No.</u>	<u>Indicated Tensile Strength (psi)</u>	<u>Bulk Density (gms/cc)</u>	<u>Per Cent Theoretical Density</u>
23-1-H	12470	3.6	90.7
23-2-H	10930	3.4	85.6
23-3-H	7460	3.5	88.2
23-4-H	12570	3.5	88.2
23-5-H	12500	3.5	88.2
23-6-H	3740	3.6	90.7

Arc-Spray Equipment Parameters: Same as Group 1

Chamber Parameters: Chamber pressure 88 cm Hg, mandrel  
rotation 488 RPM, mandrel traverse  
32.5 P/M on 2-1/2 inch spray length

TABLE III

ARC-SPRAY EQUIPMENT PARAMETERS  
USED IN FABRICATING NOZZLE THROAT INSERTS

Number	Powder	Volts	Amperes	Plasma Gas		Powder Carrier		Hopper Opening (Turns)	Standoff Distance (Inches)	Remarks
				(SCFH A)	(SCFH H <sub>2</sub> )	Gas	(SCFH A)			
1264-22-1	Tungsten	65	600	110	15	6		3/4	2	Insert ob- tained
1264-24-1	Alumina	65	600	110	15	7		1/2	5	Cracked on mandrel
1264-26-1	Alumina	65	600	110	15	7		1/2	2	Insert obtained Extremely porous
1264-27-1	Chrome Carbide	65	600	110	15	10		1/8	3-4	Insert obtained
1264-331-1	Tungsten- zirconia	62	600	110	10	10 10		1/4 1/2	2	Insert obtained

These studies were primarily exploratory in nature with the exception of the tungsten insert. This throat insert was fabricated for evaluation in the solid fuel rocket motor to ascertain the validity of testing arc-sprayed materials by this method.

The chrome carbide and alumina powders were selected to determine the releasing characteristics of these classes of compounds from the oxidized inconel surface. In both cases releasing was excellent.

The tungsten-zirconia insert was fabricated to obtain information on the mixing characteristics of two dissimilar powders and also to observe the consistency of deposition of the two materials. Visual observation of the effluent powder mixture indicated that segregation of the components of the mixture was not occurring as was the case when the individual powders were injected into different ports on the arc-gun nozzle. The photomicrograph (Figure 6) taken from the end surface of the throat insert showed gradation of the two powders on deposition. This indicates closer control of powder flow rates will be necessary before studies of two-components systems are made.

A PRELIMINARY INVESTIGATION OF THE THERMAL HISTORY  
OF POWDER PARTICLES DURING PLASMA SPRAYING

S. J. GRISAFFE

Lewis Research Center, NASA  
Cleveland, Ohio

Prepared for fifth meeting of  
Refractory Composites Working Group  
August 8-10, 1961, Dallas, Texas

A PRELIMINARY INVESTIGATION OF THE THERMAL HISTORY  
OF POWDER PARTICLES DURING PLASMA SPRAYING

S. J. Grisaffe, Materials Research Engineer

Lewis Research Center, NASA

Cleveland, Ohio

Many industrial concerns and research laboratories have plasma spray equipment, and have presented much data concerning the optimum parameters for operating these devices. An area that needs greater attention is the thermal history of the powder particles from hopper to substrate. Generally, this history consists of a particle at room temperature being introduced into an intensely hot plasma, heated, and then carried downstream by the flowing gases to some point where it collides with a substrate and is deposited. As a particle moves downstream, it loses heat by radiation and conduction and its temperature decreases as shown schematically in Fig. 1. A quantitative description of this temperature distribution does not exist. Therefore, a preliminary study was made to determine the temperature of the particles in the plasma stream and the temperature at which the particles deposit. This type of information would be very practical; for, by knowing these values, a more complete insight into the spray process would be possible. For example, data on the deposition temperature, coupled with the thermal expansion coefficients of the substrate and of the deposit, would permit much better control of residual stress in a coating or fabricated body.

To examine a typical plasma spray operation, 14.5-micron average particle diameter, stabilized zirconium dioxide of the type supplied

commercially was chosen. Spraying was done with a rigidly mounted Thermal Dynamics F-40 torch with a No. 1 spray nozzle operated at 450 amps, 60 volts using 80 cu ft/hr  $N_2$  and 10 cu ft/hr  $H_2$  as the plasma gas and 10 cu ft/hr  $N_2$  as the carrier gas. The powder flow rate was 1.25 lb/hr but no apparent change in the readings occurred when the flow rate was varied from 0.8 to 2.5 lb/hr. A Shawmeter was used to get approximate values of the particle temperature in the stream as a function of the distance from the spray nozzle. Two parallel shields painted with flat optical black paint were positioned on each side of the spray. One shield had a 1/4-in.-diameter sight hole in it, and this shield was movable so that the area of highest particle density could be observed at varying distances from the spray nozzle. (A distance restriction existed, for very close to the nozzle the Shawmeter went off-scale because of the intensely bright cone of the plasma flame.) The results are shown in Fig. 2; these values are only rough approximations, since the exact values of the emissivity of this material should be known at both wavelengths used by the Shawmeter. This instrument reads true temperatures only when the ratio of these emissivities is unity; at other ratios a correction must be made. Another possible source of error is the particles themselves, which act as reflectors and reflect light from the intense plasma arc in the nozzle.

For determining the deposition temperatures, the following procedure was employed.

Platinum - platinum-13 percent rhodium thermocouples were fabricated with oversized junctions, and these junctions were then hammered into thin flat disks approximately 0.010-in. thick and of 1/8-in.

diameter. This provided a recording surface of very low heat capacity. Then, a profile of temperature vs. distance from the nozzle was made in the plasma gases without any spray. A second profile was made by spraying the zirconium dioxide on the thermocouple at varying distances from the nozzle. In this case it was not possible to determine temperatures at a point closer than  $4\frac{1}{2}$  in. from the nozzle, since the upper limit of the thermocouples is 3000° F. The data are shown in Fig. 2. At each position the thermocouple was sprayed until a temperature maximum was reached - usually after about 0.5 sec. The coating was removed from the thermocouple after each spraying.

On comparing the data in Fig. 2, it is seen that the temperatures measured optically are much higher than those measured by thermocouple. This is due to the uncertainties in the spectral emissivities and possibly to the reflection of the plasma arc by the particles.

In conclusion, this work is the result of a preliminary investigation, and the measurements are not the most refined. However, it is felt that this type of approach needs attention and that further refinements would be of definite value for a more complete understanding of the plasma spray process.

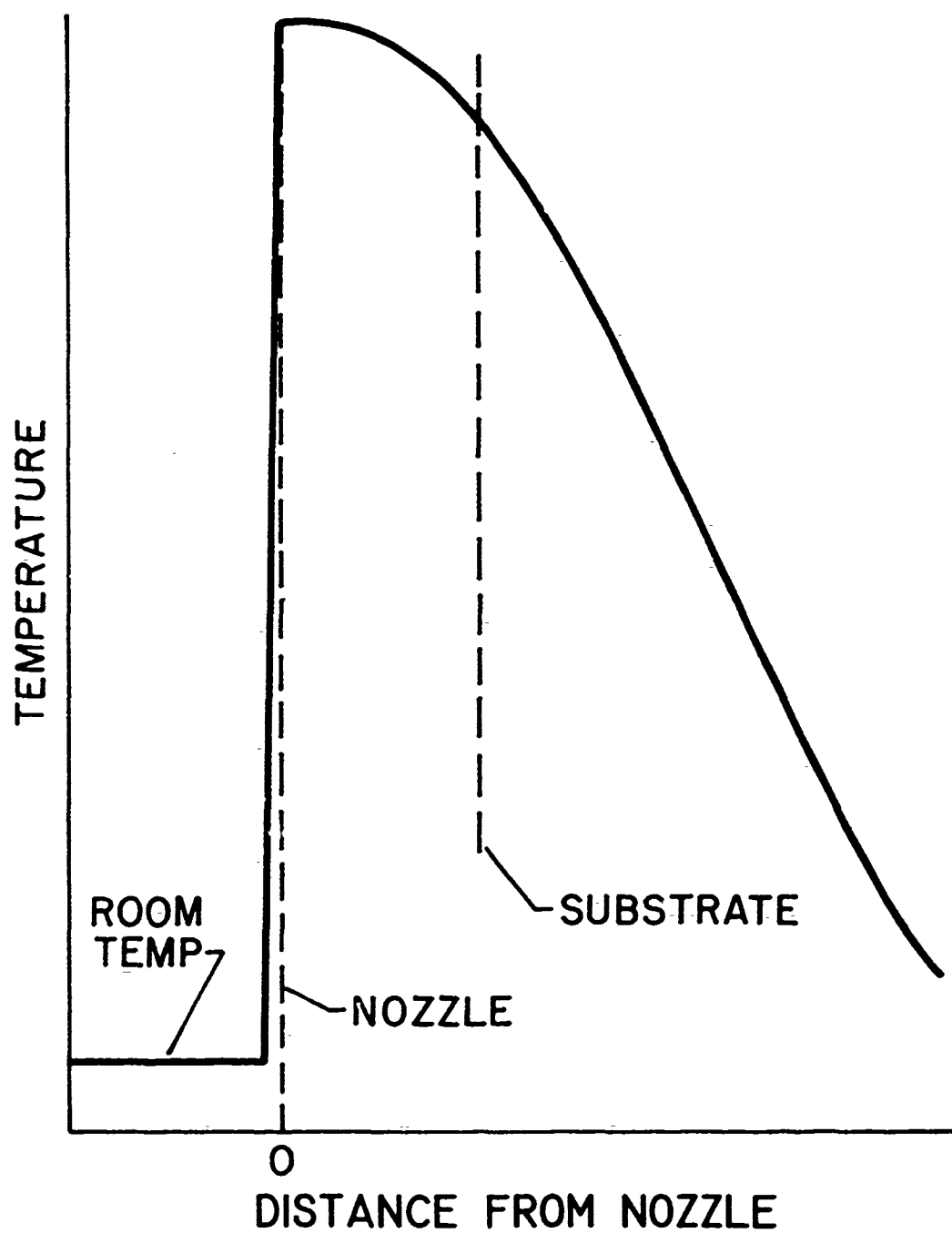


Fig. 1. - Schematic description of particle temperature as a function of distance from the spray nozzle.



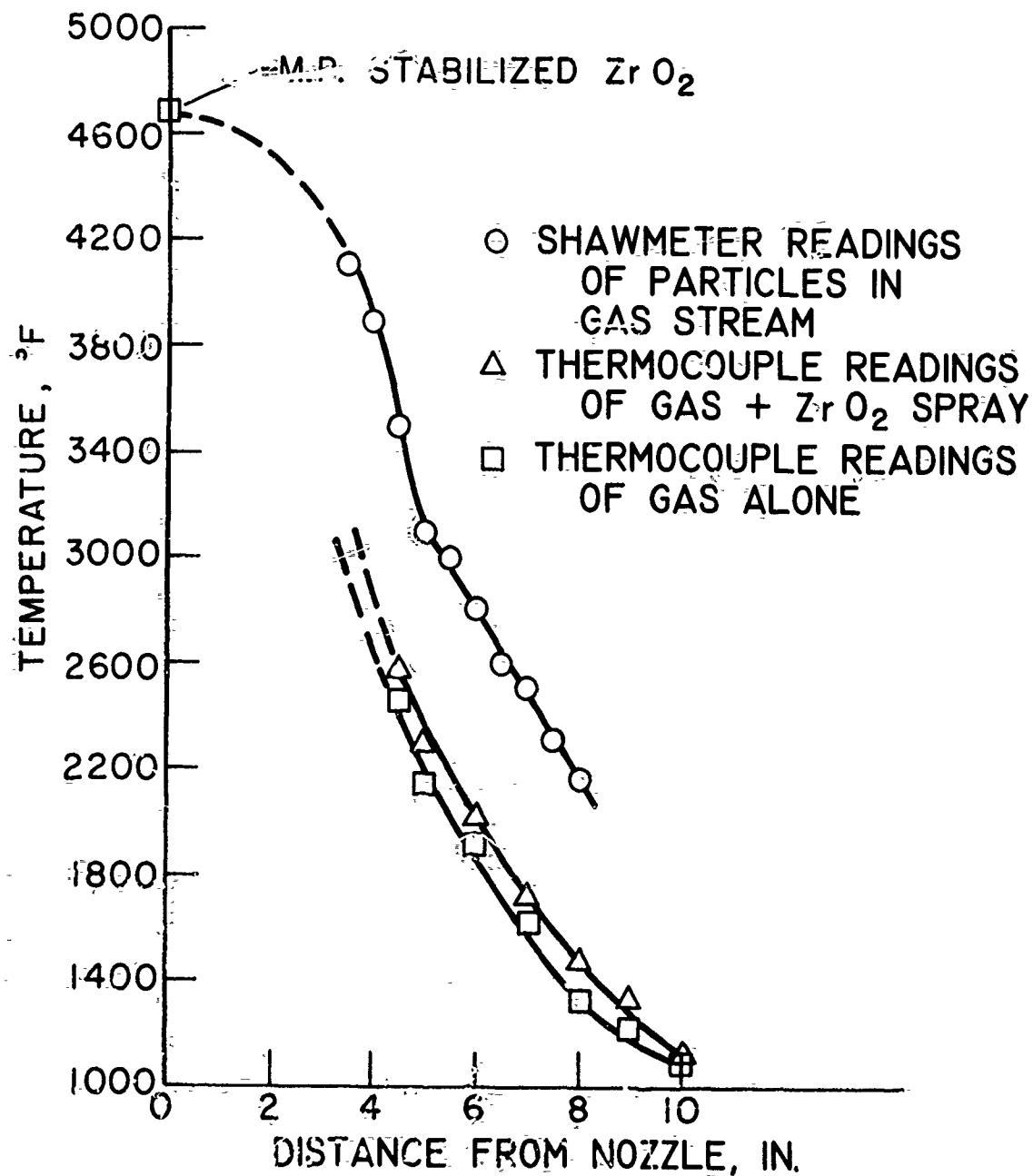


Fig. 2. - Temperature versus distance from spray nozzle.

DEVELOPMENT AND EVALUATION OF A ROKHIDE-  
PLASMA SYSTEM

R. L. JOHNSON  
W. M. WHEILDON

Norton Company  
Worcester, Massachusetts

By: W. M. Wheildon  
Norton Company, Worcester, Mass.

A major field of interest of the Norton Company is ceramic coatings. Three areas: processes, materials, and equipment, have remained under investigation and constant pursuit since the creation of the ROKIDE process of flame-spraying by atomization directly from solid bodies in the form of rods.

Of particular interest has been combustion heat sources for melting of the flame-spray materials and efficient equipment for handling. A variety of gases and finely powdered metals have been considered as fuels but none have proved as practical as oxyacetylene until recent practical development of the arc plasma flame torch.

Because of the possible advantages of plasma as a heat source for the ROKIDE process, the Norton Company is blending talents with the Plasmadyne Corporation of Santa Ana, California, in a co-operative program to create a ROKIDE plasma gun expected to effect economies of coating application and produce superior or different wanted characteristics. This paper is to deal briefly with this program, some of the approaches, and the current status from which perhaps a few predictions can be made.

One of the first questions that arose when consideration was given to developing a plasma system to spray ROKIDE rods of  $3/16"$  to  $3/8"$  diameter was the nominal power rating that would be required. The following is data calculated for the present oxyacetylene ROKIDE guns in current use.

Rod Diameter	Rod Feed Rate (inches/minute)		Flame Temperature	Heating Rate Btu/Hr.	Equivalent KW Rating
	A	Z			
$1/8"$	6-8	5.5-6	5,500	46,500	13.7
$3/16$	6-8	4.5-5	5,500	55,200	16.2
$1/4$	6-8	3.5-4	5,500	72,600	21.3

An extrapolation of these data indicates that an equivalent of approximately 35 KW would be required to handle a  $3/8"$  diameter rod. Thus it appears that considering the worst situations with respect to efficiency and heat transfer that 75KW could be expected to allow increased rates of coating deposition with  $3/8"$  diameter rods.

With this background information indicating the possibility of constructing a ROKIDE-Plasma gun of superior output within reasonable power limits, it was decided to proceed with development of a 40 KW unit for handling 3/16" zirconia rods to determine equipment and operating parameters.

Figure 1 shows schematically the first trial approach with the rod feed at right angles to the flame. This system melts satisfactorily but feed control presents too much of a problem. Obviously, if we feed too fast we strike the other side of the nozzle and upset the whole flame configuration. Particle shape and control is poor as the rod is not burning or melting to a point.

Figure 2 shows schematically the second trial approach with the rod feed directly through the rear negative electrode. This system interferes with the arc control and makes handling much too critical. In fact, there was practically no control of arc emission from this annular electrode and concentration of the arc in one spot eventually destroyed the electrode by fusion.

Figure 3 represents the system employed in the third trial. Actually three separate arcs were used in a single chamber, only two of which are shown schematically. The rod feed does not interfere with the electrodes but does pass directly through the arcs. This system appears to have too much concentrated heat on the rod. Apparently, the rod should be kept clear of the arc proper and be involved with the flame only. Attempts to spray with this unit resulted in vaporizing considerable of the rod while ejecting very large particles at intervals similar in size to B-B shot.

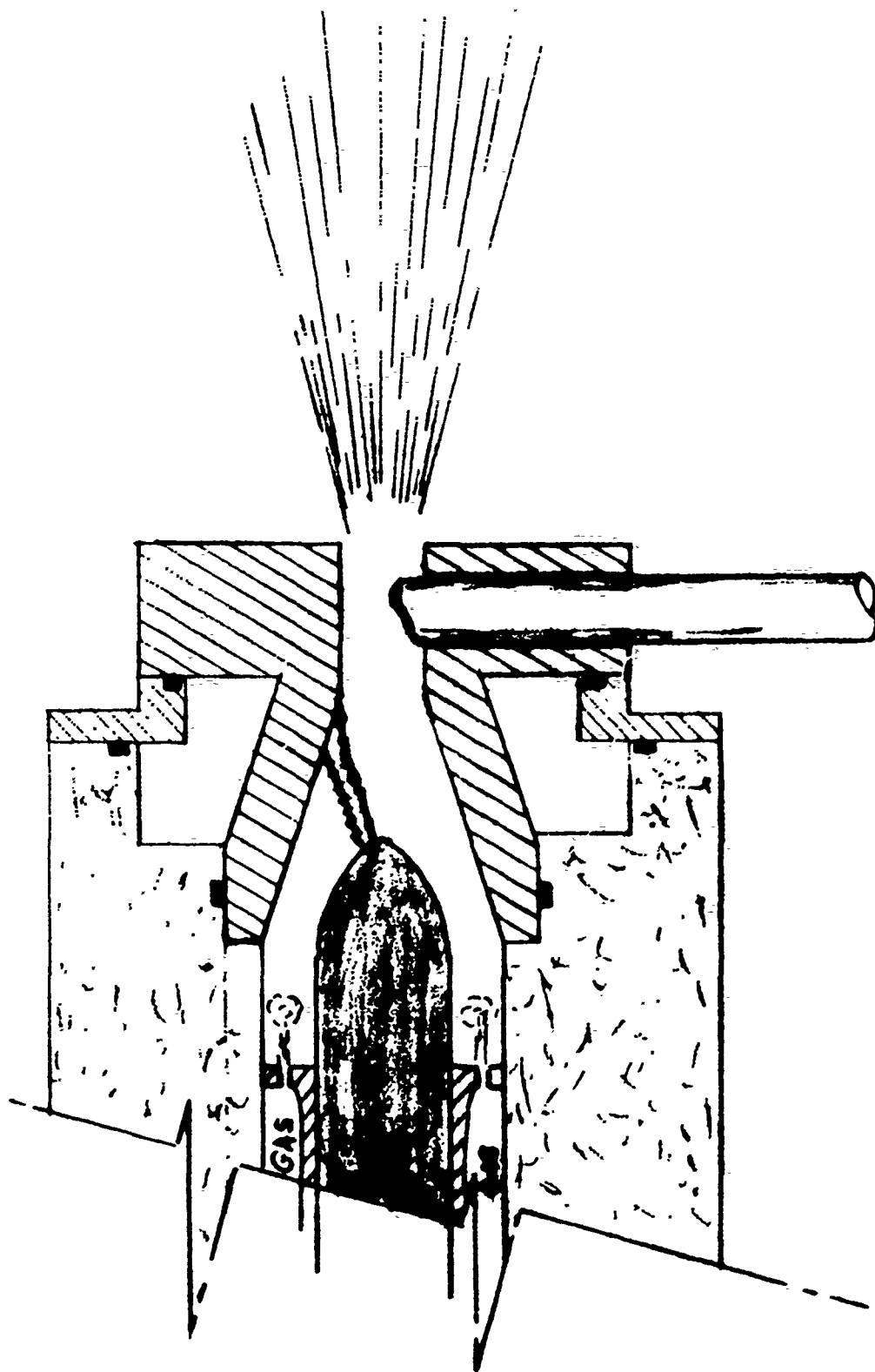
Figure 4 indicates the current design system which has produced spray patterns and coatings in the range of our interest. This is a versatile unit based on knowledge gained from the earlier units. Arcs are adjustable and rod enters into the flame only.

This system will now be employed to make a systematic investigation of operating and coating parameters prior to developing the final gun design.

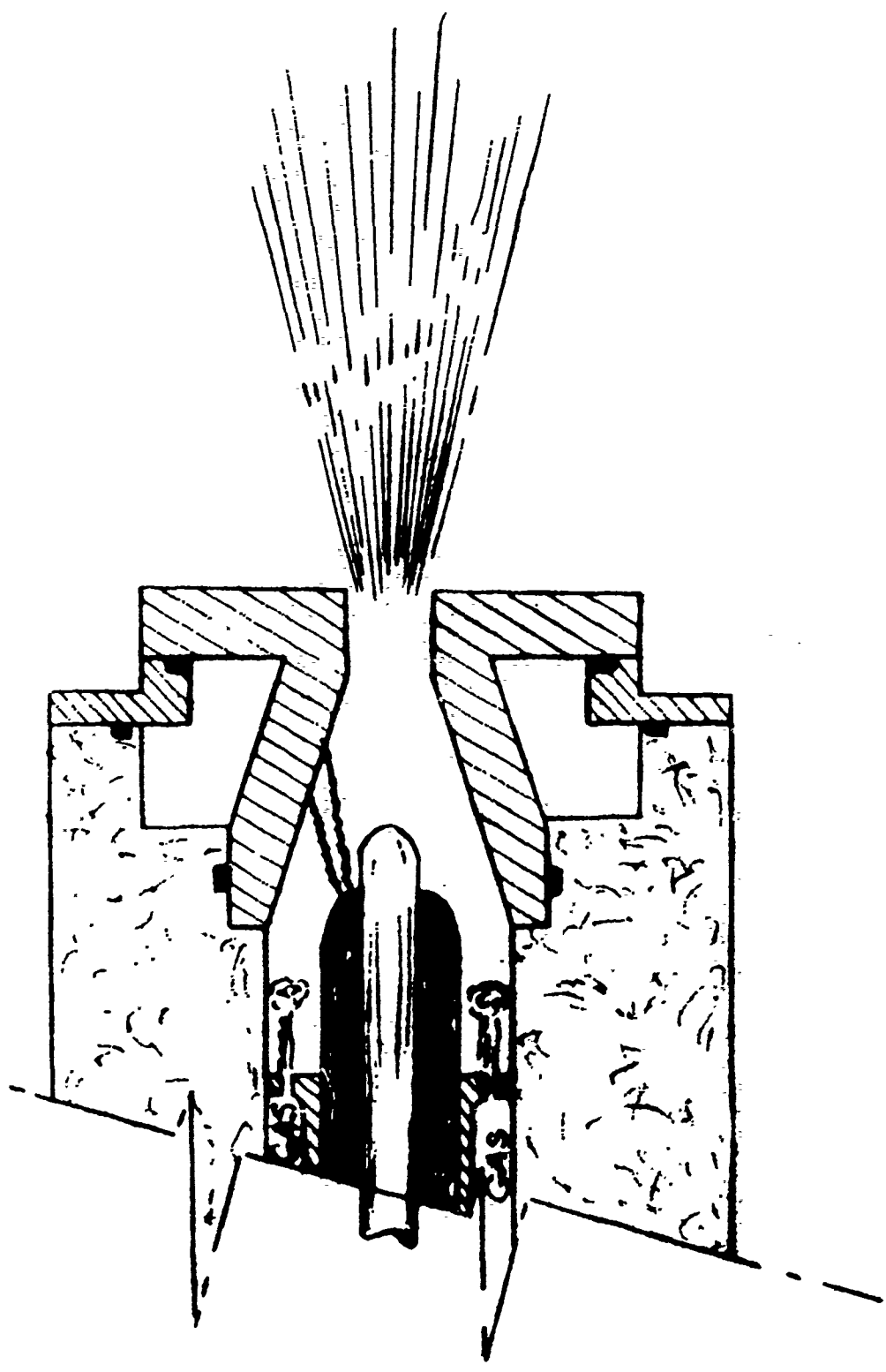
Based on the work done thus far, however, a couple of predictions can be made.

1. 40 KW appears to be sufficient power to handle up to and including 1/4" zirconia rods.
2. Rates of coating laydown are expected to be at least twice that achieved by present combustion equipment.

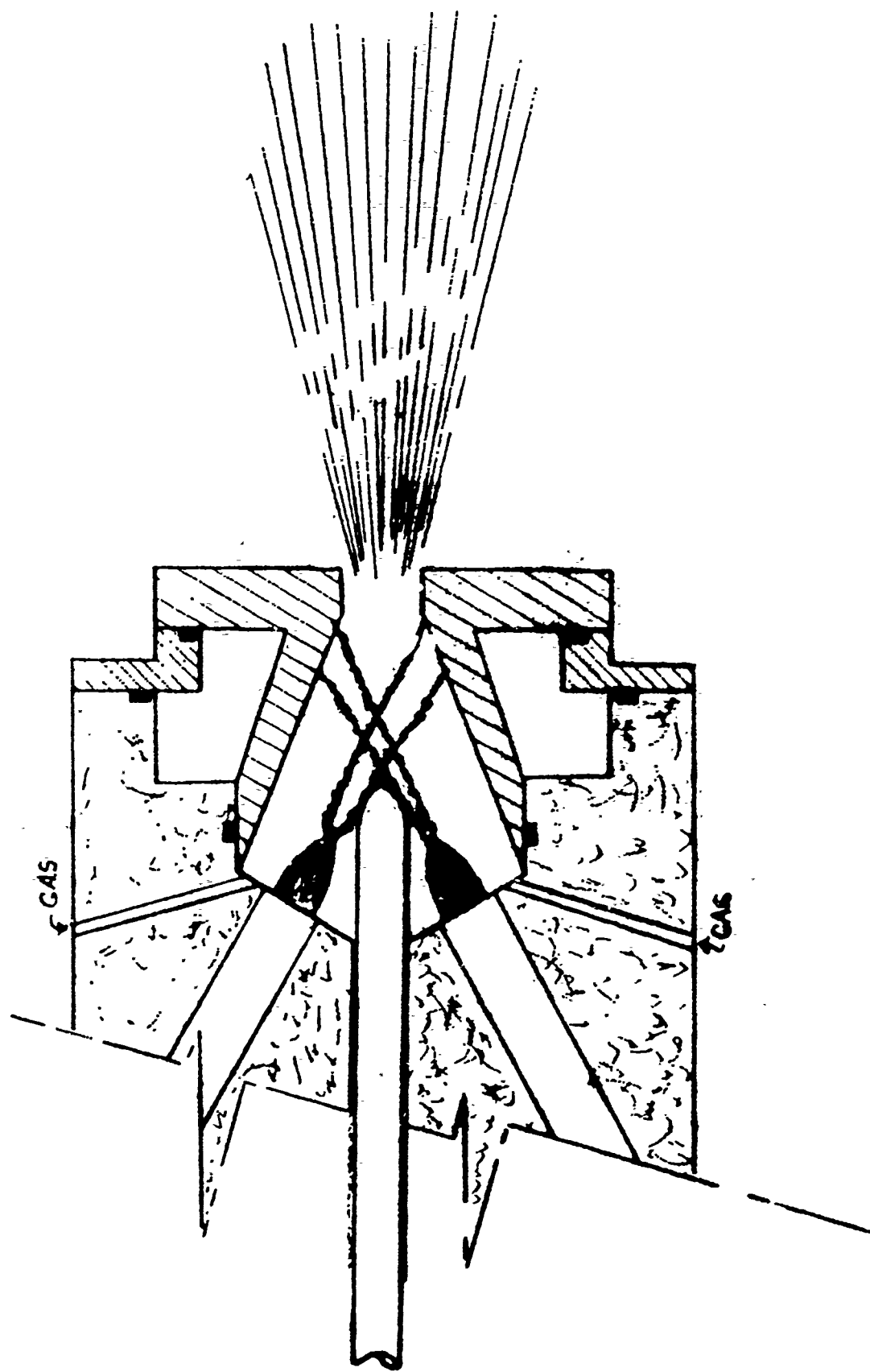
All the actual hardware designs have been developed by the Plasmadyne engineers and their representative can best go into the technical aspects of the equipment handling and performance.



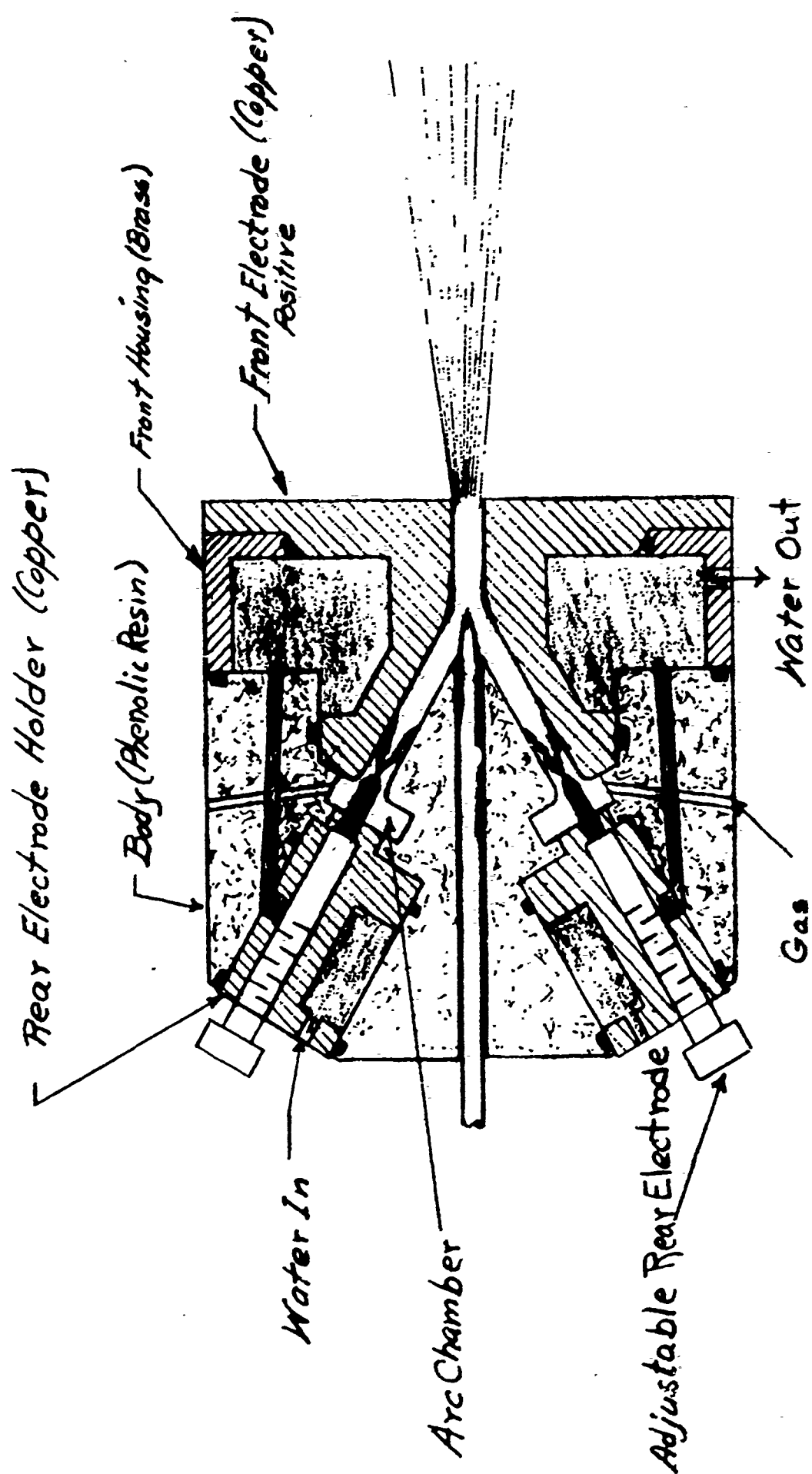
1st Trial



2nd Trial



3rd Trial



4th Trial



TRANSITION TEMPERATURE AND FLEXURAL STRENGTH  
OF TUNGSTEN MATERIALS

V. L. HILL

Allison Division  
Indianapolis, Indiana

# TRANSITION TEMPERATURE AND FLEXURAL STRENGTH OF TUNGSTEN MATERIALS

## FOREWORD:

This presentation is intended as an addendum to the paper, "Tungsten Fabrication by Arc Spraying", which was published in the July 1961 issue of the Journal of Metals. Recent work at Allison has been concerned with the evaluation of the mechanical properties of Allison plasma arc sprayed and sintered tungsten (Plasma-Tung C\*) as compared to forged tungsten and also to cold pressed and sintered tungsten. The measurement of transition temperatures and flexural strengths, which was completed by means of bend tests, has been the primary consideration.

## MATERIALS:

1. Plasma-Tung C - fully recrystallized
2. Commercial cold pressed and sintered tungsten - fully recrystallized
3. Forged commercial cold pressed and sintered tungsten with the following degrees of recrystallization:
  - a. 0%
  - b. 25%
  - c. 100%

All samples were taken from massive pieces of hardware (>25 pounds).

The grain sizes of the materials used are shown in Table I.

## BEND TEST PROCEDURE:

Transition temperature and flexural strengths were determined employing a simple beam bend test. The test specimens were 0.700 inch wide by 0.052 inch thick and were deflected over a span of one inch by a 0.0625 inch radius mandrel.

\*Plasma-Tung C is the designated name for Allison produced plasma arc sprayed and sintered tungsten.

In the basic test, the outer fiber strain rate was 0.008 in./in./min. which corresponds to a deflection rate of 0.025 in./min. All tests were conducted either to failure or to a maximum deflection of 0.250 inch. Load and deflection were automatically plotted and failure was determined by a rapid drop in load. Test samples were considered to have reached their transition temperature when they exceeded a calculated value of 5% outer fiber strain. This value corresponds to a deflection of approximately 0.150 inch in this test.

#### TRANSITION TEMPERATURES:

The transition temperatures of the various materials are shown in Figure 1. Forged non-recrystallized tungsten has a transition temperature of approximately 300°F, while the 25% recrystallized material exhibits a transition temperature of 475°F. Plasma-Tung C has a transition temperature of approximately 600°F whereas forged 100% recrystallized and cold pressed and sintered materials have transition temperatures above 800°F.

The effect of strain rate on the apparent transition temperature of 25% recrystallized forged tungsten is shown in Figure 2. The higher strain rate results in an apparent transition temperature approximately 175°F higher than the standard test rate.

#### FLEXURAL STRENGTH:

Flexural strength, or outer fiber stress at failure, of the tungsten materials was obtained from the load plot obtained in the bend test. Outer fiber stress at failure,  $\sigma_m$ , may be calculated employing the beam formula:

$$\sigma_m = \frac{1.5S}{WT^2} P \quad \text{where:}$$

P = Load at failure

T = Thickness of the specimen

W = Width of the specimen

S = Span

A plot of maximum outer fiber stress,  $\sigma_m$ , vs. temperature for the tungsten materials is shown in Figure 3. Notice that the strength values at 600 °F are about equal for those materials which exhibit transition temperatures below 800 °F.

Figure 4 indicates the effect of strain rate on the maximum outer fiber stress at various temperatures. This plot reveals that strain rate has little effect on the strength for 25% recrystallized forged material, despite the fact that the apparent transition temperature is increased as shown by Figure 2.

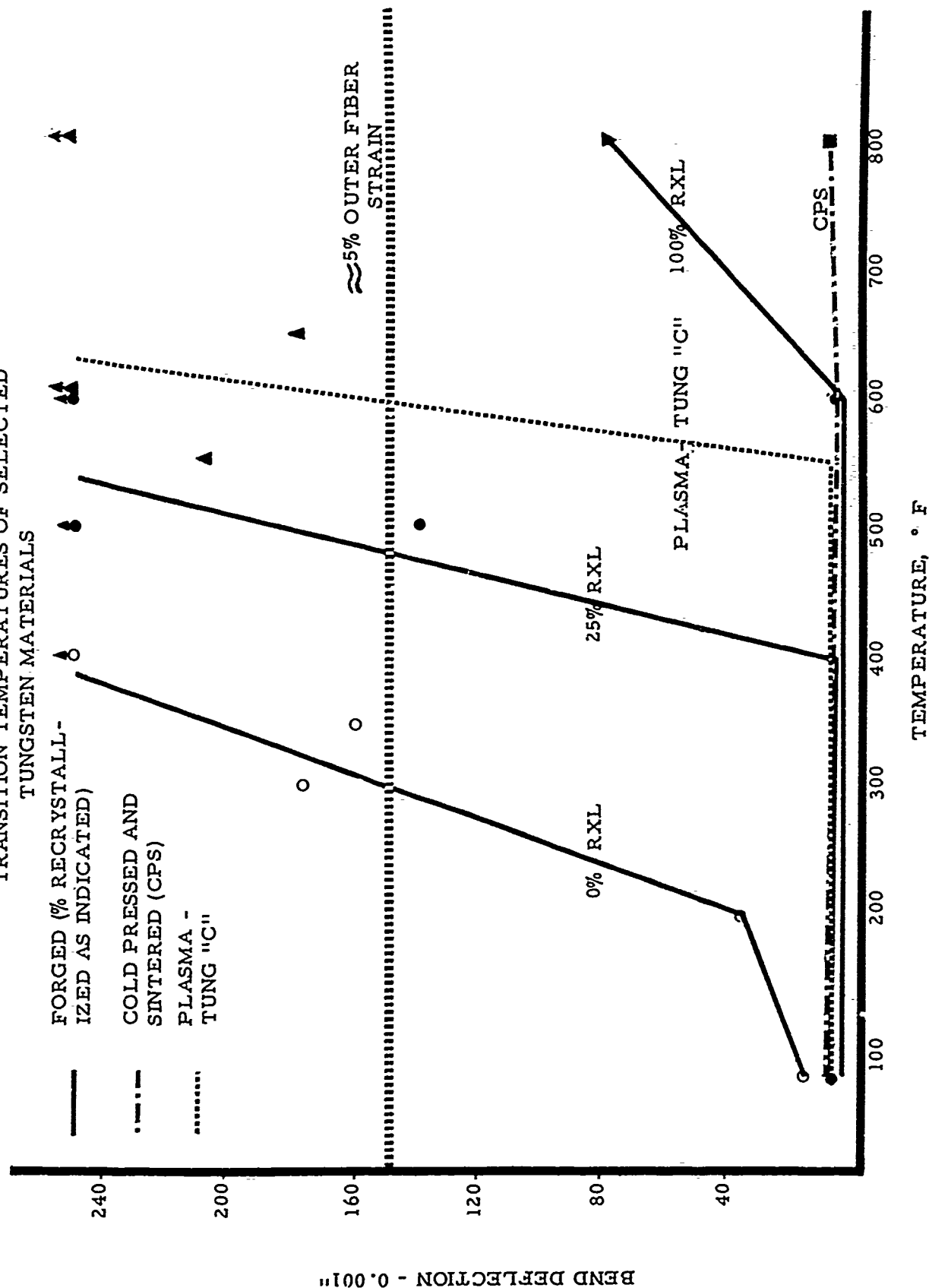
TABLE I

GRAIN SIZE\* OF RECRYSTALLIZED TUNGSTEN MATERIALS

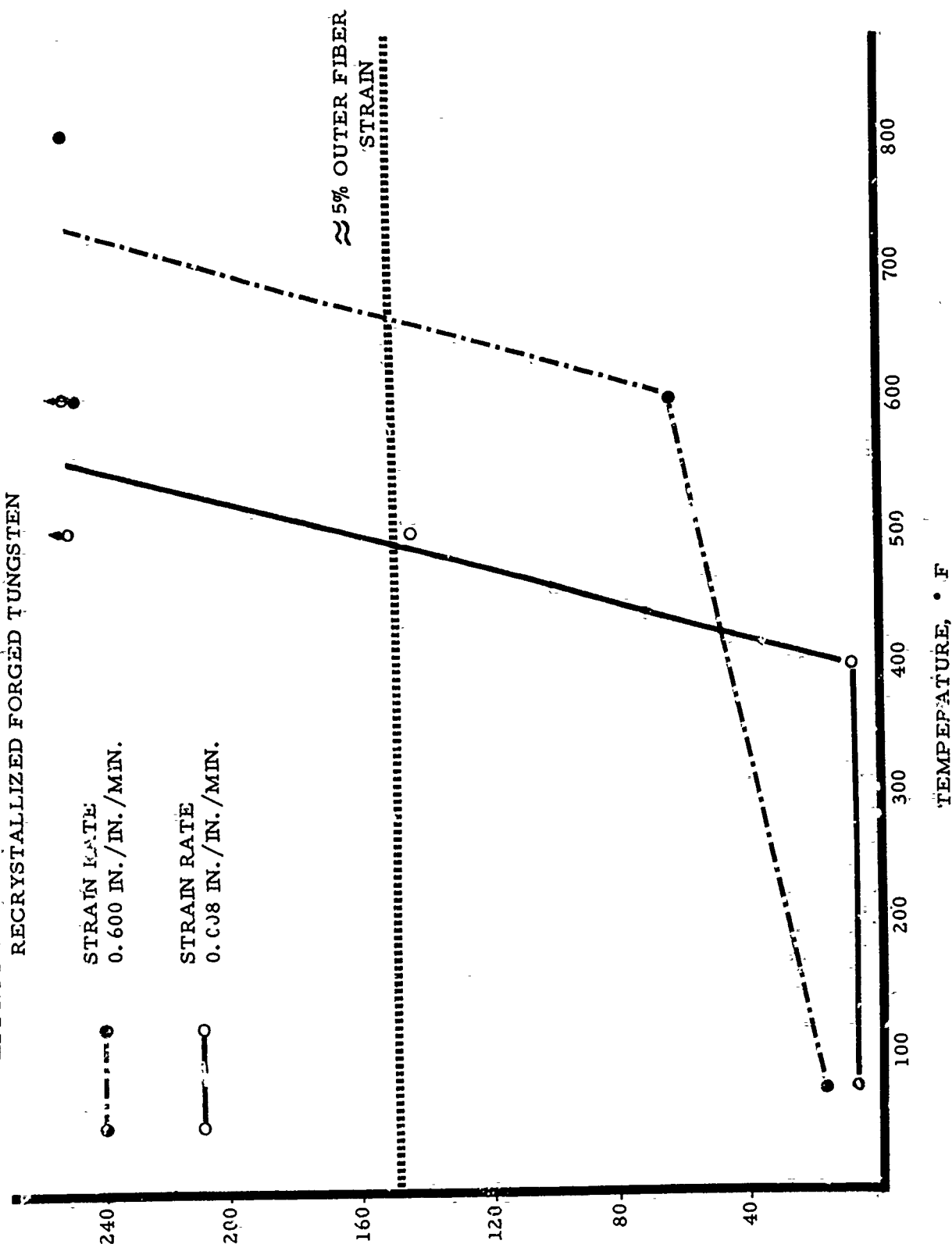
<u>Material</u>	<u>Average Grain Diameter - mm</u>	<u>Grains/sq. mm</u>
Forged	0.250	16
Cold pressed and Sintered	0.015	4,400
Plasma-Tung "C"	0.018 - 0.030	2,800 - 1,100

\*per ASTM E112-58T

# TRANSITION TEMPERATURES OF SELECTED TUNGSTEN MATERIALS



# EFFECT OF STRAIN RATE ON TRANSITION TEMPERATURE OF 25% RECRYSTALLIZED FORGED TUNGSTEN



BEND DEFLECTION TO FAILURE - 0.001 INCH

# MAXIMUM OUTER FIBER STRESS IN BENDING OF SELECTED TUNGSTEN MATERIALS

- FORGED - 0% RXL
- FORGED -25% RXL
- FORGED -100% RXL
- PLASMA-TUNG "C"
- CPS

- 
- 
- ▼
- 
- 

FORGED 0% RXL

25% RXL

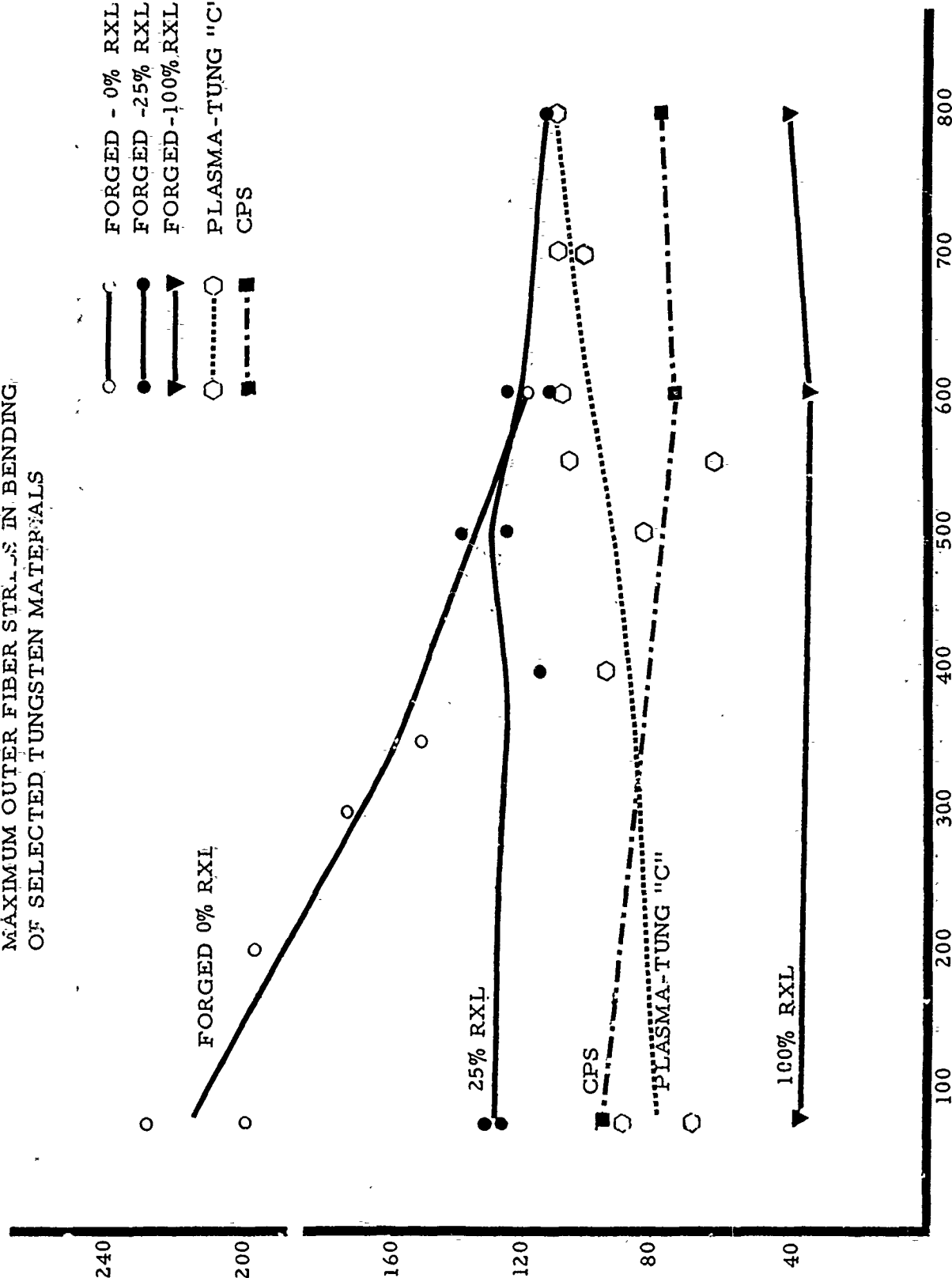
CPS

PLASMA-TUNG "C"

100% RXL

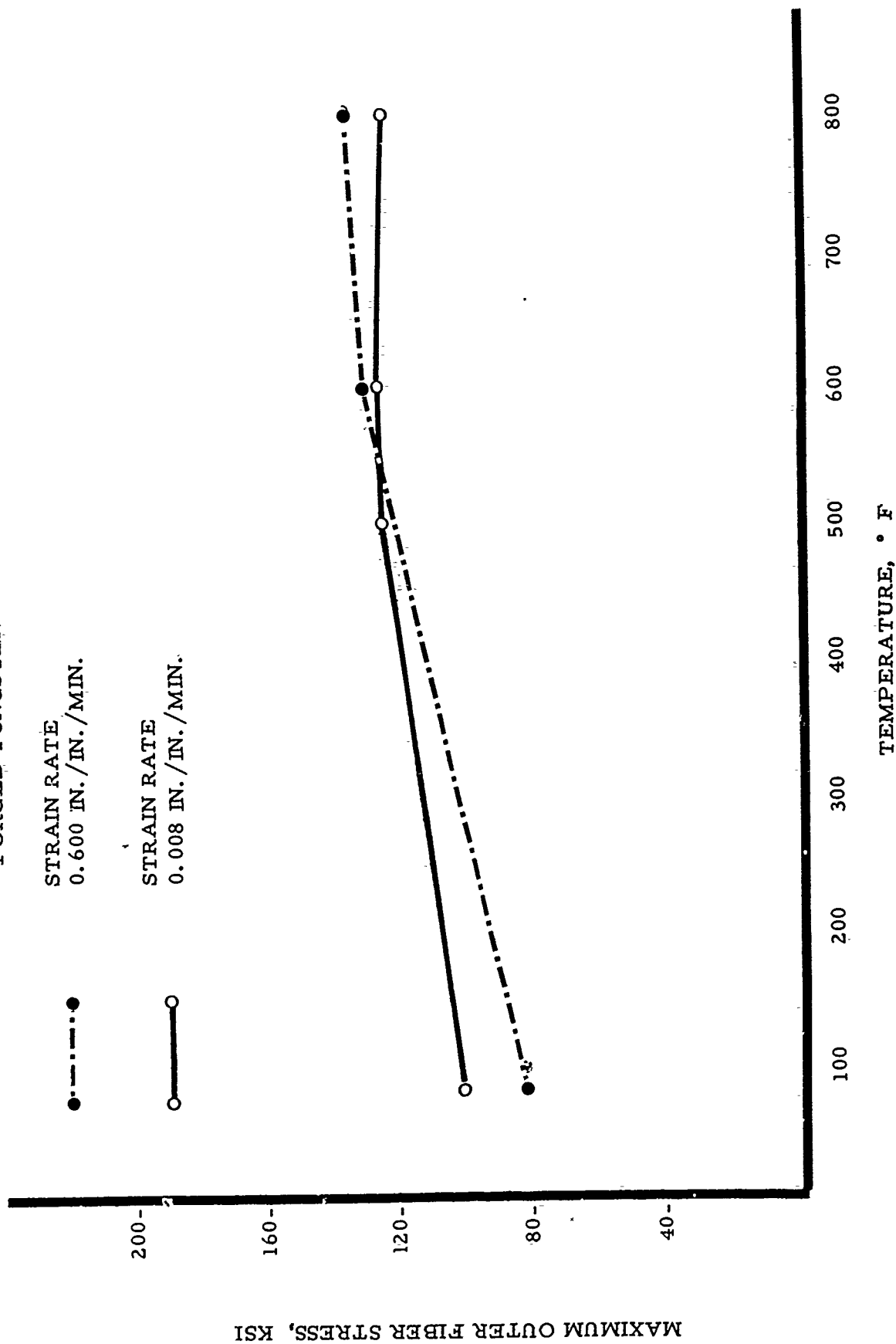
MAXIMUM OUTER FIBER STRESS, KSI

TEMPERATURE, ° F





EFFECT OF STRAIN RATE ON MAXIMUM OUTER  
FIBER STRESS OF 25% RECRYSTALLIZED  
FORGED TUNGSTEN



ACTIVITIES IN THE FIELD  
OF REFRACTORY COMPOSITES

ROGER A. LONG

Narmco Industries, Inc.  
San Diego 11, California

NARMCO ACTIVITIES IN THE FIELD  
OF REFRACTORY COMPOSITES

By

Roger A. Long, Manager  
Refractories Research Department

NARMCO INDUSTRIES, INC.  
RESEARCH AND DEVELOPMENT DIVISION  
TELECOMPUTING CORPORATION  
3540 Aero Court  
San Diego 11, California

The Narmco Refractories Research Department is continuing the investigations described in last year's meeting with two programs dealing with the bonding of tungsten sheet metal to graphite and the coating and bonding of ceramic glasses to refractory metals.

Recent Narmco publications have shown the capability of solid phase diffusion bonding of tungsten to graphite where the tungsten is carbide coated and the graphite carbide coated, and the bond results due to the diffusion of the carbides under heat and contact pressure. This is applicable to systems in which the carbides have complete or partial solid solubility with each other. Examples are: WC-TaC; WC-HfC; TaC-HfC;  $\text{Mo}_2\text{C}$ -WC, etc. The carbides are coated on the surfaces either by plasma spraying or by metal coating techniques and subsequent controlled carborization.

Recent work has indicated that certain carbides like tungsten, zirconium and titanium, in a carbonicous furnace atmosphere, will fuse to the graphite substrate at about  $4800^\circ\text{T}$ . This has the benefit of penetrating the graphite pores and thus increasing the bond strength. The same has been shown with a mixture of

refractory metal borides, carbides and silicides. Attempts to obtain higher remelt temperatures to at least 6000°F have been initiated.

Another approach has been to utilize the exothermic behavior which results upon formation of some of the refractory metal carbides and borides and silicides as a possible heat source implement.

The second investigative program on ceramic adhesive bonding of refractory metals, has resulted in the publication of a final report under Air Force Contract No. 33(616)-7196. This project was a feasibility study as to utilizing ceramic adhesives to join together the refractory metals, tungsten, tantalum, molybdenum and columbium. Ceramic adhesives were developed consisting either of mixtures of alumina, silica, titania or zirconia or based on tantalum pentoxide base system. Room temperature and 1900°F tensile shear strengths of approximately 1000 psi were obtained. There was considerable evidence that the coatings were oxidation protective, although this characteristic was not examined in detail. The coatings were applied at temperatures in excess of 3000°F in a vacuum atmosphere. Base metal oxide additions up to 30% by weight were necessary to achieve strong bonding on all refractory metals.

In addition to the above programs, Narmco is examining metal and oxide reactions with various substrates at temperatures ranging up to 7000°F, by use of arc image equipment and developing new ceramic composites based on liquid phase sintering of the refractory oxides for uses at temperatures in excess of 2300°F. These latter materials seem to have considerable resistance to thermal shock, although the flexural strengths are not high.

REFRACTORY COATING RESEARCH AND DEVELOPMENT

MILTON LEVY

Watertown Arsenal Laboratories

Watertown, Massachusetts

REFRACTORY COATING RESEARCH AND DEVELOPMENT  
WATERTOWN ARSENAL LABORATORIES

---

By: Milton Levy

The increased demand for a highly mobile military force requires that weapons must be developed with a minimum of constructional weight and a maximum of strength. The Ordnance Corps of the U. S. Army has been actively searching for materials which will reduce the weight of components of Ordnance weapons systems. A new titanium alloy containing about 6%Al-6%V-2%Sn was developed which on a strength-weight basis, is equivalent to steel at a yield strength of 325,000 psi. This alloy was developed under a materials research program at Watertown Arsenal Laboratories, aimed at improving materials for Ordnance applications. There are commercially available a variety of proven alpha-beta type titanium alloys with yield strengths varying from 130,000-170,000 psi. Steels having yield strengths varying from 230,000-300,000 psi would be comparable to these titanium alloys on a strength-weight basis. However, the severe galling tendency of titanium is a decided handicap to its usefulness. Until means of eliminating or reducing galling has been found, the use of titanium shapes in many applications will be limited in spite of its several very favorable properties. Electroless nickel-phosphorous plate was investigated as an anti-galling coating for titanium alloys. In the electroless-plating technique a nickel salt is reduced on the surface being coated by sodium hypophosphite. A modified National Bureau of Standards alkaline plating bath was used to deposit the electroless-nickel

phosphorous on several titanium alloys. The adhesion of the deposit to substrate was poor. Subsequent heat treatments were studied with the objective of achieving improved adhesion through diffusion bonding with a minimum of beta transformation. Plate adhesion and diffusion-zone structure were assessed by metallographic and x-ray-diffraction techniques. A significant improvement in adhesion was achieved by interdiffusion during the elevated-temperature treatment for a series of temperatures between 1250°F and 1550°F in vacuo. X-ray-diffraction data indicated the formation of a solid solution of 85%Ni-15%Ti(+ 3%),  $TiNi_3$ ,  $TiNiO_3$ ,  $Ti_2Ni$  as diffusion-zone layers. The abrasion resistance of the electroless-nickel deposits, both diffused and undiffused, were determined with a Taber Abraser and compared with untreated titanium. The undiffused nickel plate offered no improvement over bare titanium. However, the diffusion-bonding treatment increased the abrasion resistance of titanium between two- and seven-fold, depending upon the temperature of the treatment. In general, the abrasion resistance increased with increasing temperature between 1250°F and 1550°F, the latter temperature yielding optimum results. The wear characteristics of the deposits were determined with a modified MacMillan apparatus. The diffusion-bonding treatment afforded the titanium wear resistance comparable to, or better than steel under the test conditions. Watertown Arsenal Laboratories have developed a test weapon suitable for determining the erosion resistance of promising coating materials, using easily machined, inexpensive, replaceable, short length smooth bore or rifled inserts. This erosion-gage weapon can produce maximum internal pressures of 35,000 psi when standard caliber .60 ball ammunition loaded with double base powder is used.

An uncoated titanium alloy insert was tested in the erosion-gage weapon. At the end of 50 rounds at half charge (about 10,000 psi), little or no erosion was observed. An additional round at full charge (about 25,000 psi) was fired, resulting in a heavily eroded area at the breech end. A similar titanium alloy insert, electroless-nickel plated and diffusion bonded was tested under the same conditions. No erosion was produced. Electrodeposited coatings of hard metals, such as chromium or nickel, afford an inexpensive means of obtaining a wear- and erosion-resistant surface. Difficulties have been experienced in the application of adherent deposits to titanium. The success achieved in the deposition of electroless nickel to titanium and the formation of a diffusion-bonded zone of nickel-rich material, suggests its use as an intermediate for the subsequent deposition of chromium. This is currently being investigated.

A broad knowledge of the properties of graphite and other high-temperature materials is essential for the design of the hot components of missiles and space craft. Oxidation data concerning pyrolytic graphite, a specialized polycrystalline form of graphite has not been reported previously in the literature. The oxidation of pyrolytic graphite was studied as a function of time and temperature. Pyrolytic graphite does not oxidize as rapidly as commercial graphite at temperatures below 1450°F, but approaches that of commercial graphite at 1550°F (slide). Oxidation of pyrolytic graphite proceeds preferentially in the c-direction (perpendicular to the plane of deposition) and may be explained by the available energy associated with the strained condition of the crystal lattice and the exposed edges of the layer planes. The break in



the Arrhenius plot for pyrolytic graphite occurring at 1550°F may be attributed to the change in control mechanism from chemical reactivity to diffusion control, or to the difference between the ambient furnace temperature and the specimen-surface temperature, or to both. An activation energy of 37,180 cal/mol was calculated for a commercial graphite. The activation energy calculated for pyrolytic graphite was 23,350 cal/mol. The lower activation energy for pyrolytic graphite is associated with a lower reaction rate. This anomalous behavior is attributed to its lower porosity since a less porous material exposes a smaller surface area for molecular collisions. The technique used permitted the continuous and automatic recording of oxidation rate (slide) and may be readily applied to studies of coating materials.

Thermal shock and drop data were obtained for various ceramic oxide and hard-metal flame-sprayed deposits on several substrate materials (Table I).

TABLE I

THERMAL SHOCK AND DROP DATA

<u>Base Metal</u>	<u>Coating</u>	<u>Thermal Shock (Cycles)</u>	<u>Thermal Drop °F</u>
Mild Steel	Metco 201 (ZrO <sub>2</sub> )	3	543
Mild Steel	Metco 101 (Al <sub>2</sub> O <sub>3</sub> )	4	385
Mild Steel	Rokide "Z" (ZrO <sub>2</sub> )	6	515
Mild Steel	Rokide "A" (Al <sub>2</sub> O <sub>3</sub> )	6	475
Mild Steel	Rokide "C" (Cr <sub>2</sub> O <sub>3</sub> )	4	315
Mild Steel	Metco 32C (WC)	No spalling 50 cycles	440
Titanium	Metco 201	4	505
Titanium	Metco 101	6	287

TABLE I (Continued)

THERMAL SHOCK AND DROP DATA

<u>Base Metal</u>	<u>Coating</u>	<u>Thermal Shock (Cycles)</u>	<u>Thermal Drop °F</u>
Titanium	Rokide "Z"	12	520
Titanium	Rokide "A"	16	250
Titanium	Rokide "C"	16	420
Titanium	Metco 32C	No spalling 50 cycles	800
Stainless Steel	Metco 201	3	680
Stainless Steel	Metco 101	3	325
Stainless Steel	Rokide "Z"	9	615
Stainless Steel	Rokide "A"	2	435
Stainless Steel	Rokide "C"	5	170
Stainless Steel	Metco 32C	No spalling 50 cycles	275
Aluminum	Metco 201	1	660
Aluminum	Metco 101	2	500
Aluminum	Rokide "Z"	1	715
Aluminum	Rokide "A"	1	655
Aluminum	Rokide "C"	1	1380
Aluminum	Metco 32C	1	---
Copper	Metco 201	No spalling after 50	785
Copper	Metco 101	No spalling after 50	415
Copper	Rokide "Z"	No spalling after 50	620
Copper	Rokide "A"	No spalling after 50	300
Copper	Rokide "C"	31	400
Copper	Metco 32C	No spalling after 50	335

An oxy-acetylene flame is impinged on a coated test panel. At the end of the heating cycle (1 minute) the flame is shut off and cold air blasted on the heated zone (1 minute). Alternate periods of heating and cooling are used until the coating fails by cracking or spalling. Temperature measurements of the front and back surfaces are made with an optical pyrometer and rayotube sighted on the flamed zone and by a thermocouple attached to the rear of the specimen on the flamed area. The difference in apparent surface temperature is obtained by subtracting the rayotube reading from the optical pyrometer reading. To equate the difference in apparent temperature to emissivity, curves were derived from emissivity correction data for each of the instruments. The emissivity value is then applied to the emissivity correction curves for the optical pyrometer to obtain the true front surface temperature. The thermal drop value is obtained by subtracting the thermocouple reading from the true front surface temperature. Of the coatings investigated, tungsten carbide exhibited the greater thermal shock resistance for all substrate materials. Zirconium oxide was superior to aluminum oxide and chromic oxide. On a copper substrate, all coatings exhibited good thermal shock characteristics. In general, the largest thermal drop value was calculated for zirconium oxide.

To evaluate the adhesion of flame-sprayed ceramic coatings to several substrate materials, an apparatus and test method developed by the Porcelain Enamel Institute Research Associateship at National Bureau of Standards was used. This consists of deforming the specimen far beyond the yield point of the metal and then sampling the deformed area with a cluster of 169 needle-like

probes to determine the relative amounts of bare metal and attached coating present. Adhesion of the following coatings to medium steel, stainless steel, copper, aluminum and titanium was determined: Metco 101 ( $\text{Al}_2\text{O}_3$ ), Metco 201 ( $\text{ZrO}_2$ ), Rokide "A" ( $\text{Al}_2\text{O}_3$ ), Rokide "Z" ( $\text{ZrO}_2$ ), Rokide "C" ( $\text{Cr}_2\text{O}_3$ ). Values are contained in Table II.

TABLE II  
ADHESION INDICES (%)

<u>Coating</u>	<u>Intermediate</u>	<u>Substrate</u>		<u>Copper</u>	<u>Titanium</u>	<u>Aluminum</u>
		<u>Mild Steel</u>	<u>Stainless Steel</u>			
Rokide "A"	None	94.8	90.1	83.9	96.4	78.2
Rokide "A"	Ni-Cr	98.6	99.1	99.2	99.1	99.4
Rokide "A"	Mo	99.0	95.5	96.4	99.1	99.7
Metco 101	None	88.6	73.6	94.8	93.7	95.7
Metco 101	Ni-Cr	95.4	99.0	94.5	96.7	97.1
Metco 101	Mo	96.1	93.1	98.5	95.0	98.4
Rokide "Z"	None	97.2	97.6	96.4	96.4	98.4
Rokide "Z"	Ni-Cr	98.0	99.1	99.5	99.3	99.9
Rokide "Z"	Mo	96.2	97.2	99.8	99.5	94.2
Metco 201	None	97.2	99.3	91.6	98.4	97.3
Metco 201	Ni-Cr	98.9	99.4	98.7	99.8	94.7
Metco 201	Mo	95.0	95.0	97.2	98.6	99.6
Rokide "C"	None	83.4	58.4	77.7	94.3	99.6
Rokide "C"	Ni-Cr	97.3	95.8	99.9	89.7	99.6
Rokide "C"	Mo	94.9	89.6	99.2	89.0	99.8

It was found that subsequent to deformation loose particles of ceramic remained. Consequently, the effect of dropping the specimen and soaking in water for removal of loose particles was investigated. The adhesion in each case was appreciably decreased, indicative of the effectiveness of the procedure. Generally, the  $ZrO_2$  coatings, rod and powder, exhibited the best adhesion to the substrates, with the exception of aluminum, where Rokide "C" afforded the best adhesion. In all other cases the adhesion of Rokide "C" was poorest. The literature indicates that a nickel-chromium intermediate coating enhances the bond between ceramic and metal substrate. The above-mentioned coatings were applied over a nickel-chromium alloy intermediate to corroborate this information. In almost every instance the intermediate Ni-Cr alloy effectively improved the bond between ceramic and substrate. The greatest effect was realized with Rokide "C" on stainless steel, where adhesion was increased from 58.4% to 95.8%. Similar results were achieved with a molybdenum intermediate coating.

A solid-propellant Variable Parameter Rocket Engine was developed for the simple, rapid, and economical screening and firing testing of promising rocket nozzle materials over a wide range of conditions which are representative of both current and future Ordnance rocket engines (slide). The operating range and parameters of this test engine are as follows:

Chamber pressure:	Up to 1600 psi
Burning time:	Up to 100 seconds
Nozzle throat diameter:	0.2" to 1.0"
Propellant:	Selected solid propellant charges

A series of tests to determine reproducibility of results are being conducted with graphite nozzles. Subsequently, other nozzle materials will be evaluated for erosion resistance as the engine parameters are varied.

Currently, plasma-sprayed coatings of refractory metals, oxides and hard metals are being evaluated for adhesion to basis materials, resistance to thermal shock and oxidation. Metal phases will be introduced into ceramics to increase thermal conductivity and ductility. When subjected to thermal shock, higher conductivity means lower temperature gradients to thermal stress gradients. Metals and ceramics will be combined and plasma sprayed. These coatings will be examined for cermet formation using metallographic and x-ray-diffraction techniques. Adhesion, thermal shock and oxidation resistance will be determined. Promising coating systems will be further evaluated, using the Watertown Arsenal Laboratories Variable Parameter Rocket Engine. In addition, solid-body structures of various refractory materials will be prepared by the plasma-spray process for subsequent determination of porosity, structure and phase distribution, impact resistance and transverse bend strengths. The data obtained with these materials will be compared with that reported for like materials prepared by conventional powder-metallurgical techniques.

PERTINENT ACTIVITIES IN REFRACTORY COMPOSITES

J. L. BLITON  
S. W. BRADSTREET

Armour Research Foundation  
Chicago, Illinois

## PERTINENT ACTIVITIES IN REFRACTORY COMPOSITES

### COATINGS RESEARCH

#### I. Barium Metatitanate Coatings (ARF)

BaTiO<sub>3</sub> coatings on a variety of substrates have now been formed with flame- and plasma-spray equipment. They will be reported in detail by Mr. Bliton at the Fall Meeting of the Enamels Division, American Ceramic Society, French Lick, Indiana, September 20-23. Conclusions drawn are:

- 1) By careful control of particle size, residence time, gas stoichiometry, and chill rate, a variety of BaTiO<sub>3</sub> or oxygen-deficient modifications thereof can be reproducibly deposited as adherent dielectric coatings,
- 2) Such coatings can be made to exhibit unusual microstructures and possess properties in accord with these, and
- 3) X-ray diffraction and electronic measurements of these coatings indicate that thin, high dielectric constant coatings can easily be obtained.

Typical property data are given in Table I.

---

Table I  
PHYSICAL PROPERTIES OF BaTiO<sub>3</sub> ON INCONEL\*

---

<u>Tensile Bond Strength</u>	<u>Bond Strength</u>
Fine blast (-60 mesh SiC)	500 psi
Rough blast (20 grit SiC)	1030 psi
Cohesive strength	2340 psi
Air permeability (13 cm Hg)	less than 10 <sup>-5</sup> cm <sup>2</sup> /sec
Surface condition as sprayed	130-140 microinch RMS

\*Spray distance 6 inches, substrate 500° F max.

---

#### II. Lime-Stabilized ZrO<sub>2</sub> Coatings (ARF)

Because of its low thermal conductivity and chemical inertness, stabilized ZrO<sub>2</sub> has been continually studied. For fine-particle flame-sprayed material, techniques for forming coatings and for measuring their



more important properties have been developed. Properties measured now include those shown in Table II.

Table II  
TYPICAL VALUES FOR STABILIZED  $ZrO_2$  COATINGS

<u>Tensile Bond Strength</u> (in psi with error coefficient, %)				
	<u>-40 +60 SiC</u>	<u>-20 +40 SiC</u>	<u>or 1 mil Ni-Cr</u>	
Armco iron 200-400° F	733 (33)	897 (14)	1450 (10)	
200-800° F	1433 ( 4)	1306 (17)	1520 (13)	
Cohesive Strength:	2640 psi			
<u>Air Permeability</u>	(cc air through cm <sup>3</sup> /min-cm Hg)			
200-400° F	0.031			
200-800° F	0.012			
200-1000° F	0.0039			
Thermal Conductivity (normal to thickness): 4.1 Btu hr <sup>-1</sup> ft <sup>-2</sup> ° F <sup>-1</sup> -in (350° F)				
<u>Total Normal Emittance in air</u>				
	<u>Thickness at</u> <u>(mils)</u>	<u>400° F</u>	<u>800° F</u>	<u>1200° F</u>
Armco iron	4	0.89	0.77	0.77
	9	0.85	0.67	0.77
Aluminum	4	0.82	0.73	-
	9	0.79	0.66	-

### III. Protective Coatings for Metals (Navy BuWep)

A program aimed toward developing coatings to protect vanadium alloys from thermal oxidation has been started (B-227, NOw-61-0806-c). This will involve alloying, cladding, impregnation, and coatings.

### IV. Miscellaneous Oxide Coatings

Coatings predicted to exhibit unusual stability for protecting metals against oxidation have been identified for tantalum-magnesium ( $MgTa_2O_6$ -trirutile), iron-aluminum chromium ( $FeAlCrO_3$ -spinel), ( $Ca, MgZrO_3$ -perovskite), and further fundamental work on "tailoring" protective coatings is continuing. Testing of a  $ZrO_2$ -coated steel cupola, of cooled molds for rotary-cast iron pipe, and of mill transfer rolls for nickel-iron sheet have

been satisfactory.

#### V. Non-Destructive Tests (AF 33(616)-6396, WADD TR 61-91)

Continued study of brittle coatings on ductile substrates has recently involved experimental methods for improving the detection of small spatial variations in transmitted ultrasonic energy, better coupling having been obtained by immersion and by charge scanning the back surface of the receiving crystal with an electrical charge probe. In this way, intermodulated signals transmitted through the body can be "mapped" if ultrasonic damping of the coating is not excessive, as it is with a typical porous sprayed ceramic coating.

Surface waves can be induced in the coating and provide (if the coating is homogeneous) a reliable measure of important elastic properties of a few wave lengths thick layer at its surface. For W-2, vapor deposited, and porcelain enamel coatings this has been observed and correlated with gross flaws sites.

#### VI. Coatings for Fuel Carbides (ARF)

Exploratory studies of  $\text{UO}_2$ , UC, ThC- $\text{UC}_2$ , and  $\text{UC}_2$  particles coated with pyrolytic carbon coatings have shown maximum stability (against thermal migration and cycling) for  $\text{UC}_2$  particles of small size. In suitably dense (BANG) graphite, a 35 per cent U composite in flexural loading withstands over 12,000 psi from room temperature to at least 2000°C.

#### VII. Re-entry Body Research (Confidential, NOw-61-0482-c fbm)

Exploratory work with thin solid films is continuing under AF sponsorship; emphasis has shifted from electronic and optical behavior to chemical properties and structure. A closely allied program sponsored by the Institute of Gas Technology is concerned with fluorite-type solid oxide electrolytes and conductive catalyst suboxide electrodes for fuel cell applications. Film thicknesses range from submicrons to a few mils.

EMITTANCE COATINGS FOR THE ENHANCEMENT  
OF RADIATION HEAT TRANSFER  
FROM SOLIDS

RONALD L. JOHNSON

Plasmadyne Corporation  
Santa Ana, California

## INTRODUCTION:

The most stable materials for high temperature usages in air are the simple oxides. Not only do the oxides possess chemical stability at high temperature but they also have other inherent physical qualities that make them outstanding for numerous extreme temperature applications.

In general, the oxides are lightweight, have low thermal conductivities, are strong in compression, have low thermal expansions, low vapor pressures, and a few other outstanding features.

Some disadvantages of the oxides for flight applications in air are (1) low tensile strength, (2) low thermal shock resistance, (3) low total emissivities, and (4) difficulty in fabrication to useful shapes.

Numerous investigators have developed techniques to overcome the low tensile strength properties of oxides, solved the difficult fabrication problems associated with the oxides, and have increased the thermal shock resistance of the bodies.

Very little has been done to increase the total radiation capabilities of the oxides. The objective of this paper is to present techniques to increase the emittance abilities of materials to increase radiation heat transfer.

## SUMMARY:

The work presented depicts methods to increase the surface emittance of materials notably, the common oxides of Aluminum, Zirconium, Thorium and metals.

The increase in surface emittance increases the radiation transfer capabilities of these materials.

THEORY:

The basic relation for thermal radiation is given by the Stefan-Boltzmann equation:

$$Q = \sigma \cdot E (T^4 - T_o^4) \quad \text{Equation 1}$$

where

$$Q = \text{v. radiant flux emitted per unit area}$$

$$\frac{\text{Btu}}{\text{ft}^2 \cdot \text{hr}}$$

$$\sigma = \text{Boltzmann constant}$$

$$1.797 \times 10^{-8} \frac{\text{Btu}}{\text{ft}^2 \cdot \text{OR}^4 \cdot \text{hr}}$$

$$T = \text{absolute temperature of the radiating body} - ^\circ\text{R}$$

$$T_o = \text{absolute temperature of the surroundings}$$

$$E = \text{emittance factor}$$

The relation is simple to follow. It says that radiation energy transfer is governed by a constant, the emissivity, and the temperature of the bodies to the fourth power.

The emittance term is simply defined as the ratio of radiation from a given body compared to a blackbody radiation at the same temperature. A blackbody is a body whose surface absorbs all radiation received and reflects none. (It also emits the greatest amount of thermal radiation possible at a given temperature).

Thus emittance is an efficiency ratio of the radiation emitted by a surface with respect to the maximum radiation capable of being emitted. It is physically a surface property and not a bulk property of a material system. Equation-wise it is proportional to:

$$E \approx \left( \frac{T_{\text{blackbody}}}{T_{\text{actual}}} \right)^4 \quad \text{Equation 2}$$

Emittance may vary from 0-1.0 in range. From Equation 1 it is noted that as emittance increases the radiation increases at a fixed surface temperature. Thus to take full advantage of a high temperature oxide type thermal insulator system it is important that the emittance term be as close to unity as possible. Rejection of energy by radiation is an extremely important mode of energy transfer. The success of leading edges, nose cones, and other like parts of high speed aircraft in an atmosphere depends highly on radiation energy transfer.

This paper will describe methods to increase the emittance of surfaces by a few conventional techniques and introduce a new technique to accomplish the same.

DISCUSSION:

Techniques to increase emittance of a surface involve methods to make the surface appear as a blackbody. They include (1) surface finish, and (2) surface composition. The remaining discussion will describe surface finish, surface materials, and some chemical reactions for increasing emittance.

SURFACE FINISH:

Increasing the surface area increases the radiation transfer. References 4 and 5 substantiate this effect.

Physical methods to accomplish this are: (1) abrasive roughening, (2) controlled sprayed roughness, (3) chemical etching, and (4) mechanical scribing and/or machining.

It has been shown that if a length to diameter ratio of greater than 12 is achieved by a hole on a surface, the hole will radiate as a blackbody. It appears then that a surface containing minute holes (let's say, approximately  $10^6$  holes/sq. inch of surface) would radiate as a blackbody.

It is believed that plasma jet-spray techniques can be controlled to achieve this condition. Development techniques are being evaluated to prove the hypothesis. Test data will be available within a short period.

As-sprayed coatings possess a partial "holed" surface as noted from profilometer readings and photomicrographs.

Using results obtained by the "dissolvable mandrel" techniques, composites can be sprayed as a mixture and a single constituent can be "dissolved away". This method lends itself to providing the million holes/sq. inch of surface desired.

SURFACE MATERIALS AND/OR COMPOSITION:

Specific materials are known to have high total emittances at relatively low temperatures. There is some data at high temperature  $2000^{\circ}\text{F}$ , but it is primarily data obtained under vacuum conditions on the refractory metals and graphites.

The only material investigated with a high total emittance is graphite and/or graphite type materials. All data reported on the simple oxides such as  $\text{Al}_2\text{O}_3$ ,  $\text{ZrO}_2$ ,  $\text{ThO}_2$ , etc., show that these materials have low total emittance, in fact, they are good reflectors. These same materials are being used in the construction of high speed, high temperature vehicles. It is necessary to increase the surface emittance characteristics of these materials. Logical solutions for this are surface coatings. The authors experience gained under AF33 (616)-5441 has shown that a 300% increase in emittance can be obtained by surface treating  $\text{ZrO}_2$  with a small quantity of Chromia. With wise selection so as not to upset temperature limits, compatible

Surface Materials and/or Composition (continued)

coatings can upgrade the oxides emittance abilities.

Cer. materials that merit direct investigation for increasing emittance of oxides for use in air are certain of the borides, notably silicon and columbium diboride.

Another oxide logical to investigate although physical data is scant is Praseodymium oxide in one form or another, probably  $\text{Pr}_2\text{O}_3$ .

Techniques to apply high emittance coatings onto the oxides involves the usage of flamespray or plasma spray equipment.

Normal surface preparation such as grit blasting is necessary to increase the roughness of the substrate to be coated. Only a few mils of thickness are sufficient to give the materials the desired high emittance surface property.

Final success of this method can only be proved by rigid testing under simulated test conditions. Tests will determine emittances and compatibility limits.

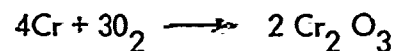
LOWER TEMPERATURE HIGH EMITTANCE SURFACES:

High surface emittance is also required frequently on metal structures such as the superalloys and the stainless steels. One of the easiest ways to increase the emittance of these materials is to oxidize the surface. The iron and chromium ingredients form a blackened surface upon oxidizing. Surface roughness is also accomplished by oxidation.

However, sometimes the required heat treat to oxidize surfaces of fabricated shapes is undesirable. A way around this has been developed. Using a sprayed on coating a few mils thick can increase the emittance properties of the steel alloys without heating the part. This is done by following the sequence schematically shown in Figure 3.

When like materials are being processed, gradation spraying can be omitted. When unlike materials are being processed, gradation spraying should be used.

The chemical reaction taking place in the plasma jet spraying is depicted for example, as:



This would apply in plasma spraying Hastelloy C powder onto a Hastelloy C fabricated part. The chromium content of the Hastelloy C alloy powder would be oxidized to give the high emittance coating desired by adding oxygen during spraying. No where in the process would the substrate (part being coated) become hotter than  $300^\circ\text{F}$ .

Experimental data should be as good or better than shown in Figures 1 and 2.

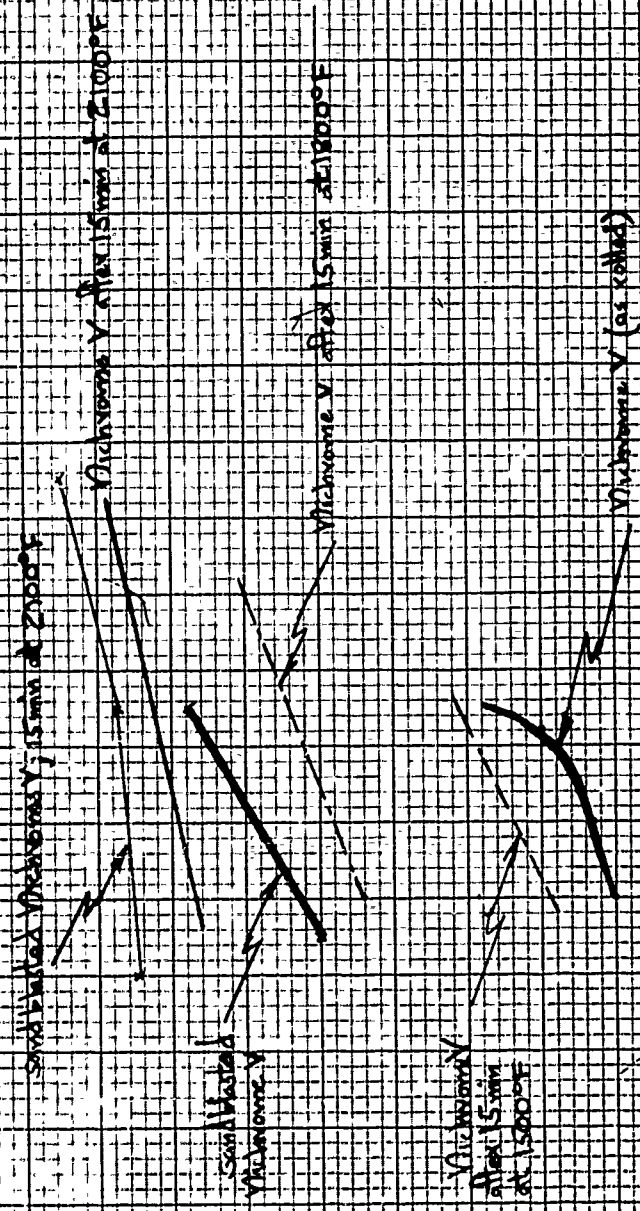
REFERENCES:

1. Suppression of Radiations at High Temperatures, by Means of Ceramic Coatings.  
D.G. Bennett, Journal of Am. Cer. Soc., October, 1947
2. The Perkin-Elmer Instrument News for Science and Industry  
Summer 1959 Vol. 10, No. 4  
Norwalk, Conn.
3. High Temperature Technology  
I.E. Campbell, 1956 - Wiley and Sons
4. Some Measurements of the Total Emissivity of Metals and Pure Refractory Oxides and the Variation of Emissivity with Temperature  
Sully, Brandes, and Waterhouse, Fulmer Research Institute, Ltd.,  
Stoke Poges, Bucks, British Journal of Applied Physics, October 1951
5. Measurement of Total Emissivity of Gas Turbine Combustor Materials  
S.M. Corso and R.L. Coit, Transaction of the ASME, November 1955



# Total Reflected Emissivity versus Temperature

for Nichrome V with various  
surface finishes and heat treatments  
(from reference 2)



Temperature - °F

# Total Emissivity versus Temperature for selected absorbent coatings Plasmadyne Corp 3-9-61

oxidized electrolytic iron

lampblack

oxidized steel

Fe<sub>2</sub>O<sub>3</sub>

Silicon  
Dioxide

Carbon  
(Siemens-Guthrie)

1.0

0.8

0.6

0.4

0.2

0

1000

2000

3000

Temperature - OF

Note:

Data on: Boron Carbide  
Chromium Oxide

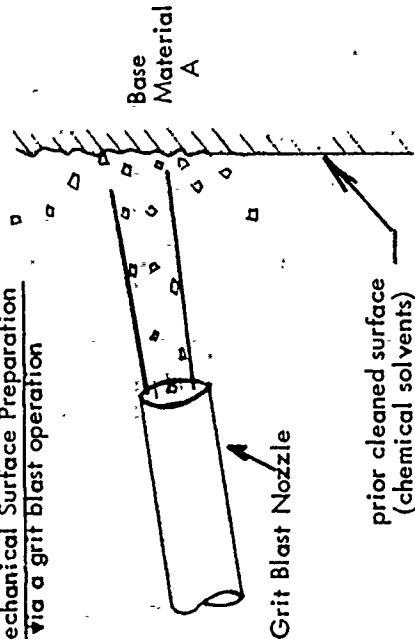
unknown to author  
expected to be > 90%  
(between 1000-3000°F)

fig 2

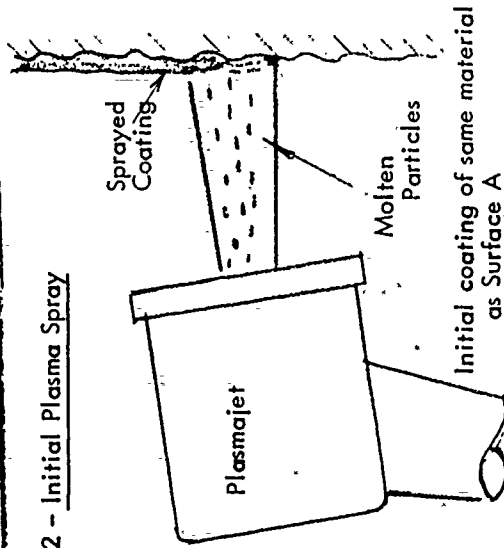
17

# SEQUENCE TO PRODUCE EMISSIVE CONTROL COATINGS VIA THE PLASMAJET

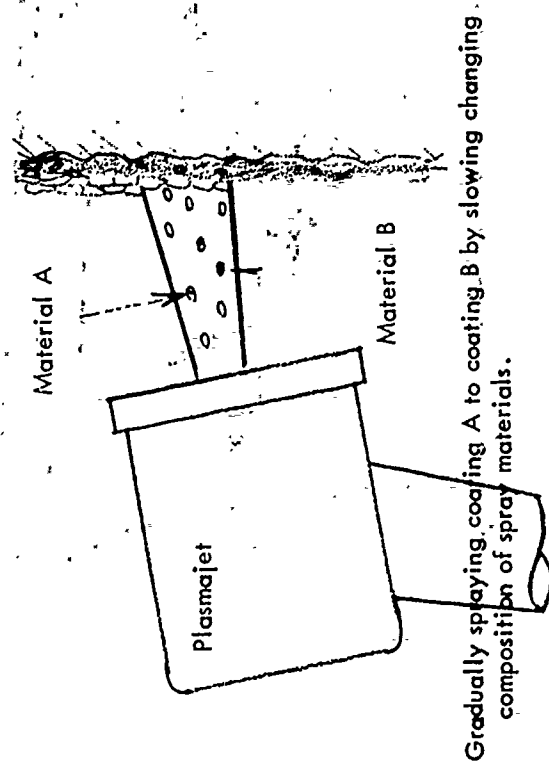
## Step 1 - Mechanical Surface Preparation via a grit blast operation



## Step 2 - Initial Plasma Spray

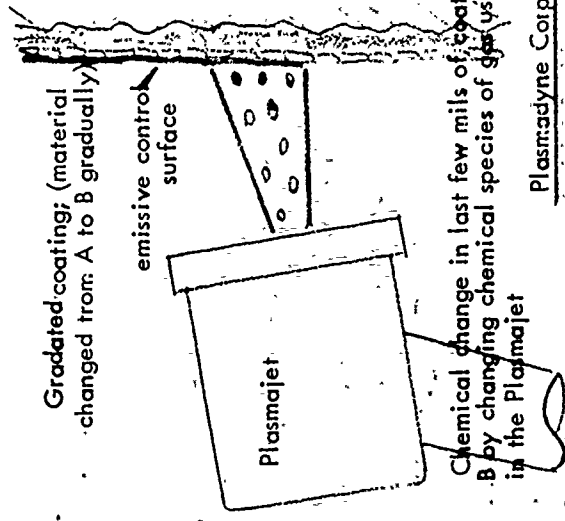


## Step 3 - Gradation Plasma Spray



Gradually spraying coating A to coating B by slowly changing composition of spray materials.

## Step 4 - Surface Chemical Reaction Via Plasmajet



Chemical change in last few mils of coating B by changing chemical species of gas used in the Plasmajet

Figure 3

Aeronautical Systems Division, Dir/Materials and Processes, Air Force Systems Command, Wright-Patterson Air Force Base, Ohio, Tech. Doc. Report No. ASD-TDR-63-96. SUMMARY OF THE FIFTH REFRACTORY COMPOSITES WORKING GROUP MEETING. August 1961. p. 520

Unclassified Report

This report is a compilation of 37 papers describing most of the information discussed at the 5th Refractory Composites Working Group Meeting held at the Chance Vought Corp., Dallas, Texas, on 8-10 August 1961. The representatives of approximately 50 organizations presented informal discussions of their current

( over )

activities in the fields of development, evaluation, and application of inorganic refractory composites for use over approximately 2500°F.

1. High temperature materials
2. Protective coatings
3. Refractory materials
  - I. AFSC Project 7381,
  - II. Directorate of Materials and Processes, Aeronautical Systems Division
  - III. L. N. Hjelm
  - IV. Not avail. fr OTS
  - V. In ASTIA collection